SIXTH EDITION

Infrared and Raman Spectra of Inorganic and Coordination Compounds

Part B

APPLICATIONS IN COORDINATION, ORGANOMETALLIC, AND BIOINORGANIC CHEMISTRY

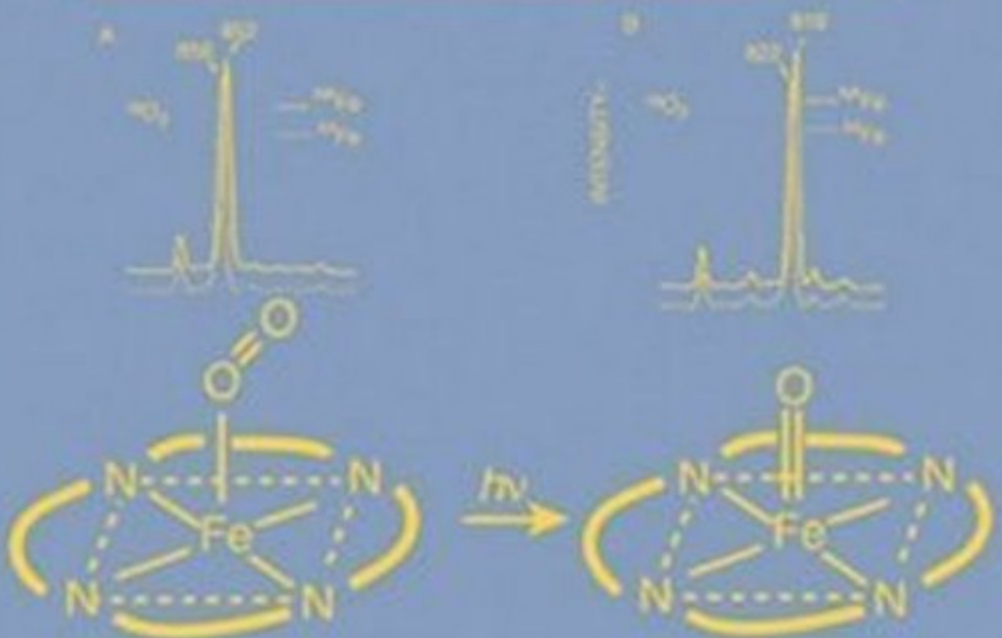

KAZUO NAKAMOTO

WILEY

Infrared and Raman Spectra of Inorganic and Coordination Compounds

Infrared and Raman Spectra of Inorganic and Coordination Compounds

Part B: Applications in Coordination, Organometallic, and Bioinorganic Chemistry

Sixth Edition

Kazuo Nakamoto
Wehr Professor Emeritus of Chemistry
Marquette University

WILEY

A JOHN WILEY & SONS, INC., PUBLICATION

Published by John Wiley & Sons, Inc., Hoboken, New Jersey
Published simultaneously in Canada

Library of Congress Cataloging-in-Publication Data is available.

ISBN 978-0-471-74493-1

Printed in the United States of America

10 9 8 7 6 5 4 3 2 1

Contents

Preface to the Sixth Edition

Since the fifth edition was published in 1996, a number of new developments have been made in the field of infrared and Raman spectra of inorganic and coordination compounds. The sixth edition is intended to emphasize new important developments as well as to catch up with the ever-increasing new literature. Major changes are described below.

Part A. Chapter 1 (''Theory of Normal Vibrations'') includes two new sections. Section 1.24 explains the procedure for calculating vibrational frequencies on the basis of density functional theory (DFT). The DFT method is currently used almost routinely to determine molecular structures and to calculate vibrational parameters. Section 1.26 describes new developments in matrix cocondensation techniques. More recently, a large number of novel inorganic and coordination compounds have been prepared by using this technique, and their structures have been determined and vibrational assignments have been made on the basis of results of DFT calculations. Chapter 2 (''Applications in Inorganic Chemistry'') has been updated extensively, resulting in a total number of references of over 1800. In particular, sections on triangular X_3- and tetrahedral X_4-type molecules have been added as Secs. 2.2 and 2.5, respectively. In Sec. 2.8, the rotational–vibrational spectrum of the octahedral UF_6 molecule is shown to demonstrate how an extremely small metal isotope shift by $^{235}U/^{238}U$ substitution (only $0.6040\,cm^{-1}$) can be measured. Section 2.14 (''Compounds of Carbon'') has been expanded to show significant applications of vibrational spectroscopy to the structural determination of fullerences, endohedral fullerenes, and carbon nanotubes. Vibrational data on a number of novel inorganic compounds prepared most recently have been added throughout Chapter 2.

Part B. Chapter 1 (''Applications in Coordination Chemistry'') contains two new Sections: Sec. 1.6 (''Metallochlorins, Chlorophylls, and Metallophthalocyanines'')

and Sec. 1.19 (“Complexes of Carbon Dioxide”). The total number of references has approached 1700 because of substantial expansion of other sections such as Secs. 1.5, 1.18, 1.20, 1.22, and 1.28. Chapter 2 (“Applications in Organometallic Chemistry”) includes new types of organometallic compounds obtained by matrix cocondensation techniques (Sec. 2.1). In Chapter 3 (“Applications in Bioinorganic Chemistry”), a new section (Sec. 3.4) has been added, and several sections such as Secs. 3.3, 3.7, and 3.9 have been expanded to include many important new developments.

I would like to express my sincere thanks to all who helped me in preparing this edition. Special thanks go to Prof. J. R. Kincaid (Marquette University), Prof. R. S. Czernuszewicz (University of Houston), and Dr. T. Kitagawa (Institute for Molecular Science, Okazaki, Japan) for their help in writing new sections of Chapter 3 of Part B. My thanks also go to all the authors and publishers who gave me permission to reproduce their figures in this and previous editions.

Finally, I would like to thank the staff of John Raynor Science Library of Marquette University for their help in collecting new references.

Milwaukee, Wisconsin
March 2008

KAZUO NAKAMOTO

Abbreviations

Several different groups of acronyms and other abbreviations are used:

1. IR, infrared; R, Raman; RR, resonance Raman; *p*, polarized; *dp*, depolarized; *ap*, anomalous polarization; *ia*, inactive.
2. ν, stretching; δ, in-plane bending or deformation; ρ_w, wagging; ρ_r, rocking; ρ_t, twisting; π, out-of-plane bending. Subscripts, *a*, *s*, and *d* denote antisymmetric, symmetric, and degenerate modes, respectively. Approximate normal modes of vibration corresponding to these vibrations are given in Figs. 1.25 and 1.26.
3. DFT, density functional theory; NCA, normal coordinate analysis; GVF, generalized valence force field; UBF, Urey–Bradley force field.
4. M, metal; L, ligand; X, halogen; R, alkyl group.
5. g, gas; l, liquid; s, solid; m or mat, matrix; sol'n or sl, solution; (gr) or (ex), ground or excited state.
6. Me, methyl; Et, ethyl; Pr, propyl; Bu, butyl; Ph, phenyl; Cp, cyclopentadienyl; OAc^-, acetate ion; py, pyridine; pic, pycoline; en, ethylenediamine. Abbreviations of other ligands are given when they appear in the text.

In the tables of observed frequencies, values in parentheses are calculated or estimated values unless otherwise stated.

Chapter 1

Applications in Coordination Chemistry

1.1. AMMINE, AMIDO, AND RELATED COMPLEXES

1.1.1. Ammine (NH_3) Complexes

Vibrational spectra of metal ammine complexes have been studied extensively, and these are reviewed by Schmidt and Müller [1]. Figure 1.1 shows the infrared spectra of typical hexammine complexes in the high-frequency region. To assign these NH_3 group vibrations, it is convenient to use the six normal modes of vibration of a simple 1 : 1 (metal/ligand) complex model such as that shown in Fig. 1.2. Table 1.1 lists the infrared frequencies and band assignments of hexammine complexes. It is seen that the antisymmetric and symmetric NH_3 stretching, NH_3 degenerate deformation, NH_3 symmetric deformation, and NH_3 rocking vibrations appear in the regions of 3400–3000, 1650–1550, 1370–1000, and 950–590 cm^{-1}, respectively. These assignments have been confirmed by NH_3/ND_3 and $NH_3/^{15}NH_3$ isotope shifts.

The NH_3 stretching frequencies of the complexes are lower than those of the free NH_3 molecule for two reasons. One is the effect of coordination. On coordination, the N−H bond is weakened and the NH_3 stretching frequencies are lowered. The stronger the M−N bond, the weaker is the N−H bond and the lower are the NH_3 stretching frequencies if other conditions are equal. Thus the NH_3 stretching frequencies may be used as a rough measure of the M−N bond strength. The other reason is the effect of the counterion. The NH_3 stretching frequencies of the chloride

Infrared and Raman Spectra of Inorganic and Coordination Compounds, Part B: Applications in Coordination, Organometallic, and Bioinorganic Chemistry, Sixth Edition, by Kazuo Nakamoto

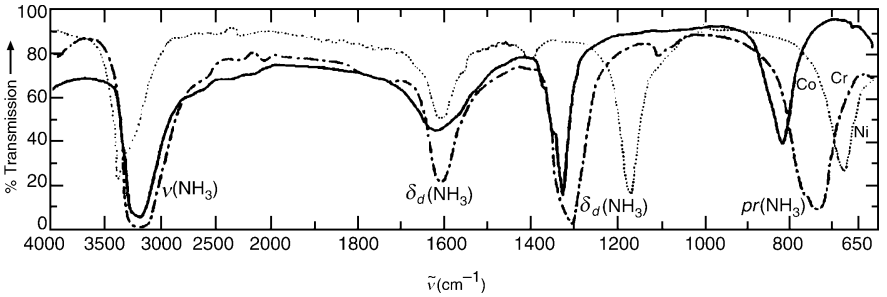

Fig. 1.1. *Infrared spectra of hexammine complexes: $[Co(NH_3)_6]Cl_3$ (solid line), $[Cr(NH_3)_6]Cl_3$ (dotted–dashed line), and $[Ni(NH_3)_6]Cl_2$ (dotted line).*

are much lower than those of the perchlorate, for example. This is attributed to the weakening of the N−H bond, due to the formation of the N−H···Cl-type hydrogen bond in the former.

The effects of coordination and hydrogen bonding mentioned above shift the NH_3 deformation and rocking modes to higher frequencies. Among them, the NH_3 rocking mode is most sensitive, and the degenerate deformation is least sensitive, to these effects. Thus the NH_3 rocking frequency is often used to compare the strength of the M−N bond in a series of complexes of the same type and anion. As will be shown in

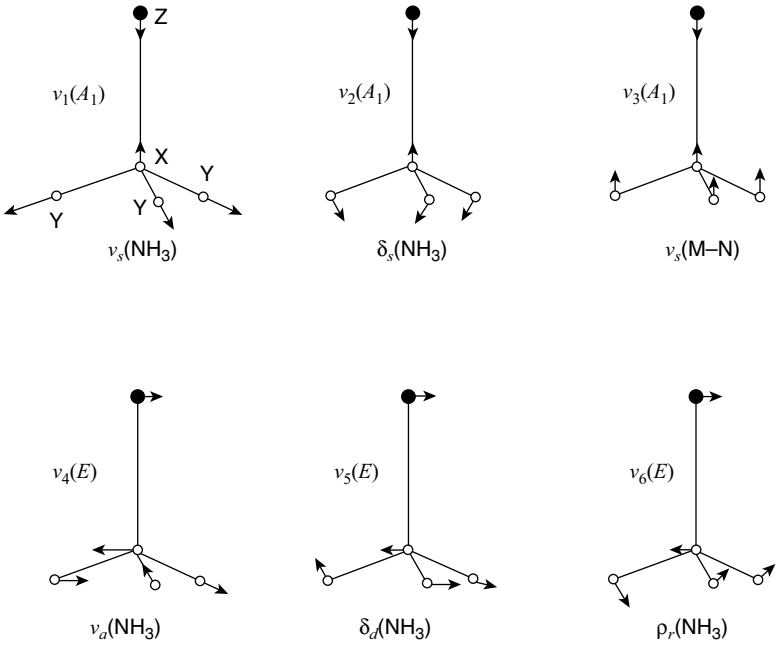

Fig. 1.2. *Normal modes of vibration of tetrahedral ZXY_3 molecules. (The band assignment is given for an M−NH_3 group.)*

TABLE 1.1. Infrared Frequencies of Octahedral Hexammine Complexes (cm^{-1})[a]

Complex	$\nu_a(NH_3)$		$\nu_s(NH_3)$	δ_a(HNH)	δ_s(HNH)	$\rho_r(NH_3)$	ν(MN) IR	ν(MN) Raman	δ(NMN)	Ref.
$[Mg(NH_3)_6]Cl_2$	3353		3210	1603	1170	660	363	335 (A_{1g}) 243 (E_g)	198	2
$[Cr(NH_3)_6]Cl_3$	3257		3185 3130	1630	1307	748	495 473 456	465 (A_{1g}) 412 (E_g)	—	3
$[^{50}Cr(NH_3)_6](NO_3)_3$	3310		3250 3190	1627	1290	770	471	—	270	4
$[Mn(NH_3)_6]Cl_2$	3340		3160	1608	1146	592	302	330 (A_{1g})	165	1,5
$[Fe(NH_3)_6]Cl_2$	3335		3175	1596	1156	633	315	—	170	1,5
$[Ru(NH_3)_6]Cl_2$	3315		3210	1612	1220	763	409	—	—	6
$[Ru(NH_3)_6]Cl_3$		3077		1618	1368 1342	788	463	500 (A_{1g}) 475 (E_g)	283 263	7
$[Os(NH_3)_6]OsBr_6$		3125		1595	1339	818	452	—	256	7
$[Co(NH_3)_6Cl_2$	3330		3250	1602	1163	654	325	357 (A_{1g}) 255 (E_g)	92	5
$[Co(ND_3)_6]Cl_3$	3240		3160	1619	1329	831	498 477 449	500 (A_{1g}) 445 (E_g)	331	8∼10
$[Co(ND_3)_6]Cl_3$	2440		2300	1165	1020	667	462 442 415	—	294	4
$[Rh(NH_3)_6]Cl_3$		3200		1618	1352	845	472	515 (A_{1g}) 480 (E_g)	302	7,10
$[Ir(NH_3)_6]Cl_3$		3155		1587	1350 1323	857	475	527 (A_{1g}) 500 (E_g)	279 264	7,10
$[^{58}Ni(NH_3)_6]Cl_2$	3345		3190	1607	1176	685	335	370 (A_{1g}) 265 (E_g)	217	8,11
$[Zn(NH_3)_6]Cl_2$	3350		3220	1596	1145	645	300	—	—	1
$[Cd(NH_3)_6]Cl_2$	—		—	1585	1091	613	298	342 (A_{1g})	—	5
$[Pt(NH_3)_6]Cl_4$	3150		3050	1565	1370	950	530 516	569 (A_{1g}) 545 (E_g)	318	12,13

[a]All infrared frequencies are those of the F_{1u} species.

the next subsection, a simple 1 : 1 complex such as that shown in Fig. 1.2 has been prepared in inert gas matrices [30].

To assign the skeletal modes such as the MN stretching and NMN bending modes, it is necessary to consider the normal modes of the octahedral MN_6 skeleton ($\mathbf{O}_h$ symmetry). The MN stretching mode in the low-frequency region is of particular interest since it provides direct information about the structure of the MN skeleton and the strength of the M−N bond. The octahedral MN_6 skeleton exhibits two ν(M−N) (A_{1g} and E_g) in Raman and one ν(M−N) (F_{1u}) in infrared spectra (see Sec. 2.8 of Part A). Most of these vibrations have been assigned on the basis of observed isotope shifts (including metal isotopes, NH_3/ND_3 and $NH_3/^{15}NH_3$) and normal coordinate calculations. Although the assignment of the ν(Co−N) in the infrared spectrum of $[Co(NH_3)_6]Cl_3$ had been controversial, Schmidt and Müller [4] confirmed the assignments that the three weak bands at 498, 477, and 449 cm^{-1} are the split components of the triply degenerate F_{1u} mode (Fig. 1.4). The intensity of the MN stretching mode in the infrared increases as the M−N bond becomes more ionic and as the MN stretching frequency becomes lower. Relative to the Co(III)−N bond of the $[Co(NH_3)_6]^{3+}$ ion, the Co(II)−N bond of the $[Co(NH_3)_6]^{2+}$ ion is more ionic, and its stretching frequency is much lower (325 cm^{-1}). This may be responsible for the strong appearance of the Co(II)−N stretching band in the infrared. As listed in Table 1.1, two Raman-active MN stretching modes (A_{1g} and E_g) are observed for the octahedral hexammine salts. In general, $\nu(A_{1g})$ is higher than $\nu(E_g)$. However, the relative position of $\nu(F_{1u})$ with respect to these two vibrations changes from one compound to another. Another obvious trend in ν(MN) is $\nu(M^{4+}-N) > \nu(M^{3+}-N) > \nu(M^{2+}-N)$. This holds for all symmetry species. Table 1.1 shows that the NH_3 rocking frequency also follows the same trend as above.

Normal coordinate analyses on metal ammine complexes have been carried out by many investigators. Among them, Nakagawa, Shimanouchi, and coworkers [13] have undertaken the most comprehensive study, using the UBF (Urey–Bradley Force) field. The MN stretching force constants of the hexammine complexes follow this order:

$$\underset{2.13}{Pt(IV)} \gg \underset{1.05}{Co(III)} > \underset{0.94}{Cr(III)} > \underset{0.34}{Ni(II)} \approx \underset{0.33}{Co(II)} \quad \text{mdyn/Å}$$

Acevedo and coworkers carried out normal coordinate calculations on the $[Cr(NH_3)_6]^{3+}$ and $[Ni(NH_3)_6]^{2+}$ ions [14,15]. On the other hand, Schmidt and Müller [4,5] and other workers [8] calculated the GVF (generalized valence Force) constants of a number of ammine complexes by using the point mass model (where the NH_3 ligand is regarded as a single atom having the mass of NH_3), and refined their values with isotope shift data (H/D, $^{14}N/^{15}N$, and metal isotopes). For the hexammine series, they obtained the following order:

$$\underset{2.75}{Pt^{4+}} > \underset{2.28}{Ir^{3+}} > \underset{2.13}{Os^{3+}} > \underset{2.10}{Rh^{3+}} > \underset{2.01}{Ru^{3+}} > \underset{1.86}{Co^{3+}} >$$

$$\underset{1.66}{Cr^{3+}} > \underset{0.85}{Ni^{2+}} > \underset{0.80}{Co^{2+}} > \underset{0.73}{Fe^{2+}} \sim \underset{0.69}{Cd^{2+}} > \underset{0.67}{Zn^{2+}} > Mn^{2+} \quad \text{mdyn/Å}$$

TABLE 1.2. Infrared Frequencies of Other Ammine Complexes (cm^{-1})

Complex	$\nu_a(NH_3)$	$\nu_s(NH_3)$	$\delta_a(HNH)$	$\delta_s(HNH)$	$\rho_r(NH_3)$	ν(MN) IR	ν(MN) Raman	δ(NMN)	Ref.
Tetrahedral									
$[Co(NH_3)_4](ReO_4)_2$	3340	3260	1610	1240	693	430	405 (A_1)	195	16
$[^{64}Zn(NH_3)_4]I_2$	3275	3150	1596	1253	685	—	432 (A_1)	156	17,18
	3233			1239			412 (F_2)		
$[Cd(NH_3)_4](ReO_4)_2$	3354	3267	1617	1176	670	370	—	166	1,19
								160	
Square-planar									
$[^{104}Pd(NH_3)_4]Cl_2 \cdot H_2O$	3270	3170	1630	1279	849	495	502 (A_{1g})	325	4,20,21
					802		482 (B_{1g})	300	
$[Pt(NH_3)_4]Cl_2$	3236	3156	1563	1325	842	510	543 (A_{1g})	301	13,22,21
							522 (B_{1g})		
$[Cu(NH_3)_4]So_4 \cdot H_2O$	3327	3169	1669	1300	735	426	420 (A_{1g})	256	4,23
	3253		1639	1283			375 (B_{1g})	227	
$[Au(NH_3)_4(NO_3)_3$	3490	3105	1571	1331	936	555	566	327	24
	3220				914		544	307	
								272	
Linear									
$[Ag(NH_3)_2So_4$	3320	3150	1642	1236	740	476	372 (A_1)	221	25,26
	3230		1626	1222	703	400		211	27
$[Hg(NH_3)_2Cl_2$	3265	3197	1605	1268	719	513	412	—	

For a series of divalent metals, this order is parallel to the Irving–Williams series ($Mn^{2+} < Fe^{2+} < Co^{2+} < Ni^{2+} < Cu^{2+} > Zn^{2+}$). Schmidt and Müller [1] discussed the relationship between the MN stretching force constant and the stability constant or the bond energy.

Table 1.2 lists the observed infrared frequencies and band assignments of tetrahedral, square–planar, and linear metal ammine complexes. The Raman-active MN stretching frequencies are also included in Table 1.2. Normal coordinate analyses have been made by Nakagawa et al. [13] by using the UBF field; the following values were obtained for the MN stretching force constants:

$$\underset{2.05}{Hg^{2+}} > \underset{1.92}{Pt^{2+}} > \underset{1.71}{Pd^{2+}} > \underset{0.84}{Cu^{2+}} \quad \text{mdyn/Å}$$

Normal coordinate calculations have also been made by Tellez [28] on the tetrahedral $[Zn(NH_3)_4]^{2+}$ and $[Cd(NH_3)_4]^{2+}$ ions. Using the GVF field and the point mass approximation, Schmidt and Müller [5] obtained the following values:

$$\underset{2.54}{Pt^{2+}} > \underset{2.15}{Pt^{2+}} \gg \underset{1.44}{Co^{2+}} \sim \underset{1.43}{Zn^{2+}} \sim \underset{1.42}{Cu^{2+}} > \underset{1.24}{Cd^{2+}} \quad \text{mdyn/Å}$$

As stated above, NH_3 frequencies of ammine complexes are determined by the strength of the M−N bond as well as the strength of the N−H···X hydrogen bond. The order of this synergetic effect has been studied for $[M(NH_3)_6]X_2$-type complexes [29].

1.1.2. Ammine Complexes in Inert Gas Matrices

Infrared spectra of cocondensation products of alkali halide (MX) vapors with NH_3 diluted in argon were measured by Ault [34]. ln the case of KCl, for example, the bands at 3365, 3177, and 1103 cm^{-1} have been assigned to the $\nu_a(NH_3)$, $\nu_s(NH_3)$, $\delta_s(HNH)$, respectively, of the 1 : 1 ion pair of type I shown below:

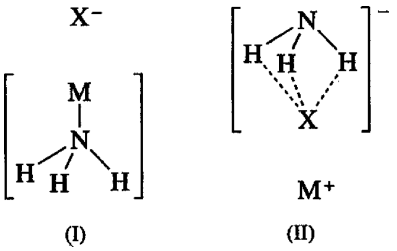

The type II structure was ruled out because of the following reasons: (1), the $\delta_s(HNH)$ frequency should be sensitive to the metal ion in (I) and to the anion in (II) [the fact that it shows relatively large shifts by changing the metal ion, but almost no shifts by changing the anion, supports (I)]; and (2) the $\nu_a(NH_3)$ and $\nu_s(NH_3)$ in (II) are expected to be highly sensitive to the anion, owing to formation of the N−H···X hydrogen bonds; this is not the case in (I). The fact that they show only small shifts in going from CsCl to CsI supports (I). Further supports for structure (I) are given by the appearance of the $\rho_r(NH_3)$ and ν(M−N) at 458 and 232 cm^{-1} (KCl), respectively. These frequencies are much lower than those of transition metal complexes discussed earlier, because their M−N bonds are much weaker (more ionic).

Süzer and Andrews [31] studied the IR spectra of cocondensation products of alkali metal (M) vapors with NH_3/Ar. They assigned the following bands:

	Li	Na	K	Cs	
$\nu_s(NH_3)$	3277	3294	3292	3287	(all in cm^{-1})
$\delta_s(NH_3)$	1133	1079	1064	1049	

to the 1 : 1 adduct of $\mathbf{C}_{3v}$ symmetry which is similar to that of the $M(NH_3)^+$ cation discussed earlier. The M−NH_3 bonding has been attributed to a small charge transfer from NH_3 to M in the case of Li and Na, and to a reverse charge transfer in the case of K and Cs. At high concentrations of M and NH_3, large aggregates of undefined stoichiometries were formed. Similar work including Fe and Cu was carried out by Szczepanski et al. [32] Loutellier et al. [33] have made the most extensive IR study on the Li(K)/NH_3/Ar system. By varying the concentrations and relative ratios of M/NH_3 in a wide range, they were able to observe bands characteristic of the 1 : 1, 1 : 2, . . ., 1 : n,

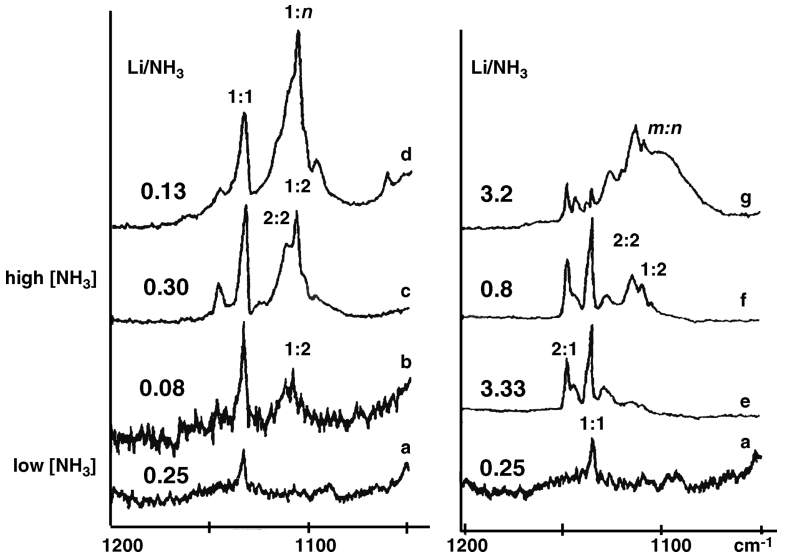

Fig. 1.3. *IR spectra (1200–1050 cm^{-1}) of cocondensation products of Li atoms with NH_3 molecules in Ar matrices. Left column: (a) Li/NH_3/Ar = 0.1/0.4/1000, (b) 0.1/1.2/1000, (c) 3/10/1000, and (d) 2.5/20/1000. Right column: (a) Li/NH_3/Ar = 0.1/0.4/1000, (e) 2/0.6/1000, (f) 2/2.5/1000, and (g) 8/2.5/1000 [33].*

and $2:1, 3:1 \cdots m:1$ adducts. As an example, Fig. 1.3 shows the IR spectra of the Li/NH_3/Ar system in the $\delta_s(NH_3)$ region. The molar ratios (Li/NH_3) and the peaks characteristic of each species are indicated in the figure. In general, the 1 : 1 adduct is formed when the concentrations of Li and NH_3 are close. If the concentration of NH_3 is high relative to Li, the $1:n$ ($n = 2,3,4,\ldots$) adducts are formed. On the other hand, the $m:1$ ($m = 2,3,4\ldots$) adducts result when the concentration of Li is high relative to NH_3. For the 1 : 1 adduct of Li, the bands at 381 and 320 cm^{-1} have been assigned to the $\rho_r(NH_3)$ and ν(Li−N), respectively. The Li−N stretching force constant was found to be 0.3 mdyn/Å.

Photolysis of ammine complexes in inert gas matrices has been used to produce a number of new species. For example, Ault [34] obtained $Cl_2V(O)NH_2$ by the reaction

$$OVCl_3 + NH_3 \xrightarrow{\text{in Ar}} OVCl_3 - NH_3 \xrightarrow{h\nu} Cl_2V(O)NH_2 + HCl$$

and its infrared spectrum was assigned by isotopic substitution (H/D and $^{14}N/^{15}N$) and DFT calculations. Similar reactions have been utilized to prepare $HSiNH_2$ [35] and $HMNH_2$(M = Al,Ga, In) [36].

1.1.3. Halogenoammine Complexes

If the NH_3 groups of a hexammine complex are partly replaced by other groups, the degenerate vibrations are split because of lowering of symmetry, and new

TABLE 1.3. Skeletal Vibrations of Pentammine and *trans*-Tetrammine Co (III) Complex (cm^{-1}) [37,38]

Complex	ν(CoN)	ν(CoX)	Skeletal Bending
Pentammine ($\mathbf{C}_{4v}$)			
$[Co(NH_3)_5F]^{2+}$			
A_1	480, 438	343	308
E	498	—	345, 290, 219
$[Co(NH_3)_5Cl]^{2+}$			
A_1	476, 416	272	310
E	498	—	292, 287, 188
$[Co(NH_3)_5Br]^{2+}$			
A_1	475, 410	215	287
E	497	—	290, 263, 146
$[Co(NH_3)_5I]^{2+}$			
A_1	473, 406	168	271
E	498	—	290, 259, 132
trans-Tetrammine ($\mathbf{D}_{4h}$)			
$[Co(NH_3)_4Cl_2]^{+}$			
A_{2u}	—	353	186
E_u	501	—	290, 167
$[Co(NH_3)_4Br_2]^{+}$			
A_{2u}	—	317	227
E_u	497	—	280, 120

bands belonging to other groups appear. Here we discuss only halogenoammine complexes. The infrared spectra of $[Co(NH_3)_5X]^{2+}$- and *trans*-$[Co(NH_3)_4X_2]^{+}$-type complexes have been studied by Nakagawa and Shimanouchi [37,38]. Table 1.3 lists the observed frequencies and band assignments obtained by these workers. The infrared spectra of some of these complexes in the CoN stretching region are shown in Fig. 1.4. Normal coordinate analyses on these complexes [37] have yielded the following UBF stretching force constants (mdyn/Å): K(Co−N), 1.05; K(Co−F), 0.99; K(Co−Cl), 0.91; K(Co−Br), 1.03; and K(Co−I), 0.62.

Using the GVF force field, Chen et al. [39,40] also carried out normal coordinate analysis on $[M(NH_3)_5X]$-type complexes (M = Co, Cr; X = NH_3, Cl, H_2O, OH, etc.) to obtain the ν(M−N) and ν(M−X) force constants.

Raman spectra of some chloroammine Co(III) complexes have been assigned [41]. In the series of the $[Cr(NH_3)_5X]^{2+}$ ions, the ν(Cr−N) are in the 475–400 cm^{-1} region, and the ν(Cr−X) are at 540, 302, 264, and 184 cm^{-1}, respectively, for X = F, Cl, Br, and I [42]. For more information on halogenoammine complexes of Cr(III), see Ref. [43]. Detailed vibrational assignments are available for halogenoammine complexes of Os(III) [44] and of Ru(III), Rh(III), Os(III), and Ir(III) [45].

In regard to $M(NH_3)_4X_2$- and $M(NH_3)_3X_3$-type complexes, the main interest has been the distinction of stereoisomers by vibrational spectroscopy. As shown in

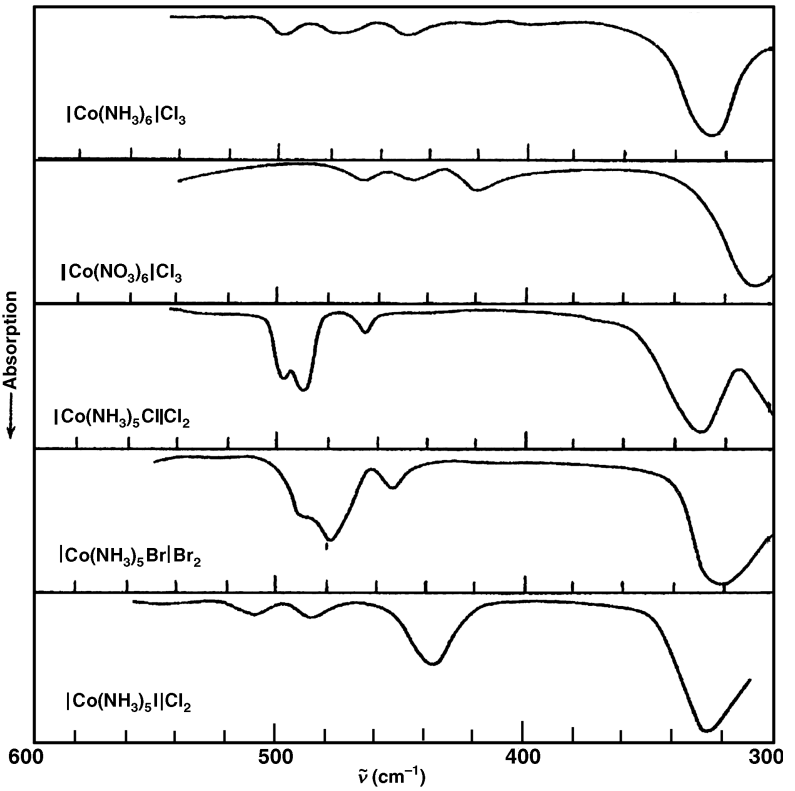

Fig. 1.4. *Infrared spectra (600–300 cm^{-1}) of Co(III) halogenoammine complexes.*

Appendix V of Part A, *trans*-MN_4X_2 ($\mathbf{D}_{4h}$) exhibits one MN stretching (E_u) and one MX stretching (A_{2u}), while *cis*-MN_4X_2 ($\mathbf{C}_{2v}$) shows four MN stretching (two A_1, B_1, and B_2) and two MX stretching (A_1 and B_1) vibrations in the infrared. For *mer*-MN_3X_3 ($\mathbf{C}_{2v}$), three MN stretching and three MX stretching vibrations are infrared-active, whereas only two MN stretching and two MX stretching vibrations are infrared-active for *fac*-MN_3X_3 ($\mathbf{C}_{3v}$). Nolan and James [12] have measured and assigned the Raman spectra of a series of $[Pt(NH_3)_nCl_{6-n}]^{(n-2)+}$-type complexes. Li et al. [46] carried out normal coordinate analysis on *cis*-$Pt(NH_3)_2Cl_4$.

Vibrational spectra of the planar $M(NH_3)_2X_2$-type complexes [M = Pt(II), Pd(II)] have been studied by many investigators. Table 1.4 summarizes the observed frequencies and band assignments of their skeletal vibrations, including those of "*cis*-platin"—the well-known anticancer drug. Figure 1.5 shows the infrared spectra of *cis*- and *trans*-$[Pd(NH_3)_2Cl_2]$ obtained by Layton et al. [51]. As expected, both the PdN and PdCl stretching bands split into two in the *cis*-isomer. Durig et al. [52] found that the PdN stretching frequencies range from 528 to 436 cm^{-1}, depending on the

TABLE 1.4. Skeletal Frequencies of Square–Planar $M(NH_3)_2X_2$-Type Complexes (cm^{-1})[a]

Complex	ν(MN)	ν(MX)	Bending	Ref.
trans-$[Pd(NH_3)_2Cl_2]$				
IR	496	333	245, 222, 162, 137	47,21
R	492	295	224	
cis-$[Pd(NH_3)_2Cl_2]$				
IR	495, 476	327, 306	245, 218, 160, 135	47
trans-$[Pd(NH_3)_2Br_2]$				
IR	490	—	220, 220, 122, 101	47
R	483	182	172	21
cis-$[Pd(NH_3)_2Br_2]$				
IR	480, 460	258	225, 225, 120, 100	47
trans-$[Pd(NH_3)_2I_2]$				
IR	480	191	263, 218, 109	47
trans-$[Pt(NH_3)_2Cl_2]$				
IR	572	365	220, 195	48,49
R	538	334	—	21,48
cis-$[Pt(NH_3)_2Cl_2]$[b]				
IR	510	330, 323	250, 198, 155, 123	49
R	507	253	160	21
trans-$[Pt(NH_3)_2Br_2]$				
IR	504	260	230	48,49
R	535	206	—	48
trans-$[Pt(NH_3)_2I_2]$				
R	532	153	—	48

[a]For band assignments, see also Refs. 13 and 50.
[b]See Sec. 3.9.1.

nature of other ligands in the complex. In general, the PtN stretching band shifts to a lower frequency as a ligand of stronger *trans* influence is introduced in the position *trans* to the Pt−N bond. Using infrared spectroscopy, Durig and Mitchell [53] studied the isomerization of *cis*-$[Pd(NH_3)_2X_2]$ to its *trans*-isomer.

Other studies on halogenoammine complexes include $[Zn(NH_3)_2X_2]$ (X = Cl,Br, I) [54] and $[Ir(NH_3)Cl_5]^{2-}$ [55].

1.1.4. Linear Chain Ammine Complexes

Mixed-valence compounds such as $Pd^{II}Pt^{IV}(NH_3)_4Cl_6$ and $Pd^{II}Pd^{IV}(NH_3)_4Cl_6$ take the form of a chain structure as shown below:

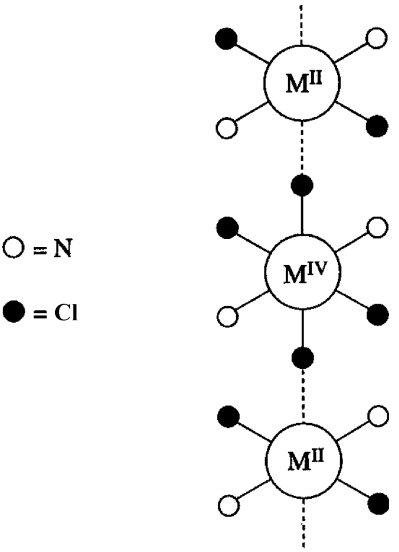

Both compounds exhibit an intense, extremely broad electronic absorption band in the visible region. The IR spectra of these mixed-valence compounds are approximately superpositions of those of each of the components. However, the RR spectra (Secs. 1.22 and 1.23 of Part A) obtained by using exciting lines in this

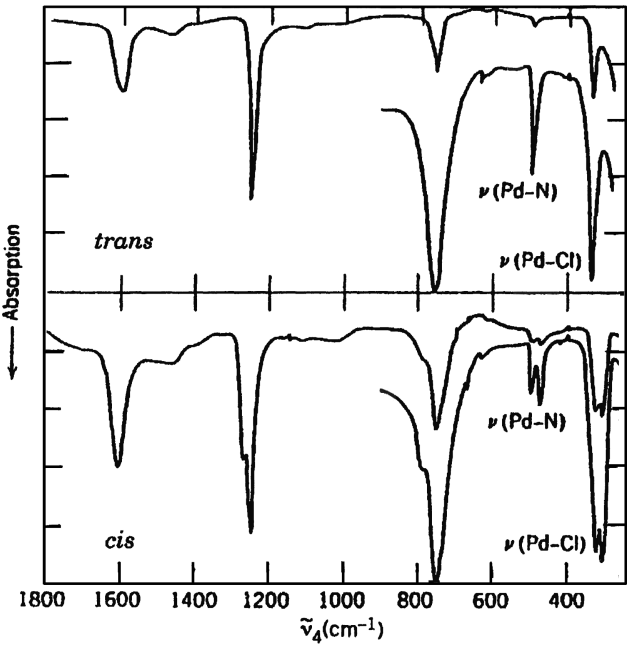

Fig. 1.5. *Infrared spectra of trans-* and *cis-*$[Pd(NH_3)_2Cl_2]$ *[51].*

region are markedly different from the IR spectra. In the case of the Pd−Pt complex, RR spectra involving the progressions of three totally symmetric metal–chlorine stretching vibrations were observed. Thus, the visible spectrum was attributed to a metal–metal mixed-valence transition. On the other hand, the Pd−Pd complex exhibits a RR spectrum involving several stretching and bending fundamentals and their combinations and overtones that originate in the Pd $(NH_3)_2Cl_4$ component only. Thus, Clark and Trumble [56] attributed the visible spectrum to the metal–ligand charge transfer transitions within this component. Later, this work was extended to the Ni−Pt complex of ethylenediamine (Sec. 1.2.3).

In the Magnus green salt, $[Pt(NH_3)_4]$ $[PtCl_4]$, the Pt(II) atoms form a linear chain structure with relatively short Pt−Pt distances (∼3.3 Å). Originally, Hiraishi et al. [13] assigned the infrared band at 200 cm^{-1} to a lattice mode that corresponds to the stretching mode of the Pt−Pt−Pt chain. This high frequency was justified on the basis of the strong Pt−Pt interaction in this salt. Adams and Hall [57], on the other hand, assigned this mode at 81 cm^{-1}, and the 201 cm^{-1} band to a NH_3 torsion. In fact, the latter is shifted to 158 cm^{-1} by the deuteration of NH_3 ligands [58]. Different from the mixed-valence complexes, the Raman spectrum of the Magnus green salt obtained by excitation in the visible absorption band does not display long overtone series [58]. This is expected since it has no axial bonds that would change the bond lengths on electronic excitation. Resonance Raman spectra of these and other linear chain complexes are reviewed by Clark [59].

1.1.5. Lattice Vibrations of Ammine Complexes

Vibrational spectra of metal ammine complexes in the crystalline state exhibit lattice vibrations below 200 cm^{-1}. Assignments of lattice modes have been made for the hexammine complexes of Mg(II),[2] Co(II) [60], Ni(II) [60,61], $[Co(NH_3)_6]$/$[Co(CN)_6]$ [62], and $[Pt(NH_3)_4]Cl_2$ [63]. Lattice modes and low-frequency internal modes of hexammine complexes have also been studied by Janik et al. [64,65] using the inelastic neutron-scattering technique.

1.1.6. Amido (NH_2) Complexes

The vibrational spectra of amido complexes may be interpreted in terms of the normal vibrations of a pyramidal ZXY_2-type molecule. Niwa et al. [66] carried out normal coordinate analysis on the $[Hg(NH_2)_2]_\infty^+$ ion (infinite-chain polymer); the results are given in Table 1.5. Brodersen and Becher [67] studied the infrared spectra of a number of compounds containing Hg−N bonds and assigned the HgN stretching bands at 700–400 cm^{-1}. Alkylamido complexes of the type $M(NR_2)_{4,5}$ (M = Ti,Zr,Hf,V,Nb,Ta) exhibit their MN stretching bands in the 700–530 cm^{-1} region [68].

TABLE 1.5. Infrared Frequencies and Band Assignments of Amido Complexes (cm^{-1}) [66]

Compound	$\nu(NH_2)$	$\delta(NH_2)$	$\rho_w(NH_2)$	$\rho_r(NH_2)$	ν(HgN)
$[Hg(NH_2)]^+_\infty(Cl)^-_\infty$	3200 3175	1540	1025	673	573
$[Hg(NH_2)]^+_\infty(Br)^-_\infty$	3220 3180	1525	1008	652	560

1.1.7. Amine(RNH_2) Complexes

Infrared spectra of methylamine complexes, $[Pt(CH_3NH_2)_2X_2]$ (X: a halogen), have been studied by Watt et al. [69]. Far-infrared spectra of $[M(R_2NH)_2X_2]$−[M = Zn(II) or Cd(II); R = ethyl or *n*-propyl; X = Cl or Br] type complexes have also been reported [70]. The ν(Pt−I) vibrations of $Pt(RNH_2)_2I_2$-type complexes are in the 200–150 cm^{-1} region [71]. Infrared and Raman spectra of metal complexes of aniline have been reviewed by Thornton [72].

1.1.8. Complexes of Hydrazine and Hydroxylamine

Hydrazine (H_2N-NH_2) coordinates to a metal as a unidentate or a bridging bidentate ligand. No chelating (bidentate) hydrazines are known. For example, the hydrazine ligands in $[M(N_2H_4)_2]Cl_2$ [M(II) = Mn,Fe,Co,Ni,Cu,Zn,Cd] are bridging bidentate (polymeric):

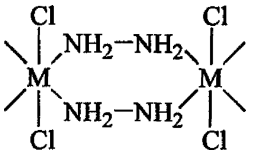

On the other hand, all hydrazine ligands in $[Co(N_2H_4)_6]Cl_2$ are coordinated to the Co atom as a unidentate ligand. According to Nicholls and Swindells [73], the complexes of the former type exhibit the ν(N−N) near 970 cm^{-1}, whereas those of the latter type show it near 930 cm^{-1}. The IR spectra of hydrazine complexes of M(II)(M = Ni,Co, Zn,Cd) [74], Os(II) [75], and Ln(III) (Ln = Pr,Nd,Sm) [76] have been reported. In these compounds, hydrazine acts as a unidentate or bridging bidentate ligand.

The vibrational spectra of hydroxyalmine(NH_2OH) have been reported by Kharitonov et al. [77]. Other related ligands include diazene (N_2H_2). Lehnert et al. [78] prepared a diazene-bridged Fe(II) dimer, $[FeL(PPr_3)_2]_2(\mu\text{-}N_2H_2)$, where L denotes 1,2-bis(2-mercaptophenylthio)ethane, and assigned the N_2H_2 vibrations on the basis of isotope shifths (H/D and $^{14}N/^{15}N$) and normal coordinate analysis. Andersen and Jensen [79] assigned the IR spectra of $M(I)_2[M(IV)L_2]$, where M(I) is an alkali metal ion; M(IV) is Ni, Fe, Mn, and V; and L is the $C_3H_6N_3O_3^{3-}$ ion (hexahydro-1,3,5-triazine-1,3,5-triol). Assignments were based on isotope shift data

(H/D, ($^{14}N/^{15}N$, $^{12}C/^{13}C$, $^{58}Ni/^{62}Ni$, and $^{54}Fe/^{57}Fe$), and the IR spectrum of the free ligand, $C_3H_6N_3(OH)_3$.

1.2. COMPLEXES OF ETHYLENEDIAMINE AND RELATED LIGANDS

1.2.1. Chelating Ethylenediamine

When ethylenediamine(en) coordinates to a metal as a chelating ligand, it may take a *gauche* (δ and λ) or a *cis* conformation, as shown in Fig. 1.6. Then, eight different conformations are probable for the $[M(en)_3]^{n+}$ ion if we consider all possible combinations of conformations of the three chelate rings (δ or λ) around the chiral metal center. They are designated as $\Lambda(\delta\delta\delta)$, $\Lambda(\delta\delta\lambda)$, $\Lambda(\delta\lambda\lambda)$, $\Lambda(\lambda\lambda\lambda)$, $\Delta(\lambda\lambda\lambda)$, $\Delta(\lambda\lambda\delta)$, $\Delta(\lambda\delta\delta)$, and $\Delta(\delta\delta\delta)$. According to X-ray analysis, all the en ligands in the $[Co(en)_3]^{3+}$ ion take the *gauche* conformation (δ), and the configuration of the whole ion is $\Lambda(\delta\delta\delta)$ [80,81]. Although it is rather difficult to obtain such information from vibrational spectra, Cramer and Huneke [82] have shown that some of these conformers can be distinguished by the number of IR-active C−C stretching vibrations. For example, $[Cr(en)_3]Cl_3 \cdot 3.5H_2O$ [$\Lambda(\delta\delta\delta)$, $\mathbf{D}_3$ symmetry] exhibits only one band at 1003 cm^{-1}, whereas $[Cr(en)_3][Ni(CN)_5] \cdot 1.5H_2O$ [$\Lambda(\delta\delta\lambda, \delta\lambda\lambda)$, $\mathbf{C}_2$ symmetry] exhibits three bands at 1008, 1002 (shoulder), and 995 cm^{-1}. Gouteron has shown [83] that racemic (*dl*) and optically active (*d*) forms of $[Co(en)_3]Cl_3$ can be distinguished in the crystalline state by comparing vibrational spectra below 200 cm^{-1}.

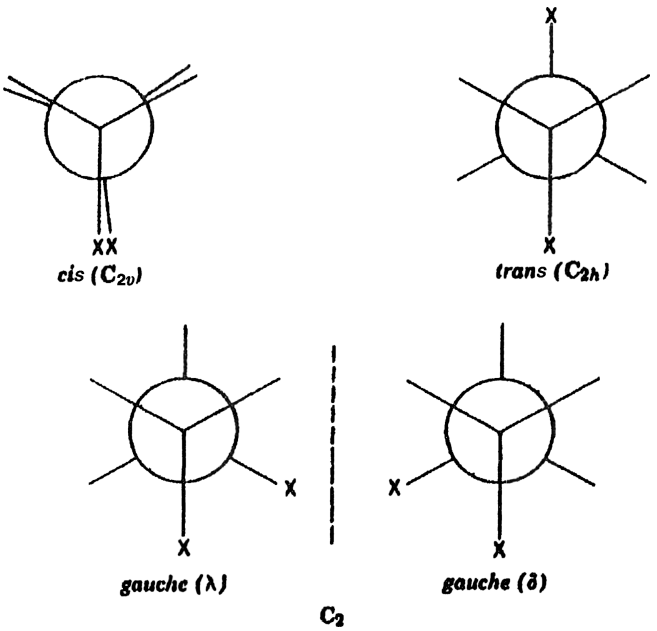

Fig. 1.6. *Rotational isomers of 1,2-disubstituted ethane. X = NH_2 for en.*

Normal coordinate analyses on metal complexes of ethylenediamine have been made by several groups of workers. Fleming and Shepherd [84] carried out normal coordinate calculations on the 1:1(Cu/en) model of the $[Cu(en)_2]^{2+}$ ion. These workers considered a 9-atom system of $\mathbf{C}_{2v}$ symmetry, assuming that the two hydrogen atoms bonded to the C and N atoms are single atoms having the double mass of hydrogen. The IR bands at 410 and 360 cm^{-1} have been assigned to the ν(Cu−N) that are coupled with other skeletal modes. The corresponding Cu−N stretching force constant (GVF) was 1.25 mdyn/Å. Borch and coworkers [85–87] have carried out more complete calculations by considering all the 37 atoms of the $[Rh(en)_3]^{3+}$ ion ($[\Lambda(\delta\delta\delta)]$ configuration of $\mathbf{D}_3$ symmetry), and the force constants (GVF) have been refined by using the vibrational frequencies obtained for the N–d_{12}, C–d_{12}, N,C–d_{24}, and their ^{15}N analogs. In total, 38 force constants were employed, including the Rh−N stretch of 1.607 mdyn/Å. Three ν(Rh−N) vibrations are at 545 (A_1), 445 (A_2), and 506 (E), although they are strongly coupled with other skeletal bending modes. Figure 1.7 shows the IR and Raman spectra of (N–d_{12}) $[Rh(en)_3]Cl_3 \cdot D_2O$ obtained by Borch et al. [87]. Later, their calculations (E modes) were improved by Williamson et al. [88], who assigned the polarized Raman spectra of tris(ethylenediamine) complexes of Co(III) and Rh(III) on the basis of similar calculations.

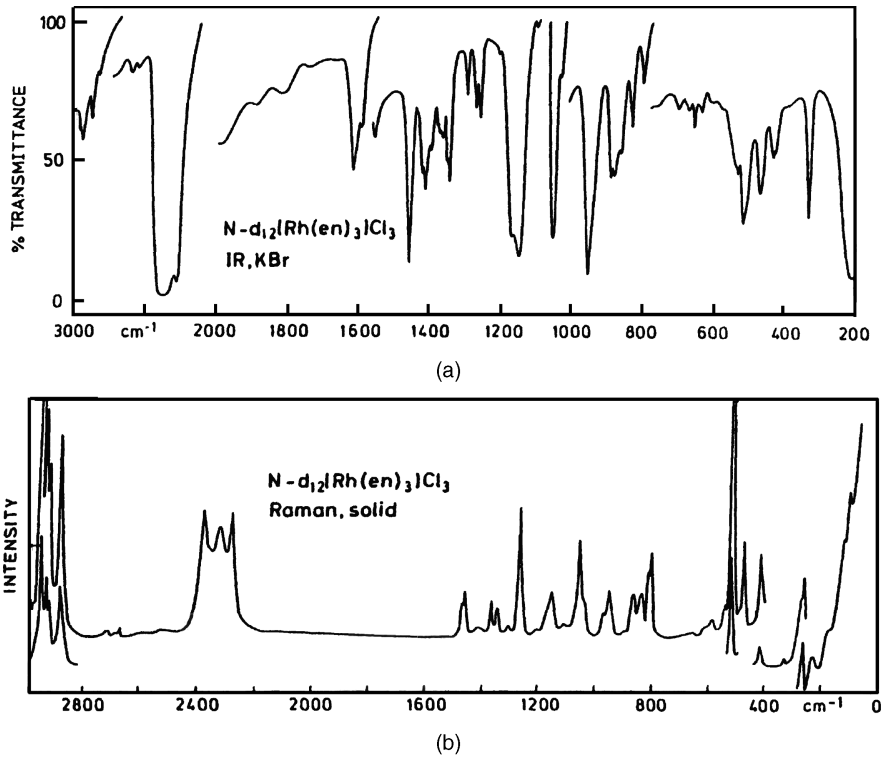

Fig. 1.7. *Infrared (a) and Raman spectra (b) of N-deuterated (N-d_{12}) $[Rh(en)_3]Cl_3 \cdot D_2O$ [87].*

Empirical assignments of ν(M–N) have been reported for $[M(en)_3]^{3+}$ (M = Cr, Co) [89] $[M(en)_3]^{2+}$ (M = Zn, Cd, Fe, etc.) [90], and $[M(en)_2]^{2+}$ (M = Cu,Pd,Pt) [91]. Bennett et al. [92,93] found that, in a series of the $M(en)_3SO_4$ complexes, the ν(M–N) frequencies follow the order

	M = Mn(II)		Fe(II)		Co(II)		Ni(II)		Cu(II)		Zn(II)	
ν_4	391	<	397	<	402	<	410	<	485	>	405	(cm^{-1})
ν_5	303	<	321	≈	319	<	334	<	404	>	291	

As mentioned in Sec. 1.1.1, this is the order of stability constants known as the *Irving–Williams series*. These assignments have been confirmed by extensive isotope substitutions, including metal isotopes.

Stein et al. [94] observed that the Raman intensities of the totally symmetric stretching and chelate deformation modes of the $[Co(en)_3]^{3+}$ ion at 526 and 280 cm^{-1}, respectively, display minima near 21.5 kK,* where the *d–d* transition shows its absorption maximum. Figure 1.8 shows the excitation profiles of these totally symmetric vibrations, as well as that of non-totally symmetric ν(Co–N) (E_g) at 444 cm^{-1}. Since this result is opposite to what one expects from resonance Raman spectroscopy (Sec. 1.22 of Part A), it is called "antiresonance." These workers

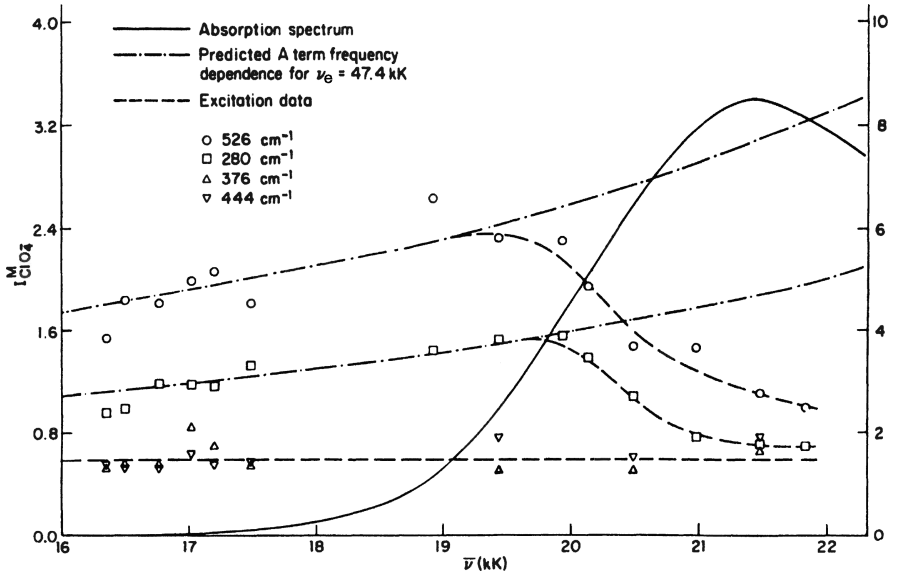

Fig. 1.8. *Excitation profiles for the $[Co(en)_3]^{3+}$ ion. The left-hand scale pertains to the excitation data and the right-hand scale, to the absorption spectrum. $I^M_{ClO_4^-}$ is the molar intensity relative to that of the ν_1 band of ClO_4^-: $(I_{Co}/C_{Co})(C_{ClO_4^-}/I_{ClO_4^-})$. The theoretical curves (– · – · –) are calculated with the A term frequency dependence given by A. C. Albrecht and M. C. Hutley [J. Chem. Phys.* ***55****, 4438 (1971)].*

* 1 kK = 1 kilokayser = 10^3 cm^{-1}.

attributed its origin to "interference" between the weak scattering from the ligand-field state and strong preresonance scattering from higher energy allowed electronic states. For more theoretical study on this phenomenon, see Ref. 95.

Lever and Mantovani [96] assigned the MN stretching bands of $M(N-N)_2X_2$-[M = Cu(II), Co(II), Ni(II); N−N = en, dimethyl-en, etc.; X = Cl, Br, etc.]-type complexes by using the metal isotope technique. For these compounds, the CoN and NiN stretching bands have been assigned to 400–230 cm^{-1} [96], and the CuN stretching vibrations have been located in the 420–360 cm^{-1} [97]. A straight-line relationship between the square of the CuN stretching frequency and the energy of the main electronic *d–d* band was found [98], with some exceptions [97].

The infrared spectra of *cis*- and *trans*-$[M(en)_2X_2]^+$ [M = Co(III), Cr(III), Ir(III), Rh (III); X = Cl, Br, etc.] have been studied extensively [99–102]. These isomers can be distinguished by comparing the spectra in the regions of 1700–1500 (NH_2 bending), 950–850 (CH_2 rocking), and 610–500 cm^{-1} (MN stretching).

1.2.2. Bridging Ethylenediamine

Ethylenediamine takes the *trans* form when it functions as a bridging group between two metal atoms. Powell and Sheppard [103] were the first to suggest that ethylenediamine in $(C_2H_4)Cl_2Pt(en)PtCl_2(C_2H_4)$ is likely to be *trans*, since the infrared spectrum of this compound is simpler than that of other complexes in which ethylenediamine is *gauche*. However, an NMR study on this complex ruled out this possibility [104]. The *trans* configuration of ethylenediamine was found in $(AgCl)_2en$ [105], $(AgSCN)_2en$ [106], $(AgCN)_2en$ [107], $Hg(en)Cl_2$ [108], and $M(en)Cl_2$ (M = Zn or Cd) [105]. The structure of these complexes may be depicted as follows:

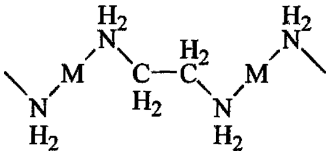

A more complete study, including the infrared and Raman spectra, of $M(en)X_2$-type complexes [M = Zn(II),Cd(II),Hg(II); X = Cl,Br,SCN] has been done by Iwamoto and Shriver [108]. Mutual exclusion of infrared and Raman spectra, along with other evidence, supports the $\mathbf{C}_{2h}$ bridging structure of the en ligand in the Cd and Hg complexes (see Fig. 1.9).

1.2.3. Mixed-Valence Complexes

In Sec. 1.1.3 we discussed the RR spectra of mixed-valence complexes such as $PdPt(NH_3)_4Cl_6$ and $Pd_2(NH_3)_4Cl_6$. Analogous complexes can be prepared by changing the metal and the N-donor ligand. For example, Clark and Croud [109] measured the RR

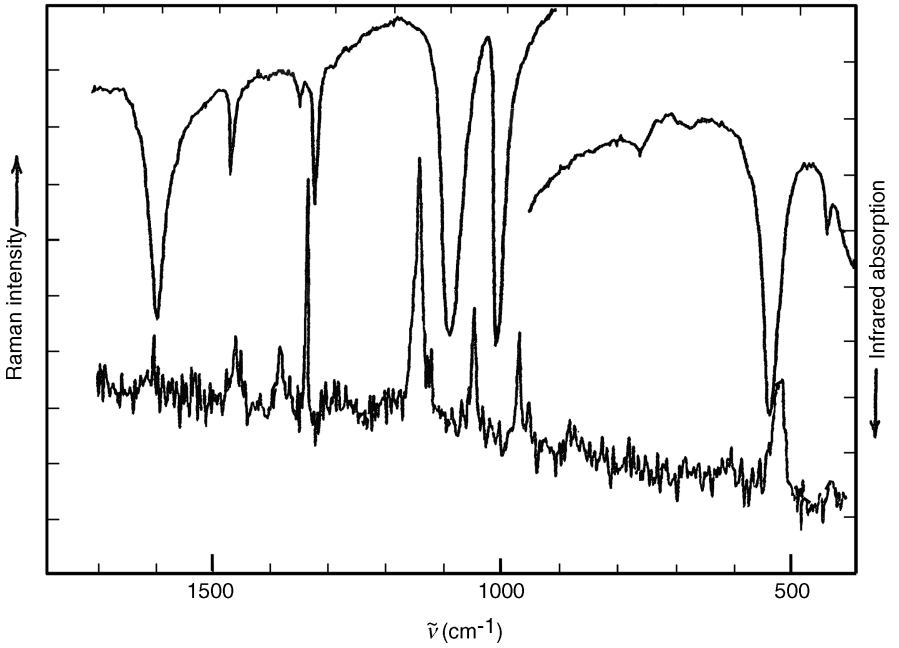

Fig. 1.9. *Infrared (top) and Raman (bottom) spectra of [Cd(en)Br$_2$]$^-$.*

spectra of single crystals of $[Ni(en)_2]$ $[Pt(en)_2X_2]$ $(ClO_4)_4$ (X = Cl, Br, I) in which a linear chain such as

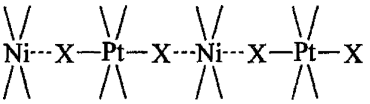

is formed via halogen bridges. These complexes exhibit strong, broad bands due to the Ni(II)–Pt(IV) charge transfer transition in the visible region. Figure 1.10 shows the RR spectra of the chloro complex obtained by 488 nm excitation at 20 K. It is seen that the complex exhibits a series of overtones of the symmetric ν_s(Cl−Pt−Cl) vibration up to 6ν, which split into three peaks, due to mixing of ^{35}CI/^{37}CI isotopes. Similar overtone series were observed for X = Br and I. Using these data, the frequencies corrected for anharmonicity and anharmonicity constants have been calculated (Sec. 1.23 of Part A). Polarized RR studies show that these vibrations are completely polarized along the Ni···X−Pt−X···Ni axis. Similar work is reported for $[Pt(en)_2][Pt(en)_2Cl_2]$ $(ClO_4)_4$[110]. In the $[Pt(en)_2][Pt(en)_2X_2](ClO_4)_4$ series, the IR-active chain phonon frequencies (antisymmetric stretching) are 359.1, 238.7, and 184.2 cm^{-1}, respectively, for X = Cl, Br, and I [111].

The mixed-valence complex $[Pt(en)_2I_2][Pt(CN)_4]$ forms a quasi-one-dimensional chain, $\{-Pt(II)-I-Pt(IV)-I-\}_n$, in the axial direction. The RR spectrum of its single crystal exhibits three totally symmetric vibrations at 138, 111, and 49 cm^{-1} in the

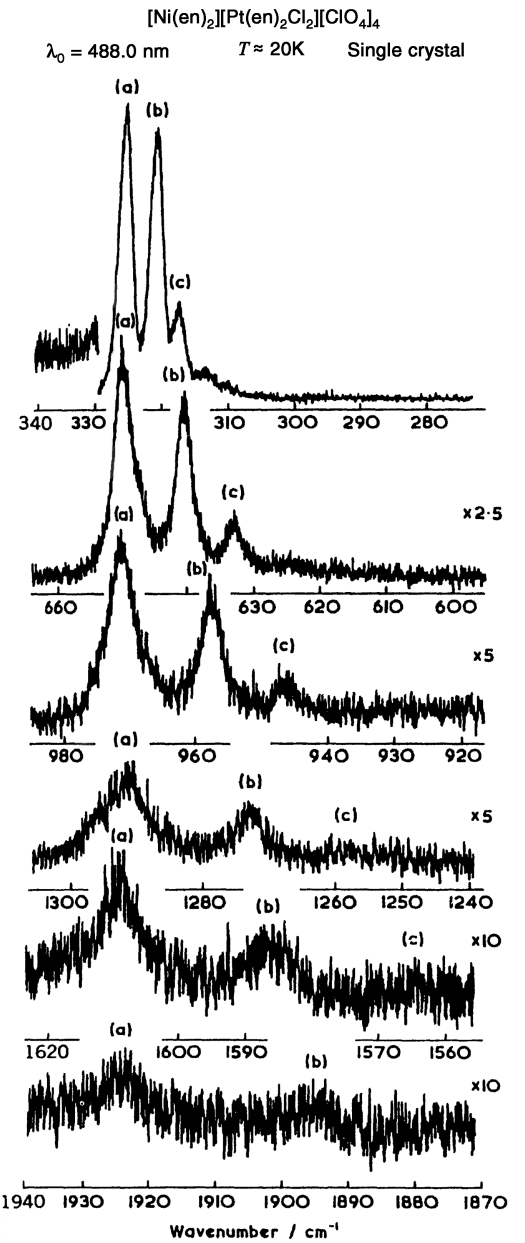

Fig. 1.10. *Isotopomer band intensities for $\nu_1 - 6\nu_1$ of a single crystal of $[Ni(en)_2][Pt(en)_2Cl_2](ClO_4)_4$. For ease of presentation, the $^{35}ClPt^{35}Cl$ component (a) of each harmonic is lined up with the same abscissa value; (b) and (c) refer to the $^{35}ClPt^{37}Cl$ and $^{37}ClPt^{37}Cl$ components, respectively [109].*

low-frequency region. The band at 138 cm^{-1} was assigned to the ν_s(I−Pt−I) since the same mode was observed at 140 cm^{-1} for the $[Pt(IV)(en)I_2]^{2+}$ ion [112].

Omura et al. [113] reported the far-IR spectra of Magnus-type salts $[M(en)_2][M'Cl_4]$ [M,M′ = Pt(II) or Pd(II)]. Berg and Rasmussen [114] measured the IR and far-IR spectra of the analogous complexes $[M(en)_2][M'Br_4]$ [M,M′ = Pt(II) or Pd(II)] and $[M(en)_2][HgI_4]$. No bands assignable to the metal–metal stretching were observed in these complexes.

1.2.4. Complexes of Polyamines

Polyamines such as these shown below coordinate to a metal as tridentate or tetradentate ligands:

Diethylenetriamine(dien):

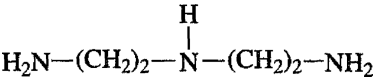

Triaminotriethylamine(tren):

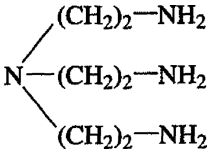

Triethylenetetramine(trien):

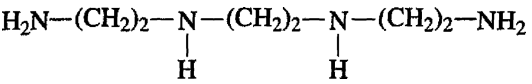

The infrared spectra of diethylenetriamine (dien) complexes have been reported for [Pd(dien)X]X (X = Cl,Br,I) [115] and $[Co(dien)(en)Cl]^{2+}$ [116]. The latter exists in the four isomeric forms shown in Fig. 1.11. Their infrared spectra revealed that the ω- and κ-isomers contain dien in the *mer* configuration; the π- and ε-isomers contain dien in the *fac* configuration. The *mer*- and *fac*-isomers of $[M(dien)X_3]$ [M = Cr(III), Co (III), and Rh(III); X: a halogen] can also be distinguished by infrared spectra [117].

The infrared spectra of β, β', β''-triaminotriethylamine(tren) complexes with Co(III) [118] and lanthanides [119] have been reported. Buckingham and Jones [120] measured the infrared spectra of $[M(trien)X_2]^+$, where trien is triethylene-tetramine, M is Co(III), Cr(III), or Rh(III), and X is a halogen or an acido anion. These compounds give three isomers (Fig. 1.12) that can be distinguished, for example, by the CH_2 rocking vibrations in the 920–869 cm^{-1} region. For $[Co(trien)Cl_2]ClO_4$, *cis*-α-isomer exhibits two strong bands at 905 and 871 cm^{-1} and *cis*-β-isomer shows four bands at 918, 898, 868, and 862 cm^{-1}; *trans*-isomer gives only one band at 874 cm^{-1} with a weak band at 912 cm^{-1}. Far-infrared spectra of some of these trien complexes have been reported [121].

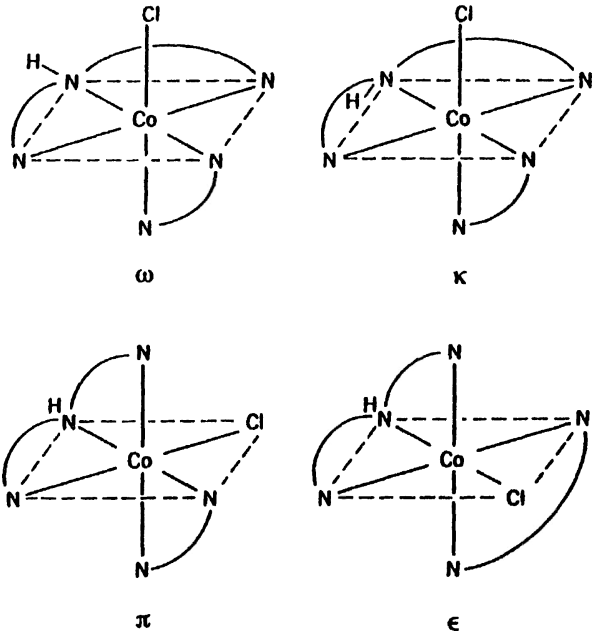

Fig. 1.11. *Structures of the* $[Co(dien)(en)Cl]^{2+}$ *ion.*

1.2.5. Complexes of 1,2-Disubstituted Ethanes

As is shown in Fig. 1.6, 1,2-disubstituted ethane may exist in the *cis*, *trans*, or *gauche* form, depending on the angle of internal rotation. The *cis* form may not be stable in the free ligand because of steric repulsion between two X groups. The *trans* form belongs to point group $\mathbf{C}_{2h}$, in which only the *u* vibrations (antisymmetric with respect to the center of symmetry) are infrared-active. On the other hand, both *gauche* forms belong to point group $\mathbf{C}_2$, in which all the vibrations are infrared-active. Thus the *gauche* form exhibits more bands than the *trans* form. Mizushima and coworkers [122] have shown that 1,2-dithiocyanatoethane ($NCS-CH_2-CH_2-SCN$) in the crystalline state

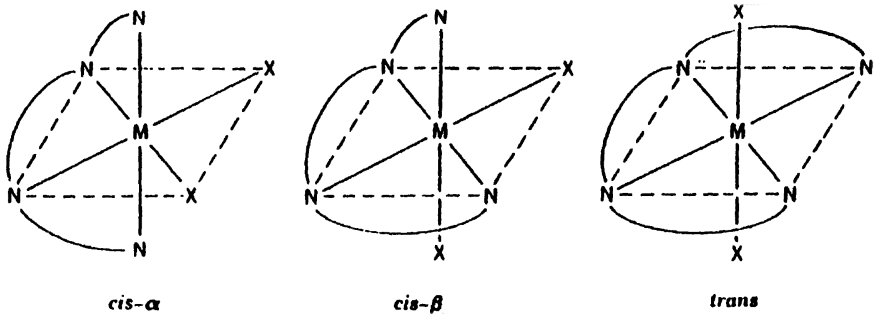

Fig. 1.12. *Structures of the* $[M(trien)X_2]^+$ *ions.*

definitely exists in the *trans* form, because no infrared frequencies coincide with Raman frequencies (mutual exclusion rule). By comparing the spectrum of the crystal with that of a $CHC1_3$ solution, they concluded that several extra bands observed in solution can be attributed to the *gauche* form. Table 1.6 summarizes the infrared frequencies and band assignments obtained by Mizushima et al. It is seen that the CH_2 rocking vibration provides the most clear-cut diagnosis of conformation: one band (A_u) at 749 cm^{-1} for the *trans* form, and two bands (*A* and *B*) at 918 and 845 cm^{-1} for the *gauche* form.

The compound 1,2-dithiocyanatoethane may take the *cis* or *gauche* form when it coordinates to a metal through the S atoms. The chelate ring formed will be completely planar in the *cis*, and puckered in the *gauche*, form. The *cis* and *gauche* forms can be distinguished by comparing the spectrum of a metal chelate with that of the ligand in $CHCl_3$ solution (*gauche* + *trans*). Table 1.6 compares the infrared spectrum of 1,2-dithiocyanatoethanedichloroplatinum(II) with that of the free ligand in a $CHCl_3$ solution. Only the bands characteristic of the *gauche* form are observed in the Pt(II) complex. This result definitely indicates that the chelate ring in the Pt(II) complex is *gauche*. The method described above has also been applied to the metal complexes of 1,2-dimethylmercaptoethane ($CH_3S-CH_2-CH_2-SCH_3$) [123]. In this case, the free ligand exhibits one CH_2 rocking at 735 cm^{-1} in the crystalline state (*trans*), whereas the metal complex always exhibits two CH_2 rockings at 920–890 and 855–825 cm^{-1} (*gauche*). In the case of ethylenediamine complexes discussed earlier, the CH_2 rocking mode does not provide a clear-cut diagnosis since it couples strongly with the NH_2 rocking and C−N stretching modes.

TABLE 1.6. Infrared Spectra of 1,2-Dithiocyanatoethane and Its Pt(II) Complex (cm^{-1}) [122]

Ligand			
Crystal *trans*	$CHCl_3$ Solution (*gauche* + *trans*)	Pt Complex (*gauche*)	Assignment
—	2170(*g*)	2165(*g*)	ν(C≡N)
2155(*t*)	2170(*t*)	—	
1423(*t*)	1423(*t*)	—	$\delta(CH_2)$
—	1419(*g*)	1410(*g*)	
1291[a](*t*)	—	—	
—	1285(*g*)	1280(*g*)	$\rho_w(CH_2)$
1220(*t*)	1215(*t*)	—	
1145(*t*)	1140(*t*)	—	$\rho_t(H_2)$
—	1100(*g*)	1110(*g*)	
—	—(*g*)[b]	1052(*g*)	$\nu(CC)$
1037[a]	—	—	
—	918(*g*)	929(*g*)	$\rho_r(CH_2)$
—	845(*g*)	847(*g*)	
749(*t*)	—[b]	—	
680(*t*)	677(*t*)	—	ν(CS)
660(*t*)	660(*t*)	—	

[a]Raman frequencies in the crystalline state.
[b]Hidden by $CHCl_3$ absorption.

1.3. COMPLEXES OF PYRIDINE AND RELATED LIGANDS

1.3.1. Complexes of Pyridine

On complex formation, the pyridine (py) vibrations in the high-frequency region are not shifted appreciably, whereas those at 604 (in-plane ring deformation) and 405 cm^{-1} (out-of-plane ring deformation) are shifts to higher frequencies. Clark and Williams [124] carried out an extensive far-infrared study on metal pyridine complexes. Table 1.7 lists the observed frequencies of these metal-sensitive py vibrations and metal–py stretching vibrations. Clark and Williams showed that ν(M−py) and ν(MX) (X = a halogen) are very useful in elucidating the stereochemistry of these py complexes. For example, *fac*-$[Rh(py)_3Cl_3]$ exhibits two ν(Rh—py) ($\mathbf{C}_{3v}$ symmetry), whereas *mer*-$Rh(py)_3Cl_3$ shows three ν(Rh—py) ($\mathbf{C}_{2v}$ symmetry) near 250 cm^{-1}. The infrared spectra of these two compounds are shown in Fig. 1.13.

Vibrational spectra in the low-frequency region have been assigned for other halogeno pyridine complexes, including *trans*-$[Tc(py)_2X_4]$ [128], *cis*/*trans*-$[Os(py)_2X_4]^-$[129], *cis*/*trans*-$[Pt(py)_2Cl_4]$ [130], *mer*-$[Os(py)_3X_3]$ [131], *trans*-$[Os(py)_4X_2]$ [132], and *trans*-$[Pt(py)_4F_2]^{2+}$ [133].

The metal isotope technique has been used to assign the ν(M−py) and ν(MX) vibrations of $Zn(py)_2X_2$ [134] and $Ni(py)_4X_2$ [135]. The former vibrations have been located in the 225–160 and 250–225 cm^{-1} regions, respectively, for the Zn(II) and Ni (II) complexes. Figure 1.14 shows the infrared and Raman spectra of $[^{64}Zn(py)_2Cl_2]$ and its ^{68}Zn analog. As expected from its $\mathbf{C}_{2v}$ symmetry, two ν(Zn−py) and two ν(ZnCl) are metal-isotope-sensitive.

Thornton and coworkers [136,137] carried out an extensive study on a variety of pyridine complexes with emphasis on band assignments based on isotope shift data (py-d_5, ^{15}N-py, and metal isotopes). As an example, Fig. 1.15 illustrates the IR spectra and band assignments of a series of the $M(py)_2Cl_2$-type complexes [137]. The shaded

TABLE 1.7. Vibrational Frequencies of Pyridine Complexes (cm^{-1}) [124]

Complex	Structure	py[a]	py[a]	ν(M−py)
$Co(py)_2Cl_2$	Monomeric, tetrahedral	642	422	253[b]
$Ni(py)_2I_2$	Monomeric, tetrahedral	643	428	240
$Cr(py)_2Cl_2$	Polymeric, octahedral	640	440	219
$Cu(py)_2Cl_2$	Polymeric, octahedral	644	441	268
$Co(py)_2Cl_2$	Polymeric, octahedral	631	429	243,235[b]
mer-$[Rh(py)_3Cl_3]$	Monomeric, octahedral	650	468	265,245,230
fac-$[Rh(py)_3Cl_3]$	Monomeric, octahedral	643	464	266,245
trans-$[Ni(py)_4Cl_2]$	Monomeric, octahedral	626	426	236
trans-$Ir(py)_4Cl_2]Cl$	Monomeric, octahedral	650	469	260,(255)
cis-$[Ir(py)_4Cl_2]Cl$	Monomeric, octahedral	656	468	287,273
trans-$[Pt(py)_2Br_2]$	Monomeric, square–planar	656	476	297
cis-$[Pt(py)_2Br_2]$	Monomeric, square–planar	659 644	448	260,234

[a]For band assignments of pyridine, see Refs. 125 and 126.
[b]Assignments made by Postmus et al. [127].

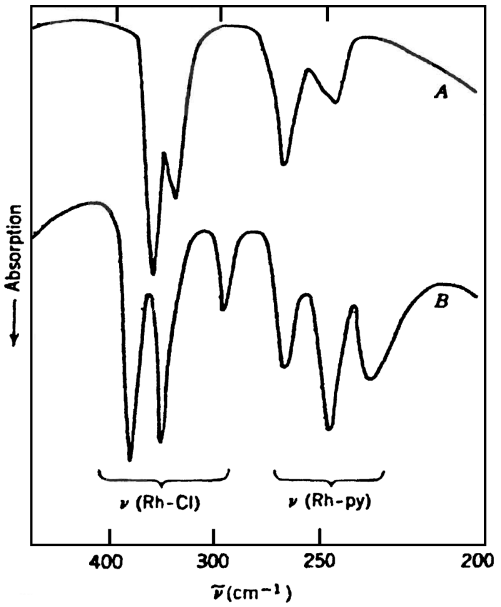

Fig. 1.13. *Far-IR spectra of (A) fac-* and *(B) mer-*$[Rh(py)_3Cl_3]$ [*124*].

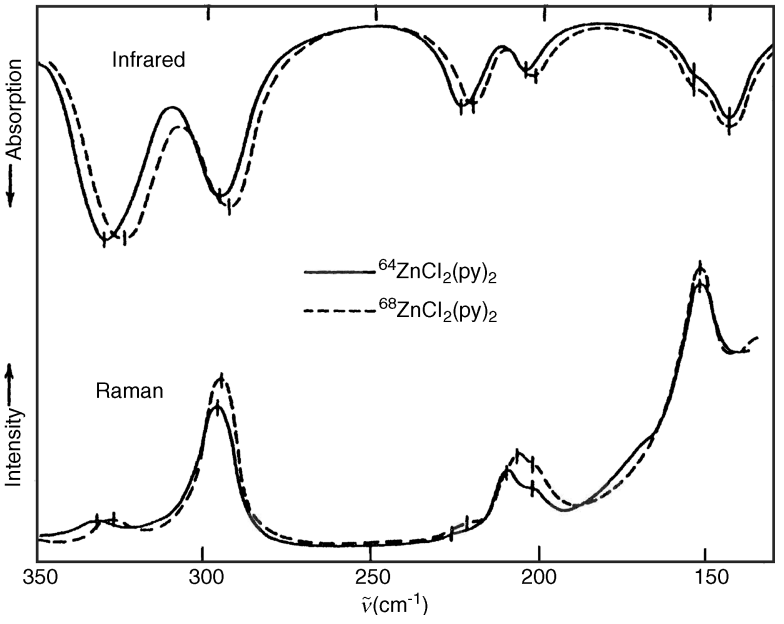

Fig. 1.14. *Infrared and Raman spectra of* $^{64}Zn(py)_2Cl_2$ *and its* ^{68}Zn *analog [134].*

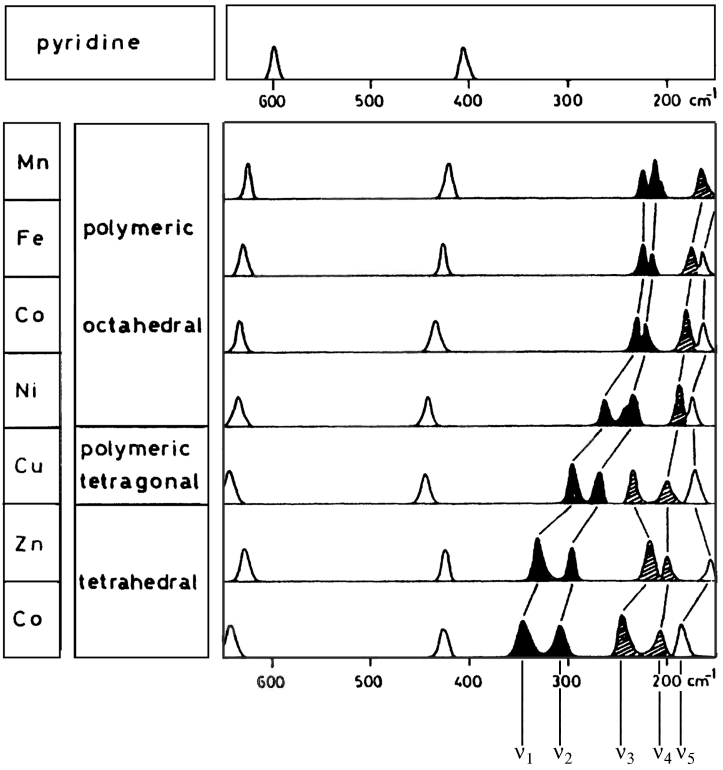

Fig. 1.15. *Infrared spectra (650–150 cm^{-1}) of the M(py)$_2$Cl$_2$ complexes: solid bands, ν(M–Cl) and shaded bands, ν(M–N) [139].*

bands (ν_3 and ν_4) are assigned to the ν(M—N), while the solid bands (ν_1 and ν_2) are due to the ν(M–Cl). The ν_5 is assigned to a bending mode. In a series of polymeric octahedral complexes shown in Fig. 1.15, both ν(M—N) and ν(M—Cl) follow the Irving–Williams order shown in Sec. 1.2.1.

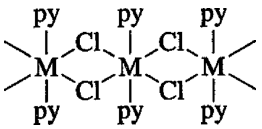

Two ν(M—Cl) and one ν(M—N) are expected in IR spectra of polymeric octahedral complexes ($\mathbf{C}_1$ symmetry), whereas two ν(M–Cl) and two ν(M—N) are expected in IR spectra of tetrahedral complexes ($\mathbf{C}_{2v}$ symmetry). The latter also holds for polymeric tetragonal Cu(II) complex. It should be noted that the violet Co(II) complex is polymeric octahedral while the blue Co(II) complex is monomeric tetrahedral. An Infrared and Raman spectra of metal pyridine complexes have been reviewed extensively by Thornton [137]. Far-infrared spectra of metal pyridine nitrate complexes, M(py)$_x$(NO$_3$)$_y$, have been reported [138,139].

1.3.2. Surface-Enhanced Raman Spectra of Pyridine

In 1974, Fleischmann et al. [140] made the first observation of surface-enhanced Raman spectra (SERS) of pyridine adsorbed on a silver electrode. Figure 1.16 shows the Raman that spectra of pyridine in solution [(a) and (b)] and SERS of pyridine on an Ag electrode that has the potential 0 to -1.0 V [(c)–(h)] relative to the SCE. It is seen that the intensities of the bands at 1037, 1025, and 1008 cm^{-1} (ring stretch) are changed markedly by changing the potential. The 1025 cm^{-1} band was assigned to the uncharged species, that is, pyridine bonded directly on the electrode surface (Lewis acid site) since its intensity is maximized near zero potential. The remaining two bands were attributed to the pyridine that is hydrogen-bonded to water molecules on the electrode surface. These two environments of pyridine are illustrated in Fig. 1.17. As expected, the relative intensity of the 1025 cm^{-1} band decreases and those of the 1037 and 1008 cm^{-1} bands increase as the negative potential increases.

While verifying these results in 1977, Jeanmaire and Van Duyne [141,142] noted that the Raman signals (3067, 1036, and 1008 cm^{-1}) from pyridine on Ag electrodes are enhanced by a huge factor (10^4–10^6) relative to normal Raman spectra in solution. In addition, they noted that the Raman intensity depends not only on the electrode potential but also on several other factors such as electrode surface preparation, concentration of pyridine in solution, and the nature and concentration of the supporting electrolyte anion. Almost simultaneously, Albrecht and Creighton [143] noted anomalous enhancements of Raman bands of pyridine adsorbed on a Ag electrode. These bands include those at 3076 (CH stretch), 1600 and 1050–1000 (ring stretch), 669 (ring deformation), and 239 cm^{-1} [Ag–N(py) stretch] [144].

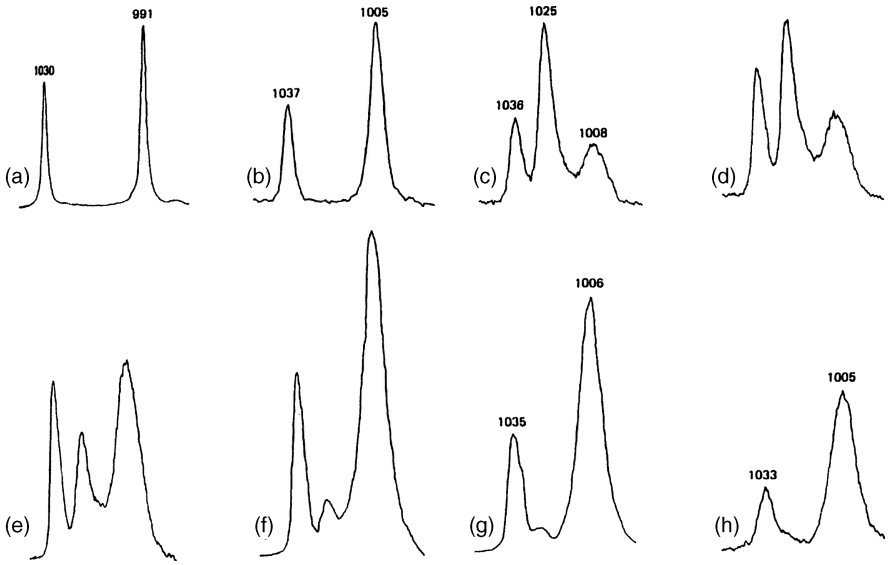

Fig. 1.16. *Raman spectra of pyridine in solution and at the silver electrode: (a) liquid pyridine; (b) 0.05 M aqueous pyridine; (c) silver electrode, 0 V (SCE); (d) −0.2 V; (e) −0.4 V; (f) −0.6 V; (g) −0.8 V; (h) −1.0 V (514.5 nm excitation, 100 mW) [140].*

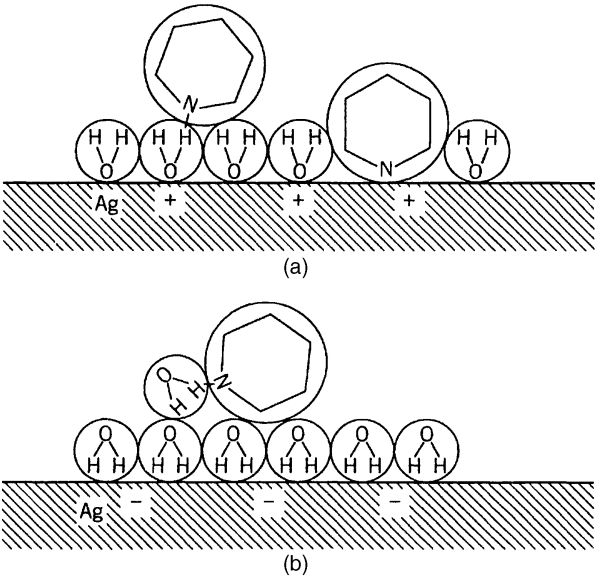

Fig. 1.17. *A possible model of the structure of the double layer between silver and KCl solution containing pyridine: (a) At positive potentials, showing pyridine adsorbed to silver via nitrogen and in an "aqueous acidic environment"; (b) at negative potentials, showing adsorbed pyridine in "aqueous environment" [140].*

Yamada and Yamamoto [145,146] measured the SERS of pyridine adsorbed on metal oxides with UV excitation (363.8 nm). These workers were able to distinguish three types of adsorbed pyridine, as shown in Fig. 1.18:

Type H Pyridine hydrogen-bonded to the surface OH group ($\sim$3075 and 999 cm^{-1})
Type L Pyridine adsorbed on a Lewis acid site ($\sim$3075 and 1025 cm^{-1})
Type B Pyridine adsorbed on a Bronsted acid site (3090 and 1005 cm^{-1})

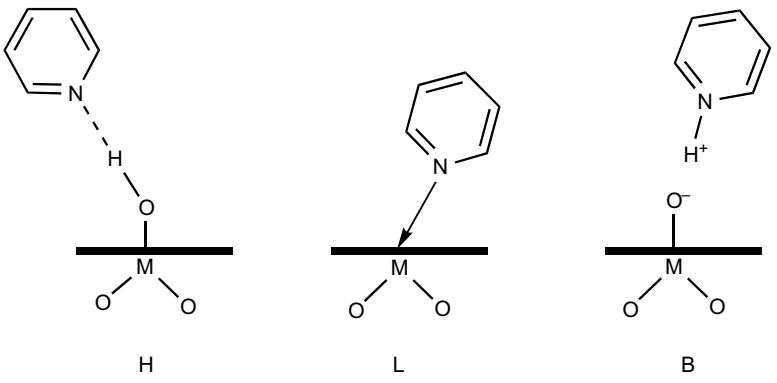

Fig. 1.18. *Three types of adsorbed pyridines on metal oxide surfaces [146].*

The frequencies in the brackets are those observed for γ-alumina. SERS of pyridine adsorbed on rhodium oxide have also been reported [147].

The SERS of the $[Os(NH_3)_5py]^{n+}$ ($n = 2,3$) and $[Ru(NH_3)_5py]^{2+}$ ions adsorbed at the silver–aqueous interface exhibit internal modes of pyridine as well as metal–ligand modes, although the lone-pair electrons of pyridine nitrogen atoms in these ions are not available for bonding to the surface silver atoms. This result demonstrates the utility of SERS in obtaining vibrational data of coordination compounds that are sometimes difficult to obtain in bulk media [e.g., Os(II) complex] [148].

As stated in Sec. 1.21 of Part A, Raman intensity is proportional to P^2, where P (induced dipole moment) is equal to αE (where a = polarizability; E = electric field strength). Thus, surface enhancement must be caused by the enhancement of either E or α or both. E increases significantly on the surface of fine metal particles or on rough metal surfaces (electromagnetic enhancement). In this case, the incident beam excites conduction electrons and generates "surface plasma resonance (plasmon resonance)" α increases through charge transfer or bond formation between the adsorbate and the metal surface (chemical enhancement).

1.3.3. Complexes of Pyridine Derivatives and Related Ligands

The infrared spectra of metal complexes with alkyl pyridines have been studied extensively [149,150]. Using the metal isotope technique, Lever and Ramaswamy [151] assigned the M−pic stretching bands of $M(pic)_2X_2$ M = Ni(II), Cu(II); pic = picoline; X = Cl,Br,I] in the 300–230 cm^{-1} region. The infrared spectra of metal complexes with halogenopyridines have been reported [152,153]. Infrared spectra have been used to determine whether coordination occurs through the nitrile or the pyridine nitrogen in cyanopyridine complexes. It was found that 3- and 4-cyanopyridines coordinate to the metal via the pyridine nitrogen [154], whereas 2-cyanopyridine coordinates to the metal via the nitrile nitrogen [155].

Vibrational spectra of $M(3,5\text{-lutidine})_4X_2$ [156] (M = Mn or Cu; X = Cl or Br), and Zn{Hpic)(pic)Cl [157] and $[Mn(Hpic)(pic)Cl]_2$ [158], where Hpic is 2-picolic acid, have been assigned.

Infrared spectra of aromatic amine *N*-oxides and their metal complexes have been reviewed by Garvey et al. [159]. The N=O stretching band of pyridine *N*-oxide (1265 cm^{-1}) is shifted by 70–30 cm^{-1} to a lower frequency on complexation. The following references are given for three complexes: Fe(II) [160], Hg(II) [161], and Fe (III) [162].

Imidazole (Im) and its derivatives form complexes with a number of transition metal ions. Infrared spectra are reported for metal complexes of

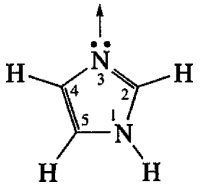

imidazole [163–165], 2-methylimidozole [166,167] 1 (or *N*)-methylimidazole [168], 4- and 5-bromoimidazole [169], and benzimidazole [170,171]. Among them, imidazole is biologically most important since imidazole nitrogens of histidyl residues coordinate to metal ions in many metalloproteins. Thus, the identification of M−N (Im) vibrations in biological systems provides valuable information about the structure of the active site of a metalloprotein (Sec. 3.1). Using metal isotope techniques, Cornilsen and Nakamoto [165] assigned and M−N stretching vibrations of 16 imidazole complexes of Ni(II), Cu(II), Zn(II), and Co(II) in the 325–210 cm^{-1} region. Hodgson et al. [172] also assigned these vibrations in the same region. Salama and spiro [173] were first to assign the Co−N stretching vibrations in resonance Raman spectra of $Co(ImH)_2Cl_2$ (274 and 232 cm^{-1}), $[Co(ImH)_4]^{2+}$ (301 cm^{-1}), and $[Co(Im^-)_4]^{2-}$ (306 cm^{-1}).

Caswell and Spiro [174] studied excitation profiles of imidazole, histidine, and related ligands including the $[Cu(ImH)_4]^{2+}$ ion in the UV region. These compounds exhibit maxima near 218 and 204 nm, where the π–π^* transitions of the heterocyclic rings occur.

Drozdzewski and coworkers prepared the $\{M(IA)_2]$ [M = Cu(II), Ni(II), Co(II), HIA = 4-imidazoleacetic acid] and their IR spectra on the basis of isotopic shift data (H/D, $^{63}Cu/^{65}Cu$) and DFT calculations [175], The far-IR spectrua of polymeric Zn (II) complexes, $[ZnCl(IA)(HIA)]$ H_2O ($^{64}Zn/^{68}Zn$), were also assigned [176]. Their work was extended to Pd(II) complexes of the type $[Pd(hi)X_2]$ [177] (X = Cl,Br) and $[Pd(hi)_2]Br_2$ [178], where hi is 2-hydrazino-2-imidazoline.

1.4. COMPLEXES OF BIPYRIDINE AND RELATED LIGANDS

1.4.1. Complexes of 2,2′-Bipyridlne

Infrared spectra of metal complexes of 2,2′-bipyridine (bipy) have been studied extensively. In general, the bands in the high-frequency region are not metal-sensitive since they originate in the heterocyclic or aromatic ring of the ligand. Thus, the main interest has been focused on the low-frequency region, where *v*(MN) and other metal-sensitive vibrations appear. It has been difficult, however, to assign *v*(MN) empirically since several ligand vibrations also appear in the same frequency region. This difficulty was overcome by using the metal isotope technique. Hutchinson et al. [179] first applied this method to the tris-bipy complexes of Fe(II), Ni(II), and Zn(II), Later, this work was extended to other metals in various oxidation states [180]. Table 1.8 lists *v*(MN), magnetic moments, and the electronic configuration of these tris-bipy complexes. The results revealed several interesting relationships between *v*(MN) and the electronic structure:

(1) In terms of simple MO theory, Cr(III), Cr(II), Cr(I), Cr(0), V(II), V(0), Ti(0), Ti (–I), Fe(III), Fe(II), and Co(III) have filled or partly filled t_{2g} (bonding) and empty e_g (antibonding) orbitals. The *v*(MN) of these metals (group A) are in the 300–390 cm^{-1} region.

TABLE 1.8. MN Stretching Frequencies and Electronic Structures in $[M(bipy)_3]^{n+}$-Type Compounds (cm^{-1})[a]

	–I	0	I	II	III
d^3				374 V 335 (3.67) $(t_{2g})^3$	385 Cr 349 (3.78) $(t_{2g})^3$
d^4		374 Ti 339 (0) $(t_{2g})^4$-ls		351 Cr 343 (2.9) $(t_{2g})^4$-ls	
d^5	365 Ti 322 (1.74) $(t_{2g})^5$-ls	371 V 343 (1.68) $(t_{2g})^5$-ls	371 Cr 343 (2.0) $(t_{2g})^5$-ls	224 Mn 191 (5.95) $(t_{2g})^3$ (e_g)-hs	384 Fe 367 (?)
d^6		382 Cr 308 (0) $(t_{2g})^6$		386 Fe 376 (0) $(t_{2g})^6$	378 Co 370 (0) $(t_{2g})^6$
d^7		258 Mn 227 (4.10) $(t_{2g})^5(e_g)^2$		266 Co 228 (4.85) $(t_{2g})^5(e_g)^2$	
d^8	235 Mn 184 (3.71) $(t_{2g})^6(e_g)^2$		244 Co 194 (3.3) $(t_{2g})^6(e_g)^2$	282 Ni 258 (3.10) $(t_{2g})^6(e_g)^2$	
d^9		280 Co 257 (2.23) $(t_{2g})^6(e_g)^3$		291 Cu 268 (?) $(t_{2g})^6(e_g)^3$	
d^{10}				230 Zn 184 (0) $(t_{2g})^6(e_g)^4$	

[a] The numbers at the upper right of each group indicate the MN stretching frequencies (cm^{-1}). The numbers in parentheses give the observed magnetic moments in Bohr magnetons. Is = low spin; hs = high spin.

(2) On the other hand, Co(II), Co(I), Co(0), Mn(II), Mn(0), Mn(–I), Ni(II), Cu(II), and Zn(II) have filled or partly filled e_g orbitals. The ν(MN) of these metals (group B) are in the 180–290 cm^{-1} region.

(3) Thus no marked changes in frequencies are seen in the Cr(III)–Cr(0) and Co (II)-Co(0) series, although a dramatic decrease in frequency is observed in going from Co(III) to Co(II).

(4) The fact that the ν(MN) do not change appreciably in the former two series indicates that the M−N bond strength remains approximately the same.

These results also suggest that, as the oxidation state is lowered, increasing numbers of electrons of the metal reside in essentially ligand orbitals that do not affect the M−N bond strength.

Other work on bipy complexes includes a far-infrared study of tris-bipy complexes with low-oxidation-state metals [Cr(0), V(–I), Ti(0), etc.] [181], the assignments of infrared spectra of M(bipy)Cl_2 (M = Cu, Ni, etc.) [182], normal coordinate analysis on Pd(bipy)Cl_2 and its bipy-d_8 analog [183].

The $[Fe(bipy)_3]^{2+}$ ion and its analogs exhibit strong absorption near 520 nm, which is due to Fe(3*d*)–ligand(π) CT transition. When the laser wavelength is tuned in this region, a number of bipy vibrations (all totally symmetric) are strongly resonance-enhanced, as shown in Fig. 1.19 [184]. Excitation profile studies show that the intensities of all these bands are maximized at the main absorption maximum at 19,100 cm^{-1} (524 nm) and that no maxima are present at the sideband near 20,500 cm^{-1} (488 nm). Thus, Clark et al. [184] concluded that the latter band is due to a vibronic transition. The resonance Raman spectrum of the $[Fe(bipy)_3]^{2+}$ ion was also observed near the iron electrode surface in borate buffer solution containing bipy [185]. The electronic spectrum of the singly reduced $[Fe(bipy)_3]^{+}$ ion has also been assigned based on excitation profile studies [186].

1.4.2. Time-Resolved Resonance Raman (TR^3) Spectra

The $[Ru(bipy)_3]^{2+}$ ion and related complexes have attracted much attention as potential compounds of solar energy conversion devices because of their excited-state redox properties. When solutions of this ion are irradiated with 7-ns, high-intensity pulses from the third harmonic (354.5 nm) of a Nd–YAG laser, the irradiated volume can be saturated with the longlived (~600 ns) triplet M−L CT state (A_3) via efficient ($\phi \cong 1$) and rapid ($\tau < 10$ ps) intersystem crossing ($A_2 \rightarrow A_3$) as shown in Fig. 1.20. Since the A_3–A_4 (π–π^*) transition is close to the 354.5-nm exciting line, conditions are favorable for efficient resonance Raman scattering from the A_3 state; namely, it is possible to obtain the time-resolved resonance Raman (TR^3) spectrum of the ion in the electronic excited state. The first observation of such spectra was made by Dallinger and Woodruff [187], who were followed by many investigators [188–191]. These workers found that the TR^3 spectrum consists of two series of bipy vibrations; one series of bands are the same as those observed in the A_1 state and the other correspond to those of $Li^+(bipy^{\cdot -})$. Figure 1.21 shows the spectra obtained by Mallick et al. [192]. It is seen that the TR^3 spectrum (middle trace) is the addition of the RR

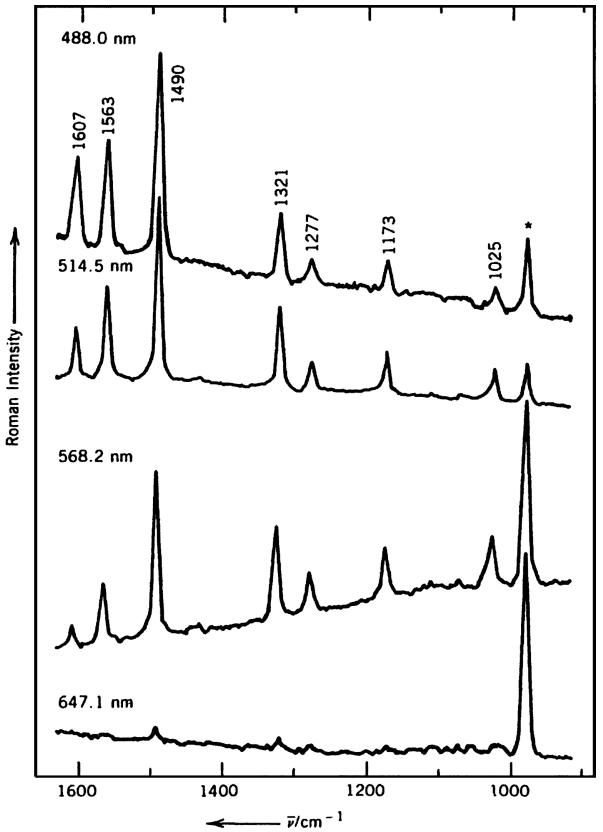

Fig. 1.19. *The RR spectra of the* $[Fe(bipy)_3]^{2+}$ *ion. The asterisk indicates the 981* cm^{-1} *band of the* SO_4^{2-} *ion (internal standard) [184].*

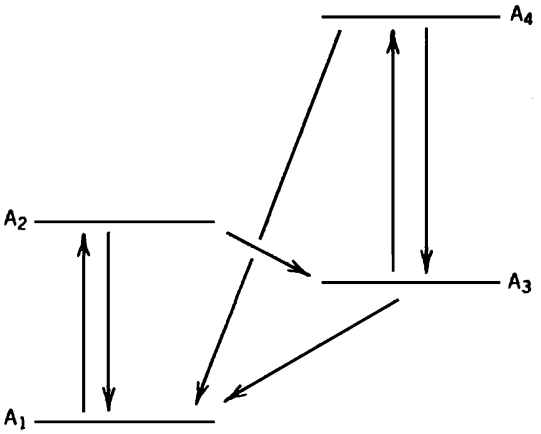

Fig. 1.20. *Energy-level diagram for the* $[Ru(bipy)_3]^{2+}$ *ion.*

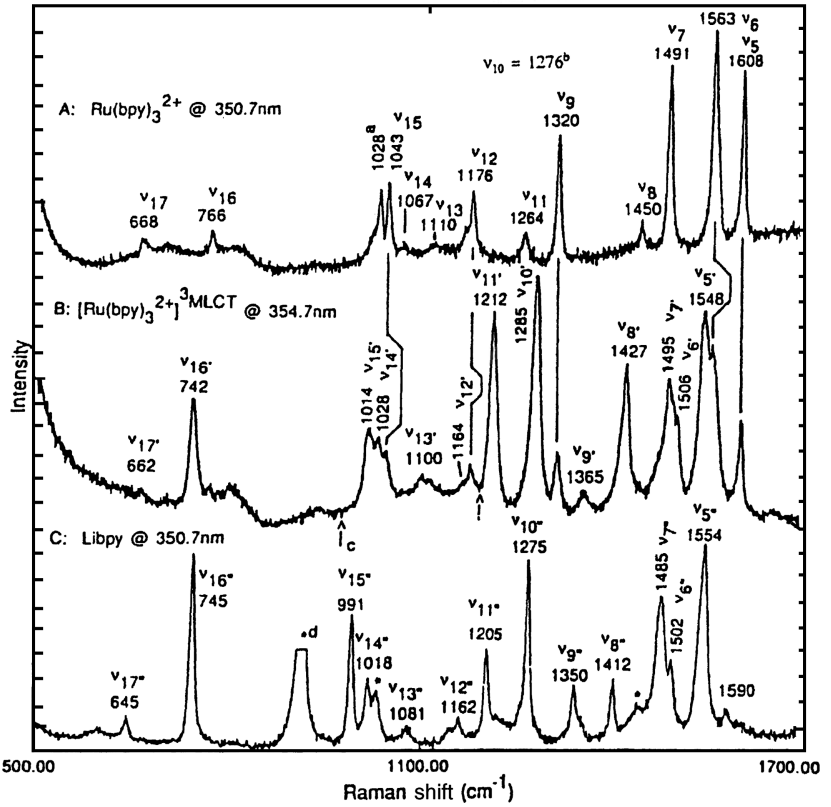

Fig. 1.21. *The RR and TR³ spectra of the $[Ru(bipy)_3]^{2+}$ ion. (A) RR spectrum with 350.7 nm excitation. (B) TR³ spectrum with 354.7 nm excitation. (C) RR spectrum of Li (bipy) with 350.7 nm excitation [192].*

spectra of the $[Ru(bipy)_3]^{2+}$ ion (top trace) and $Li^+(bipy^{\cdot -})$ (bottom trace). Thus, the triplet M−L CT state (A_3) is formulated as $[Ru(III)(bipy)_2(bipy^{\cdot -})]^{2+}$, that is, the electron is localized on one bipy rather than delocalized over all three ligands (at the least vibrational time scale). The RR spectra of electron reduction products of several $[Ru(bipy)_3]^{2+}$ derivatives show similar electron localization [193].

Kincaid and coworkers [194,195] carried out normal coordinate analyses on the 1 : 1 (metal/ligand) model of the $[Ru(bipy)_3]^{2+}$ ion in the ground and the M−L CT states. As expected, extensive vibrational couplings exist among those represented by local internal coordinates. The Ru−N stretching force constant was 2.192 mdyn/Å in both states.

In heteroleptic complexes, selective population of individual ligand-localized excited states is possible by using TR^3 spectroscopy. For example, Danzer and Kincaid [196] have demonstrated that the triplet M−L CT state of the $[Ru(bipy)_2(bpz)]^{2+}$ ion (bpz = bipyrazine) should be formulated as $[Ru(III)(bipy)_2(bpz^{\cdot -})]^{2+}$, whereas that of the $[Ru(bipy)(bpz)_2]^{2+}$ ion should be formulated as $[Ru(III)(bipy)(bpz)(bpz^{\cdot -})]^{2+}$.

This work was extended to many other heteroleptic complexes such as $[Ru(bipy)_2(bpm)]^{2+}$ [197] and $[Ru(bipy)_2(dpp)]^{2+}$ [198,199], where bpm and dpp denote 4,4′-bipyrimidine and 2,3-bis(2-pyridyl)pyrazine, respectively. TR[3] studies show selective population of the bpm-localized excited state in the former, and polarization of electron density toward the pyrazyl fragment in the latter. In the case of $[Ru(pypz)_3]^{2+}$, where pypz is an inherently asymmetric ligand, 2-(2-pyridyl)pyrazine, the electronic charge is polarized toward the pyrazine fragment [200]. Other complexes studied include $[Ru(bipy)_2(bpdz)]^{2+}$(bpdz = 3,3′-bipyridazine) [201] and $[Ru(bipy)_2L]^{2+}$ (L; alkylated 2,2′-bipyridine) [202].

1.4.3. Complexes of Phenanthroline and Related Ligands

The metal isotope technique has been used to study the effect of magnetic crossover on the low-frequency spectrum of $Fe(phen)_2(NCS)_2$ (phen = 1,10-phenanthroline). This compound exists as a high-spin complex at 298 K and as a low-spin complex at 100 K. Figure 1.22 shows the infrared spectra of $^{54}Fe(phen)_2(NCS)_2$ obtained by Takemoto and Hutchinson [203]. On the basis of observed isotopic shifts, along with other evidence, they made the following assignments (cm^{-1}):

	ν(Fe−NCS)	ν[Fe−N(phen)]
High spin	252(4.0)	222(4.5)
Low spin	532.6(1.6)	379(5.0)
	528.5(1.7)	371(6.0)

The numbers in parentheses indicate the isotope shift, $\nu(^{54}Fe) - \nu(^{57}Fe)$. Both vibrations show large shifts to higher frequencies in going from the high- to

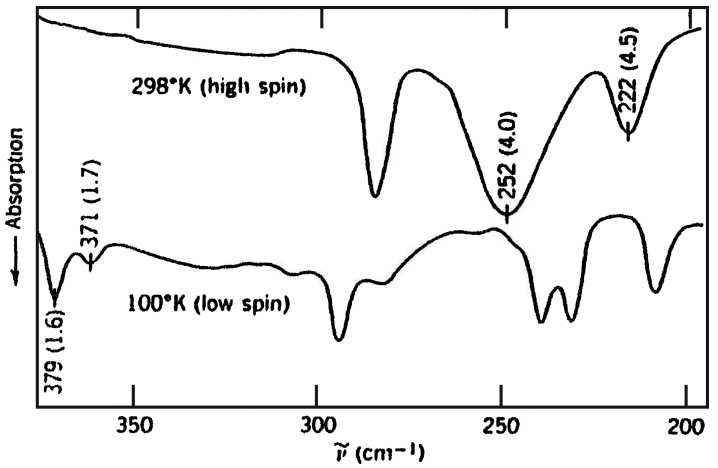

Fig. 1.22. *Infrared spectra of $^{54}Fe(phen)_2(NCS)_2$. Numbers in parentheses indicate isotope shifts due to $^{54}Fe/^{57}Fe$ substitution.*

the low-spin complexes. This result suggests the marked strengthening of these coordinate bonds in goine from the high- to the low-spin complexes, as confirmed by X-ray analysis [204]. The work of Takemoto and Hutchinson has been extended to $Fe(bipy)_2(NCS)_2$ and $Fe(phen)_2(NCSe)_2$ [205].

Spin crossover by changing the temperature was also observed for $[Fe(btr)_2(NCS)_2]H_2O$ (btr = 4,4′-bis-1,2,4-triazole). Thus, the ν_a (NCS) of the low-spin (~115 K) and high-spin (~141 K) species were observed at 2099 and 2054 cm^{-1}, respectively. However, a large hysteresis effect was noted in this temperatural spin conversion [206]. It has been shown by infrared spectroscopy that a partial high- → low-spin conversion occurs under high pressure [207]. Barnard et al. [208] studied the vibrational spectra of bis[tri-(2-pyridyl)amine]Co(II) perchlorate in the high-spin (293 K) and low-spin (100 K) states. In the infrared, the CoN stretching band is at 263 cm^{-1} for the high-spin complex, whereas it splits and shifts to 312 and 301 cm^{-1} in the low-spin complex.

As stated above, $Fe(phen)_2(NCS)_2$ exhibits the room-temperature high-spin state (HS-1) and the low-temperature low-spin state (LS-1). Herber and Casson [209] found that, when the latter is irradiated by white light below ~50 K, another high-spin state (HS-2) is obtained (light-induced excited-state trapping), and annealing of this HS-2 state above ~30 K produces another low-spin state (LS-2). These workers have shown that the ν(CN) of the NCS ligands near the 2100-cm^{-1} region are different among these four states. This work has been extended to $Fe(bt)_2(NCX)_2$ (bt = 2,2′-bi-2-thiazoline and X = S or Se) [210], and to $Fe(5,6\text{-dmp})_2(NCS)_2$ (dmp = dimethylphenanthroline) [211].

The TR^3 spectrum of the $[Cu(I)(DPP)_2]^+$ ion (DPP = 2,9-diphenyl-phenanthroline) shows that its M−L CT state is formulated as $[Cu(II)(DPP)(DPP^{\cdot -})]^+$ [212].

Similar to the case of the $[Ru(bipy)_3]^{2+}$ ion, the TR^3 spectrum of the $[Ru(phen)_3]^{2+}$ ion at the M−L CT state was expected to show the bands due to the $phen^{\cdot -}$ fragment. Since no such bands were observed, Turro et al. [213] concluded that charge localization seen for the corresponding bipy complex does not occur in this case.

1.4.4. Complexes of Other Ligands

Simple α-diimines such as shown below form metal chelate compounds similar to bipy and phen, discussed earlier:

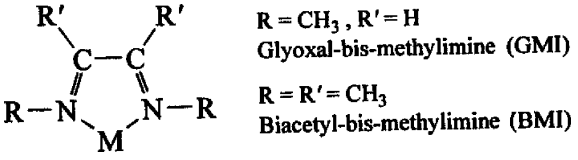

Figure 1.23 shows the IR spectra of Fe(II) and Ni(II) complexes of these ligands [214]. Normal coordinate calculations indicate extensive vibrational couplings among those represented by individual internal coordinates.

Depending on the nature of the alkyl group (R), an alkyl-substituted α-diimine (R−N=CH−CH=N−R) coordinates to the metal [Pt(II) or Pd(II)] as a unidentate or

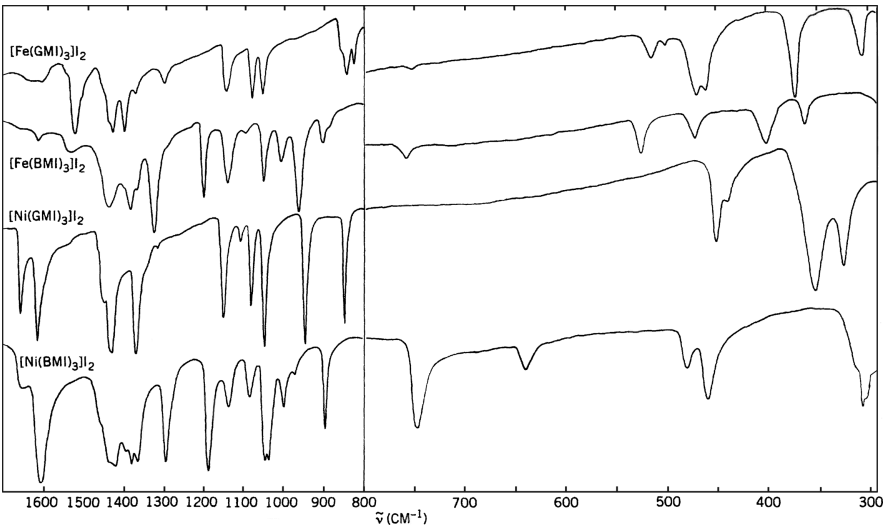

Fig. 1.23. *Infrared spectra of α-diimine complexes of Fe(II) and Ni(II) [214].*

bidentate (chelating) ligand. Van der Poel et al. [215] observed the C=N stretching bands at 1615–1624 and 1590–1604 cm^{-1} for the unidentate and bidentate coordinations, respectively.

The metal isotope technique has been used to assign the MN vibrations of metal complexes with many other ligands. For example, Takemoto [216] assigned the NiN_2 and NiN_1 stretching vibrations of $[Ni(DAPD)_2]^{2-}$ at 416–341 and 276 cm^{-1}, respectively:

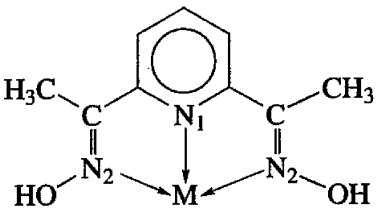

DAPD = 2,6-diacetylpyridine dioxime

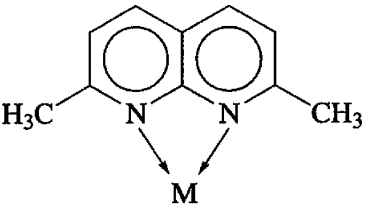

DMNAPY = 2,7-dimethyl-1,8-naphthyridine

In $Ni(DAPD)_2$, where the Ni atom is in the +IV state, the NiN_2 and NiN_1 stretching bands are located at 509.8–472.0 and 394.8 cm^{-1}, respectively. These high-frequency shifts in going from Ni(II) (d^8) to Ni(IV) (d^6, diamagnetic) have also been observed for diarsine complexes (Sec. 1.25.2). Hutchinson and Sunderland [217] have noted that the MN stretching frequencies of the Ni(II) and Zn(II) complexes of 2,7-dimethyl-1,8-naphthyridine (DMNAPY), shown above, are lower than those of the corresponding tris-bipy complexes by 16–24%. This was attributed to weakening of the M−N bond due to the strain in the four-membered chelate rings of the DMNAPY complexes. Normal coordinate analysis has been carried out on the $M(DMG)_2$ series (DMG =

dimethylglyoximate ion) [218] and the MN stretching force constants (mdyn/Å) have been found to be as follows:

Pt(II)	Pd(II)	Cu(II)	Ni(II)	
3.77	>2.84 >	1.92	> 1.88	(GVF)

This work was extended to bis(glyoximato) complexes of Pt(II), Pd(II), and Ni(II) [219]. The Co−N(DMG) and Co−N(py) stretching bands of $Co(DMG)_2(py)X$ (X = a halogen) were assigned at 512 and 453 cm^{-1}, respectively, based on ^{15}N and py-d_5 isotope shifts [220]. The metal isotope technique has been used to assign the MN stretching vibrations of metal complexes with 8-hydroxyquinoline [221] and 1,8-naphthyridine [222].

Spectra–structure correlations [223] and detailed assignments [224] were made for metal complexes of 8-hyroxyquinoline. Assignments of the IR/Raman spectra of the $[Ru(tpy)_2]^{2+}$ ion (tpy = 2,2′,6′,2″-terpyridine) were based on normal coordinate analysis [225].

1.5. METALLOPORPHYRINS

Vibrational spectra of metalloporphyrins have been studied exhaustively because of their biological importance as prosthetic groups of a variety of heme proteins (Chapter 3). Thus, many review articles have been published on this subject, and most of them discuss vibrational spectra of metalloporphyrins together with those of heme proteins. A review by Kitagawa and Ozaki [226], however, is focused on metalloporphyrins.

1.5.1. Normal Coordinate Analysis

Because of relatively high symmetry and biological significance, normal coordinate analyses on metalloporphyrins have been carried out by many investigators [227–234]. Figure 1.24 shows the planar $\mathbf{D}_{4h}$ structure of a metalloporphyrin. The simplest

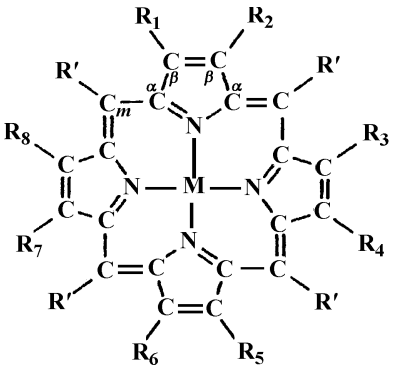

Fig. 1.24. *Structures of metalloporphyrins. Porphin (Por), $R_1 \sim R_8 = H$ and $R' = H$. Octaethylporphyrin (OEP), R_1–R_8 = ethyl and $R' = H$. Tetraphenylporphyrin (TPP), $R_1 \sim R_8 = H$ and $R' =$ phenyl. Tetramesitylporphyrin (TMP), R_1–$R_8 = H$ and $R' =$ mesityl. Protoporphyrin IX (PP), $R_1 = R_3 = R_5 = R_8 = CH_3$, $R_2 = R_4 =$ vinyl, $R' = H$ and $R_6 = R_7 = (CH_2)_2COOH$.*

TABLE 1.9. Classification of Normal Vibrations of a Metal Porphin Complex of D_{4h} Symmetry[a] [227].

In-Plane Vibrations		Out-of-Plane Vibrations	
A_{1g} (R)	9	A_{1u}	3
A_{2g}[b]	8	A_{2u} (IR)	6
B_{1g} (R)	9	B_{1u}	5
B_{2g} (R)	9	B_{2u}	4
E_u(IR)	18	E_g(R)[c]	8

[a] R = Raman-active; IR = IR-active.
[b] The A_{2g} vibrations become Raman-active under resonance conditions (see Sec. 1.23 of Part A).
[c] The E_g vibrations are weak even under resonance condtions.

porphyrin, porphin (Por), has 105 ($3 \times 37-6$) normal vibrations, which are classified as shown in Table 1.9 [227]. As stated in Sec. 1.23 of Part A, metalloporphyrins are ideal for resonance Raman (RR) studies because they exhibit strong absorption bands in the visible and near-UV regions. It is well established that RR spectra obtained by excitation near the Q_0 (or α) band are dominated by those of the B_{1g} and B_{2g} species (*dp*), while those obtained by excitation between the Q_0 and Q_1 (or β) band are dominated by those of the A_{2g} species (*ap*). On the other hand, the RR spectra obtained by excitation near the **B** (or Soret) band are dominated by those of the A_{1g} species (*p*). This information, combined with isotope shift data (H/D, $^{14}N/^{15}N$, and metal isotopes), has been used extensively to refine the results of normal coordinate calculations.

Spiro and coworkers [232–234] carried out the most extensive normal coordinate calculations on metalloporphyrins. As expected from their conjugated ring structures, strong vibrational couplings occur among vibrational modes represented by local internal coordinates. Thus, it is rather difficult to describe the normal modes by single internal coordinates. Table 1.10 lists the observed frequencies and major local coordinates responsible for the IR/Raman-active in-plane skeletal modes of Ni(Por), Ni(OEP), and Ni(TPP) (the RR spectra of Ni(OEP) are shown in Fig. 1.35 of Part A). Figure 1.25 shows the normal modes of the eight A_{1g} vibrations obtained for Ni(OEP) and Ni(Por). Table 1.11 lists the normal modes to which the ν(Ni−N) coordinates make significant contributions. Previously, empirical assignments have been made for IR-active M−N stretching vibrations of a series of M(II)(TPP) complexes using metal isotopes such as $^{58}Ni/^{62}Ni$, $^{63}Cu/^{65}Cu$, and $^{64}Zn/^{68}Zn$ [235]. For normal coordinate analysis on the out-of-plane modes, see Ref. 234.

It should be noted that the internal vibrations of the peripheral substituents such as the ethyl and phenyl groups also couple with the porphyrin core vibrations [232,233]. The vinyl group vibrations of Fe(PP) (PP = protoporphyrin IX; see Fig. 1.24), which are commonly found in natural heme proteins, can be resonance-enhanced by excitation near 200 nm (near the π–π^* transition of the vinyl group) [236,237].

Density Functional Theory (DFT) calculations (Sec. 1.24 of Part A) were carried out on large metalloporphyrin molecules to obtain structural information and to make band assignments. Spiro and coworkers [238,239] calculated both in-plane and

TABLE 1.10. In-Plane Skeletal-Mode Frequencies (cm^{-1}) and Local-Mode Assignments for Ni(II) Complexes of OEP, Porphin, and TPP [232,233]

Symmetry	ν_i	Description[a]	NiOEP	NiPor	NiTPP
A_{1g}	ν_1	$\nu(C_m\text{-}X)$	[3041][b]	[3042]	1235
	ν_2	$\nu(C_\beta\text{-}C_\beta)$	1602	1579	1572
	ν_3	$\nu(C_\alpha\text{-}C_m)_{sym}$	1520	1463	1470
	ν_4	ν(Pyr. half-ring)$_{sym}$	1383	1380	1374
	ν_5	$\nu(C_\beta\text{-}Y)_{sym}$	1138	[3097]	[3097]
	ν_6	ν(Pyr. breathing)	804	999	1004
	ν_7	δ(Pyr. def.)$_{sym}$	674	735	889
	ν_8	ν(Ni-N)	360/343	372	402
	ν_9	$\delta(C_\beta\text{-}Y)_{sym}$	263/274	1070	1078
B_{ig}	ν_{10}	$\nu(C_\alpha\text{-}C_m)_{asym}$	1655	1654	1594
	ν_{11}	$\nu(C_\beta\text{-}C_\beta)$	1577	1509	1504
	ν_{12}	ν(Pyr. half-ring)$_{sym}$	1331	1319	1302
	ν_{13}	$\delta(C_m\text{-}X)$	1220	1189	238
	ν_{14}	$\nu(C_\beta\text{-}Y)_{sym}$	1131	[3097]	[3097]
	ν_{15}	ν(Pyr. breathing)	751	1007	1004
	ν_{16}	δ(Pyr. def.)$_{sym}$	746	734	[900]
	ν_{17}	$\delta(C_b\text{-}Y)_{sym}$	305	1064	1084
	ν_{18}	ν(Ni-N)	168	241	277
A_{2g}	ν_{19}	$\nu(C_\alpha\text{-}C_m)_{asym}$	1603	1615	1550
	ν_{20}	ν(Pyr. quarter-ring)	1394	1358	1341
	ν_{21}	$\delta(C_m\text{-}X)$	1307	1143	[257]
	ν_{22}	ν(Pyr. half-ring)$_{asym}$	1121	1009	1016
	ν_{23}	$\nu(C_\beta\text{-}Y)_{asym}$	1058	[3087]	[3087]
	ν_{24}	δ(Pyr. def.)$_{asym}$	597	810	828
	ν_{25}	δ(Pyr. rot.)	551	433	560
	ν_{26}	$\delta(C_\beta\text{-}Y)_{asym}$	[243]	1321	1230
B_{2g}	ν_{27}	$\nu(C_m\text{-}X)$	[3040]	[3041]	1269
	ν_{28}	$\nu(C_\alpha\text{-}C_m)_{asym}$	1483	[1492]	[1481]
	ν_{29}	ν(Pyr. quarter-ring)	1407	1372	1377
	ν_{30}	ν(Pyr. half-ring)$_{asym}$	1160	1007	1004
	ν_{31}	$\nu(C_\beta\text{-}Y)_{asym}$	1015	[3088]	[3087]
	ν_{32}	δ(Pyr. def.)$_{asym}$	938	823	869
	ν_{33}	δ(Pyr. rot.)	493	439	450
	ν_{34}	$\nu(C_\beta\text{-}Y)_{asym}$	197	1197	1191
	ν_{35}	δ(pyr. transl.)	144	201	109
E_u	ν_{36}	$\nu(C_m\text{-}X)$	[3040]	[3042]	
	ν_{37}	$\nu(C_\alpha\text{-}C_m)_{asym}$	[1637]	1624	
	ν_{38}	$\nu(C_\beta\text{-}C_\beta)$	1604	1547	
	ν_{39}	$\nu(C_\alpha\text{-}C_m)_{sym}$	1501	1462	
	ν_{40}	ν(Pyr. quarter-ring)	1396	1385	
	ν_{41}	ν(Pyr. half-ring)$_{sym}$	[1346]	1319	
	ν_{42}	$\delta(C_m\text{-}X)$	1231	1150	
	ν_{43}	$\nu(C_\beta\text{-}Y)_{sym}$	1153	[3097]	
	ν_{44}	ν(Pyr. half-ring)$_{asym}$	1133	1033	
	ν_{45}	$\nu(C_\beta\text{-}Y)_{asym}$	996	[3087]	

(*continued*)

TABLE 1.10. (*Continued*)

Symmetry	ν_i	Description[a]	NiOEP	NiPor	NiTPP
	ν_{46}	δ(Pyr.)$_{asym}$	927	806	
	ν_{47}	ν(Pyr. breathing)	766	995	
	ν_{48}	δ(Pyr.)$_{sym}$	[615]	745	
	ν_{49}	δ(Pyr. rot.)	[534]	366	
	ν_{50}	ν(Ni-N)	[358]	420	
	ν_{51}	δ(C$_b$-Y)$_{asym}$	328	1064	
	ν_{52}	δ(C$_\beta$-Y)$_{sym}$	263	1250	
	ν_{53}	δ(Pyr. transl.)	[167]	282	

[a]See Ref. 232 for definitions of local coordinates. X,Y = H,H for NiPor, H,C_2H_5 for NiOEP, and C_6H_5, H for NiTPP.
[b][ ], calculated values.

out- of-plane vibrations of Ni(Por), Fe(Por), and Fe(Por)CO, and found that DFT force constants can reproduce the observed frequencies more accurately than NCA force constants and can predict IR/Raman intensities that are in good agreement with the observed spectra. The results of their calculations suggested slight ruffling distortion of the Ni(Por) core. DFT calculations on Ni(TPP) [240] indicated that the molecular symmetry is lowered to $\mathbf{S}_4$ as a result of the porphyrin core ruffling and the rotation of the phenyl groups. This distortion activates two out-of-plane vibrations, $\gamma_{12}(330\,\text{cm}^{-1})$ and $\gamma_{13}(547\,\text{cm}^{-1})$, of B_{1u} symmetry that are forbidden under $\mathbf{D}_{4h}$, or $\mathbf{D}_{2d}$ symmetry in the Soret-excited RR spectrum. An X-ray diffraction study on Ni (Por) by Jentzen et al. [241] showed that the porphin ring is planar with very small ruffling, and noted that its RR spectrum in the solid state is almost identical to that in solution. Thus, they concluded that any distortion of $\mathbf{D}_{4h}$ symmetry, if it exists in solution, is rather small.

In contrast, substituent-induced distortions are noted in Ni(II) complexes of *meso-tert*-butylporphyrins [242] and tetracyclopentenyl–tetraphenyl porphyrin and its derivatives [243]. Since ethioporphyrins have one methyl and one ethyl substituent on each pyrrole ring, there are four possible isomers that differ only in the relative positions of the alkyl groups in the periphery. Etio I ($R_1 = R_3 = R_5 = R_7 = CH_3$ and $R_2 = R_4 = R_6 = R_8 = C_2H_5$ in Fig. 1.24) is the most symmetric, whereas Etio-III ($R_1 = R_3 = R_5 = R_8 = CH_3$ and $R_2 = R_4 = R_6 = R_7 = C_2H_5$) is the least symmetric. Rankin and Czernuszewicz [244] have shown that the Ni(II) and VO(II) complexes of ethioporphyrins I and III can be distinguished by RR spectra in the 1050–750 cm^{-1} region.

Li et al. [245] measured the surface-enhanced RR spectra (SERRS) of water-insoluble Ni(Por) in aqueous silver sol (low concentration, $\sim 10^{-8}$ M), and observed extra enhancement of the A_{1g}, B_{1g}, and B_{2g} modes but not of the A_{2g} modes when the excitation was made at or near the Soret band. However, an antiresonance effect was noted for the A_{1g} mode at 995 cm^{-1} when the excitation wavelength was in the valley between the Soret and Q bands. Vibrational frequencies in the SERR spectra were in good agreement with those in homogeneous solution. The effective symmetry of the adsorbed Ni(Por) must be lower than $\mathbf{D}_{4h}$, since many out-of-plane modes and IR-active in-plane modes were observed in the SERR spectra.

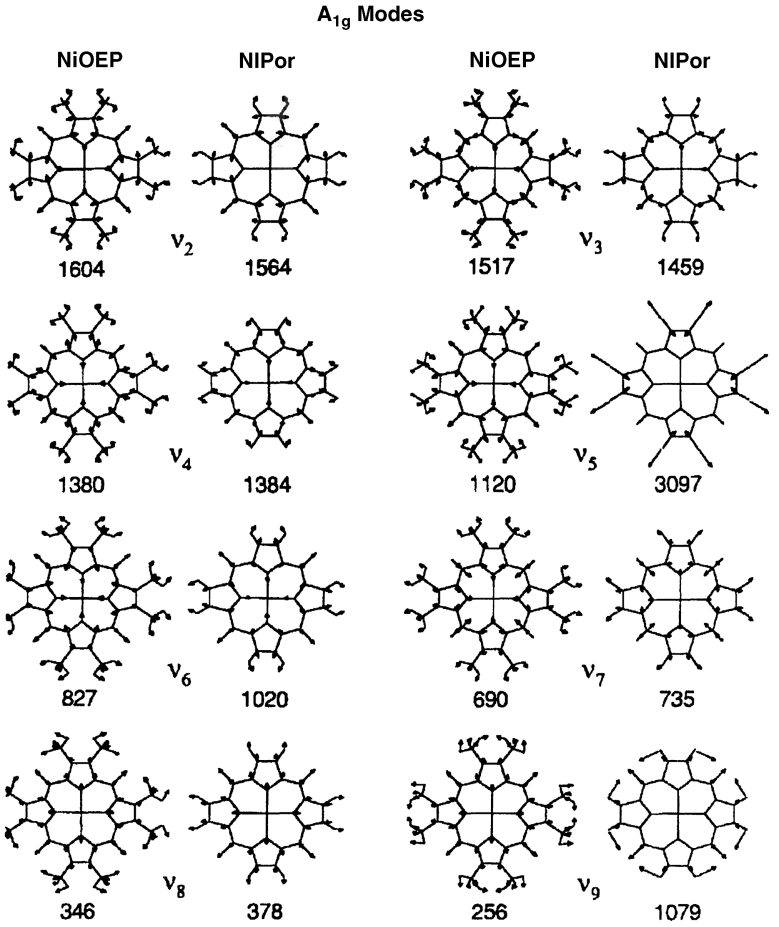

Fig. 1.25. *Atomic displacements and calculated skeletal frequencies (cm^{-1}) of A_{1g} modes compared for Ni(OEP) and Ni(Por)* [*233*].

TABLE 1.11. Normal Modes Containing Ni–N Stretching Vibrations[a,b]

Complex	$\nu_8(A_{1g})$	$\nu_{18}(B_{1g})$	$\nu_{50}(E_u)$	$\nu_{53}(E_u)$
Ni (Por)	369(27%)	237 (64%)	420 (50%)	282 (44%)
Ni (OEP)	360/343 (7%)	168 (37%)	358* (30%)	328 (28%)[c]
Ni (TPP)	402 (24%)	277 (53%)	436 (21%)	306 (32%)

[a] The Ni–N stretching force constant of 1.68 mdyn/Å was used for all three porphyrins.
[b] Numbers in front of brackets are observed frequencies (cm^{-1}) except for that with an asterisk, which is calculated. Numbers in brackets indicate % PED.
[c] ν_{51}.

1.5.2. Structure-Sensitive Vibrations

Ozaki et al. [246] measured the resonance Raman spectra of a series of Fe(OEP) complexes and found linear relationships between the frequencies of their skeletal modes (ν_2, ν_3, ν_{10}, ν_{11}, ν_{19}) and the Ct−N distances (from the center of the porphyrin ring to pyrrole N atom) shown in Fig. 1.26. Similar relationships were found in a series of Fe(OEC) complexes (OEC = octaethylchlorin) discussed in Sec. 1.6. The slope of each line increases in the order $\nu_{19} > \nu_{10} > \nu_3 > \nu_2 > \nu_{11}$, which is parallel to the percent contribution to the $\nu(C_\alpha - C_m)$ coordinate in each normal mode. This result indicates that when the core size increases, the $C_\alpha - C_m$ bonds are weakened and the corresponding frequencies are lowered. In going from low to high spin state, the porphyrin core tends to expand or be domed, and this results in weakening of the $C_\alpha - C_m$ bond. Thus, these vibrations serve as the spin state marker bands [247]. They are also metal-sensitive because the core size varies with the nature of the metal ion [248]. The ν_{10} is sensitive to the number and the nature of axial ligands [249]. The ν_{11} is sensitive to the nature of the peripheral substituents since it is due mainly to $\nu(C_\beta C_\beta)$. Finally, ν_7 is a 16-membered porphyrin ring breathing motion. Thus, it is strong for planar complexes and weak for nonplanar (or domed) complexes [250].

The totally symmetric breathing mode, ν_4, is known to be the best marker for the oxidation state. It is near 1360 cm^{-1} for Fe(II) complexes, and near 1375 cm^{-1} for Fe (III) complexes with relatively small dependence on the spin state. The frequency increase in going from Fe(II) to Fe(III) is attributed to the decrease of π-backbonding

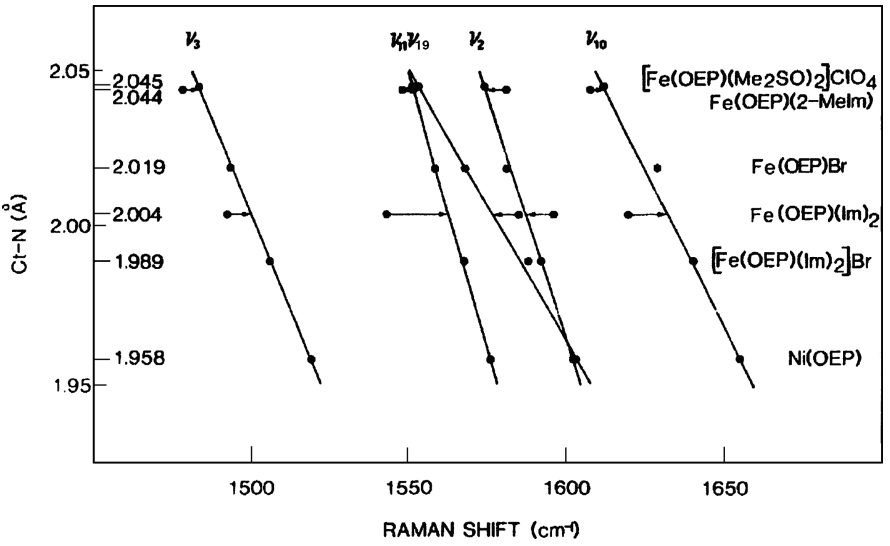

Fig. 1.26. *Correlations between the ν_{10}, ν_2, ν_{19}, ν_{11}, and ν_3 frequencies and the porphyrin core size (Ct−N, Å) for the Fe(OEP) complexes [246].*

from the metal $d\pi$ orbital to the porphyrin π^* orbital. In Fe(IV) and Fe(V) porphyrins, the ν_4 are at 1379 [251] and 1384 cm^{-1} [252], respectively. Mylrajan et al. [253] included ν_4 and ν_{28} and the crystallographically defined complexes, Fe(OEP), Fe(OEP)(NCS), $[Fe(OEP)(N\text{-}MeIm)_2]^+$, $[Fe(OEP)(DMSO)_2]^+$, Fe(OEC), and three Ni(OEP) complexes [triclinic (A and B) and tetragonal forms] in the correlations presented above.

Structure-sensitive bands of other metalloporphyrins have also been studied; Fe(OEC) [254] and water-soluble porphyrins such as Fe(TMpy-P2) [TMpy-P2: tetrakis (2-*N*-methylpyridyl)porphyrin, R_1–$R_8 = H$, $R' = 2$-*N*-methylpyridyl cation in Fig. 1.24] [255,256].

According to X-ray analysis, triclinic and tetragonal crystals of Ni(OEP) contain "flat" and "ruffled" porphyrin rings, respectively. All the frequencies above 1400 cm^{-1} (in-plane skeletal modes) are lower in the "ruffled" form than in the "flat" form. The solution frequencies are intermediate between those of the triclinic and tetragonal forms, indicating that Ni(OEP) is definitely "ruffled" in solution [257,258].

In Ni(OETPP) (R_1–$R_8 = C_2H_5$ and $R' = C_6H_5$ in Fig. 1.24), "saddle" distortion of the porphyrin ring occurs because of steric crowding of the peripheral substituents. Shelnutt and coworkers carried out RR as well as X-ray diffraction studies on this and related complexes [259–261]. Such distortion causes large-downshifts ($\sim$70 cm^{-1}) relative to the planar porphyrin in a number of porphyrin skeletal modes, and activates three out-of-plane (γ_{15}, γ_{16}, and δ_4) vibrations. Among them, the γ_{16} (tilting of the pyrrole rings) becomes one of the strongest bands in the Soret-excited RR spectrum [262].

1.5.3. Axial Ligand Vibrations

Table 1.12 lists the observed frequencies of Fe−L stretching vibrations of the iron porphyrins where L is an axial ligand. Polyatomic ligands such as N_3 and pyridine (py) exhibit their own internal modes as well. These axial ligand vibrations can be assigned by using isotopic ligands (H/D, $^{14}N/^{15}N$, $^{32}S/^{34}S$, etc.) and metal isotopes ($^{54}Fe/^{56}Fe$, etc.).

Kincaid and Nakamoto [270] observed the ν(Fe−F) of ^{54}Fe(OEP)F at 595 cm^{-1} with the 514.5 nm excitation. Kitagawa et al. [271] also observed the ν(Fe−X) of Fe(OEP)X at 364 and 279 cm^{-1} for X = Cl and Br, respectively, and the ν_s(L−Fe−L) of $[Fe(OEP)L_2]^+$ (L = ImH) at 290 cm^{-1} using the 488 nm excitation. These results show that the axial vibrations can be enhanced via resonance with in-plane π–π^* transitions (α and β bands). According to the latter workers, vibrational coupling between these axial vibrations and totally symmetric in-plane porphyrin-core vibrations is responsible for their resonance enhancement. On the other hand, Spiro [272] prefers electronic coupling; namely, the π–π^* transition induces the changes in the Fe−X (or L) distance, thus activating the axial vibration. Direct excitation is possible if the metal–axial ligand CT transition is in the visible region. Thus, Asher and Sauer [273] observed the ν(Mn−X) of Mn(EP)X (X = F,Cl,Br,I) with exciting lines in the

TABLE 1.12. Observed Frequencies of Iron-Axial Ligand Stretching Vibrations

Complex[a]	Mode	Obs. Freq. (cm^{-1})	Ref.
Fe(OEP) $(ImH)_2^+$	ν_a(L−Fe−L)	385,319[b]	263
Fe(PP) $(ImH)_2^+$	ν_s(L−Fe−L)	200	263
Fe(OEP) $(\gamma\text{-pic})_2^+$	ν_a(L−Fe−L)	373	264
Fe(PP) $(ImH)_2$	ν_s(L−Fe−L)	200	263
Fe(MP) $(py)_2$	ν_s(I−Fe−L)	179	265
Fe(OEP)F	ν(Fe−L)	605.5	264
Fe(OEP)Cl	ν(Fe−L)	357	264
Fe(OEP)Br	ν(Fe−L)	270	264
Fe(OEP)I	ν(Fe−L)	246	264
Fe(OEP)NCS	ν(Fe−L)	315	264
Fe(OEP)N_3	ν(Fe−L)	420	266
Fe(OEP) (SC_6H_5)	ν(Fe−L)	341	267
Fe(TPP) $(SC_6H_5)_2^-$	ν_a(L−Fe−L)	345	267
Fe(TPP)$(THT)_2^+$	ν_a(L−Fe−L)	328	267
Fe(TPP)F_2^-	ν_s(L−Fe−L)	453	268
Fe(TPP)CCl_2	ν(Fe−L)	1274[c]	269
Fe(TPP)CBr_2	ν(Fe−L)	1270[c]	269

[a] MP = mesoporphyrin IX dimethyl ester; THT = tetrahydrothiophene; pic = picoline.
[b] These two bands are due to ~50 : 50 mixing of two modes (antisymmetric Fe−L stretching and pyrrole tilting) [263].
[c] ν(Fe=C).

460–490 nm region where the Mn−X CT bands appear. Here EP denotes etioporphyrin ($R_1 = R_3 = R_5 = R_7 = CH_3$, $R_2 = R_4 = R_6 = R_8 = C_2H_5$ in Fig. 1.24). Similarly, Wright et al. [265] were able to observe totally symmetric pyridine (py) vibrations as well as ν_s[Fe−N(py)] of Fe(MP)$(py)_2$ with exciting lines near 497 nm that are in resonance with the Fe($d\pi$)–py(π^*) CT transition. Here, MP denotes mesoporphyrin IX dimethylester ($R_1 = R_3 = R_5 = R_8 = CH_3$, $R_2 = R_4 = C_2H_5$, and $R_6 = R_7 = -CH_2-CH_2COOCH_3$ in Fig. 1.24).

Ogoshi et al. [274] reported the IR spectra of M(OEC) (M = Zn,Cu,Ni), Mg(OEC)$(py)_2$, and Fe(OEC)X (X = F,Cl,Br,I), and assigned ν[M−N(OEC)] and ν[Mg−N(py)] using metal isotope techniques. Ozaki et al. [275] report RR spectra of these and other OEC complexes.

Vibrations of axial ligands such as O_2, NO, CO, and so on are discussed in later sections. Axial ligand vibrations provide valuable information about the structure and bonding of heme proteins containing these ligands.

1.5.4. Metal–Metal-Bonded Porphyrins

As shown in Sec. 2.11.2 of Part A, RR spectra of metal–metal bonded complexes such as $Re_2F_8^{2-}$ exhibit the strong ν(Re−Re) at 320 cm^{-1} and a series of its overtones and combination bands. The metal–metal bonded porphyrin dimer, $[Ru(OEP)]_2^{n+}$, exhibits the ν(Ru−Ru) at 285, 301, and 310 cm^{-1} for $n = 0$, 1, and 2, respectively [276]. The observed frequency increase indicates that the electron density of the Ru−Ru bond is removed from its antibonding π^* orbital as the complex ion is oxidized.

However, this removal has almost no effect on the porphyrin core vibrations since the metal–metal bond is perpendicular to the porphyrin plane. Similar results are reported for the $[Os(OEP)]_2^{n+}$ series (233, 254, and 266 cm^{-1} for $n = 0$, 1, and 2, respetively) [277]. The RR spectra of asymmetric sandwich compounds such as Ce(OEP)(TPP) [278], triple-decker sandwich compounds such as $Eu_2(OEP)_3$, and their singly oxidized compounds are available [279].

1.5.5. π–π Complex Formation and Dimerization

The Cu(II) uroporphyrin I (R_1–$R_8 = -CH_2COO^-$ in Fig. 1.24) forms molecular adducts with a variety of aromatic heterocyclic compounds in aqueous alkaline solution. Using Raman difference spectroscopy, Shelnutt [280] observed small shifts (from $+2.9$ to -2.7 cm^{-1}) of the porphyrin skeletal vibrations resulting from the π–π charge-transfer (porphyrin to heterocycle), and showed that the planes of these two components are parallel to each other. This work has been extended to the study of dimerization of the Cu(II) and Ni(II) complexes of uroporphyrin I. In this case, the porphyrin skeletal modes were upshifted by 1–3 cm^{-1} as a result of dimerization [281].

1.5.6. Reduction of Metalloporphyrins

Reduction of a metalloporphyrin results in lowering of the oxidation state of the central metal or the formation of a porphyrin anionic radical, depending on whether an electron enters in a metal or porphyrin orbital. One-electron reduction of Zn(TPP) yields Zn $(TPP^{\cdot -})$ containing an anionic radical of TPP, as confirmed by the observed pattern of isotopic shifts and polarizations [282]. In this case, an extra electron enters in the porphyrin e_g* orbital causing Jahn–Teller effect. One-electron reduction of VO(OEP) also yields $VO(OEP^{\cdot -})$ [283]. Teraoka et al. [284] have shown by electronic absorption and RR and ESR spectroscopy that two- and three-electron reduction of Fe(III)(OEP)Cl in THF solution yield low-oxidation-state porphyrins that are formulated as $[Fe(I)(OEP)]^{2-}$ and $[Fe(I)(OEP^{\cdot -})]^{2-}$, respectively. Anxolabéhére et al. [285] carried out UV–visible and RR spectroelectrochemical studies of Fe(TPP) and its pentafluorophenyl derivative, and concluded that the two-electron reduced species should be formulated as Fe(0) complexes because their RR spectra did not provide any evidence for the formation of the porphyrin anion radical. On the other hand, De Silva et al. [286] obtained $[Fe(TPP)]^{2-}$ by three-electron reduction of Fe(III)(TPP)Cl, and observed the RR spectrum which is qualitatively similar to that of the two-electron reduction product, $[Fe(I)(TPP)]^-$. Thus, these workers formulated it as $[Fe(I)(TPP^{\cdot -})]^{2-}$.

1.6. METALLOCHLORINS, CHLOROPHYLLS, AND METALLOPHTHALOCYANINES

1.6.1. Metallochlorins

Metallochlorins differ from metalloporphyrins in that one of the four pyrrole rings of $C_\beta C_\beta$ bonds is saturated, and serve as model compounds of chlorophylls that are

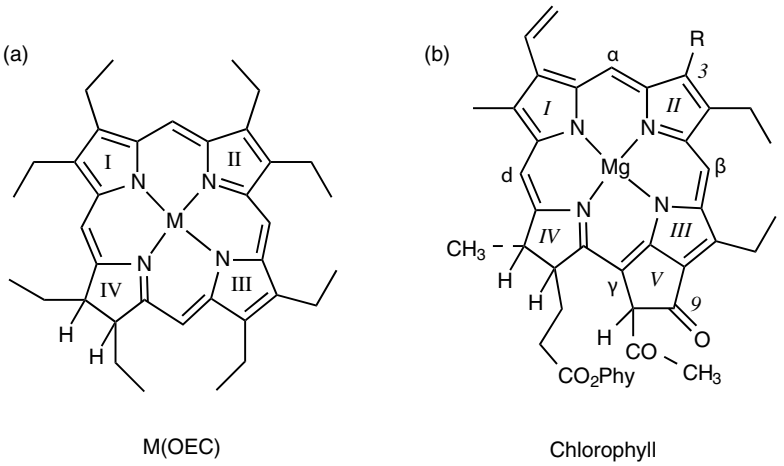

M(OEC) Chlorophyll

Fig. 1.27. *Structures of M(OEC) (a) and chlorophyll; in (b) R = CH_3 for Chl a*, and CHO for Chl *b*. *[Phy = phytyl = $C_{20}H_{39}$ = $-CH_2-CH=C(CH_3)-\{(CH_2)_3-C(CH_3)\}_3-CH_3$].*

involved in photosynthetic processes. Figure 1.27 shows the structures of metallooctaethylchlorin [M(OEC)] and chlorophyll *a*. The symmetry of a metallochlorin is regarded as $\mathbf{C}_{2v}$ because the substituents on the reduced pyrrole ring normally take a *trans* conformation. Infrared and Raman selection rules of metallochlorins are markedly different from those of metalloporphyrins as a result of symmetry lowering from $\mathbf{D}_{4h}$, to $\mathbf{C}_{2v}$. According to the correlation table (Appendix IX of Part A), the symmetry species of the in-plane skeletal modes of a metalloporphyrin listed in Table 1.9 are changed as follows: $A_{1g}(A_1), A_{2g}(B_1), B_{1g}(A_1), B_{2g}(B_1)$, and $E_u(A_1 + B_1)$. Here, the corresponding symmetry species under $\mathbf{C}_{2v}$ symmetry are shown in parentheses. Since A_1, B_1, and B_2 species are all IR-active, the IR spectrum of M (OEC) is expected to show more bands than the corresponding M(OEP). This is clearly demonstrated in Fig. 1.28 obtained by Ogoshi et al. [287]. These workers also located the metal isotope-sensitive bands of Zn(OEC), Cu(OEC), and Mg(OEC)$(py)_2$ at 212.0 (1.0), 233.0 (1.6), and 176.5 (4.0) cm^{-1}, respectively, by $^{64}Zn/^{68}Zn$, $^{63}Cu/^{65}Cu$, and $^{24}Mg/^{26}Mg$ substitutions. Here, the vibrational frequencies are listed for the first isotopic species of each metal, and the numbers in parentheses indicate the magnitudes of the isotope shifts. The corresponding mode of Ni(OEC) was assigned at 256 cm^{-1}. The number of vibrations observed in RR spectra also increases as a result of symmetry lowering. Normal coordinate analysis on M(OEC) was made by Bocian and coworkers [288,289].

Boldt et al. [290] carried out vibrational analysis of in-plane vibrations of Ni(OEC) and its derivatives using a semiempirical quantum mechanical force field (QCFF/PI) method [291]. On the basis of their theoretical calculations, these workers assigned 45 bands of the RR spectrum of Ni(OEC) observed in the 1650–340 cm^{-1} region. The results show that few of the high-frequency modes of Ni(OEC) can be correlated with a single Ni(OEP) mode but the vibrations below 950 cm^{-1} can be correlated with it. Their work was extended to Cu(OEC) and its isotopic species (H/D and $^{14}N/^{15}N$) [292].

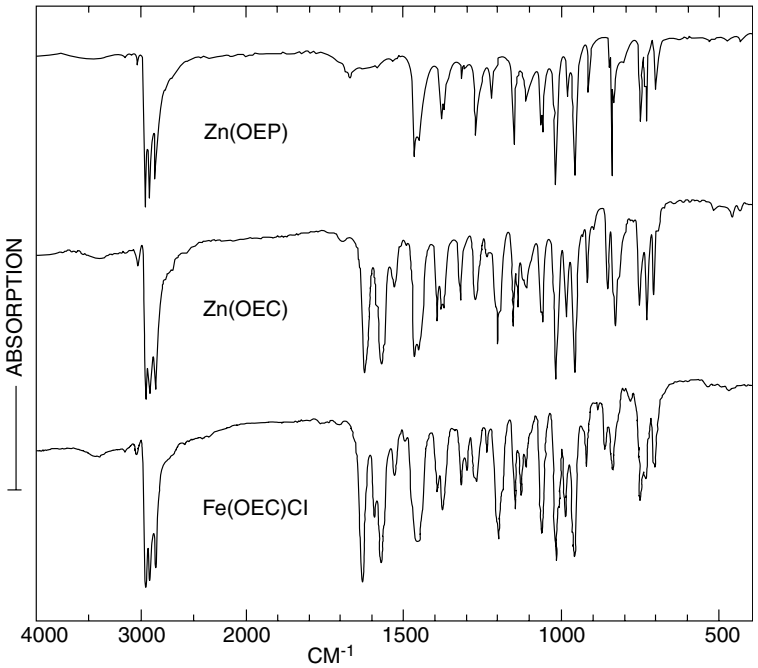

Fig. 1.28. *IR spectra of Zn(OEP), Zn(OEC), and Fe(OEC)Cl [287].*

Anderson et al. [293] compared the spectral properties of *cis*- and *trans*-isomers of planar Cu(OEC) and $\mathbf{S}_4$-ruffled Ni(OEC), and found that conformational differences of the peripheral substituents have marked effects on the spectral properties and that such localized changes strongly perturb the overall properties of chlorins. Ozaki et al. [294] measured the far-IR spectra (Fig. 1.29) of the Fe(OEC)X (X = F,Cl,Br,I) and assigned the ν(Fe−X) bands at 589 (605.5), 352 (357), 270 (270), and 240.5 (246) cm^{-1} for X = F, Cl, Br, and I, respectively. Here, the numbers in parentheses indicate the corresponding frequency of Fe(OEP)X. Ozaki et al. [295,296] also compared the RR spectra of Fe(OEC)L- and Fe(OEC)L_2-type compounds with those of the corresponding Fe(OEP) complexes in the high- and low-frequency regions. RR spectra of *meso*-substituted chlorin complexes of Ni(II) and Cu(II) [297], Cu(II) [298], and Zn(II) [299] were measured and assigned by comparing them with the corresponding porphyrin complexes.

1.6.2. Chlorophylls

Chlorophylls (Chl) and bacteriochlorophylls (BChl) are another "reduced" pigments that are involved in the process of photochemical energy transduction (Sec. 3.4). As shown in Fig. 1.27b, Chl is a Mg(II) macrocycle in which one pyrrole ring (ring IV) is reduced and ring V is fused to ring III. The peripheral R group on ring II is CH_3 for Chl *a* and CHO for Chl *b*. Assignments of the vibrational spectra of Chls in the

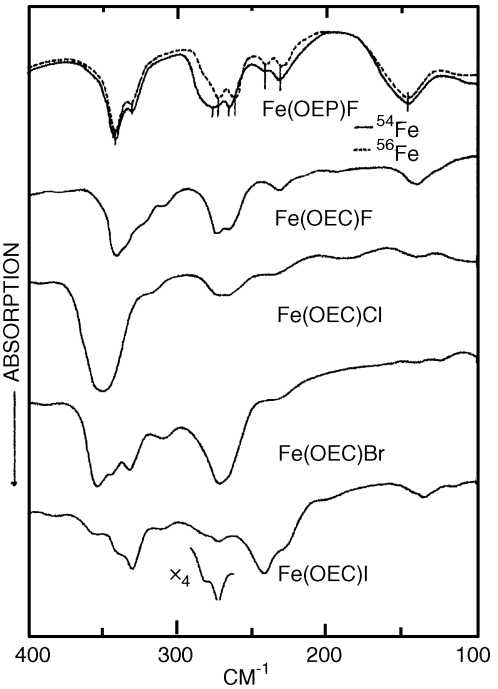

Fig. 1.29. *Far-IR spectra of Fe(OEP)F and Fe(OEC)X (X = F,Cl,Br,I) [294].*

high-frequency region were based on the results of theoretical calculations obtained for in-plane vibrations of Ni(OEC) [290]. A similar approach was taken to assign low-frequency vibrations (below 1000 cm^{-1}) of Mg(OEP), Mg(OEC), and Chl *a* [300].

Fujiwara and Tasumi [301,302] measured the Raman spectra (441.6 nm excitation) of Chl *a* and *b* in various solvents. Figure 1.30 compares their spectra obtained in diethylether and THF. The bands in the 1710–1690 cm^{-1} region observed for both compounds are assigned to the ν(C=O) of the free C-9 carbonyl group of ring V, while those in the 1670–1669 cm^{-1} of Chl *b* are assigned to the free C-3 formyl carbonyl group. The Raman spectrum of Chl *a* exhibits three bands at 1607 (weak), 1554 (strong), and 1529 (medium) cm^{-1} in diethylether (group I solvent), and these bands are shifted to 1596, 1545, and 1521 cm^{-1}, respectively, in THF (group II solvent). Similar solvent behaviors were observed in going other group I solvents (*n*-hexane. CCl_4, CS_2, etc.) to group II solvents (dioxane, pyridine, and methanol). On the basis of these results together with other information, these workers concluded that Chl *a* in group I solvents is five-coordinate (with one axial ligand) whereas it becomes six-coordinate (two axial ligands) in group II solvents. These two species coexist in I,II-mixed solvents, although the six-coordinate species is dominant in pyridine solution. Similar results were obtained for Chl *b*.

Heald and Cotton [303] observed that the RR spectrum (407.6 nm excitation) of the electrochemically generated cation radical of Chl *a* in CH_2Cl_2 exhibits the C-9 ν(C=O) vibration at 1717 cm^{-1}, which is 32 cm^{-1} higher than that of Chl *a*

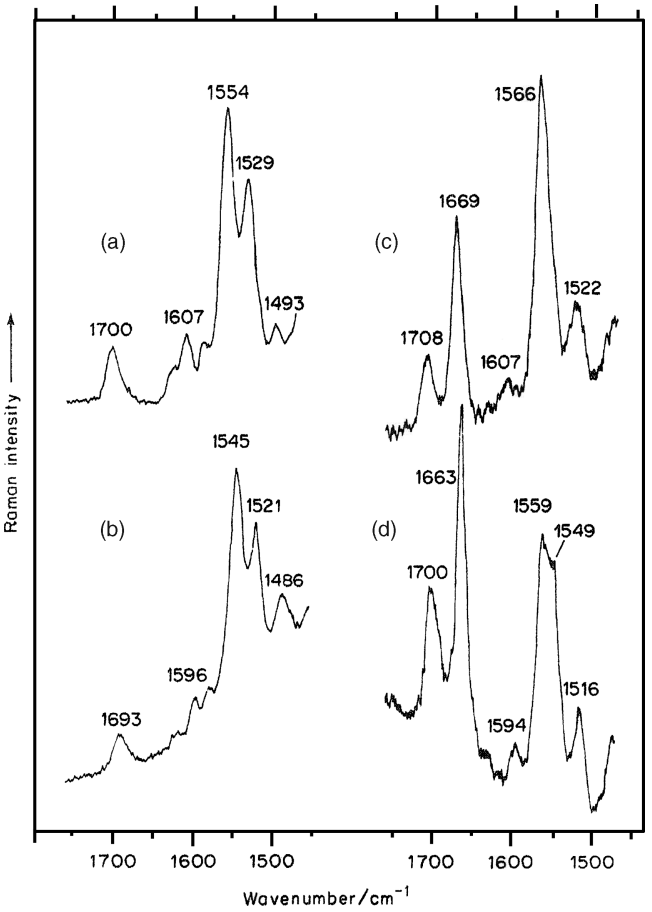

Fig. 1.30. *Raman spectra (1750–1450 cm^{-1}) of chlorophylls* a *and* b: *(a) Chl* a *in diethylether; (b) Chl* a *in THF; (c) Chl* b *in diethylether; (d) Chl* b *in THF [302].*

(1685 cm^{-1}). This was attributed to a decrease in conjugation between the C-9 keto group and the macrocyclic ring caused by one-electron oxidation. It was suggested that the C-9 keto group plays a role in chlorophyll redox reaction *in vivo*.

Vibrational spectra of chlorophylls and related compounds have been reviewed by several groups of investigators [302,304,305].

1.6.3. Metallophthalocyanines

Metallophthalocyanines [M(Pc)], shown in Fig. 1.31, are known for their exceptional thermal stability and extremely low solubility in any solvents. Under $\mathbf{D}_{4h}$, symmetry, their 165 ($3 \times 57 - 6$) normal vibrations are classified into $14A_{1g} + 13A_{2g} + 14B_{1g}$ $14B_{2g} + 13E_g + 6A_{1u} + 8A_{2u} + 7B_{1u} + 7B_{2u} + 28E_u$, of which the A_{1g}, A_{2g}, B_{1g}, B_{2g}, and E_u vibrations are in-plane modes, and the A_{1u}, A_{2u}, B_{1u}, B_{2u}, and E_g vibrations are

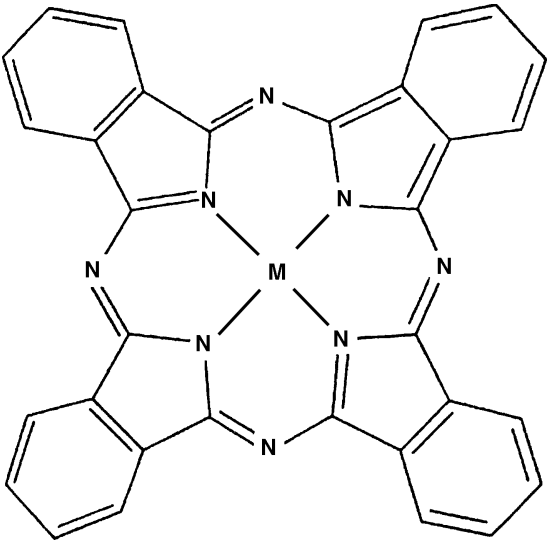

Fig. 1.31. *Structure of metallophthalocyanine.*

out-of-plane modes. Only the A_{2u} and E_u vibrations are IR-active, whereas the A_{1g}, B_{1g}, B_{2g}, and E_g vibrations are Raman-active. Similar to metalloporphyrins, the A_{2g} vibrations become Raman-active under resonance conditions. Melendres and Maroni [306] carried out normal coordinate analysis on Fe(Pc). As expected, extensive vibrational couplings occur among the local coordinates so that simple descriptions of normal modes by local coordinates cannot be justified. They estimated the Fe−N stretching force constant to be 1.00 mdyn/Å. Using metal isotope techniques, Hutchinson et al. [307] assigned primary ν(M−N) modes of M(Pc) at 240.7 (^{64}Zn), 284.0 (^{63}Cu), 376.0 and 317.8 (^{58}Ni), and 308.4 cm^{-1} (^{54}Fe).

SERR and IR spectra of other M(Pc^2) (M = Mg,Cu,Zn,Pt,Pb) are reported together with band assignments (totally symmetric in-plane modes) obtained by normal coordinate analysis [308].

Homborg and coworkers carried out extensive IR and Raman studies of a variety of metallophthalocyanines. In a series of $[Bi(III)(Pc^{2-})_2]^n$ ($n = -1,0,+1$), the Bi(III) atom is coordinated by eight N atoms of two slightly distorted Pc^{2-} ligands in a square–antiprismatic conformation, and the ν_a(Bi−N) and ν_s(Bi−N) were located at 116 (IR) and 150 cm^{-1}(RR), respectively [309]. The RR spectra (1064 nm excitation) of [M$(Pc)_2$] [M = a lanthanide(III) ion] obtained by anodic oxidation of $[M(Pc^{2-})]^-$ exhibit the ν_s(M−N) in the range of 141 (La) to 168 cm^{-1} (Lu), and show equal presence of the Pc^- π-radical($Pc^{-\cdot}$)[310]. Thus, it may be formulated as $[M(Pc^{2-})(Pc^{-\cdot})]$. The IR spectra of the $[M(Pc^{2-})_2]^-$ ion (M = Y(III) or In(III)) show the ν_a(M−N) at 182 and 137 cm^{-1}, for M = Y and In, respectively [311]. The ν(Re−Re) and ν_a(Re−N) vibrations of dimeric $[Re(Pc^{2-})_2]$ are at 240 and 355 cm^{-1}, respectively [312]. The IR and Raman spectra of a monolayer film of Eu$(Pc)_2$ were assigned by Berno et al. [313] on the basis of $\mathbf{C}_{4v}$ symmetry.

Figure 1.32 shows the IR and Raman spectra of a series of $[Cr(III))(Pc^{2-})X_2]^-$ (X = F,Cl,Br,I) below 600 cm^{-1} obtained by Sievertsen et al. [314]. The shaded bands indicate the $\nu_a(CrX_2)$(IR) and $\nu_s(CrX_2)$(Raman) vibrations. Axial ν(M−X) vibrations of other $[M(Pc^{2-})X_2]$-type complexes have been reported for M = Ir(III) [315], Os(II) [316], Ru(III) [317], and Tl(III) [318]. The ν(M−X) vibrations of $[Ru(III)(Pc^{2-})(py)X]^-$-type complexes are at 390, 360, 337, 260, and 204 cm^{-1} for $X = CN^-$, N_3^-, NCO^-, NCS^-, and NO_2^- respectively [319]. In the case of $[M(O)(Pc^{2-})X_2]$-type complexes [M = Nb(V) and Ta(V) and $X = F^-, Cl^-, NCS^-$ and N_3^-], three axial ligands (2X and O) are on one side of the Pc^{2-} plane, and their ν(M=O), ν_s(M−X)

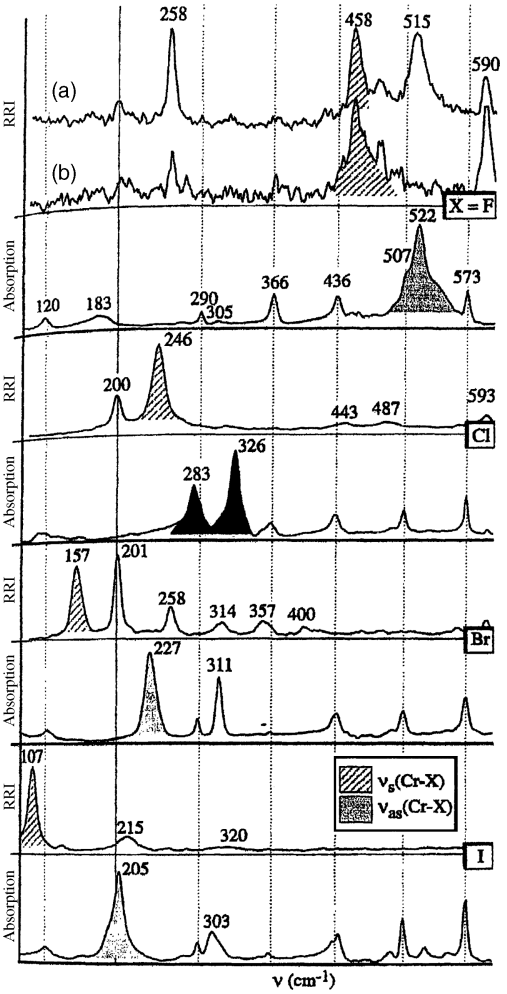

Fig. 1.32. *Vibrational spectra of $[^nBu_4N][CrX_2(Pc^{2-})]$: (a) 476.5 nm excitation, X = F; (b) 496.5 nm excitation, X = Cl, Br, I (all 496.5 nm excitation) (RRI = relative Raman intensity) [314].*

and ν_a(M−X) vibrations have been assigned [320]. In μ-carbido diphthalocyanines of [$(MPc^{2-})_2$(μ-C)] (M = Fe,Ru), the M−C−M bond is linear, and the ν_a(MCM) and ν_s(MCM) vibrations are at 997 and 477 cm^{-1}, respectively, for M = Fe [321]. The ν_a and ν_s vibrations of the Mn−N−Fe bridge in (TPP)Mn−N−Fe(Pc) are at 956/945 and 381 cm^{-1}, respectively [322]. Electronic and IR spectra of phthalocyanine molecular assemblies are reviewed by Cook [323].

1.7. NITRO AND NITRITO COMPLEXES

The NO_2^- ion coordinates to a metal in a variety of ways:

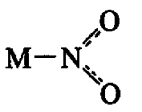

Nitro complex

I

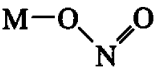

Nitrito complex

II

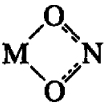

Chelating nitrito complex

III

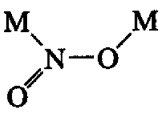

IV

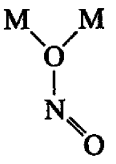

V

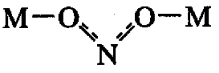

VI

Bridging complexes

Vibrational spectroscopy is very useful in distinguishing these structures.

1.7.1. Nitro Complexes

The normal vibrations of the unidentate N-bonded nitro complex may be approximated by those of a planar ZXY_2 molecule, as shown in Fig. 1.33. In addition to these modes, the NO_2 twisting and skeletal modes of the whole complex may appear in the low-frequency region. Table 1.13 summarizes the observed frequencies and band assignments for typical nitro complexes. It is seen that these complexes exhibit $\nu_a(NO_2)$ and $\nu_s(NO_2)$ in the 1470–1370 and 1340–1320 cm^{-1} regions, respectively. On the other hand, the free NO_2^- ion exhibits these modes at 1250 and 1335 cm^{-1}, respectively. Thus $\nu_a(NO_2)$ shifts markedly to a higher frequency, whereas $\nu_s(NO_2)$ changes very little on coordination.

Nakagawa and Shimanouchi [60] and Nakagawa et al. [324] carried out normal coordinate analyses to assign the infrared spectra of crystalline hexanitro cobaltic salts; both internal and lattice modes were assigned completely by factor group analysis. The results indicate that the complex ion takes the $\mathbf{T}_h$, symmetry in K, Rb, and

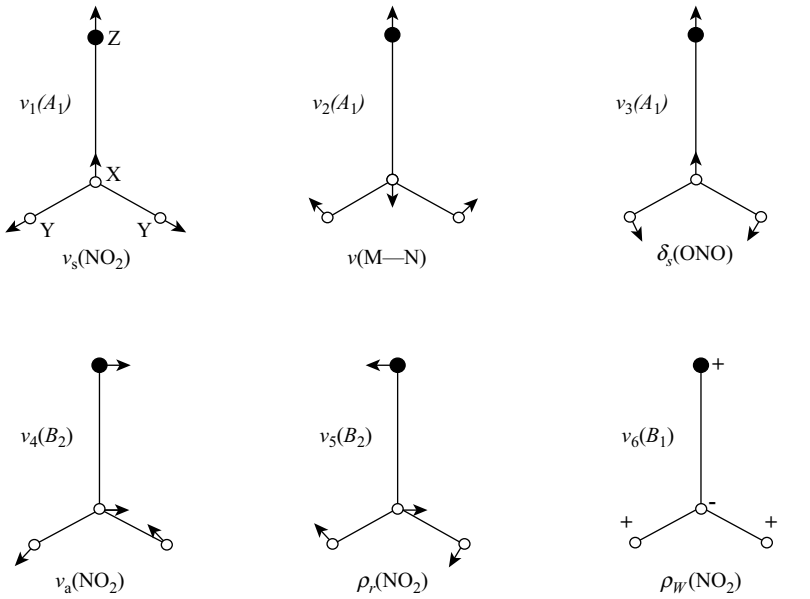

Fig. 1.33. *Normal modes of vibration of planar ZXY_2 molecules (the band assignment is given for an $M-NO_2$ group).*

TABLE 1.13. Observed Infrared Frequencies and Band Assignments of Nitro Complexes (cm^{-1})

Complex	$\nu_a(NO_2)$	$\nu_s(NO_2)$	δ(ONO)	$\rho_w(NO_2)$	ν(MN)	$\rho_r(NO_2)$[a]	Refs.
$K_3[Co(NO_2)_6]$	1386	1332	827	637	416	293	324
$Na_3[Co(NO_2)_6]$	1425	1333	854 831	623	449 372	276 249	324
$K_2Ba[Ni(NO_2)_6]$	1343	1306	838	433	291	255	324
$K_3[Ir(NO_2)_6]$	1395 1375	1330	830	657	390	300	325
$K_3[Rh(NO_2)_6]$	1395	1340	833	627	386	283	325
$K_3[Ir(NO_2)Cl_5]$	1374	1315	835	644	325	288	326
$[Pt(NO_2)_6]^{4-}$	1488 1458	1328	834	621	368	294	327
$K_2[Pt(^{15}NO_2)_4]$	1466 1397	1343	847 839 833	640 623	421		328,329
$[Pd(NO_2)_4]^{2-b}$	1408	1364 1320	834 824	440	290		329
$K_2[Pt(NO_2)Cl_3]$	1401	1325	844	614	350	304	326

[a] This mode may couple with other low-frequency modes.
[b] Raman data in aqueous solution.

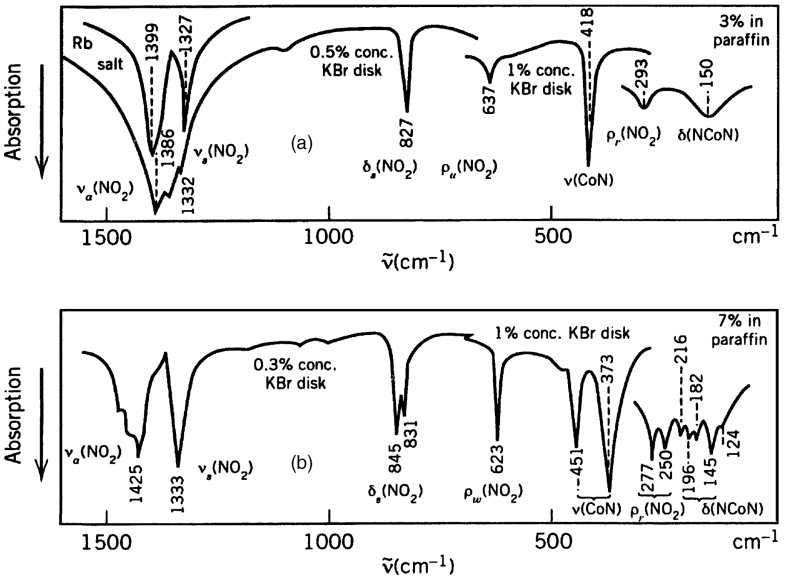

Fig. 1.34. *Infrared spectra of (a) $K_3[Co(NO_2)_6]$ and (b) $Na_3[Co(NO_2)_6]$ [330].*

Cs salts but the $\mathbf{S}_6$ symmetry in the Na salt (see Fig. 1.10 of Part A). The IR spectra of K and Na salts are compared in Fig. 1.34. Kanamori et al. [330] obtained the RR spectra (632.8 nm excitation, ~80 K) of these complexes, and showed that resonance enhancement occurs via the B term since nontotally as well as totally symmetric vibrations are observed.

There are many nitro complexes containing other ligands such as NH_3 and Cl. In these cases, the main interest has been the distinction of stereoisomers by the symmetry selection rules and the differences in frequency between isomers. It is possible to distinguish *cis*- and *trans*-$[Co(NH_3)_4(NO_2)_2]^+$ [331] by the rule that the *cis*-isomer exhibits more bands than the *trans*-isomer, and to distinguish *fac*- and *mer*-$[Co(NH_3)_3(NO_2)_3]$ [332] by the observation that $\delta(NO_2)$ and $\rho_w(NO_2)$ are higher for the *fac*-isomer ($\mathbf{C}_3$, 832 and 625 cm^{-1}, respectively) than for the *mer*-isomer ($\mathbf{C}_{2v}$, 825 and 610 cm^{-1}, respectively). Nakagawa and Shimanouchi [333] measured the infrared spectra of the $[Co(NO_2)_n(NH_3)_{6-n}]^{(3-n)+}$ series and carried out normal coordinate analysis on the mononitro and dinitro complexes. Nolan and James [334] studied the infrared and Raman spectra of $[Pt(NO_2)_nCl_{6-n}]^{2-}$-type salts in the crystalline state.

1.7.2. Nitrito Complexes

If the NO_2 group is bonded to a metal through one of its O atoms, it is called a *nitrito complex*. Table 1.14 lists the NO stretching frequencies of typical nitrito complexes. The two $\nu(NO_2)$ of nitrito complexes are well separated, ν(N=O) and ν(NO) with at 1485–1400 and 1110–1050 cm^{-1}, respectively. Distinction between the nitro and nitrito coordination can be made on this basis. It is to be noted that nitrito complexes

TABLE 1.14. Vibrational Frequencies of Nitrito Complexes (cm^{-1})

Complex	ν(N=O)	ν(NO)	δ(ONO)	Ref.
$[Co(NH_3)_5(ONO)]Cl_2$	1468	1065	825	335
$[Cr(NH_3)_5(ONO)]Cl_2$	1460	1048	839	335
$[Rh(NH_3)_5(ONO)]Cl_2$	1461 1445	1063	830	326
$[Ni(py)_4(ONO)_2]$	1393	1114	825	336
trans-$[Cr(en)_2(ONO)_2]ClO_4$	1485 1430	—	835 825	337
$[Co(py)_4(ONO)_2](py)_2$	1405	1109	824	338

lack the wagging modes near 620 cm^{-1} that appear in all nitro complexes. The ν(MO) of nitrito complexes were assigned in the 360–340 cm^{-1} region for metals such as Cr (III), Rh(III), and Ir(III) [326].

Infrared spectra of nitro–nitrito isomeric pairs are reported for *cis*-$[Ru(II)(bipy)_2(NO)X]^{2+}$, where X is $-NO_2$ and $-ONO$ [339].

In many nitro complexes several types of nitro coordination are mixed. Goodgame, Hitchman, and their coworkers carried out an extensive study on vibrational spectra of nitro complexes containing various types of coordination. For example, all six nitro groups in $K_4[Ni(NO_2)_6]\cdot H_2O$ are coordinated through the N atom. However, its anhydrous salt exhibits the bands characteristic of nitro as well as nitrito coordination. From UV spectral evidence, Goodgame and Hitchman [340] suggested the structure $K_4[Ni(NO_2)_4(ONO)_2]$ for the anhydrous salt. Table 1.15 lists the observed frequencies of two Ni(II) complexes containing both nitro and nitrito groups.

The red nitritopentammine complex, $[Co(NH_3)_5(ONO)]Cl_2$, is unstable and is gradually converted to the stable yellow nitro complex. The kinetics of this conversion can be studied by observing the disappearance of the nitrito bands [342,343], and the rate of the photochemical isomerization in the solid state has been determined [344]. Burmeister [345] reviewed the vibrational spectra of these and other linkage isomers.

1.7.3. Chelating Nitrito Complexes

If the nitrito group is chelating, the ν(N=O) and ν(N−O) of the nitrito group will be shifted to a lower and a higher frequency, respectively, relative to those of unidentate

TABLE 1.15. Vibrational Frequencies of Ni(II) Complexes Containing Nitro and Nitrito Groups (cm^{-1})

	Nitro Group			Nitrito Group		
Complex	$\nu_a(NO_2)$	$\nu_s(NO_2)$	ρ_w(ONO)	ν(N=O)	ν(NO)	Ref.
$K_4[Ni(NO_2)_6]H_2O$	1346	1319	427	—	—	340
$K_4[Ni(NO_2)_4(ONO)_2]$	1347	1325	423 414	1387	1206	340
Ni[2-(aminomethyl)-py]$_2$-(NO_2)(ONO)	1338	1318	—	1368	1251	341

TABLE 1.16. Vibrational Frequencies of Chelating Nitrito Groups (cm^{-1})

Complex	$\nu_a(NO_2)$	$\nu_s(NO_2)$	δ(ONO)	Δ^a	Ref.
$Co(Ph_3PO)_2(NO_2)_2$	1266	1199 1176	856	78	346
$Ni(\alpha\text{-pic})_2(NO_2)_2$	1272	1199	866 862	73	346
$Re(CO)_2(PPh_3)_2(NO_2)$	1241	1180	887	61	347
[Ni(*N,N′*-dimethyl-en)-(NO_2)] ClO_4	1300	1230	—	70	348
$Cs_2[Mn(NO_2)_4]$	1302	1225	841	77	349
$Co(Me_4\text{-en})(NO_2)_2$	1290	1207	850	83	338
$Zn(py)_2(NO_2)_2$	1351	1171	850	180	350
$Zn(isoquinoline)_2(NO_2)_2$	1370	1160	—	210	350
(*o*-cat) $[Co(NO_2)_4]^b$	1390	1191	—	199	349

[a] $\Delta = \nu_a - \nu_s$.
[b] *o*-cat = [*o*-xylylenebis(triphenylphosphonium)]$^{2+}$ ion.

nitrito complexes. As a result, the separation between these two modes (Δ) becomes much smaller than those of unidentate complexes. Table 1.16 lists the vibrational frequencies of chelating nitrito groups. It should be noted that the Δ value depends on the degree of asymmetry of the coordinated nitrito group; it is expected that the Δ value is the smallest when the two N−O bonds are equivalent and increases as the degree of asymmetry increases. Relatively large Δ values observed for the last three compounds in Table 1.16 may be accounted for on this basis.

According to X-ray analysis, the orange compound, $K_4[Ni(NO_2)_6]\cdot H_2O$, is an octahedral complex with six N-bonded nitro ligands and a water of crystallization. On dehydration at 100°C, it forms a mixture of red $K_3[Ni(NO_2)_4$(chelated $O_2N)]$ and KNO_2. The former exhibits the ν_a, ν_s, and δ vibrations of the chelated nitrite group at 1385, 1225, and 866 cm^{-1} in IR spectra [351]. The corresponding vibrations are observed at 1293, 1223, and 826 cm^{-1} in the IR spectrum of $NaNO_2$ in Ar matrices, indicating the formation of a chelate ring with Na atom ($\mathbf{C}_{2v}$ symmetry). On photoirradiation (248 nm), it is converted to the unidentate *trans*-Na–ONO complex with the three bands at 1446, 1159, and 787 cm^{-1} [352].

1.7.4. Bridging Nitro Complexes

The nitro group is known to form a bridge between two metal atoms. Nakamoto et al. [335] suggested that among the three possible structures, IV, V, and VI, shown earlier, IV is most probable for

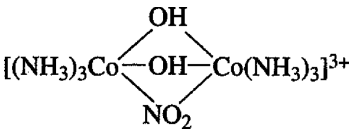

since its NO_2 stretching frequencies (1516 and 1200 cm^{-1}) are markedly different from those of other types discussed thus far. Later, this structure was found by X-ray

analysis of [353]

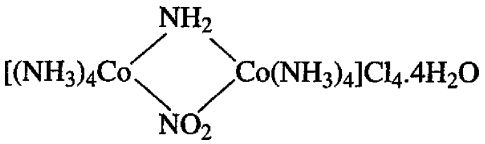

This compound exhibits the NO_2 stretching bands at 1492 and 1180 cm^{-1}. On $^{16}O \rightarrow {}^{18}O$ substitution of the bridging oxygen, the latter is shifted by $-10\,cm^{-1}$ while the former is almost unchanged. Thus, these bands are assigned to the $\nu(N{=}O)$ (outside the bridge) and $\nu(N{-}O)$ (bridge), respectively [354]. The $[Co_2\{(NO_2)(OH)_2\}(NO_2)_6]^{3-}$ ion exhibits the NO_2 bands at 1516, 1190, and 860 cm^{-1}, indicating the presence of a bridging nitro group [355]:

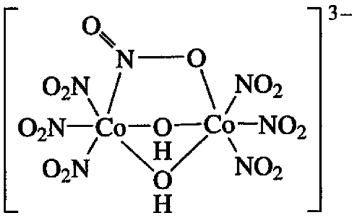

$[Ni(\beta\text{-pic})_2(NO_2)_2]_3 \cdot C_6H_6$ exhibits a number of bands due to coordinated nitro groups. Goodgame et al. [356] suggested the presence of two different types of bridging nitro groups (IV, V) and III, on the basis of the crystal structure and infrared data for this compound. Type IV absorbs at 1412 and 1236, type V at 1460 and 1019, and type III at 1299 and 1236 cm^{-1}. Goodgame et al. [357] also studied the infrared spectra of other bridging nitro complexes of Ni(II). For example, they found that $Ni(en)(NO_2)_2$ contains a type IV bridge (1429 and 1241 cm^{-1}), while $Ni(py)_2(NO_2)_2(\frac{1}{3}C_6H_6)$ is similar to that of the analogous β-picoline complex.

1.8. LATTICE WATER AND AQUO AND HYDROXO COMPLEXES

Water in inorganic salts may be classified as lattice or coordinated water. There is, however, no definite borderline between the two. The former term denotes water molecules trapped in the crystalline lattice, either by weak hydrogen bonds to the anion or by weak ionic bonds to the metal, or by both:

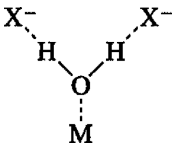

The latter term denotes water molecules bonded to the metal through partially covalent bonds. Although bond distances and angles obtained from X-ray and neutron

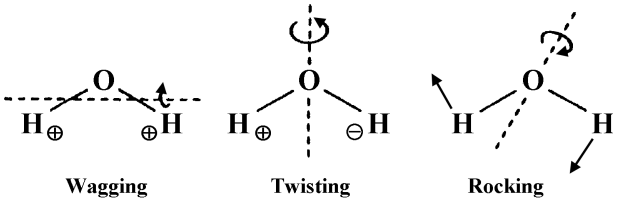

Fig. 1.35. *The three rotational modes of H_2O in the solid state.*

diffraction data provide direct information about the geometry of the water molecule in the crystal lattice, studies of vibrational spectra are also useful for this purpose. It should be noted, however, that the spectra of water molecules are highly sensitive to their surroundings.

1.8.1. Lattice Water

In general, lattice water absorbs at 3550–3200 cm^{-1} (antisymmetric and symmetric OH stretchings) and at 1630–1600 cm^{-1} (HOH bending). If the spectrum is examined under high resolution, the fine structure of these bands is observed. For example, $CaSO_4 \cdot 2H_2O$ exhibits eight peaks in the 3500–3400 cm^{-1} region [358], and its complete vibrational analysis can be made by factor group analysis (Sec. 1.28 of Part A). In the low-frequency region (600~200 cm^{-1}) lattice water exhibits "librational modes" that are due to rotational oscillations of the water molecule, restricted by interactions with neighboring atoms. As shown in Fig. 1.35, they are classified into three types depending on the direction of the principal axis of rotation. It should be noted, however, that these librational modes couple not only among themselves but also with internal modes of water (HOH bending) and other ions (SO_4^{2-}, NO_3^-, etc.) in the crystal. Tayal et al. [359] reviewed librational modes of water in hydrated solids.

The presence of the hydronium (H_3O^+) ion in crystalline acid hydrates is well established, and their spectra were discussed in Sec. 2.3.1 of Part A. The existence of the $H_5O_2^+$ ion was first detected by X-ray analysis [360]. Pavia and Giguère [361] further confirmed its presence in $HClO_4 \cdot 2H_2O$ (namely, $[H_5O_2]ClO_4$) by the absence of some characteristic bands of the H_3O^+ and H_2O species. Its structure is suggested to be centrosymmetric $H_2O-H-OH_2$ of approximately $\mathbf{C}_{2h}$ symmetry. Both X-ray [362] and neutron diffraction [363] studies suggest the presence of the $H_5O_2^+$ ion in *trans*-$[Co(en)_2Cl_2]Cl \cdot HCl \cdot 2H_2O$. Thus it should be formulated as *trans*-$[Co(en)_2Cl_2]Cl \cdot [H_5O_2]Cl$. The existence of the $H_7O_3^+$ ion in crystalline $HNO_3 \cdot 3H_2O$ and $HClO_4 \cdot 3H_2O$ was confirmed by infrared studies [364]. The spectra are consistent with a structure in which two of the hydrogens of the H_3O^+ ion are bonded to two H_2O molecules through short, asymmetric hydrogen bonds.

1.8.2. Aquo (H_2O) Complexes

In addition to the three fundamental modes of the free water molecule, coordinated water exhibits other modes, such as those shown in Fig. 1.33. Nakagawa and

TABLE 1.17. Observed Frequencies, Band Assignments, and MO Stretching Force Constants of Aquo Complexes [365]

Compound	$\rho_r(H_2O)$	$\rho_w(H_2O)$	ν(MO)	K(M−O)[a]
$[Cr(H_2O)_6]Cl_3$	800	541	490	1.31
$[Ni(H_2O)_6]SiF_6$	(755)[b]	645	405	0.84
$[Ni(D_2O)_6]SiF_6$	—	450	389	0.84
$[Mn(H_2O)_6]SiF_6$	(655)[c]	560	395	0.80
$[Fe(H_2O)_6]SiF_6$	—	575	389	0.76
$[Cu(H_2O)_4]SO_4 \cdot H_2O$	887, 855	535	440	0.67
$[Zn(H_2O)_6]SO_4 \cdot H_2O$	—	541	364	0.64
$[Zn(D_2O)_6]SO_4 \cdot D_2O$	467	392	358	0.64
$[Mg(H_2O)_6]SO4 \cdot H_2O$	—	460	310	0.32
$[Mg(D_2O)_6]SO_4 \cdot D_2O$	474	391	—	0.32

[a] UBF field (mdyn/Å).
[b] $Ni(H_2O)_4Cl_2$.
[c] $Mn(H_2O)_4Cl_2$.

Shimanouchi [365] carried out normal coordinate analyses on $[M(H_2O)_6]$- ($\mathbf{T}_h$, symmetry) and $[M(H_2O)_4]$-type ions (with $\mathbf{D}_{4h}$ symmetry) to assign these low-frequency modes. Table 1.17 lists the frequencies and band assignments, and Fig. 1.36 illustrates the far-infrared spectra of aquo complexes obtained by these authors. According to Stefov et al. [366], $[Cr(H_2O)_6]Cl_3$ exhibits the rocking (ρ_r), twisting (ρ_t), and wagging (ρ_w) modes of the coordinate water molecule at 825 (629), 575 (420),

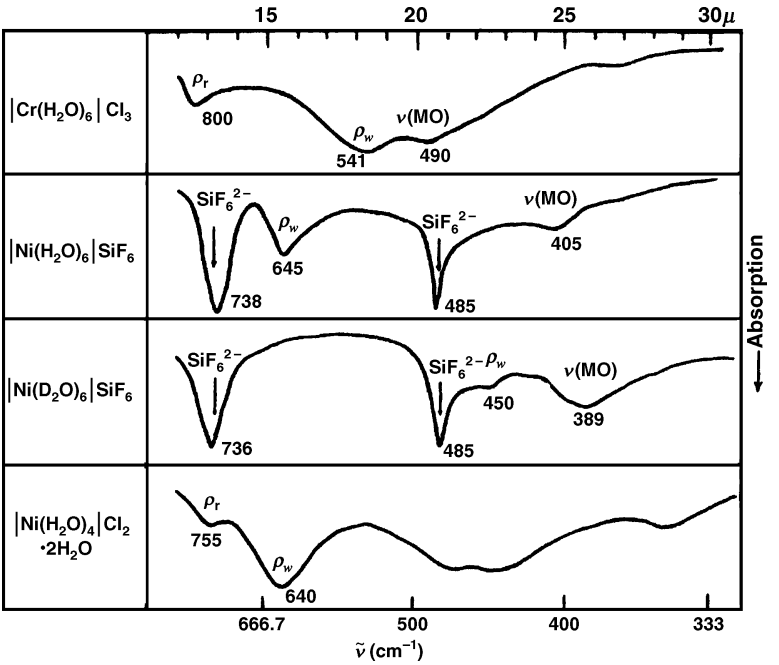

Fig. 1.36. *Infrared spectra of aquo complexes in the low-frequency region [365].*

and 500 (390) cm^{-1}, respectively, in IR spectrum (the number in the brackets indicates the frequency of the D_2O complex).

The MO_6 skeletal vibrations of the octahedral $[M(H_2O)_6]^{n+}$ ions have been assigned for M = Mg(II) [367], Cd(II) [368], Al(III) [369], and Ga(III) [370]. In $Cs_2[InBr_5(H_2O)]$, the ρ_r, ρ_w, and ν(In−O) were assigned at 520, 380, and 260 cm^{-1}, respectively [371]. In solid $K_2[FeCl_5(H_2O)]$, however, the frequency order of these bands is different; $600(\rho_w) > 460(\rho_t) > 390\ cm^{-1}$ [ν(Fe−O)] [372]. The ν(Co−O) of $[Co(NH_3)_5(H_2O)]Cl_3$ and $[Co(NH_3)_5(OH)]Cl_2$ are assigned at 502 and 531 cm^{-1}(respectively [373]. Complete vibrational analysis has been made for single crystals of $Ni(H_2O)_4Cl_2 \cdot 2H_2O$ and related Co(II) complex [374]. α-Alums such as $CsM(SO_4)_2 \cdot 12H_2O$ (M = Co or Ir) contain the $[M(H_2O)_6]^{3+}$ ions, and their single-crystal Raman spectra have been assigned by Best et al. [375]. An *ab initio* method has been employed to calculate vibrational frequencies of the $[Na(H_2O)_n]^+$ ion (n = l–4) [376].

Raman spectra of aqueous solutions of inorganic salts have been studied extensively. For example, Hester and Plane [377] observed polarized Raman bands in the 400–360 cm^{-1} region for the nitrates, sulfates, and perchlorates of Zn(II), Hg(II), and Mg(II), and assigned them to the MO stretching modes of the hexa-coordinated aquo complex ions. Kameda et al. [378] measured the Raman spectra of NaX (X = Cl,Br. ClO_4,NO_3) in concentrated (10 M%) aqueous solutions to determine the hydrated structure of the Na^+ ion. The polarized bands at 183–187 cm^{-1} were assigned to totally symmetric vibrations of the $Na^+(H_2O)_n$ ion because they are downshifted by ∼10 cm^{-1} in D_2O solution. The value of n was close to 4. In the case of concentrated LiBr solution, the totally symmetric vibration of the $Li(H_2O)_4^+$ ion and the ion-pair $[Li(H_2O)_4^+ - Br^-]$ vibration were assigned at 190 and 340 cm^{-1}, respectively [379].

Vibrational spectroscopy is very useful in elucidating the structures of aquo complexes. For example, $TiCl_3 \cdot 6H_2O$ should be formulated as *trans*-$[Ti(H_2O)_4Cl_2]Cl \cdot 2H_2O$ since it exhibits one TiO stretching (500 cm^{-1}, E_u) and one TiCl stretching (336 cm^{-1}, A_{2u}) mode [380]. Chang and Irish [381] showed from infrared and Raman studies that the structures of the tetrahydrates and dihydrates resulting from the dehydration of $Mg(NO_3)_2 \cdot 6H_2O$ are as follows:

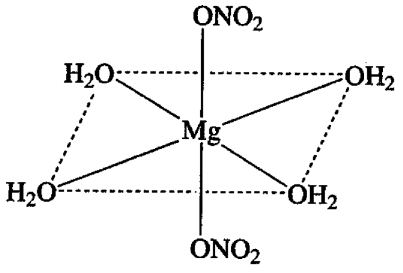

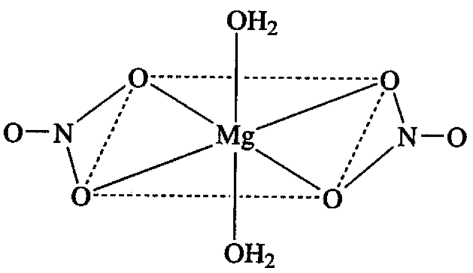

A number of hydrated inorganic salts have also been studied by the inelastic neutron scattering (INS) technique [382,383]. Since the proton scattering cross section is quite large, the INS spectrum reflects mainly the motion of the protons in the crystal. Furthermore, INS spectroscopy has no selection rules involving dipole moments or

polarizabilities. Thus, it serves as a complementary tool to vibrational spectroscopy in studying the hydrogen vibrations of hydrated salts.

1.8.3. Aquo Complexes in Inert Gas Matrices

Cocondensation reactions of alkali halide vapors with H_2O in Ar matrices (14 K) produce 1 : 1 adducts of a pyramidal structure ($\mathbf{C}_s$ symmetry):

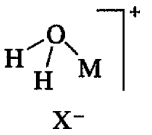

These aquo complexes exhibit two ν(OH) at 3300–3000 and two δ(OH) at 700–400 cm^{-1} in agreement with $\mathbf{C}_s$ symmetry [384]. Cocondensation reaction of Li vapor with H_2O in Kr matrices yields the 1 : 1 complex, Li(H_2O), which can be characterized by three internal modes of water [385]. Similar studies with alkaline-earth metal vapors show that the $\delta(H_2O)$ is downshifted by 15 cm^{-1} for Mg and 30 cm^{-1} for Ca, Sr, and Ba on complex formation [386].

As stated in Sec. 1.26.2 of Part A, the reaction of a laser-ablated metal atom with a molecule such as CO in inert gas matrices produces a mixtures of a variety of novel species. In the case of metal atom–H_2O reactions, assignments of IR frequencies and structures of reaction products were based on isotopic shifts (H/D and $^{16}O/^{18}O$) and DFT calculations. For example, the reaction of laser-ablated Th atom with H_2O in excess of Ar produced over 15 intriguing species [387]. Similar investigations were carried out with laser-ablated metal atoms such as Mn [388], Sc [389], Ti [390], Zr [390] and Hf [390].

1.8.4. Hydroxo (OH) Complexes

The spectra of hydroxo complexes are supposedly similar to those of the metal hydroxides discussed in Sec. 2.1 of Part A. The hydroxo group can be distinguished from the aquo group since the former lacks the HOH bending mode near 1600 cm^{-1}. Furthermore, the hydroxo complex exhibits the MOH bending mode below 1200 cm^{-1}. For example, this mode is at 1150 cm^{-1} for the $[Sn(OH)_6]^{2-}$ ion [391] and at ~1065 cm^{-1} for the $[Pt(OH)_6]^{2-}$ ion [392]. The $[P(OH)_4]^+$ ion exhibits ν(OH), δ_a(POH), and δ_s(POH) vibrations at 3379/3262, 1112, and 1017 cm^{-1}, respectively [393].

The OH group also forms a bridge between two metals. For example

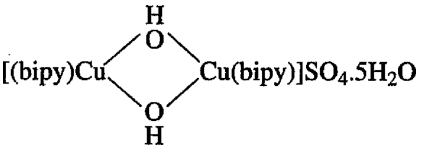

exhibits the bridging OH bending mode at 955 cm^{-1}; this is shifted to 710 cm^{-1} on deuteration [394]. For bridging hydroxo complexes of Pt(II), see Refs. [395] and [396].

The hydroperoxo ligand in the $[Cu(II)(bppa)(OOH^-)]^+$ ion [bppa = bis(6-pivalamide-2-pyridylmethyl)(2-pyridylmethyl)amine] exhibits ν(O−OH) vibration at 856 cm^{-1}, which is shifted to 810 cm^{-1} by $^{16}O/^{18}O$ substitution [397].

1.9. COMPLEXES OF ALKOXIDES, ALCOHOLS, ETHERS, KETONES, ALDEHYDES, ESTERS, AND CARBOXYLIC ACIDS

1.9.1. Complexes of Alkoxides and Alcohols

Metal alkoxides, $M(OR)_n$ (R: alkyl), exhibit ν(CO) at ~1000 cm^{-1} and ν(MO) at 600–300 cm^{-1} [398]. Infrared spectra have been reported for various alkoxides of Er(III) [399]. and isopropoxides of rare-earth metals [400]. Complete assignments of the IR and Raman spectra of $M(OCH_3)_6$ (M = Mo,W) and the $Sb(OCH_3)_6^-$ ion have been based on normal coordinate analysis ($\mathbf{C}_{3i}$, $\equiv \mathbf{S}_6$ symmetry). The $\nu(MO_6)$ and $\delta(MO_6)$ vibrations are at 600–450 and 400–200 cm^{-1}, respectively [401]. The ν(TiO) vibration of $TiCl_3(OCH_3)$ in Ar matrices was assigned at 636 cm^{-1} [402], and the ν(Fe−O) frequencies of $[Fe(III)(catecholato)]^{2-}$ were 583 and 283 cm^{-1} according to DFT calculations [403].

The infrared spectra of alcohol complexes, $[M(EtOH)_6]Y_2$, where M is a divalent metal and Y is ClO_4^-, BF_4^-, and NO_3^-, have been measured by van Leeuwen [404]. As expected, the anions have considerable influence on ν(OH) and δ(MOH). In ethylene glycol complexes with MX_2 (X = Cl,Br,I), ν(OH) are shifted to lower frequencies and δ(CCO) to higher frequencies relative to those of free ligand. It was shown that ethylene glycol serves as a bidentate chelating as well as a unidentate ligand, and that the *gauche* form prevails in the complexes [405]. Normal coordinate analyses have been carried out to assign the IR spectra of $[M(ROH)_6]X_2$ (M = Mg,Ca; R = CH_3, C_2H_5; and X = Cl,Br). The bands at 305 and 275 cm^{-1} of $Mg(CH_3OH)_6Br_2$ and its Ca analog are primarily the ν(M−O), and the corresponding force constants are 0.42 and 0.35 mdyn/Å, respectively [406].

1.9.2. Complexes of Ethers

The vibrational spectra of diethyl ether complexes with $MgBr_2$ and MgI_2 have been assigned completely [407]; ν(MgO), at 390–300 cm^{-1}. The solid-state Raman spectra of 1 : 1 and 1 : 2 adducts of 1,4-dioxane with metal halides show that the ligand is bridging between metals in the chair conformation [408].

When the oxygen atoms of the crown ether (l8-crown-6) coordinate to Ba(II) [409] and Sb(III) [410], the ν(COC) band near 1100 cm^{-1} is shifted by 14 and 30 cm^{-1}, respectively, to a lower frequency.

The ν(Ga−O) vibrations of the $[Ga(III)I_2(18\text{-crown-}6)]^+$ ion are located at 396 and 352 cm^{-1} [411]. In the case of $Ln(NCS)_3$ (13-crown-4)·$2H_2O$ (Ln = La, Pr, etc.), the redshift of the ν(COC) band is in the range of 76–64 cm^{-1}, and the ν(Ln−O) band

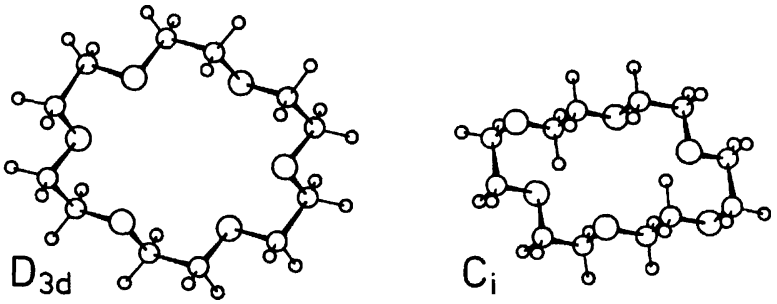

Fig. 1.37. *Two conformers of the 18-crown-6 ring [437].*

appears at 390–370 cm^{-1} [412]. According to X-ray analysis, the 18-crown-6 ring takes the $\mathbf{D}_{3d}$ structure in the K^+ complex and the $\mathbf{C}_i$ structure in the uncomplexed state (Fig. 1.37). Takeuchi et al. [413] assigned the IR/Raman spectra of these two compounds in the solid state via normal coordinate analysis, and elucidated the ring conformations of other metal complexes in methanol solution by comparing their Raman spectra with those of the known structures.

1.9.3. Complexes of Other Oxygen Donors

There are many coordination compounds with weakly coordinating ligands containing oxygen donors. These include ketones, aldehydes, esters, and some nitro compounds. Driessen and Groeneveld [414–416] and Driessen et al. [417] prepared metal complexes of these ligands (L) through the reaction

$$MCl_2 + 6L + 2FeCl_3 \xrightarrow[CH_3NO_2]{} [ML_6](FeCl_4)_2$$

in a moisture-free atmosphere; CH_3NO_2 was chosen as the solvent because it is the weakest ligand available. In acetone complexes, ν(C=O) are lower, and δ(CO), π(CO), and δ(CCC) are higher than those of free ligand [414]. Similar results have been obtained for complexes of acetophenone, chloracetone, and butanone [415]. In the $[Li(acetone)_4]^+$ ion, however, the ν(C=O), ν_a(CC), and ν_s(CC) all shift to higher frequencies on coordination to the Li ion [418].

In metal complexes of acetaldehyde, ν(C=O) are lower and δ(CCO) are higher than those of free ligand [416]. In ester complexes [417] ν(C=O) shifts to lower and ν(C−O) to higher frequencies by complex formation. When these shifts are dependent on the metal ions, the magnitudes of the shifts follow the well-known Irving–Williams order: Mn(II) < Fe(II) < Co(II) < Ni(II) < Cu(II) > Zn(II).

Formamide($HCONH_2$) coordinates to metal ions via the O atom, and the ν(M−O) vibrations appear in the 304–230 cm^{-1} range. In $NiCl_2(NMF)_4$ and $NiCl_2(DMF)_4$ (NMF = *N*-methylformamide; DMF = dimethylformamide), the Ni(II) ion is coordinated by the N as well as O atoms, and the ν(Ni−N) and ν(Ni−O) vibrations are observed at 500–480 and 420–380 cm^{-1}, respectively [419].

1.9.4. Complexes of Carboxylic Acids

Extensive infrared studies have been performed on metal complexes of carboxylic acids. Table 1.18 gives the infrared frequencies and band assignments for the formate and acetate ions obtained by Itoh and Bernstein [420]. The carboxylate ion may coordinate to a metal in one of the following modes:

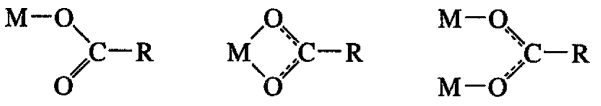

I II III

Deacon and Phillips [421] made careful examinations of IR spectra of many acetates and trifluoroacetates having known X-ray crystal structures, and arrived at the following conclusions:

(1) Unidentate complexes (structure I) exhibit Δ values $[\nu_a(CO_2^-) - \nu_s(CO_2^-)]$ that are much greater than the ionic complexes.
(2) Chelating (bidentate) complexes (structure II) exhibit Δ values that are significantly less than the ionic values.
(3) The Δ values for bridging complexes (structure III) are greater than those of chelating (bidentate) complexes, and close to the ionic values.

TABLE 1.18. Infrared Frequencies and Band Assignments for Formate and Acetate Ions (cm^{-1}) [420]

$[HCOO]^-$		$[CH_3COO]^-$			
Na Salt	Aqueous Solution	Na Salt	Aqueous Solution	C_{2v}	Band Assignment
2841	2803	2936	2935	A_1	ν(CH)
—	—	—	1344		$\delta(CH_3)$
1366	1351	1414	1413		ν_s(COO)
—	—	924	926		ν(CC)
772	760	646	650		δ(OCO)
—	—	—	—	A_2	$\rho_t(CH_3)$
—	—	2989	3010 or 2981	B_1	ν(CH)
1567	1585	1578	1556		ν_a(COO)
—	—	1430	1429		$\delta(CH_3)$
—	—	1009	1020		$\rho_r(CH_3)$
1377	1383	460	471		δ(CH) or ρ_r(COO)
—	—	2989	2981 or 3010	B_2	ν(CH)
—	—	1443	1456		$\delta(CH_3)$
—	—	1042	1052		$\rho_r(CH_3)$
1073	1069	615	621		π(CH) or π(COO)

The bridging 2-thiopheneacetate (taa) ligand in $[Cu(taa)_2(DMF)]_2$ exhibits the ν_a(COO) and ν_s(COO) at 1620 and 1284 cm^{-1}, respectively ($\Delta = 336\ cm^{-1}$) [422]. Assignments of IR and Raman spectra of dimeric $[Cu(OAc^-)_2(H_2O)]_2$ were based on $^{63}Cu/^{65}Cu$ isotopic shift data and DFT calculations. The ν(Cu−Cu) vibration was located at 178 cm^{-1} in Raman spectra [423]. In $[Mn_2(dmb)_4(bipy)_2(H_2O)_2](bipy)$, where dmb is 2.6-dimethylbenzoate, terminal and bridging dmb ligands are mixed; the terminal unidentate dmb exhibits the ν_a(COO) and ν_s(COO) at 1566 and 1404 cm^{-1}, respectively ($\Delta = 162\ cm^{-1}$), whereas the bridging, chelating dmb exhibits these vibrations at 1604 and 1358 cm^{-1}, respectively ($\Delta = 146\ cm^{-1}$) [424].

As seen in Table 1.19, these criteria hold except for asymmetric bidentates such as $Ph_2Sn(CH_3COO)_2$ where the two Sn−O bond distances are markedly different:

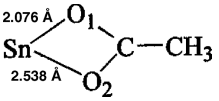

In these cases, Δ values are comparable to those of unidentate complexes [427]. Table 1.19 also shows three carboxylate complexes in which two modes of coordination are mixed. Figure 1.38 shows the Raman spectra of $Si(OAc)_4$ and $Ge(OAc)_4$ that contain only unidentate acetato ligands [426]. According to Stoilova et al., [435],

TABLE 1.19. Carboxyl Stretching Frequencies and Structures of Carboxylate Complexes (cm^{-1})

Compound	ν_a(COO)[a]	ν_s(COO)[a]	Δ	Structure	Ref.
$HCOO^-$	1567	1366	201	Ionic	420
CH_3COO^- (OAc^-)	1578	1414	164	Ionic	420
$Rh(OAc)(CO)(PPh_3)_2$	1604	1376	228	Unidentate	425
$Ru(OAc)(CO)_2(PPh_3)$	1613	1315	298	Unidentate	425
$Si(OAc)_4$	1745[b]	1290[b]	455	Unidentate	426
$Ge(OAc)_4$	1710[b]	1280[b]	430	Unidentate	426
$RuCl(OAc)(CO)(PPh_3)_2$	1507	1465	42	Bidentate	425
$RuH(OAc)(PPh_3)_2$	1526	1449	77	Bidentate	425
$Ph_2Sn(CH_3{-}COO)_2$	1610	1335	265	Asym. bidentate	427
$Ph_2Sn(CH_2Cl{-}COO)_2$	1620	1240	380	Asym. bidentate	427
$Ph_2Te(CCl_3{-}COO)_2$	1705	1270	435	Asym. bidentate	427
$Rh_2(OAc)_2(CO)_3(PPh_3)$	1580	1440	140	Bridging	428
$[Ru(CO)_2(C_2H_5COO)]_n$	1548	1410	138	Bridging	429
$[Cr_3O(OAc)_6(H_2O_3)]^+$	1621	1432	189	Bridging	430
$[Mn_2O_2(OAc)]^{2+}$	1548	1387	171	Bridging	431
$[Pd(OAc)_2(PPh_3)]_2$	1629	1314	315	Unidentate	432
	1580	1411	169	Bridging	
$CrO_2(OAc)_2$	1710	1240	470	Unidentate	433
	1610	1420	190	Bidentate	
$Cp_2Zr[Cr(CO)_3(RCOO)]_2$[c]	1641	1329	312	Unidentate	434
	1542	1377	165	Bidentate	

[a] These correspond to the ν(C=O) (free) and ν(C−O) (coordinated) of the unidenlate carboxylates, respectively.
[b] IR frequency.
[c] $R = C_6H_5$.

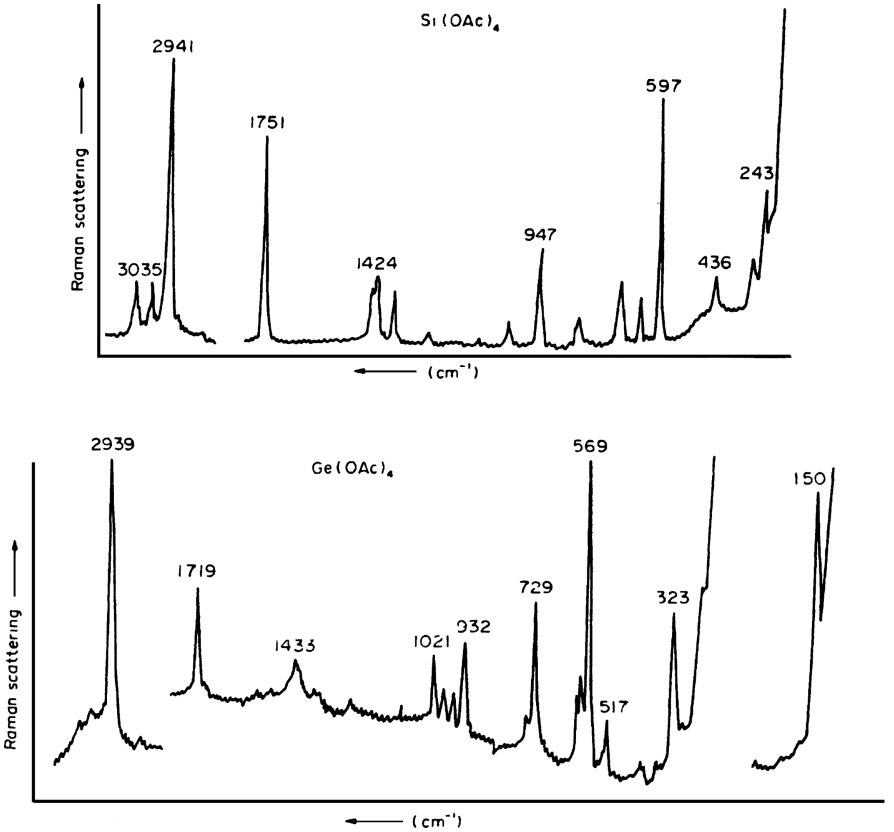

Fig. 1.38. *Raman spectra of $Si(OAc)_4$ and $Ge(OAc)_4$ in the solid state (514.5 nm excitation) [426].*

unidentate acetates exhibit three bands (COO deformation) at 920–720 cm^{-1} and a strong band [$\pi(CO_2)$] at 540 cm^{-1} that are absent in bridging complexes and reduced in number in bidentate complexes. Infrared spectra of formates have been reviewed by Busca and Lorenzelli. [436].

The linkage isomerism involving the acetate group has been reported by Baba and Kawaguchi [437]:

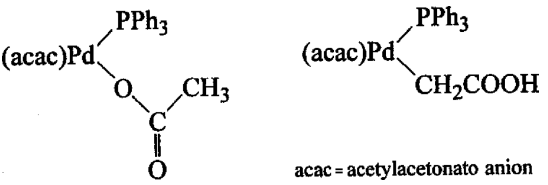

The O-isomer exhibits ν(C=O) at 1640 cm^{-1}, whereas the C-isomer shows ν(C=O) at 1670 and 1650 and ν(OH) at 2700–2500 cm^{-1}. It is also possible to

distinguish two acetato groups having different *trans* ligands by their frequencies:

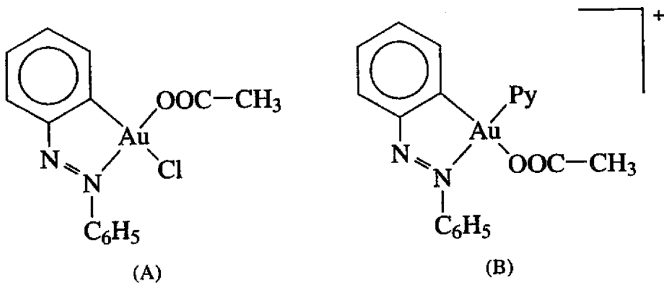

Complex A exhibits the ν_a(COO) and ν_s(COO) at 1665 and 1360 cm^{-1}, respectively, whereas complex B exhibits these vibrations at 1620 and 1300 cm^{-1}, respectively [438]. Assignments of the IR spectra of metal glycolato ($CH_2(OH)-COO^-$) complexes have been based on normal coordinate calculations [439].

Citric acid [$C(OH)(COOH)(CH_2COOH)_2$] contains one hydroxyl and three carboxylate groups. X-Ray analysis by Matzapetakis et al. [440] shows that the Mn(II) ion in $[Mn(II)(C_6H_5O_7)_2]^{4-}$ ion is octahedrally coordinated by two citrate ligands in which three carboxyl groups are deprotonated and the C−OH group is not ionized. Although the structure of the $[Mn(III)(C_6H_4O_7)_2]^{5-}$ ion is similar, the C−OH group is also deprotonated. The IR spectrum of the former complex exhibits the ν_a(COO) and ν_s(COO) at 1621–1588 and 1436–1386 cm^{-1}, respectively, while these vibrations are at 1636–1596 and 1441–1397 cm^{-1}, respectively, in the latter complex.

1.10. COMPLEXES OF AMINO ACIDS, EDTA, AND RELATED LIGANDS

1.10.1. Complexes of Amino Acids

Amino acids exist as zwitterions in the crystalline state. Table 1.20 lists band assignments for the zwitterions of glycine [441] and α-alanine [442]. According to X-ray analysis, two glycino anions (gly) in $[Ni(gly)_2]\cdot 2H_2O$, [443], for example, coordinate to the metal by forming a *trans*-planar structure, and the noncoordinating C=O groups are hydrogen-bonded to the neighboring

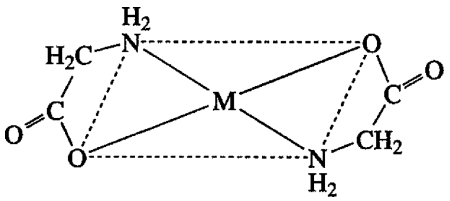

molecule or water of crystallization, or weakly bonded to the metal of the neighboring complex. Thus $\nu(CO_2)$ of amino acid complexes are affected by coordination as well as by intermolecular interactions.

TABLE 1.20. Infrared Frequencies and Band Assignments of Glycine and α-Alanine in the Crystalline State (cm^{-1}) [441,442]

Glycine	α-Alanine	Band Assignment
1610	1597	$\nu_a(COO^-)$
1585	1623	$\delta_d(NH_3^+)$
1492	1534	$\delta_s(NH_3^+)$
—	1455	$\delta_d(CH_3)$
1445	—	$\delta(CH_2)$
1413	1412	$\nu_s(COO^-)$
—	1355	$\delta_s(CH_3)$
1333	—	$\rho_w(CH_2)$
—	1308	$\delta(CH)$
1240 (R)	—	$\rho_t(CH_2)$
1131, 1110	1237, 1113	$\nu_r(NH_3^+)^a$
1003	1148	$\nu_a(CCN)^a$
—	1026, 1015	$\rho_r(CH_3)^a$
910	—	$\rho_r(CH_2)$
893	918, 852	$\nu_s(CCN)^a$
694	648	$\rho_w(COO^-)$
607	771	$\delta(COO^-)$
516	492	$\rho_t(NH_3^+)$
504	540	$\rho_r(COO^-)$

[a] These bands are coupled with other modes in α-alanine.

To examine the effects of coordination and hydrogen bonding, Nakamoto et al. [444] performed extensive IR measurements of the COO stretching frequencies of various metal complexes of amino acids in D_2O solution, in the hydrated crystalline state, and in the anhydrous crystalline state. The results showed that, in any one physical state, the same frequency order is found for a series of metals, regardless of the nature of the ligand. The antisymmetric frequencies increase, the symmetric frequencies decrease, and the separation between the two frequencies increases in the following order of metals:

$$\text{Ni(II)} < \text{Zn(II)} < \text{Cu(II)} < \text{Co(II)} < \text{Pd(II)} \approx \text{Pt(II)} < \text{Cr(III)}$$

Although there are several exceptions to this order, these results generally indicate that the effect of coordination is still the major factor in determining the frequency order in a given physical state. The frequency order shown above indicates the increasing order of the metal–oxygen interaction since the COO group becomes more asymmetrical as the metal–oxygen interaction becomes stronger.

To give theoretical band assignments on metal glycino complexes, Condrate and Nakamoto [445] carried out a normal coordinate analysis on the metal–glycino chelate ring. Figure 1.39 shows the infrared spectra of bis(glycino) complexes of Pt(II), Pd(II), Cu(II), and Ni(II). Table 1.21 lists the observed frequencies and theoretical band assignments. The CH_2 group frequencies are not listed, since they

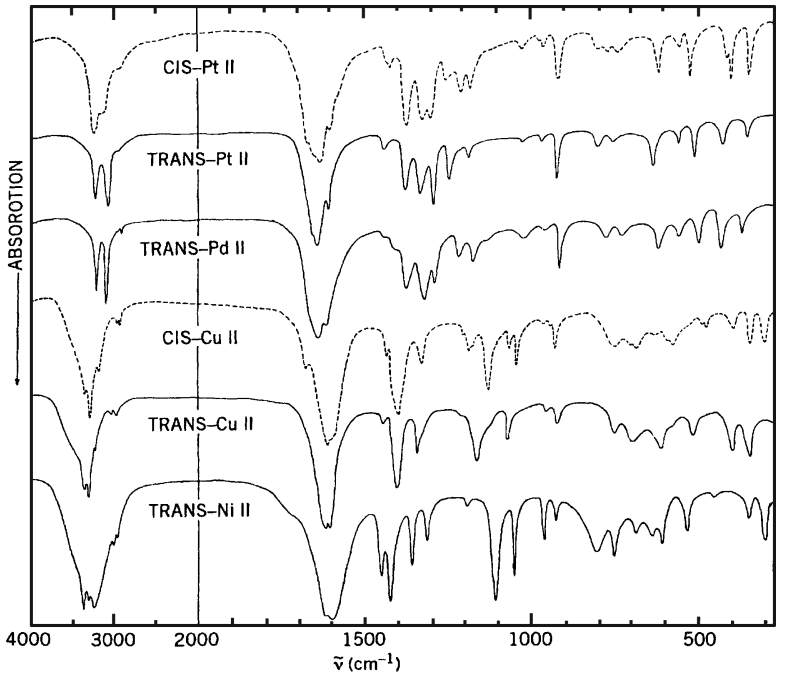

Fig. 1.39. *Infrared spectra of cis- or trans-bis(glycino) complexes of Pt(II), Pd(II), Cu(II), and Ni(II) [445].*

TABLE 1.21. Observed Frequencies and Band Assignments of Bis(glycino) Complexes (cm^{-1}) [445]

trans-[Pt(gly)$_2$]	*trans*-[Pd(gly)^2]	*trans*-[Cu(gly)$_2$]	*trans*-[Ni(gly)$_2$]	Band Assignment
3230 3090	3230 3120	3320 3260	3340 3280	$\nu(NH_2)$
1643	1642	1593	1589	$\nu(C{=}O)$
1610	1616	1608	1610	$\delta(NH_2)$
1374	1374	1392	1411	$\nu(C{-}O)$
1245	1218	1151	1095	$\rho_t(NH_2)$
1023	1025	1058	1038	$\rho_w(NH_2)$
792	771	644	630	$\rho_r(NH_2)$
745	727	736	737	$\delta(C{=}O)$
620	610	592	596	$\pi(C{=}O)$
549	550	481	439	$\nu(MN)$
415	420	333	290	$\nu(MO)$
2.10	2.00	0.90	0.70	$K(M{-}N)(mdyn/Å)^a$
2.10	2.00	0.90	0.70	$K(M{-}O)(mdyn/Å)^a$

[a]UBF.

are not metal-sensitive. It is seen that the C=O stretching, NH_2 rocking, and MN and MO stretching bands are metal-sensitive and are shifted progressively to higher frequencies as the metal is changed in the order Ni(II) < Cu(II) < Pd(II) < Pt(II). Table 1.21 shows that both the MN and MO stretching force constants also increase in the same order of the metals. These results provide further support to the preceding discussion of the M−O bonds of glycino complexes.

To give definitive band assignments in the low-frequency region of bis(glycino) complexes of Ni(II), Cu(II), and Co(II), Kincaid and Nakamoto [446] carried out H−D, $^{14}N - {}^{15}N$, $^{58}Ni - {}^{62}Ni$, and $^{63}Cu - {}^{65}Cu$ substitutions, and performed normal coordinate analyses on the skeletal modes of bis(glycino) complexes. Their results show that, in *trans*-$[M(gly)_2]\cdot 2H_2O$, the infrared-active ν(MN) and ν(MO) are at 483 and 337 cm^{-1}, respectively, for the Cu(II) complex, and at 442 and 289 cm^{-1}, respectively, for the Ni(II) complex. Both modes are coupled strongly with other skeletal modes, however. Use of multiple isotope labeling techniques in assigning IR spectra of amino acid complexes has been extended to $[Cd(gly)_2]\cdot H_2O$ [447], *cis*-$[Ni(gly)_2(ImH)_2]$ [448], and $[M(L\text{–}Ala)_2]$ [M = Ni(II),Cu(II)] [449].

Square–planar bis(glycino) complexes can assume the *cis* or the *trans* configuration. As expected from symmetry consideration, the *cis*-isomer exhibits more bands in infrared spectra than does the *trans*-isomer (see Fig. 1.39). In the low-frequency region, the *cis*-isomer exhibits two ν(MN) and two ν(MO), whereas the *trans*-isomer exhibits only one for each of these modes [445]. This criterion has been used by Herlinger et al. to assign the geometry of a series of bis(aminoacidato)Cu(II) complexes [450,451]. Octahedral tris(glycino) complexes may take the *fac* and *mer* configurations shown in Fig. 1.40. For example, $[Co(gly)_3]$ exists in two forms: purple crystals (dihydrate, α-form) and red crystals (mono-hydrate, β-form). The α-form is assigned to the *mer* configuration since it exhibits more infrared bands than does the β-form (*fac* configuration) [452].

Glycine also coordinates to the Pt(II) atom as a unidentate ligand:

The carboxyl group is not ionized in *trans*-$[Pt(glyH)_2X_2]$ (X = a halogen), whereas it is ionized in *trans*-$[Pt(gly)_2(NH_3)_2]$. The former exhibits the un-ionized COO stretching band near 1710 cm^{-1}, while the latter shows the ionized COO stretching band near 1610 cm^{-1} [453].

The distinction between unidentate and bidentate glycino complexes of Pt(II) can be made readily from their infrared spectra. Figure 1.41 illustrates the infrared spectra of *trans*-$[Pt(glyH)_2Cl_2]$ and $K[Pt(gly)Cl_2]$ in the COO stretching and PtO stretching regions. The bidentate (chelated) glycino group absorbs at 1643 cm^{-1}, unlike either the ionized unidentate group (1610 cm^{-1}) or the un-ionized unidentate group (1708 cm^{-1}). Furthermore, the bidentate glycino group exhibits the PtO stretching band at 388 cm^{-1}, whereas the unidentate glycino group has no absorption between

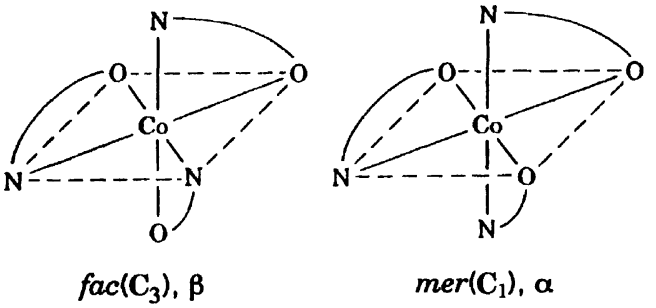

Fig. 1.40. Structures of fac- and mer-tris(glycino) complexes.

470 and 350 cm^{-1}. Figure 1.41 also shows the spectrum of [Pt(gly)(glyH)Cl], in which both the unidentate and bidentate glycino groups are present. It is seen that the spectrum of this compound can be interpreted as a superposition of the spectra of the former two compounds [453].

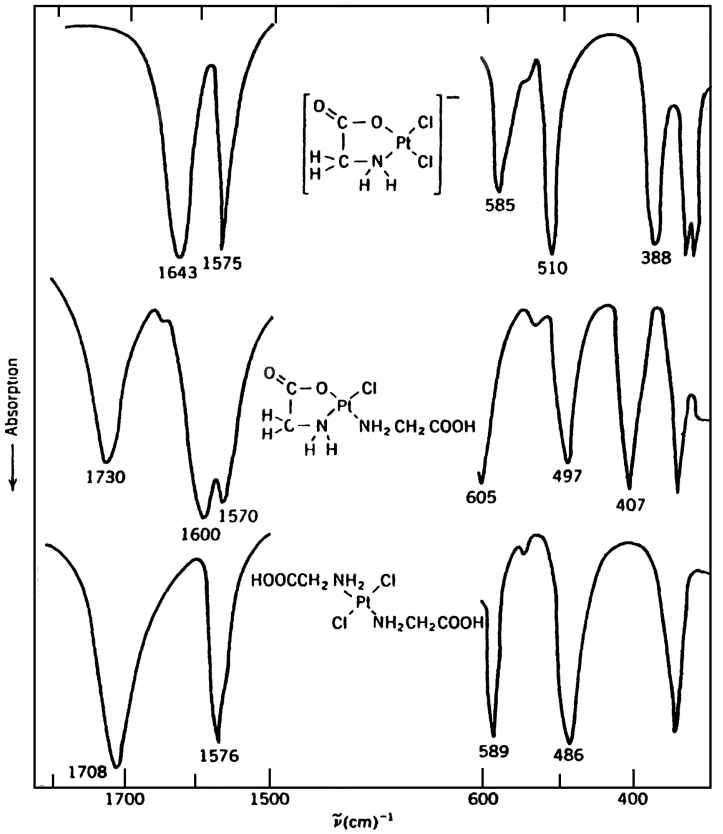

Fig. 1.41. IR spectra of K[Pt(gly)Cl2], [Pt(gly)(glyH)Cl], and trans-[Pt(glyH)2Cl2] [453].

The Cu(III) complexes of tetraglycine and tetraglycineamide exhibit the N(amide)–Cu(III) CT absorption at 365 nm. Using the 363.8 nm excitation, Kincaid et al. [454] were able to resonance-enhance the ν(Cu−N) vibrations at 420 and 417 cm^{-1}, respectively.

Metal complexes with *N*-methylglycine (sarcosine) and *N*-phenylglycine, of the $ML_2.nH_2O$ type, take the chelate ring structures similar to those of the glycine complexes, and their IR spectra have been assigned by Inomata et al. [455] on the basis of normal coordinate calculations. These ligands also form metal complexes of the type $CoCl_2(HL)\cdot 2H_2O$ and $MCl_2(HL)$ (M = Zn, Cd) in which the zwitterion of the amino acid is coordinated to the metal via the carboxyl oxygen atom [455].

Drożdżewski et al. [456–459] assigned the metal–nitrogen stretching vibrations of histamine (hm) complexes on the basis of isotope shifts (H/D and metal isotopes) and DFT calculations. Histamine forms a chelate ring via its NH_2 group and imidazole (Im) nitrogen:

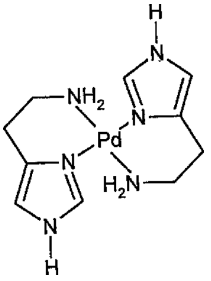

Table 1.22 lists the ν(M−NH_2) and ν[M−N(Im)] frequencies of the Ni(II), Cu(II), and Pd(II) complexes in IR spectra.

1.10.2. Complexes of EDTA and Related Ligands

From the infrared spectra observed in the solid state, Busch and coworkers [460] determined the coordination numbers of the metals in metal chelate compounds of EDTA and its derivatives:

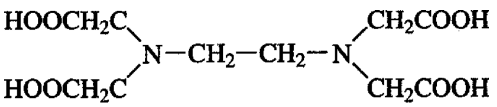

Ethylenediaminetetraacetic acid
(EDTA) or (H_4Y)

This method is based on the simple rule that the un-ionized and uncoordinated COO stretching band occurs at 1750–1700 cm^{-1}, whereas the ionized and coordinated

TABLE 1.22. Metal-Nitrogen Stretching Frequencies (cm^{-1}) of Histamine Complexes[a]

Compound	Metal Isotopes	ν(M-NH_2)	ν(M-N(Im))	Ref.
[Ni(hm)Cl_2] $2H_2O$	$^{58}Ni/^{62}Ni$	423(2.5)	266(3.5) 249(2.0)	456
[Cu(hm)Cl_2]	$^{62}Cu/^{65}Cu$	417(1.0)	285(1.5) 270(3.5)	457
[Pd(hm)$_2$]Cl_2	^{104}Pd ^{110}Pd	464(2.0)	311(4.5)	458,459

[a]Numbers in parentheses indicate the magnitude of metal isotope shift.

COO stretching band is at 1650–1590 cm^{-1}. The latter frequency depends on the nature of the metal: 1650–1620 cm^{-1} for metals such as Cr(III) and Co(III), and 1610–1590 cm^{-1} for metals such as Cu(II) and Zn(II). Since the free ionized COO^- stretching band is at 1630–1575 cm^{-1}, it is also possible to distinguish the coordinated and free COO^- stretching bands if a metal such as Co(III) is chosen for complex formation.

Table 1.23 summarizes the ν_a(COO) of the un-ionized COOH, coordinated COO^-, and free COO^- groups of EDTA complexes. Faulques et al. [462] obtained the IR/Raman spectra of $[Co(H_2O)(H_2Y)]\cdot 2H_2O$ and $[Co(H_2O)_6][Co(H_2O)(HY)]_2\cdot 2H_2O$ by microspectroscopy.

TABLE 1.23. Antisymmetric COO Stretching Frequencies and Number of Functional Groups Used for Coordination in EDTA Complexes (cm^{-1}) [460,461]

Compound[a]	Un-ionized COOH	Coordinated $COO^-\cdots M$	Free COO^-	Number of Coordinated Groups
$H_4[Y]$	1698[b]	—	—	
$Na_2[H_2Y]$	1668[b]	—	1637[b]	
$Na_4[Y]$	—	—	1597[b]	
$Ba[Co(Y)]_2\cdot 4H_2O$	—	1638	—	6
$Na_2[Co(Y)Cl]$	—	1648	1600	5
$Na_2[Co(Y)NO_2]$	—	1650	1604	5
$Na[Co(HY)Cl]\cdot\frac{1}{2}H_2O$	1750	1650	—	5
$Na[Co(HY)NO_2]\cdot H_2O$	1745	1650	—	5
$Ba[Co(HY)Br]\cdot 9H_2O$	1723	1628	—	5
$Na[Co(YOH)Cl]\cdot\frac{3}{2}H_2O$	—	1658	—	5
$Na[Co(YOH)Br]\cdot H_2O$	—	1654	—	5
$Na[Co(YOH)NO_2]$	—	1652	—	5
$[Pd(H_2Y)]\cdot 3H_2O$	1740	1625	—	4
$[Pt(H_2Y)]\cdot 3H_2O$	1730	1635	—	4
$[Pd(H_4Y)Cl_2]\cdot 5H_2O$	1707, 1730	—	—	2
$[Pt(H_4Y)Cl_2]\cdot 5H_2O$	1715, 1530	—	—	2

[a]Y = tetranegative ion; HY = trinegative ion; H_2 Y = dinegative ion; H_4Y = neutral species of EDTA; YOH = trinegative ion of HEDTA (hydroxyethylenediaminetriacetic add).
[b]Reference 461.

Tomita and Ueno [463] studied the infrared spectra of metal complexes of NTA, using the method described above. They concluded that NTA

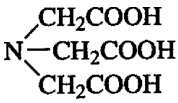

Nitrilotriacetic acid (NTA)

acts as a quadridentate ligand in complexes of Cu(II), Ni(II), Co(II), Zn(II), Cd(II), and Pb(II), and as a tridentate in complexes of Ca(II), Mg(II), Sr(II), and Ba(II).

Krishnan and Plane [464] studied the Raman spectra of EDTA and its metal complexes in aqueous solution. They noted that ν(MN) appears strongly in the 500–400 cm^{-1} region for Cu(II), Zn(II), Cd(II), Hg(II), and so on, and that its frequency decreases with an increasing radius of the metal ion, independently of the stability of the metal complex. McConnell and Nuttall [465] assigned the ν(MN) and ν(MO) of $Na_2[M(EDTA)]2H_2O$ (M = Sn, Pb) in their Raman and infrared spectra.

1.11. INFRARED SPECTRA OF AQUEOUS SOLUTIONS

Since water is a weak Raman scatterer, Raman spectra of samples in aqueous solution can be measured without major interference from water vibrations. On the other hand, infrared spectroscopy of aqueous solution suffers from strong absorption of bulk water that interferes with IR absorption of the sample. Even so, it is sometimes necessary to measure aqueous IR spectra because some vibrations are inherently weak in Raman spectra.

To measure IR spectra of aqueous solution, it is common to use very thin layers (0.01–0.05 mm thick) of solutions of relatively high concentrations (5–20%) which are sandwiched between two plates of water-insoluble crystals such as CaF_2 and KRS-5 (TlBr/TlI). Figure 1.42 displays the IR spectra of H_2O and D_2O obtained by

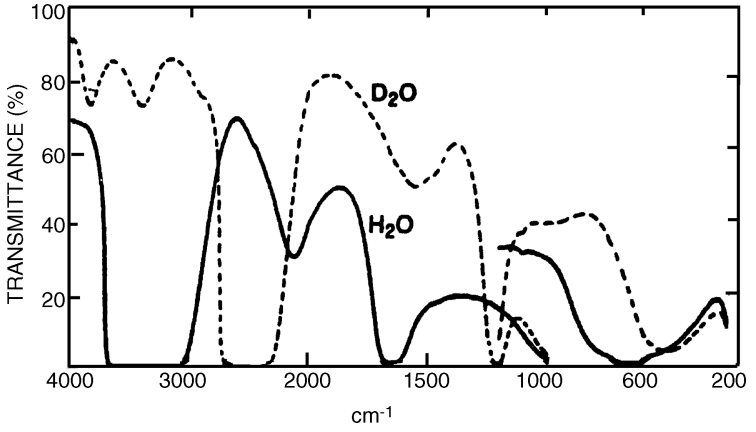

Fig. 1.42. *Infrared spectra of H_2O versus air and D_2O versus air [466].*

using a CaF_2 cell (4000–1000 cm^{-1}, 0.03 mm thick) and a KRS-5 cell (1200–250 cm^{-1}, 0.015 mm thick), showing that at least two regions, 2800–1800 and 1500–950 cm^{-1} are relatively free from H_2O absorption. These spectral "window" regions can be shifted to 2150–1250 and 1100–750 cm^{-1}, respectively, in D_2O [466]. The combination of a more recently developed cylindrical internal reflection (CIR) cell [467] with a FTIR spectrometer may be best suited to IR studies of aqueous solution [468]. The following examples demonstrate the utility of aqueous IR spectroscopy in elucidating the structures of complex ions in solution equilibria.

The C≡N stretching band (2200–2000 cm^{-1}) can be measured in aqueous solution since it is in the "window" region. Thus, the solution equilibria of cyano complexes have been studied extensively by using aqueous infrared spectroscopy (Sec. 1.16). Fronaeus and Larsson [469] extended similar studies to thiocyanato complexes that exhibit the C≡N stretching bands in the same region. They [470] also studied the solution equilibria of oxalato complexes in the 1500–1200 cm^{-1} region, where the CO stretching bands of the coordinated oxalato group appear. Larsson [471] studied the infrared spectra of metal glycolato complexes in aqueous solution. In this case, the C−OH stretching band near 1060 cm^{-1} was used to elucidate the structures of the complex ions in equilibria.

The COO stretching bands of NTA, EDTA, and their metal complexes appear between 1750 and 1550 cm^{-1} (Sec. 1.10). As stated above, this region is free from D_2O absorption. Nakamoto et al. [472], therefore, studied the solution (D_2O) equilibria of NTA, EDTA, and related ligands in this frequency region. By combining the results of potentiometric studies with the spectra obtained as a function of the pH (pD) of the solution, it was possible to establish the following COO stretching frequencies:

Type A Un-ionized carboxyl (R_2N-CH_2COOH), 1730–1700 cm^{-1}
Type B α-Ammonium carboxylate ($R_2N^+H-CH_2COO^-$), 1630–1620 cm^{-1}
Type C α-Aminocarboxylate ($R_2N-CH_2COO^-$), 1585–1575 cm^{-1}

As stated in Sec. 1.10, the coordinated (ionized) COO group absorbs at 1650–1620 cm^{-1} for Cr(III) and Co(III), and at 1610–1590 cm^{-1} for Cu(II) and Zn(II). Thus it is possible to distinguish the coordinated COO group from those of types B and C if a proper metal ion is selected.

Tomita et al. [473] studied the complex formation of NTA with Mg(II) by aqueous infrared spectroscopy. Figure 1.43 shows the infrared spectra of equimolar mixtures of NTA and $MgCl_2$ at concentrations of ∼5–10% by weight. The spectra of the mixture from pD 3.2 to 4.2 exhibit a single band at 1625 cm^{-1}, which is identical to that of the free $H(NTA)^{2-}$ ion in the same pD range [474]. This result indicates that no complex formation occurs in this pD range, and that the 1625 cm^{-1} band is due to the $H(NTA)^{2-}$ ion (type B). If the pD is raised to 4.2, a new band appears at 1610 cm^{-1}, which is not observed for the free NTA solution over the entire pD range investigated. Figure 1.43 shows that this 1610 cm^{-1} band becomes stronger, and the 1625 cm^{-1} band becomes weaker, as the pD increases. It was concluded that this change is due mainly to a shift of the following equilibrium in the direction of complex formation:

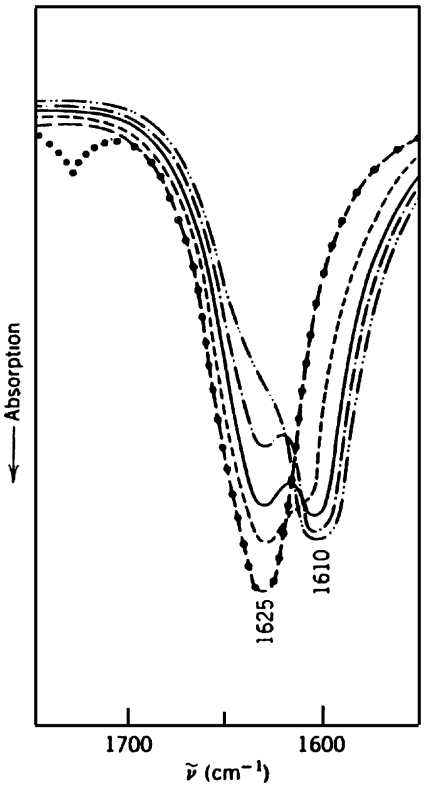

Fig. 1.43. *Infrared spectra of Mg-NTA complex in D_2O solutions: (●●●●) pD 3.2; (– – – –) pD 4.2; (– – –) pD 5.5; (—) pD 6.8; (–•–•–), pD 10.0; (–••–••–), pD 11.6 [473].*

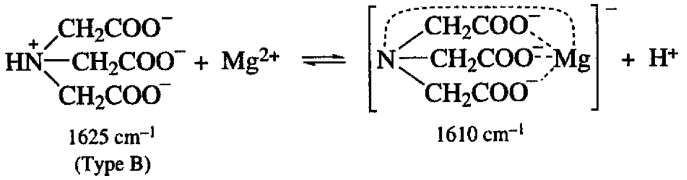

By plotting the intensity of these two bands as a function of pD, the stability constant of the complex ion was calculated to be 5.24. This value is in good agreement with that obtained from potentiometric titration (5.41).

Martell and Kim [475–478] carried out an extensive study on solution equilibria involving the formation of Cu(II) complexes with various polypeptides. As an example, the glycylglycino–Cu(II) system is discussed below [476]. Figure 1.44 illustrates the infrared spectra of free glycylglycine in D_2O solution as a function of

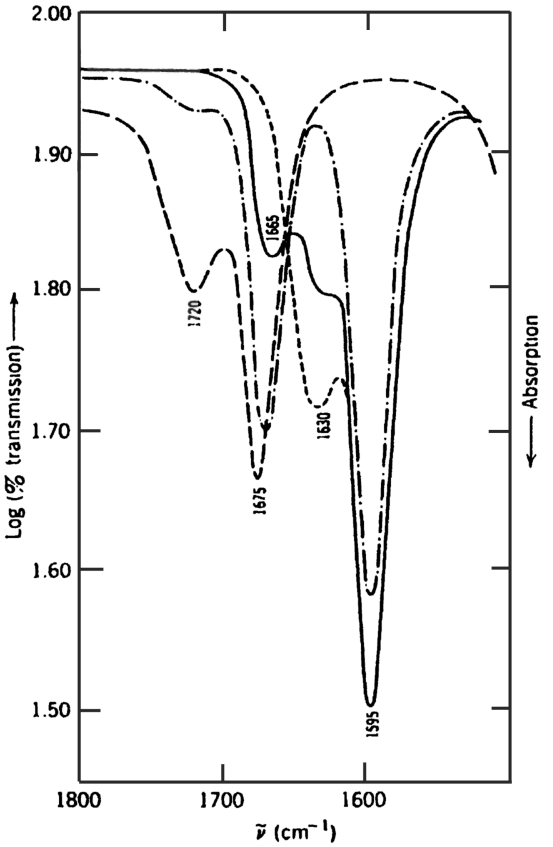

Fig. 1.44. *Infrared spectra of glycylglycine in D_2O solutions: (– – – –) pD 1.75; (–•–•–) pD 4.31; (—) pD 8.77; (– – – – –) pD 10.29 [476].*

pD. The observed spectral changes were interpreted in terms of the solution equilibria shown below:

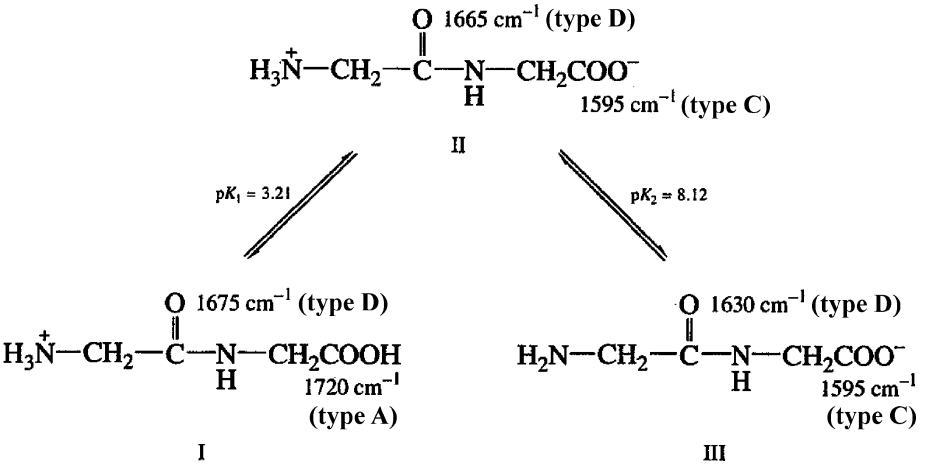

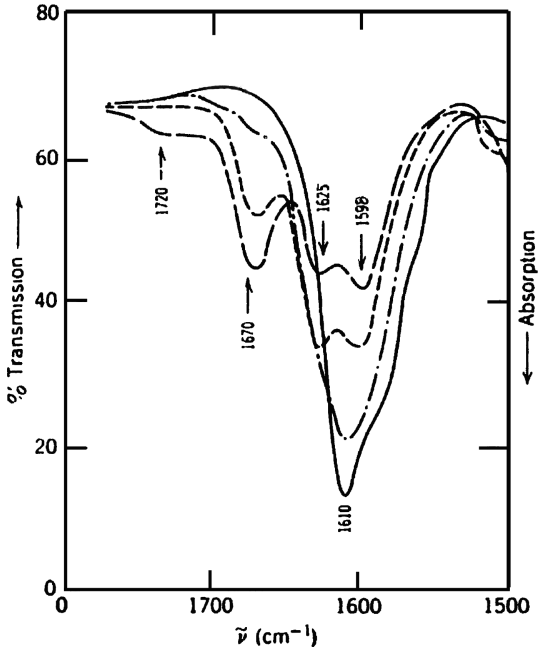

Fig. 1.45. *Infrared spectra of Cu(II)-glycylglycino complexes in D_2O solutions: (——) pD 3.58; (– – – – –) pD 4.24; (–•–•–) pD 5.18; (—) pD 10.65 [477].*

Band assignments have been made by using the criteria given previously. In addition, Type D frequency (1680–1610 cm^{-1}) was introduced to denote the peptide carbonyl group. The exact frequency of this group depends on the nature of the neighboring groups.

Figure 1.45 shows the infrared spectra of glycylglycine mixed with copper chloride at equimolar ratio in D_2O solution [477]. At pD = 3.58, the ligand exhibits three bands at 1720, 1675, and 1595 cm^{-1} (Fig. 1.44). This result indicates that I and II are in equilibrium. At the same pD value, however, the mixture exhibits one extra band at 1625 cm^{-1}. This band was attributed to the metal complex (IV), which was formed by the following reaction:

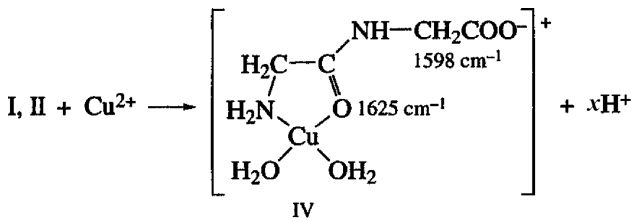

IV

At pD = 5.18, the solution exhibits one broad band at ~1610 cm^{-1}. This result was interpreted as an indication that the following equilibrium was shifted almost

completely to the right side, and that the 1610-cm^{-1} band is an overlap of two bands at 1610 and 1598 cm^{-1}:

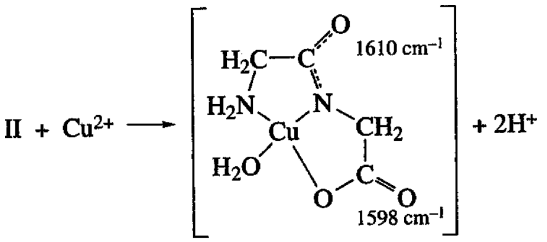

V

The shift of the peptide carbonyl stretching band from 1625 (IV) to 1610 (V) cm^{-1} may indicate the ionization of the peptide NH hydrogen, since such an ionization results in the resonance of the O−C−N system, as indicated by the dotted line in structure V. Kim and Martell [478] also studied the triglycine and tetraglycine Cu(II) systems. Later, Tasumi et al. [479] carried out similar studies in a wider frequency range (1800–1200 cm^{-1}). Kruck and Sarker [480] studied the equilibria of the Cu(II)-L-histidine system in D_2O.

1.12. COMPLEXES OF OXALATO AND RELATED LIGANDS

1.12.1. Oxalato Complexes

The oxalato anion (ox^{2-}) coordinates to a metal as a unidentate (I) or bidentate (II) ligand:

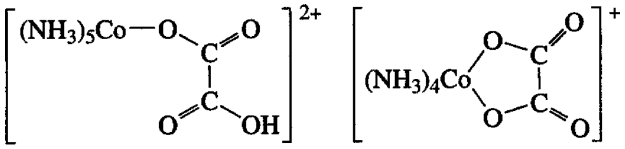

I II

The bidentate chelate structure (II) is most common. Fujita et al. [481] carried out normal coordinate analyses on the 1 : 1 (metal–ligand) model of the $[M(ox)_2]^{2-}$ and $[M(ox)_3]^{3-}$ series, and obtained the band assignments listed in Table 1.24. In the divalent metal series, ν(C=O) (average of ν_1 and ν_7) becomes higher, and $\nu(C-O)$ (ν_2 and ν_8) becomes lower, as ν_4(MO) becomes higher in the order Zn(II) < Cu(II) < Pd(II) < Pt(II) (see Fig. 1.46). This relation holds despite the fact that ν_2, ν_4, and ν_8 are all coupled with other vibrations.

In the trivalent metal series, Hancock and Thornton [482] found that ν_{11} (MO stretching) follows the same trend as the crystal field stabilization energies (CFSE) of these metals, namely:

TABLE 1.24. Frequencies and Band Assignments of Chelating Oxalato Complexes (cm^{-1}) [481]

$K_2[Zn(ox)_2]\cdot 2H_2O$	$K_2[Cu(ox)_2]\cdot 2H_2O$	$K_2[Pd(ox)_2]\cdot 2H_2O$	$K_2[Pt(ox)_2]\cdot 3H_2O$	$K_3[Fe(ox)_3]\cdot 3H_2O$	$K_3[V(ox)_3]\cdot 3H_2O$	$K_3[Cr(ox)_3]\cdot 3H_2O$	$K_3[Co(ox)_3]\cdot 3H_3O$	$K_3[Al(ox)_3]\cdot 3H_2O$	$[Cr(NH_3)_4(ox)]\cdot Cl$	Band Assignment	
1632	(1720) 1672	1698	1709	1712	1708	1708	1707	1722	1704	ν_a(C=O)	ν_7
—	1645	1675, 1657	1674	1677, 1649	1675, 1642	1684, 1660	1670	1700, 1683	1668	ν_a(C=O)	ν_1
1433	1411	1394	1388	1390	1390	1387	1398	1405	1393	ν_s(CO) + ν(CC)	ν_2
1302	1277	1245 (1228)	1236	1270, 1255	1261	1253	1254	1292, 1269	1258	ν_s(CO) + δ(O−C=O)	ν_8
890	886	893	900	885	893	893	900	904	914, 890	ν_s(CO) + δ(O−C=O)	ν_3
785	795	818	825	797, 785	807, 797	810, 798	822, 803	820, 803	804	δ(O−C=O) + ν(MO)	ν_9
622	593	610	—	580	581	595	—	—	—	Crystal water?	
519	541	556	575, 559	528	531	543	565	587	545	ν(MO) + ν(CC)	ν_4
519	481	469	469	498	497	485	472	436	486,469	Ring. def. + δ(O−C=O)	ν_{10}
428, 419	420	417	405	366	368	415	446	485	366	ν(MO) + ring def.	ν_{11}
377, 364	382, 370	368	370	340	336	358	364	364	347	δ(O−C=O) + ν(CC)	ν_5
291	339	350	328	—	—	313	332	—	328	π	

	Sc d^0		V d^2		Cr d^3		Mn d^4		Fe d^5		Co d^6		Ga d^{10}
ν(MO) $(cm)^{-1}$	340	<	367	<	416	>	372	>	354	<	446	>	368
CFSE $(10^3\,cm^{-1})$	0	<	10.2	<	21.2	>	10.2	>	0	<	27.0	>	0

Both quantities are maximized at the d^3 and d^6 configurations (d^4 and d^5 ions are in high-spin states). The IR spectra of $[Ir(ox)Cl_4]^{3-}$ ($\mathbf{C}_{2v}$), $[Ir(ox)_2Cl_2]^{3-}$ (*trans*, $\mathbf{D}_{2h}$; *cis*, $\mathbf{C}_2$), and $[Ir(ox)_3]^{3-}$ ($\mathbf{D}_3$) have been assigned by Gouteron [483]. The IR and Raman spectra of the $[Co(ox)_2]^{2-}$ ($\mathbf{D}_{2h}$) [484] and $[Os(ox)X_4]^{2-}$ (X = Cl,Br,I) ($\mathbf{C}_{2v}$) ions have been assigned [485]. Vibrational spectra of bidentate chelating oxalato complexes were also assigned for $[Os(ox)Cl_4]^{2-}$ [486], $[Pt(ox)X_2]^{2-}$ [487] and *trans*-{$Pt(ox)_2X_2]^{4-}$ (X = a halogen)) [488]. DFT calculations were made for $[Fe(III)(ox)_3]^{3-}$ and $[Fe(0)(ox)]^{2-}$ [489].

The oxalato anion may act as a bridging group between metal atoms. According to Scott et al. [490], the oxalato anion can take the following four bridging structures:

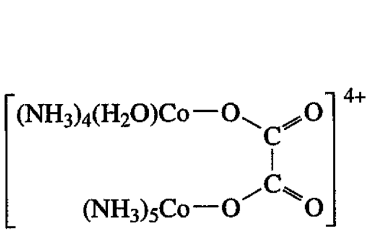

III

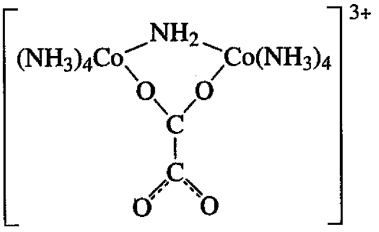

IV

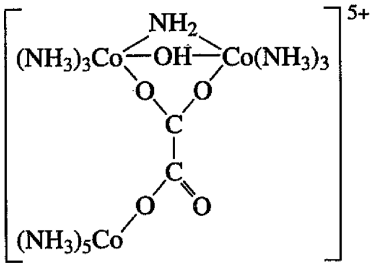

V

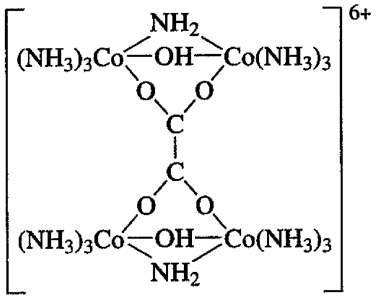

VI

Table 1.25 lists the ν(CO) of each type. The spectrum of the tetradentate complex (VI) is the most simple. Because of its high symmetry [$\mathbf{D}_{2h}$ (planar) or $\mathbf{D}_{2d}$ (twisted)], it exhibits only two ν(CO). The spectra of bidentate complexes (III and IV) show four ν(CO), as expected from the $\mathbf{C}_{2v}$ symmetry. The spectrum of the tridentate complex (V) should show four ν(CO), although only three are observed. The tetradentate bridging structure (VI) is also found in $[(MoFe_3S_4Cl_4)_2(ox)]^{4-}$, which exhibits the ν(CO) at 1630 cm^{-1}:

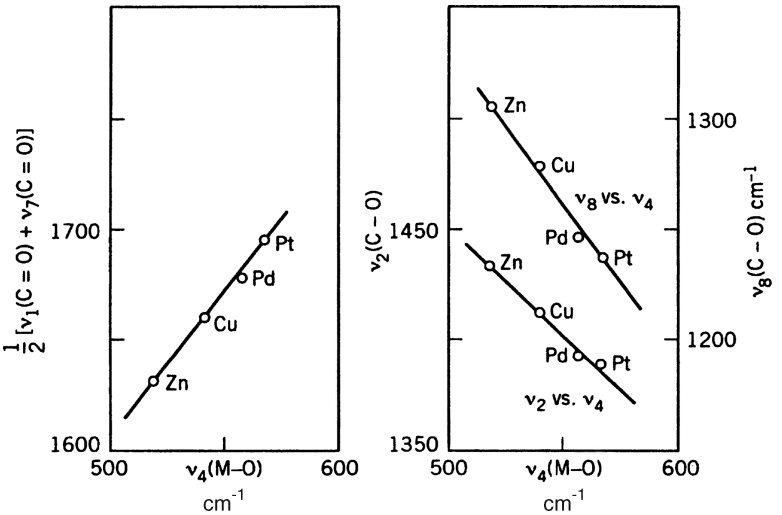

Fig. 1.46. *M–O stretching frequency versus C=O and C–O stretching frequencies in oxalato complexes of divalent metals [481].*

This frequency is much lower than that of the chelating oxalato group in $[MoFe_3S_4Cl_4(ox)]^{3-}$ ($1670\,cm^{-1}$) [491].

The $[Cr_2(ox)_5]^{4-}$ ion contains four bidentate chelating ligands and one bridging oxalato ligand. The former exhibits the ν_a(CO), ν_s(CO), and δ(OCO) at 1678,1384, and 884 cm^{-1}, respectively, whereas the latter exhibits these vibrations at 1655,1357, and 804 cm^{-1}, respectively [492]. The Raman spectra of metal oxalato complexes have also been examined to investigate the solution equilibria and the nature of the M–O bond [493].

TABLE 1.25. CO Stretching Vibrations of Co(III) Oxalato Complexes (cm^{-1})

Compound	Symmetry	ν(CO)			
I	C_s/C_1	1761	1682 1665	1400	1260
II	C_{2v}	1696	1667	1410	1268
III	C_{2v}/C_2	1721 1701	1629 1670	1439 1430	1276 1250
IV	C_{2v}/C_2	1755	1626	1318	1284
V	C_s/C_1	1650	1610	1322	—
VI	D_{2h}/D_{2d}	—	1628	1345	—

1.12.2. Complexes of Related Ligands

Vibrational assignments have been made on metal oxamido complexes of $\mathbf{V}_h$ symmetry [494].

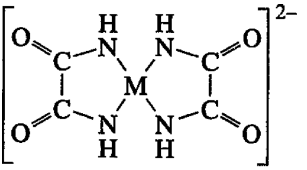

(M = Ni or Cu)

and the *cis*- and *trans*-dimethyloxamido complexes of dimethylgallium [495]:

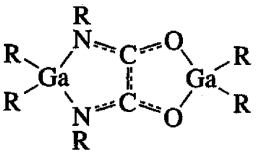

cis(C_{2v})

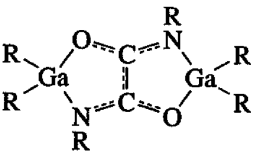

trans(C_{2h})

The IR and Raman spectra of the Ni(II) and Cu(II) complexes of oxamic hydrazine have been assigned using ^{58}Ni and ^{62}Ni isotopes [496]:

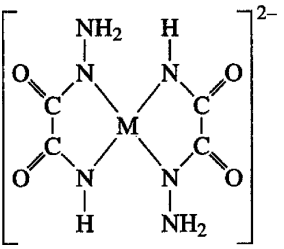

(D_{2h})

The ν(Ni−NH) and ν[Ni−N(NH_2)] of the ^{58}Ni complex are at 439 and 428 cm^{-1}, respectively, in the IR spectrum.

Biuret ($NH_2CONHCONH_2$) is known to form the following two types of chelate rings:

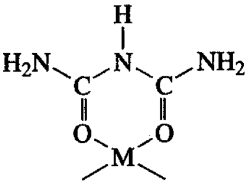

VII

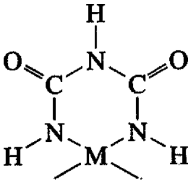

VIII

Violet crystals of composition $K_2[Cu(biureto)_2]\cdot 4H_2O$ are obtained when the Cu(II) ion is added to an alkaline solution of biuret, whereas pale blue-green crystals of composition $[Cu(biuret)_2]Cl_2$ result when the Cu(II) ion is mixed with biuret in neutral (alcoholic) solution. The former contains the N-bonded chelate ring structure (VIII), while the latter consists of the O-bonded chelate rings (VII). Kedzia et al. [497] carried out normal coordinate analyses of both compounds. The Co(II) complex forms the N-bonded chelate ring, whereas the Zn complex forms the O-bonded ring structure [497]. In $[Cd(biuret)_2]Cl_2$, the biuret molecules are bonded to the metal as follows [498]:

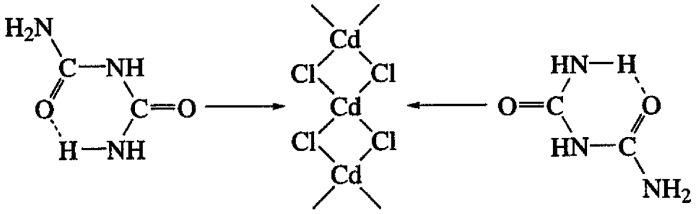

IX

Saito et al. [499] carried out normal coordinate analysis on the ligand portion of the Cd complex. Thamann and Loehr [500] assigned the Raman spectra of N-bonded Cu(II) and Cu(III) complexes of biuret and oxamide based on normal coordinate calculations. The vibrations that are predominantly ν(Cu−N) appear at 320–291 cm^{-1} for the Cu(II) and at 344–320 cm^{-1} for the Cu(III) complexes. The corresponding force constants were 1.04–0.96 mdyn/Å for the former and 1.46–1.35 mdyn/Å for the latter.

1.13. COMPLEXES OF SULFATE, CARBONATE, AND RELATED LIGANDS

When a ligand of relatively high symmetry coordinates to a metal, its symmetry is lowered and marked changes in the spectrum are expected because of changes in the selection rules. This principle has been used extensively to determine whether acido anions such as SO_4^{2-} and CO_3^{2-} coordinate to metals as unidentate, chelating bidentate, or bridging bidentate ligands. Although symmetry lowering is also caused by the crystalline environment, this effect is generally much smaller than the effect of coordination.

1.13.1. Sulfato (SO_4) Complexes

The free sulfate ion belongs to the high-symmetry point group $\mathbf{T}_d$. Of the four fundamentals, only ν_3 and ν_4 are infrared-active. If the symmetry of the ion is lowered by complex formation, the degenerate vibrations split and Raman-active modes appear in the infrared spectrum. The lowering of symmetry caused by coordination

is different for the unidentate and bidentate complexes, as shown below:

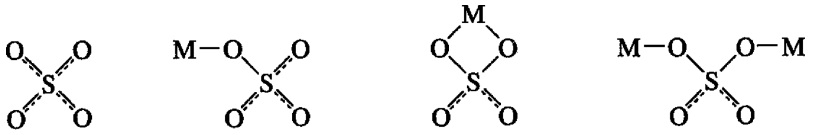

Free ion (T_d) | Unidentate complex (C_{3v}) | Bidentate complex (C_{2v}) | Bridged bidentate complex (C_{2v})

The change in the selection rules caused by the lowering of symmetry was shown in Table 2.6F of Part A. Table 1.26 and Fig. 1.47 give the frequencies and the spectra of typical Co(III) sulfato complexes obtained by Nakamoto et al. [501]. In $[Co(NH_3)_6]_2(SO_4)3\cdot 5H_2O$, ν_3 and ν_4 do not split and ν_2 does not appear, although ν_1 is observed, it is very weak. They concluded, therefore, that the symmetry of the SO_4^{2-} ion is approximately $\mathbf{T}_d$. In $[Co(NH_3)_5SO_4]Br$, both ν_1 and ν_2 appear with medium intensity; moreover, ν_3 and ν_4 each splits into two bands. This result can be explained by assuming a lowering of symmetry from $\mathbf{T}_d$ to $\mathbf{C}_{3v}$ (unidentate coordination). In

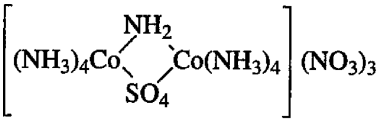

both ν_1 and ν_2 appear with medium intensity, and ν_3 and ν_4 each splits into three bands. These results suggest that the symmetry is further lowered and probably reduced to $\mathbf{C}_{2v}$, as indicated in Table 1.26. Thus, the SO_4^{2-} group in this complex is concluded to be a bridging bidentate as depicted in the preceding diagram.

The chelating bidentate SO_4^{2-} group was discovered by Barraclough and Tobe [502], who observed three bands (1211, 1176, and 1075 cm^{-1}) in the ν_3 region of $[Co(en)_2SO_4]Br$. These frequencies are higher than those of the bridging bidentate complex listed in Table 1.26. Eskenazi et al. [503] also found the same trend in Pd(II) sulfato complexes. Thus the distinction between bridging and chelating sulfato complexes can be made on this basis. Table 1.27 lists the observed frequencies of the sulfato groups and the modes of coordination as determined from the spectra.

TABLE 1.26. Vibrational Frequencies of Co(III) Sulfato Complexes (cm^{-1}) [501]

Compound	Symmetry	ν_1	ν_2	ν_3	ν_4
Free SO_4^{2-} ion	$\mathbf{T}_d$	—	—	1104 (vs)[a]	613 (s)
$[Co(NH_3)_6]_2(SO_4)_3\cdot 5H_2O$	$\mathbf{T}_d$	973 (vw)	—	1130–1140 (vs)	613 (s)
$[Co(NH_3)_6]_5SO_4]Br$	$\mathbf{C}_{3v}$	970 (m)	438 (m)	1032–1044 (s) 1117–1143 (s)	645 (s) 604 (s)
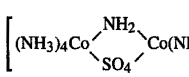	$\mathbf{C}_{2v}$	995 (m)	462 (m)	1050–1060 (s) 1170 (s) 1105 (s)	641 (s) 610 (s) 571 (m)

[a] vs = very strong; s = strong; m = medium; vw = very weak.

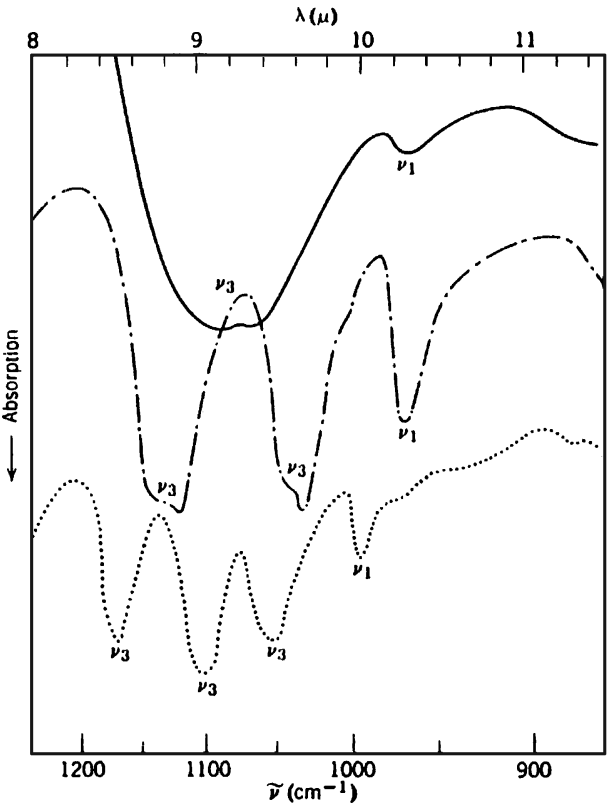

Fig. 1.47. *Infrared spectra of* $[Co(NH_3)_6]_2(SO_4)_3 \cdot 5H_2O$ *(solid line);* $[Co(NH_3)_6]_5SO_4]Br$ *(dot–dash line); and*

$$\left[(NH_3)_4Co\begin{matrix}NH_2\\ \diagup\ \ \diagdown\\ SO_4\end{matrix}Co(NH_3)_4\right] (No_3)_3$$ *(dotted line) [501].*

Unidentate coordination of the sulfato group in *trans*-$[Ru(SO_4)(NH_3)_4$(nitotinamide)] Cl has also been confirmed [504].

The symmetries of the sulfate ions in metal sails at various stages of hydration have been studied using IR spectra [505]. Normal coordinate analyses have been carried out on Co(III) ammine complexes containing sulfato groups [506,507].

1.13.2. Perchlorato (ClO_4) Complexes

In general, the perchlorate (ClO_4^-) ion coordinates to a metal when its complexes are prepared in nonaqueous solvents. The structure and bonding of metal complexes containing these weakly coordinating ligands have been reviewed briefly by Rosenthal [517]. Infrared and Raman spectroscopy has been used extensively to determine the mode of coordination of the ClO_4^- ligand.

TABLE 1.27. Vibrational Frequencies and Modes of Coordination of Various Sulfato Complexes (cm^{-1})

Compound	Mode of Coordination	ν_1	ν_2	ν_3	ν_4	Ref.
$[Cr(H_2O)_5SO_4]Cl\cdot\frac{1}{2}H_2O$	Unidentate	1002	—	1118 1068	—	508
$[VO(SO_4)_2(H_2O)_3]^{2-}$	Unidentate	—	483	1140 1046	640 619	509
$[Cu(bipy)SO_4]\cdot 2H_2O$ (polymeric)	Bridging bidentate	971	—	1163 1096 1053–1035	—	510
$Ni(morpholine)_2SO_4$ (polymeric)	Bridging bidentate	973	493	1177 1094 1042	628 612 593	511
$[Co_2\{(SO_4)_2OH\}(NH_3)_6]Cl$	Bridging bidentate	966	—	1180 1101 1048	645 598	512
$Pd(NH_3)_2SO_4$	Bridging bidentate	960	—	1195 1110 1035	—	503
$Pd(phen)SO_4$	Chelating bidentate	955	—	1240 1125 1040–1015	—	503
$Pd(PPh_3)_2SO_4$	Chelating bidentate	920	—	1265 1155 1110	—	513
$Ir(PPh_3)_2(CO)I(SO_4)$	Chelating bidentate	856	549	1296 1172 880	662 610	514
$K_3[Fe(SO_4)F]$	Chelating bidentate	—	—	1225 1130 1020	—	515
$Tl[VO_2SO_4]$	Chelating bidentate	1000	455 400	1255 1160 1125	720 570	516

The structures listed in Table 1.28 were determined on the basis of the same symmetry selection rules as used for sulfato complexes. The ν_3 and ν_4 frequencies of unidentate perchlorato complexes are 1194 and 1008 cm^{-1}, respectively, for $[Au(ClO_4)_4](ClO_2)$ [524], and 1204 and 1065 cm^{-1}, respectively, for $[Pd(ClO_4)_4](NO_2)_2$ [525]. In $Pd(ClO_4)_2$, two ClO_4 ligands form a square–planar complex around the Pd atom, and Cunin et al. [525] made complete band assignments of its IR/Raman spectra on the basis of DFT calculations. The terminal ClO_2 group exhibits the $\nu_a(ClO_2)$ at 1288 and 1272 cm^{-1} and $\nu_s(ClO_2)$ at 1152 and 1130 cm^{-1}, whereas the coordinating ClO_2 group exhibits these vibrations at 864 and 820 cm^{-1}, respectively, in IR spectra.

Causse et al. [526] concluded from their IR and Raman study that $[Al(ClO_4)_n]^{-(n-3)}$ contain two unidentate and two bidentate for $n=4$, four unidentate ligands and one bidentate for $n=5$, and six unidentate ligands for $n=6$. In polymeric $M(ClO_4)_3$ ($M=In$, Tl), the ClO_4^- ion acts as a bridging bidentate ligand [527].

TABLE 1.28. ClO Stretching Frequencies of Perchlorato Complexes (cm^{-1})

Complex	Structure	ν_3	ν_4	Ref.
$K[ClO_4]$	Ionic	1170–1050	(935)[a]	
$Cu(ClO_4)_2 \cdot 6H_2O$	Ionic	1160–1085	(947)[a]	518
$Cu(ClO_4)_2 \cdot 2H_2O$	Unidentate	1158 1030	920	518
$Cu(ClO_4)_2$	Bidentate	1270–1245 1130 948–920	1030	518
$Mn(ClO_4)_2 \cdot 2H_2O$	Bidentate	1210 1138 945	1030	519
$Co(ClO_4)_2 \cdot 2H_2O$	Bidentate	1208 1125 935	1025	519
$[Ni(en)_2(ClO_4)_2]$[b]	Bidentate	1130 1093 1058	962	520
$Ni(CH_3CN)_4(ClO_4)_2$	Unidentate	1135 1012	912	521
$Ni(CH_3CN)_2(ClO_4)_2$	Bidentate	1195 1106 1000	920	521
$[Ni(4\text{-Me-py})_4](ClO_4)_2$	Ionic	1040–1130	(931)[a]	522
$Ni(3\text{-Br-py})_4(ClO_4)_2$	Unidentate	1165–1140 1025	920	522
$GeCl_3(ClO_4)$	Unidentate	1265, 1240	1030	523

[a]Weak.
[b]Blue form.

According to Pascal et al., the ClO_4^- ligands in $M(ClO_4)_2$ (M = Ni, Co) are bridging tridentate [528]:

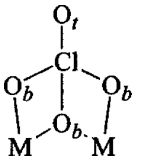

In $Ni(ClO_4)_2$ (IR), the $\nu(ClO_t)$, $\nu_a(ClO_b)$, and $\nu_s(ClO_b)$ are at 1300, 1030, and 960 cm^{-1}, respectively. This type of coordination has also been proposed for $M(ClO_4)_3$ (M = Y, La, Nd, Sm, etc.) [529] and for $Ce(ClO_4)_3$ [530] and $Mn(ClO_4)_2$ [531].

1.13.3. Complexes of Other Tetrahedral Ligands

Many tetrahedral anions coordinate to a metal as unidentate and bidentate ligands, and their modes of coordination have been determined by the same method as is used for

the SO_4^{2-} and ClO_4^- ions. Thus, the PO_4^{3-} ion is a unidentate in $[Co(NH_3)_5PO_4]$ and a bidentate in $[Co(NH_3)_4PO_4]$ [532]. Vibrational spectra have been reported for unidentate and bidentate complexes of the AsO_4^{3-} [533], CrO_4^{2-}, and MoO_4^{2-} ions [534]. The SeO_4^{2-} ion in $[Co(NH_3)_5SeO_4]Cl$ is a unidentate [535], whereas it is a bridging bidentate ligand and in $[Co_2\{SeO_4)_2OH\}\text{-}(NH_3)_6]Cl$ [512]. The latter structure is also reported for $(NH_4)_2UO_2(SeO_4)_2 \cdot 4H_2O$ [536].

The Raman spectrum of solid $Ni(H_2PO_2)_2$ is interpreted as that of the two ions, $[Ni(H_2PO_2)]^+$ and $H_2PO_2^-$; the hypophosphite ion in the former is a chelating bidentate [537]. In polymeric $UCl(H_2PO_2)_3 \cdot 2H_2O$, however, the $H_2PO_2^-$ ion serves as a bridging bidentate with $\nu_a(PO_2)$ and $\nu_s(PO_2)$ at 1234 and 1058 cm^{-1}, respectively [538]. Bridging bidentate phosphinates ($R_2PO_2^-$ where R is a phenyl) of Ru(I) exhibit the $\nu_a(PO_2)$ and $\nu_s(PO_2)$ at approximately 1145 and 1035 cm^{-1}, respectively [539].

The $S_2O_3^{2-}$ ion can coordinate to a metal in a variety of ways. According to Freedman and Straughan [540], $\nu_a(SO_3)$ near 1130 cm^{-1} is most useful as a structural diagnosis: >1175 (S-bridging); 1175–1130 (S-coordination); ~1130 (ionic $S_2O_3^{2-}$); < 1130 cm^{-1} (O-coordination). On the basis of this criterion, they proposed polymeric structures linked by O-bridges for thiosulfates of UO_2^{2+} and ZrO_2^{2+}. In the $[OsO_2(S_2O_3)_2]^{2-}$ ion, the thiosulfate ion is a S-bonded unidentate with the $\nu(S-S)$ at 409 cm^{-1}, which is much lower than that of the free ligand (434 cm^{-1}) [541].

The fluorosulfate (SO_3F^-) ion is a unidentate in $[Sn(SO_3F)_6]^{2-}$ [542], but is a unidentate as well as a bidentate in $VO(SO_3F)_3$ [543]. Similarly, only unidentate coordination is seen in $[Ru(SO_3F)_6]^{2-}$, whereas $[Ru(SO_3F)_5]^-$ may contain both unidentate and bidentate ligands [544]. The $\nu_a(SO_2)$, $\nu_s(SO_2)$, and $\nu(S-O)/\nu(S-F)$ vibrations of $Cs[Sb(SO_3F)_6]$ were assigned at 1451(IR), 1256(R) and 958(IR)/903 (R) cm^{-1}, respectiuvely. Band assignments are also reported for $Cs_2[M(SO_3F)_6]$ (M = Sn, Pt) [545].

1.13.4. Carbonato(CO_3) Complexes

The unidentate and bidentate (chelating) coordinations shown below are found in the majority of carbonato complexes:

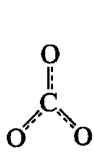

Free ion (D_{3h})

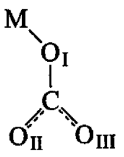

Unidentate (C_s)

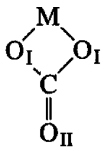

Bidentate (C_{2v})

The selection rule changes as shown in Table 1.18 of Part A. In C_{2v} and C_s*, the ν_1 vibration, which is forbidden in the free ion, becomes infrared-active and each of the doubly degenerate vibrations, ν_3 and ν_4, splits into two bands. Although the number of infrared-active fundamentals is the same for C_{2v} and C_s, the splitting of the degenerate

*The symmetry of the unidentate carbonato group is C_{2v} if the metal atom is ignored.

vibrations is larger in the bidentate than in the unidentate complex [501]. For example, $[Co(NH_3)_5CO_3]Br$ exhibits two CO stretchings at 1453 and 1373 cm^{-1}, whereas $[Co(NH_3)_4CO_3]Cl$ shows them at 1593 and 1265 cm^{-1}. In organic carbonates such as dimethyl carbonate, $(CH_3O_I)_2CO_{II}$, this effect is more striking because the CH_3-O_I bond is strongly covalent. Thus, the CO_{II} stretching is observed at 1870 cm^{-1}, whereas the CO_I stretching is at 1260 cm^{-1}. Gatehouse and co-workers [546] showed that the separation of the CO stretching bands increases along the following order:

$$\text{Basic salt} < \text{carbonato complex} < \text{acid} < \text{organic carbonate}$$

Fujita et al. [547] carried out normal coordinate analysis on unidentate and bidentate carbonato complexes of Co(III). According to their results, the CO stretching force constant, which is 5.46 for the free ion, becomes 6.0 for the $C-O_{II}$ bonds and 5.0 for the $C-O_I$ bond of the unidentate complex, whereas it becomes 8.5 for the $C-O_{II}$ bond and 4.1 for the $C-O_I$ bonds of the bidentate complex (all are UBF force constants in units of mdyn/Å). The observed and calculated frequencies and theoretical band assignments are shown in Table 1.29. Normal coordinate analyses on carbonato complexes have also been carried out by other workers [548,549]. Vibrational spectra of bidentate carbonato complexes are reported for $Na_5[Sc(CO_3)_4]\cdot 2H_2O$ [550] and for $GaCO_3$ radical formed in inert gas matrices [551].

As is shown in Table 1.29, normal coordinate analysis predicts that the highest-frequency CO stretching band belongs to the B_2 species in the unidentate and the A_1 species in the bidentate complex. Elliott and Hathaway [552] studied the polarized infrared spectra of single crystals of $[Co(NH_3)_4CO_3]Br$ and confirmed these symmetry properties. As will be shown later for nitrate complexes, Raman polarization studies are also useful for this purpose.

According to X-ray analysis, the carbonate groups in $[(NH_3)_3Co(\mu\text{-}OH)_2(\mu\text{-}CO_3)Co(NH_3)_3]SO_4\cdot 5H_2O$ [553] and [(teed)CuCl(CO_3)CuCl(teed)] (teed: *N*,*N*,*N*′,*N*′-tetraethyl-ethylenediamine) [554] take the bridging bidentate and tridentate structures, respectively:

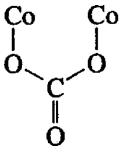

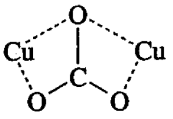

Vibrational spectra of bridging bidentate and tridentate complexes are also reported for $[Ru(III)_2(tacn)_2(\mu\text{-}OH)_2(\mu\text{-}CO_3)]Br_2\cdot 3.75H_2O$ (tacn=1.4.7-triazacyclononane) [555] and $(\mu\text{-}CO_3)[Ni(II)_3(Medpt)_3(NCS)_4]$ [Medpt=bis(3-aminopropyl)methylamine] [556].

No simple criteria have been established to distinguish these structures from common unidentate and bidentate (chelating) coordination on the basis of vibrational frequencies. However, Greenaway et al. [557] have demonstrated that the bridging and bidentate carbonate ligands can be distingished if the angular distortion ($\Delta\alpha$), the

TABLE 1.29. Calculated and Observed Frequencies of Unidentate and Bidentate Co(III) Carbonato Complexes (cm^{-1}) [547]

Species (C_{2v})[a]	$\nu_1(A_1)$	$\nu_2(A_1)$	$\nu_3(A_1)$	$\nu_4(A_1)$	$\nu_5(B_2)$	$\nu_6(B_2)$	$\nu_7(B_2)$	$\nu_8(B_1)$
Calculated Frequency	1376	1069	772	303	1482	676	92	—
Assignment	$\nu(CO_{II})$ $+\nu(CO_I)$	$\nu(CO_I)$ $+\nu(CO_{II})$	$\delta(O_{II}CO_{II})$	$\nu(CoO_I)$	$\nu(CoO_{II})$	$\rho_r(O_{II}CO_{II})$	$\delta(CoO_IC)$	π
$[Co(NH_3)_5CO_3]Br$	1373	1070	756	362	1453	678	—	850
$[Co(ND_3)_5CO_3]Br$	1369	1072	751	351	1471	687	—	854
$[Co(NH_3)_5CO_3]I$	1366	1065	776	360	1449	679	—	850
$[Co(ND_3)_5CO_3]I$	1360	1063	742	341	1467	687	—	853

Species (C_{2v})[a]	$\nu_1(A_1)$	$\nu_2(A_1)$	$\nu_3(A_1)$	$\nu_4(A_1)$	$\nu_5(B_2)$	$\nu_6(B_2)$	$\nu_7(B_2)$	$\nu_8(B_2)$
Calculated Frequency	1595	1038	771	370	1282	669	429	—
Assignment	$\nu(CO_{II})$	$\nu(CO_I)$	+ Ring Def. $\nu(CoO_I)$	$\nu(CoO_I)$ + Ring Def.	$\nu(CO_I)$ $+\delta(O_ICO_{II})$	$\delta(O_ICO_{II})$ $+\nu(CO_I)$ $+\nu(CoO_I)$	$\nu(CoO_I)$	π
$[Co(NH_3)_4CO_3]Cl$	1593	1030	760	395	1265	673	430	834
$[Co(ND_3)_4CO_3]Cl$	1635 / 1607	(1031)[b]	753	378	1268	672	418	832
$[Co(NH_3)_4CO_3]ClO_4$	1602	—[c]	762	392	1284	672	428	836
$[Co(ND_3)_4CO_3]ClO_4$	1603	—[c]	765	374	1292	676	415	835

[a]Symmetry assuming a linear Co−O−C bond (see Ref. 547).
[b]Overlapped with $\delta_s(ND_3)$.
[c]Hidden by $[ClO_4]^-$ absorption.

difference between the largest and smallest OCO angles, is known from X-ray analysis. These workers found that the frequency separation ($\Delta\nu$) between the two highest ν(CO) bands increases linearly with $\Delta\alpha$. As an example, $Na_2[Cu(CO_3)_2]$ contains one bidentate ligand and one bridging carbonate ligand. Using their correlation, they were able to assign the 1610 and 1328 cm^{-1} bands to the bidentate ($\Delta\alpha = 11.2^\circ$ and $\Delta\nu = 282\ cm^{-1}$) and the 1525 and 1380 cm^{-1} bands to the bridging carbonate ligands ($\Delta\alpha = 7.7^\circ$ and $\Delta\nu = 145\ cm^{-1}$).

The IR spectrum of K_2CO_3 in a N_2 matrix indicates that the CO_3 group coordinates in a bidentate fashion to one of the K atom and in a unidentate fashion to the other K atom [558]. Busca and Lorenzelli [559] reviewed the IR spectra and modes of coordination of carbonate, bicarbonate, and formate ions, and of CO_2 in metal complexes.

1.13.5. Nitrato (NO_3) Complexes

The structures and vibrational spectra of a large number of nitrato complexes have been reviewed by Addison et al. [560] and Rosenthal [513]. X-Ray analyses show that the NO_3^- ion coordinates to a metal as a unidentate, symmetric, and asymmetric chelating bidentate, and bridging bidentate ligand of various structures. It is rather difficult to differentiate these structures by vibrational spectroscopy since the symmetry of the nitrate ion differs very little among them ($\mathbf{C}_{2v}$ or $\mathbf{C}_s$). Even so, vibrational spectroscopy is still useful in distinguishing unidentate and bidentate ligands.

Originally, Gatehouse et al. [561] noted that the unidentate NO_3 group exhibits three NO stretching bands, as expected for its $\mathbf{C}_{2v}$ symmetry. For example, $[Ni(en)_2(NO_3)_2]$ (unidentate) exhibits three bands as follows:

$\nu_5\ (B_2)$	1420 cm^{-1}	$\nu_a(NO_2)$
$\nu_1\ (A_1)$	1305 cm^{-1}	$\nu_s(NO_2)$
$\nu_2(A_1)$	(1008) cm^{-1}	ν(NO)

whereas $[Ni(en)_2NO_3]ClO_4$ (chelating bidentate) exhibits three bands at the following:

$\nu_1(A_1)$	1476 cm^{-1}	ν(N=O)
$\nu_5(B_2)$	1290 cm^{-1}	$\nu_a(NO_2)$
$\nu_2(A_1)$	(1025) cm^{-1}	$\nu_s(NO_2)$

The separation of the two highest-frequency bands is 115 cm^{-1} for the unidentate complex, whereas it is 186 cm^{-1} for the bidentate complex. Thus Curtis and Curtis [562] concluded that $[Ni(dien)(NO_3)_2]$ contains both types, since it exhibits bands due to unidentate (1440 and 1315 cm^{-1}) and bidentate (1480 and 1300 cm^{-1}) groups. Table 1.30 lists the three NO stretching frequencies mentioned above. The order of these frequencies is $\nu_5 > \nu_1 > \nu_2$ for unidentate, and $\nu_1 > \nu_5 > \nu_2$ for chelating bidentate complexes. In general, the separation of the first two bands of the latter is larger than that of the former if the complexes are similar. As seen in Table 1.30, however, this rule does not hold if the complexes are markedly different. More examples are found

TABLE 1.30. NO Stretching Frequencies of Unidentate and Bidentate Nitrato Complexes (cm^{-1})

Compound	Mode of Coordination	ν_5	ν_1	ν_2	ν_5–ν_1	Ref.
$Re(CO)_5NO_3$	Unidentate	1497	1271	992	226	563
cis-$[Pt(NH_3)_2(NO_3)_2]$	Unidentate	1510	1275	997	235	564
$Sn(NO_3)_4$	Chelating bidentate	1630	1255	983	375	565
$K[UO_2(NO_3)_3]$	Chelating bidentate	1555 1521	1271	1025	284 250	566
$Co(NO_3)_3$	Chelating bidentate	1619	1162	963	457	567
$Na_2[Mn(NO_3)_4]$	Chelating bidentate	1490	1280	1041 1036	210	568
$Cu(NO_3)_2MeNO_2$	Bridging bidentate	1519	1291	1008	228	569
$Zn(bt)_2(NO_3)_2$[a]	Chelating bidentate	1485	1300	—	185	570
$Ni(dmpy)_2(NO_3)_2$[b]	Chelating bidentate	1513	1270	1013	243	571
$Th(NO_3)_4\ (tmu)_2$[c]	Chelating bidentate	1530	1278	1023	252	572
$Ln(NO_3)_3\ (DMSO)_n$ (Ln = La,Ce,.)	Chelating bidentate	1500	1295	1030	305	573

[a] bt = benzothiazole.
[b] dmpy = 2,6-dimethyl-4-pyrone.
[c] tmu = tetramethylurea.

for $C\{Hg(NO_3)\}_4 \cdot H_2O$ (unidentate, 223 cm^{-1}) [574], $[V_2O_3Cl_4(NO_3)_2]^{2-}$ (chelatuig bidentate, 232 cm^{-1}) [575], and $CrO_2(NO_3)_2$ (chelating bidentate. ~280 cm^{-1}) [576].

Lever et al. [577] proposed the use of the combination band, $\nu_1 + \nu_4$, of free NO_3^- that appears in the 1800–1700 cm^{-1} region for structural diagnosis. On coordination, ν_4 (E', in-plane bending) near 700 cm^{-1} splits into two bands, and the magnitude of this splitting is expected to be larger for bidentate than for unidentate ligands. This should be reflected on the separation of two ($\nu_1 + \nu_4$) bands in the 1800–1700 cm^{-1} region. According to Lever et al. [577], the NO_3^- ion is bidentate if the separation is ~66–20 cm^{-1} and is unidentate if it is ~26–5 cm^{-1}.

As stated previously, the highest-frequency CO stretching band of the carbonato complexes belongs to the A_1 species in the bidentate and to the B_2 species in the unidentate complex. The same holds true for the nitrato complex. Ferraro et al. [578] showed that all the nitrato groups in $Th(NO_3)_4(TBP)_2$ coordinate to the metal as bidentate ligands since the Raman band at 1550 cm^{-1} is polarized (TBP = tributylphosphate). This rule holds very well for other compounds [579]. According to Addison et al. [560], the intensity pattern of the three NO stretching bands in the Raman spectrum can also be used to distinguish unidentate and symmetric bidentate NO_3 ligands. The middle band is very strong in the former, whereas it is rather weak in the latter.

The use of far-infared spectra to distinguish unidentate and bidentate nitrato coordination has been controversial. Nuttall and Taylor [580] suggested that unidentate and bidentate complexes exhibit one and two MO stretching bands, respectively, in the

350–250 cm^{-1} region. Bullock and Parrett [581] showed, however, that such a simple rule is not applicable to many known nitrato complexes. Ferraro and Walker [582] assigned the MO stretching bands of anhydrous metal nitrates such as $Cu(NO_3)_2$ and $Pr(NO_3)_3$.

Several workers studied the Raman spectra of metal nitrates in aqueous solution and molten states. For example, Irish and Walrafen [583] found that E'-mode degeneracy is removed even in dilute solutions of $Ca(NO_3)_2$. This, combined with the appearance of the A_1' mode in the infrared, suggests $\mathbf{C}_{2v}$ symmetry of the NO_3^- ion. Using FTIR and Raman spectroscopy, Castro and Jagodzinski [584] have shown that the $Cu(NO_3)^+$ ion of $\mathbf{C}_{2v}$ symmetry is formed when copper nitrate hydrate is dissolved in H_2O and acetone at a high solute concentration. The Raman band at 335 cm^{-1} was assigned to the ν_s(Cu−O) of this chelating bidentate complex. Hester and Krishnan [585] studied the Raman spectra of $Ca(NO_3)_2$ dissolved in molten KNO_3 and $NaNO_3$. Their results suggest an asymmetric perturbation of the NO_3^- ion by the Ca^{2+} ion through ion-pair formation.

Wick et al. [586] prepared the first peroxynitrite($OONO^-$) complex, $Na_3[Co(CN)_5(OONO)]$, which exhibits the ν(N=O), ν(N−O), and ν(O−O) vibrations at 1621,1399, and 915 cm^{-1}, respectively.

1.13.6. Sulfito (SO_3), Selenito (SeO_3), and Sulfinato (RSO_2) Complexes

The pyramidal sulfite (SO_3^{2-}) ion may coordinate to a metal as a unidentate, bidentate, or bridging ligand. The following two structures are probable for unidentate coordination:

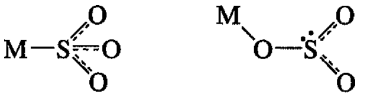

$\mathbf{C}_{3v}$ $\mathbf{C}_s$

If coordination occurs through sulfur, the $\mathbf{C}_{3v}$ symmetry of the free ion will be preserved. If coordination occurs through oxygen, the symmetry may be lowered to $\mathbf{C}_s$. In this case, the doubly degenerate vibrations of the free ion will split into two bands. It is anticipated [587] that coordination through sulfur will shift the SO stretching bands to higher frequencies, whereas coordination through oxygen will shift them to lower frequencies, than those of the free ion. On the basis of these criteria, Newman and Powell [588] showed that the sulfito groups in $K_6[Pt(SO_3)_4]\cdot 2H_2O$ and $[Co(NH_3)_5(SO_3)]Cl$ are S-bonded and those in $Tl_2[Cu(SO_3)_2]$ are O-bonded. Baldwin [589] suggested that the sulfito groups in *cis*- and *trans*-$Na[Co(en)_2(SO_3)_2]$ and $[Co(en)_2(SO_3)X]$ (X = Cl or OH) are S-bonded, since they show only two SO stretchings between 1120 and 930 cm^{-1}. According to Nyberg and Larsson [590], the appearance of a strong SO stretching band above 975 and below 960 cm^{-1} is an indication of S- and O-coordination, respectively. Table 1.31 lists typical results obtained for unidentate complexes.

The IR spectrum of *fac*-$[Rh(SO_3)_3(NH_3)_3]\,Na_3\cdot 2H_2O$ in the crystalline state [592] shows that the symmetry of the S-bonded unidentate sulfite ligand is lowered from $\mathbf{C}_{3v}$ to $\mathbf{C}_s$. Comparison of the Raman spectra of *cis*- and *trans*-$[Rh(SO_3)_2(NH_3)_4]^+$ ions

TABLE 1.31. Infrared Spectra of Unidentate Sulfito Complexes (cm^{-1})

Compound	Structure	$\nu_3(E)$	$\nu_1(A_1)$	$\nu_2(A_1)$	$\nu_4(E)$	Ref.
Free SO_3^{2-}	—	933	967	620	469	
$K_6[Pt(SO_3)_4]\cdot 2H_2O$	S-bonded	1082–1057	964	660	540	588
$[Co(NH_3)_5(SO_3)]Cl$	S-bonded	1110	985	633	519	588
trans-$Na[Co(en)_2(SO_3)_2]$	S-bonded	1068	939	630	—	589
$[Co(en)_2(SO_3)Cl]$	S-bonded	1117–1075	984	625	—	589
$Tl_2[Cu(SO_3)_2]$	O-bonded	902 862	989	673	506 460	588
$(NH_4)_9[Fe(SO_3)_6]$	O-bonded	943	815	638	520	591

reflects the difference between these geometries on the numbers of the observed SO_3 vibrations [593].

The structures of complexes containing bidentate sulfito groups are rather difficult to deduce from their infrared spectra. Bidentate sulfito groups may be chelating or bridging through either oxygen or sulfur or both, all resulting in $\mathbf{C}_s$ symmetry. Baldwin [589] prepared a series of complexes of the type $[Co(en)_2(SO_3)]X$ (X = Cl, I, or SCN), which are monomeric in aqueous solution. They show four strong bands in the SO stretching region (one of them may be an overtone or a combination band). A chelating structure in which two oxygens of the sulfito group coordinate to the Co(III) atom was suggested. Newman and Powell [588] obtained the infrared spectra of $K_2[Pt(SO_3)_2]\cdot 2H_2O$, $K_3[Rh(SO_3)_3]\cdot 2H_2O$, and other complexes for which bidentate coordination of the sulfito group is expected. It was not possible, however, to determine their structures from infrared spectra alone. Krieglstein and Breitinger [594] prepared $[(en)Pt(SO_3)_2Pt(en)]\cdot 3H_2O$ and its Pd analog. According to X-ray analysis, the former contains two parallel μ-S,O bridges whereas the latter contains two antiparallel (μ-S,O bridges:

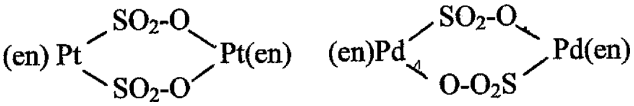

The former exhibits the $\nu_s(SO_2)$, $\nu_a(SO_2)$, and $\nu(SO)$ at 1116/1062, 1178/1153 and 923 cm^{-1}, respectively, while the corresponding frequencies of the latter are 1108, 1188, and 927 cm^{-1}, respectively.

The mode of coordination of the selenite ion (SeO_3^{2-}) is similar to that of the sulfite ion. Two types of unidentate complexes are expected. The O-coordinated complex exhibits $\nu_3(E)$ and $\nu_1(A_1)$ at 755 and 805 cm^{-1}, respectively, for $[Co(NH_3)_5(SeO_3)]Br\cdot H_2O$, [595] whereas the Se-coordinated complex, $[Co(NH_3)_5(SeO_3)]ClO_4$ [596], shows them at 823 and 860 cm^{-1}, respectively.

Four types of coordination are probable for sulfinato (RSO_2^-, R = CH_3, CF_3, Ph, etc.) groups:

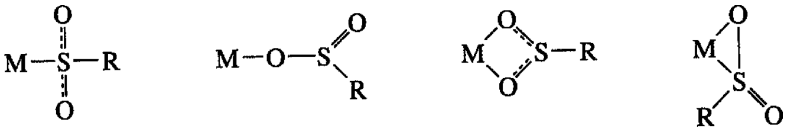

The SO stretching bands at 1200–850 cm^{-1} are useful in distinguishing these structures [597,598].

1.14. COMPLEXES OF β-DIKETONES

1.14.1. Complexes of Acetylacetonato Ion

A number of β-diketones form metal chelate rings of type A:

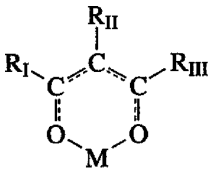

Type A

Among them, acetylacetone (acacH) is most common ($R_I = R_{III} = CH_3$ and $R_{II} =$ H). Infrared spectra of $M(acac)_2$- and $M(acac)_3$-type complexes have been studied extensively. Theoretical band assignments were first made by Nakamoto and Martell [599], who carried out normal coordinate analysis on the 1 : 1 model of $Cu(acac)_2$. Mikami et al. [600] performed normal coordinate analyses on the 1 : 2 (square–planar) and 1 : 3 (octahedral) models of various acac complexes. Figure 1.48 shows the infrared spectra of six acac complexes, and Table 1.32 lists the observed frequencies and band assignments for the Cu(II), Pd(II), and Fe(III) complexes obtained by Mikami et al. In this table, the 1577- and 1529-cm^{-1} bands of $Cu(acac)_2$ are assigned to ν(C⋯C) coupled with ν(C⋯O) and ν(C⋯O) coupled with ν(C⋯C), respectively. Junge and Musso [601] have measured the ^{13}C and ^{18}O isotope shifts of these bands and concluded that the above assignments must be reversed.

The ν(MO) of acac complexes are most interesting since they provide direct information about the M−O bond strength. Using the metal isotope technique, Nakamoto et al. [602] assigned the MO stretching bands of acetylacetonato complexes at the following frequencies (cm^{-1}):

$Cr(acac)_3$	$Fe(acac)_3$	$Pd(acac)_2$	$Cu(acac)_2$	$Ni(acac)_2(py)_2$
463.4	436.0	466.8	455.0	438.0
358.4	300.5	297.1	290.5	270.8
		265.9		

Both normal coordinate calculations and isotope shift studies show that the bands near 450 cm^{-1} are coupled with the $C-CH_3$ bending mode, whereas those in the low-frequency region are relatively pure MO stretching vibrations. Figure 1.49 shows the actual tracings of the infrared spectra of $^{50}Cr(acac)_3$ and its ^{53}Cr analog. It is seen that two bands at 463.4 and 358.4 cm^{-1} of the former give negative shifts of 3.0 and 3.9 cm^{-1}, respectively, whereas other bands (ligand vibrations) produce negligible shifts by the $^{50}Cr - {}^{53}Cr$ substitution.

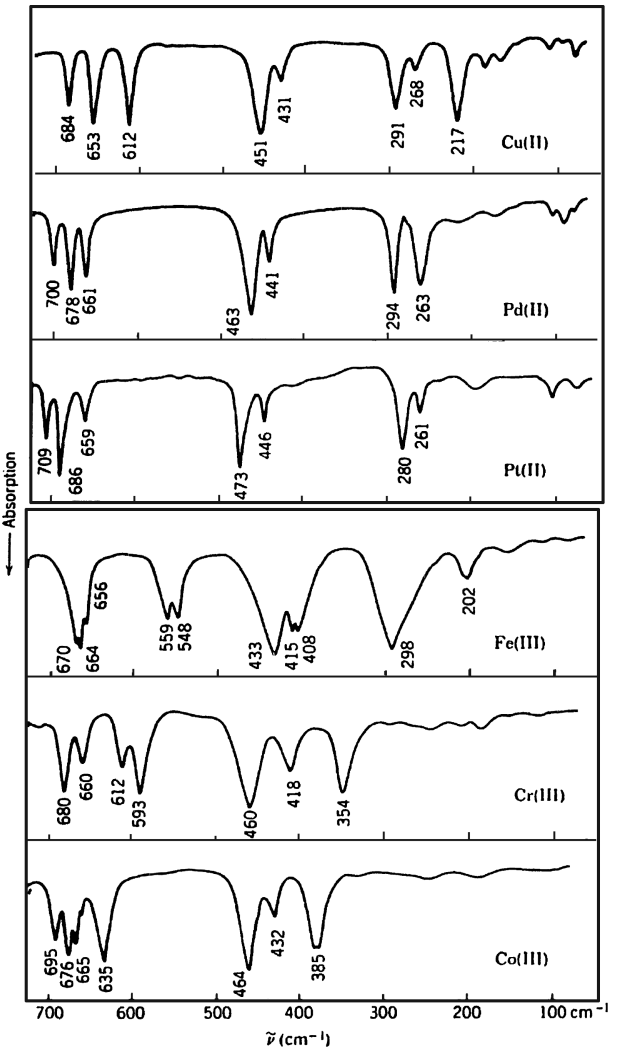

Fig. 1.48. *Infrared spectra of bis- and tris-(acetylacetonato) complexes [600].*

Schönherr et al. [603] carried out normal coordinate analysis on $Sn(acac)Cl_4$. The Sn−O stretching force constant (GVF) was 1.56 mdyn/Å. Handa et al. [604] observed the following trends (cm^{-1}) in the RR spectra of the Fe(III)–acac system in CH_3CN solution:

	$Fe(acac)^{2+}$		$Fe(acac)_2^+$		$Fe(acac)_3$
ν(CC)+ν(CO)	1554	<	1578	<	1603
ν(Fe−O)	474	>	462	>	451

TABLE 1.32. Observed Frequencies[a] and Band Assignments of Acetylacetonato Complexes (cm^{-1}) [600]

$Cu(acac)_2$	$Pd(acac)_2$	$Fe(acac)_3$	Predominant Mode
3072	3070	3062	ν(CH)
2987 2969 2920	2990 2965 2920	2895 2965 2920	$\nu(CH_3)$
1577	1569	1570	$\nu(C{=}C) + \nu(C{=}C)$
1552	1549	—	combination
1529	1524	1525	$\nu(C{=}O) + \nu(C{=}C)$
1461	(1425)	1445	$\delta(CH) + \nu(C{=}C)$
1413	1394	1425	$\delta_d(CH_3)$
1353	1358	1385 1360	$\delta_s(CH_3)$
1274	1272	1274	$\nu(C{-}CH_3) + \nu(C{=}C)$
1189	1199	1188	$\delta(CH) + \nu(C{-}CH_3)$
1019	1022	1022	$\rho_r(CH_3)$
936	937	930	$\nu(C{=}C) + \nu(C{=}O)$
780	786 779	801 780 771	π(CH)
684	700	670 664	$\nu(C{-}CH_3)$ + ring deformation + ν(MO)
653	678	656	$\pi\left(CH_3{-}C\begin{matrix}C\\O\end{matrix}\right)$
612	661	559 548	Ring deformation + ν(MO)
451	463	433	ν(MO) + $\nu(C{-}CH_3)$
431	441	415 408	Ring deformation
291	294	298	ν(MO)
1.45	1.85	1.30	K(M−O) (mdyn/Å) (UBF)

[a]IR spectra in the solid state.

These orders suggest that the Fe−O bond becomes weaker as the number of the coordinated acac ligand increases because the Lewis acidity of the metal ion decreases in the same order.

Complexes of the $M(acac)_2X_2$ type may take the *cis* or *trans* structure. Although steric and electrostatic considerations would favor the *trans*-isomer, the greater stability of the *cis*-isomer is expected in terms of metal–ligand π-bonding. This is the case for $Ti(acac)_2F_2$, which is "*cis*" with two ν(TiF) at 633 and 618 cm^{-1} [605]. In the case of $Re(acac)_2Cl_2$, however, both forms can be isolated; the *trans*-isomer exhibits ν(ReO) and ν(ReCl) at 464 and 309 cm^{-1}, respectively, while each of these bands splits into two in the *cis*-isomer [472 and 460 cm^{-1} for ν(ReO) and 346 and 333 cm^{-1} for ν(ReCl) in the infrared] [606]. For $VO(acac)_2L$, where L is a substituted

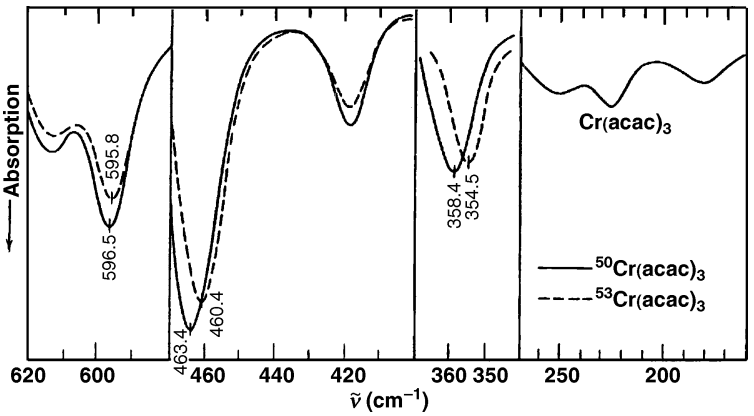

Fig. 1.49. *Infrared spectra of* $^{50}Cr(acac)_3$ *and its* ^{53}Cr *analog [625].*

pyridine, *cis*- and *trans*-isomers are expected. According to Caira et al. [607], these structures can be distinguished by their infrared spectra. The ν(V=O) and ν(V−O) of the *cis*-isomer are lower than those of the *trans*-isomer. For example, ν(V=O) of VO $(acac)_2$ is 999 cm^{-1}, and this band shifts to 959 cm^{-1} for 4-Et-py (*cis*) and to 973 cm^{-1} for py (*trans*). Furthermore, the ν(V−O) of the *cis*-isomer splits into two bands:

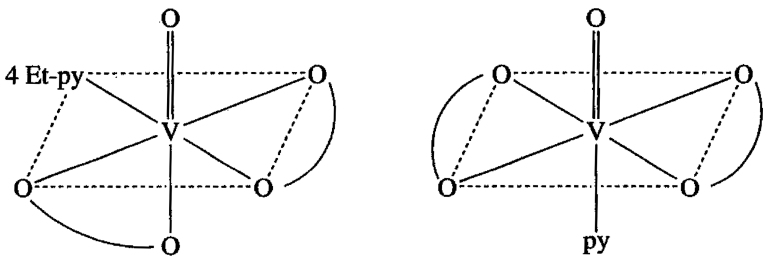

cis-isomer *trans*-isomer

Vibrational spectra of acac complexes have been studied by many other investigators. References are cited only for the following: $Cs[Os(acac)X_4]$ (X = Cl,Br,I) [608], $[Os(acac)_3]$ [609], $[M(acac)_3]$ (M = Ti,V,Cr,Mn,Fe,Co,Ni,Sc,Al) [610], $[UO_2(acac)_2]$ [611], and $[Ce(acac)_3(H_2O)]\cdot H_2O$ [612]. Infrared spectra of metal complexes of β-diketones have been reviewed extensively by Thornton [613].

According to X-ray analysis [614], the hexafluoroacetylacetonato ion (hfa) in $[Cu(hfa)_2\{Me_2N–(CH_2)_2–NH_2\}_2]$ coordinates to the metal as a unidentate via one of its O atoms. This compound exhibits ν(C=O) at 1675 and 1615 cm^{-1}, values slightly higher than those for $Cu(hfa)_2$, in which the hfa ion is chelated to the metal (1644 and 1614 cm^{-1}). The ν(C=O) of a mixed-ligand complex, [Ru(II)(hfa)(acac)], is assigned at 1583 for the hfa ring and 1579 cm^{-1} for the acac ring. These bands are shifted to 1550 and 1521 cm^{-1}, respectively, in the $[Ru(I)(hfa)(acac)]^-$ ion [615].

The following dimeric bridging structure has been proposed for [CoBr(acac)]$_2$:

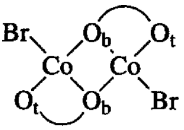

ν(CoO$_t$) and ν(CoO$_b$) were assigned at 435 and 260 cm^{-1}, respectively [616]. In [Ni(acac)$_2$]$_3$ and [Co(acac)$_4$]$_4$, the O atoms of the acac ion serve as a bridge between two metal atoms [617]. However, no band assignments on these polymeric species are available.

1.14.2. Complexes of Neutral Acetylacetone

In some compounds, the keto form of acetylacetone forms a chelate ring of type B:

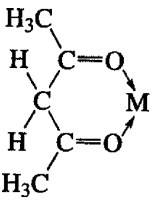

Type B

This particular type of coordination was found by van Leeuwen [618] in [Ni(acacH)$_3$](ClO$_4$)$_2$ and its derivatives, and by Nakamura and Kawaguchi [619] in Co(acacH)Br$_2$. These compounds were prepared in acidic or neutral media, and exhibit strong ν(C=O) bands near 1700 cm^{-1}. Similar ketonic coordination was proposed for Ni(acacH)$_2$Br$_2$ [620] and M(acacH)Cl$_2$ (M = Co,Zn) [621].

According to X-ray analysis [622], the acetylacetone molecule in Mn(acacH)$_2$Br$_2$ is in the enol form and is bonded to the metal as a unidentate via one of its O atoms:

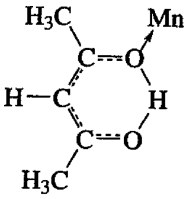

Type C

The C ⋯ O and C ⋯ C stretching bands of the enol ring were assigned at 1627 and 1564 cm^{-1}, respectively.

1.14.3. C-Bonded Acetylacetonato Complexes

Lewis and coworkers [623] reported the infrared and NMR spectra of a number of Pt(II) complexes in which the metal is bonded to the γ-carbon atom of the acetylacetonato ion:

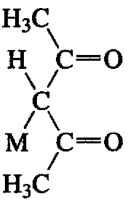

Type D

Behnke and Nakamoto carried out normal coordinate analysis on the $[Pt(acac)Cl_2]^-$ ion, in which the acac ion is chelated to the metal (type A) [624], and on the $[Pt(acac)_2Cl_2]^{2-}$ ion, in which the acac ion is C-bonded to the metal (type D) [625]. Table 1.33 lists the observed frequencies and band assignments for these two types, and Fig. 1.50 shows the infrared spectra of these two compounds. The results indicate that (1) two ν(C=O) of type D are higher than those of type A, (2) two ν(C−C) of type D are lower than those of type A, and (3) ν(PtC) of type D is at 567 cm^{-1}, while ν(PtO) of

TABLE 1.33. Observed Frequencies, Band Assignments, and Force Constants for $K[Pt(acac)Cl_2]$ and $Na_2[Pt(acac)_2C]_2]\cdot 2H_2O$

$K[Pt(acac)Cl_2]$ (O-Bonded, Type A)	$Na_2[Pt(acac)_2Cl_2]\cdot 2H_2O$ (C-Bonded, Type D)	Band Assignment
—	1652, 1626	ν(C=O)
1563, 1380	—	ν(C ⋯ O)
1538, 1288	—	ν(C ⋯ C)
—	1350, 1193	ν(C−C)
1212, 817	1193, 852	δ(CH) or π(cH)
650, 478	—	ν(PtO)
—	567	ν(PtC)
K(C ⋯ O) = 6.50	K(C=O) = 8.84	
K(C ⋯ C) = 5.23	K(C−C) = 2.52	UBF constant
K(C−CH_3) = 3.58	K(C−CH_3) = 3.85	(mdyn/Å)
K(Pt−O) = 2.46	K(Pt−C) = 2.50	
K(C−H) = 4.68	K(C−H) = 4.48	
$\rho = 0.43$[a]		

[a] The stretching–stretching interaction constant (ρ) was used for type A because of the presence of resonance in the chelate ring.

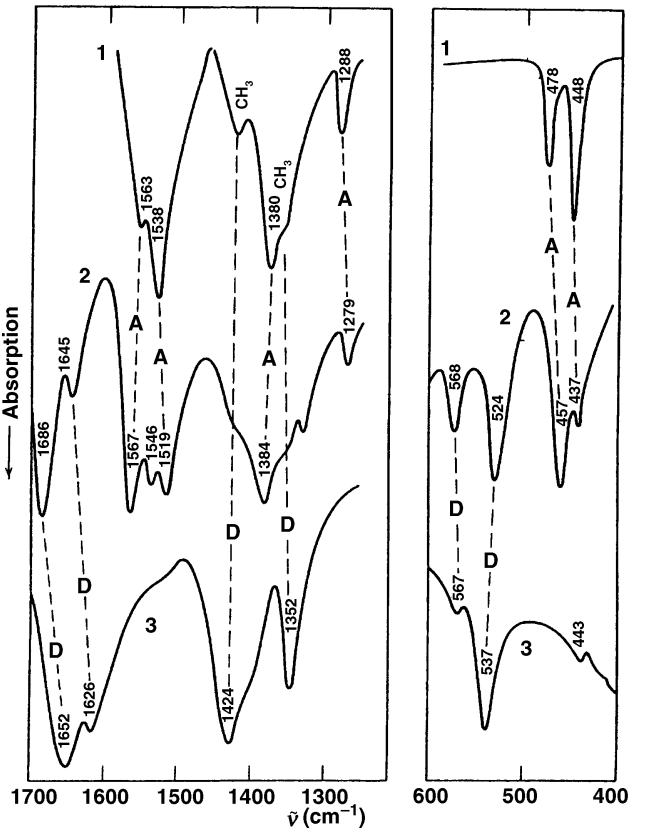

Fig. 1.50. *Infrared spectra of Pt(II) acetylacetonato complexes: (1) K[Pt(acac)Cl$_2$]; (2) K[Pt (acac)$_2$Cl]; (3) Na$_2$[Pt(acac)$_2$Cl$_2$]H$_2$O, where A and D denote the bands characteristic of types A and D, respectively [624,625].*

type A are at 650 and 478 cm^{-1}. Figure 1.50 also shows that the structure of K[Pt (acac)$_2$Cl] is as follows

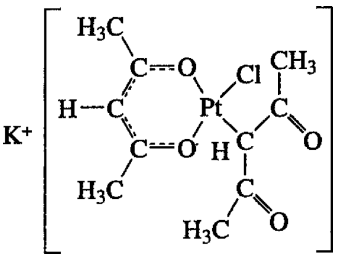

since its spectrum is roughly a superposition of those types A and D. Similarly, the infrared spectrum of K[Pt(acac)$_3$] [623] is interpreted as a superposition of spectra of types A, D, and D′, in which two C−O bonds are transoid [626]:

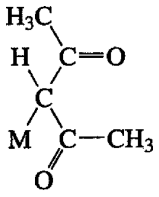

Type D′

The C-bonded acac ion was found in Hg_2Cl_2(acac) [627], Au(acac)(PPh_3), [628], and Pd(acac)$_2$(PPh_3) [629]. In the last compound, one acac group is type A and the other, type D. In all these cases, the ν(C=O) of the type D acac groups are at 1700–1630 cm^{-1}.

As discussed above, K[Pt(acac)$_2$Cl] contains one type A acac group and one type D acac group. If a solution of K[Pt(acac)$_2$Cl] is acidified, its type D acac group is converted into type E:

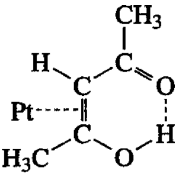

Type E

This structure was first suggested by Allen et al. [630], based on NMR evidence. Behnke and Nakamoto [631] showed that the infrared spectrum of [Pt(acac)(acacH)Cl] thus obtained can be interpreted as a superposition of spectra of types A and E.

That the two O atoms of the C-bonded acac group (type D) retain the ability to coordinate to a metal was first demonstrated by Lewis and Oldham [632], who prepared neutral complexes of the following type:

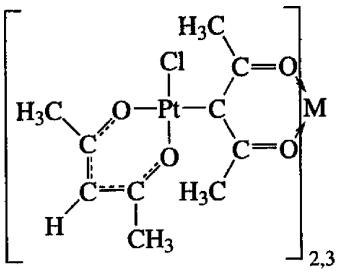

M = Co(II), Ni(II), Fe(III), etc.

Using the metal isotope technique, Nakamura and Nakamoto [633] assigned the ν(NiO) of Ni[Pt(acac)$_2$Cl]$_2$ at 279 and 266 cm^{-1}. These values are relatively close to

the ν(NiO) of $Ni(acacH)_2Br_2$ (264 and 239 cm^{-1}), discussed previously. Thus, the newly formed Ni-acac ring retains its keto character and is close to type B. Other types prepared by Kawaguchi and coworkers include the following:

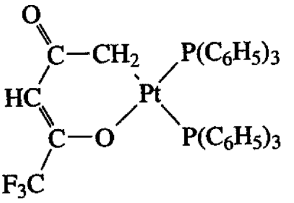

C,O-chelate[634]

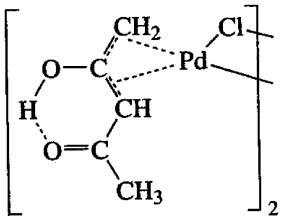

η^3-allylic[635]

Kawaguchi [636] reviewed the modes of coordination of β-diketones in a variety of metal complexes.

Gerisch et al. [637] determined the crystal structures of novel anionic tetranuclear platina-β-diketonates of platina-β-diketones, $\frac{1}{2}(BH)_2[Cl_2Pt(\mu\text{-}COMe)_2Pt(COMe)_2H)]_2$ (B = *n*-$BuNH_2$, NEt_3, etc.), shown below:

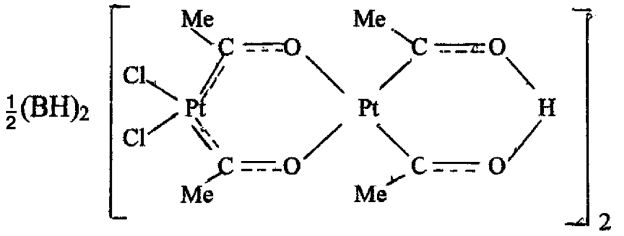

The IR spectra exhibit the ν(CO) of the bridging μ-acyl group in the platina-β-diketonato unit at 1524–1534 cm^{-1} and those of the platina-β-diketone unit, at 1552–1556 cm^{-1}.

1.14.4. Complexes of Other β-Diketones

In a series of metal tropolonato complexes, Hulett and Thornton [638] noted a parallel relationship between the ν(MO) and the CFSE energy. These workers assigned the ν(MO) of trivalent metal tropolonates in the 660–580 cm^{-1} region, based on the $^{16}O - {}^{18}O$ isotope shifts observed for the Cu(II) complex [639]. Using the metal

isotope technique, Hutchinson et al. [640] assigned the ν(MO) at the following frequencies (cm^{-1}):

V(III)		Cr(III)		Mn(III)		Fe(III)		Co(III)
377	$\sim$	361	$>$	338	$>$	317	$<$	371
319	$<$	334	$>$	268	$>$	260	$<$	360

It was found that these frequencies still follow the order predicted by the CFSE.

2,4,6-Heptanetrione forms 1 : 1 and 1 : 2 (metal: ligand) complexes with Cu(II) [641]:

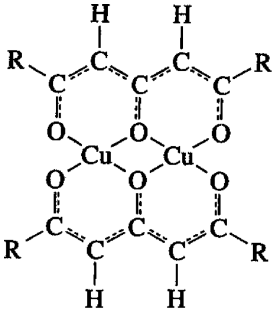

1:1 complex

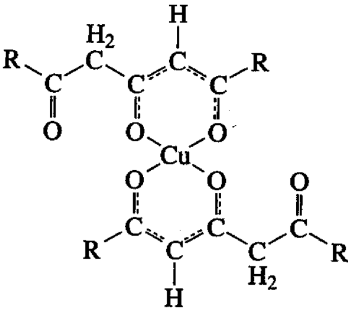

1:2 complex

Both complexes exhibit multiple bands due to type A rings in the 1600–1500 cm^{-1} region. However, the 1 : 2 complex exhibits ν(C=O) of the uncoordinated C=O groups near 1720 cm^{-1}.

1.15. COMPLEXES OF UREA, SULFOXIDES, AND RELATED LIGANDS

1.15.1. Complexes of Urea and Related Ligands

Penland et al. [642] first studied the infrared spectra of urea complexes to determine whether coordination occurs through nitrogen or oxygen. The electronic structure of urea may be represented by a resonance hybrid of structures I, II, and III, with each contributing roughly an equal amount:

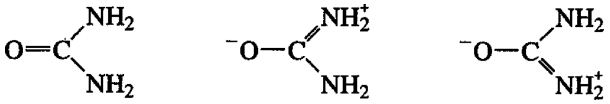

I II III

If coordination occurs through nitrogen, the contributions of structures II and III will decrease. This results in an increase of the CO stretching frequency with a decrease in the CN stretching frequency. The NH stretching frequency in this case may fall in the same range as the value for the amido complexes (Sec. 1.1). If coordination occurs

TABLE 1.34. Some Vibrational Frequencies of Urea and Its Metal Complexes (cm^{-1}) [642]

$[Pt(urea)_2Cl_2]$	Urea	$[Cr(urea)_6]Cl_3$	Predominant Mode
3390 3290	3500 3350	3440 3330	$\nu(NH_2)$, free
3130 3030		3190	$\nu(NH_2)$, bonded
1725	1683	1505[a]	ν(C=O)
1395	1471	1505[a]	ν_a(CN)

[a] ν(C=O) and ν(C−N) couple in the Cr complex.

through oxygen, the contribution of structure I will decrease. This may result in a decrease of the CO stretching frequency but no appreciable change in the NH stretching frequency. Since the spectrum of urea itself has been analyzed completely [643], band shifts caused by coordination can be checked immediately. The results shown in Table 1.34 indicate that coordination occurs through nitrogen in the Pt(II) complex, and through oxygen in the Cr(III) complex. It was also found that Pd(II) coordinates to the nitrogen, whereas Fe(III), Zn(II), and Cu(II) coordinate to the oxygen of urea. The infrared spectra of tetramethylurea (tmu) complexes of lanthanide elements, $[Ln(tmu)_6](ClO_4)_3$, indicate the presence of O-coordination [644]. Similar conclusions have been obtained for ThL_3Cl_4 (L = *N*,*N*′-dialkylurea) inasmuch as the ν(CO) is downshifted by 110–60 cm^{-1} on coordination [645].

The ν(Sn−O) vibrations of *cis*- and *trans*-$[Sn(dmu)_2Br_4]$ (dmu = 1,3-dimethylurea) have been assigned in the 405–397 cm^{-1} region [646].

From infrared studies on thiourea $[(NH_2)_2CS]$ complexes, Yamaguchi et al. [647] found that all the metals studied (Pt, Pd, Zn, and Ni) form M−S bonds, since the CN stretching frequency increases and the CS stretching frequency decreases on coordination, without an appreciable change in the NH stretching frequency. On the basis of the same criterion, thiourea complexes of Fe(II) [648], Mn(II), Co(II), Cu(I), Hg(II), Cd(II), and Pb(II) were shown to be S-bonded [649]. Several investigators [650–652] studied the far-infrared spectra of thiourea complexes and assigned the MS stretching bands between 300 and 200 cm^{-1}. For example, the ν(Te−S) vibrations of *cis*-[Te(thiourea)$_2Cl_2$] are observed at 276 and 262 cm^{-1} [653]. Thus far, the only metal reported to be N-bonded is Ti(IV) [654].

Infrared spectra of alkylthiourea complexes have also been studied. Lane and colleagues [655] studied the infrared spectra of methylthiourea complexes and concluded that methylthiourea forms M−S bonds with Zn(II) and Cd(II) and M−N bonds with Pd(II), Pt(II), and Cu(I). The ν(C=S) of $[ReO(Me_4tu)_4](PF_3)_3$ (Me_4tu = tetramethylthiourea) at 458 cm^{-1} is 30 cm^{-1} lower than that of the free ligand [656]. For other alkylthiourea complexes, see Refs. 657 and 658.

Infrared spectra of selenourea (su) complexes of Co(II), Zn(II), Cd(II), and Hg(II) exhibit ν(MSe) in the 245–167 cm^{-1} region [659]. The Raman spectra of $[Pd(su)_4]^{2+}$ and $[Pt(su)_4]^{2+}$ ions exhibit the A_{1g} ν(MSe) at 178 and 191 cm^{-1}, respectively [660].

Linkage isomerism was found for the formamidopentamminecobalt(III): $[(NH_3)_5Co(-NH_2CHO)]^{3+}$ and $[(NH_3)_5Co(-OCHNH_2)]^{3+}$. Although little difference was found in the ν(C=O) region, the N-isomer showed the aldehyde ν(CH) at 2700 cm^{-1}, whereas such a band was not obvious in the O-isomer [661].

1.15.2. Complexes of Sulfoxides and Related Compounds

Cotton et al. [662] studied the infrared spectra of sulfoxide complexes to see whether coordination occurs through oxygen or sulfur. The electronic structure of sulfoxides may be represented by a resonance hybrid of these structures:

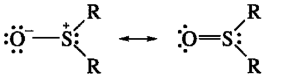

IV V

If coordination occurs through oxygen, the contribution of structure V will decrease and result in a decrease in ν(S=O). If coordination occurs through sulfur, contribution of structure IV will decrease and may result in an increase in ν(S=O). It has been concluded that coordination occurs through oxygen in the $Co(DMSO)_6^{2+}$ ion, since the ν(S=O) of this ion absorbs at 1100–1055 cm^{-1}. On the other hand, coordination may occur through sulfur in $PdCl_2(DMSO)_2$ and $PtCl_2(DMSO)_2$, since ν(S=O) of these compounds (1157–1116 cm^{-1}) are higher than the value for the free ligand. Other ions such as Mn(II), Fe(II,III), Ni(II), Cu(II), Zn(II), and Cd(II) are all coordinated through oxygen, since the DMSO complexes of these metals exhibit ν(S=O) between 960 and 910 cm^{-1}. Drago and Meek [663], however, assigned ν(S=O) of O-bonded complexes in the 1025–985 cm^{-1} region, since they are metal sensitive. The bands between 960 and 930 cm^{-1}, which were previously assigned to ν(S=O) are not metal-sensitive and assigned to $\rho_r(CH_3)$. Even so, ν(S=O) of O-bonded complexes are lower than the value for free DMSO. To confirm ν(S=O) assignments, it is desirable to compare the spectra of the corresponding DMSO-d_6 complexes since $\rho_r(CD_3)$ is outside the ν(S=O) region. Table 1.35 lists ν(S=O) of typical compounds.

Wayland and Schramm [664] found the first example of mixed coordination of DMSO in the $[Pd(DMSO)_4]^{2+}$ ion; it exhibits two S-bonded ν(S=O) at 1150 and 1140 cm^{-1}, and two O-bonded ν(S=O) at 920 and 905 cm^{-1}. Thus, the infrared spectrum is most consistent with a configuration in which two S-bonded and two O-bonded DMSO are in the *cis* position. The infrared and NMR spectra of $Ru(DMSO)_4Cl_2$ suggested a mixing of O- and S-coordination; ν(S=O) at 1120 and 1090 cm^{-1} for S-coordination and at 915 cm^{-1} for O-coordination [674]. X-Ray analysis [675] has since shown that two Cl atoms are in the *cis* positions of an octahedron and the remaining positions are occupied by one O-bonded and three S-bonded DMSO ligands. Infrared spectra show that all DMSO ligands in $Ru(DMSO)_3Cl_3$ are O-bonded while O- and S-bonded DMSO ligands are mixed in $M(DMSO)_3Cl_3$ (M = Os,Rh) [676]. In contrast, all the DMSO ligands are S-bonded in the *fac*-isomer of $RuCl_3(DMSO)_3$ but O- and S-bonded DMSO ligands are mixed in the *mer*-isomer [677]. In *mer*,*cis*-$RuCl_3(DMSO)_2(NH_3)$, one DMSO that is *trans* to

TABLE 1.35. SO Stretching Frequencies of DMSO Complexes (cm^{-1})

Compound	ν(S=O)	Bonding	Ref.
$Sn(DMSO)_2Cl_4$	915	O	664
$[Cr(DMSO)_6](ClO_4)_3$	928	O	664
$[Ni(DMS0)_6](ClO_4)_2$	955	O	664
$[Ln(DMSO)_8](ClO_4)_3$, (Ln = La, Ce, Pr, Nd)	998–992	O	665
$[Al(DMSO)_6]X_3$, (X = Cl, Br, I)	1000–1008	O	666
$CdAg_6I_8(DMSO)_8$	1000	O	667
$[Ru(NH_3)_5(DMSO)](PF_6)_2$	1045	S	668
trans-$[Pd(DMSO)_2Cl_2]$	1116	S	669
cis-$[Pt(DMSO)_2Cl_2]$	1135 1160	S	670
cis-$[PtCl_2$(quinoline) (DMSO)]	1120	S	671
$[Pt(R_2SO)\ (\mu\text{-Cl})Cl]_2$[a]	1142	S	672
cis-$RuCl_2\ [CH_3C(CH_2S\text{-}Et)_3]$ (DMSO)	1080	S	673

[a] $R = C_2H_5$.

the NH_3 is S-bonded, and the other DMSO, which is *trans* to the Cl, is O-bonded. These two DMSO ligands exhibit the ν(S=O) at 1088 and 910 cm^{-1}, respectively [678]:

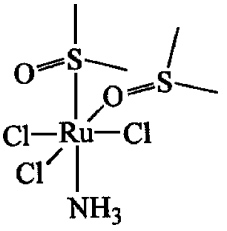

In *trans,cis,cis*-$[Ru(CO)(DMSO)_3Cl_2]$, two DMSO ligands *trans* to Cl are S-bonded while one DMSO ligand *trans* to CO is O-bonded. The former exhibits the ν(S=O) and ν(Ru−S) at 1134 and 422 cm^{-1}, respectively, whereas the latter exhibits the ν(S=O) and ν(Ru−O) at 924 and 472 cm^{-1}, respectively [679]. The first example of a rare double-bridging Ru(II) complex of DMSO, $[Ru_2(\mu\text{-Cl})(\mu\text{-DMSO})Cl_3(DMSO)_3(CO)_2]$, contains three S-bonded and one bridging DMSO ligands. The two Ru(II) atoms are connected via a Cl bridge as well as via a Ru−S−O−Ru bridge by forming a five-membered ring. The ν(S=O) of the terminal S-bonded DMSO are at 1141 and 1107 and that of the bridging DMSO is at 1010 cm^{-1} [680].

Interaction of DMSO with lanthanide perchlorates in anhydrous CH_3CN has been studied by FTIR and Raman spectroscopy [681]. The magnitude of downshifts of the ν(S=O) increases with the increasing atomic number of the Ln(III) ion from −49 to −58 cm^{-1}. In free $(CF_3)_2SO$, the ν(S=O) is at 1242 cm^{-1}. This band is shifted to 1130 cm^{-1} (IR) in $[\{(CF_3)_2SO\}XeF]SbF_6$, indicating O-coordination of the sulfrane ligand [682].

Complete assignments on infrared and Raman spectra of *trans*-$Pd(DMSO)_2X_2$ (X = Cl,Br) and their deuterated analogs have been made by Tranquille and Forel

[683]. Berney and Weber [684] found the order of ν(MO) in the $[M(DMSO)_6]^{n+}$ ion to be as follows:

	M =	Cr(III)		Ni(II)		Co(II)		Zn(II)		Fe(II)		Mn(II)
ν(MO)	(cm^{-1})	529	>	444	>	436	>	431	>	438 415	>	418

Griffiths and Thornton [685] made band assignments of these DMSO complexes based on d_6 and ^{18}O substitution of DMSO.

Ligands such as DPSO (diphenylsulfoxide) and TMSO (tetramethylenesulfoxide) do not exhibit the CH_3 rocking bands near 950 cm^{-1}. Thus, the SO stretching bands of metal complexes containing these ligands can be assigned without difficulty. In a series of O-bonded DMSO and TMSO complexes, the S=O stretching force constant decreases linearly as the M−O stretching force constant increases [686]. Table 1.36 lists the SO stretching frequencies and the magnitude of band shifts in DPSO complexes [560]. Van Leeuwen and Groeneveld [687] noted that the shift becomes larger as the electronegativity of the metal increases. In Table 1.36, the metals are listed in the order of increasing electronegativity.

In $[M(DTHO_2)_3]^{2+}$ [M = Co(II), Ni(II), Mn(II), etc.], the metals are O-bonded since the ν(S=O) of free ligand (1055–1015 cm^{-1}) are shifted to lower frequencies by 40–22 cm^{-1}:

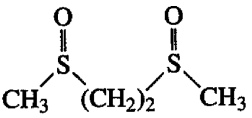

2,5-Dithiahexane-2,5-dioxide ($DTHO_2$)

On the other hand, the metals are S-bonded in $M(DTHO_2)Cl_2$ [M = Pt(II), Pd(II)] since ν(S=O) are shifted to higher frequencies by 108–77 cm^{-1} [688]. Dimethylselenoxide, $(CH_3)_2Se{=}O$, forms complexes of the MCl_2,$(DMSeO)_n$ type, where M is Hg(II), Cd

TABLE 1.36. Shifts of SO Stretching Bands in DPSO and DMSO Complexes (cm^{-1}) [687]

	DPSO Complex		DMSO Complex
Metal	ν(SO)	Shift	Shift
Ca(II)	1012–1035	0– (–23)	—
Mg(II)	1012	–23	—
Mn(II)	983–991	–45	–41
Zn(II)	987–988	–47	—
Fe(II)	987	–48	—
Ni(II)	979–982	–55	–45
Co(II)	978–980	–56	–51
Cu(II)	1012, 948	–23, –87	–58
Al(III)	942	–93	—
Fe(III)	931	–104	—

(II), Cu(II), and so on, and n is 1, $1\frac{1}{2}$, or 2. The ν(Se=O) of the free ligand (800 cm^{-1}) is shifted to the 770–700 cm^{-1} region, indicating the O-bonding in these complexes [689].

1.16. CYANO AND NITRILE COMPLEXES

1.16.1. Cyano Complexes

The vibrational spectra of cyano complexes have been studied extensively and these investigations are reviewed by Sharp [690], Griffith [691], Rigo and Turco [692], and Jones and Swanson [693].

1.16.1.1. CN Stretching Bands Cyano complexes can be identified easily since they exhibit sharp ν(CN) at 2200–2000 cm^{-1}. The ν(CN) of free CN^- is 2080 cm^{-1} (aqueous solution). On coordination to a metal, the ν(CN) shift to higher frequencies, as shown in Table 1.37. The CN^- ion acts as a σ-donor by donating electrons to the metal and also as a π-acceptor by accepting electrons from the metal. σ-Donation tends to raise the ν(CN) since electrons are removed from the 5σ orbital, which is weakly antibonding, while π-backbonding tends to decrease the ν(CN) because the electrons enter into the antibonding $2p\pi^*$ orbital. In general, CN^- is a better σ-donor and a poorer π-acceptor than is CO. Thus, the ν(CN) of the complexes are generally higher than the value for free CN^-, whereas the opposite prevails for the CO complexes (Sec. 1.18).

According to El-Sayed and Sheline [702], the ν(CN) of cyano complexes are governed by (1) the electronegativity, (2) the oxidation state, and (3) the

TABLE 1.37. C≡N Stretching Frequencies of Cyano Complexes (cm^{-1})

Compound	Symmetry	ν(CN)	Ref.
$Tl[Au(CN)_2]$	$\mathbf{D}_{\infty h}$	2164 ($\sum_g^+$), 2141 ($\sum_u^+$)	694,695
$K[Ag(CN)_2]$	$\mathbf{D}_{\infty h}$	2146 ($\sum_g^+$), 2140 ($\sum_u^+$)	696
$K_2[Ni(^{12}C^{14}N)_4]$	$\mathbf{D}_{4h}$	2143.5 (A_{1g}), 2134.5 (B_{1g}), 2123.5 (E_u)	697
$K_2[Pd(^{12}C^{14}N)_4]$	$\mathbf{D}_{4h}$	2160.5 (A_{1g}), 2146.4 (B_{1g}), 2135.8 (E_u)	697
$K_2[Pt(^{12}C^{14}N)_4]$	$\mathbf{D}_{4h}$	2168.0 (A_{1g}), 2148.8 (B_{1g}), 2133.4 (E_u)	697
$Na_3[Ni(CN)_5]$	$\mathbf{C}_{4v}$	2130(A_1), 2117 (B_1), 2106 (E), 2090 (A_1)	698
$Na_3[Co(CN)_5]$	$\mathbf{C}_{4v}$	2115 (A_1), 2110 (B_1), 2096 (E), 2080 (A_1)	698
$K_3[Mn(CN)_6]$	$\mathbf{O}_h$	2129 (A_1), 2129 (E_g), 2112 (F_{1u})	699,700
$K_4[Mn(CN)_6]$	$\mathbf{O}_h$	2082 (A_{1g}), 2066 (E_g), 2060 (F_{1u})	699
$K_3[Fe(CN)_6]$	$\mathbf{O}_h$	2135 (A_{1g}), 2130 (E_g), 2118 (F_{1u})	699
$K_4[Fe(CN)_6]\cdot 3H_2O$	$\mathbf{O}_h$	2098 (A_{1g}), 2062 (E_g), 2044 (F_{1u})	699
$K_3[Co(CN)_6]$	$\mathbf{O}_h$	2150 (A_{1g}), 2137 (E_g), 2129 (F_{1u})	699
$K_4[Ru(CN)_6]\cdot 3H_2O$	$\mathbf{O}_h$	2111 (A_{1g}), 2071 (E_g), 2048 (F_{1u})	699
$K_3[Rh(CN)_6]$	$\mathbf{O}_h$	2166 (A_{1g}), 2147 (E_g), 2133 (F_{1u})	699
$K_2[Pd(CN)_6]$	$\mathbf{O}_h$	2185 (F_{1u})	701
$K_4[Os(CN)_6]\cdot 3H_2O$	$\mathbf{O}_h$	2109 (A_{1g}), 2062 (E_g), 2036 (F_{1u})	699
$K_3[Ir(CN)_6]$	$\mathbf{O}_h$	2167 (A_{1g}), 2143 (E_g), 2130 (F_{1u})	699

coordination number of the metal. The effect of electronegativity is seen in the following order:

$$\underset{2128}{[Ni(CN)_4]^{2-}} < \underset{2143}{[Pd(CN)_4]^{2-}} < \underset{2150}{[Pt(CN)_4]^{2-}} \quad cm^{-1}$$

Since the electronegativity of Ni(II) is smallest, the σ-donation will be the least, and the ν(CN) is expected to be the lowest. The effect of oxidation state is seen in the following frequency order [703]:

$$\underset{1910}{[V(CN)_6]^{5-}} < \underset{2065}{[V(CN)_6]^{4-}} < \underset{2077}{[V(CN)_6]^{3-}} \quad cm^{-1}$$

The higher the oxidation state, the stronger the σ-bonding, and the higher the ν(CN). The effect of coordination number [704] is evident in the frequency order:

$$\underset{2092}{[Ag(CN)_4]^{3-}} < \underset{2105}{[Ag(CN)_3]^{2-}} < \underset{2135}{[Ag(CN)_2]^{-}} \quad cm^{-1}$$

Here an increase in the coordination number results in a decrease in the positive charge on the metal, which, in turn, weakens the σ-bonding, thus decreasing the ν(CN). The ν(CN) of $A_3[M(CN)_6]$-type salts (M = Fe,Co) are sensitive to the nature of the counterion (A). Thus, Fernandez-Beltran et al. [705] used this fact to examine the CN ligand–counterion interaction quantitatively.

Other cyano complexes that are not included in Table 1.37 are $Na[Cu(CN)_2]2H_2O$ (polymeric chain) [706], $Na_2[Cu(CN)_3]\cdot 3H_2O$ ($\mathbf{D}_{3h}$) [707], $Cs[Hg(CN)_3]$ ($\mathbf{D}_{3h}$) [708], $K_2[Zn(CN)_4]$ ($\mathbf{T}_d$) [709], $(Bu_4N)[B(CN)_4]$ ($\mathbf{T}_d$) [710] and $[PPN]_2[Mn(II)(CN)_4]$ (PPN: $[PH_2P{=}N{=}PPh_2]^+$)($\mathbf{T}_d$) [711].

The symmetry of the $[Mo(CN)_7]^{4-}$ ion may be $\mathbf{D}_{5h}$ [712] or $\mathbf{C}_{2v}$ [713]. The pentagonal–bipyramidal structure ($\mathbf{D}_{5h}$) has been proposed for $[Re(CN)_7)]^{4-}$ [714], $[Tc(CN)_7]^{4-}$ [715], and $[W(CN)_7]^{5-}$ [716] on the basis of their IR and Raman spectra in either the solid state, solution, or both. According to X-ray analysis [717], the $[Mo(CN)_8]^{4-}$ ion in $K_4[Mo(CN)_8]\cdot 2H_2O$ is definitely $\mathbf{D}_{2d}$ (dodecahedron). On the other hand, a Raman study [718] supported the $\mathbf{D}_{4d}$ (archimedean–antiprism) structure of the $[Mo(CN)_8]^{4-}$ ion in aqueous solution. The stereochemical conversion of the $[Mo(CN)_8]^{4-}$ ion from $\mathbf{D}_{2d}$ (solid) to $\mathbf{D}_{4d}$ (solution) symmetry was confirmed by Hartman and Miller [719] and Parish et al. [720]. Similar conversions were proposed for the $[W(CN)_8]^{4-}$ [719,720], and $[Nb(CN)_8]^{4-}$ [721] ions. However, Long and Vernon [722] claim that the $\mathbf{D}_{2d}$ geometry is maintained even in aqueous solution. Both X-ray and Raman studies confirm the $\mathbf{D}_{2d}$ structure for $K_5[Nb(CN)_8]$ in the solid state, although the $\mathbf{D}_{4d}$ structure prevails in solution [723].

According to the results of X-ray analysis [724], the unit cell of $[Cr(en)_3]$-$[Ni(CN)_5]\cdot 1\frac{1}{2}H_2O$ contains both square–pyramidal ($\mathbf{C}_{4v}$) and trigonal–bipyramidal ($\mathbf{D}_{3h}$) structures of the $[Ni(CN)_5]^{3-}$ ion. Terzis et al. [725] showed that the complicated vibrational spectrum of this crystal in the ν(CN) region is simplified

dramatically when it is dehydrated. These spectral changes suggest that the $\mathbf{D}_{3h}$ (somewhat distorted) units have been converted to $\mathbf{C}_{4v}$ geometry on dehydration. Basile et al. [726] showed that such conversion from $\mathbf{D}_{3h}$ to $\mathbf{C}_{4v}$ also occurs when the crystal is subjected to high pressure. Hellner et al. [727] observed the splitting of the degenerate ν(CN) of $K_2[Zn(CN)_4]$ and a partial reduction of the central metal in $K_3[M(CN)_6]$ [M = Fe(III), Mn(III)] when these crystals are under high external pressure.

Penneman and Jones [704] made an extensive infrared study of the equilibria of cyano complexes in aqueous solution. (For aqueous infrared spectroscopy, see Sec. 1.11.) Figure 1.51 shows the infrared spectra of aqueous silver cyano complexes obtained by changing the ratio of Ag^+ to CN^- ions.

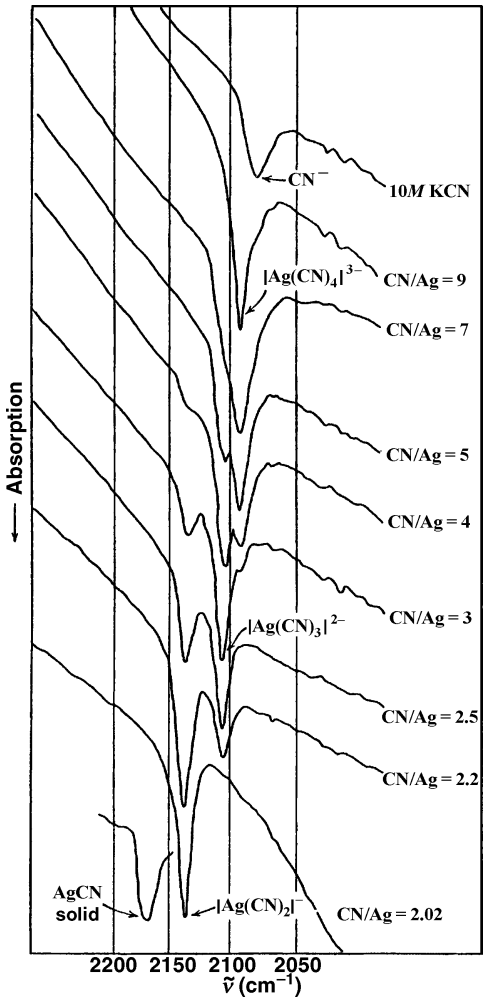

Fig. 1.51. *Infrared spectra of silver cyano complexes in aqueous solutions.*

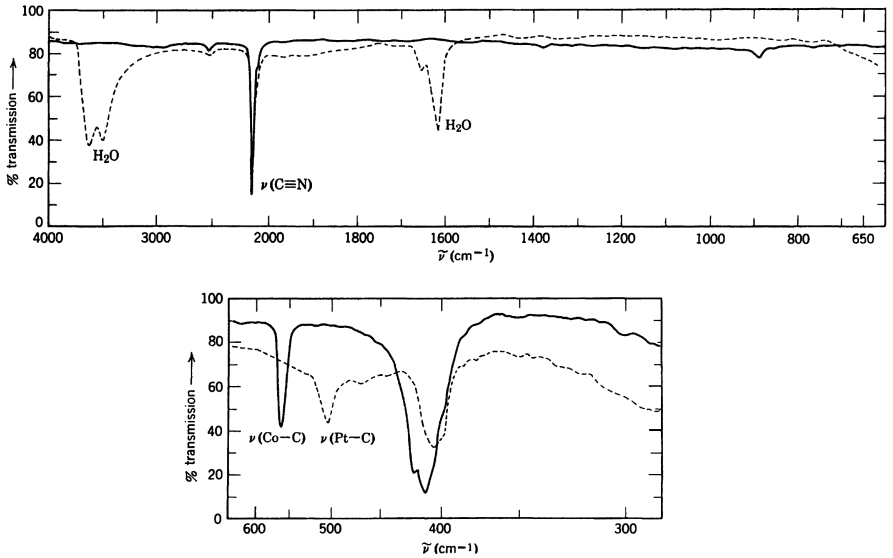

Fig. 1.52. *Infrared spectra of $K_3[Co(CN)_6]$ (solid line) and $K_2[Pt(CN)_4]\cdot 3H_2O$ (broken line).*

1.16.1.2. Lower-Frequency Bands In addition to ν(CN), the cyano complexes exhibit ν(MC), δ(MCN), and δ(CMC) bands in the low-frequency region Figure 1.52 shows the infrared spectra of $K_3[Co(CN)_6]$ and $K_2[Pt(CN)_4]\cdot 3H_2O$. Normal coordinate analyses have been carried out on various hexacyano complexes to assign these low-frequency bands (Table 1.38). The results of these calculations indicate that the ν(MC), δ(MCN), and δ(CMC) vibrations appear in the regions 600–350, 500–350, and 130–60 cm^{-1}, respectively. The MC and C≡N stretching force constants obtained are also given in Table 1.38.

Nakagawa and Shimanouchi [730] noted that the MC stretching force constant increases in the order Fe(III) < Co(III) < Fe(II) < Ru(II) < Os(II), and the C≡N stretching force constant decreases in the same order of metals. This result was interpreted as indicating that the M−C π-bonding increases in the above-mentioned order. The degree of M−C π-bonding may be proportional to the number of d-electrons in the t_{2g} electronic level. According to Jones [731], the integrated absorption coefficient of the C≡N stretching band (F_{1u}) becomes larger as the number of d-electrons in the t_{2g} level increases. Thus the results shown in Table 1.39 suggest that the M−C π-bonding increases in the order Cr(III) < Mn(III) < Fe(III) < Co(III). The order of ν(MC) shown in the same table confirms this conclusion. Griffith and Turner [699] found a similar trend in the Fe(II) < Ru(II) < Os(II) series. Nakagawa and Shimanouchi [732] carried out complete normal coordinate analyses on $K_3[M(CN)_6]$ [M = Fe(III),Cr(III)] crystals, including all lattice modes. Jones et al. [733] also performed complete normal coordinate analyses on crystalline $Cs_2Li[Fe(CN)_6]$, including its ^{13}C, ^{15}N, and ^{6}Li analogs.

TABLE 1.38. Vibrational Frequencies and Band Assignments of Hexacyano Complexes (cm^{-1})

	$[Cr(CN)_6]^{3-}$	$[Co(CN)_6]^{3-}$	$[Ir(CN)_6]^{3-}$	$[Rh(CN)_6]^{3-}$	$[Co(CN)_6]^{3-}$	$[Fe(CN)_6]^{4-}$	$[Fe(CN)_6]^{3-}$	$[Ru(CN)_6]^{4-}$	$[Os(CN)_6]^{4-}$
A_{1g} ν(MC)	374	408	469	445	406	(410)	(390)	(460)	(480)
E_g ν(MC)	336	(391)	450	435	(375)	(390)	—	(410)	(450)
F_{1g} δ(MCN)	536	(358)	(415)	(380)	(380)	(350)	—	(340)	(360)
F_{1u} δ(MC)	457	564	520	520	565	585	511	550	554
δ(MCN)	694	416	398	386	414	414	387	376	392
δ(CMC)	124	(84)	(82)	(88)	—	—	89	—	—
F_{2g} δ(MCN)	536	(480)	483	(475)	—	(420)	—	(400)	(430)
δ(CMC)	106	98	95	94	98	—	99	—	—
F_{2u} δ(MCN)	496	(440)	445	—	(395)	—	—	(365)	(390)
δ(CMC)	95	(72)	(69)	—	—	—	70	—	—
Force field	GVF	GVF	GVF	GVF	UBF	UBF	UBF	UBF	UBF
K(M−C) (mdyn/Å)	1.928	2.063	2.704	2.366	2.308	2.428	1.728	2.793	3.343
K(C≡N) (mdyn/Å)	16.422	16.767	16.678	16.831	16.5	15.1	17.0	15.3	14.9
References	728	729	729	729	730	730	730	730	730

TABLE 1.39. Relation between Infrared Spectrum and Electronic Structure in Hexacyano Complexes [731]

Compound	Number of *d*-Electrons in t_{2g} Level	ν(CN) (cm^{-1})	ν(MC) (cm^{-1})	Integrated Absorption Coefficient ($mol^{-1}\,cm^{-2}$)
$K_3[Cr(CN)_6]$	3	2128	339	2,100
$K_3[Mn(CN)_6]$	4	2112	361	8,200
$K_3[Fe(CN)_6]$	5	2118	389	12,300
$K_3[Co(CN)_6]$	6	2129	416	18,300

Normal coordinate analyses have been made on tetrahedral, square–planar, and linear cyano complexes of various metals; Table 1.40 gives the results of these studies. Far-infrared spectra of various cyano complexes have been measured [745]. An ultraviolet–infrared study [746] showed that the $[Ni(CN)_4]^{2-}$ and $[Ni(CN)_5]^{3-}$ ions are in equilibrium in a solution containing $Na_2[Ni(CN)_4]$, KCN, and KF. The

TABLE 1.40. Frequencies and Band Assignments of the Lower-Frequency Bands of Cyano Complexes (cm^{-1})

Ion	Symmetry	ν(MC)	δ(MCN)	δ(CMC)	Force Constant[a] K(M−C)	Force Constant[a] K(C≡N)	Ref.
$[Cu(CN)_4]^{3-}$	$\mathbf{T}_d$	364(IR) 288(R)	324(R) 306(IR)	(74) (63)	1.25 – 1.30	16.10 – 16.31	734 735
$[Zn(CN)_4]^{2-}$	$\mathbf{T}_d$	359(IR)[b] 342(R)	315(IR)[b] 230(R)	71(R)	1.30	17.22	736 709
$[Cd(CN)_4]^{2-}$	$\mathbf{T}_d$	316(IR)[b] 324(R)	250(R)[b] 194(R)	61(R)	1.28	17.13	736
$[Hg(CN)_4]^{2-}$	$\mathbf{T}_d$	330(IR)[b] 335(R)	235(R)[b] 180(R)	54(R)	1.53	17.08	736
$[Pt(CN)_4]^{2-}$	$\mathbf{D}_{4h}$	505(IR) 465(R) 455(R)	318(R) 300(IR)	95(R)	3.425	16.823	737 738
$[Ni(CN)_4]^{2-}$	$\mathbf{D}_{4h}$	543(IR) (419) (405)	433(IR) 421(IR) 488(IR)	(54)	2.6	16.67	739
$[Au(CN)_4]^{-}$	$\mathbf{D}_{4h}$	462(IR) 459(R) 450(R)	(325) 415(IR)	110(R)	3.28 – 3.42	17.40 – 17.44	740
$[Hg(CN)_2]$	$\mathbf{D}_{\infty h}$	442(IR) 412(R)	341(IR) 275(R)	(100)	2.607	17.62	741 742
$[Ag(CN)_2]^{-}$	$\mathbf{D}_{\infty h}$	390(IR) (360)	(310) 250(R)	(107)	1.826	17.04	743
$[Au(CN)_2]^{-}$	$\mathbf{D}_{\infty h}$	427(IR) 445(R)	(368) 305(R)	(100)	2.745	17.17	744

[a]Force constants (mdyn/Å) were obtained by using the GVF field for all ions except the $[Pt(CN)_4]^{2-}$ ion, for which the UBF field was used.

[b]Coupled vibrations between ν(MC) and δ(MCN).

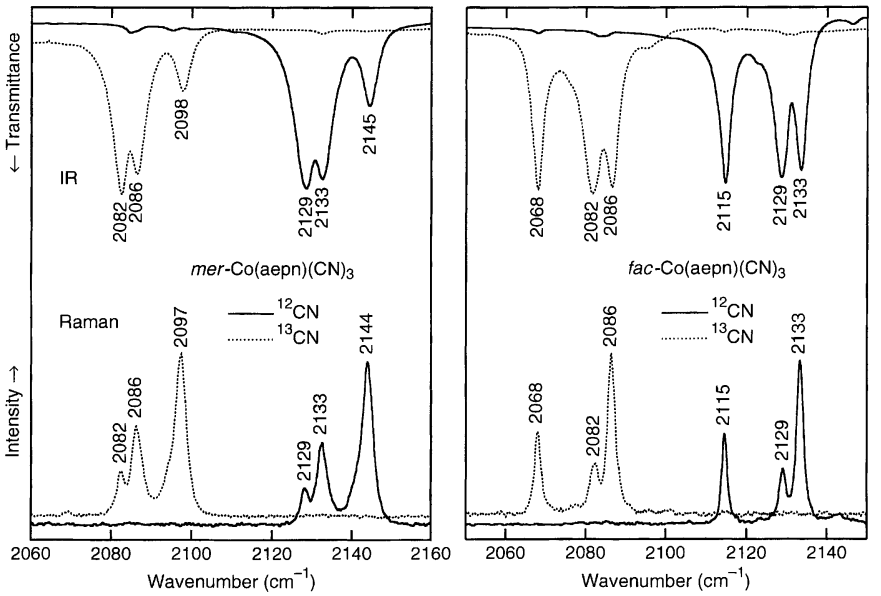

Fig. 1.53. *IR and Raman spectra of mer- and fac-Co(aepn)(^{12}CN)$_3$ and their ^{13}CN isotopomers [753].*

integrated absorption coefficient of the C≡N stretching band increases in the order Hg (II) < Ag(I) < Au(I) in linear dicyano complexes, indicating that the M−C π-bonding increases in the same order [731]. From the measurements of infrared dichroism, Jones determined the orientation of $[Ag(CN)_2]^-$ and $[Au(CN)_2]^-$ ions in their potassium salts [743,744]. His results are in good agreement with those of X-ray analysis.

Vibrational spectra are reported for a number of cyano complexes of mixed ligands. Some examples are $[Au(CN)_2X_2]^-$ [747], $K_2[Pt(CN)_4X_2]$ [748], and $K_2[Pt(CN)_5X]$ ($X = Cl^-$, Br^-, I^-) [749], and $Na_3[Fe(II)(CN)_5(CO)]\cdot 2H_2O$ [750]. Complete band assignments including $^{54}Fe/^{56}Fe$, $^{12}C/^{13}C$, $^{14}N/^{15}N$ isotope shift data coupled with normal coordinate analysis [751] and DFT calculations [752] were made for $Na_2[Fe(CN)_5(NO)]\cdot 2H_2O$. Chun et al. [753] synthesized two stereoisomers, *fac*- and *mer*-{Co $(CN)_3$(aepn)] [aepn = *N*-(2-aminoethyl)-l,3-propanediamine]. Figure 1.53 compares the IR and Raman spectra of the two isomers and their ^{13}C analogs in the high-frequency region. Both complexes exhibit three ν(CN) bands, indicating approximate $\mathbf{C}_s$ symmetry.

1.16.1.3. Bridged Cyano Complexes If the M−C≡N group forms a M−C≡N−M′-type bridge, ν(C≡N) shifts to a higher, and ν(MC) to a lower, frequency. The higher-frequency shift of ν(C≡N) should be noted since the opposite trends are observed for bridging carbonyl and halogeno complexes. Shriver [754] observed that ν(C≡N) of $K_2[Ni(CN)_4]$ at 2130 cm^{-1} shifts to 2250 cm^{-1} in $K_2[Ni(CN)_4]\cdot 4BF_3$ because of the formation of the Ni−C≡N−BF_3-type bridge. They [755] also found that, for $KFeCr(CN)_6$, the green isomer containing the Fe(II)−C≡N−Cr(III) bridges exhibits ν(C≡N) at 2092 cm^{-1}, while the red isomer containing the

Cr(III)−C≡N−Fe(II) bridges shows ν(C≡N) at 2168 and 2114 cm^{-1}. Brown et al. [756] studied the mechanism of conversion from green to red isomer by combining infrared and Mössbauer spectroscopy with other techniques. The ν(C≡N) and ν(Fe−C) of crystalline $Cs_2Mg[Fe(CN)_6]$ are higher by 40 cm^{-1} than those of the $[Fe(CN)_6]^{4-}$ ion in aqueous solution [757]. The same trend is seen for crystalline $Mn_3[Co(CN)_6]\cdot xH_2O$ and the $[Co(CN)_6]^{3-}$ ion in aqueous solution [758]. These observations suggest the presence of strong interaction of the Fe−C≡N···Mg or Co−C≡N···Mn type in the solid state. The bridging ν(C≡N) of the $[(NC)_5Fe^{II}-CN-Co^{III}(CN)_5]^{6-}$ and $[(NC)_5Fe^{III}-CN-Co^{III}(CN)_5]^{5-}$ ions are at 2130 and 2185 cm^{-1}, respectively [759]. The infrared and Mössbauer spectra of $K_4[Fe(CN-SbX_3)_6]$ (X = F,Cl) and $K_4[Fe(CN-SbX_3)_4(CN)_2]$ (X = Cl,Br) have been studied [760]. As expected, the infrared spectrum of Prussian blue is identical to that of Turnbull's blue [761].

The Pt(II) and Cu(II) atoms in $[(CN)_3Pt(\mu\text{-}CN)Cu(NH_3)_4]$ are linked by a bent CN bridge (CN−Cu angle, ∼ 120°), and the terminal ν(CN) are at 2157–2121 while the bridging ν(CN) is at 2181 cm^{-1} [762]. The crystal structures of CN bridged polymers of the compositions, $(NBu_4)[Cu(I)(CN)X]$ (X = Br,I) and $(NBu_4)[Cu(I)_3(CN)_4]\cdot CH_3CN$ have been determined; the former takes a one-dimensional polymeric chain structure, whereas the latter forms two-dimensional polymer sheets. The low-frequency skeletal vibrations such as ν(Cu−X) and ν(Cu−CN) of these polymers have been assigned [763]. Vibrational spectra of CN bridging complexes containing mixed-valence metal atoms are reported for $K_5[(NC)_5M(II)-CN-Ru(III)(EDTA)]$ (M = Fe, Ru,Os) [764], $[(H_3N)_5Ru(III)-NC-Os(II)(CN)_5]^-$ [765], $[(NC)_5Fe(III)-CN–Pt(II)(NH_3)_4-NC-Fe(III)(CN)_5]^{4-}$ [766], and $[(H_3N)_5Pt(IV)-CN-Fe(II)(CN)_5]$ [767]. The ν(CN) frequencies are reported for the former three complexes, and the low-frequency modes were assigned for the last complex.

Partially oxidized tetracyanoplatinates such as $K_2[Pt(CN)_4]Br_{0.3}\cdot 3H_2O$ are known as one-dimensional (linear chain) conductors [768]. In these compounds, the planar $Pt(CN)_4^{2-}$ ions are stacked in one direction, and the Pt···Pt distances (2.88 Å) are much shorter than that of the parent compound, $K_2[Pt(CN)_4]\cdot 3H_2O$ (3.478 Å), The oxidation state of the Pt atom in $K_2[Pt(CN)_4]Br_{0.33}\cdot 3H_2O$ is +2.33. As a result, its ν(CN) [2182(A_{1g}), 2165(B_{1g}) cm^{-1}] are between those of $K_2[Pt^{II}(CN)_4]\cdot 3H_2O$ (2168, 2149 cm^{-1}) and $K_2[Pt^{IV}(CN)_4Cl_2]$ (2196 and 2186 cm^{-1}) [769]. Vibrational spctra of cyano complexes containing metal–metal bonds are reported For $[(NC)_5Pt(III)-Pt(III)(CN)_5]^{4-}$ [770] and $[(NC)_5Pt(II)-Tl(III)(CN)_n]^{n-}$ (n = 1,2,3) [771]. The Raman spectrum of the former exhibits the ν(Pt−Pt), ν(Pt−C) (equatorial) and ν(Pt−C) (axial) at 145, 467, and 400 cm^{-1}, respectively. The Raman spectra of the latter series in aqueous solution exhibit the ν(Pt−Tl) at 163.7, 162.6, and 159.1 cm^{-1} for n = 1, 2, and 3, respectively.

1.16.2. Nitrile and Isonitrile Complexes

Nitriles (R−C≡N, R = alkyl or phenyl) form a number of metal complexes by coordination through their N atoms. Again, ν(CN) becomes higher on complex formation. For example, Walton [772] measured the infrared spectra of $MX_2(RCN)_2$-type compounds, where M is Pt(II) and Pd(II) and X is Cl^- and Br^-.

When R is phenyl, the ν(CN) are near 2285 cm^{-1}, which is higher than the value for the ν(CN) of free benzonitrile (2231 cm^{-1}). It was noted that the ν(CN) of benzonitrile (2231 cm^{-1}) shifts to a higher frequency (2267 cm^{-1}) when it coordinates to the pentammine Ru(III) species but to a lower frequency (2188 cm^{-1}) when coordinated to the pentammine Ru(II) species. This result may indicate that the latter species has unusually strong π-backbonding ability [773]. Similarly, the ν(CN) of $[(NH_3)_5Os(III)(NC{-}CH_3)]^{3+}$ (2300 cm^{-1}) is higher and that of $[(NH_3)_5Os(II)(NC{-}CH_3)]^{2+}$ (2200 cm^{-1}) is lower than the ν(CN) of free acetonitrile (2254 cm^{-1}) [774]. The totally symmetric ν(M–N) vibrations of $[M(NC{-}CH_3)_4]^{2+}$ were assigned at 440 and 430 cm^{-1}, respectively, for M = Pt(II) and Pd(II) [775]. A strong band at 174 cm^{-1} of $ZnCl_2(CH_3CN)_2$ was suggested to be ν(ZnN) [776]. The ν(MN) bands of other acetonitrile complexes have been assigned in the 450–160 cm^{-1} region [777].

In solution, $Fe(PEt_3)_2(CO)_2(Et{-}C{\equiv}N)$ exists as a mixture of the following isomers:

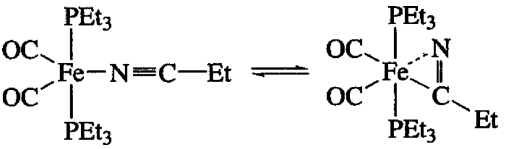

The end-on and side-on isomers exhibit the ν(CN) at 2112 and 1625 cm^{-1}, respectively [778]. The latter frequency is extremely low because of its η^2-bonding. This type of bonding is also found in $Mo(Cp)_2(CH_3CN)$, which exhibits the ν(CN) at 1725 cm^{-1} [779].

Farona and Kraus [780] observed ν(CN) of $Mn(CO)_3(NC{-}CH_2{-}CH_2{-}CN)Cl$ at 2068 cm^{-1}, although ν(CN) of free succinonitrile (sn) is at 2257 cm^{-1}. This large shift to a lower frequency was attributed to the chelating bidentate coordination through its CN triple bonds:

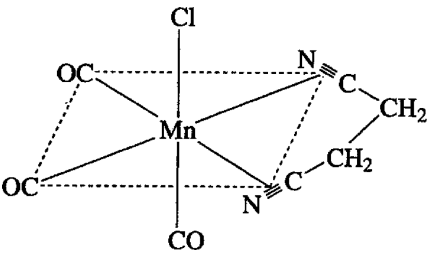

According to X-ray analysis [781], the complex ion in $[Cu(sn)_2]NO_3$ takes a polymeric chain structure in which the ligand is in the *gauche* conformation:

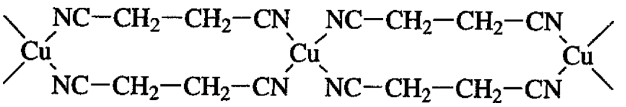

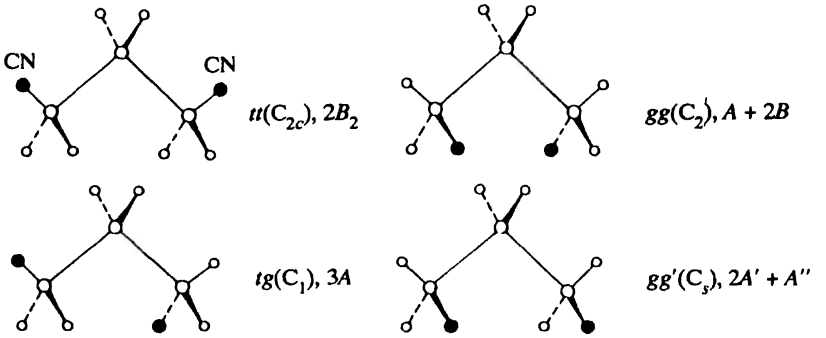

Fig. 1.54. *Rotational isomers of glutaronitrile.*

In these dinitrile complexes, ν(CN) are shifted to higher frequencies on coordination. As in the case of ethylenediamine complexes (Sec. 1.2), infrared spectroscopy has been used to determine the conformation of the ligand in metal complexes. The Cu(I) complex, which is known to contain the *gauche* conformation, exhibits two CH_2 rocking modes at 966 and 835 cm^{-1}, whereas the Ag(I) complex, $Ag(sn)_2BF_4$, shows a single CH_2 rocking mode at 770 cm^{-1}, which is characteristic of the *trans* conformation [782].

There are four rotational isomers for glutaronitrile (gn), $NC-CH_2-CH_2-CH_2-CN$, which are spectroscopically distinguishable. Figure 1.54 shows the conformation, the symmetry, and the number of infrared-active CH_2 rocking vibrations for each isomer. According to X-ray analysis on $Cu(gn)_2NO_3$ [783], the ligand in this complex is in the *gg* conformation. The infrared spectrum of this complex is very similar to that of solid glutaronitrile in the stable form. Matsubara [784] therefore concluded that the latter also takes the *gg* conformation. However, the spectrum of solid glutaronitrile in the metastable form (produced by rapid cooling) is different from that of the *gg* conformation and it could have been *tt*, *tg*, or *gg′*. The *tt* conformation was excluded because of the absence of the 730 cm^{-1} band characteristic of the *trans*-planar methylene chain [785], and the *gg′* conformation was considered to be improbable because of steric repulsion between two CN groups. This left only the *tg* conformation for the metastable solid. The complicated spectrum of liquid glutaronitrile was accounted for by assuming that it is a mixture of the *tg*, *gg*, and *tt* conformations. Kubota and Johnston [786], using these results, have been able to show that the glutaronitrile molecules in $Ag(gn)_2ClO_4$ and $Cu(gn)_2ClO_4$ are in the *gg* conformation, while those in $TiCl_4gn$ and $SnCl_4gn$ have the *tt* confonnation. Table 1.41 summarizes the CH_2 rocking frequencies of glutaronitrile and its metal complexes. An infrared study similar to the above has been extended to adiponitrile [$NC-(CH_2)_4-CN$] and its Cu(I) complex [787].

Cotton and Zingales [788] studied the N≡C stretching bands of isonitrile complexes. When isonitriles are coordinated to zero-valence metals such as Cr(O), backdonation of electrons from the metal to the ligand is extensive and the N≡C stretching band is shifted to a lower frequency. For monopositive and dipositive metal ions, little or no backdonation occurs and the N≡C stretching band is shifted to a higher

TABLE 1.41. Infrared-Active CH_2 Rocking Frequencies of Glutaronitrile and Its Metal Complexes (cm^{-1})

Liquid[a]	945 (*tg*)	904 (*gg*)	835 (*tg, gg*)	757 (*tg, gg*)	737 (*tt*)[b]
Solid (metastable)	943 (*tg*)	—	839 (*tg*)	757 (*tg*)	—
Solid[a] (stable)	—	903 (*gg*)	837 (*gg*)	768 (*gg*)	—
$Cu(gn)_2NO_3$[a]	—	913 (*gg*)	830 (*gg*)[c]	778 (*gg*)	—
$Cu(gn)_2ClO_4$[d]	—	908 (*gg*)	875 (*gg*)	767 (*gg*)	—
$Ag(gn)_2ClO_4$[d]	—	904 (*gg*)	872 (*gg*)	772 (*gg*)	—
$SnCl_4(gn)$[d]	—	—	—	—	733 (*tt*)
$TiCl_4(gn)$[d]	—	—	—	—	730 (*tt*)

[a]Reference 784.
[b]The *tt* form should exhibit two infrared-active CH_2 rocking vibrations. The other one is not known, however.
[c]Overlapped with a NO_3^- absorption.
[d]Reference 786.

frequency as a result of the inductive effect of the metal ion. Sacco and Cotton [789] obtained the infrared spectra of $Co(CH_3NC)_4X_2$- and $[Co(CH_3NC)_4][CoX_4]$-type compounds (X = Cl, Br, etc.). Dart et al. [790] report the ν(NC) of bis(phosphine) tris (isonitrile) complexes of Co(I). Boorman et al. [791] made rather complete assignments of vibrational spectra of some isonitrile complexes of Co(I) and Co(II) in the 4000–33 cm^{-1} region. Nitrile and isonitrile ligands are mixed in *trans*, *trans*, *trans*-$[Ru(II)Cl_2(-NCR)_2(-CNR')_2]$ (R = methyl/phenyl and R′ = *t*-buthyl, xylyl or cyclohexyl), and their $\nu(-NC)$ and $\nu(-CN)$ vibrations are observed at 2121–2150 and 2251–2291 cm^{-1}, respectively [792].

1.17. THIOCYANATO AND OTHER PSEUDOHALOGENO COMPLEXES

The CN^-, OCN^-, SCN^-, $SeCN^-$, CNO^-, and N_3^- ions are called *pseudohalide ions*, since they resemble halide ions in their chemical properties. These ions may coordinate to a metal through either one of the end atoms. As a result, the following linkage isomers are possible:

M−CN, cyano complex	M−NC, isocyano complex
M−OCN, cyanato complex	M−NCO, isocyanato complex
M−SCN, thiocyanato complex	M−NCS, isothiocyanato complex
M−SeCN, selenocyanato complex	M−NCSe, isoselenocyanato complex
M−CNO, fulminato complex	M−ONC, isofulminato complex

Two compounds are called *true linkage isomers* if they have exactly the same composition and two of the different linkages mentioned above. A well-known example is nitro (and nitrito) pentammine Co(III) chloride, discussed in Sec. 1.6. A pair of true linkage isomers is difficult to obtain since, in general, one form is much more stable than the other. As will be shown later, a number of new linkage isomers have been isolated, and infrared spectroscopy has proved to be very useful in distinguishing them. Burmeister [793] reviewed linkage isomerism in

metal complexes. Bailey et al. [794] and Norbury [795] reviewed the infrared spectra of SCN, SeCN, NCO, and CNO complexes and their linkage isomers in detail.

1.17.1. Thiocyanato (SCN) Complexes

The SCN group may coordinate to a metal through the nitrogen or the sulfur or both (M−NCS−M′). In general, class A metals (first transition series, such as Cr, Mn, Fe, Co, Ni, Cu, and Zn) form M−N bonds, whereas class B metals (second half of the second and third transition series, such as Rh, Pd, Ag, Cd, Ir, Pt, Au, and Hg) form M−S bonds [796]. However, other factors, such as the oxidation state of the metal, the nature of other ligands in a complex, and steric consideration, also influence the mode of coordination.

Several empirical criteria have been developed to determine the bonding type of the NCS group in metal complexes.

(1) The CN stretching frequencies are generally lower in N-bonded complexes (near and below 2050 cm^{-1}) than in S-bonded complexes (near 2100 cm^{-1}) [797]. The bridging (M−NCS−M′) complexes exhibit ν(CN) well above 2100 cm^{-1}. However, this rule must be applied with caution since ν(CN) are affected by many other factors [794].

(2) Several workers [798,799] considered ν(CS) as a structural diagnosis: 860–780 cm^{-1} for N-bonded, and 720–690 cm^{-1} for S-bonded, complexes. However, this band is rather weak and is often obscured by the presence of other bands in the same region.

(3) It was suggested [798,799] that the N-bonded complex exhibits a single sharp δ(NCS) near 480 cm^{-1}, whereas the S-bonded complex shows several bands of low intensity near 420 cm^{-1}. However, these bands are also weak and tend to be obscured by other bands.

(4) Several workers [800–802] used the integrated intensity of ν(CN) as a criterion; it is larger than $9 \times 10^4 M^{-1} cm^{-2}$ per NCS^- for N-bonded complexes, and close to or smaller than $2 \times 10^4 M^{-1} cm^{-2}$ for S-bonded complexes. However, this rule is also difficult to apply when the spectrum consists of multiple components or when the dissociation occurs in solution.

(5) Some workers [803,804] proposed using ν(MN) and ν(MS) in the far-infrared region as a criterion; in general, ν(MN) is higher than ν(MS). However, these frequencies are very sensitive to the overall structure of the complex and the nature of the central metal. Thus extreme caution must be taken in applying this criterion.

It is clear that only a combination of these five criteria would provide reliable structural diagnosis. Table 1.42 lists the vibrational frequencies of typical isothiocyanato and thiocyanato complexes. The ν(MN) and ν(MS) vibrations of some of these and other complexes were assigned by using metal isotopes [808] and ^{15}N-substituted

TABLE 1.42. Vibrational Frequencies of Isothiocyanato and Thiocyanato Complexes (cm^{-1})[a]

Compound	ν(CN)	ν(CS)	δ(NCS)	Ref.
K[NCS]	2053	748	486, 471	513 [Chapter 2 (Part A)]
$(NEt_4)_2[Co(-NCS)_4]$	2062 (s)	837 (w)	481 (m)	794
$K_3[Cr(-NCS)_6]$	2098 (vs)	820 (vw)	474 (s)	805
	2058 (vs)			
$(NEt_4)_2[Cu(-(NCS)_4]$	2074 (s)	835 (w)	—	806
$(NEt_4)_3[Fe(-NCS)_6]$	2098 (sh)	822 (w)	479 (m)	794
	2052 (s)			
$(NEt_4)_4[Ni(-NCS)_6]$	2109 (sh)	818 (w)	469 (m)	794
	2102 (s)			
$(NEt_4)_2[Zn(-NCS)_4]$	2074 (s)	832 (w)	480 (m)	794
$(NH_4)[Ag(-SCN)_2]$	2101 (s)	718 (w)	453 (m)	794
	2086 (s)			
$K[Au(-SCN)_4]$	2130 (s)	700 (w)	458 (w)	794
			413 (s)	
$K_2[Hg(-SCN)_4]$	2134 (m)	716 (m)	461 (m)	794
	2122 (sh)	709 (sh)	448 (m)	
	2109 (s)	703 (sh)	432 (sh)	
			419 (m)	
$(NBu_4)_3[Ir(-SCN)_6]$	2127 (m)	822 (m)	430 (w)	807
	2098 (s)	693 (w)		
$K_2[Pd(-SCN)_4]$	2125 (s)	703 (w)	474 (w)	794
	2095 (s)	697 (sh)	467 (w)	
			442 (m)	
			432 (m)	
$K_2[Pt(-SCN)_4]$	2128 (s)	696 (w)	477 (w)	794
	2099 (s)		469 (w)	
	2077 (sh)		437 (m)	
			426 (m)	

[a]vs = very strong; s = strong; m = medium; w = weak; sh = shoulder.

ligands [809]. Figure 1.55 shows the IR and Raman spectra of $(TBA)_3$ $[Ru(NCS)_6]$ (TBA = tetrabutylammonium ion) obtained by Fricke and Preetz [810]. Bütje and Preetz [811] obtained the IR and Raman spectra of all 10 isomeric complexes of $[Os(NCS)_n(SCN)_{6-n}]^{3-/2-}$ ($n = 0$–6). Preetz and coworkers also reported the vibrational spectra of N-bonded NCS complexes of Re(IV) [812,813] and Os(IV) [814,815] complexes, and S-bonded $[Pt(-SCN)_6]^{2-}$ [816], $[Ir(-SCN)_6]^{3-}$ [817], and $[Os(-SCN)_6]^{3-}$ [818]. Karbowiak et al. [819] assigned the IR and Raman spectra of $(Et_4N)_4[M(-NCS)_7]$ (M = U, Nd) In the $[M(NCS)_4]^{2-}$ (M = Zn,Cd,Hg) series, aqueous Raman studies by Yamaguchi et al. [820] show that all the ligands are N-bonded in the Zn and S-bonded in the Hg complexes, but both types coexist in the Cd complex. The Raman spectra of $Cd(NCS)_2$ dissolved in DMSO suggests that the Cd atom is S-bonded in this case [821].

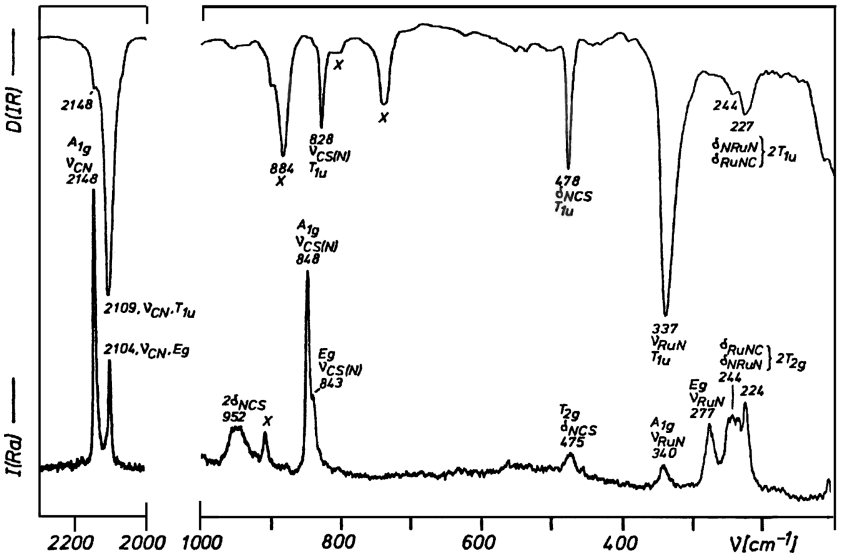

Fig. 1.55. *Infrared and Raman spectra of $(TBA)_3[Ru(NCS)_6]$; the symbol × indicates the TBA (tetrabutylammonium ion) band [810].*

Clark and Williams [803] measured the infrared spectra of tetrahedral $M(NCS)_2L_2$, monomeric octahedral $M(NCS)_2L_4$, and polymeric octahedral $M(NCS)_2L_2$-type complexes (M = Fe, Co, Ni, etc.; L = py, α-pic, etc.), and studied the relationship between the spectra and stereochemistry. They found that ν(CS) are higher by 40–50 cm^{-1} for tetrahedral than for octahedral complexes for the same metal, although ν(CN) are very similar for both.

The *cis*- and *trans*-isomers of $[Co(en)_2(NCS)_2]Cl \cdot H_2O$, for example, can be distinguished by infrared spectra in the ν(CN) region: *trans*, 2136 cm^{-1}; *cis*, 2122 and 2110 cm^{-1} [822]. Lever et al. [823] have found, however, that no splittings of ν(CN) are observed at room temperature for *cis*-octahedral $ML_2(NCS)_2$, where M is Co(II) and Ni(II) and L is 1,2-bis-(2′-imidazolin-2′-yl)benzene. The splitting of ν(CN) of this complex was observed only at liquid-nitrogen temperature.

Turco and Pecile [824] noted that the presence of other ligands in a complex influences the mode of the NCS bonding. For example, in $Pt(NCS)_2L_2$, the NCS ligand is N-bonded if L is a phosphine (π-acceptor), and is S-bonded if L is an amine. In the solid state, $Ni(NCS)_2(PMePh_2)_2$ is N-bonded (*trans*) but its Pd analog is S-bonded (*trans*), and the Pt analog is N-bonded (*cis*) [825]. For $[Cr(NCS)_4L_2]^{n-}$ ions, Contreras and Schmidt [826] proposed, on the basis of the ν(CN) and ν(CS) of these ions, N-bonding for L = urea, glycinate ion, and so on, and S-bonding for L = thiourea, acetamide, and so on. These results have been explained in terms of the steric and electronic effects of L.

TABLE 1.43. Vibrational Frequencies of True Linkage Isomers Involving the NCS Group (cm^{-1})

Compound	Type	ν(CN)	ν(CS)	Ref.
trans-$[Pd(AsPh_3)_2(NCS)_2]$	N-bonded	2089	854	827–829
	S-bonded	2119	—	
$Pd(bipy)(NCS)_2$	N-bonded	2100	842	830,828
	S-bonded	2117 2108	700	
(π-Cp)$Mo(CO)_3(NCS)$	N-bonded	2099	—	831
	S-bonded	2114	699	
$K_3[Co(CN)_5(NCS)]$	N-bonded	2065	810	832
	S-bonded	2110	718	
trans-$[Co(DMG)_2(py)(NCS)]$	N-bonded	2128	—	833
	S-bonded	2118	—	

A variety of true linkage isomers involving the NCS group have been prepared. Table 1.43 lists the ν(CN) and ν(CS) of typical pairs of these linkage isomers. Epps and Marzilli [834] isolated three linkage isomers of $AsPh_4[Co(DMG)_2(NCS)_2]$:

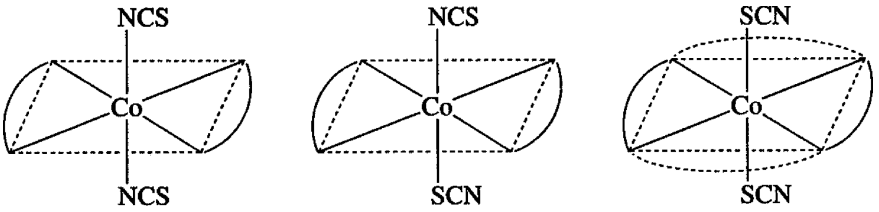

Although all these isomers exhibit ν(CN) at 2110 cm^{-1}, they can be distinguished by the differences in the intensity of the ν(CN) band; the (NCS,NCS) isomer is the strongest, the (SCN,SCN) isomer is the weakest, and the (NCS,SCN) isomer is in between. Preetz and coworkers also reported the vibrational spectra of true linkage isomers for $[OsCl_5(-NCS)]^{2-}$ [835], $OsBr_5(-NCS)]^{2-}$ [836], and $[ReCl_5(-NCS)]^{2-}$ [837].

Both N-bonded and S-bonded NCS ligands are mixed in *cis*- and *trans*-$[ReBr_4(NCS)(SCN)]^{2-}$ [838], *trans* -$[IrCl_2(NCS)(SCN)_3]^{3-}$ [839] [Pd(4,4′-dimethyl-bipy)(NCS)(SCN)] [840], [Pd{$Ph_2P(CH_2)_3NMe_2$}(NCS)(SCN)] [841], and other Pd complexes [842,843]. Similar mixed NCS−SCN bonding was found for [PdL(NCS)(SCN)], where L is $Ph_2P(o\text{-}C_6H_4)AsPh_2$ and $Ph_2P(CH_2)_2NMe_2$ [844]. These bidentate ligands contain two different donor atoms that give different electronic effects on the NCS groups *trans* to them. Thus, the *trans* effect, together with the steric effect of these ligands, may be responsible for the mixing of the N- and S-bonding. Using the ν(CS) as a marker, Coyer et al. [845] have shown that the yellow isomer of $Pt(bipy)(SCN)_2$ containing two *cis*, S-bonded ligands is converted into the red isomer with two *cis*, N-bonded ligands. This "flip" can occur by heating in solution or in the solid state. In the case of $[Ni(DPEA)(NCS)_2]_2$[DPEA = di(2-pyridyl-β-ethyl)amine], IR spectra suggest that terminal N-bonded and bridging NCS groups are mixed [ν(CN) = 2094 and 2128 cm^{-1}, respectively] [846].

Burmeister et al. [847] found that in the ML_2X_2-type complexes [M = Pd(II),Pt(II); L = a neutral ligand; X = SCN, SeCN, NCO, etc.], the mode of bonding of X to the metal is determined by the nature of the solvent. For example, $Pd(AsPh_3)_2(NCS)_2$ is N-bonded in pyridine and acetone solution, whereas it is S-bonded in DMF and DMSO solution. However, the bonding of the NCO group is insensitive to the nature of the solvent.

The NCS group also forms a bridge between two metal atoms. The CN stretching frequency of a bridging group is generally higher than that of a terminal group. For example, $HgCo(NCS)_4$(Co−NCS−Hg) absorbs at 2137 cm^{-1}, whereas $(NEt_4)_2$[Co(−NCS)$_4$] absorbs at 2065 cm^{-1}. According to Chatt and Duncanson [848], the CN stretching frequencies of Pt(II) complexes are 2182–2150 cm^{-1} for the bridging and 2120–2100 cm^{-1} for the terminal NCS group. [$(P(n\text{-}Pr)_3)_2Pt_2(SCN)_2Cl_2$] (compound I) exhibits one bridging CN stretching, whereas [$(P(n\text{-}Pr)_3)_2Pt_2(SCN)_4$] (compound II) exhibits both bridging and terminal CN stretching bands. Thus the IR spectra suggest that the structure of each compound is as follows:

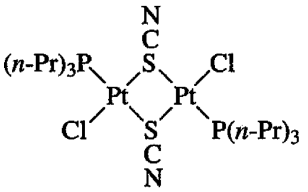

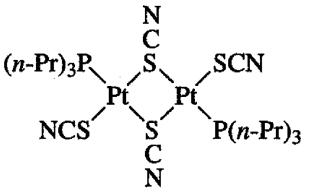

(*n*-pr = *n*-propyl)

I II

Compound I, however, exhibits as two isomers, α and β, which absorb at 2162 and 2169 cm^{-1}, respectively. Chatt and Duncanson [848] originally suggested a geometric isomerism in which two SCN groups were in a *cis* or *trans* position with respect to the central ring. Later [849–851], "bridge isomerism" of end-to-end type such as the following was found by X-ray analysis:

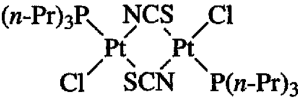

α β

The IR spectra of metal complexes containing bridging NCS groups have been reported for $Sn(NCS)_2$ [852], $M(py)_2(NCS)_2$[M = Mn(II),Co(II),Ni(II)] [853], $[Me_3Pt(NCS)]_4$ [854], and M[$Pt(SCN)_6$] [M = Co(II), Ni(II), Fe(II), etc.] [855].

According to X-ray analysis [856], the $[Re_2(NCS)_{10}]^{3-}$ ion contains solely N-bonded bridging thiocyanate groups that exhibit ν(CN) near 1900 cm^{-1}.

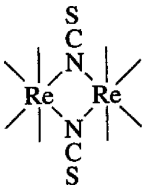

(All terminal NCS groups are also N-bonded.)

In polymeric bridging complex, $[Cu(dach)(\mu\text{-}NCS)(NCS)]_n$, (dach = 1,4-diazacycloheptane), the Cu(dach)(−NCS) units are connected via the novel single NCS bridge of the end-to-end type, and exhibits the ν(CN) at 2140 and 2088 cm^{-1} [857].

1.17.2. Selenocyanato (SeCN) Complexes

The SeCN group also coordinates to a metal through the nitrogen (M−NCSe) or the selenium (M−SeCN) or both (M−NCSe−M′). Again, class A metals tend to form M−N bonds, while class B metals prefer to form M−Se bonds. Although the number of SeCN complexes studied is much smaller than that of SCN complexes, these studies suggest the following trends:

(1) ν(CN) is below 2080 cm^{-1} for N-bonded, but higher for Se-bonded complexes. The ν(CN) of a bridged complex $[HgCo(NCSe)_4]$ is at 2146 cm^{-1} [858].
(2) The ν(CSe) is at 700–620 cm^{-1} for N-bonded and at 550–500 cm^{-1} for Se-bonded complexes.
(3) The δ(NCSe) of N-bonded complexes are above 400 cm^{-1}, whereas Se-bonded complexes show at least one component of δ(NCSe) below 400 cm^{-1}.
(4) The integrated intensity of ν(CN) is larger for the N-bonded than for the Se-bonded group [859].

Table 1.44 lists the observed frequencies of typical N-bonded and Se-bonded complexes.

Burmeister and Gysling [864] observed that in $[PdL_2(SeCN)_2]$-type compounds the effect of changing the π-bonding ability and basicity of L on the Pd−SeCN bonding is

TABLE 1.44. Vibrational Frequencies of Isoselenocyanato and Selenocyanato Complexes (cm^{-1})

Compound[a]	ν(CN)	ν(CSe)	δ(NCSe)	Ref.
K[NCSe]	2070	558	424, 416	514 [Chapter 2 (Part A)]
$R_2[Mn(-NCSe)_6]$	2079, 2082 2070	640 617	424	859
$R_2[Fe(-NCSe)_4]$	2067, 2055	673, 666	432	859
$R_4[Ni(-NCSe)_6]$	2118, 2102	625	430	859
$[Ni(pn)_2(-NCSe)_2]$	2096, 2083	692	—	860
$R'_2[Co(-NCSe)_4]$	2053	672	433, 417	861
$[Co(NH_3)_5(-NCSe)](NO_3)_2$	2116	624	—	862
$R_2[Zn(-NCSe)_4]$	2087	661	429	859
$[Cu(pn)_2(-SeCN)_2]$	2053, 2028	—	—	860
$R_3[Rh(-SeCN)_6]$	2104, 2071	515	—	859
$R''_2[Pd(-SeCN)_4]$	2114, 2105	521	410,374	863
$R_2[Pt(-SeCN)_4]$	2105, 2060	516	—	859
$[Pt(bipy)(-SeCN)_2]$	2135, 2125	532, 527	—	862
$K_2[Pt(-SeCN)_6]$	2130	519	390, 379 367	861

[a] R = $[N(n\text{-}C_4H_9)_4]'$; R′ = $[N(C_2H_5)_4]'$; R″ = $[N(CH_3)_4]'$; pn = propylenediamine; bipy = 2,2′-bipyridine.

negligible in contrast to the analogous SCN complexes. A pair of true linkage isomers has been isolated and characterized by infrared spectra for [(π-Cp)Fe(CO)(PPh_3)(SeCN) [865] and [Pd(Et_4dien)(SeCN)]BPh_4 [866], where Et_4dien is 1,1,7,7-tetraethyldiethylenetriamine. Vibrational spectra of osmium complexes containing −NCSe and −SeCN ligands have been reported by Preetz and coworkers [867,868]. Their work was extended to *mer*-$[ReCl_3(NCSe)_2{}^{cis}(SeCN)]^{2-}$ [869], $[ReCl_4(NCSe)(SeCN)]^{2-}$ [870], and $M(SeCN)_4]^{2-}$ (M = Pd,Pt) [871]. The IR spectra of $[Ru(NH_3)_5(NCSe)]I_2\cdot 2H_2O$ and its true linkage isomer, $[Ru(NH_3)_5(SeCN)]I_2\cdot 2H_2O$, are reported [872].

1.17.3. Cyanato (OCN) Complexes

The OCN group may coordinate to a metal through the nitrogen (M−NCO) or the oxygen (M−OCN) or both. Thus far, the majority of complexes are reported to be N-bonded. Table 1.45 lists the observed frequencies of N-bonded NCO groups in typical complexes; v_a(NCO) and v_s(NCO) denote vibrations consisting mainly of v(CN) and v(CO), respectively.

Other N-bonded complexes include $ML_2(NCO)_2$ [M = Pd(II),Pt(II); L = NH_3, py, etc.] [881], In(III)$(NCO)_3L_3$ (L = py, DMSO, etc.) [882], and *mer*-[Re(III)$(NCO)_3$($PMe_2Ph)_3$] [883]. Forster and Horrocks [874] carried out normal coordinate analyses

TABLE 1.45. Vibrational Frequencies of Isocyanato Complexes (cm^{-1})

Compound	v_a(NCO)[b]	v_s(NCO)[b]	δ(NCO)	Refs.
K[NCO]	2155	1282, 1202	630	512 [Chapter 2 (Part A)]
$Si(NCO)_4$	2284	1482	608, 546	873
$Ge(NCO)_4$	2247	1426	608, 528	873
$[Zn(NCO)_4]^{2-}$	2208	1326	624	874
$[Mn(NCO)_4]^{2-}$	2222	1335	623	875,876
$[Fe(NCO)_4]^{2-}$	2182	1337	619	875,876
$[Co(NCO)_4]^{2-}$	2217, 2179	1325	620, 617	875,876
$[Ni(NCO)_4]^{2-}$	2237, 2186	1330	619, 617	875
$[Fe(NCO)_4]^{-}$	2208, 2171	1370	626, 619	875
$[Pd(NCO)_4]^{2-}$	2200 –, 2190	1319	613, 604, 594	877
$[Sn(NCO)_6]^{2-}$	2270, 2188	1307	667, 622	877
$[Zr(NCO)_6]^{2-}$	2205	1340	628	878
$[Mo(OCN)_6]^{3-}$	2205	1296, 1140	595	879
$Ln(NCO)_6]^{3-,a}$	2190	1333	633	880

[a] Ln = Yb or Lu.

[b] The notations v_a and v_b are used because the separation of the v(NC) and v(CO) is not distinct.

on $Zn(NCX)_4^{2-}$ (X = O, S, or Se). Complete vibrational assignments are available for the IR spectra of $Zn(NCO)_2L_2$, where L is NH_3 or pyridine [884].

Thus far, O-bonded structures have been suggested for $[M(OCN)_6]^{n-}$ [M = Mo (III),Re(IV),Re(V)] [879]. Anderson and Norbury [885] prepared the first example of linkage isomers: yellow $Rh(PPH_3)_3(NCO)$ and orange $Rh(PPh_3)_3(OCN)$. The integrated ν(CN) intensity of the former is smaller than that of the free ion, whereas the intensity of the latter is larger than that of the free ion. Also, the latter exhibits two δ(OCN) at 607 and 590 cm^{-1}, whereas the former shows only one band at 592 cm^{-1}. An electron diffraction study shows that the previously reported structure of $F_5Se-NCO$ is not correct; it is $F_5Se-OCN$, with the ν_2(NCO) and ν_s(NCO) occurring at 2290 and 1104 cm^{-1}, respectively [886].

Bridging NCO groups may take one of the following structures:

I

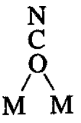

II

III

Structure I has been proposed for $ML_2(NCO)_2$ (M = Mn,Fe,Co,Ni; L = 3- or 4-CN-py) [887] and $Re_2(CO)_8(NCO)_2$ [888] Thus far, II is not known. Structure III has been proposed for $[(NH_3)_5Cr(NCO)Cr(NH_3)_5]Cl_5$. It exhibits the ν_a(NCO), ν_s(NCO), δ(NCO), ν(Cr−NCO), and ν(Cr−OCN) at 2248, 1315, 605, 350, and 303 cm^{-1}, respectively [889]. X-Ray analysis confinned the presence of such a bridge in $[\{CuL(\mu\text{-}NCO)\}_n]^{n+}$ $(ClO_4)_n$ (L = *N*,*N*,*N*′,*N*′,*N*″-pentamethyl-3-azapentane-l,5-diamine). It exhibits ν_a(NCO) at 2271 and 2204 and ν_s(NCO) at 1323 cm^{-1} [890].

1.17.4. Fulminato (CNO) Complexes

The fulminato (CNO^-) ion may coordinate to a metal through the carbon (M−CNO), the oxygen (M−ONC), or both as a bridging ligand. As stated in Sec. 2.5.2 of Part A, fulminic acid (HCNO) is linear, whereas isofulminic acid (HONC) is bent. The same trend may hold for their metal complexes. Thus far, all the complexes containing the CNO group are presumed to be C-bonded. Beck and coworkers have carried out an extensive vibrational study on metal fulminato complexes. Table 1.46 lists the vibrational frequencies of typical complexes obtained by these workers. A more complete listing is found in a review by Beck [897].

Beck and Fehlhammer observed rapid isomerization:

$$NEt_4[W(CO)_5(CNO)] \xrightarrow[\text{in } CH_2Cl_2]{} NEt_4[W(CO)_5(NCO)]$$

The fulminato complex shows the 2ν(NO), ν(CN), and ν(NO) at 2190, 2110, and 1087 cm^{-1}, respectively, while its isocyanato isomer exhibits the ν_a and ν_s at 2235 and 1318 cm^{-1}, respectively [898].

TABLE 1.46. Observed Frequencies of Typical Fulminate Complexes (cm^{-1})

Ion	ν(CN)	ν(NO)	δ(CNO)	Ref.
$[CNO]^-$	2052	1057	471	891
$[Ag(CNO)_2]^-$	2119	1144	—	892
$[Au(CNO)_2]^-$	2173	1180	—	892
$[Fe(CNO)_6]^{4-}$	2187	1040	514 466	892
$[Hg(CNO)_4]^{2-}$	2130	1143	—	893
$[Ni(CNO)_4]^{2-}$	2184	1122	479 470	894
$[Zn(CNO)_4]^{2-,a}$	2146 (A_1) 2130 (F_2)	1177 (A_1) 1154 (F_2)	498 (E) 475 (F_2)	895
$[Pt(CNO)_4]^{2-,b}$	2194 (A_{1g}) 2189 (B_{1g})	1174 (A_{1g}) 1140 (B_{1g})	476 (B_{2g}) 453 (E_g)	895
$Pt(PPh_3)_2(CNO)_2$	2183	1171	—	896

[a] $\mathbf{T}_d$ symmetry.
[b] $\mathbf{D}_{4h}$ symmetry.

1.17.5. Azido (N_3) Complexes

Table 1.47 lists the observed frequencies of typical azido complexes. The two N_3 groups around the Hg atom in $Hg_2(N_3)_2$ are in the *trans* position ($\mathbf{C}_{2h}$), whereas they are in a twisted configuration ($\mathbf{C}_2$) in $Hg(N_3)_2$. The former exhibits one $\nu_a(N_3)$ at 2080 cm^{-1}, whereas the latter shows two $\nu_a(N_3)$ at 2090 and 2045 cm^{-1} [904]. For Co(III) azido ammine complexes and $[M(N_3)_2(py)_2]$ (M = Cu,Zn,Cd), see Refs. 905 and 906, respectively. Forster and Horrocks [901] made complete assignments of vibrational spectra of the $[Co(N_3)_4]^{2-}$ and $[Zn(N_3)_4]^{2-}$ ($\mathbf{D}_{2d}$) and $[Sn(N_3)_6]^{2-}$ ($\mathbf{D}_{3d}$) ions. The spectra suggest that the M−NNN bonds in these anions are not linear.

Vibrational spectra are reported for many other azido complexes. These include $[Au(N_3)_4]^{4-}$ [907], $[As(N_3)_4]^+$ [908], $[Sb(N_3)_4]^+$ [908], $[Pt(N_3)_6]^{2-}$ [909,910], $[Sb(N_3)_2Cl]$ [911], *trans*-$[Pd(N_3)_2(2\text{-Cl-py})_2]$ [912], *trans*-$[Pt(N_3)_4X_2]^{2-}$ (X = a halogen) [913], and $[OsN(N_3)_5](PPh_4)_2$ [914]. Figure 1.56 shows the RR spectra of $[Mn(N_3)_4(bipy)]$ and its $^{15}N^{14}N_2$ isotopomer. The $^{14}N_3$ complex shows two ν(Mn−N_3) bands at 373 and 362 cm^{-1} that exhibit identical isotope shifts (3 cm^{-1}). X-Ray studies show that the Mn−N distance of the N_3 ligand *trans* to bipy(1.914Å) is shorter than that of *cis* to bipy(1.965Å). Thus, these bands were assigned to the ν(Mn−N_3) of the N_3 ligands that are *trans* and *cis* to the bipy ligand, respectively [915].

The bridging azido groups are found in

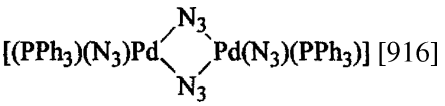

and

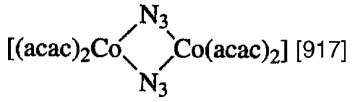

TABLE 1.47. Vibrational Frequencies of Azido Complexes (cm^{-1})[a]

Compound[a]	ν_a(NNN)	ν_s(NNN)	δ(NNN)	ν(MN)	Ref.
$[N_3]^-$	2041	1343	638	48	459 [Chapter 2 (Part A)]
$R_2[Pt(N_3)_4]$	2075, 2060 2024, 2029	1276	582	394	899,900
$R[Au(N_3)_4]$	2030, 2034	1261 1251	578	432	899,900
$R''_2[Zn(N_3)_4]$	2097, 2058	1330 1282	—	—	899,900
$R_2[VO(N_3)_4]$	2088, 2051 2092, 2060 2005	1340	652	442 405	899,900
$R_2[Pd(N_3)_6]$	2045, 2056 2037	1262 1253	640 597	327 313	899,900
$R_2[Pt(N_3)_6]$	2022, 2028	1275 1262 1253	578	402 397 320	899,900
$R'_2[Co(N_3)_4]$	2089, 2050	1338 1280	642 610	368	901
$R''_2[Mn(N_3)_4]$	2058	1330 1267	650 630	317 288	902
$R'_2[Sn(N_3)_4]$	2115, 2080	1340	659 601	390 330	901
trans-$R_2[TiCl_4(N_3)_2]$	2072, 2060	1344	610	—	903

[a] $R = [As(Ph)_4]^+$; $R' = [N(C_2H_5)_4]^+$; $R'' = [P(Ph)_4]^+$.

The azido bridge can be either the end-on or the end-to-end type shown below:

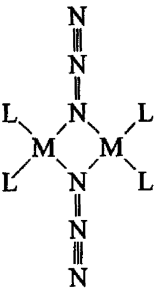

End-on (μ-1,1)

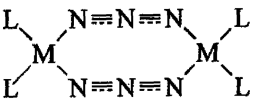

End-to-end (μ-1,3)

These two types may be distinguished by using an isotopically scrambled ligand such as $^{14}N - {}^{14}N - {}^{15}N$ since one expects three and two isotopomers for the end-on and end-to-end complexes, respectively.

X-Ray analysis [918] shows that the azido bridges in $(\mu\text{-}N_3)_2NiL_2(ClO_4)_2$ take the end-on structure with the $\nu_a(N_3)$ at $\sim 2050\,cm^{-1}$. Here, L is 2,4,4-trimethyl-1,5,9-triazacyclododeca-l-ene. Both terminal and bridging (end-on) azido groups are present

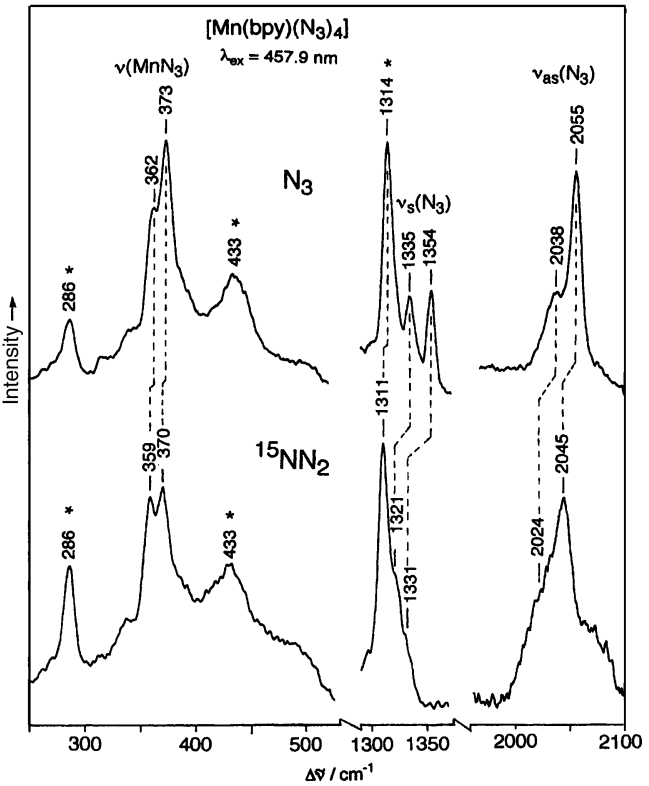

Fig. 1.56. *Room temperature RR spectra of [Mn(bpy)(N$_3$)$_4$] and its $^{15}N^{14}N_2$-labeled isotopomer in CH_2Cl_2 solution excited at 457.9 nm; 50-mW laser power, 6-cm^{-1} slit widths; the bands marked by asterisks are due to bpy vibrations (bpy = bipy) [916].*

in [Rh$_3$(μ-dpmp)$_2$(CO)$_3$(μ-N$_3$)N$_3$] (BPh$_4$). Here, dpmp is bis((diphenylphosphino)-methyl)phenylphosphine. The ν_a(N$_3$) of the former is at 2035 cm^{-1}, whereas that of the latter is at 2085 cm^{-1} [919].

Similar mixing of azido coordination is found in [Cp*TaCl(N$_3$)(μ-N$_3$)]$_2$(μ-O) [920], and [Cp*V(N$_3$)$_2$(μ-N$_3$)]$_2$ [921] (Cp* = pentamethyl Cp). End-on and end-to-end bridgings are mixed in polymeric [Cu(N$_3$)$_3$](Me$_4$N) [922]. The ν(N$_3$) frequencies of these bridging azide groups are reported.

A novel azidoimido(-N$_4$) complex, *mer*-[Os(IV)(bipy)Cl$_3$(N$_4$)] (PPN) complex {PPN = [(PPh$_3$)$_2$N]$^+$ ion} was synthesized by the following reaction:

$$\textit{mer}\text{-}\{Os(VI)(bipy)Cl_3(N)\} + N_3^- \xrightarrow{CH_3CN} \textit{mer}\text{-}[(bipy)Cl_2Os(IV)=N\text{-}N{=}N{=}N]^-$$

The IR spectrum (all ^{14}N except for bipy) exhibits the $\nu_a(N_3^-)$ and ν(Os−N) at 2058 and 1092 cm^{-1}, respectively [923].

1.18. COMPLEXES OF CARBON MONOXIDE

In the last few decades, a large number of carbonyl complexes have been synthesized, and their spectra and structures have been studied exhaustively. This section describes only typical results obtained from these investigations. For more comprehensive information, several review articles [924–928] should be consulted.

Most carbonyl complexes exhibit strong and sharp ν(CO) bands at ~2100–1800 cm^{-1}. Since ν(CO) is generally free from coupling with other modes and is not obscured by the presence of other vibrations, studies of ν(CO) alone often provide valuable information about the structure and bonding of carbonyl complexes. In the majority of compounds, ν(CO) of free CO (2155 cm^{-1}) is shifted to lower frequencies. In terms of simple MO theory, this observation has been explained as follows: (1) the σ-bond is formed by donating 5σ electrons of CO to the empty orbital of the metal (see Fig. 1.57), which tends to raise ν(CO), since the 5σ orbital is slightly antibonding; and (2) the π-bond is formed by backdonating the $d\pi$-electrons of the metal to an empty antibonding orbital, the $2p\pi^*$ orbital of CO. This tends to lower ν(CO). Although these two components of bonding are synergic, the net result is a drift of electrons from the metal to CO when the metal is in a relatively low oxidation state. Thus the ν(CO) of metal carbonyl complexes are generally lower than the value for free CO. The opposite trend is observed, however, when CO is complexed with metal halides in which the metals are in a relatively higher oxidation state (see Sec. 1.18.6).

If CO forms a bridge between two metals, its ν(CO) (1900–1800 cm^{-1}) is much lower than that of the terminal CO group (2100–2000 cm^{-1}). An extremely low ν(CO) (~1300 cm^{-1}) is observed when the bridging CO group forms an adduct via its O atom (see Sec. 1.18.2) [929].

1.18.1. Mononuclear Carbonyls

Table 1.48 lists the observed frequencies and band assignments of mononuclear carbonyls of tetrahedral ($\mathbf{T}_d$), trigonal–bipyramidal ($\mathbf{D}_{3h}$), and octahedral ($\mathbf{O}_h$) structures. Complete normal coordinate analyses have been made on most of these carbonyls. Jones and coworkers [935,936] carried out extensive vibrational studies on

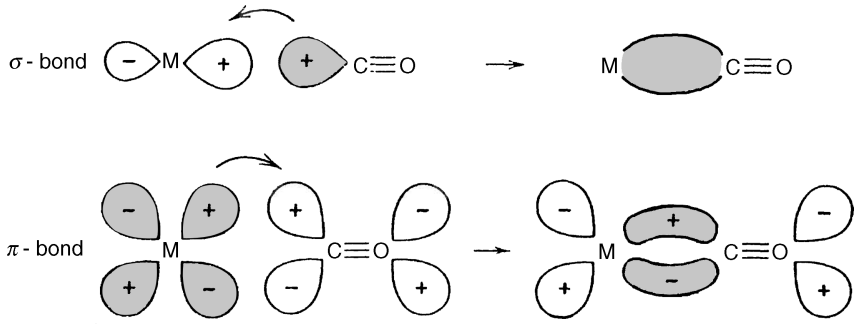

Fig. 1.57. *The σ and π bonding in metal carbonyls.*

TABLE 1.48. Vibrational Frequencies and Band Assignments of Mononuclear Metal Carbonyls[a]

Compound	Symmetry	State	ν (CO)	ν (MC)	δ (MCO)	δ (MCC)	Ref.
$Ni(CO)_4$	$\mathbf{T}_d$	Gas	2131(A_1) 2057.6(F_2)	367.5(A_1) 421(F_2)	380(E) 458.8(F_2) 300(F_1)	64(E) 80(F_2)	930
$[Co(CO)_4]^-$	$\mathbf{T}_d$	Solution	2002(A_1) 1890(F_2)	431(A_1) 556(F_2)	523(F_2)	91(E)	931
$[Fe(CO)_4]^{2-}$	$\mathbf{T}_d$	Solution	1788(A_1) 1788(F_2)	464(A_1) 644(F_2)	550(F_2) 785(E)	100-85 (E,F_2)	932
$[Rh(CO)_4]^+$	$\mathbf{D}_{4h}$	Solid	2214(A_{1g}) 2174(B_{1g}) 2137(E_u)	406(A_{1g}) 406(B_{1g}) 331(E_u)	465(A_{2u}) 306(E_g) 543(E_u)		933
$[Pd(CO)_4]^+$	$\mathbf{D}_{4h}$	Solid	2278(A_{1g}) 2263(B_{1g}) 2249(E_u)	383(A_{1g}) 363(B_{1g}) 336(E_u)	427(A_{2u}) 484(E_u)	 95(B_{2g})	933
$[Pt(CO)_4]^+$	$\mathbf{D}_{4h}$	Solid	2289(A_{1g}) 2267(B_{1g}) 2244(E_u)	436(A_{1g}) 408(B_{1g}) 360(E_u)	473(A_{2u}) 341(E_g) 518(E_u)	 99(B_{2g})	933
$Fe(CO)_5$	$\mathbf{D}_{3h}$	Liquid	2116(A'_1) 2030(A'_1) 1989(E')	418(A'_1) 381(A'_1) 482(E')	278(A'_2) 653(E') 559(E') 491(E'') 448(E'')	107(E') 64(E')	934 935
$Cr(CO)_6$	$\mathbf{O}_h$	Gas	2118.7(A_{1g}) 2026.7(E_g) 2000.4(F_{1u})	379.2(A_{1g}) 390.6(E_g) 440.5(F_{1u})	364.1(F_{1g}) 668.1(F_{1u}) 532.1(F_{2g}) 510.9(F_{2v})	97.2(F_{1u}) 89.7(F_{2g}) 67.9(F_{2u})	936
$Mo(CO)_6$	$\mathbf{O}_h$	Gas	2120.7(A_{1g}) 2024.8(E_g) 2000.3(F_{1u})	391.2(A_{1g}) 381(E_g) 367.2(F_{1u})	341.6(F_{1g}) 595.6(F_{1u}) 477.4(F_{2g}) 507.2(F_{2u})	81.6(F_{1u}) 79.2(F_{2g}) 60(F_{2u})	936
$W(CO)_6$	$\mathbf{O}_h$	Gas	2126.2(A_{1g}) 2021.1(E_g) 1997.6(F_{1u})	426(A_{1g}) 410(E_g) 374.4(F_{1u})	361.6(F_{1g}) 586.6(F_{1u}) 482.0(F_{2g}) 521.3(F_{2u})	82.0(F_{1u}) 81.4(F_{2g}) 61.4(F_{2u})	936
$[Fe(CO)_6]^{2+}$	$\mathbf{O}_h$	Solid	2241(A_{1g}) 2220(E_g) 2204(F_{1u})	347(A_{1g}) 361(E_g) 380(F_{1u})	(336)(F_{1g}) 586(F_{1u}) 501(F_{2g}) 468(F_{2u})	170(F_{1u}) 138(F_{2g}) 114(F_{2u})	937
$[Os(CO)_6]^{2+}$	$\mathbf{O}_h$	Solid	2258(A_{1g}) 2214(E_g) 2189(F_{1u})	429(A_{1g}) 409(E_g) 344(F_{1u})	345(F_{1g}) 560(F_{1u}) 509(F_{2u}) 480(F_{2g})	145(F_{1u}) 142(F_{2g}) 96(F_{2u})	938
$[V(CO)_6]^-$	$\mathbf{O}_h$	Solution	2020(A_{1g}) 1894(E_g) 1858(F_{1u})	374(A_{1g}) 393(E_g) 460(F_{1u})	356(F_{1g}) 650(F_{1u}) 517(F_{2g}) 506(F_{2u})	92(F_{1u}) 84(F_{2g})	939

(*continued*)

TABLE 1.48. (*Continued*)

Compound	Symmetry	State	ν(CO)	ν(MC)	δ(MCO)	δ(MCC)	Ref.
$[Re(CO)_6]^+$	O_h	Solution	2197(A_{1g}) 2122(E_g) 2085(F_{1u})	441(A_{1g}) 426(E_g) 356(F_{1u})	354(F_{1g}) 584(F_{1u}) 486(F_{2g}) 522(F_{2u})	82(F_{1u}) 82(F_{2g})	939
$[Mn(CO)_6]^+$	O_h	Solution	2192(A_{1g}) 2125(E_g) 2095(F_{1u})	384(A_{1g}) 390(E_g) 412(F_{1u})	347(F_{1g}) 636(F_{1u}) 500(F_{2g}) 500(F_{2u})	101(F_{1u}) 101(F_{2g})	940

[a] Vibrational coupling may occur among the three low-frequency modes.
[b] IR in solution, and Raman in solid.

$Fe(CO)_5$ and $M(CO)_6$ (M = Cr,Mo,W), including their ^{13}C and ^{18}O species. They obtained the following F_{1u} force constants (mdyn/Å) from gas-phase spectra:

	$Cr(CO)_6$	$Mo(CO)_6$	$W(CO)_6$	
F(C≡O)	17.22	17.39	17.21	(GVF)
F(M−C)	1.64	1.43	1.80	

This result indicates that the M−C bond strength increases in the order Mo < Cr < W, an order also supported by a Raman intensity study of these compounds [941]. On the other hand, Hendra and Qurashi [942] related the Raman intensity ratio of two A_{1g} modes, $I(\nu_1, \text{CO stretching})/I(\nu_2, \text{MC stretching})$, to the π-character of the M−C bond, and concluded that the M−C bond strength increases in the order Cr < W < Mo < Re(I). Kettle et al. [943] noted that the relative intensities of Raman bands of these metal carbonyls are anomalous. For example, the intensity ratios, $I(A_{1g})/I(E_g)$, are only about 0.15 for the $M(CO)_6$ series mentioned above. The origins of these anomalies have been discussed by these workers [944,945]. Raman spectra of hexacarbonyls in the vapor phase [946] and in Ar matrices [947] have been reported. Adelman and Gerrity [948] measured the UVRR spectra of $Cr(CO)_6$ and $W(CO)_6$ (cyclohexane solution) in the regions of the two lowest allowed ($A_{1g} \rightarrow F_{1u}$) CT transitions (excitation at 355–253 nm), and obtained evidence for Jahn–Teller distortion in their excited states.

In general, the ν(CO) is lowered as the negative charge on the metal carbonyl increases. For example, the ν(CO) (average value; see Table 1.48) is in the following order:

$$\underset{2094}{Ni(CO)_4} > \underset{1946}{[Co(CO)_4]^-} > \underset{1788\ (cm^{-1})}{[Fe(CO)_4]^{2-}}$$

In terms of the bonding scheme mentioned earlier, this result indicates that the metal-CO π-backbonding increases as the negative charge increases. The ν(CO) of the $[Nb(CO)_6]^-$ ion are at 2019 (A_{1g}), 1878–1887 (E_g), and 1860 cm^{-1} (F_{1u}) [949]. The ν(CO) of the $[Ir^{3-}(CO)_3]^{3-}$ ion is at 1665 cm^{-1} in hexamethylphosphoamide solution (IR) [950], and that of the $[Co(CO)_3]^-$ ion is as low as ~1610 cm^{-1} (a shoulder at 1740 cm^{-1}) [951]. Highly reduced species such as $Na_4[M(CO)_4]$ (M = Cr,Mo,W of formal oxidation state, −IV) exhibit very low ν(CO) at 1530–1460 cm^{-1} [952].

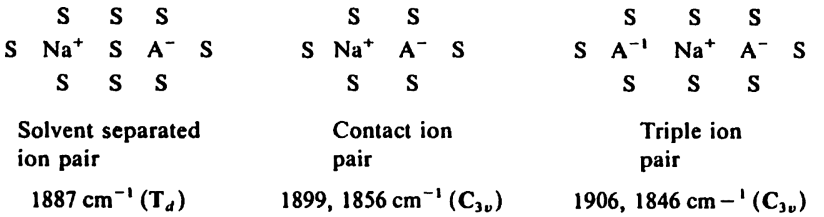

Fig. 1.58. *Structures and ν(CO) of Na[Co(CO)$_4$] at three ion sites in THF solution; A^- and S indicate the anion and solvent, respectively [957].*

Conversely, as the positive charge of the complex increases, the ν(CO) is shifted to higher frequency because the σ-bonding becomes more predominant Thus, metal carbonyl cations such as $[Hg(CO)_2]^{2+}$ (ν_s, 2281 and ν_a, 2278 cm^{-1}) [953] and $[Au(CO)_2]^+$ (ν_s, 2246.0 and ν_a, 2210.5 cm^{-1}) [954] show extremely high ν(CO). The $[Pt(CO)_4]^{2+}$ ion exhibits three ν(CO) at 2281 (A_{1g}), 2257 (B_{2g}), and 2235 cm^{-1} (E_u), which are much higher than those of neutral Pt(CO)$_4$ (2067 cm^{-1}) [955].

Edgell and coworkers [956] attributed the band at 413 cm^{-1} of Li[Co(CO$_4$)] in a THF solution to the vibrations of the alkali ions, which form ion pairs with $[Co(CO)_4]^-$. For sodium and potassium salts, the corresponding bands are observed at 192 and 142 cm^{-1} respectively. From computer-aided curve analysis of IR spectra of Na[Co(CO)$_4$] in the ν(CO) region, they [957] also demonstrated that there are three kinds of ion sites in THF solution, each of which exhibits different spectra. Their structures and ν(CO) are shown in Fig. 1.58.

Infrared spectroscopy has been utilized to elucidate the modes of CO bonding on the surfaces of metal single crystals [958,959] and metal oxide catalysts. In general, the observed ν(CO) frequencies were used to distinguish various modes of binding. The IR spectra of CO adsorbed on the (111) surface of platinum metal at 85–300 K show the terminal ν(CO) at 2110 cm^{-1} and bridging ν(CO) at 1842 (two-fold bridge) and 1822 (three-fold bridge) cm^{-1} [960]. Ichikawa and Fukushima [961] studied the modes of adsorption of CO on SiO_2 supported Rh−Mn catalyst. They observed that, by increasing the percentage of Mn, the bridging ν(CO) at 1880 cm^{-1} is progressively shifted to 1700 cm^{-1} and a new weak shoulder band appears near 1520 cm^{-1}. To account for these results, two types of bridging structures involving the Rh and Mn atoms on the SiO_2 surfaces were proposed as shown:

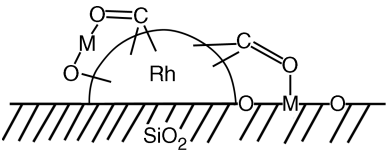

M~Mn^{2+}, Ti^{3+} / Ti^{4+}, ...

1.18.2. Polynuclear Carbonyls

Since polynuclear carbonyls take a variety of structures, elucidation of their structures by vibrational spectroscopy has been a subject of considerable interest. The principles involved in these structure determinations were described in Sec. 1.11 of Part A.

However, the structures of some polynuclear complexes are too complicated to allow elucidation by simple application of selection rules based on symmetry. Thus the results are often ambiguous. In these cases, one must resort to X-ray analysis to obtain definitive and accurate structural information. However, vibrational spectroscopy is still useful in elucidating the structures of metal carbonyls in solution.

In general, the terminal ν(CO) is higher than the bridging ν(CO). Thus, the $[Pd_2(\mu\text{-}CO)_2]^{2+}$ ion, which contains two bridging and no terminal CO ligands ($\mathbf{D}_{2h}$, structure I of Fig. 1.59), exhibits two bridging ν(CO) at 2027(R) and 1977(IR) cm^{-1} [962], whereas the $[Pt(I)_2(CO)_6]^{2+}$ ion, which has no bridging CO ligands ($\mathbf{D}_{2d}$, structure II), exhibits five terminal ν(CO) between 2233 and 2173 cm^{-1} (Raman spectrum in concentrated H_2SO_4 solution) [963]. According to X-ray analysis [964], $Co_2(CO)_8$ takes structure III. For this $\mathbf{C}_{2v}$ structure, five terminal and two bridging ν(CO) are expected to be IR-active; the former were observed at 2075, 2064, 2047, 2035, and

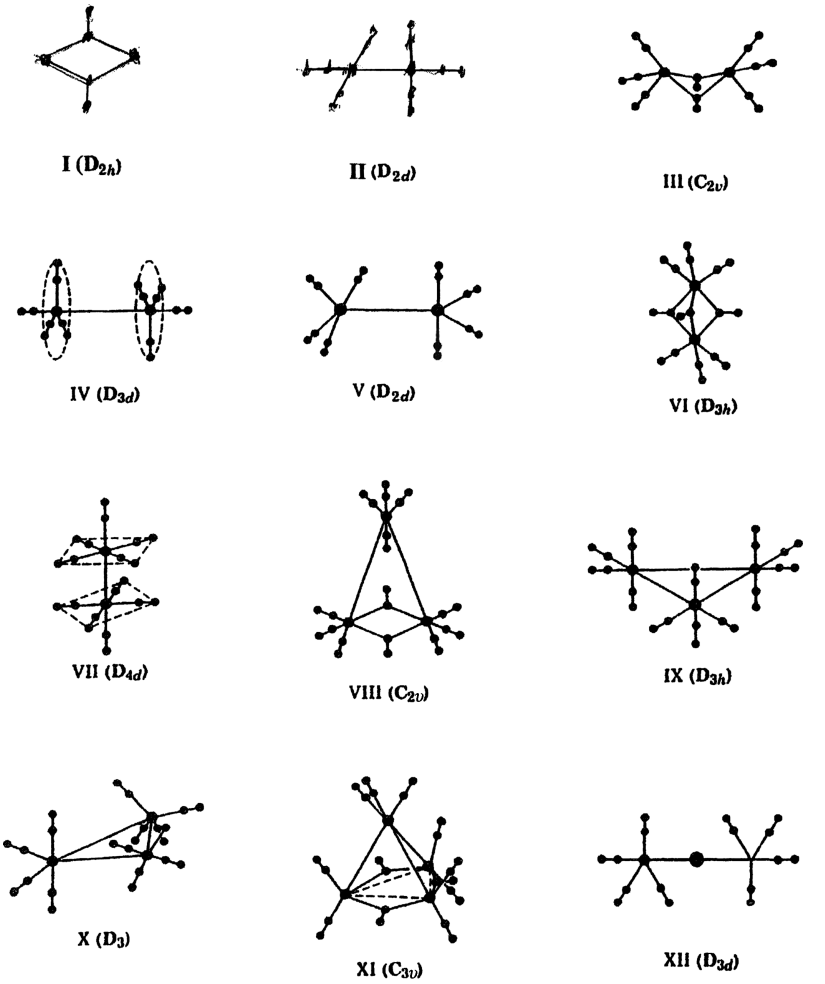

Fig. 1.59. *Structures of polynuclear metal carbonyls.*

2028 cm^{-1}, and the latter were located at 1867 and 1859 cm^{-1} [965]. When the $Co_2(CO)_8$ in various gas matrices are photolyzed, the IR spectra show the presence of the third isomer (structure V) in addition to two isomers(III and IV) [966].

Sheline and Pitzer [967] first measured the IR spectrum of $Fe_2(CO)_9$ and observed two terminal (2080 and 2034 cm^{-1}) and one bridging(1828 cm^{-1}) ν(CO) bands. Their result agrees with that expected from structure VI determined by X-ray analysis [968]. Figure 1.59 (VII) shows the structure of $Mn_2(CO)_{10}$ obtained by X-ray analysis [969]. This $\mathbf{D}_{4d}$ structure predicts four Raman- and three IR-active ν(CO) bands. Adams et al. [970] observed the former at 2116 (A_1), 1997 (A_1), 2024 (E_2), and 1981 (E_3) cm^{-1}, and Bor [971] bserved the latter at 2046 (B_2), 1984 (B_2), and 2015 (E_1) cm^{-1} in solution. Levenson et al. [972] confirmed these infrared assignments by studying the polarization properties of the three bands in a nematic liquid crystal. The structures of $Re_2(CO)_{10}$ and $T_2(CO)_{10}$ are similar to that of $Mn_2(CO)_{10}$. The vibrational spectra of $Re_2(CO)_{10}$, $Tc_2(CO)_{10}$, $MnTc(CO)_{10}$, and $TcRe(CO)_{10}$ are reported [970,973–976]. High-pressure IR and Raman studies show that the symmetries of $Mn_2(CO)_{10}$ and $Re_2(CO)_{10}$ change from $\mathbf{D}_{4d}$ to $\mathbf{D}_{4h}$ at pressures of 8 and 5 kbar, respectively, owing to phase transitions [977].

Figure 1.59 (VIII) shows the structure of $Fe_3(CO)_{12}$ determined by X-ray analysis [978]. This structure can account for Mössbauer [979] and solid-state infrared spectra. In solution, the infrared spectrum does not agree with that expected for structure VIII; the bridging ν(CO) is very weak and the terminal ν(CO) region is broad without resolution. Cotton and Hunter [980] suggest that a whole range of structures varying from $\mathbf{D}_{3h}$ (structure IX) to $\mathbf{C}_{2v}$ (structure VIII) are in equilibrium, with the majority close to $\mathbf{D}_{3h}$. Johnson suggests the presence of a new isomer of $\mathbf{D}_3$ symmetry, shown by structure X [981]. DFT calculations on $Fe_2(CO)_9(\mathbf{D}_{3h})$ and $Fe_3(CO)_{12}$ ($\mathbf{C}_{2v}$) [982] suggest reassignments of their vibrational spectra.

According to X-ray analysis [983], $Os_3(CO)_{12}$ takes the $\mathbf{D}_{3h}$ structure (IX), for which four terminal ν(CO) should be infrared-active. Huggins et al. [984] assigned them at 2068 (E'), 2035 (A''_2), 2014 (E'), and 2002 (E') cm^{-1}. Quicksall and Spiro [985] assigned the Raman spectra of $Os_3(CO)_{12}$ and analogous $Ru_3(CO)_{12}$, for which six ν(CO) are expected in the Raman spectrum. For $Os_3(CO)_{12}$, they are observed at 2130 (A'_1), 2028 (E''), 2019 (E'), 2006 (A'_1), 2000 (E'), and 1989 (E') cm^{-1}. Vibrational spectra of solid $M_3(CO)_{12}$ (M = Ru,Os) in the ν(CO) region have been assigned on the basis of factor group analysis [986]. The ν(CO) of $Ru_3(CO)_{12}$ and $Os_3(CO)_{12}$ ($\mathbf{D}_{3h}$) were correlated with those of their mixed metal carbonyls, $Ru_2Os(CO)_{12}$ and $RuOs_2(CO)_{12}$ ($\mathbf{C}_{2v}$) [987]. The IR spectrum of $[CoRh(\mu\text{-}CO)_2(CO)_5]$ exhibits five terminal and two bridging ν(CO) vibrations [988].

Accoiding to X-ray analysis [989], $Co_4(CO)_{12}$ takes the $\mathbf{C}_{3v}$ structure (XI of Fig. 1.59), for which six terminal and two bridging ν(CO) are infrared-active. Vibrational analyses have been made on $Co_4(CO)_{12}$ and $Rh_4(CO)_{12}$ [990]. The ν(CO) frequencies are reported for $[CoRu_3(CO)_{13}]$ [991]. The ν(M−M) of $Ir_4(CO)_{12}$ ($\mathbf{T}_d$) are at 209 (A_1) and 162 (F_2) cm^{-1}, and those of its derivatives such as $Ir_3Mo(CO)_{11}$ (η^5–C_5H_4Me) were assigned [992]. Stammreich et al. [993] proposed structure XII of $\mathbf{D}_{3d}$ symmetry from a Raman study of $M[Co(CO)_4]_2$ (M = Cd or Hg). For this structure, three ν(CO) are Raman-active and the other three are infrared-active. The former were observed at 2107 (A_{1g}), 2030 (A_{1g}), and 1990 (E_g) cm^{-1} [993], and the latter were located at 2072 (A_{2u}), 2022 (A_{2u}), and 2007 (E_u) cm^{-1} [994]. Ziegler et al.

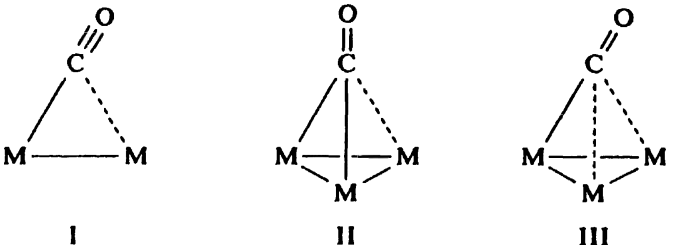

Fig. 1.60. *Structures of unusual bridging carbonyls.*

[995] made complete vibrational assignments of the $M[Co(CO)_4]_2$ series, where M is Zn, Cd, and Hg.

Figure 1.60 shows the structures of unusual bridging carbonyl compounds found by X-ray analysis. "Semibridging" carbonyls (structure I) are present in $(Cp)_2V_2(CO)_5$, and their ν(CO) have been assigned to the bands at 1871 and 1832 cm^{-1} [996]. A "semitriple bridging" carbonyl group (structure II) was found in $[(Cp)_2Rh_3(CO)_4]^-$ [997], and the band at 1693 cm^{-1} is probably due to this carbonyl. The IR band at 1662 cm^{-1} of $PtCo_2(CO)_5(\mu\text{-dppm})$ (dppm = $Ph_2P{-}CH_2{-}PPh_2$) has bee assigned to a "semitriple bridging" carbonyl stretching vibration [998]. Another "semitriple bridging" carbonyl group (structure III) in $(Cp)_3Nb_3(CO)_7$ exhibits an extremely low ν(CO) at 1330 cm^{-1} [999].

The ν(CO) frequencies of a series of trigonal bipyramidal $[MRh_4(CO)_{15}]^{2-}$ ions (M = Fe,Ru,Os) show that the spectra in the bridging region are more structure-sensitive than are those in the terminal region [1000]. Vibrationai spectra are reported for polynuclear complexes of unusual structures such as $[Fe_6N(CO)_{15}]^{3-}$ ($\sim\mathbf{O}_h$) [1001] and $H_3C{-}C{-}Co_3(CO)_9$ [1002].

The structures of large metal carbonyl clusters such as $[Rh_{23}N_4(CO)_{38}]^{3-}$ have been determined by X-ray analysis and characterized by IR spectroscopy [1003]. These include $[Pd_{13}N_{13}(CO)_{34}]^{4-}$ [1004], $[Ag_{16}Ni_{24}(CO)_{40}]^{4-}$ [1005], and $[Ni_{38}Pt_6(CO)_{48}]^{n-}$ (n = 5–9) [1006].

According to Roth et al. [1007,1008], $[Pt_{24}(CO)_{30}]^n$ exhibits six reversible one-electron redox steps (n = 0 to −6) in organic solvents, and each redox form gives characteristic ν(CO) (terminal and bridged) bands that are shifted to lower frequencies in a near-linear fashion as n becomes more negative. Such IR spectroelectrochemistry was found to be highly important in comparing the electronic and bonding properties of large ionizable metal clusters with those of chargeable metal surfaces.

Shriver et al. [1009] found that the O atom of the bridging CO group can form a bond with a Lewis acid such as $AlEt_3$. Kristoff and Shriver [929] observed that $Co_2(CO)_8$ forms an adduct of the following type:

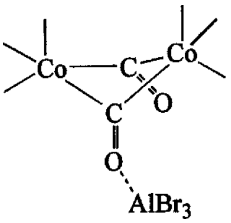

As expected from this structure, the adduct exhibits two bridging ν(CO) in the infrared: one at 1867 cm^{-1}, which is 15 cm^{-1} higher, and the other at 1600 cm^{-1}, which is 232 cm^{-1} lower, than that of the parent compound. In the case of $Fe_2(CO)_9AlBr_3$, only one bridging ν(CO) is observed at 1557 cm^{-1}. This suggests the following structure, which resulted from rearrangement of the CO groups of the parent compound:

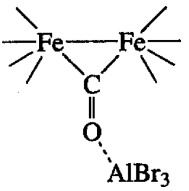

Metal–carbon vibrations in carbonyl carbide clusters have been assigned by several investigators. The iron butterfly carbide in the $[Fe_4C(CO)_{12}]^{2-}$ ion has an idealized symmetry of $\mathbf{C}_{2v}$ as shown in Fig. 1.61. Using $^{12}C/^{13}C$ isotope shift data, Stanghellini et al. [1010] carried out normal coordinate calculations on this skeleton. Figure 1.61 illustrates the four normal modes together with their frequencies. It is seen that the first three normal modes involve the motions of the carbide carbon atom and their frequencies are between 930 and 600 cm^{-1}. The frequency of the last mode is low because it involves the motions of the Fe atoms.

For other metal carbide clusters, the metal–carbide stretching vibrations have been assigned empirically. In $[M_5C(CO)_{15}]$ (M = Ru, Os), for example, these vibrations are located in the 800–730 cm^{-1} region [1011]. The C atom in $Co_6C(CO)_{12}S_2$ is located at the center of the trigonal prism formed by six Co atoms, and its Co–C (carbide) vibrations were assigned at 819 and 548 cm^{-1} based on $^{12}C/^{13}C$ isotope shift data [1012]. In the $[Os_{10}C(CO)_{24}]^-$ ion, the carbide C atom is at the center of the Os_{10} skeleton [1013]. The $^{12}C/^{13}C$ isotope experiments show the presence of three Os–C (carbide) stretching vibrations at 772.8, 760.3, and 735.4 cm^{-1} [1014].

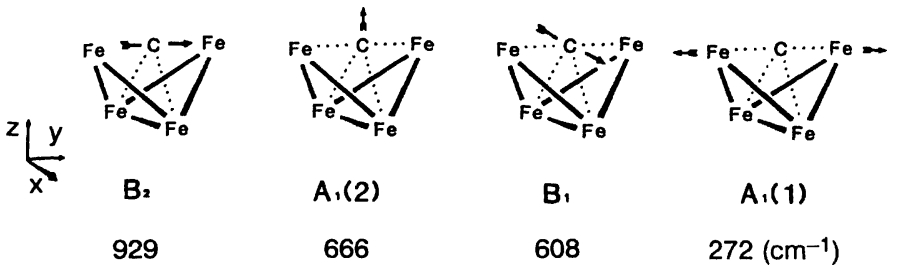

Fig. 1.61. *Normal modes, symmetries, and vibrational frequencies of the iron butterfly carbide in the* $[Fe_4C(CO)_{12}]^{2-}$ *ion [1010].*

A carbon atom capping a three-metal array may form a CCO ligand owing to its strong affinity for CO. Sailor and Shriver [1015] have demonstrated the formation of such a ligand in solid $(PPN)_2[Ru_3(CO)_6(\mu\text{-}CO)_3(\mu_3\text{-}CCO)]$ [PPN = $(PPh_3)_2N^+$ ion).

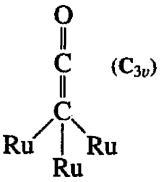

The Raman spectra exhibits four polarized bands (A_1) that are sensitive to the $^{12}C/^{13}C$ substitution of the CCO moiety; the $\nu(CRu_3)$ (319 cm^{-1}), $\nu(C{=}C)$ (1309 cm^{-1}), and $\nu(C{=}O)$ (2024 and 1980 cm^{-1}). The last two bands are presumably due to vibrationally coupled modes between the ν(CCO) and the ν(CO) of terminal CO groups directly bonded to the Ru atoms.

For metal–metal stretching vibrations of polynuclear carbonyls, see Sec. 1.26.

1.18.3. Metal Carbonyls Containing Other Ligands

There are many metal carbonyls in which some of the CO groups are replaced by other ligands such as halogens, phosphorus derivatives, and cyclopentadienyl groups. Vibrational spectroscopy has been utilized to study the effects of these substitutions on the metal–CO bonding.

If one of the CO groups is substituted by a halogen (X), the ν(CO) tends to shift to a higher frequency since the metal–CO π-backbonding decreases as the metal becomes more electropositive by forming a M−X bond. Thus, we obtain a series such as

$Pt(CO)_4$		$[Pt(CO)Cl_3]^-$		*cis*-$[Pt(CO)_2Cl_2]$		$[Pt(CO)Cl_5]^-$
2067 (av) [1016]	<	2097 [1017]	<	2163 (av) [1018]	<	2184 [1019] (cm^{-1})

It should be noted that the oxidation state of the Pt atom has been changed from Pt (O) to Pt(II) to Pt(IV) in the series shown above. As discussed earlier, the ν(CO) is lowered as the negative charge on the metal carbonyl increases. Thus, the ν(CO) of $[Os(CO)Cl_5]^-$ (2121 cm^{-1}) is 170 cm^{-1} higher than that of $[Os(CO)Cl_5]^{2-}$ [1020].

Table 1.49 lists the observed frequencies of typical compounds for which complete band assignments have been made. Figure 1.62 shows the RR spectrum of solid (TBA) [*trans*-$OsBr_4(CO)_2$] (TBA = tetra-*n*-butylammonium ion) obtained by Johannsen and Preetz [1025]. It shows a series of overtones of the totally symmetric $\nu(Os{-}Br)$ (ν_3, 209.3 cm^{-1}) up to 10 ν_3 together with many combination bands involving other totally symmetric fundamentals [ν_1(CO), 2122.1 and ν_2 (OsC), 460.4 cm^{-1}].

Goggin and Mink [1026] prepared the planar bridging carbonyl halide complexes of Pd(I), $[Pd_2(CO)_2X_4]^{2-}$ (X = Cl or Br) (structure I in Fig. 1.63) and observed the ν_s(CO) and ν_a(CO) of the bridging CO at 1969 and 1907 cm^{-1}, respectively, in IR spectra.

TABLE 1.49. Vibrational Frequencies of Metal Carbonyl Halides (cm^{-1})

Compound	IR or Raman and Symmetry		ν(CO)	ν(MX)	Ref.
$Mn(CO)_5Cl$	IR	($\mathbf{C}_{4v}$)	2138 (A_1) 2056 (E) 2000 (A_1)	291 (A_1)	1021
$Mn(CO)_5Br$	IR	($\mathbf{C}_{4v}$)	2138 (A_1) 2052 (E) 2007 (A_1)	222 (A_1)[a]	1022
fac-$[Os(CO)_3Cl_3]^-$	Raman	($\mathbf{C}_{3v}$)	2125 (A_1) 2022 (E) 2033 (E)	321 (A_1) 287 (E)	1023
cis-$[Os(CO)_2Cl_4]^{2-}$	Raman	($\mathbf{C}_{2v}$)	2016 (A_1) 1910 (B_2)	316 (A_1) 281 (A_1) 308 (B_2)	1023 1024
$[Os(CO)Cl_5]^{3-}$	IR	($\mathbf{C}_{4v}$)	1968 (A_1)	332 (A_1)[a] 316 (A_1)[a] 306 (E)	1023
$[Pt(CO)Cl_3]^-$	IR	($\mathbf{C}_{2v}$)	2120 (A_1)	331 (A_1) 310 (A_1)	1023 1017,1018

[a] Raman frequency.

El-Sayed and Kaesz [1027] studied the ν(CO) of $M_2(CO)_8X_2$ (M = Mn,Tc,Re; X = Cl,Br,I), and proposed the halogen-bridging structure II shown in Fig. 1.63. Four infrared-active ν(CO) have been observed in accordance with this structure. Garland and Wilt [1028] interpreted the infrared spectrum of $Rh_2(CO)_4X_2$ (X = Cl,Br) on the basis of the $\mathbf{C}_{2v}$ structure III (Fig. 1.63) found by X-ray analysis [1029]. As predicted, three infrared-active ν(CO) have been observed for this compound. Johnson et al. [1030] studied the exchange of $\mathbf{C}^{18}O$ with CO groups of $Rh_2(CO)_4X_2$ (X = Cl, Br, I, etc.) with time by following the variation of infrared spectra in the ν(CO) region.

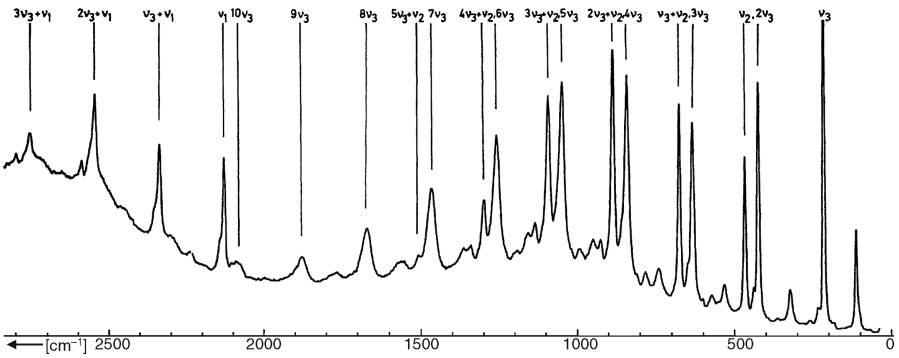

Fig. 1.62. *The RR spectrum of (TBA) [trans-$OsBr_4(CO)_2$] in a KBr disk at 80 K (496.5 nm excitation) [1025].*

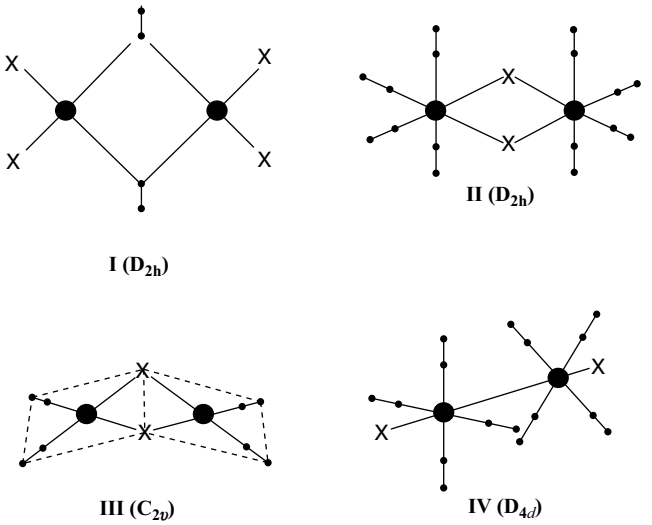

Fig. 1.63. *Structures of metal carbonyl halides.*

Cotton and Johnson [1031] proposed the staggered structure IV for $Fe_2(CO)_8I_2$, since only two ν(CO) were observed in the infrared.

If CO is replaced by a phosphine, ν(CO) decreased since the latter is a strong σ-donor but a weak π-acceptor. In the $[Ni_{12-n}(PMe_3)_n(CO)_{24-3n}]^{2-}$ series ($n = 2,3,4$), both terminal and bridging ν(CO) are downshifted as n increases [1032]. Ligands such as arsines, amines, and isonitriles give similar results. Table 1.50 lists the ν(CO) of typical compounds. Vibrational assignments have been reported for *cis*-$[M(CO)_4(L{-}L)]$ [M = Cr,Mo,W, and L−L is $Ph_2P{-}(CH_2)_n{-}PPh_2$, n = l–3] [1038], $[CpW(CO)_2(PMe_3)(SiH_2Me)]$ [1039], and $[M(CO)_5(CS)]$ (M = Cr,W), and their CSe

TABLE 1.50. CO Stretching Frequencies of Metal Carbonyls Containing Other Ligands (cm^{-1})

Compound	IR or Raman and Symmetry		ν(CO)	Ref.
$Ni(CO)_3(PMe_3)$	Raman	(C_{3v})	2069 (A_1), 1980 (E)	1033
$Fe(CO)_4(PMe_3)$	Raman	(C_{3v})	2051 (A_1), 1967 (A_1) 1911 (E)	1034
$Fe(CO)_4(AsMe_3)$	Raman	(C_{3v})	2050 (A_1), 1964 (A_1) 1911 (E)	1034
$Co(CO)_5(PEt_3)$	IR	(C_{4v})	2060 (A_1), 1973 (B_1) 1943 (A_1), 1935 (E)	1035
$W(CO)_5(NMe_3)$	IR	(C_{4v})	2073 (A_1), 1932 (E) 1920 (A_1)	1036
$W(CO)_4$(bipy)	IR	(C_{2v})	2010 (A_1), 1900 (B_1) 1874 (A_1), 1832 (B_2)	1037
$W(CO)_2(bipy)_2$	IR	(C_2)	1778 (A_1), 1719 (B_2)	1037

analogs [1040]. The IR spectra of $M(CO)_5L$, where M is Mo or W and L is Kr or Xe, have been measured. The lifetime of the Kr complex is ~0.1 s in liquid Kr at 150 K [1041].

Low-frequency infrared species have been reported for $M(CO)_{6-n}(PR_3)n$ (M = Cr, Mo,W) [1042], $M(CO)_{6-n}(CH_3CN)_n$ (M = Cr, W; $n = 1,2$) [1043], and $Fe(CO)_4L$ ($L = PPh_3$, $AsPh_3$, and $SbPh_3$) [1044]. References on vibrational spectra of metal carbonyls containg other ligands include $B(CO)(CF_3)_3$ [1045] and *mer*-$[Ir(CO)_3(SO_3F)_3]$ [1046].

1.18.4. CO Adducts of Metalloporphyrins

Vibrational spectra of CO adducts of metalloporphyrins have been reviewed by Kitagawa and Ozaki [226] and Yu [1047]. In general, these compounds exhibit the ν(CO) in the 2100–1900 cm^{-1} region. In the M(TPP)$(CO)_2$ series, the ν_a(CO) follows the order:

$Co(TPP)(CO)_2$ [1048]		$Fe(TPP)(CO)_2$ [1049]		$Ru(TPP)(C0)_2$ [1050]	
2078	>	2042	>	2005	(cm^{-1})

This result indicates that the degree of the M → CO π-backdonation increases in going from Co(II) to Fe(II) to Ru(II). The 1 : 1 adduct, Fe(TPP)(CO), exhibits the ν(CO) at 1973 cm^{-1}, which is lower than that of $Fe(TPP)(CO)_2$ because the net M → CO π-backdonation decreases in the latter due to competition between the two CO ligands [1049].

Yu and coworkers carried out an extensive RR study on CO adducts of metalloporphyrins by using isotopic ligands, $^{13}C^{16}O$, $^{12}C^{18}O$, and $^{13}C^{18}O$. In the 700–100 cm^{-1} region, $Fe(T_{piv}PP)(CO)$(1-MeIm) ($T_{piv}PP$: "picket-fence" porphyrin shown in Fig. 1.64a) shows only one isotope-sensitive band at 489 cm^{-1}. This band has been assigned to the ν (Fe−C) because it shifts from 485 to 481 to 477 cm^{-1} in the order

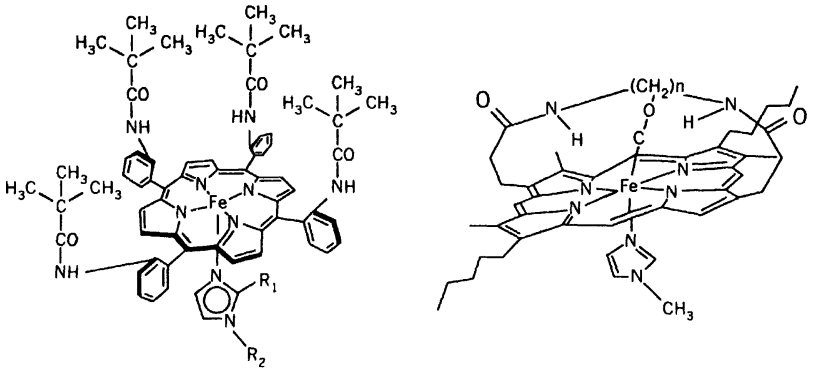

Fig. 1.64. *Structures of (a) "picket-fence" and (b) "strapped" porphyrins.*

shown above for the isotopic CO ligands. It is also sensitive to the nature of the *trans*-ligand (L); the weaker the M−L bond is, the stronger the Fe−CO bond. However, no bands assignable to the δ(FeCO) were resonance-enhanced [1051].

In CO adducts of simple metalloporphyrins such as Fe(TPP)(CO), the Fe−C−O bond is linear and normal to the porphyrin plane. In the "strapped" porphyrins (Fig. 1.64b), the Fe−C−O (linear) bond is tilted because of steric hindrance of the "strap." According to Yu [1047], this tilting increases the electron donation from a pyrrole ring (π) to the CO (π^*) orbital because of a better overlap between these orbitals. This would decrease the CO bond order and increase the Fe−C bond order. Thus, the following trends are observed as the "strap" is shortened [1052]:

	SP-15		SP-14		SP-13
ν(CO)(cm^{-1})	1945	>	1939	>	1932
ν(Fe−C)(cm^{-1})	509	<	512	<	514
	—		504		506

In the latter two complexes, the ν(Fe−C) bands are split into two bands; the higher- and lower-frequency components were attributed to the "tilted" and "upright" conformers, respectively. Similar trends in frequency were observed for a hybrid of the "picket-fence" and the "basket-handle" porphyrins [1053].

The RR spectra of these "strapped" porphyrins exhibit the δ(FeCO), which shows the "zigzag" isotope shift pattern. For example, SP-14 exhibits this band at 578 cm^{-1}, which is shifted to 563 ($^{13}C^{16}O$), 575 ($^{12}C^{18}O$), and 561 ($^{13}C^{18}O$) cm^{-1} by the isotopic substitutions indicated in the parentheses. In contrast, the ν(Fe−C) vibration near 510 cm^{-1} shows a normal (monotonous) isotopic shift pattern. This difference has often been used to distinguish these two models. It should be noted, however, that the observation of a "zigzag" isotope shift pattern does not necessarily indicate the bending mode (Sec. 3.2.1). Yu et al. [1052] also observed that the degree of resonance enhancement of the δ(FeCO) relative to the ν(Fe−C) mode increases as the distortion of the Fe−C≡O linkage increases by shortening the "strap" length.

As described above, Yu and coworkers originally assigned the δ(FeCO) near 560 cm^{-1}, which are higher than the ν(Fe−C) near 510 cm^{-1}, and their assignments have been followed by many other workers. However, an alternative assignment has been proposed for the CO adducts of heme proteins (Sec. 3.2.1).

1.18.5. Hydrocarbonyls

Hydrocarbonyls exhibit bands characteristic of both M−H and M−CO groups. Kaesz and Saillant [1054] reviewed the vibrational spectra of metal carbonyls containing the hydrido group. Vibrational spectra of hydrido complexes containing other groups are discussed in Sec. 1.24. In general, the terminal M−H group exhibits a relatively sharp- and medium-intensity ν(MH) band in the 2200–1800 cm^{-1} region. The MH stretching band can be distinguished easily from the CO stretching band by the deuteration experiment.

Edgell and coworkers [1055] assigned the infrared bands at 1934 and 704 cm^{-1} of $HCo(CO)_4$ to ν(CoH) and δ(CoH), respectively, and proposed structure I of Fig. 1.65,

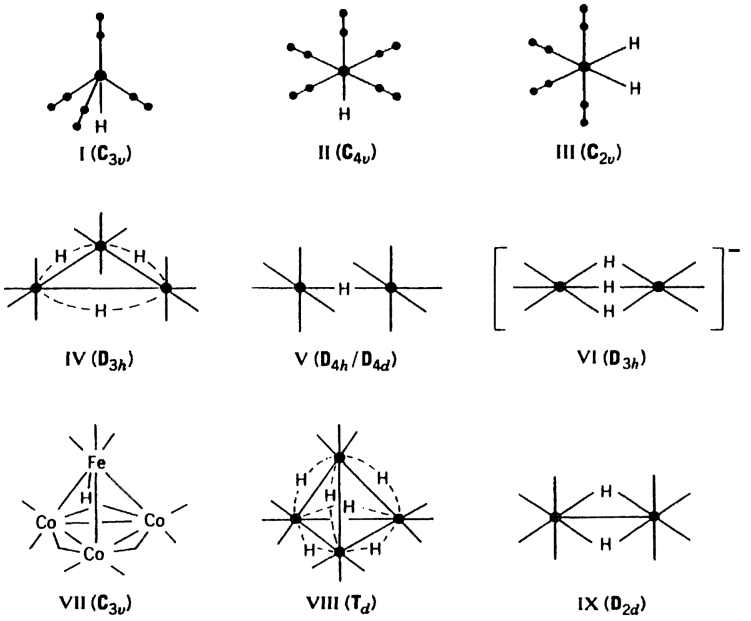

Fig. 1.65. *Structures of hydrocarbonyls.*

in which the H atom is on the C_3 axis. Stammreich et al. [932] reported the Raman spectrum of $HFe(CO)_4^-$, which is expected to have a structure similar to that of $HCo(CO)_4$. According to X-ray analysis [1056], the $Mn(CO)_5$ skeleton of $HMn(CO)_5$ takes the $\mathbf{C}_{4v}$ structure shown in structure II. Kaesz and coworkers [1057,1058] assigned the infrared spectrum of $HMn(CO)_5$ in the ν(CO) region on the basis of this structure. The Raman spectra of $HMn(CO)_5$ and $HRe(CO)_5$ exhibit their ν(MH) at 1780 and 1824 cm^{-1}, respectively [1059].

Edgell et al. [1061] have completed a complete vibrational assignment of gaseous $HMn(CO)_5$. The infrared spectrum of $H_2Fe(CO)_4$ in hexane at $-78°C$ exhibits three or more ν(CO) above 2000 cm^{-1} and a weak, broad ν(FeH) at 1887 cm^{-1}. Thus, Farmery and Kilner [1061] suggested structure III. Table 1.51 lists the observed frequencies of other hydrocarbonyl compounds.

It is rather difficult to locate the bridging ν(MH) in polynuclear hydrocarbonyls. These vibrations appear in the region from 1600 to 800 cm^{-1}, and are rather broad at room temperature although they are sharpened at low temperatures. Higgins et al. [1066] were the first to suggest the presence of bridging hydrogens in $Re_3H_3(CO)_{12}$ (structure IV) since no terminal ν(ReH) bands were observed. Smith et al. [1067] observed a very weak and broad band at 1100 cm^{-1} in the Raman spectrum of $Re_3H_3(CO)_{12}$ and assigned it to the bridging ν(ReH) since it shifted to 787 cm^{-1} on deuteration.

Although structure V was proposed for $[M_2H(CO)_{10}]^-$ (M = Cr, Mo and W) [1068], the W–H–W angle of the tungsten complex was found to be 137° [1069]. Shriver et al. [1070] located the antisymmetric and symmetric stretching vibrations of the W–H–W

TABLE 1.51. Vibrational Frequencies of Metal Hydrocarbonyl Compounds (cm^{-1})[a]

Compound	ν(CO)	ν(MH)	δ(MH)	Ref.
$RhH(CO)(PPh_3)_3$	1926	2004	784	1062
$IrH(CO)(PPh_3)_3$	1930	2068	822	1062
$IrHCl_2(CO)(PEt_2Ph)_2$	2101	2008	—	1063
$IrHBr_2(CO)(PEt_2Ph)_2$	2035	2232	—	1063
$IrHCl_2(CO)(PPh_3)_2$	2027	2240	—	1064
$OsHCl(CO)(PPh_3)_2$	1912	2097	—	1064
$OsH_2(CO)(PPh_3)_2$	2014	1928	—	1065
	1990	1873		

[a]For the configurations of these molecules, see the original references.

bridge at 1683 and ~900 cm^{-1}, respectively. At ~80 K, the latter splits into four bands at 960, 869, 832, and 702 cm^{-1}. Although the origin of this splitting is not clear, the possibility of Fermi resonance with an overtone or a combination band involving the ν(WC) or δ(WCO) was ruled out on the basis of $CO-C^{18}O$ isotopic shifts [1070].

Ginsberg and Hawkes [1071] suggested structure VI for $[Re_2H_3(CO)_6]^-$ since they could not observe any terminal ν(ReH) vibrationals. The bridging ν(FeH) band of $FeHCo_3(CO)_{12}$ in the infrared was finally located at 1114 cm^{-1} by Mays and Simpson [1072], using a highly concentrated KBr pellet. This band shifts to 813 cm^{-1} on deuteration. On the basis of mass spectroscopic and infrared evidence, they proposed structure VII, in which the H atom is located inside the metal atom cage. From the spectra in the ν(CO) region, together with X-ray evidence, Kaesz et al. [1073] proposed the $\mathbf{T}_d$ skeleton (structure VIII) for $[Re_4H_6(CO)_{12}]^{2-}$. It showed no terminal ν(ReH), but a broad bridging ν(ReH) centered at 1165 cm^{-1} was observed in its Raman spectrum. This band shifts to 832 cm^{-1} with less broadening on deuteration. Bennett et al. [1074] found no terminal ν(ReH) in the infrared spectrum of $Re_2H_2(CO)_8$. However, its Raman spectrum exhibits bands at 1382 and 1272 cm^{-1}, which shift to 974 and 924 cm^{-1}, respectively, on deuteration. The $\mathbf{D}_{2h}$ structure (IX) was proposed for this compound.

Figure 1.66 shows the Raman spectra of $Ru_4H_4(CO)_{12}$ and $Ru_4D_4(CO)_{12}$ obtained by Knox et al. [1075]. Two ν(RuH) bands at 1585 and 1290 cm^{-1} of the former compound are shifted to 1153 and 909 cm^{-1}, respectively, on deuteration. Its infrared spectrum exhibits five ν(CO) instead of the two expected for $\mathbf{T}_d$ symmetry. Thus a structure of $\mathbf{D}_{2d}$ symmetry, which lacks two H atoms from structure VIII, was proposed [1076]. The ν(OsH) vibrations of the analogous Os complex have also been assigned [1077]. In the $[Ru_6H(CO)_{18}]^-$ ion, the H atom is located at the center of an octahedron consisting of six Ru atoms [1078]. Oxton et al. [1079] located its ν(R−H) at 845 and 806 cm^{-1} (95 K), which are probably split by Fermi resonance.

As stated in Sec. 1.8 (on aquo complexes), the inelastic neutron scattering (INS) technique is very effective in locating hydrogen vibrations. White and Wright [1080] found two hydrogen vibrations at 608 and 312 cm^{-1} in the INS spectrum of $Mn_3H_3(CO)_{12}$. However, the nature of these vibrations is not clear.

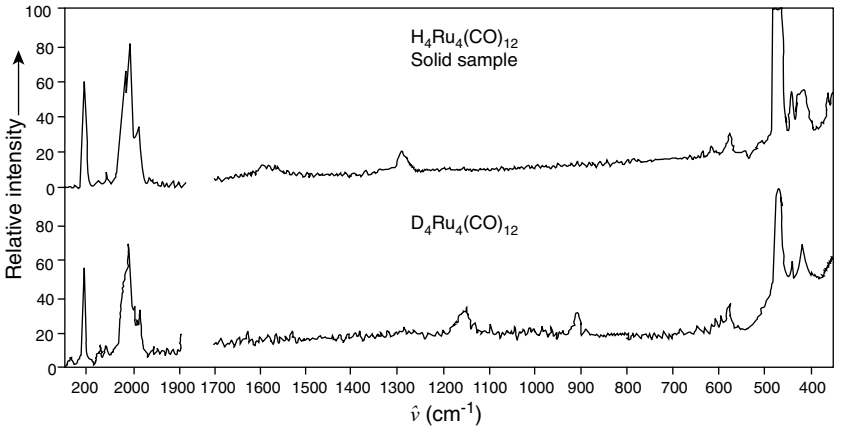

Fig. 1.66. *Raman spectra of $Ru_4H_4(CO)_{12}$ and its deuterated analog [1075].*

1.18.6. Metal Carbonyls in Inert Gas Matrices

General theory of matrix isolation spectroscopy and examples of matrix cocondensation reactions are given in Secs. 1.25 and 1.26 of Part A, respectively. Cocondensation reaction of metal atom vapors with CO yields a mixture of different compositions

$$M + nCO \rightarrow M(CO)_n \quad (n = 1 \sim 6)$$

and photolysis of coordinatively saturated metal carbonyls yields metal carbonyls of lower coordination numbers:

$$M(CO)_n \xrightarrow{h\nu} M(CO)_{n-1} \xrightarrow{h\nu} M(CO)_{n-2} \rightarrow$$

Andrews and co-workers [1081] prepared a variety of metal carbonyls and determined their structures using the methods described in Sec. 1.26. In most cases, their structures were elucidated on the basis of IR spectra in the high-frequency region, because Raman spectra are technically difficult to measure in inert gas matrices and because the spectra in the low-frequency region are difficult to measure even by IR spectroscopy. Table 1.52 lists the symmetry, structure, and the number of IR-active ν(CO) vibrations of $M(CO)_n$ ($n = 1$–6)-type molecules. As an example, Fig. 1.38 of Part A shows the IR spectra of $Sc(CO)_n$ obtained by cocondensation reaction in Ar matrices.

$Ni(CO)_2$ in Ar matrices is bent ($\mathbf{C}_{2v}$) and not linear as previously proposed. This was confirmed by complete assignments of all the nine modes, including $^{58/60}$Ni and $^{12/13}$C isotopomers [1082]. The linear Pd(CO) molecule in Ar matrices (site I) exhibits five palladium isotope peaks (^{104}Pd, ^{105}Pd, ^{106}Pd, ^{108}Pd, and ^{110}Pd) of the ν(Pd−C) vibrations at 472.97, 472.48, 472.06, 471.18, and 470.32 cm^{-1}, respectively [1083]. As stated in Sec. 1.26, cationic $M(CO)_n^+$ species such as $Fe(CO)^+$ and $Fe(CO)_2^+$ are produced by laser ablation techniques [1084], whereas anionic species such as

TABLE 1.52. Number of Infrared-Active CO Stretching Vibrations for $M(CO)_x$

Molecule	Symmetry and Structure		IR-Active ν(CO)
M(CO)	$\mathbf{C}_{\infty v}$	Linear	$\sum^+$
$M(CO)_2$	$\mathbf{D}_{\infty h}$	Linear	$\sum_u^+$
$M(CO)_2$	$\mathbf{C}_{2v}$	Bent	$A_1 + B_2$
$M(CO)_3$	$\mathbf{D}_{3h}$	Trigonal–planar	E'
$M(CO)_3$	$\mathbf{C}_{3v}$	Trigonal–pyramidal	$A_1 + E$
$M(CO)_4$	$\mathbf{T}_d$	Tetrahedral	F_2
$M(CO)_4$	$\mathbf{D}_{4h}$	Square–planar	E_u
$M(CO)_5$	$\mathbf{C}_{4v}$	Tetragonal–pyramidal	$2A_1 + E$
$M(CO)_5$	$\mathbf{D}_{3h}$	Trigonal–bipyramidal	$A_2'' + E'$
$M(CO)_6$	$\mathbf{O}_h$	Octahedral	F_{1u}

$Ni(CO)_n^-$ ($n = 1$–3) are produced by UV irradiation and electron bombardment [1085]. For all metal carbonyls, ν(CO) frequencies follow the order, cations > neutrals > anions. For example, $Ni(CO)^+$ (2206.3) > Ni(CO)(2006.6) > $Ni(CO)^-$(1860.6) (all in cm^{-1}) [1081].

Ultraviolet photolysis of $Ni(CO)_4$ in O_2-doped Ar matrices produces mixed-ligand species such as (η^2 –O_2)$Ni(CO)_2$, (η^2-O_2)$Ni(CO)_3$, and O=$Ni(CO)_2$. The $\nu(^{16}O_2)$ of the side-on O_2 of the first species is at 978 cm^{-1} [1086]. The ν(CO) of linear M(CO)Cl-type molecules are at 2218.7, 2156.8, and 2184.0 cm^{-1} for M = Ni, Cu, and Ag, respectively [1087].

Photon-induced isomerization reactions such as shown below are known to occur for

$$M(CO) \xrightarrow{h\nu} C{-}M{-}O \; (M = Nb,Th,U)$$

$$M(CO)_2 \xrightarrow{h\nu} O{-}M{-}C{-}C{-}O \; (M = Ti,Zr,Hf,Nb,Ta,Th,U)$$

For example, C−Nb−O thus obtained exhibits two bands at 919.8 and 783.7 cm^{-1} [1088]. The ν(CO) of Li−CO and Li−OC were observed at 1806 and 1614 cm^{-1}, respectively, in Kr matrices [1089]. Such an "isocarbonyl" structure, O=C−Au−O=C, was also proposed for $Au(CO)_2$ [1090]. The pair of OC−BeO and CO−BeO was produced by the cocondensation reaction of pulsed-laser-evaporated Be atoms with CO_2/Ar. The former exhibits the ν(CO) and ν(Be−O) at 2139.4 and 1498.2 cm^{-1}, respectively, whereas the latter exhibits these bands at 2056.5 and 1533.9 cm^{-1} [1091].

Poliakoff and Turner [1092] carried out UV photolysis of ^{13}CO-enriched $Fe(CO)_5$ in SF_6 and Ar matrices [$Fe(CO)_5 \xrightarrow{h\nu} Fe(CO)_4 + CO$], and concluded that the structure of $Fe(CO)_4$ is $\mathbf{C}_{2v}$ since it exhibits four ν(CO) ($2A_1 + B_1 + B_2$) in the infrared spectrum. Graham et al. [1093] proposed the $\mathbf{C}_{4v}$ structure for $Cr(CO)_5$ produced by the photolysis of $Cr(CO)_6$ in inert gas matrices. On the other hand, Kündig and Ozin [1094] proposed the $\mathbf{D}_{3h}$ structure for $Cr(CO)_5$ prepared by cocondensation of Cr atoms with CO in inert gas matrices. They derived a general rule that $M(CO)_5$ species take the $\mathbf{D}_{3h}$ structure when the number of valence-shell electrons is even [Cr (16), Fe (18)], and the $\mathbf{C}_{4v}$ structure when it is odd [V (15), Mn (17)]. However, the $\mathbf{D}_{3h}$, structure of $Cr(CO)_5$ has been questioned by Black and Braterman [1095] and Perutz and Turner [1096].

The UV photolysis of $Fe_2(CO)_9$ in Ar matrices produces $Fe_2(CO)_8$ of $\mathbf{C}_{2v}$ symmetry having two bridging CO groups [1097]. Photolysis of $Mn_2(CO)_{10}$ by plane-polarized light in Ar matrices produces $Mn_2(CO)_9$, which exhibits the ν(CO) at 1764 cm^{-1} [1098,1099]. Dunkin et al. [1098] proposed the semibridging structure on the basis of its polarization properties:

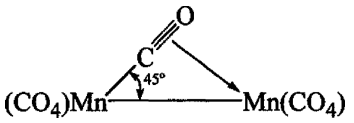

Ultraviolet photolysis of $MnRe(CO)_{10}$ in Ar matrices yields $MnRe(CO)_9$ with the ν(CO) at 1759.8 cm^{-1} [1100]. A semibridging structure similar to that proposed above may be expected.

Carbonyl complexes of the type MX_2CO are formed by reacting metal halide vapor directly with CO in inert gas matrices [1101,1102]. In this case, ν(CO) shifts to higher frequencies by complexation, since the bonding is dominated by the donation of σ-electrons to the metal. On the other hand, ν(MX) shifts to lower frequencies because the oxidation state of the metal is lowered by accepting σ-electrons from CO. Figure 1.67 shows infrared spectra of the PbF_2–L system (L = CO,NO,N_2) in Ar matrices obtained by Tevault and Nakamoto [1102].

In this series, the magnitudes of the shifts of the PbF_2 and L stretching bands (cm^{-1}) relative to the free state are as follows:

	PbF_2CO	PbF_2NO	PbF_2N_2
$\nu_s(PbF_2)$	−10.8	−8.8	−5.8
ν_a (PbF_2)	−10.9	−8.5	−5.0
ν(L)	+38.4	+16.4	—

This result definitely indicates that CO is the best, NO is the next best, and N_2 is the poorest σ-donor.

Other work involves the direct deposition of stable carbonyls in inert gas matrices, mainly to study the effect of matrix environments on the structure. Both $Fe(CO)_5$ [1103] and $M_3(CO)_{12}$ (M = Ru,Os) [1104] were found to be distorted from $\mathbf{D}_{3h}$ symmetry in inert gas matrices. If a thick deposit is made on a cryogenic window while maintaining a relatively high sample/inert gas dilution ratio, it is possible to observe low-frequency modes such as ν(MC) and δ(MCO). It was found that these bands show splittings due to the mixing of metal isotopes. For example, the F_{1u} ν(CrC) of $Cr(CO)_6$ in a N_2 matrix exhibits four bands due to ^{50}Cr, ^{52}Cr, ^{53}Cr, and ^{54}Cr (see Fig. 1.36 of Part A). The magnitude of these isotope splittings may be used to estimate the degree of the ν(MC)–δ(MCO) mixing in the low-frequency vibrations [1105].

1.18.7. Theoretical Calculations of Vibrational Frequencies

Normal coordinate analyses on metal carbonyl compounds have been carried out by many investigators. Among them, Jones and coworkers have made the most

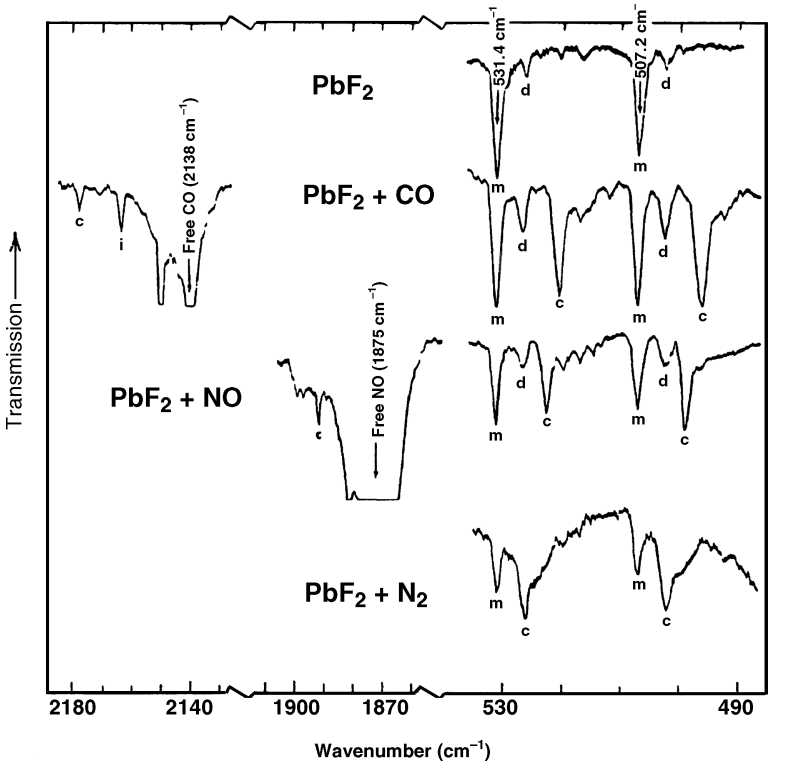

Fig. 1.67. *Infrared spectra of PbF_2, PbF_2CO, PbF_2NO, and PbF_2N_2 in Ar matrices: (m) monomeric PbF_2; (d) dimeric PbF_2; (c) complex; (i) impurity (HF–CO) [1101].*

extensive study in this field. For example, they performed rigorous calculations on the $M(CO)_6$ (M = Cr,Mo,W) series [936], $Fe(CO)_5$ [935], and $Mn(CO)_5Br$ [1022], including their ^{13}C and ^{18}O analogs. For the last compound, 5 stretching, 16 stretching–stretching interaction, and 33 bending–bending interaction constants (GVF) were used to calculate its 30 normal vibrations.

On the other hand, Cotton and Kraihanzel (C–K) [1106] developed an approximation (C–K) method for calculating the CO stretching and CO−CO stretching interaction constants, while neglecting all other low-frequency modes. For $Mn(CO)_5Br$, they used only the five force constants [1107] shown in Fig. 1.68. Since only four CO stretching bands are observed for this type of compound, it was assumed that $\frac{1}{2}k_t = k_c = k_d$ holds. This was justified on the basis of the symmetry properties of the metal $d\pi$ orbitals involved. This C–K method has since been applied to many other carbonyls in making band assignments, in interpreting intensity data, and in discussing the bonding schemes of metal carbonyls [924]. It is clear that the choice of a rigorous approach (Jones) or a simplified method (C–K) depends on the availability of observed data and the purpose of the

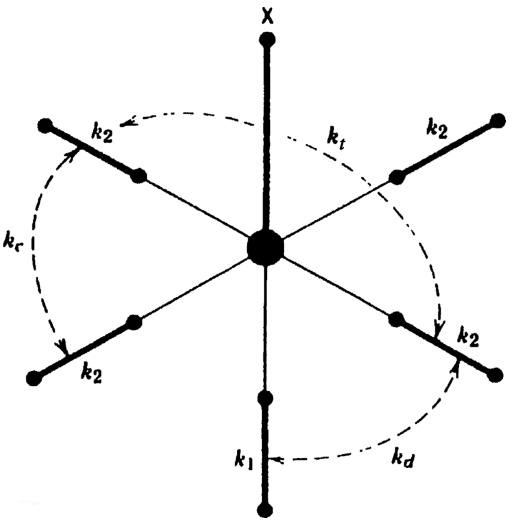

Fig. 1.68. *Definition of force constants for $M(CO)_5X$.*

investigation. Jones [1108] and Cotton [1109] discuss the merits of their respective approaches relative to the alternative.

As mentioned earlier, ν(CO) of metal carbonyls are determined by two factors: (1) donation of the 5σ-electrons to the empty metal orbital tends to raise the ν(CO) since the 5σ orbital is slightly antibonding; and (2) backdonation of metal $d\pi$-electrons to the $2p\pi$ orbitals of CO tends to lower ν(CO) since the $2p\pi$ orbitals are antibonding. Vibrational spectroscopy does not allow observation of these two effects separately since the observed ν(CO) and the corresponding force constant reflect only the net result of the two counteracting components. It is possible, however, to correlate the CO stretching force constants (C–K) with the occupancies of the 5σ and $2p\pi$ orbitals as calculated by MO theory. Table 1.53 lists the results obtained for d^6 carbonyl halides and dihalides by Hall and Fenske [1110]. It is interesting that the *trans*-CO in $Fe(CO)_4I_2$ and the *cis*-CO in $Mn(CO)_5Cl$ have almost the same force constants since the 5σ occupancy of the former is smaller by 0.102 than that of the latter, while the $2p\pi$ occupancy of the former is larger by 0.108 than that of the latter. It is also noteworthy that the *trans*-CO in $Fe(CO)_4I_2$ and the *cis*-CO in $Cr(CO)_5Cl^-$ have identical $2p\pi$ occupancies (0.537) but substantially different force constants (17.43 and 15.58 mdyn/Å, respectively). In this case, the difference in force constants originates in the difference in the 5σ occupancies (1.293 vs. 1.457). Hall and Fenske [1110] found a linear relationship between the C–K CO stretching force constants and the occupancies of the 5σ and $2p\pi$ levels:

$$k = -11.73[2\pi_x + 2\pi_y + (0.810)5\sigma] + 35.81$$

TABLE 1.53. Carbonyl Orbital Occupancies[a] and Force Constants

Compound	Structure	5σ	$2\pi_x$	$2\pi_y$	k (mdyn/Å)[b]
$Cr(CO)_5Cl^-$	*trans*	1.407	0.355	0.355	14.07
$Cr(CO)_5Br^-$	*trans*	1.405	0.353	0.353	14.10
$Mn(CO)_4I_2^-$	*trans*	1.354	0.302	0.330	15.48
$Mn(CO)_4IBr^-$	*trans*	1.355	0.302	0.327	15.48
$Mn(CO)_4Br_2^-$	*trans*	1.357	0.302	0.325	15.50
$Cr(CO)_5Br^-$	*cis*	1.456	0.261	0.282	15.56
$Cr(CO)_5Cl^-$	*cis*	1.457	0.261	0.276	15.58
$Mn(CO)_5Cl$	*trans*	1.352	0.286	0.286	16.28
$Mn(CO)_5Br$	*trans*	1.350	0.286	0.286	16.32
$Mn(CO)_5I$	*trans*	1.349	0.286	0.286	16.37
$Mn(CO)_4I_2^-$	*cis*	1.402	0.251	0.251	16.75
$Mn(CO)_4IBr^-$	*cis*	1.404	0.241	0.252	16.77
$Mn(CO)_4Br_2^-$	*cis*	1.406	0.242	0.242	16.91
$Mn(CO)_5I$	*cis*	1.394	0.213	0.240	17.29
$Mn(CO)_5Br$	*cis*	1.394	0.212	0.228	17.39
$Fe(CO)_4I_2$	*trans*	1.293	0.252	0.285	17.43
$Mn(CO)_5Cl$	*cis*	1.395	0.211	0.218	17.46
$Fe(CO)_4Br_2$	*trans*	1.295	0.250	0.272	17.53
$Fe(CO)_5Br^+$	*trans*	1.287	0.233	0.233	17.93
$Fe(CO)_5Cl^+$	*trans*	1.289	0.233	0.233	17.95
$Fe(CO)_4I_2$	*cis*	1.337	0.221	0.221	17.95
$Fe(CO)_4Br_2$	*cis*	1.338	0.205	0.205	18.26
$Fe(CO)_5Cl^+$	*cis*	1.325	0.171	0.177	18.99
$Fe(CO)_5Br^+$	*cis*	1.325	0.171	0.193	19.00

[a]The *cis* and *trans* designations of the CO groups are made with respect to the position of the halogen or halogens.
[b]Cotton–Kraihanzel force constants (see Ref. 1110).

A similar attempt has been made for a series of Mn carbonyls containing isocyanide groups [1111].

As described in Sec. 1.24 of Part A, density functional theory (DFT) has been used to determine the structures of a variety of compounds and to calculate their vibrational frequencies. In particular, this method was indispensable in elucidating the structures and in making vibrational assignments of novel metal carbonyls produced in inert gas matrices (Sec. 1.26).

1.19. COMPLEXES OF CARBON DIOXIDE

Although CO_2 is highly inert, a few complexes with metal atoms and metal ions in the low oxidation state are known. These complexes have been a subject of considerable interest because they have the potential to become catalysts in activating CO_2, which is the most abundant source of C_1 compounds.

Thus far, vibrational studies on metal complexes of CO_2 are limited to a small number of compounds, because stable complexes of CO_2 are rare. The CO_2 ligand may

coordinate to a metal in any one of the following schemes:

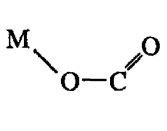

End-on (C_s)

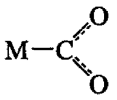

C-bonded (C_{2v})

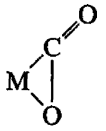

Side-on (C_s)

Different from the linear CO_2 molecule in the free state, the CO_2 ligand in metal complexes is generally bent. Furthermore, the bond orders of the two CO bonds change markedly on coordination. Thus, the three vibrations observed for free CO_2 show large downshifts in metal complexes. Table 1.54 lists the observed frequencies of typical complexes and their modes of coordination. The CO_2 vibrations in metal complexes can easily be identified since they are sensitive to $^{13}C^{12}O$ and $^{12}C^{18}O$ substitutions. According to Jegat et al. [1115,1116], it is possible to distinguish the three modes of coordination on the basis of $\nu_3 - \nu_1$ values and the magnitudes of isotopic shifts due to ^{13}C and ^{18}O substitutions.

A variety of CO_2 complexes were prepared by reacting CO_2 with metal atom vapor produced by thermal heating. According to Mascetti and Tranquille [1120], matrix cocondensation reaction of Ti atom with pure CO_2($\sim$ 1/1000, 15 K) yields a side-on type complex, $OTi(CO_2)$:

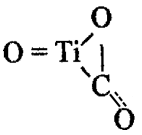

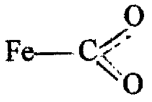

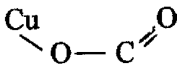

TABLE 1.54. Observed CO_2 Stretching Frequencies (cm^{-1}) and Modes of Coordination

Compound	ν_3	ν_1	Mode of Coordination	Ref.
Free CO_2	2349	1337	—	330 (Chapter 2, Part A)
$[U(IV)(CO_2)L]^a$	2188	—	End-on[b]	1112
cis-$[Ru(bipy)_2(CO)(CO_2)]$	1443	—	End-on	1113
$[\{Ir_4S_2CH_2CN\}(CO_2)]^+$	1682	—	End-on	1114
$Cp_2Ti(CO_2)(PMe_3)$	1671	1187	C-bonded	1115
$Mo(CO_2)_2(PMe_3)_4$	1668	1153	Side-on	1116
		1102		
$Fe(CO_2)(PMe_3)_4$	1623	1106	Side-on	1116
$Ni(CO_2)(PCy_3)_2$[c]	1741	1150	Side-on	1117
		1093		
$Ni(CO_2)(PEt_3)_2$	1660	1203	Side-on	1118
	1635	1009		
$RhCl(CO_2)(PBu_3)_2$	1668	1165	Side-on	1119
	1630	1120		

[a] L = (^{ad}ArOH)$_3$tacn = l,4,7-tris(3-adamantyl-5-*tert*-butyl-2-hydroxybenzyl)1,4,7-triazacyclononane.
[b] Almost linear end-on coordination. The UOC and OCO angles are 171° and 178°, respectively.
[c] Cy = cyclohexyl.

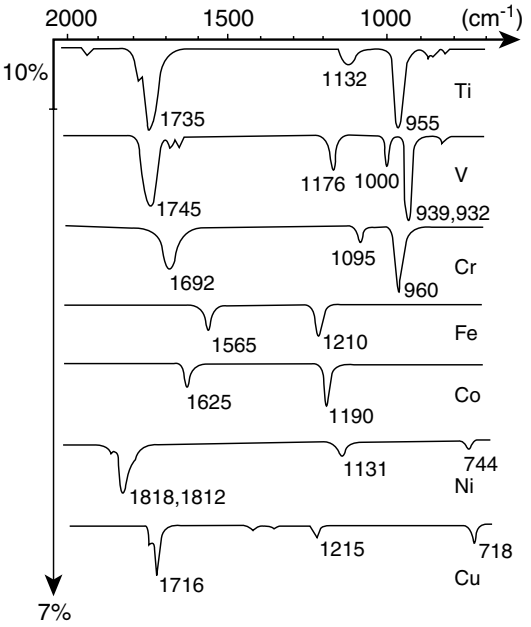

Fig. 1.69. *IR spectra of the cocondensation reaction products of transition metal atoms with pure CO_2 at 15 K ($M/CO_2 \sim 1/1000$) (bands arising from H_2O at 1615 cm^{-1} and CO_2 have been omitted for clarity) [1120].*

It exhibits the ν(C=O), ν(C−O), ν(Ti=O), and ν(Ti−O) at 1776/1735, 1132, 955, and 455 cm^{-1}, respectively. No simple Ti(CO_2) was detected in this case because it is unstable and its decomposition product, Ti−O, reacts with the second CO_2 to form OTi(CO_2). The cocondensation product of Fe atom with CO_2 exhibits IR bands at 1565 (ν_3) and 1210 (ν_1) cm^{-1}, which suggests a C-bonded structure. On the other hand, the cocondensation product of Cu atom with CO_2 exhibits the ν(C=O), ν(C−O), and δ(OCO) at 1722/1716, 1215, and 718 cm^{-1}, respectively. The end-on structure of *cis*-conformation shown above was proposed. Figure 1.69 shows the IR spectra of these and other cocondensation products at 15 K [1120].

Solov'ev et al. [1121] measured the IR spectra of the cocondensation products of pure CO_2 with Mg atom vapor produced by thermal heating. Three bands were observed at 1580, 1385, and 866 cm^{-1}. Theoretical calculations suggested the formation of a four-membered ring in which the Mg atom is chelated to the two oxygen atoms of CO_2. Le Quere et al. [1122] carried out cocondensation reactions of thermally produced Al atom vapor with CO_2/Ar, and found two geometric isomers of Al(CO_2) that are reversibly interconvertable. The low-temperature form takes an end-on structure of $\mathbf{C}_s$ symmetry and exhibits the ν(C=O), ν(C−O), δ(OCO), and ν(Al−O) at 1780, 1146.5, 773, and 468.5 cm^{-1}, respectively, whereas the high-temperature form takes a four-membered ring structure of $\mathbf{C}_{2v}$ symmetry similar to that of Mg(CO_2) mentioned above. It exhibits the ν_a(C−O), ν_s(C−O), δ(OCO), ν_s(Al−O), and ν_a(Al−O) at 1443.5, 1265,5, 796,5, 428, and 213,5 cm^{-1}, respectively. In the case

of Ag atom with CO_2, the CO_2 vibrations are essentially unperturbed, indicating only a weak interaction [1123].

Reactions of laser-ablated rhenium atoms with CO_2 in Ar produce ORe(CO), $ORe(CO)_2$, $O_2Re(CO)$, $O_2Re(CO)_2$, and anionic species, $[ORe(CO)]^-$ and $[ORe(CO)_2]^-$, and elucidation of their structures has been based on the results of isotope shifts, warmup experiments, and DFT calculations [1124]. Reactions of laser-ablated CuX_2 (X = Cl,Br) with CO_2/Ar yield XCuOCO-type complexes, which are linear and exhibit the ν(CO) vibration at 2383.9 and 2381.4 cm^{-1}, respectively, for X = Cl, and Br [1125].

1.20. NITROSYL COMPLEXES

Like CO, NO acts as a σ-donor and a π-acceptor. The NO contains one more electron than CO, and this electron is in the $2p\pi^*$ orbital. The loss of this electron gives the nitrosonium ion, $(NO)^+$, which is much more stable than NO. Thus, the ν(NO) of the nitrosonium ion (2273 cm^{-1}) is much higher than that of the latter (1880 cm^{-1}). On the other hand, the addition of one electron to this orbital produces the $(NO)^-$ ion, which is less stable and gives a lower frequency ($\sim$1366 cm^{-1}) than does NO. Such a charge effect has already been discussed in Sec. 2.1 of Part A.

In nitrosyl complexes, ν(NO) ranges from 1900 to 1500 cm^{-1}. X-Ray studies on nitrosyl complexes have revealed the presence of linear and bent M−NO groups:

I II

In the valence-bond theory, the hybridizations of the N atom in (I) and (II) are *sp* and sp^2, respectively. If the pair of electrons forming the M−N bond is counted as the ligand electrons, the nitrosyl groups in (I) and (II) are regarded as NO^+ and NO^-, respectively. Thus, one is tempted to correlate ν(NO) with the charge on NO and the MNO angle. It was not possible, however, to find simple relationships between them since ν(NO) is governed by several other factors (electronic effects of other ligands, nature of the metal, structure, and charge of the whole complex etc.) [1126]. According to Haymore and Ibers [1127], the distinction between linear and bent geometry can be made by using properly corrected ν(NO) values; the MNO group is linear or bent, respectively, if this value is above or below 1620–1610 cm^{-1}. Several review articles are available for vibrational spectra of nitrosyl complexes [1126,1128–1132].

1.20.1. Inorganic Nitrosyl Complexes

Table 1.55 lists the vibrational frequencies of typical nitrosyl complexes. Although the M−NO group is expected to show ν(NO), ν(MN), and δ(MNO), only ν(NO) have been observed in most cases. The latter two modes are often coupled since their frequencies are

TABLE 1.55. Vibrational Frequencies of Inorganic Nitrosyl Complexes (cm^{-1})

Compound	ν(NO)	ν(MN)	δ(MNO)	Ref.
$Cr(NO)_4$	1721	650	496	1133
$Co(NO)_3$	1860 1795	—	—	1134
$[Mo(NO)_5]^{5+}$	1912, 1816, 1675	665, 633, 560, 516, 380	470, 320, 186	1135
$Cr(CO)_3(NO)_2$	1705	—	—	1136
$Co(CO)_3(NO)$	1822	609	566	1137
$Mn(CO)_4(NO)$	1781	524	657	1138
$Mn(PF)_3(NO)_3$	1836, 1744	—	—	1139
$cis[MoCl_4(NO)_2]^{2-}$	1720, 1600	—	—	1140
$NiCl_2(NO)_2$	1872, 1842	—	—	1141
$[RuCl_5(NO)]^{2-}$	1904	606	588	1142
$[RuBr_5(NO)]^{2-}$	1870	572	300	1143
$[Tc(NO)(CNCMe_3)_5]^{2+,a}$	1865	—	—	1144

[a] $CNCMe_3$: *tert*-butyl isocyanide. This complex is formulated as $[Tc(I)(NO)^+(CNCMe_3)_5]^{2+}$ because of its high ν(NO).

close to each other. Jones et al. [1137] carried out a complete analysis of the vibrational spectra of $Co(CO)_3(NO)$ and its ^{13}C, ^{18}O, and ^{15}N analogs. According to Quinby-Hunt and Feltham [1145], vibrational spectra of a wide variety of nitrosyl complexes can be accounted for on the basis of the simple three-body (M−N−O) model as long as the complex does not contain two or more NO groups attached to the metal.

Vibrational spectra of nitroprusside salts have been studied extensively [1146]. Khanna et al. [1147,1148] assigned the IR and Raman spectra of the $Na_2[Fe(CN)_5(NO)]\cdot 2H_2O$ crystal and its deuterated analog. On the basis of a comparison of ν(CN), δ(FeCN), and ν(Fe−CN) between the Fe(II) and Fe(III) complexes of the $[Fe(CN)_5X]^{n-}$-type ions, Brown [1149] suggested that the Fe−NO bonding of the $[Fe(CN)_5(NO)]^{2-}$ ion be formulated as Fe(III)−NO and not as Fe(II)−NO^+. Tosi and Danon [1150] studied the IR spectra of $[Fe(CN)_5X]^{n-}$ ions ($X = H_2O, NH_3, NO_2^-$, NO^-, SO_3^{2-}). The ν(CN) of the nitroprusside (2170, 2160, and 2148 cm^{-1}) are unusually high in this series because the Fe−CN π-backbonding in this ion is much less than in other compounds owing to extensive Fe−NO π-backbonding. Vibrational spectra of nitroprusside salts of various forms have been assigned [1151–1153]. The IR spectra of $K_3[Mn(CN)_5(NO)]$ and its ^{15}NO analog have been reported [1154,1155].

According to X-ray analysis, $RuCl(NO)_2(PPh_3)_2PF_6$ contains one linear M−NO group and one bent M—NO group that exhibit the ν(NO) at 1845 and 1687 cm^{-1}, respectively [1156]. $CoCl_2(NO)L_2$ [$L = P(CH_3)Ph_2$] exists in two isomeric forms:

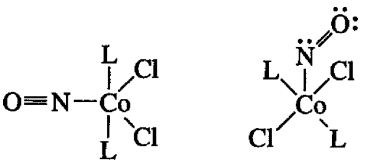

The ν (NO) of the former is at 1750 cm^{-1}, whereas that of the latter is at 1650 cm^{-1} [1157].

The ν(NO) of the bridging nitrosyl group is much lower than that of the terminal nitrosyl group. For example, $(C_5H_5)_2Cr_2(NO)_3(NXY)$ (X = OH,Y = *t*-Bu) shown below exhibits the terminal ν(NO) at 1683 and 1625 cm^{-1} and the bridging ν(NO) at 1499 cm^{-1} [1158].

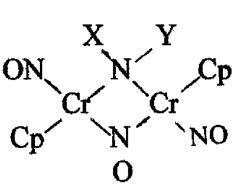

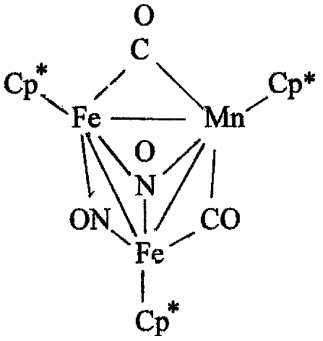

Similar frequencies are reported for an analogous compound [X = Et, Y = $B(Et)_2$] [1159]. The structure of $M_3(CO)_{10}(NO)_2$ (M = Ru,Os) resembles that of $Fe_3(CO)_{12}$ (structure VIII in Fig. 1.59) with double nitrosyl bridges in place of the double carbonyl bridges in the latter. As expected, ν(NO) of these nitrosyl groups are very low: 1517 and 1500 cm^{-1} for the Ru compound, and 1503 and 1484 cm^{-1} for the Os compound [1160]. The bridging ν(NO) of $[Ru_2(\mu\text{-}NO^-)_2(bipy)_4]$ $(ClO_4)_2$ is much lower (1363 cm^{-1}) than that of $[Ru_2(\mu\text{-}NO)_2(acac)_4]$ (1575 cm^{-1}), which contains formally neutral NO bridges [1161]. In $[Cp^*_3\ Fe_2Mn(\mu\text{-}CO)_2(\mu_2\text{-}NO)(\mu_3\text{-}NO)]$ shown above, the $\nu(\mu_2$-NO) and $\nu(\mu_3$-NO) are observed at 1518 and 1320 cm^{-1}, respectively [1162].

The ν(NO) is spin-state-sensitive in Fe(NO)(salphen) [salphen - N,N′-*o*-phenylenebis(salicylideneimine)]: 1724 cm^{-1} for the high-spin (room temperature) and 1643 cm^{-1} for the low-spin (liquid N_2 temperature) states [1163]. Photolysis of $Cr(NO)_4$ in Ar matrices produces $Cr(NO)_3(NO^*)$ where NO* denotes a bent NO group with an unusually low ν(NO) (1450 cm^{-1}) [1164]. Similar observations were made for the photolysis products of $Mn(CO)(NO)_3$ [1165] and $Ni(C_5H_5)(NO)$ [1166].

1.20.2. NO Adducts of Metalloporphyrins

Table 1.56 lists the ν(NO) of metalloporphyrins in which the NO groups take linear geometry. In $Fe(TPP)(NO)_2$, however, the two ν(NO) bands at 1870 and 1690 cm^{-1} have been assigned to the linear $Fe(II)-(N0)^+$ and the bent $Fe(II)-(NO)^-$, respectively [1168].

The low-frequency modes, such as ν(M−NO) and δ(MNO), have been observed by RR studies (Soret excitation). For example, a "strapped" porphyrin, Mn(SP-15)(NO) (N-MeIm) (Fig. 1.64) exhibits the ν(NO), ν(M−NO), and δ(MNO) at 1727, 631, and 578 cm^{-1}, respectively [1173]. A simple porphyrin such as Mn(PPDME)(NO)

TABLE 1.56. NO Stretching Frequencies of Metalloporphyrins (cm^{-1})

Compound	IR/Raman	ν(NO)	Ref.
Cr(TPP) (NO)	IR	1700	1167
Mn(TPP) (NO)	IR	1760	1167
Fe(TPP) (NO)	IR	1700	1168
Ru(TPP)(NO)Cl	IR	1845	1169
Ru(TPP)(NO)(ONO)	IR	1852	1170
Fe(TPP) $(NO)_2$	IR	1870	1168
		1690	
Fe(PPDME) (NO)	IR	1660	1171
Fe(PPDME) (NO)-(N-MeIm)	IR	1676	1171
Fe(TPP) (NO)	RR (in THF)	1681	1172
Fe(TPP) (NO^-)	RR (in THF)	1496	1172

[a]PPDME = protoporphyrin IX dimethyl ester.

(N-MeIm) (PPDME = protoporphyrin IX dimethylester) shows the ν(NO) and ν(M−NO) at 1733 and 628 cm^{-1}, respectively. Thus, introduction of steric hindrance lowers the ν(NO) and raises the ν(M−NO). Lipscomb et al. [1174] observed the RR spectra of NO adducts of iron porphyrins by Soret excitation. The ν[Fe(II)−NO] and ν[Fe(III)−NO] are at ∼527 and ∼600 cm^{-1}, respectively. The NO adducts of heme proteins exhibit the ν(NO) at ∼554 cm^{-1}, which is much higher than that of simple porphyrins (∼527 cm^{-1}). Thus, the cage effect of proteins raises the ν(NO) in this case. It was also noted that the ν[Fe(II)−NO] is insensitive to the nature of the *trans* ligand. This is markedly different from the ν[Fe(II)−CO], ν[Fe(II)−O_2], and ν[Fe(II)−CN], which are sensitive to the *trans* ligand. The δ(MNO) vibrations were not observed for iron porphyrins.

1.20.3. Metastable States of Nitroprussides

When a sample of $Na_2[Fe(CN)_5(NO)]\cdot 2H_2O$ is irradiated by the 488.0-nm line of an Ar–ion laser at 20 K, two electronically excited metastable states (MS_1 and MS_2) are produced. Güida et al. [1175,1176] have measured the IR spectra of these metastable states using an orientated single crystal. The upper traces of Fig. 1.70 show the polarized IR spectra of the ground-state complex (GS) with the electric vectors parallel to the *a* and *c* axes, respectively. The ν(NO) near 1950 cm^{-1} is strong and broad in the former but rather weak in the latter, because the linear Fe−N−O axis [1177] is on the *ab* plane of the orthorhombic crystal. The δ(FeNO) and ν(Fe−NO) bands are seen at 667 and 658 cm^{-1}, respectively.

On irradiation at 20 K, two sets of new bands appear as shown in the lower traces of Fig. 1.70. The bands at 1834, 583, and 565 cm^{-1} (marked by 1) are assigned to the ν(NO), δ(FeNO), and ν(Fe−NO) of MS_1, and those at 1663, 597, and 547 cm^{-1} (marked by 2) are assigned to the corresponding modes of MS_2. Thus, all three bands are shifted markedly in going from GS to MS_1 and MS_1 to MS_2. Similar redshifts are observed for the ν(CN) near 2150 cm^{-1}, although the magnitudes of their shifts are much smaller than those observed for the FeNO group vibrations. This result indicates

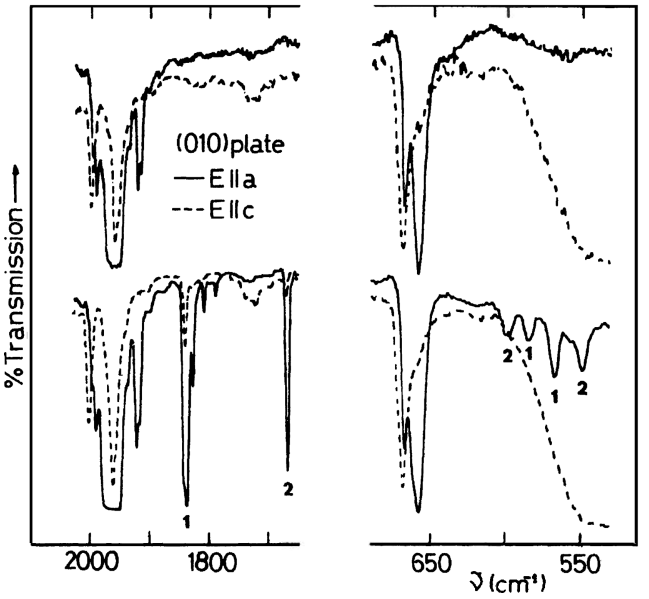

Fig. 1.70. *Low-temperature polarized IR spectra of ground-state (top traces) and metastable (bottom traces) anions in $Na_2[Fe(CN)_5NO]\cdot 2H_2O$ single-crystal plate that was cut along the 010 plane; 1 and 2 denote the peaks resulting from the MS_1 and MS_2 states, respectively [1196].*

that the electronic transitions mainly involve the FeNO bond. The MS_1 is stable below 200 K, whereas MS_2 is stable only below 150 K.

According to the X-ray analysis at 50 K by Carducci et al. [1178], the NO ligand in the MS_1 state is a linear O-bonded isonitrosyl (Fe−O−N), and the results of polarized Raman studies by Morioka et al. [1179] are consistent with such a structure. Extensive IR and DFT studies including $^{14}N/^{15}N$, $^{16}O/^{18}O$, and $^{54}Fe/^{56}Fe$ isotope shift data by Aymonino and coworkers [1180,1181] also support this structure. On the other hand, X-ray analysis [1178] shows that the NO ligand in the MS_2 state is side-on with the Fe−N, Fe−O, and N−O distances of 1.89(2), 2.07(2) and 1.14(2) Å, respectively. This structure was also supported by the IR studies cited above [1181].

Similar photo-induced isomerization occurs for Ru(II) complxes. X-Ray analysis of *trans*-$K_2[Ru(NO_2)_4(OH)(NO)]$ indicates that the NO ligand in the MS_1 state takes an almost linear Ru−O−N structure (RuON angle, 169°) while it takes a side-on structure in the MS_2 state [1182]. IR studies [1183] show that the ν(NO) at 1914 cm^{-1} in the ground state is shifted to 1790 cm^{-1} in the MS_1 state. Although *trans*-$[Ru(NH_3)_4(NO)(nicotinamide)]^{3+}$ shows that the ν(NO) at 1974 cm^{-1} (with a shoulder at 1918) in the ground state is shifted to 1826 cm^{-1} in the MS_1 state, it was not observed in the MS_2 state [1184]. IR and Raman studies were also carried out on $K_2[RuCl_5(NO)]$ [1185]. The ν(NO) was observed at 1765 in the MS_1 state and 1554/1550 cm^{-1} in the MS_2 state. Kawano et al. [1186] carried out X-ray analysis on *trans*-$[Ru(en)_2(H_2O)(NO)]Cl_3$, and confirmed the Ru−O−N bonding in the MS_1 state. These workers

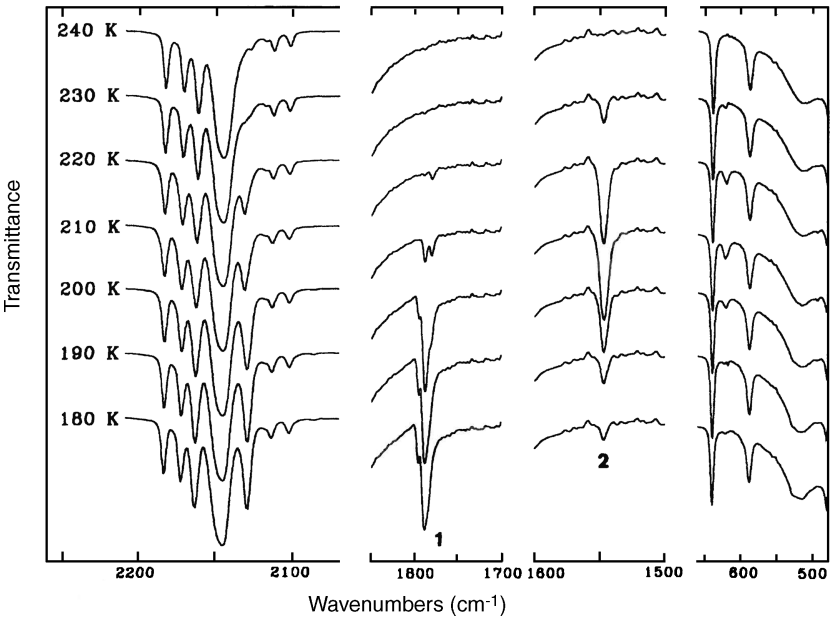

Fig. 1.71. *Effect of heating on the IR spectrum of $Na_2[Os(CN)_5NO]\cdot 2H_2O$ in the MS_1 state, which was produced by irradiation with an Ar–ion laser (457.9 nm) at 80 K; 1 and 2 denote the ν(NO) bands of the MS_1 and MS_2 states, respectively [1211].*

assigned the ν(Ru−O) and δ(RuON) at 492 and 484 cm^{-1}, respectively. The corresponding ν(Ru−N) and δ(RuNO) in the ground state are observed at $\sim$ 590 cm^{-1}. IR/Raman studies on metastable states are reported for *trans*-$[Ru(H_{ox})(en)_2(NO)]Cl_2$ (H_{ox} = oxalic acid monoanion) [1187] and *cis*- and *trans*-$[RuX(en)_2(NO)]X_2$ (X = Cl, Br) [1188]. For $[Ru(OEP)(O\text{-}iC_5H_{11})(NO)]$, the ν(NO) are at 1791, 1645, and 1497 cm^{-1} for the ground, MS_1, and MS_2 states, respectively [1189].

In the case of the analogous osmium complex, $Na_2[Os(CN)_5(NO)]\cdot 2H_2O$ [1190], the GS, MS_1, and MS_2 states exhibit the ν(NO) at 1897, 1790, and 1546 cm^{-1}, respectively. The MS_1 and MS_2 states can selectively be populated by irradiating the sample with an Ar–ion laser (457.9 nm) and a mercury lamp (280–340 nm), respectively, at 80 K. Figure 1.71 shows the effect of heating on the IR spectrum of MS_1 thus produced. It is seen that the onset decay temperature (T_2) of MS_2 ($\sim$220 K) is higher than that of MS_1 (T_1, $\sim$190 K). This is opposite to the case of the nitroprusside discussed above. Furthermore, the population of the MS_2 state begins to increase at the expense of the MS_1 state near the decay temperature T_1.

The photoexcited MS_1 state was also detected for [Ni(Cp(NO)]. The ν(NO) of the ground and MS_1 states are observed at 1820–1786 and 1576/1566 cm^{-1}, respectively [1191]. Coppens and co-workers [1192] reviewed photoinduced linkage isomers of transition metal nitrosyl complexes and other linkage isomers of di- and triatomic ligands such as N_2, NO_2, and SO_2. Gütlich et al. [1193] reviewed photoswitchable coordination compounds including $Na_2[Fe(CN)_5(NO)]\cdot 2H_2O$.

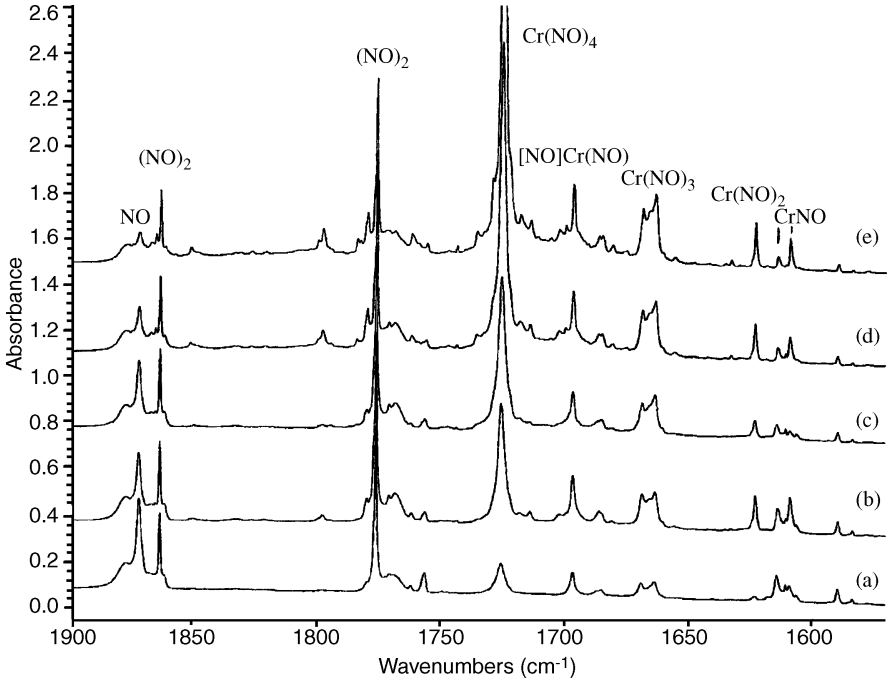

Fig. 1.72. *Infrared spectra in the 1900–1570 cm^{-1} region for laser-ablated chromium atoms codeposited with 0.4% NO in excess argon on a 10 K CsI window: (a) after 1-h sample codeposition at 10 K; (b) after annealing to 25 K; (c) after broadband photolysis for 30 min; (d) after annealing to 30 K; and (e) after annealing to 35 K. Labels in the diagrams employ NO or (NO) to denote η^1- and [NO] to denote η^2-bonding to Cr [1195].*

1.20.4. Matrix Cocondensation Reactions

Similar to the reactions of CO complexes discussed in Sec. 1.18.6, matrix cocondensation reactions of laser-ablated metal atoms with NO have been studied by Andrews and coworkers [1194]. As an example, Fig. 1.72 shows the IR spectra of Cr atoms cocondensed with 0.4% NO in excess Ar [1195]. The band assignments shown were based on the results of warmup experiments, isotope shifts, and DFT calculations. The bands at 1726.0, 1696.8, 1663.5, 1623.3, and 1614.3 cm^{-1} were assigned to Cr $(-NO)_4$, [NO]Cr(−NO), Cr$(-NO)_3$, Cr$(-NO)_2$, and Cr(−NO), respectively. Here, (−NO) and [NO] denote the end-on and side-on coordinations, respectively. Other products such as N−Cr−O (976.1 and 866.2 cm^{-1}) and Cr[NO] (1108.8, 528.2, and 478.0 cm^{-1}) were identified.

1.21. COMPLEXES OF DIOXYGEN

Dioxygen (molecular oxygen) adducts of metal complexes have been studied extensively because of their importance as oxygen carriers in biological systems (Sec. 3.2)

and as catalytic intermediates in oxidation reactions of organic compounds. A number of review articles are available on the chemistry of dioxygen adducts [1126,1196–1205].

As discussed in Sec. 2.1 of Part A, the bond order of the O−O linkage decreases as the number of electrons in the antibonding $2p\pi^*$ orbital increases in the following order:

	$[O_2^+]AsF_6$		O_2		$K[O_2^-]$		$Na_2[O_2^{2-}]$
Bond order	2.5	>	2.0	>	1.5	>	1.0
Bond distance (Å)	1.123	<	1.207	<	1.28	<	1.49
$\nu(O_2)(cm^{-1})$	1858	>	1555	>	1108	>	~760

The decrease in bond order causes an increase in O−O distance and a decrease in $\nu(O_2)$. In fact, there is a good linear relationship between the O−O bond order and the $\nu(O_2)$ of these simple dioxygen compounds.

Dioxygen adducts of more complex molecules are generally classified into two groups; complexes that exhibit $\nu(O_2)$ in the 1200–1100 cm^{-1} region are called "superoxo" because their frequencies are close to that of KO_2, and complexes whose $\nu(O_2)$ are in the 920–750 cm^{-1} region are called "peroxo" because their frequencies are close to that of Na_2O_2. As will be shown later, many compounds exhibit $\nu(O_2)$ outside these regions. Thus, this distinction of dioxygen adducts is not always clear-cut.

Structurally, the dioxygen adducts are classified into four types:

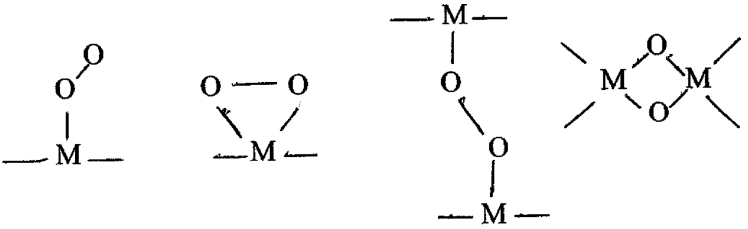

I **End-on (η^1)** II **Side-on (η^2)** III **Bridging end-on** IV **Bridging side-on**

In structure I, two oxygens are not equivalent, whereas they are equivalent in other structures. Thus, the $\nu(^{16}O^{18}O)$ vibration splits into two bands in I, but not in II, III and IV.

1.21.1. Dioxygen Adducts of Metal Atoms

As stated in Sec. 1.26 of Part A, a number of stable and unstable complexes of the ML_n type have been synthesized via matrix cocondensation reactions of metal vapor (M) with gaseous ligands (L). Table 1.57 lists typical results obtained for the $M(O_2)$-type compounds. It is seen that the $\nu(O_2)$ of these dioxygen adducts scatter over a wide range from 1120 to 920 cm^{-1}. Previously, we noted that the $\nu(O_2)$ decreases as the negative

TABLE 1.57. Vibrational Frequencies of $M(O_2)$-Type Compounds (cm^{-1})

Compound	$\nu(O_2)$	$\nu_s(MO)$	$\nu_a(MO)$	Ref.
$^6LiO_2$	1097.4	743.8	507.3	1206
$^7LiO_2$	1096.9	698.8	492.4	1206
NaO_2	1094	390.7	332.8	1206
KO_2	1108	307.5	—	1206
RbO_2	1111.3	255.0	282.5	1206
CsO_2	1115.6	236.5	268.6	1206
AgO_2	1082/1077	—	—	1207
RhO_2	900	—	422	1208
InO_2	1084	332	277.7	1209
GaO_2	1089	380	285.5	1209
AuO_2	1092	—	—	1210
TlO_2	1082	296	250	1211
PdO_2	1024.0	427	—	1212
NiO_2	966.2	504	—	1212
FeO_2	946	—	—	1213
PtO_2	926.6	—	—	1212

charge on the O_2 increases. Thus, these results seem to suggest that the negative charge on the O_2 can be varied continuously by changing the metal. In fact, Lever et al. [1214] noted that there is a linear relationship between the electron affinity of the M^{2+} ion and the $M-O_2$ CT transition energy in the $M(O_2)_2$ series and that the latter is linearly related to the $\nu(O_2)$.

The dioxygen ligand may coordinate to a metal in the end-on or side-on fashion. These two structures can be distinguished by using the isotope scrambling technique. Andrews [1215] first applied this method to the structure determination of the ion-pair complex $Li^+O_2^-$; a mixture of $^{16}O_2$, $^{16}O^{18}O$, and $^{18}O_2$ was prepared by Tesla coil discharge of a $^{16}O_2 - {}^{18}O_2$ mixture, and reacted with Li vapor in an Ar matrix. Three $\nu(O_2)$ were observed in the Raman spectrum:

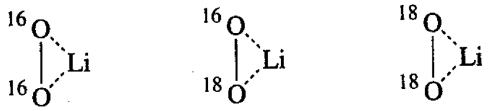

1096.1 cm^{-1} 1065.7 cm^{-1} 1034.6 cm^{-1}

This result clearly indicates side-on coordination since four bands are expected for end-on coordination (see above). Using the same technique, Ozin and co-workers [1210–1212] showed that, in all cases they studied, O_2 coordinates to a metal in the side-on fashion and that, in $M(O_2)_2$ (M = Ni,Pd,Pt), the complexes take the spiro $\mathbf{D}_{2d}$ structure. Some metal superoxides and peroxides are prepared by ordinary methods, and their $\nu(O_2)$ are reported by Evans [1216] and Eysel and Thym [1217].

Andrews and coworkers prepared a variety of novel complexes via cocondensation reactions of transition metal vapors produced by laser ablation with O_2 diluted by inert

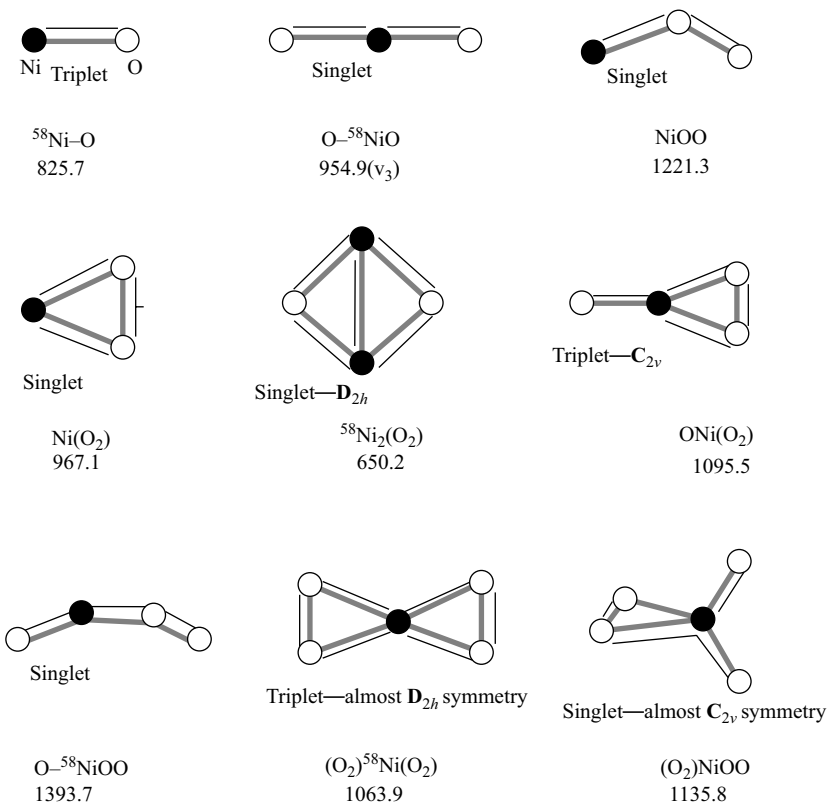

Fig. 1.73. *Optimized structures and IR frequencies (cm^{-1}) [1218].*

gases. As an example, Fig. 1.73 shows the structures and vibrational frequencies of nine species obtained by the reaction of Ni atom vapor with O_2/Ar [1218]. Here, (O_2) denotes the side-on η^2-bonding. It is interesting to note that NiO_2 takes three isomeric structures, while NiO_3 and NiO_4 take two isomeric forms.

1.21.2. Dioxygen Adducts of Transition Metal Complexes

There are many transition metal complexes containing superoxo and peroxo ligands. Examples of superoxo complexes are $[Cr(\eta^1\text{-}O_2)(H_2O)_5]^{2+}$ [1240] and $[Sm(\eta^2\text{-}O_2)(Tp^{Me2})_2]$ [$Tp^{Me2} = HB(3,5\text{-}Me_2pz)_3$] [1241]. The former exhibits the $\nu(O_2)$ and $\nu(CrO)$ at 1166 and 503 cm^{-1}, respectively, whereas the latter is a rare example of the side-on-type superoxo complex with the $\nu(O_2)$ at 1124 cm^{-1}.

Peroxo complexes take the symmetric side-on structure and exhibit the $\nu(O_2)$ in the 900–800 cm^{-1} region and the $\nu_a(MO_2)$ and $\nu_s(MO_2)$ in the 650–430 cm^{-1} region. In general, the $\nu_a(MO_2)$ is higher than the $\nu_s(MO_2)$. Table 1.58 lists the observed frequencies of typical peroxo complexes. Some of these assignments have been

TABLE 1.58. Observed Frequencies of Peroxo Complexes (cm^{-1})

Complex	$\nu(O_2)$	$\nu(MO_2)$	Ref.
$(NH_4)_3[Ti(O_2)F_5]$	905	600, 530	1221
$K_2[Ti(O_2)(C_2O_4)]$	895	611, 536	1222
$Zr(O_2)(H_2EDTA)$	840	650, 600	1223
$(NH_4)_2$ $[ZrO(O_2)F_2]$	850	640, 585	1224
$(NH_4)_3$ $[Zr(O_2)F_5]$	837	550, 471	1225
$K_3[V(O_2)_4]$	854	620, 567	1226
$K_3[Ta(O_2)F_4]$	866	592, 518	1227
$A_3[PO_4\{WO(O_2)_2\}_4]$[a]	843	591, 526	1228
$[Fe(EDTA)(O_2)]^{3-}$ (aq.)	815	—, —	1229
$Na_2[UO_2(O_2)(CO_3)]$	980	615, 550	1230
$Pt(O_2)$ $(PPh_3)_2$	821	460, 437	1231

[a] A: $[N(C_6H_{13})_4]^+$ ion.

confirmed by $^{16}O_2/^{18}O_2$ substitution. Nakamura et al. [1232] have made nonnal coordinate calculations on peroxo complexes.

According to X-ray analysis [1233], $[Cu(HB(3,5\text{-}R_2pz)_3)]_2(O_2)$ (R = *i*-Pr,Ph; pz = pyrazole) contains a rare symmetric side-on bridge:

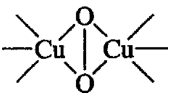

The O−O distance (1.412 Å) is typical of peroxo complexes, and all the Cu−O distances are essentially the same (1.90–1.93 Å). The RR spectrum exhibits the $\nu(O_2)$ at 741 cm^{-1}, which is much lower than those shown in Table 1.58. This compound serves as a model for dioxygen binding in hemocyanin (Sec. 3.6).

1.21.3. Dioxygen Adducts of Cobalt Ammine and Schiff-Base Complexes

Extensive vibrational studies have been made on dioxygen adducts of cobalt ammine and Schiff base complexes. Table 1.59 lists the $\nu(O_2)$ and $\nu(CoO)$ of representative compounds.

The $\nu(O_2)$ of dinuclear cobalt complexes such as $\{[Co(NH_3)_5]_2O_2\}^{n+}$ ($n = 4$ or 5) are markedly different depending on whether the O_2 group is of superoxo or peroxo type. The $\nu(O_2)$ of the $\{[Co(NH_3)_5]_2O_2\}^{5+}$ ion appears strongly in Raman spectra (1122 cm^{-1}) but is forbidden in IR spectra because the O−O bridge is centrosymmetric. However, the $\nu(O_2)$ of a dibridged complex ion, $[(NH_3)_4Co(NH_2)(O_2)Co(NH_3)_4]^{4+}$, is observed as 1068 cm^{-1} in IR spectra [1236].

N,*N*′-Ethylenebis(salicylideniminato)cobalt, Co(salen), binds dioxygen reversibility in the solid state [1243]. Figure 1.74 shows the resonance Raman spectra of $[Co(salen)]_2O_2$ at ~100 K [1239]. The bands at 1011 and 533 cm^{-1} are shifted to 943 and 514 cm^{-1}, respectively, by $^{16}O_2 - {}^{18}O_2$ substitution, and thus assigned to the $\nu(O_2)$ and $\nu(CoO)$, respectively. The former frequency is unique in that it is between those of

TABLE 1.59. Vibrational Frequencies and Structures of Dioxygen Adducts of Cobalt Ammine and Schiff Base Complexes (cm^{-1})

Compound	Structure	$\nu(O_2)$	ν(Co–O)	Ref.
Co(J-en)(py)O_2[a]	Superoxo end-on	1146	—	1234
Co(salen)(py)O_2	Superoxo end-on	1144	527	1235
{[Co$(NH_3)_5]_2O_2$}$Cl_5 \cdot 3H_2O$	Superoxo bridging	1122	620, 441	1236
{[Co$(NH_3)_5]_2O_2$}$(NO_3)_5$	Superoxo bridging	1122	—	1237
K_5[[Co$(CN)_5]_2O_2$}H_2O	Superoxo bridging	1104	493	1238
[Co(salen)$]_2O_2$	Superoxo bridging	1011	533	1239
				1240
[Co(salen)(pyO)$]_2O_2$[b]	Peroxo bridging	910	535	1241
[Co(salen)(py)$]_2O_2$	Peroxo bridging	884	543	1240
[Co(J-en)(py)$]_2O_2$	Peroxo bridging	841	562	1234
[Co(DMG)$(PPh_3)]_2O_2$[c]	Peroxo bridging	818	551	1242
K_6[[Co$(CN)_5]_2O_2$}H_2O	Peroxo bridging	804	602	1238
{[Co$(NH_3)_5]_2O_2$}$(NO_3)_4$	Peroxo bridging	805	642, 547	1236
{[Co$(NH_3)_5]_2O_2$}$(NCS)_4$	Peroxo bridging	786	—	1237

[a]J-en = *N,N′*-ethylenebis(2,2′-diacetylethylideneaminato) anion.
[b]pyO = pyridine *N*-oxide.
[c]DMG = dimethylglyoximato anion.

superoxo and peroxo complexes. However, this band is shifted to the normal peroxo range when the base ligands are coordinated *trans* to the dioxygen. Evidently, electron donation from the base to the bridging dioxygen is responsible for the shift of $\nu(O_2)$ to a lower frequency.

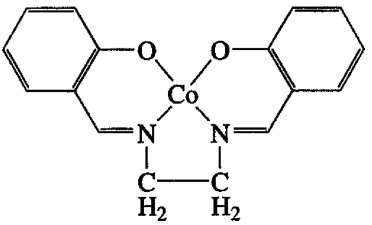

When a Co Schiff base (SB) complex in a nonaqueous solvent absorbs oxygen in the presence of a base (B), the following equilibria are established:

$$[Co(SB)B] + O_2 \rightleftharpoons [Co(SB)B]O_2$$
$$[Co(SB)B]O_2 + [Co(SB)B] \rightleftharpoons [Co(SB)B]_2O_2$$

The $\nu(O_2)$ of the 1 : 1 (Co/O_2) adduct is near 1140 cm^{-1}, whereas that of the 1 : 2 adduct is between 920 and 820 cm^{-1}. Using these bands as the markers, it is possible to examine the effects of oxygen pressure, temperature, and solvent polarity on the equilibria shown above. Figure 1.75 shows the RR spectra of Co(J-en) in CH_2Cl_2 containing pyridine that were saturated with oxygen at various oxygen pressures and temperatures. [1234]. It is seen that the concentration of the 1 : 1 adduct (1143 cm^{-1})

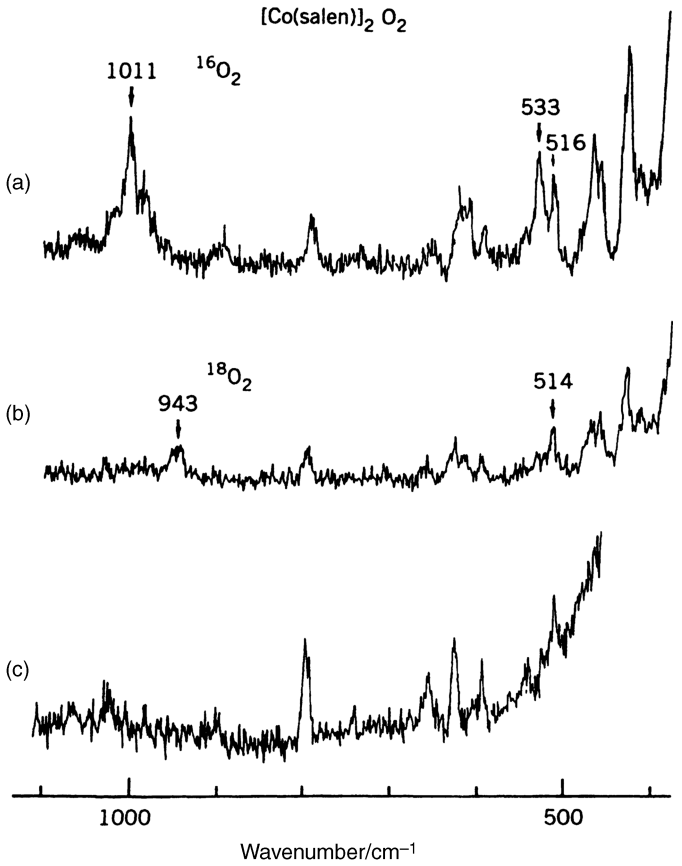

Fig. 1.74. *The RR spectra of (a) [Co(salen)]$_2$ $^{16}O_2$, (b) [Co(salen)]$_2$ $^{18}O_2$, and (c) Co(salen) (579 nm excitation, ~100 K) [1239].*

increases and that of the 1 : 2 adduct (836 cm^{-1}) decreases as the oxygen pressure increases (A → B) and as the temperature decreases (D → C → B). It was also noted that 1 : 1 adduct is favored in a polar solvent containing a relatively strong base.

1.21.4. "Base-Free" Dioxygen Adducts of Metalloporphyrins and Related Compounds

Table 1.60 lists the structures and observed frequencies of "base-free" dioxygen adducts of metalloporphyrins that were prepared mostly by matrix cocondensation reactions at low temperatures. The $\nu(O_2)$ varies continuously from the superoxo to the peroxo regions. The $\nu(O_2)$ is the highest in $Co(TPP)O_2$ (superoxo) and the lowest in $[MoO(TPP)O_2]^-$ (peroxo), although some complexes exhibit the $\nu(O_2)$ in the intermediate region. The $\nu(O_2)$ of "base-free" $Co(TPP)O_2$ is 133 cm^{-1} higher than that of

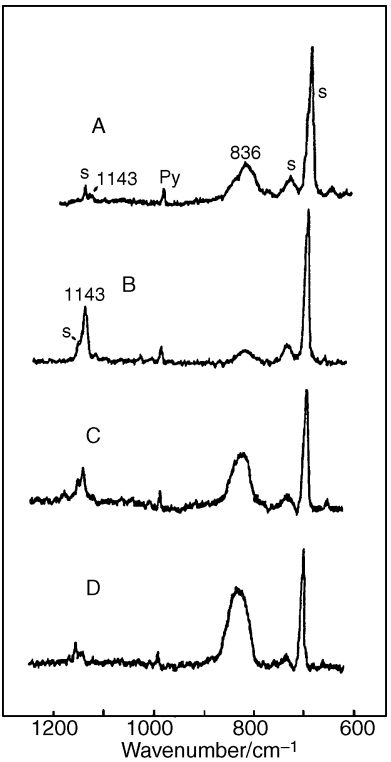

Fig. 1.75. *The RR spectra of Co(J-en) in CH_2Cl_2 containing 3% pyridine that was saturated with O_2 at various O_2 pressures and temperatures (580 nm excitation): (A) 1 atm, −78°C, (B) ~3 atm, −80°C; (C) ~3 atm, −30°C; (D) ~3 atm, +20°C, where S and py denote the solvent and pyridine bands, respectively [1234]. For the structure of J-en, see footnote* a *in Table 1.59.*

"base-bound" Co(TPP)(1-MeIm)O_2 (1143 cm^{-1}) discussed in the following section. A shift of similar magnitude (127 cm^{-1}) is observed in going from $[Co(salen)]_2O_2$ to its pyridine adduct. Evidently, these shifts are caused by the base ligands, which increase the negative charge on the dioxygen ("base ligand effect").

Table 1.60 also indicates the "metal ion effect"; the $\nu(O_2)$ is lowered and the mode of coordination is shifted from the end-on to the side-on as the metal ion is changed in the following order:

	$Co(TPP)O_2$		$Fe(TPP)O_2$		$Mn(TPP)O_2$
$\nu(O_2)$ (cm^{-1})	1278 (end-on)	>	1195 (end-on)		
			1106 (side-on)	>	983 (side-on)

The IR spectra of $Fe(TPP)O_2$ shown in Fig. 1.76 are of particular interest since it exhibits two $\nu(O_2)$ at 1195 and 1106 cm^{-1}, corresponding to the end-on and side-on isomers, respectively [1248].

TABLE 1.60. Structures and Observed Frequencies (cm^{-1}) of "Base-Free" Dioxygen Adducts

Complex	Structure	$\nu(^{16}O_2)$	$\nu(^{18}O_2)$	Δ^a	$\nu(MO_2)$	Refs.
$Co(TPP)O_2$	End-on	1278	1209	69	345	1244
$Co(OEP)O_2$	End-on	1275	1202	73		1245
$Co(TMP)O_2$	End-on	1270	1200	70	404	1246
$Co(J\text{-}en)O_2$	End-on	1260	1192	68		1234
$Co(salen)O_2$	End-on	1235	1168	67		1247
$[Co(salen)]_2O_2$	Bridging	1011	943	68		1239
$Fe(TPP)O_2$	End-on	1195	1127	68	509	1248,1238
	Side-on	1106	1043	63		
$Fe(OEP)O_2$	End-on	1190	1124	66		1248
	Side-on	1104	1042	62		
$Fe(Pc)O_2$	End-on	1207	1144	63	488	1248,1250
$Fe(salen)O_2$	Side-on	1106	1043	63		1248
$[Fe(salen)]_2O_2$	Bridging	1001	943	58		1251
$Ru(TPP)O_2$	End-on	1167	1101	66		1252
$[Ru(TPP)]_2O_2$	Bridging	1114	1057	57		1252
$[Os(TPP)]_2O_2$	Bridging	1090	1030	70		1252
$Mn(TPP)O_2$	Side-on	983	933	50	433	1253,1254
$Mn(Pc)O_2$	Side-on	992	935	57		1255
$[MoO(TPP)O_2]^-$	Side-on	876	—	—	521 490	1256

[a] $\Delta = \nu(^{16}O_2) - \nu(^{18}O_2)$.

Table 1.60 reveals another interesting trend; the $\nu(O_2)$ becomes lower as the in-plane ligand is changed in the order

$$\begin{array}{cccccc} & Fe(Pc)O_2 & & Fe(TPP)O_2 & & Fe(salen)O_2 \\ \nu(O_2)(cm^{-1}) & 1207 & > & 1195,\ 1106 & \geq & 1106 \end{array}$$

Here, Pc denotes the phthalocyanato ion. This result indicates that the larger the π-conjugated system of the in-plane ligand is, the less the negative charge on the dioxygen, and the higher the $\nu(O_2)$ ("in-plane ligand effect").

1.21.5. "Base-Bound" Dioxygen Adducts of Metalloporphyrins

"Base-bound" dioxygen adducts of metalloporphyrins are highly important as models of respiratory heme proteins (Secs. 3.1, 3.2). Several reviews [1257,1126,226] are available on vibrational spectra of base-bound dioxygen adducts of metalloporphyrins. Table 1.61 lists the $\nu(^{16}O_2)$, $\nu(M - {}^{16}O_2)$, and $^{16}O_2/^{18}O_2$ isotope shifts observed for end-on, base-bound dioxygen adducts.

As mentioned previously, the $\nu(O_2)$ of these base-bound adducts are lower than those of the corresponding "base-free" adducts because of the "base ligand effect." In a series of base-bound adducts such as $Co(TPP\text{-}d_8)(B)O_2$ (B = nitrogen donor base), the $\nu(O_2)$ decreases linearly as the pK_a of the base increases [1264]. Thus, the $\nu(O_2)$ is the highest ($1167\ cm^{-1}$) for the most acidic base (4-cyanopyridine, $pK_a = 1.90$) and

TABLE 1.61. Observed Frequencies of "Base-Bound" Dioxygen Adducts of Metalloporphyrins (cm^{-1}, in Solution)

Compound[a]	$\nu(^{16}O_2)$	$\Delta\nu(O_2)$[b]	$\nu(M-^{16}O_2)$	$\Delta\nu(MO_2)$[c]	Ref.
$Co(TPP)(py)O_2$	1144	60	519	21	1258
$Co(TPP)(pip)O_2$	1142	64	509	20	1259
$Fe(TPP)(pip)O_2$	1157	64	575	24	1259
$Co(T_{piv}PP)(1,2\text{-}Me_2Im)O_2$	1153	65	—	—	1259
$Co(T_{piv}PP)(1\text{-}MeIm)O_2$	—	—	517	23	1259
$[Co(T_{piv}PP)(SC_6HF_4)O_2]^-$	1126	66	—	—	1260
$Fe(T_{piv}PP)(l,2\text{-}Me_2Im)O_2$	1159	66	—	—	1261
$Fe(T_{piv}PP)(1\text{-}MeIm)O_2$	—	—	568	23	1262
$[Fe(T_{piv}PP)(SC_6HF_4)O_2]^-$	1140	60	—	—	1263

[a] T_{piv} PP = picket-fence porphyrin (see Fig. 1.64a).
[b] $\Delta\nu(O_2) = \nu(^{16}O_2) - \nu(^{18}O_2)$.
[c] $\Delta\nu(M{-}O_2) = \nu(M{-}^{16}O_2) - \nu(M{-}^{18}O_2)$.

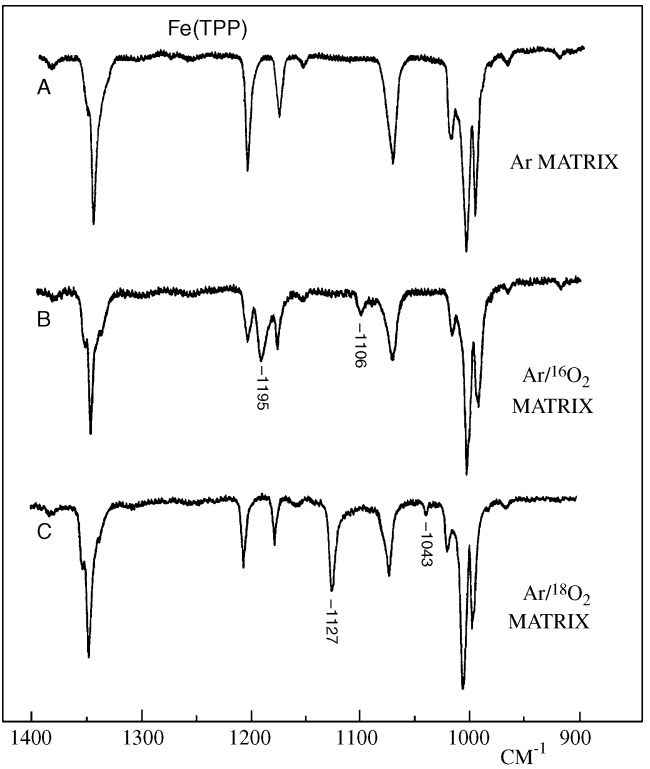

Fig. 1.76. *Infrared spectra of (A) Fe (TPP) in Ar matrix, (B) Fe(TPP) cocondensed with $^{16}O_2/Ar$ (1/10), and (C) Fe(TPP) cocondensed with $^{18}O_2/Ar$ (1/10) at ~15 K [1248].*

the lowest (1151 cm^{-1}) for the most basic base (4-dimethylaminopyridine, pK_a = 9.70). If the pK_a value is regarded as a rough measure of σ-donation, this result suggests that the $\nu(O_2)$ is governed largely by the degree of σ-donation of these bases.

The $\nu(O_2)$ is shifted markedly to lower frequency when a thiolate ligand such as $SC_6H_5^-$ coordinates to a metal. For example, the $\nu(O_2)$ of the $[Co(TPP)(SC_6H_5)O_2]^-$ ion (1122 cm^{-1}) is 21 cm^{-1} lower than that of Co(TPP)(py)O_2 (1144 cm^{-1}) in the same solvent (CH_2Cl_2) [1265]. As shown in Table 1.61, a similar downshift is noted for Fe(II) porphyrins. Since the pK_a of $SC_6H_5^-$ (6.5) does not differ appreciably from that of py (5.25), the observed shift must be attributed largely to an increase in π-donation. This π-donation is promoted by two factors: (1) relative to py, the thiolate ligand possesses an extra electron on the $2p$ orbital that overlaps on the $d\pi$ orbital of the metal, and (2) the $SC_6H_5^-$ ligand tends to take an orientation that maximizes the $p\pi - d\pi$ overlap and minimizes the steric repulsion from the mesophenyl groups.

As discussed in Sec. 3.3.2, the active site of cytochomes $P450_{cam}$ is an iron porphyrin that has the mercaptide sulfur of a cystenyl residue as an axial ligand. When O_2 coordinates to the axial position *trans* to the sulfur, it exhibits the $\nu(O_2)$ at 1140 cm^{-1}. Matsu-ura et al. [1266] synthesized a novel model compound of cytochrome P450, a twin-coronet porphyrin with a thioglycolate group. The hydrogen-bonded O_2 adduct of this model compound exhibits the $\nu(O_2)$ at 1137 cm^{-1}, which is shifted to 1073 cm^{-1} by $^{16}O_2/^{18}O_2$ substitution.

Table 1.61 also shows the "metal-ion effect"—the $\nu(O_2)$ of the Fe(II) adduct is higher than that of the corresponding Co(II) adduct. Although this is opposite to the case of base-free adducts discussed previously, the metal ion effect on the $\nu(M-O_2)$ is the same in both cases; the $\nu(Fe-O_2)$ is always higher than the $\nu(Co-O_2)$. These results can be accounted for in terms of the following bonding schemes [1251]:

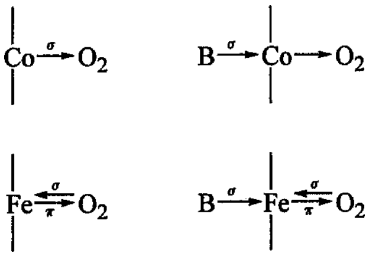

When the O_2 is bound to Co(II) (d^7), the $Co-O_2$ bond is formed mainly by σ-donation from Co(d_{z^2}) to the antibonding O_2 (π_g^*) orbital [i.e., Co(III)$-O_2^-$]. In the case of Fe(II) (d^6), however, the $Fe-O_2$ bond is formed by σ-donation from O_2 (π_g^*) to Fe(d_{z^2}), which is counteracted by a stronger π-donation in the opposite direction. This would strengthen the $Fe-O_2$ bond and weaken the O$-$O bond relative to those of the corresponding Co(II) adduct. In fact, "base-free" Fe(II) adducts exhibit lower $\nu(O_2)$ and higher $\nu(M-O_2)$ than do the corresponding Co(II) adducts. In base-bound Co(II) complexes, σ-donation from die base ligand causes a marked increase in the negative charge on O_2, thus causing a large downshift in $\nu(O_2)$ relative to base-free complexes. However, the base ligand effect is much smaller in Fe(II) complexes because σ-donation from the base is opposed by σ-donation from the O_2. As a result, the

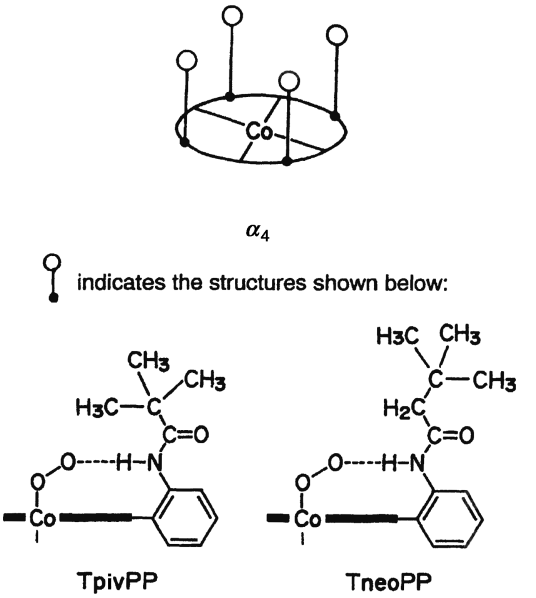

Fig. 1.77. *Structure of O_2 adducts of "picket-fence" Co(II) porphyrin and its derivative. See also Fig. 1.64a.*

O_2 in Fe(II) adducts is less negative than that of Co(II) complexes. Thus, the $\nu(O_2)$ of Fe(II) adducts become higher than those of Co(II) adducts. The $\nu(Fe-O_2)$ is always higher than the $\nu(Co-O_2)$ because of the multiple bond character of the former.

It is well established that the O_2 bound to myoglobin and hemoglobin is stabilized by forming the $N-H\cdots O_2$ hydrogen bond with the distal imidazole of the peptide chain (Sec. 3.2). To mimic this "cavity effect," "protected" porphyrins such as "picket-fence" and "strapped" porphyrins (Fig. 1.64) have been prepared. Figure 1.77 compares the structures of the pickets in picket-fence porphyrin, $Co(\alpha_4\text{-}T_{piv}PP)$ and its derivative, $Co(\alpha_4\text{-}T_{neo}PP)$. It was found that the $\nu(O_2)$ decreases in the following order:

	$Co(TPP\text{-}d_8)(B)O_2$		$Co(T_{piv}PP)(B)O_2$		$Co(T_{neo}PP)(B)O_2$
$\nu(O_2)(cm^{-1})$	1167	>	1161	>	1148

Here, B is 4-cyanopyridine and the spectra were measured in toluene [1264,1267]. Presumably, the $N-H\cdots O_2$ hydrogen bonding is weaker in $Co(T_{piv}PP)$ than in Co $(T_{neo}PP)$ because the repulsive force between the $C(CH_3)_3$ group and the bound dioxygen tends to push the pivalamide group outward. This repulsive force would be decreased when the pivalamide group is replaced by the neo-pentylcarboxamide group (T_{neo}). Odo et al. [1267] carried out an extensive RR study on $\nu(O_2)$ of Co(II) complexes of a variety of picket-fence porphyrins.

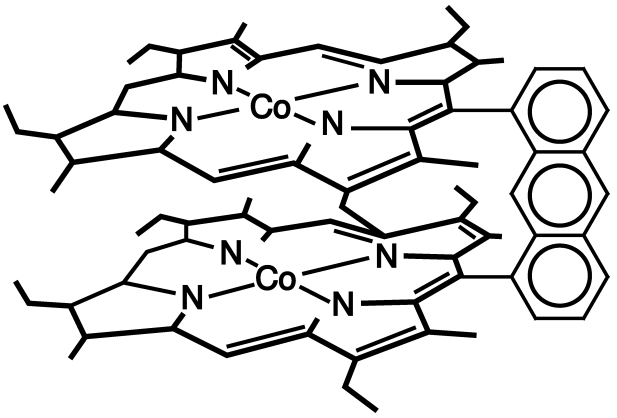

Fig. 1.78. *Structure of "Pillard" dicobalt cofacial diporphyrin.*

Pillard dicobalt cofacial diporphyrin, shown in Fig. 1.78, is another type of modified porphyrin which is of great interest in structural chemistry. Since a large base ligand such as 4-(dimethylamino)pyridine cannot enter the inter-porphyrin cavity, it forms a bridging O_2 adduct that exhibits the $\nu(O_2)$ at 1098 cm^{-1} (superoxo type) in RR spectra. This band is not observed if a small base such as γ-picoline is first added to the Co−Co complex solution and then the solution is oxygenated. This result indicates that a small base occupies the interporphyrin space so that formation of the $Co-O_2-Co$ bridge is blocked [1268]. However, the 1098-cm^{-1} band is observed if the Co−Co complex solution is first saturated by O_2 and then a small base is added. Apparently, the $Co-O_2-Co$ bond once formed is too stable to be cleaved by the addition of a base ligand.

The RR spectrum of Co(TPP-d_8)(py)O_2 in CH_2Cl_2 exhibits a single $\nu(O_2)$ band at 1143 cm^{-1}. However, this band becomes a doublet (1155 and 1139 cm^{-1}) when 1,2-dimethylimidazole is used as the base. An extensive study involving a variety of base ligands [1258] has shown that vibrational coupling between $\nu(O_2)$ and a nearby base ligand vibration of the same symmetry is responsible for the observed doublet structure and resonance enhancement. In the case of Co(TPP-d_8)(py)$^{18}O_2$ in CH_2Cl_2, a weak py band appears at 1067 cm^{-1} in addition to the $\nu(^{18}O_2)$ at 1084 cm^{-1}. The 1067 cm^{-1} band of py is not observed in the case of the $^{16}O_2$ adduct. This is another example of vibrational coupling between the py mode and the $\nu(^{18}O_2)$ [1258].

Similar vibrational couplings were noted between the $\nu(O_2)$ and the axial ligand (3.5-dichloropyridine) for three picket-fence Co(II) porphyrins [1269].

The internal mode of a solvent molecule can also be resonance-enhanced via a similar mechanism [1264]. As shown in Fig. 1.79 the RR spectrum of Co(TPP-d_8)(py)O_2 in toluene exhibits two strong bands at 1160 and 1151 cm^{-1} where the $\nu(^{16}O_2)$ band is expected (trace A). This doublet structure does not appear in toluene-d_8 (trace C) and is not observed in the $\nu(^{18}O_2)$ region (trace B). Toluene exhibits three bands at 1210 (T_1), 1178 (T_2), and 1155 cm^{-1} (T_3) with an intensity ratio of approximately 6 : 1 : 1

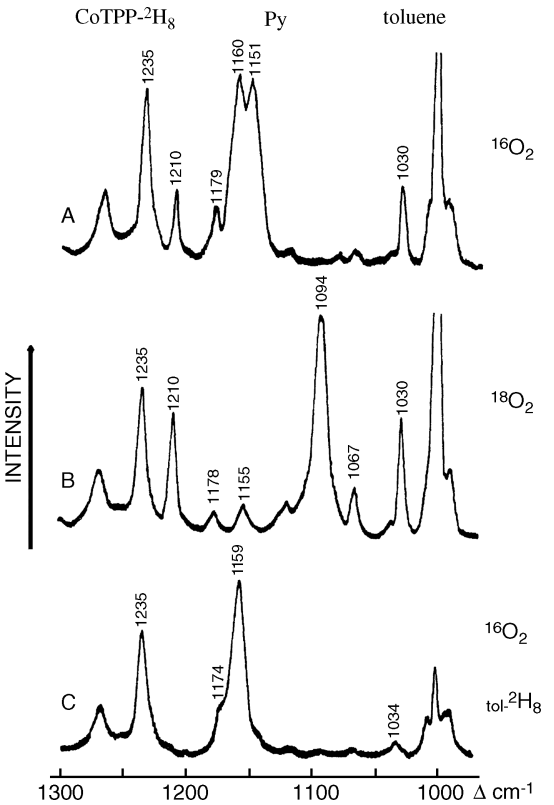

Fig. 1.79. *The RR spectra of Co(TPP-d_8) in toluene containing 3% pyridine at −85° C under ~4 atm O_2 pressure:* (A) $^{16}O_2$; (B) $^{18}O_2$; (C) $^{16}O_2$ *in toluene-d_8 [1264].*

(trace B). Thus, it is reasonable to attribute the observed splitting to a strong vibrational coupling between $\nu(^{16}O_2)$ and T_3, which are very close in frequency. If $\nu(^{16}O_2)$ is shifted between T_2 and T_3 by using a weaker base (4-cyanopyridine), both internal modes of toluene are resonance-enhanced, as seen in Fig. 1.80. In this case, the magnitudes of frequency perturbation and resonance enhancement are less, relative to the previous case, since $\nu(^{16}O_2)$ is further from the solvent modes. As seen in Fig. 1.80, the multiple structure observed for Co(TPP-d_8) disappears completely when picket-fence porphyrin, Co(T_{piv}PP), is employed. This result indicates that the vibrational coupling observed for "unprotected porphyrin" cannot occur in picket-fence porphyrin because the four pivaloyl groups prevent the access of toluene to bound dioxygen. Thus, not only "frequency matching" but also "direct O_2 solvent association" is necessary to cause such vibrational coupling. Vibrational couplings between $\nu(O_2)$ of bound dioxygen and internal modes of base ligands and/or solvents have been found in many other systems [1270,1271]. Thus, RR spectra of dioxygen adducts of metalloporphyrins must be interpreted with caution. Proniewicz and Kincaid [1272] carried out quantitative treatments of these vibrational couplings using a Fermi resonance scheme.

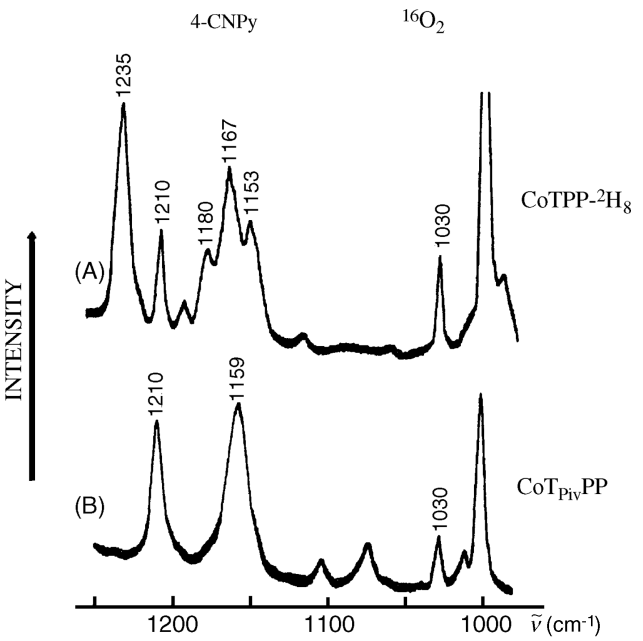

Fig. 1.80. *The RR spectra of* (A) *Co(TPP-d_8) and* (B) *Co(T_{piv}PP) in toluene containing 3% 4-cyanopyridine at −85° C under ∼4 atom O_2 pressure [1264].*

1.22. METAL COMPLEXES CONTAINING OXO GROUPS

1.22.1. Metal Complexes Containing Monooxo Groups

There are many compounds containing monooxo groups (M=O) in which relatively heavy metal atoms are bonded to oxygen via double bonds. In most cases, their ν(M=O) vibrations can be assigned without difficulty since they are relatively free from vibrational couplings and appear strongly in the 1100–900 cm^{-1} region of IR spectra. Examples of M=O group vibrations in inorganic compounds are found in the ν(ZX) vibrations of ZXY_3 (Table 2.6g), ZXY_4 (Table 2.7b), and ZXY_5 (Table 2.8c)-type compounds discussed in Part A. Table 1.62 lists the ν(M=O) of metal complexes containing monooxo groups.

A new type of isomerism involving monooxo groups was found by Wieghardt et al. [1277]. For example, the crystals of $[PF_6][W(O)LCI_2]$ (L = a tridentate ligand) can be obtained in the blue and green forms. X-Ray analyses show that the structures of these two forms are identical except for the W=O and W−N (*trans* to W=O) distances; the W=O bond length in the blue form (1.72 Å) is shorter than that in the green form (1.89 Å). Correspondingly, the ν(W=O) of the former (980 cm^{-1}) is higher than that of the latter (960 cm^{-1}).

Similar isomerism has been reported for complexes containing the Nb=O and Nb=S groups [1278]. Thus, the yellow form of $Nb(O)Cl_3(PMe_3)_3$ exhibits the

TABLE 1.62. Vibrational Frequencies (cm^{-1}) of Monooxo Complexes

Complex	Oxo Group	ν(M=O)	Ref.
$(VO)(TBP)_8(CzH)^a$	V(IV)=O	976(939)[b]	1273
$(MnO)(TBP)_8(Cz)^a$	Mn(V)=O	979(938)[b]	1274
$H(TcO)(cys)_2^c$	Tc(V)=O	940	1275
$[(ReO)(cys)_2]^{-,c}$	Re(V)=O	969	1275
$[(RhO)(bipy)_2(py)]^{3+}$	Rh(V)=O	845	1276

[a] $(TBP)_8(Cz)$ = octakis(*p-tert*-butylphenyl)corroiazine.
[b] $\nu(M={}^{18}O)$.
[c] Cys = cysteine.

ν(Nb=O) at 882 cm^{-1} (Nb=O distance, 1.78 Å), whereas its green isomer shows it at 871 cm^{-1} (Nb=O distance, 1.93 Å). In $Nb(S)Cl_3(PMe_3)_3$, the orange form exhibits the ν(Nb=S) at 455 cm^{-1} (Nb=S distance, 2.196 Å), while the green form shows it at 489 cm^{-1}, although its Nb=S distance (2.296 Å) is longer than that of the orange form. The origin of this anomaly is not clear. Moreover, the origin of this new type of isomerism ("bond-stretch" isomerism) is not understood.

1.22.2. Metal Complexes Containing Dioxo Groups*

As stated in Sec. 2.2 of Part A, the dioxo groups (O=M=O) such as $Mo(O)_2$, $Ru(O)_2$, $W(O)_2$, $Re(O)_2$, $Os(O)_2$, and $U(O)_2$ exhibit strong- to medium-intensity IR bands in the 1100–850 cm^{-1} region. Although the *trans* (linear) dioxo group exhibits only the ν_a(O=M=O) vibration in IR spectra and only the ν_s(O=M=O) vibration in Raman spectra, the *cis* (bent) dioxo group is expected to show both vibrations in either spectra [1279]. Thus, *trans*-$[Os(O)_2(bipy)_2]$ (bipy = 2,2′-bipyridine) exhibits only one band at 872 cm^{-1}, whereas its *cis*-isomer shows two bands at 833 (ν_s) and 863 cm^{-1} (ν_a) in IR spectra [1280]. However, the *trans*-$[Re(O)_2(py)_4]^+$ ion exhibits both symmetric and antisymmetric ν(O=Re=O) at 907 and 822 cm^{-1}, respectively, in RR spectra (CH_3CN solution) [1281]. The reason for this anomaly is not clear. The *cis*-$V(O)_2$ groups show the ν_s and ν_a(O=Ru=O) at 922–910 and 907–876 cm^{-1}, respectively [1282]. Similar results are reported for *cis*-$Mo(O)_2$ [1283–1285] and *cis*-$W(O)_2$ groups [1286,1287]. In the case of $Ru(TPP)(O)_2$, the ν_s(O=Ru=O) vibration is observed at 808 cm^{-1} in RR spectra in solution [1288]. The corresponding ν_a(O=Ru=O) vibration appears at 821 cm^{-1} in IR spectra [1289].

More recent references on dioxo complexes are summarized in Table 1.63.

1.22.3. Metal Complexes Containing Oxo Bridges

If the oxo bridge (M−O−M) is linear, the ν_a(MOM) is only IR-active and the ν_s(MOM) is only Raman-active. Although both become IR- and Raman-active in a bent geometry, the former is stronger in IR whereas the latter is stronger in Raman spectra. Table 1.64 lists the structures and observed frequencies of monooxo bridged complexes.

* To avoid confusion with dioxygen adducts (MO_2), the dioxo groups are written as $M(O)_2$.

TABLE 1.63. IR Frequencies of Dioxo Complexes (cm^{-1})

Complex	*cis/tran*	ν_a(OMO)	ν_s(OMO)	Ref.
$[Re(O)_2(P(CH_2OH)_3))]^+$	*trans*	880	—	1290
$[Re(O)_2(pyz)_4]^{+,a}$	*trans*	810	—	1291
$[Os(O)_2(N_2H_2C_2O_2)_2]^{2-}$	*trans*	852	900 (Raman)	1292
$[U(O)_2F_6]^{4-}$	*trans*	913	951 (Raman)	1293
$[V(O)_2(HL)]^{-,b}$	*cis*	882	918	1294
$[Re(O)_2(OTeF_5)_3]$	*cis*	978	1022	1295
$[Re(O)_2F_4]^-$	*cis*	973	1011	1296
$[Os(O)_2F_4]$	*cis*	930	940	1297

[a] pyz = pyrazine.
[b] HL = Schiff base ligand containing alkoxo group.

Figure 1.81 illustrates three types of monooxo bridges. Structures II and III contain one and two μ-carboxylato groups in addition to single monooxo bridge. Structure III is important as a model compound of hemerythrin and other metalloproteins (Sec. 3.5). Sanders–Loehr et al. [1307] carried out a systematic study on electronic and RR spectra of oxo-bridged dinuclear Fe(III) complexes in proteins and their model compounds. As shown in Appendix VII of Part A, the Fe−O−Fe angle can be calculated using the observed values of ν_a(FeOFe) and ν_s(FeOFe). These workers obtained excellent agreement between the observed (X-ray) and calculated Fe−O−Fe angles. They also noted that the molar Raman intensity of ν_s(FeOFe) is much larger in proteins than in model compounds, and suggested several possible reasons for this phenomenon.

Bridging dioxo(μ-O)$_2$ and trioxo(μ-O)$_3$ complexes contain the structures shown below:

TABLE 1.64. Structures and Vibrational Frequencies (cm^{-1}) of Monooxo-Bridged Complexes

Compound	Structure	ν_a	ν_s	Ref.
$[Fe_2(\mu\text{-O})(TPP)_2]$	Linear FeOFe	885	363	1298
$[Fe_2(\mu\text{-O})(OEC)_2]$	Linear FeOFe	872	400	1299
$[Cr_2(\mu\text{-O})(TPP)_2]$	Linear CrOCr	860	—	1300
{Cr(TPP)(μ-O)Fe(TPP)}	Linear CrOFe	843	—	1301
$[Fe_2(\mu\text{-O})(H_2O)_{10}]^{4+}$	Linear FeOFe	840	—	1302
$[V_2(\mu\text{-O})(\text{L-Hist})_4]\ 2H_2O$	Bent VOV	730	436	1303
$[Fe)_2(\mu\text{-O})(\mu\text{-}CH_3CO_2)_2L_2]^{2+,a}$	Bent FeOFe	730	—	1304
$[Fe_2(\mu\text{-O})(\mu\text{-}CH_3COO)_2L'_2]^b$	Bent FeOFe	754	530	1305
$[V_2(\mu\text{-O})((\mu\text{-}CH_3COO)_2L'_2]^b$	Bent VOV	685	536	1306

[a] L = tacn = 1,4,7-triazacyclononane.
[b] L′ = HB(pz)$_3$ = tris(1-pyrazolyl)borate ion.

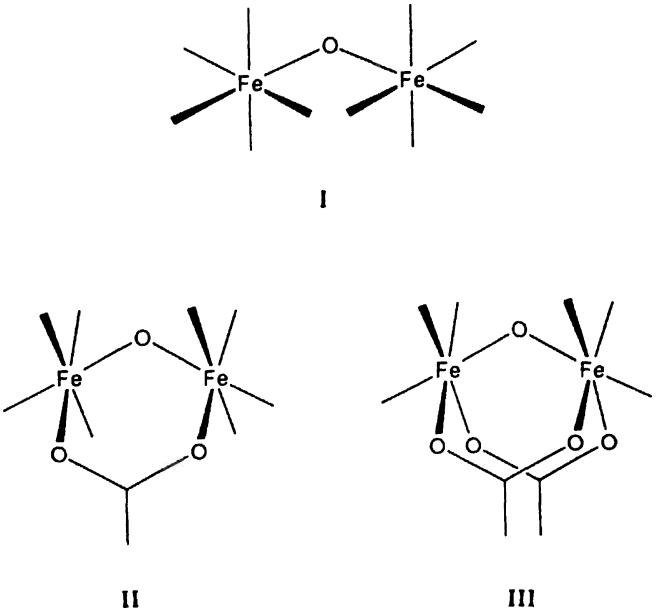

Fig. 1.81. *Structures of three types of oxo bridges [1307].*

For example, $[Au^{III}{}_2\ (bipy)_2(\mu\text{-}O)_2]^{2+}$ [1308] and $[(Cu^{III}{}_2(Sp)_2(\mu\text{-}O)_2]^{2+}$ [1309] exhibit the $\nu(M_2O_2)$ at 682(662) and 619(591) cm^{-1}, respectively. Here the numbers in brackets indicate the frequencies of the corresponding ^{18}O vibrations, and Sp is (−) sparteine. Trioxo bridging vibrations are reported for $[Cr^{III}{}_3(C_2H_5CO_2)_6F_3(\mu\text{-}O)_3]^{2-}$ [1310]. The $\nu_a(CrO_3)$ and $\nu_s(CrO_3)$ are at 663 and 165 cm^{-1}, respectively.

1.22.4. Oxoferrylporphyrins and Related Complexes

Another type of monooxo comolex is oxoferrylporphyrin. As stated in Sec. 1.21.4, the O_2 adducts of five-coordinate, base-free porphyrins such as $Fe(TPP)O_2$ were prepared via matrix cocendensation reaction, and assignments of their IR spectra were based on $^{16}O_2/^{18}O_2$ isotopic shifts. During the measurements of the corresponding RR spectra in pure O_2 at ~15 K, Bajdor and Nakamoto [1311] observed the appearance of a new band at 853 cm^{-1} on laser irradiation (406.7 nm, 1–2 mW), and noted that the intensity of this band peaks after ~20 min. As shown in Fig. 1.82, this band is shifted to 818 cm^{-1} by $^{16}O_2 - {}^{18}O_2$ substitution. Similar experiments with scrambled dioxygen ($^{16}O_2/^{16}O^{18}O^{18}O_2 \cong 1/2/1$) produce only two bands at 852 and 818 cm^{-1}. These results clearly indicate that the bands at 852 and 818 cm^{-1} are due to the $\nu(Fe = {}^{16}O)$ and $\nu(Fe^{18}O)$, respectively, of FeO(TPP), which were formed by the cleavage of the bound dioxygen in $Fe(TPP)O_2$. $^{54}Fe - {}^{56}Fe$ substitution experiments further confirmed these assignments. A simple diatomic approximation gives a FeO stretching force constant of 5.32 mdyn/Å, which is much larger than that of the FeO bond in $[Fe(TPP)]_2O$ (3.8 mdyn/Å) [1298]. A more detailed study by Proniewicz et al. [1312]

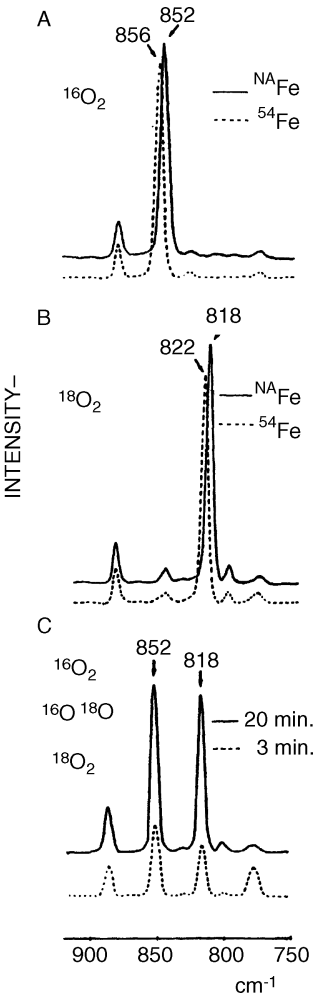

Fig. 1.82. *The RR spectra of Fe(TPP) cocondensed with O_2 at ~15 K (406.7 nm excitation):* (A) *^{NA}Fe(TPP) with $^{16}O_2$;* (B) *^{NA}Fe(TPP) with $^{18}O_2$, and* (C) *^{NA}Fe(TPP) with isotopically scrambled O_2. The broken lines in* (A) *and* (B) *denote the spectra of ^{54}Fe(TPP) cocondensed with respective gases. All the spectra in* (A), (B), *and* (C) *(solid line) were obtained after 20-min laser irradiation. The dotted line in* (C) *indicates the spectrum obtained only after 3-min laser irradiation. ^{NA}Fe (Fe in natural abundance) contains 92% ^{56}Fe [1311].*

shows that the Fe atom in oxoferryl porphyrin is Fe(IV) and low-spin, and that the FeO bond should be formulated as Fe(IV) $\cdots$ O^{2-}. Here, the arrowed line indicates a σ-bond formed via the d_{z^2}–p_z overlap and the broken lines represent two π-bonds formed via the d_{xz}–p_x and d_{yz}–p_y overlaps. It is conventionally written as Fe=O. Similar experiments readily produced FeO(OEP) and FeO(salen) but not FeO(Pc). These results suggest that the O−O bond strength decreases in the order Fe(Pc)O_2 > Fe(TPP)O_2 > Fe(salen)O_2 as indicated in their $\nu(O_2)$ (Table 1.60).

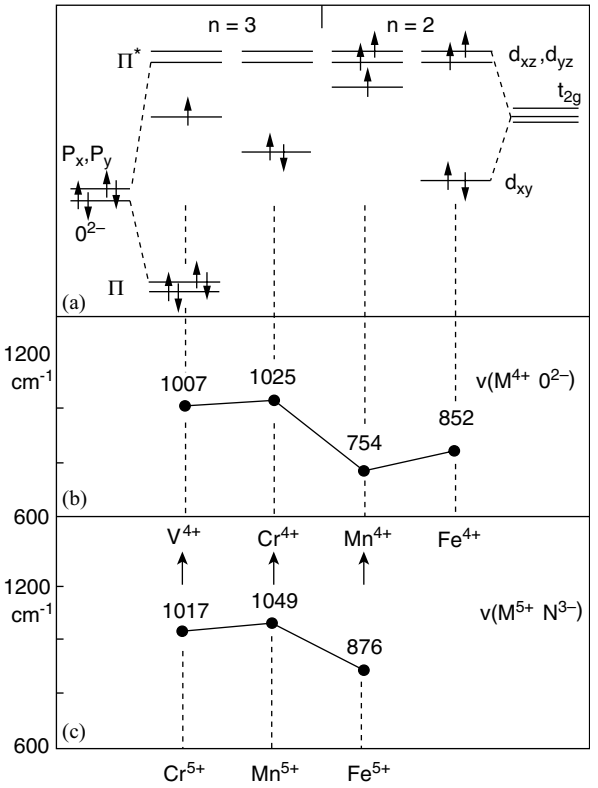

Fig. 1.83. *(a) Electron configuration of $M^{4+}O^{2-}$ porphyrin; (b) variation of $\nu(M^{4+}O^{2-})$ in $M^{4+}O^{2-}$ porphyrins; (c) variation of $\nu(M^{5+}N^{3-})$ in $M^{5+}N^{3-}$ porphyrins [1314,1315].*

Oxoferrylporphyrin, FeO(TMP) (TMP = tetramesitylporphyrin), can also be produced by electrooxidation of Fe(TMP)(OH) in CH_2Cl_2 at $-40°C$. According to Czernuszewicz and Macor [1313], it exhibits the ν(Fe=O) at 841 cm^{-1}. Cooling is necessary because it is unstable and readily reacts with CH_2Cl_2 to form Fe(TMP)Cl at higher temperature.

The ν(M=O) of stable oxo porphyrins are known for TPP(V=O) (1007 cm^{-1}), TPP (Cr=O) (1925 cm^{-1}), and (TPP)(Mn=O) (754 cm^{-1}). Figure 1.83a is a simple molecular orbital (MO) diagram showing the relationship between the ν(M=O) and the *d*-electron configuration [1314]. As seen in Fig. 1.83b, the *d* electrons enter the nonbonding (d_{xy}) orbital in V(IV) (d^1) and Cr(IV) (d^2) but antibonding orbitals (d_{xz} and d_{yz}) in Mn(IV) (d^3) and Fe(IV) (d^4) thus reducing the MO bond order from 3 to 2. As a result, the ν(M=O) drops abruptly in going from V(IV) and Cr(IV) to Mn(IV) and Fe (IV). In the Mn(IV) complex, the d_{xy} orbital is raised near the d_{xz} and d_{yz} orbitals because of the special stability of the half-filled t_{2g} subshell, resulting in the high-spin $(d_{xy})^1\ (d_{xz})^1\ (d_{yz})^1$ configuration, and this is reflected in the ν(M=O) frequencies. The ν(Mn=O) is lower than the ν(Fe=O) primarily because of the higher effective nuclear charge on Fe(IV) relative to Mn(IV).

1.22.5. Oxoferrylporphyrin π-Cation Radicals

As shown in the preceding section, oxoferrylporphyrins such as (TPP)Fe=O are formed by laser irradiation of (TPP)FeO_2 in O_2 matrices. A more detailed RR study by Proniewicz et al. [1316] revealed simultaneous formation of its π-cation radical. As shown in Fig. 1.84, (TPP)Fe=^{16}O exhibits seven bands (shown shaded) that are sensitive to $^{16}O/^{18}O$ isotope substitution. The bands at 1195 (1129) and 1105 (1043) cm^{-1} are due to the $\nu(O_2)$ of the end-on and side-on isomers of (TPP)FeO_2, respectively (Sec. 1.21.4). Here, the numbers in brackets indicate the corresponding ^{18}O frequencies. Three bands at 508(487), 349(345) and 408(402) cm^{-1} are also $^{16}O/^{18}O$ isotope-sensitive. The former two were assigned to the $\nu(Fe-O_2)$ and $\delta(FeOO)$ of the end-on isomer, respectively, whereas the last band was assigned to the $\nu_s(Fe-O)$ of the side-on isomer. In the high-frequency region, two isotope-sensitive bands are

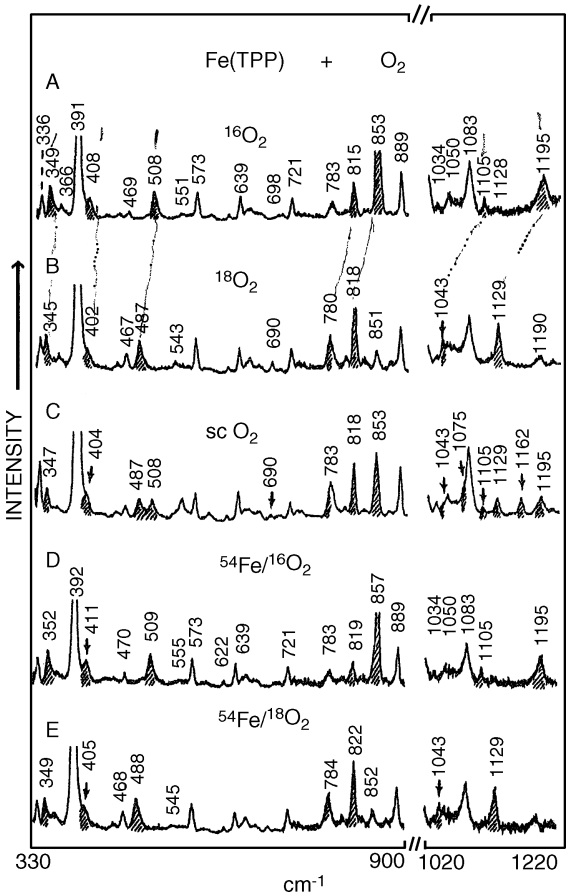

Fig. 1.84. *RR spectra of Fe(TPP) cocondensed with dioxygen at ~30 K (406.7 nm excitation): (A) $^{16}O_2$; (B) $^{18}O_2$; (C) scrambled O_2 ($^{16}O_2$: $^{16}O^{18}O$: $^{18}O_2$ = 1 : 2 : 1); (D) $^{54}Fe/^{16}O_2$; (E) $^{54}Fe/^{18}O_2$. Shaded bands are oxygen-isotope-sensitive.*

observed at 853(818) and 815(780) cm^{-1}. Although the former stronger band was previously assigned to the ν(Fe=O) of (TPP)Fe=O, the nature of the latter, weaker band was not clear. It must be another ν(Fe=O) band since the magnitude of its isotope shift (35 cm^{-1}) is close to that of the former (37 cm^{-1}). To find out the difference between these two species, the RR intensities of (TPP-d_8)Fe=O were measured as a function of laser power as well as of laser irradiation time. It was found that the intensity of the former band at 853 cm^{-1} increases rapidly as the laser power increases and reaches a maximum value after 30 min (laser power, 8.0 mW), whereas that of the latter band at 815 cm^{-1} reaches a maximum at ~3.5 mW, and then decreases exponentially with time. On the basis of these differences, the 815 cm^{-1} band was attributed to the π-cation radical, (TPP$^{\bullet+}$-d_8)Fe=O, which was formed as an intermediate species during photocleavage of the O=O bond. As will be shown in Sec. 3.3.3, such a π-cation radical serves as a model compound of HRP compound I.

Hashimoto et al. [1317] first generated O=Fe(TMP($^{\bullet+}$) in CH_2Cl_2 solution mixed with CH_3OH and observed the ν(Fe=O) at 828 cm^{-1}. On the other hand, Kincaid et al. [1318] observed it at 802 cm^{-1} in CH_2Cl_2. Later, the former band was reassigned to the six-coordinated species with CH_3OH as the axial ligand, whereas the latter band at 802 cm^{-1} was reassigned to the six-coordinate species with Cl^- as the axial ligand [1319]. Since the ν(Fe=O) of the five-coordinated species, FeO(TPP$^{\bullet,+}$) in O_2 matrices [1316] was observed at 815 cm^{-1}, the shift from 815 to 802 (13 cm^{-1}) was attributed to the *trans*-effect of the axial ligand on the Fe=O moiety. This *trans* effect was confirmed in a series of FeO(TMP$^{\bullet,+}$)L-type complexes where the ν(Fe=O) band is shifted from 828 to 801 cm^{-1} by changing L from CH_3OH to *m*-CPBA (*m*-chloroperoxybenzoic acid). Czarnecki et al. [1319] conducted an extensive study using a variety of L, and observed the ν (Fe=O) near 835 cm^{-1} for L = ClO_4^- and CF3SO_3^-, and near 800 cm^{-1} for L = F^- Cl^-, and *m*-CPBA. Their results clearly indicate that the electron-donating capabilities of the latter group are greater than that of the former group.

Metalloporphyrin π-cation radicals can take either the $^2A_{1u}$ or $^2A_{2u}$ ground state because the two highest occupied orbitals are of a_{1u} or a_{2u} symmetry, which is nearly degenerate under $\mathbf{D}_{4h}$ symmetry (Sec. 1.23 of Part A). Figure 1.85 shows the

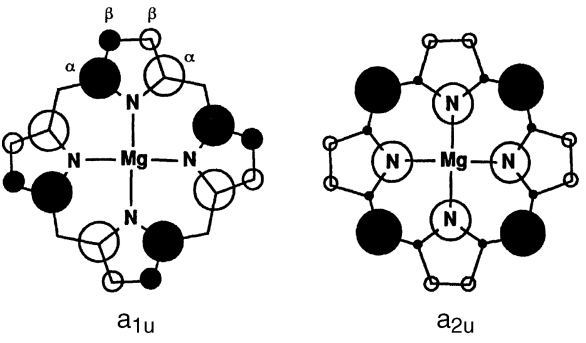

Fig. 1.85. *The atomic orbital (AO) structure of Mg (Por) in the two highest-occupied orbitals; the circle sizes are approximately proportional to the AO coefficients; the open circles represent negative signs of the upper lobe of the* pπ *AOs [1341].*

coefficients of the atomic p_z orbitals represented by the size of the circles [1320]. The open circle represents the negative sign of the upper lobes of the p_z atomic orbital. It is seen that the $C_\beta-C_\beta$ bond is antibonding in the a_{1u} orbial, whereas it is bonding in the a_{2u} orbital. As shown in Table 1.10, the $\nu_2(A_{1g})$ is due to the $\nu(C_\beta-C_\beta)$. Therefore, this vibration should be downshifted in the $^2A_{2u}$ radical and upshifted in the $^2A_{1u}$ radical. It was concluded Ni(TPP), Cu(TPP), and ClFe(TPP) produce the A_{2u} type, whereas Ni (OEP) and ClFe(OEP) form the A_{1u} type [1320,1321]. VO(OEP) [1322,1323] also forms an A_{1u} radical because its ν_2 is upshifted from 1580 to 1601 cm^{-1}. In general, TPP and OEP complexes form π-cation radicals of A_{2u} and A_{1u} types, respectively. The $\nu(V=O)$ near 1000 cm^{-1} is insensitive to the radical type [1345]. Kincaid et al. [1324] concluded that six-coordinate FeO(TMP$^{\cdot+}$)L is of A_{2u} type because both ν_2 and ν_4 are downshifted by $\sim$30 and $\sim$10 cm^{-1}, respectively, on radical formation [1318]. However, the A_{1u}-type symmetry was found for FeO(TMTMP$^{\cdot+}$) [1324]. Here, TMTMP is tetramethyl–tetramesitylporphyrin.

π-Cation radical types can also be differentiated by comparing the intensity of IR-active E_u modes. For example, the $\nu(C_\alpha-C_m)_a$ (ν_{37}) band of Cu(OEP) at 1551 cm^{-1} markedly increases its intensity on radical formation. In contrast, the corresponding band at 1574 cm^{-1} of Cu(TPP) shows almost no increase in intensity on radical formation. This result suggests that the changes in the *du/dQ* terms (Sec. 1.19 of Part A) are markedly different depending on the radical type [1325]. Resonance Raman studies on oxofenyl porphyrins and their π-cation radicals have been reviewed by Kitagawa and Mizutani [1326] and Nakamoto [1327].

1.23. COMPLEXES OF DINITROGEN AND RELATED LIGANDS

1.23.1. Dinitrogen Complexes of Transition Metals

Since Allen and Senoff [1328] prepared the first stable dinitrogen (molecular nitrogen) compounds, $[Ru(N_2)(NH_3)_5]X_2$ ($X = Br^-$, I^-, BF_4^-, etc.), a large number of dinitrogen compounds have been synthesized. The chemistry and spectroscopy of these compounds have been reviewed extensively [1126,1329–1332]. The structures of dinitrogen compounds are classified into three types:

End-on (linear) | Side-on (symmetric) | Bridging (linear)

The terminal end-on coordination is most common. The $M-N_2$ bonding is interpreted in terms of the σ-donation and π-backbonding, which were discussed in Secs. 1.16 and 1.18. Since N_2 is a weaker Lewis base than CO, π-backbonding may be more important in nitrogen complexes than in CO complexes [1333]. Free N_2 exhibits $\nu(N\equiv N)$ at 2331 cm^{-1}, and this band shifts to 2220–1850 cm^{-1} on coordination to the metal. Table 1.65 lists the $\nu(N\equiv N)$ of typical complexes. The $\nu(N_2)$ of the Fe(0) complex

TABLE 1.65. Observed N≡N Stretching Frequencies (cm^{-1})

Complex	ν(N≡N)	Ref.
$Fe(N_2)(DPE)_2$[a]	1955	1334
$[FeCl(N_2)(DPE)]^{+}$,[a]	2088	1335
$[Ru(N_2)(NH_3)_5]Br_2$	2105	1336
$[Ru(N_2)(NH_3)_5]I_2$	2124	1337
$[Os(N_2)(NH_3)_5]Cl_2$	2022, 2010	1338
$[OsH(N_2)(PPh_2OCH_3)_4]^{+}$	2197	1339
$Co(N_2)(PPh_3)_3$	2093	1340
$Co(N_2)H(PPh_3)_3$	2105	1341
$Ir(N_2)Cl(PPh_3)_2$	2105	1342
$Ir(N_2)Cl(H)(PPh_3)_2(BF_4)$	2229	1343
trans-$Mo(N_2)_2(DPE)_2$[a]	1970 (2020)	1344
cis-$W(N_2)_2(PMe_2Ph)_4$	1998, 1931	1345
$Co(N_2)(PR_3)(PR_2)_2^{2b}$	1904 ~ 1864	1346
$[Rh(I)(N_2)_2]^{+}$,[c]	2244. 2218	1347

[a] DPE = Ph_2P–$(CH_2)_2$–PPh_2.
[b] R = *n*-Bu or Ph.
[c] On zeolite surface.

[1334] is much lower than that of the Fe(II) complex [1335], indicating stronger π-backdonation of the former to the N_2 ligand.

Very little information is available for ν(M—N_2) and δ(M−N≡N) in the low-frequency region. Allen et al. [1333] assigned ν(Ru−N_2) of $[Ru(N_2)(NH_3)_5]^{2+}$-type compounds in the 508–474 cm^{-1} region, whereas other workers [1336,1337] attributed these bands to δ(Ru−N≡N). Figure 1.86 shows the infrared spectrum of $[Ru(NH_3)_5N_2]Br_2$ obtained by Allen et al.

According to Srivastava and Bigorgne [1348], $Co(N_2)H(PPh_3)_3$ exists in two forms in the solid state; one form exhibits ν(N≡N) at ~ 2087 cm^{-1}, and the other shows two bands of equal intensity at 2101 and 2085 cm^{-1}. However, their structural differences are unknown. Darensbourg [1349] obtained a linear relationship between ν(N≡N) and the absolute integrated intensity in a series of dinitrogen compounds.

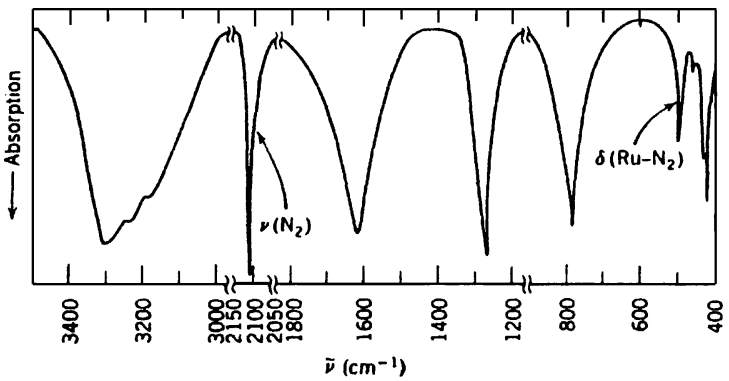

Fig. 1.86. *Infrared spectrum of $[Ru(NH_3)_5N_2]Br_2$ [1333].*

Armor and Taube [1350] postulated the occurrence of the side-on structure as a possible transition state in linkage isomerization: $[(NH_3)_5Ru-{}^{14}N \equiv {}^{15}N]Br_2 \leftrightarrow [(NH_3)_5Ru-{}^{15}N \equiv {}^{14}N]Br_2$. Krüger and Tsay [1351] carried out X-ray analysis on $[\{(C_6H_5Li)_3Ni\}_2(N_2)\{(C_2H_5)_2O\}_2]_2$ and confirmed the presence of the side-on coordination in this compound; the N−N distance was found to be extremely long (1.35 Å). Formichev et al. [1352] prepared a photoinduced metastable state of $[Os(NH_3)_5(N_2)](PF_6)_2$ and confirmed its side-on coordination by X-ray diffraction. The $\nu(N_2)$ was observed at 1838 cm^{-1}(IR), which is 187 cm^{-1} lower than that of the side-on ligand in the ground state.

The linear bridging M−N≡N−M-type complex should not show ν(N≡N) in the IR spectrum. However, it may show a strong ν(N≡N) in the Raman spectrum. Thus $[\{Ru(NH_3)_5\}_2(N_2)]^{4+}$ shows no infrared bands in the 2220–1920 cm^{-1} region, whereas a strong ν(N≡N) band appears at 2100 cm^{-1} in the Raman region [1353].

In the case of $(\mu\text{-}N_2)\{Mo(III)[N(R)\,L]_3\}_2$, where R is $C(CD_3)_2CH_3$ and L is 3.5-$C_6H_3Me_2$, the $\nu(N_2)$ of the linear Mo−N≡N−Mo bridge is at 1630 cm^{-1}, which is shifted to 1577 cm^{-1} by $^{14}N/^{15}N$ substitution (Raman). The observed low frequency suggests the NN bond order close to 2 [1354]. If N_2 forms a bridge between two different metals, ν(N≡N) is observed in the infrared. For example, ν(N≡N) is at 1875 cm^{-1} in the infrared (spectrum of $[(PMe_2Ph)_4ClRe-N_2-CrCl_3(THF)_2]$ [1355]. According to X-ray analysis [1356], an analogous compound, $[(PMe_2Ph)_4ClRe-N_2-MoCl_4(OMe)]$, has a N≡N distance of 1.2 Å, and its ν(N≡N) is at 1660 cm^{-1}. As expected, the ν(N=N) of $[(CO)_5Cr-NH=NH-Cr(CO)_5]$ is very low (1415 cm^{-1}) [1357].

The side-on bridging structure (μ–η^2–η^2–N_2), similar to that of the O_2 bridge (Sec. 1.21), was proposed for $\{[(Pr^i{}_2PCH_2SiMe_2)_2N]ZrCl\}_2(N_2)$ by Cohen et al. [1358]. An intense Raman peak at 731 cm^{-1} was assigned to one of the totally symmetric modes of the Zr_2N_2 moiety that is predominantly due to $\nu(N_2)$ in character. It is downshifted by $\sim 22\,cm^{-1}$ by $^{14}N/^{15}N$ substitution in THF solution.

1.23.2. Dinitrogen Adducts of Metal Atoms

Similar to $M(CO)_n$- and $M(O_2)_n$-type compounds discussed previously (Secs. 1.18 and 1.21), it is possible to prepare simple $M(N_2)_n$-type adducts by reacting metal atoms with N_2 in inert gas matrices. Again the distinction between end-on and side-on geometries can be made by using the isotope scrambling techniques ($^{14}N_2 + {}^{14}N{}^{15}N + {}^{15}N_2$). Figure 1.87 shows the IR spectra of Ni(N_2)(end-on) [1359] and Co(N_2)(side-on) [1360]. The observed frequencies (cm^{-1}) and assignments of the four bands of the former are as follows:

Ni−^{14}N≡^{14}N	Ni−^{14}N≡^{15}N	Ni−^{15}N≡^{14}N	Ni−^{15}N≡^{15}N
2089.9	2057.4	2053.6	2020.6

Table 1.66 lists the $\nu(N_2)$ of $M(N_2)$-type complexes. All these adducts take the end-on structure except for Co(N_2) and Th(N_2) [1365]. The structure of $M(N_2)_4$, $M(N_2)_3$, and $M(N_2)_2$ are tetrahedral, trigonal–planar, and linear respectively, although slight

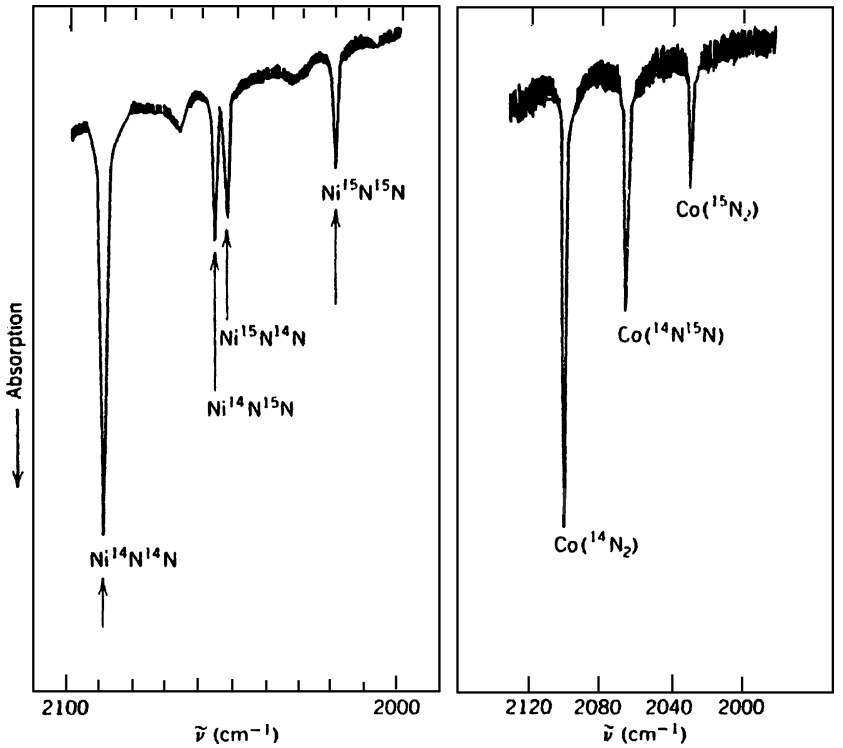

Fig. 1.87. *Matrix isolation IR spectra of Ni and Co atom vapors cocondensed with $^{14}N_2/^{14}N^{15}N/^{15}N_2$/Ar at 10 K [1359,1360].*

distortions from these ideal symmetries occur as a result of the matrix effect. In all these compounds, the N_2 ligands take end-on geometry except $Pt(N_2)_2$, for which side-on coordination has been proposed [1361].

Most of the studies described above have been made in the $\nu(N_2)$ region since low-frequency vibrations are generally weak and difficult to measure in inert gas matrics. However, the IR-active $\nu(M-N_2)$ vibrations of $Ni(N_2)_4$, $Rh(N_2)_4$, and $Pd(N_2)_2$ have

TABLE 1.66. Typical 1 : 1 (Metal/N_2) Adducts Prepared by Matrix Cocondensation Techniques

Adduct	$\nu(N_2)$	Ref.
$Ni(N_2)$	2088	1359,1359a
$Pd(N_2)$	2211	1359
$Pt(N_2)$	2173/2168	1361
$Co(N_2)$	2101	1360
$V(N_2)$	2216	1362
$Nb(N_2)$	1926/1931	1363
$Cr(N_2)$	2215	1364
$Th(N_2)$	1829	1365

been observed at 283, 345, and 340 cm^{-1}, respectively. The corresponding force constants are 0.81, 1.44, and 1.25 mdyn/Å, respectively [1366]. It should be noted that the Ni−CO stretching force constant of $Ni(CO)_4$ (1.80 mdyn/Å) is more than 2 times larger than that of $Ni(N_2)_4$ (0.81 mdyn/Å).

As stated in Chapter 2 of Part A, UN_2 and PuN_2 prepared by the spattering techniques take the linear N−M−N structures. Such insertion products are obtained by matrix cocondensation reactions of N_2 with laser-ablated metal atom vapors. For example, the Fe atom reacts with N_2/Ar at 10 K to form FeN (934.8), NFeN (903.6), cyclo-Fe_2N (779,719) in addition to end-on $Fe(N_2)$(2017.8), side-on $Fe(N_2)$(1 826.8), and side-on $Fe(N_2)_2$ (1683.7) [1367]. Here, the numbers in parentheses indicate the characteristic frequency of each species. Similar results are reported for laser-ablated Be [1368] and Pt [1369] atoms. Maier et al. [1370] found that the reaction of thermally generated Si atom vapor with N_2 produces NNSiNN, SiNNSi, SiNSiN, cyclo-SiN_2, and cyclo-Si_2N_2, and confirmed their structures by DFT calculations.

1.23.3. Nitrido Complexes

If the N^{3-} ion coordinates to a metal, it is called a *nitrido complex*. Nitrido complexes of transition metals can be prepared by several methods, and their preparations, structures, and spectra have been reviewed by Griffith [1371]. The M≡N triple bonds are formed as a result of the strong π-donating property of the N^{3-} ion. Cleare and Griffith [1372] carried out an extensive study on vibrational spectra of nitrido complexes.

As shown in Table 1.67, the ν(M≡N) of nonbridging nitrido complexes are generally found in the 1100–1000 cm^{-1} region. However, an exception was found for Fe(N)(OEP), which exhibits the ν(Fe≡N) at 876 cm^{-1}. This novel Fe(V) nitrido complex was prepared by laser photolysis of the corresponding azido complex at ∼ 30 K [1382]:

$$(OEP)Fe-N{=}N{\equiv}N \xrightarrow{h\nu} (OEP)Fe{\equiv}N + N_2$$

TABLE 1.67. Vibrational Frequencies of Nonbridging Nitrido Complexes (cm^{-1})

Complex	ν(M≡N)	Ref.
$[Nb(N)F_5]^{3-}$	1050	1373
$[Ta(N)Cl_5]^{3-}$	1040	1373
Cr(N)(TTP)[a]	1017	1374
$[Cr(N)(CN)_4]^{2-}$	1052	1375
$[Cr(N)(CN)_5]^{3-}$	972	1375
Mo(N)(*t*-BuO)$_3$	1020	1376
Mo(N)(TMP)	1038	1377
W(N)(*t*-BuO)$_3$	1010	1376
Mn(N)(TPP)	1052	1378
$[Tc(N)(py)_4]^{2+}$	1072	1379
$[Ru(N)Cl_4]^{-}$	1092	1380
$[Os(N)Cl_5]^{2-}$	1081	1372
$[Os(N)(N_3)_5](PPh_4)_2$	1054	1381

[a]TTP = tetra-*p*-tolylporphyrin.

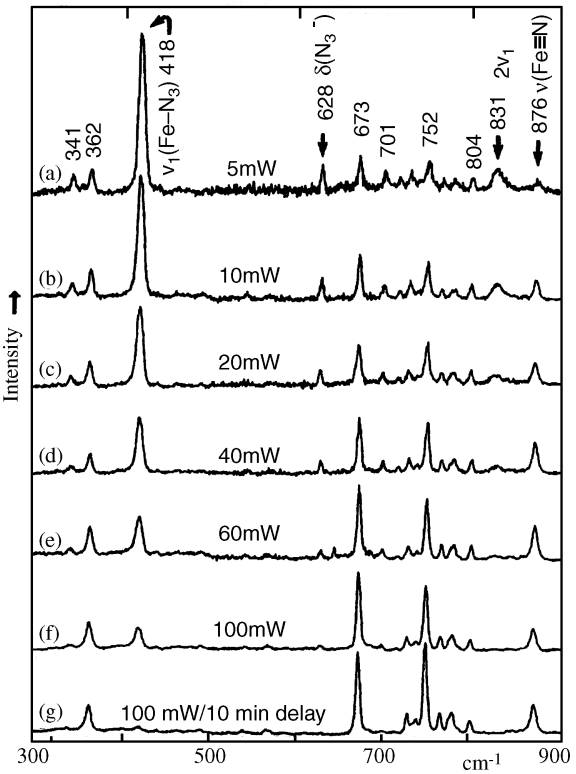

Fig. 1.88. *The RR spectra of a thin film of Fe(N_3)(OEP) at ~30 K, 488.0 nm excitation with different excitation power:* (a) *5 mW, eight scans added;* (b) *10 mW, four scans added;* (c) *20 mW, two scans added;* (d) *40 mW;* (e) *60 mW;* (f) *100 mW;* (g) *100 mW, after 10-min preirradiation with 488.0 nm (100 mW) [1382].*

Figure 1.88 shows the RR spectra of a thin film of Fe(N_3)(OEP) that was irradiated by 488.0 nm line of Ar ion laser. It is seen that, as the laser power increases, the bands characteristic of the azido group [266] become weaker and a set of new bands at 876, 752, and 673 cm^{-1} become stronger. The 876 cm^{-1} band can be assigned to the ν(Fe≡N) on the basis of the results of isotope substitution experiments involving $^{15}NN_2$, $15N_3$, and $^{54}Fe/^{56}Fe$. The remaining two bands are attributed to porphyrin core vibrations of the nitrido complex. Similar results have been obtained for the TPP analogs.

The large drop in the ν(M≡N) in going from nitrido porphyrins of Cr(V) and Mn(V) to Fe(V) may be accounted for in terms of the MO schemes shown previously (Fig. 1.83c).

Since the M(V)≡N^{3-} system is one-electron-deficient relative to the M(IV)=O^{2-} system, the Fe(V)≡N^{3-} bond is isoelectronic with the Mn(IV)=O^{2-} bond. Thus, the electronic configuration of the Fe(V)≡N system may be $(d_{xy})^1(d_{xz})^1(d_{yz})^1$ (high spin) or $(d_{xy})^2(d_{xz})^1$ (low spin). The former is preferred because of the relatively small Fe≡N

stretching force constant (5.07 mdyn/Å). This is further supported by Meyer et al. [1383], who studied the ESR and Mössbauer spectra of the *trans*-$[Fe(N)(N_3)(cyclam)]^+$ ion. The frequencies of oxidation state marker bands of OEP and TPP porphyrins discussed in Sec. 1.5 indicate the Fe(V) state for their nitrido complexes.

Dinuclear complexes containing linear and symmetric nitride bridges (M−N−M) exhibit the ν_a(MNM) in IR and ν_s(NMN) in Raman spectra. These vibrations are observed at 985 and 228 cm^{-1}, respectively, for $[Ta_2(\mu\text{-}N)Br_{10}]^{2-}$ and at 904 and 203 cm^{-1}, respectively, for $[Nb_2(\mu\text{-}N)Br_{10}]^{2-}$ [1384]. For $[W_2(\mu\text{-}N)Cl_{10}]^-$, the ν_a(WNW) was observed at 945 cm^{-1} [1385]. The ν_a(MNM) of $[Mn_2(\mu\text{-}N)(CN)_{10}]^{6-}$ is in the range of 976–935 cm^{-1} depending on the cation [1386]. Similar frequencies are reported for $[Nb_2(\mu\text{-}N)Cl_{10}]^{3-}$ (951 cm^{-1}) [1387]. In $[Fe(TPP)]_2(\mu\text{-}N)$ containing low-spin Fe(III) centers, the ν_s(FeNFe) has been observed at 424 cm^{-1} in RR spectra [1388]. The corresponding FeNFe stretching force constant (4.5 mdyn/Å) is slightly larger than the FeOFe stretching force constant (3.8 mdyn/Å) in $(Fe(TPP))_2O$ [1298]. Thus, the FeNFe bridge may be expressed as Fe≕N≕Fe (bond order, 1.5).

Clear and Griffith [1372] list the vibrational frquencies of other nitrido bridges containing Ru, Os, and Ir. In a trinuclear complex ion, $[Ir_3N(SO_4)_6(H_2O)_3]^{4-}$, the nitrido atom is bonded to three Ir atoms trigonally and the $\nu_a(Ir_3N)$ is observed at 780 cm^{-1} [1372].

1.24. COMPLEXES OF DIHYDROGEN AND RELATED LIGANDS

1.24.1. Metal Complexes of Dihydrogen

Dihydrogen is known to coordinate to a transition metal atom only in the side-on fashion. The metal H_2 bonding is interpreted in terms of a delicate balance between σ-donation to the metal and backdonation to σ^*, as illustrated below [1389]:

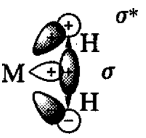

Photolysis of a mixture of $Fe(CO)_2(NO)_2$ with H_2 in liquid Xe (−104°C) produces $Fe(CO)(NO)_2(H_2)$, which exhibits the $\nu(H_2)$, $\nu_a(Fe-H_2)$, and $\nu_s(Fe-H_2)$ at 2973, 1374, and 870 cm^{-1}, respectively [1390]. These dihydrogen vibrations have been observed for $M(CO)_5(H_2)$ (M = Cr,Mo,W) [1391,1392], $M(CO)_3(Cp)(H_2)$ (M = V, Nb) [1393], and *cis*-$W(CO)_4(C_2H_4)(H_2)$ [1394], which were prepared by similar methods. In $V(CO)_3(Cp)(H_2)$, the $\nu(H_2)$ at 2642 cm^{-1} is shifted to 2377and 1998 cm^{-1}, respectively, by HD and D_2 substitution. The fact that the IR spectrum of the HD compound exhibits the ν(HD) at a frequency intermediate between those of the H_2 and D_2 compounds and is not an overlap of the ν(V−H) and ν(V−D) bands provides definitive evidence that it is a dihydrogen compound and not a dihydride.

More stable dihydrogen complexes of the type $M(CO)_3(PR_3)_2(H_2)$, where M is Mo and W and R is cyclohexyl (Cy) or isopropyl (*i*-Pr), were first prepared by Kubas et al.

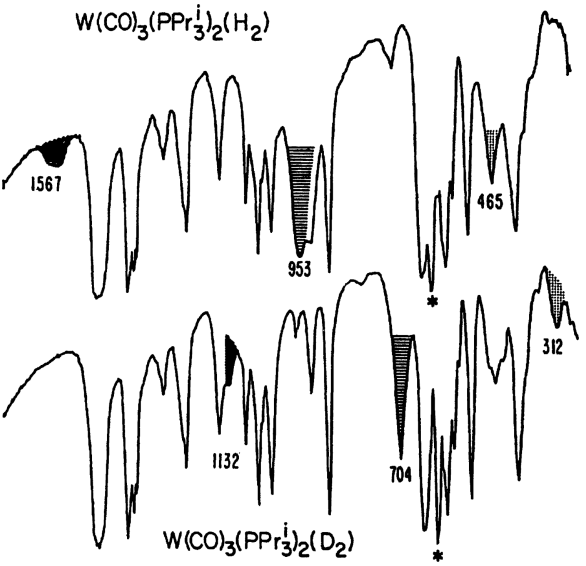

Fig. 1.89. *Infrared spectra of $W(CO)_3$ $(P(i\text{-}Pr)_3)_2(H_2)$ and its D_2 analog (Nujol mull) [1395,1396].*

[1395,1396]. Figure 1.89 shows the IR spectra of $W(CO)_3[P(i\text{-}Pr)_3]_2(H_2)$ and its D_2 analog. The $\nu(H_2)$, $\nu_a(WH_2)$, $\nu_s(WH_2)$, and $\delta(WH_2)$ are observed at 2695, 1567 ($\sim$1140), 953 (704), and 465 (312) cm^{-1}, respectively. The corresponding frequencies of the D_2 analog are given in parentheses. It should be noted that these complexes are still labile and must be kept in an H_2-enriched atmosphere.

Vibrational spectra and band assignment are also reported for *trans*-$W(CO)_3(Pcy_3)_2(H_2)$ (cy=cyclohexyl) [1397] and $[CpRu(Ph_2P{-}PPh_2)(H_2)]BF_4$ [1398], with $\nu(H_2)$ at 2690 and 2082 cm^{-1}, respectively. The latter frequency is very low, and the corresponding $\nu(D_2)$ is at 1530 cm^{-1}. X-Ray analysis shows that the H−H distance in $Cr(CO)_3(Pcy_3)_2(H_2)$ is only 0.67(5) Å, which is the shortest ligated H−H bond. However, its $\nu(H_2)$ is hidden under other bands [1399].

1.24.2. Hydrido Complexes

Vibrational spectra of hydrocarbonyls have been discussed in Sec. 1.18.5. Metal complexes containing terminal hydrido groups (M−H) exhibit the ν(M−H) and δ(M−H) in the 2250–1700 and 800–600 cm^{-1} regions, respectively; Table 1.68 lists M−H frequencies of typical complexes.

The ν(MH) is sensitive to other ligands, particularly those in the *trans* position in the square–planar Pt(II) complexes. Thus Chatt et al. [1410] found that the order of ν(PtH) in *trans*-$[Pt(H)X(PEt_3)_2]$ is as follows:

X =	NO_3^-	<	Cl^-	<	Br^-	<	I^-	<	NO_2^-	<	SCN^-	<	CN^-
ν(PtH)(cm^{-1})	2242	>	2183	>	2178	>	2156	>	2150	>	2112	>	2041

TABLE 1.68. M–H Frequencies of Hydrido Complexes (cm^{-1})

Complex	ν(MH)	δ(MH)	Ref.
$[Al(H)(NPh_2)_3]^-$	1777	—	1400
$H_2Ga(\mu\text{-}Cl)_2GaH_2$	2042–1988	—	1401
trans,trans-$[Cr(H)(CO)_2(NO)(PEt_3)_2]$	1661	—	1402
$[Mo(H)(CN)_7]^{4-}$	1805	—	1403
cis-$[Fe(H)(CO)_3P(OC_6H_5)_3]^-$	1895	—	1404
trans-$[Fe(H)Cl\{C_2H_4(PEt_2)_2\}_2]$	1849	656	1405
$[Co(H)(CN)_5]^{3-}$	1840	774	1406
$[Ru(CO)(H)(NCO)(PPh_2Me)_3]$	1920	—	1407
mer-$[Os(H)_3(NO)(PPr_3)_2]$	2032–1849	—	1408
$[Rh(H)(CN)_5]^{3-}$	1980	781	1403
$[Ir(H)(CN)_5]^{3-}$	2040	811	1403
$Ir(H)(COD)\{As(C_6H_5)_3\}_2$[a]	2030	—	1409

[a]COD = 1,5-cyclooctadiene.

This is the increasing order of *trans* influence. Church and Mays [1411] found that the NMR Pt−H coupling constant (J) and ν(PtH) decrease in the same order in the *trans*-$[Pt(H)L(PEt_3)_2]^+$ series:

L =	py	<	CO	<	PPh_3	<	$P(OPh)_3$	<	$P(OMe)^3$	<	PEt^3
J(PtH)(Hz)	1106	>	967	>	890	>	872	>	846	>	790
ν(PtH)(cm^{-1})	2216	>	2167	>	2100	>	2090	>	2067	<	2090

In this series, the σ-donor strength of L increases as the J(PtH) value decreases and ν(PtH) shifts to a lower frequency. Atkins et al. [1412] found linear relationships between the chemical shift of the hydride, the Pt−H coupling constant, ν(PtH), and the pK_a value of the parent carboxylic acid in a series of *trans*-[Pt(H)L(PEt3)$_2$], where L is a carboxylate ligand.

X-Ray analyses have shown that both terminal and bridging hydrido groups exist in each of the three complexes shown in Fig. 1.90. Compounds I and II exhibit the terminal and bridging ν(MH) in the 2100–1800 and 1200–950 cm^{-1} regions, respectively, while three ν(TaH) vibrations (1810,1720, and 1650 cm^{-1}) are reported for compound III.

Metal carbonyl ions such as $[Co_6(CO)_{15}H]^-$ contain rare interstitial hydrogens. The neutron diffraction study on its $[N(P(C_6H_5)_3)_2]^+$ salt indicates that the H atom is located at the center of the Co_6 octahedron [1416]. The same conclusion has been reached by the inelastic neutron scattering (INS) study of the Cs^+ salt since it revealed the presence of a single ν(CoH) (triply degenerate) at 1056 cm^{-1} [1417]. Figure 1.91 shows the low-temperature IR spectra of its K^+ salt obtained by Stanghellini and Longoni [1418]. It is seen that two bands at 1086 and 949 cm^{-1} are shifted to 772 and 677 cm^{-1}, respectively, by H/D substitution. Possible reasons for the observed splitting have been discussed by these workers. Corbett et al. [1419] observed two INS bands at 790 and 480 cm^{-1} for $Li_6[Zr_6Cl_{18}H]$ at ~15 K, and assigned them to the E and A_1 vibrations, respectively, of the interstitial hydrogen at the trigonal ($\mathbf{C}_{3v}$) site within the octahedral Zr_6 cluster.

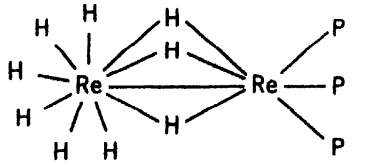

I. $[Re_2\ (\mu\text{–}H)_3\ H_6\ (triphos)]^-$ (Ref. 1413)

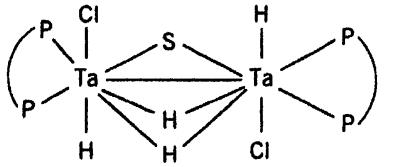

II. $[\{(i\text{–}Pr)_2\ P(CH_2)_3\ P(i\text{–}Pr)_2\}\ TaHCl]_2\ (\mu\text{–}S)(\mu\text{–}H)_2$ (Ref. 1414)

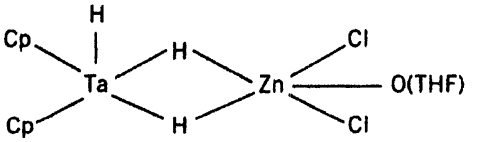

III. $(Cp)_2\ TaH\ (\mu\text{–}H)_2\ ZnCl_2\ THF$ (Ref. 1415)

Fig. 1.90. *Structures of complexes containing both terminal and bridging hydrido groups.*

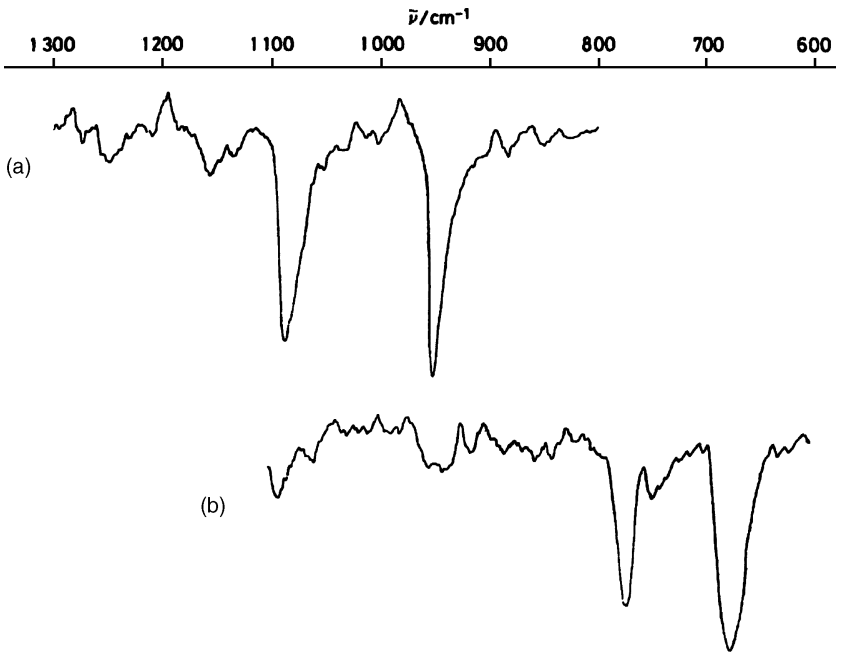

Fig. 1.91. *Infrared spectra of* (a) *$K[Co_6(CO)_{15}H]$ and* (b) *$K[Co_6(CO)_{15}D]$ in Nujol mull at ~110 K [1418].*

There are several metal hydrides of simple composition, and complete band assignments were based on their symmetries. These include $Mg_2[CoH_5](\mathbf{C}_{4v})$ [1420] and $K_2[PdH_4](\mathbf{D}_{4h})$ [1421].

1.24.3. Metal–Hydrogen Complexes in Inert Gas Matrices

Using methods similar to those described in Sec. 1.18.6, many metal–hydrogen complexes have been synthesized via matrix cocondensation reactions. Andrews and coworkers synthesized a number of novel metal–hydrogen complexes, and elucidated their structures and assigned their IR spectra on the basis of DFT calculations. Their results are summarized by Andrews [1422]. For example, the reactions of laser-ablated Mg atom vapor with H_2/Ar at 10 K produced MgH (1422), linear MgH_2 (1571.9 and 439.8), HMgMgH (1491.8), rhombic $(MgH)_2$ (1022.8 and 605.4), and the bridged species, $HMg(\mu\text{-}H)_2MgH$ (1531.0, 1164.2, 1013.7 and 613.9) [1423], where the numbers in parenthses indicate the observed frequencies in cm^{-1}.

1.25. HALOGENO COMPLEXES

Halogens (X) are the most common ligands in coordination chemistry. Several review articles [1424,1425] summarize the results of extensive infrared studies on halogeno complexes. Chapter 2 of Part A lists the vibrational frequencies of many halogeno compounds. Here the vibrational spectra of halogeno complexes containing other ligands are discussed. In most cases ν(MX) can be readily assigned by halogen or metal (isotope) substitution.

1.25.1. Terminal Metal–Halogen Bond

Terminal MX stretching bands appear in the regions of 750–500 cm^{-1} for MF, 400–200 cm^{-1} for MCl, 300–200 cm^{-1} for MBr, and 200–100 cm^{-1} for MI. According to Clark and Williams [124], the ν(MBr)/ν(MCl) and ν(MI)/ν(MCL) ratios are 0.77–0.74 and 0.65, respectively. Several factors govern ν(MX) [1426]. If other conditions are equal, ν(MX) is higher as the oxidation state of the metal is higher. Examples have already been given for tetrahedral MX_4- and octahedral MX_6-type compounds, discussed in Chapter 2 of Part A. It is interesting to note, however, that in the $[M(dias)_2Cl_2]^{n+}$ series [dias = *o*-phenylenebis(dimethylarsine)]. ν(MCl) changes rather drastically in going from Ni(III) to Ni(IV) (Fig. 1.89), while very little change is observed between Fe(III) and Fe(IV):

	d^4	d^5	d^6	d^7
	Fe(IV)	Fe(III)	Ni(IV)	Ni(III)
ν(MCl)(cm^{-1})	390	384	421	240

This was attributed to the presence of one electron in the antibonding e_g^* orbital in the Ni(III) complex [1427]. The same trend was noted for the *trans*-planar-$[NiL_2X_2]^{2+}$

TABLE 1.69. Structural Dependence of NiX Stretching Frequencies (cm^{-1})[a]

Stretching Frequency	Linear Triatomic	*trans*-Planar	*cis*-Planar	Tetrahedral	*trans*-Octahedral
ν(NiCl)	$NiCl_2$[b]	$Ni(PEt_3)_2Cl_2$[c]	Ni(DPE)Cl_2[d]	$Ni(PPh_3)_2Cl_2$[c]	$Ni(py)_4Cl_2$
	521	403	341, 328	341, 305	207
ν(NiBr)	$NiBr_2$[b]	$Ni(PEt_3)_2Br_2$[c]	Ni(DPE)Br_2[d]	$Ni(PPh_3)_2Br_2$[e]	$Ni(py)_4Br_2$
	414	338	290, 266	265, 232	140
ν(NiI)			Ni(DPE)I_2[d]	$Ni(PPh_3)_2I_2$[e]	$Ni(py)_4I_2$
			260, 212	215	105
$\frac{\nu(NiBr)}{\nu(NiCl)}$	0.80	0.84	0.83[f]	0.77[f]	0.68
$\frac{\nu(NiI)}{\nu(NiCl)}$			0.70[f]	0.67[f]	0.51

[a]DPE = l,2-bis(diphenylphosphino)ethane.
[b]Reference 1429.
[c]Reference 1430.
[d]Reference 1431.
[e]Reference 1432.
[f]This value was calculated by using average frequencies of two bands.

ion, where L is o-$C_6H_4(PMe_2)_2$ and X is Cl and Br [1428]. In the case of the bromide, the ν(Ni−Br) changes from 180 to 306 cm^{-1} in going from Ni(III) to Ni(IV).

If other conditions are equal, ν(MX) is higher as the coordination number of the metal is smaller. Table 1.69 indicates the structure dependence of ν(NiX), obtained by Saito et al. [135]. According to Wharf and Shriver [1433], the SnX stretching force constants of halogenotin compounds are approximately proportional to the oxidation number of the metal divided by the coordination number of the complex.

It is interesting to note that the ν(SnCl) of free $SnCl_3^-$ ion [289 (A_1) and 252 (E) cm^{-1}] are shifted to higher frequencies on coordination to a metal. Thus ν(SnCl) of $[Rh_2Cl_2(SnCl_3)_4]^{2-}$ are at 339 and 323 cm^{-1}. According to Shriver and Johnson [1434], the L−X force constant of the LX_n-type ligand will increase on coordination to a metal if X is significantly more electronegative than L. In the example above, chlorine is more electronegative than tin. Similar trend is reported for $[Pt(SnCl_3)_5](NBu_4)_3$ [1435]. In metal amine complexes (see Sec. 1.1), ν(NH) shifts to lower frequencies because nitrogen is more electronegative than hydrogen. As expected, the ν(GeCl) of free $GeCl_3^-$ ion [303 (A_1) and 285 (E) cm^{-1}] are also shifted to higher frequencies in [Pd(PhNC)(PPh_3)($GeCl_3$)Cl] (384 and 360 cm^{-1}) [1436].

The MX vibrations are very useful in determining the stereochemistry of the complex. Appendix V of Part A tabulates the number of infrared- and Raman-active vibrations of various MX_nY_m-type compounds. Using these tables, it is possible to determine the stereochemistry of a halogeno complex simply by counting the number of ν(MX) fundamentals observed. Examples of this method will be given in the following sections.

1.25.1.1. Square–Planar Complexes Vibrational spectra of planar $M(NH_3)_2X_2$ [M = Pt(II) and Pd(II)] were discussed in Sec. 1.l. The *trans*-isomer ($\mathbf{D}_{2h}$) exhibits one ν(MX) (B_{3u}), whereas the *cis*-isomer ($\mathbf{C}_{2v}$) exhibits two ν(MX)

(A_1 and B_2) bands in the infrared. The infrared spectra of *cis*- and *trans*-$[Pd(NH_3)_2Cl_2]$ were shown in Fig. 1.5. Similar results have been obtained for a pair of *cis*- and *trans*-$[Pt(py)_2Cl_2]$ [1437], and PtL_2X_2, where L is one of a variety of neutral ligands [1438].

In planar Pt(II) and Pd(II) complexes, ν(MX) is sensitive to the ligand *trans* to the M−X bond. Thus the effect of "*trans* influence" [1439] has been studied extensively by using infrared spectroscopy. In the $[PtCl_3L]^-$ series [1440], $\nu(PtCl_{trans})$ follows the order

L=	CO	SMe_2	C_2H_4	SEt_2	$AsEt_3$	PPh_3	PMe_3	$AsMe_3$	PEt_3
ν(PtCl) (cm^{-1})	322	> 310	~309	~307	> 280	~279	~275	~272	~271

Their order represents an increasing degree of *trans* influence, since ν(PtCl) becomes lower as a ligand of stronger *trans* influence is introduced *trans* to the Pt−Cl bond. It was found that $\nu(PtCl_{cis})$ is insensitive to the change in L. An order of *trans* influence such as

$$Cl^- < Br^- < I^- \sim CO < CH_3 < PR_3 \sim AsR_3 < H$$

was noted from the order of $\nu(M{-}Cl_{trans})$ in a series of octahedral Rh(III) and Os(III) complexes [1441].

Fujita et al. [1442] prepared two isomers of $PtCl(C_2H_4)$(L-ala), where L-ala is L-alanino anion:

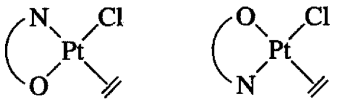

(N-isomer) I (O-isomer) II

Isomers I and II exhibit their ν(PtCl) at 360 and 340 cm^{-1}, respectively. Since the *trans* influence of the N-donor is expected to be stronger than that of the O-donor, the structures of these two isomers have been assigned as shown above.

Complexes of the type $Ni(PPh_2R)_2Br_2$ (R = alkyl) exist in two isomeric forms: tetrahedral (green) and *trans*-planar (brown). Distinction between these two can be made easily since the numbers and frequencies of infrared-active ν(NiBr) and ν(NiP) are different for each isomer. Wang et al. [1443] studied the infrared spectra of a series of compounds of this type, and confirmed that ν(NiBr) and ν(NiP) are at ~330 and ~260 cm^{-1}, respectively, for the planar form and at ~270–230 and ~200–160 cm^{-1}, respectively, for the tetrahedral form. The presence or absence of the 330-cm^{-1} band is particularly useful in distinguishing these two isomers. According to X-ray analysis [1444], the green form of $Ni(PPh_2Bz)_2Br_2$ (Bz = benzyl) is a mixture of the planar and tetrahedral molecules in a 1 : 2 ratio. Ferraro et al. [1445] studied the effect of high pressure on the infrared spectra of this compound, and found that all the bands characteristic of the tetrahedral form disappear as the pressure is increased to ~20,000 atm. This result indicates that the tetrahedral molecule can be converted to the planar form under high pressure if the energy difference between the two is relatively small. This

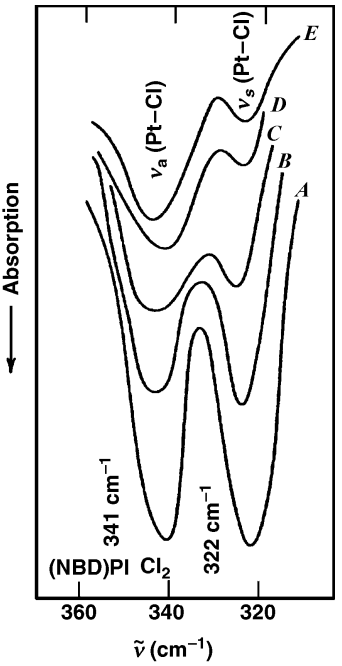

Fig. 1.92. *Effect of pressure on Pt–Cl stretching bands of Pt(NBD)Cl$_2$: (A) 1 atm; (B) 6000 atm; (C) 12,000 atm; (D) 18,000 atm; (E) 24,000 atm [1446].*

conversion is completely reversible; the original green form is recovered as the pressure is reduced. High-pressure infrared spectroscopy has also been used to distinguish symmetric and antisymmetric MX stretching vibations. For example, Fig. 1.92 shows the effect of pressure on ν_a(PtCl) and ν_s(PtCl) of Pt(NBD)Cl$_2$ (NBD = norbornadiene) [1446]. It is seen that by increasing pressure, the intensity of ν_s(PtCl) is suppressed to a greater degree than that of ν_a(PtCl). For high-pressure vibratjonal spectroscopy, see a review by Ferraro [1447,1448].

1.25.1.2. Octahedral Complexes *cis*-MX_2L_4 ($\mathbf{C}_{2v}$) should exhibit two ν(MX), while *trans*-MX_2L_4 ($\mathbf{D}_{4h}$) should give only one ν(MX) in the infrared. Thus *cis*-$[IrCl_2(py)_4]Cl$ shows two ν(IrCl) at 333 and 327 cm^{-1}, while *trans*-$[IrCl_2(py)_4]Cl$ exhibits only one ν(IrCl) at 335 cm^{-1} [124]. If MX_3L_3 is *fac* ($\mathbf{C}_{3v}$), two ν(MX) are expected in the infrared. If it is *mer* ($\mathbf{C}_{2v}$), three ν(MX) should be infrared-active. As is shown in Fig. 1.13, *fac*-$[RhCl_3(py)_3]$ gives two bands at 341 and 325 cm^{-1} and *mer*-$[RhCl_3(py)_3]$ shows three bands at 355, 322, and 295 cm^{-1}[1,124].

In MX_4L_2-type compounds, the number of IR-active ν(MX) is one for the *trans*-isomer ($\mathbf{D}_{4h}$) and four for the *cis*-isomer ($\mathbf{C}_{2v}$). For example, *trans*-$[PtCl_4(NH_3)_2]$ exhibits one ν(PtCl) at 352 cm^{-1} (with a shoulder at 346 cm^{-1}), whereas *cis*-$[ptCL_4(NH_3)_2]$ exhibits four ν(PtCl) at 353, 344, 330, and 206 cm^{-1} [1449]. Using Sn isotopes, Ohkaku and Nakamoto [1450] confirmed that *trans*-$[SnCl_4L_2]$ (L = py,

THF, etc.) exhibits one ν(SnCl) in the 342–370 cm^{-1} region, while *cis*-[$SnCl_4$(L−L)] (L−L = bipy, phen, etc.) shows four ν(SnCl) in the 340–280 cm^{-1} region. For MX_5L ($\mathbf{C}_{4v}$), one expects three ν(MX) in the infrared. The ν(InCl) of $[InCl_5(H_2O)]^{2-}$ were observed at 280, 271, and 256 cm^{-1} [1451].

1.25.2. Bridging Metal–Halogen Bond

Halogens tend to form bridges between two metal atoms. In general, bridging MX stretching frequencies [ν_b(MX)] are lower than terminal MX stretching frequencies [ν_t(MX)]. Vibrational spectra of simple M_2X_6-type ions having bridging halogens were discussed in Sec. 2.10 of Part A. Table 1.70 lists the ν_t(MX) and ν_b(MX) of bridging halogeno complexes containing other ligands.

The *trans*-planar $M_2X_4L_2$-type compounds ($\mathbf{C}_{2h}$) exhibit three infrared-active (B_u) ν(MX) modes: one $\nu(MX_t)$, and two $\nu(MX_b)$. For the latter two

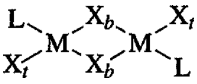

the higher-frequency band corresponds to $\nu(MX_b)$ *trans* to X, whereas the lower-frequency mode is assigned to $\nu(MX_b)$ *trans* to L since it is sensitive to the nature of L [1452]. Strong coupling is expected, however, among these modes since they belong to the same symmetry species. In the $\{[Ru(NO)(Cl)(I)_2](\mu\text{-}I)_2\}^{2-}$ ion of $\mathbf{C}_{2h}$ symmetry, the terminal ν(Ru−I) are at 214 and 208 cm^{-1} while the bridging ν(Ru−I) are at 145 and 128 cm^{-1} [1455].

TABLE 1.70. Terminal and Bridging Metal–Halogen Stretching Frequencies (cm^{-1})

Compound[a]	ν_t(MX)	ν_b(MX)	ν_b/ν_t[b]	Ref.
trans-$Pd_2Cl_4L_2$	360–339	308–294	0.86	1452
		283–241	0.75	
trans-$Pt_2Cl_4L_2$	368–347	331–317	0.91	1452
		301–257	0.78	
$Pd_2Br_4L_2$	285–265	220–185	0.74	1453
		200–165	0.66	
$Pt_2Br_4L_2$	260–235	230–210	0.89	1453
		190–175	0.74	
$Pt_2I_4L_2$	200–170	190–150	0.92	1453
		150–135	0.77	
$Ni(py)_2Cl_2$	—	193, 182	—	1454
$Ni(py)_2Br_2$	—	147	—	1454
$Co(py)_2Cl_2$				
Monomeric	347, 306	—		137
Polymeric	—	186, 174		137

[a] L = PMe_3, PEt_3, PPh_3, and so on.
[b] These values were calculated using average frequencies.

The $[Pt_3Br_{12}]^{2-}$ ion takes a structure of nearly $\mathbf{D}_{2h}$ symmetry in which two Pt(IV) Br_6 octahedra share edges with one planar Pt(II)Br_4 group:

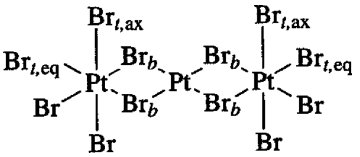

Here, subscripts ax and eq denote the axial and equatorial atoms, respectively. Figure 1.93 shows the IR and Raman spectra of $(TBA)_2[Pt_3Br_{12}]$ obtained by Hillebrecht et al. [1456]. These spectra have been assigned completely via normal coordinate analysis. Four different Pt−Br stretching force constants were necessary to distinguish the Pt(IV)−$Br_{t,eq}$, Pt(IV)–$Br_{t,ax}$, Pt(II)−Br_b, and Pt(IV)−Br_b bonds (1.75, 1.69, 1.10, and 1.05 mdyn/Å, respectively).

As discussed in Sec. 1.3.1, $Co(py)_2Cl_2$ exists in two forms: the monomeric tetrahedral (blue) and the polymeric octahedral (lilac). The $\nu(Co-Cl_b)$ of the polymer is very low relative to that of the $\nu(Co-Cl_t)$ because of an increase in coordination number and the effect of bridging [137]. Polymeric $Ni(py)_2X_2$ also exhibits $\nu(Ni-X_b)$ below 200 cm^{-1} (Table 1.68) [1454].

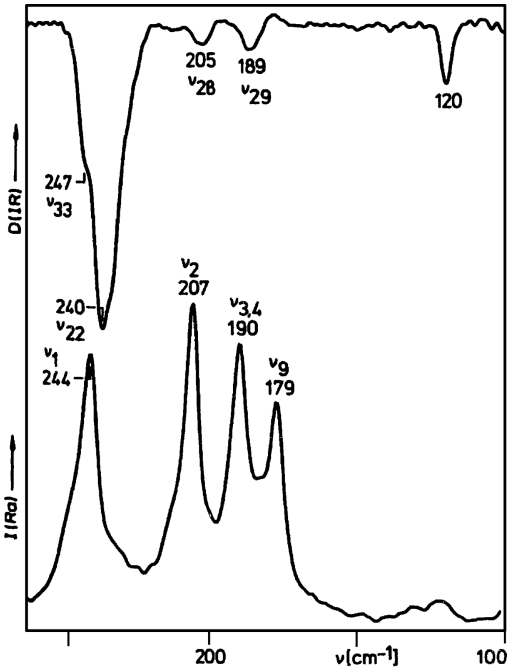

Fig. 1.93. *Infrared and Raman spectra of $(TBA)_2[Pt_3Br_{12}]$ (TBA = tetra-n-butylammonium ion) [1456].*

The mixed-valence $[Ru_2(NH_3)_6X_3]^{2+}$ ion (X = Cl, Br) contains a triple halogeno bridge:

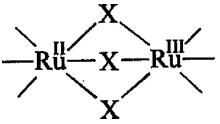

The totally symmetric ν(Ru−X) and $\delta(RuX_3)$ vibrations (310 and 145 cm^{-1} for X = Cl, and 253 and 111 cm^{-1} for X = Br, respectively) are strongly enhanced in the RR spectrum by excitation in the visible region. Armstrong et al. [1457] were able to assign the electronic transition responsible for this resonance enhancement. The mixed-valence complex ion, $[Pt_2I_8]^{2-}$, assumes a chain structure: Pt(IV)−I−Pt(II)−I−Pt(IV)−. The ν(Pt(IV)−I−Pt(II)) frequency is reported to be 120 cm^{-1} [1458].

Vibrational spectra of metal cluster ions such as $[(M_6X_8)Y_6]^{2-}$ (M = Mo,W; X = a bridging halogen; Y = a terminal halogen) and $[(M_6X_{12})Y_6]^{n-}$ (M = Nb, Ta) are discussed in Sec. 2.12 of Part A. The low-frequency spectra of these compounds are difficult to assign empirically because of strong vibrational couplings among the ν(M−X), ν(M−Y), ν(M−M), and bending modes. Finally, matrix cocondensation reactions such as

$$Al + X_2 \rightarrow AlX_n + Al_2X_6$$

(where X = F,Cl,Br, I; n = 1–3) were carried out and their IR spectra assigned by Hassanzadeh et al. [1459].

1.26. COMPLEXES CONTAINING METAL–METAL BONDS

A large number of complexes containing metal–metal (M−M) bonds are known, and their vibrational spectra have been reviewed extensively [1460–1464]. In Part A, we reviewed the vibrational spectra of the X_2Y_6-, X_2Y_8-, and X_2Y_{10}-type compounds containing M−M bonds (Secs. 2.10, 2.11) and metal clusters containing halogeno bridges (Sec. 2.12). In this section, we discuss other complexes containing M−M bonds.

In general, ν(MM) appear in the low-frequency region (250–100 cm^{-1}) because the M−M bonds are relatively weak and the masses of metals are relatively large. However, the ν(MM) of some complexes are as high as 400 cm^{-1} owing to the multiple-bond character of their M−M bonds. If the dinuclear complex is centrosymmetric with respect to the M−M bond, the ν(MM) is forbidden in IR. However, the ν(M−M′) of a heteronuclear complex is allowed in IR spectra. In contrast, Raman spectroscopy has distinct advantages in that both ν(MM) and ν(MM′) appear strongly since large changes in polarizabilities are expected as a result of stretching covalent M−M(M′) bonds. As shown in Sec. 2.11 of Part A, a long series of overtones of ν(MM) can be observed under resonance conditions. Special caution must be taken, however, in measuring Raman spectra of metal–metal bonded compounds since they may

TABLE 1.71. Metal–Metal Bond Stretching Frequencies (cm^{-1})

Complex	ν(M−M)	Ref.
$[Ag_2(\mu\text{-dcpm})]^{2+,a}$	80	1465
$[Au^{I}_2(dcpm)_2]^{2+,a}$	88	1466
$[Au^{I}_2(CS_3)_2]^{2-}$	116	1467
$[Ir^{II}(py)(Pc^{2-})]_2$	135	1468
$[(NC)_5Pt\text{-}Tl(CN)_3]^{3-}$	159	1469
$[(NC)_5Pt\text{-}Tl(phen)_2]$	172	1470
$[Pt(bipy)_2][Pt(CN)_4]$	54	1471
$Hg^{I}_2(SCN)_2$	179.158	1472

[a]dcpm = bis(dicyclohexylphosphine)methane.

undergo thermal and/or photochemical decomposition on laser irradiation. Table 1.71 lists the ν(M−M) of metal complexes containing relatively weak metal–metal bonds.

1.26.1. Compounds Containing Metal–Metal Multiple Bonds

A number of compounds containing unusually short M−M bonds exhibit unusually high ν(MM). For example, the Mo−Mo distance of $Mo_2(OAc)_4$ is only 2.09 Å and its ν(MM) is at 406 cm^{-1}. According to Cotton [1473], this Mo−Mo bond consists of one σ-bond, two π-bonds, and a δ-bond (bond order 4). Such a quadruple bond is also expected for $[Re_2Cl_8]^{2-}$, which exhibits the ν(ReRe) at 272 cm^{-1} with an Re−Re distance of 2.22 Å [1474,1475]. Table 1.72 lists ν(MM) of typical compounds. It is seen that the ν(MM) of dimolybdenum compounds of bond order 4 scatter over a wide range.

TABLE 1.72. Bond Orders, Bond Distances, and Stretching Frequencies (cm^{-1}) of Metal–Metal Multiply Bonded Compounds

Compound	Bond Order	Bond Distance	ν(MM)	Ref.
$Mo_2(O_2CCH_3)_4$	4	2.09	406	1476,1477
$Mo_2(O_2CCF_3)_4$	4	2.09	397	1478
$Mo_2(O_2CCF_3)_4(py)_2$	4	2.22	367	1478
$K_4[Mo_2Cl_8]\cdot 2H_2O$	4	2.14	345	1478
$K_3[Mo_2(SO_4)_4]\cdot 3.5H_2O$	3.5	2.16	386	1479
			373	
$Re_2(O_2CCH_3)_4Cl_2$	4	2.24	289	1476
$[Bu_4N]_2[Re_2Cl_8]$	4	2.22	272	1474
$Re_2Cl_5(DTH)_2$[a]	3	2.29	267	1476
$Re_2OCl_5(O_2CCH_2CH_3)_2(PPh_3)_2$	2	2.52	216	1476
$Re_2(CO)_{10}$	1	3.02	122	1476
$W_2(O_2C\text{−}t\text{-}Bu)_4(PPh_3)_2$	4	2.22	287	1480
$Os_2(O_2CCH_3)_4Cl_2$	3	2.31	229	1481
$Rh_2(O_2CCH_3)_4(PPh_3)_2$	4	2.45	289	1482,1483
$Rh_2(O_2CCH_3)_4(AsPh_3)_2$	4	2.43	298	1484
$Rh_2(O_2CCH_3)_4(SbPh_3)_2$	4	2.42	306	1484
$Rh_2(OSC\text{−}CH_3)_4(PPh_3)_2$	4	—	226	1485

[a]DTH = 2,5-dithiahexane.

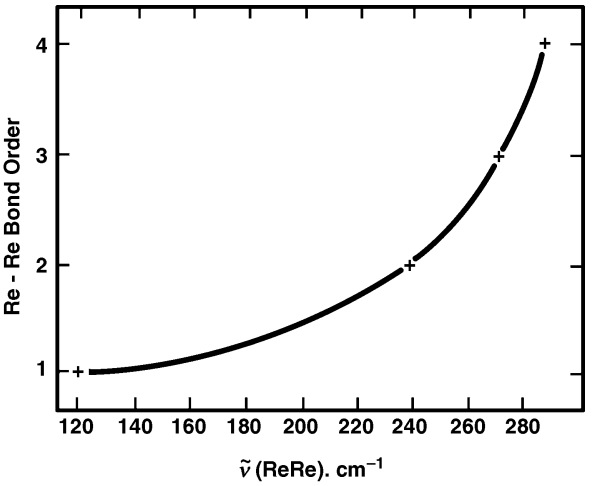

Fig. 1.94. *ν(Re–Re) versus Re–Re bond order.*

In contrast, dirhenium compounds exhibit a nice ν(MM)–bond order relationship as demonstrated by Fig. 1.94.

Thus far, the highest ν(MM) reported is 411 cm^{-1} for $[Mo_2(CN)_8]^{4-}$ [1486,1487]. Littrell et al. [1488] noted that only the band at 369 cm^{-1} of $Mo_2(CH_2SiMe_3)_6$ is shifted to 299 cm^{-1} when the Mo atom is replaced by W atom (Raman). This provides definitive support for assigning them to the ν(MM). Mixed-valence complexes such as $Ru^{II}\,Ru^{III}(O_2C_2H_3)_4Cl$ (bond order 2 or 2.5) exhibit the ν(Ru–Ru) in the range from 329 to 347 cm^{-1} [1489].

Table 1.72 also shows that the ν(RhRh) is sensitive to the nature of the axial ligand and is downshifted by ~60 cm^{-1} when the acetato group is replaced by the thioacetato group. The ν(MoMo) of $Mo_2(O_2CCH_3)_4$ is upshifted by 9 cm^{-1} when Mo in natural abundance (mainly ^{96}Mo) is replaced by the ^{92}Mo isotope. Such a metal–isotope shift provides definitive assignment for the metal–metal vibration [1490]. Normal coordinate analyses are reported for $M_2(O_2CCH_3)_4$ and $M_2X_5^{n-}$ (M = Mo, Re; X = Cl,Br). [1491,1492]. The ν(MM) of porphyrin dimers are listed in Sec. 1.5.4.

1.26.2. Polynuclear Carbonyls

The ν(CO) of polynuclear carbonyls have been discussed in Sec. 1.17.2. Here, we discuss the ν(MM) of polynuclear carbonyls in the low-frequency region. As an example, the Raman spectra of $Mn_2(CO)_{10}$, $MnRe(CO)_{10}$, and $Re_2(CO)_{10}$ are shown in Fig. 1.95, where the ν(MM) are indicated for each compound [1493]. Risen and coworkers [1494–1496] carried out normal coordinate analyses on many dinuclear and trinuclear metal carbonyls. Table 1.73 lists the observed ν(MM) and the corresponding force constants obtained by these and other workers. It is noted that the MM stretching force constants obtained by rigorous calculations are surprisingly close to those obtained by approximate calculations considering only metal atoms. There is a

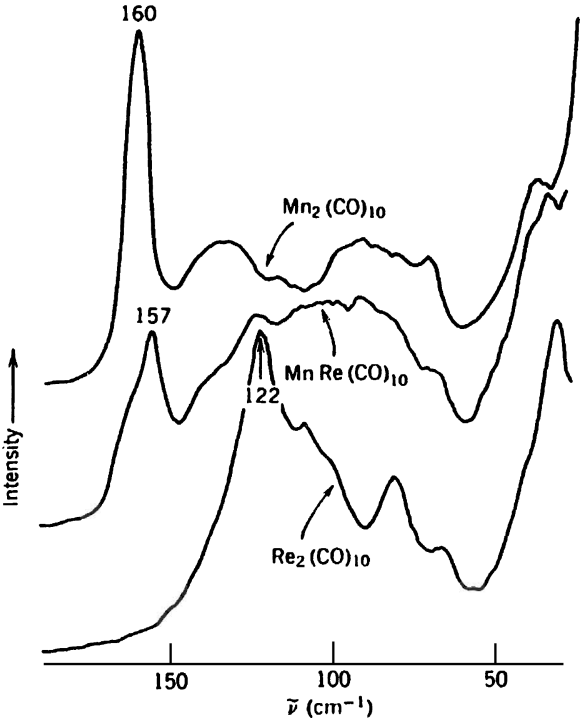

Fig. 1.95. *Low-frequency Raman spectra of polycrystalline $Mn_2(CO)_{10}$, $MnRe(CO)_{10}$, and $Re_2(CO)_{10}$ (632.8 nm excitation) [1493].*

general trend that as the MM stretching force constant increases, the ν(MM) frequency decreases in going from lighter to heavier metals in the $M_2(CO)_{10}$ (M = Mn,Tc,Re) [1493] and $[M_2(CO)_{10}]^{2-}$ (M = Cr,Mo,W) series.

In Sec. 1.18.3, we discussed the spectra of $M_2(CO)_8X_2$-type compounds (M = Mn, Tc, Re, Rh, etc.) in which the metals are bonded through halogen (X) bridges. Goggin and Goodfellow [1499] concluded, however, that the $[Pt_2(CO)_2X_4]^{2-}$ ion (X = Cl,Br) contains the direct Pt−Pt bond:

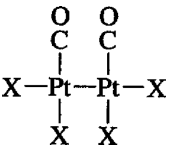

They isolated two isomers of $[N(n\text{Pr})_4]_2[Pt_2(CO)_2Cl_4]$ that differ only in the angle of rotation about the Pt−Pt bond. Both isomers exhibit ν(PtPt) at $\sim$170 cm^{-1}.

$Fe_2(CO)_9$ and $Fe_3(CO)_{12}$ exhibit very strong Raman bands at 225 and 219 cm^{-1}, respectively. San Filippo and Sniadoch [1500] assigned them to ν(FeFe). Later studies [1501] showed, however, that these bands are due to decomposition products resulting from strong laser irradiation. Thus, the appearance of strong Raman bands in the low-frequency region does not necessarily mean that they are due to ν(MM). It is also

TABLE 1.73. Metal–Metal Stretching Frequencies (cm^{-1}) and Force Constants

Compound	ν(MM)	Force Constant (mdyn/Å)		Ref.
		Rigorous Calculation	Approximate Calculation[a]	
$(CO)_5Mn-Mn(CO)_5$	160	0.59	0.41	1493
$(CO)_5Tc-Tc(CO)_5$	148	0.72	0.63	1493
$(CO)_5Re-Re(CO)_5$	122	0.82	0.82	1493
$(CO)_5Re-Mn(CO)_5$	157	0.81	0.62	1493
$(CO)_5Mn-W(CO)_5^-$	153	0.71	0.55	1494
$(CO)_5Mn-Mo(CO)_5^-$	150	0.60	0.47	1494
$(CO)_5Mn-Cr(CO)_5^-$	149	0.50	0.37	1494
$Cl_3Sn-Co(CO)_4$	204	1.23	0.97	1495
$Cl_3Ge-Co(CO)_4$	240	1.05	1.11	1495
$Cl_3Si-Co(CO)_4$	309	1.32	1.07	1495
$Br_3Ge-Co(CO)_4$	200	0.96	—	1496
$I_3Ge-Co(CO)_4$	161	0.52	—	1496
$Br_3Sn-Co(CO)_4$	182	1.05	—	1496
$I_3Sn-Co(CO)_4$	156	0.64	—	1496
$H_3Ge-Re(CO)_5$	209	—	1.34	1497
$H_3Ge-Mn(CO)_5$	219	—	0.88	1497
$H_3Ge-Co(CO)_4$	228	—	1.00	1497
$(CO)_4Co-Zn-Co(CO)_4$	170, 284[b]	1.30	—	995
$(CO)_4Co-Cd-Co(CO)_4$	163, 218[b]	1.28	—	995
$(CO)_4Co-Hg-Co(CO)_4$	163, 195[b]	1.26	—	995

[a]Calculations considering only metal atom skeletons.
[b]Under $\mathbf{D}_{3d}$ symmetry, these frequencies correspond to the A_{1g} (symmetric) and A_{2u} (antisymmetric) MCo stretching modes, respectively.

noted that $Re_2(CO)_8X_2$ (X = Cl,Br), which does not contain Re−Re bonds, shows strong Raman bands at 125 cm^{-1} where ν(ReRe) of $Re_2(CO)_{10}$ appears [1501]. Cooper et al. [1502] were able to locate the ν(MM) of $Fe_2(CO)_9$ and $Fe_3(CO)_{12}$ at 260 and at 240 and 176 cm^{-1}, respectively. These assignments are based on the ^{54}Fe–^{56}Fe isotopic shifts observed in Raman spectra at ~10 K. Onaka and Shriver [1503] observed three ν(MM) bands at 235, 185, and 159 cm^{-1} in acetone solution of $Co_2(CO)_8$ that correspond to the three isomers discussed in Sec. 1.18.2. They have shown that the ν(MM) is higher than 200 cm^{-1} for bridging carbonyls and between 190 and 140 cm^{-1} for single-bonded nonbridged complexes. The RR band at 225 cm^{-1} of $[Cp(CO)Fe]_2(\mu\text{-}CO)_2$ results from strong vibrational coupling between the ν(Fe−Fe) and Fe-(μ-CO) breathing modes [1504].

Trinuclear complexes such as $Ru_3(CO)_{12}$ and $Os_3(CO)_{12}$ contain a triangular M_3 skeleton for which two ν(MM) are expected under $\mathbf{D}_{3h}$ symmetry. Quicksall and Spiro [985] assigned the Raman bands at 185 and 149 cm^{-1} of the Ru complex to ν(RuRu) of the A_1' and E' species, respectively. The latter is coupled with other modes. The corresponding RuRu stretching force constant is 0.82 mdyn/Å. Kettle and co-workers [1505,1506] have assigned the ν(MM) of the $[Os_xRu_{3-x}(CO)_{12}]$- ($x = 0,1,2,3$)-type complexes. In $Mn_3H_3(CO)_{12}$, Martin et al. [1507] assigned the ν(MnMn) at 163 (A'_1) and 146 cm^{-1} (E') and obtained the stretching force constant, K(Mn−Mn) of 0.37

mdyn/Å with the interaction constant of −0.08 *K*. On the other hand, Jayasooriya and Skinner [1508] assigned the RR bands at 198 (A'_1) and 164 cm^{-1} (E') to the ν(MnMn), and obtained *K*(Mn−Mn) of 0.553 mdyn/Å with the interaction constant of −0.055 mdyn/Å. In $Re_3H_3(CO)_{12}$, the ν(ReRe) were observed at 126 (A'_1) and 116/103 cm^1(E') in the matrix-isolated IR spectrum [1509]. Kettle et al. [1510] carried out a detailed study on the IR and Raman spectra of the $Fe_3EE'(CO)_9$ (E,E′ = S,Se,Te)-type complexes in the low-frequency region. These polynuclear complexes take pseudotrigonal–bipyramidal structures with two E(E′) atoms at axial positions, and they noted vibrational coupling between ν(Fe−Fe) and ν(Fe−Te) modes.

Quicksall and Spiro [1511] assigned the Raman spectrum of $Ir_4(CO)_{12}$, which consists of a tetrahedral Ir skeleton; three ν(IrIr) bands were assigned at 207 (A_1), 161 (F_2), and 131 (E) cm^{-1}. The ratio of these three frequencies, 2 : 1.56 : 1.27, is far from that predicted by a "simple cluster model" (2:$\sqrt{2}$:1) [1512], indicating the substantial coupling between the individual stretching modes. Their rigorous calculations gave *K*(Ir−Ir) of 1.69 mdyn/Å, together with interaction constants of −0.13 and +0.13 mdyn/Å for the adjacent and opposite Ir−Ir bonds, respectively. The ν(MM) of $Rh_4(CO)_{12}$ [1513] and $Co_4(CO)_{12}$ [1514] have been assigned and the corresponding force constants calculated [1514]. As mentioned in Sec. 1.18.5, the M_4 skeleton of $M_4H_4(CO)_{12}$ (M = Ru,Os) take $\mathbf{D}_{2d}$ symmetry. Then, the six $(3 \times 4 - 6)$ normal vibrations are classified into $2A_1(R) + B_1(R) + B_2(IR, R) + E(IR, R)$. Kettle and Stanghellini [1515] have made complete assignments of these modes.

1.26.3. Metal Cluster Compounds

Vibrational spectra of metal clusters including $[(M_6X_8)Y_6]^{2-}$ (M = Mo,W) and $[(M_6X_{12})Y_6]^{n-}$ (M = Nb,Ta), where X and Y are bridging and terminal halogens, respectively, have been discussed in Sec. 2.12 of Part A. The ν(MM) are also reported for metal clusters of other types. In the mixed-valence ion, $[Pt_4(NH_3)_8(C_5H_4NO)_4]^{5+}$, shown in Fig. 1.96a, the intradimer (Pt_1-Pt_2) and interdimer (Pt_2-Pt_2) distances are 2.774 and 2.87 Å, respectively. Correspondingly, the $\nu(Pt_1-Pt_2)$ and $\nu(Pt_2-Pt_2)$ are observed at 149 and 69 cm^{-1}, respectively, in RR spectra [1516]. $Pt_2(EtCS_2)_4I$ ($EtCS_2^-$ = dithiopropanoic acid anion) is a one-dimensional halogeno-bridged polymer consisting of a −Pt−Pt−I−Pt−Pt−I− chain with an average valence state of Pt at +2.5. It exhibits the ν(Pt−Pt) at 74 cm^{-1} in Raman spectra [1517].

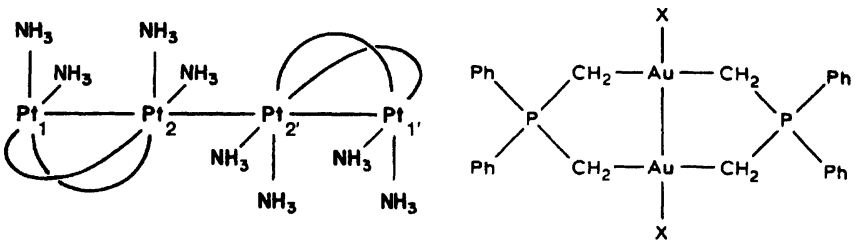

Fig. 1.96. *Structures of metal–metal bonded complex ions:* (a) $[Pt_4(NH_3)_8(C_5H_4NO)_4]^{5+}$ *(the curves indicate α-pyridonate bridges);* (b) $[Au(CH_2)_2PPh_2]_2X_2$.

The ν(PtPt) of the SO_4 bridged complex, $[Pt_2(SO_4)_4\ (H_2O)L]^{n-}$ (n = 2 or 3) is sensitive to the nature of the axial ligand (L = H_2O, OH^- and Cl^-) [1518]. Sensitivity of the ν(AuAu) to the nature of the *trans* ligand is seen in the series of $[Au(CH_2)_2PPh_2]_2X_2$ shown in Fig. 1.96b; 162, 132, and 103 cm^{-1}, respectively, for X = Cl, Br, and I [1519]. Two isomers of triangular phosphido-bridged $Pt_3(\mu\text{-}PPh_2)_3(Ph)(PPh_3)_2$ have been isolated. Their differences are in the Pt−Pt distances and Pt−(μ-PPh_2)−Pt angles. Both isomers exhibit the ν(Pt−Pt) in the range from 122 to 96 cm^{-1} [1520].

1.26.4. Metal–Metal Stretching Vibrations of Electronic Excited States

Using TR^3 spectroscopy (Sec. 1.4.2), it is possible to measure the ν(MM) of electronic excited states. As mentioned in Sec. 2.11.2 of Part A, the ν(ReRe) of die $[Re_2Cl_8]^{2-}$ ion at 275 cm^{-1} in the ground state $[(d\delta)^2, {}^1A_g]$ is shifted to 204 cm^{-1} in the excited state $[(d\delta)(d\delta^*], {}^1A_{2u}]$ since an electron is promoted from a bonding ($d\delta$) to an antibonding ($d\delta^*$) orbital [1521]. An opposite trend prevails when an electron is promoted from an antibonding to a bonding or less antibonding orbital. As an example, Figure 1.97 shows the RR spectra of the $[Rh_2b_4]^{2+}$ ion (b = 1,3-diisocyanopropane) in the electronic ground

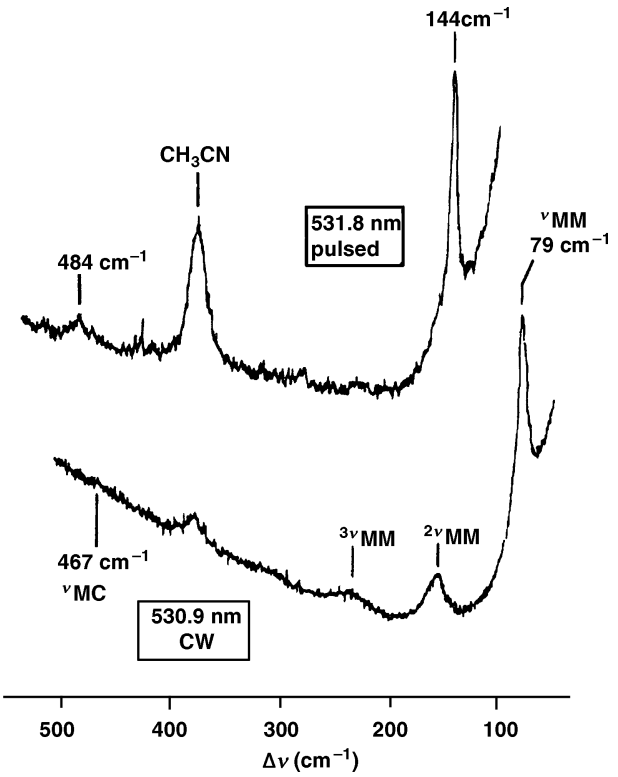

Fig. 1.97. *Lower trace—ground-state RR spectrum of the $[Rh_2b_4]^{2+}$ ion obtained by CW excitation at 530.9 nm; upper trace—excited-state RR spectrum obtained by pulsed-laser excitation at 531.8 nm [1522].*

$[(d\sigma^*)^2, {}^1A_{1g}]$ and excited $[(d\sigma^*)(p\sigma), {}^3A_{2u}]$ states obtained by Dallinger et al. [1522]. It is seen that the ν(RhRh) at 79 cm^{-1} in the ground state is upshifted to 144 cm^{-1} in the excited state. Correspondingly, the Rh−Rh stretching force constant in the ground state (0.19 mdyn/Å) is increased ~3 times (0.63 mdyn/Å) by this electronic excitation.

Similar results are reported for $[Rh_2(TMB)_4]^{2+}$(TMB = 2,5-dimethyl-2,5-diisocycano hexane); ν(RhRh) are at 50 and 151 cm^{-1}, respectively, in the ground and excited triplet states [1523]. In the case of the $[Rh_2(dimen)_4]^{2+}$ ion (dimen = 1,8-diisocyanomenthane), the Rh−Rh distance is very long (4.48 Å) in the ground state, and its ν(RhRh) frequency is very low (28 cm^{-1}). However, the lowest electronic excitation ($d\sigma^* \rightarrow p\sigma$) produces an excited state with a much shorter Rh−Rh distance (3.2 Å) although the ν(RhRh) band could not be observed because of its subnanosecond lifetime [1524]. The ν(AuAu) vibrations of $[Au_2(dmpm)_2]^{2+}$ [dmpm = bis(dimethylphosphine)methane] are observed at 79 and 165 cm^{-1}, respectively, for the ground and the first electronic excited states [1525]. In the $[Pt_2(pop)_4]^{4-}$ ion [pop = $(P_2O_5H_2)^{2-}$ ion], the ν(PtPt) at 118 cm^{-1} in the ground state is upshifted to 156 cm^{-1} when an electron is promoted from the $d\sigma^*$ to the $p\sigma$ orbital [1526]. Similar trends are observed for M_2(dppm) [M = Pd, Pt; dppm = bis(diphenylphosphino) methane] [1527]. For more details, see a review by Morris and Woodruff [1528].

1.27. COMPLEXES OF PHOSPHORUS AND ARSENIC LIGANDS

Ligands such as phosphines (PR_3) and arsines (AsR_3) (R = alkyl, aryl, halogen, etc.) form complexes with a variety of metals in various oxidation states. Vibrational spectroscopy has been used extensively to determine the structures of these compounds and to discuss the nature of the metal–ligand bonding.

1.27.1. Complexes of Phosphorus Ligands

Vibrational frequencies of pyramidal XY_3-type ligands such as PH_3, PF_3, and their halogeno analogs are found in Sec. 2.3 of Part A. The most simple phosphine ligand is PH_3. The vibrational spectra of $Ni(PH_3)_4$ [1529], $Ni(PH_3)(CO)_3$ [1530], and $Ni(PH_3)(PF_3)_3$ [1531] have been reported by Bigorgne and coworkers. All these compounds exhibit ν(PH), $\delta(PH_3)$, and ν(NiP) at 2370–2300, 1120–1000, and 340–295 cm^{-1}, respectively. A series of the $Ni(PH_3)_{n-}$ (n = 1–4)-type complexes have been prepared by matrix cocondensation reactions, and their ν(Ni−P) have been assigned at 390–395 cm^{-1} [1532]. Complete assignments based on normal coordinate calculations have been made on $Ni(P(CH_3)_3)_4$ [1533]. The A_1 and F_2 ν(Ni−P) vibrations of this compound have been assigned at 296 and 343 cm^{-1}, respectively.

Trifluorophosphine (PF_3) forms a variety of complexes with transition metals. According to Kruck [1534], the ν(PF) of free PF_3 (892, 860 cm^{-1}) are shifted slightly to higher frequencies (960–850 cm^{-1}) in $M(PF_3)_n$ (n = 4,5,6) and $HM(PF_3)_4$ and to lower frequencies (850–750 cm^{-1}) in $[M(PF_3)_4]^-$ (M = Co,Rh,Ir). These results have been explained by assuming that the P−F bond possesses a partial double-bond character that is governed by the oxidation state of the metal. For individual compounds, only references are cited: $M(PF_3)_4$ (M = Ni,Pd,Pt) [1535], $M(PF_3)_5$

[1536], $V(PF_3)_6$ [1537], $Au(PF_3)Cl$ [1538], and *cis*-$MH_2(PF_3)_4$ (M = Fe,Ru,Os) [1539]. The $\delta(PF_3)$ and ν(MP) of some of these compounds are assigned at 590–280 and 250–180 cm^{-1}, respectively. Bénazeth et al. [1540] showed that the skeletal symmetry of $HCo(PF_3)_4$ is $\mathbf{C}_{3v}$, while that of $[Co(PF_3)_4]^-$ is $\mathbf{T}_d$. The ν(CoP) of these compounds are at 250–210 cm^{-1}. Woodward and coworkers [1541] carried out complete vibrational analyses of the $M(PF_3)_4$ (M = Ni,Pd,Pt) series. Their results show the following trends:

		$Ni(PF_3)_4$	$Pd(PF_3)_4$	$Pt(PF_3)_4$
ν(MP) (cm^{-1})	A_1	195	204	213
	F_2	219	222	219
K(M−P) (mdyn/Å)		2.71	3.17	3.82

For the $Ni(PX_3)_4$ (X = a halogen) series, Edwards et al. obtained the following:

		$Ni(PF_3)_4$	$Ni(PCl_3)_4$ [1542]	$Ni(PBr_3)_4$ [1543]	$Ni(PI_3)_4$ [1544]
ν(MP) (cm^{-1})	A_1	195	135	78	(55)
	F_2	219	208	193	184
K(M−P) (mdyn/Å)		2.71	2.35	2.05	—

The ν(NiP) of $Ni(PMe_3)_4$ arc observed at 182 (A_1,) and 197 cm^{-1} (F_2) [1545]. The ν(AuP) of $Au(PMe_3)X$ are observed at 220, 209, and 219 cm^{-1}, respectively, for X = Cl,Br,I [1546]. In general, it is more difficult to assign the ν(MP) of alkyl and phenyl phosphine complexes than those of halogeno phosphine complexes because the former ligands exhibit many internal modes in the region where the ν(MP) are expected to appear. To overcome this difficulty, Shobatake and Nakamoto [1430] utilized the metal isotope technique (Sec. 1.17 of Part A).

Figure 1.98 shows the infrared spectra of *trans*-$[^{58,62}Ni(PEt_3)_2X_2]$ (X = Cl,Br), and Table 1.74 lists the observed frequencies, metal isotope shifts, and band assignments. It is clear that the ν(NiP) of these complexes must be assigned near 270 cm^{-1}, in contrast to previous investigations, which placed these vibrations near 450–410 cm^{-1} [1453,1547–1549].

Triphenylphosphine (PPh_3) is most common among phosphine ligands. It is not simple, however, to assign the ν(MP) of PPh_3 complexes since PPh_3 exhibits a number of ligand vibrations in the low-frequency region [1550–1552]. Using the metal isotope technique, Nakamoto and a colleague [1430] showed that tetrahedral $Ni(PPh_3)_2Cl_2$, for example, exhibits two ν(NiP) at 189.6 and 164.0 cm^{-1}, in agreement with the result of previous workers [1553]. The ν(MP) of $M(PPh_3)_3Cl$ [M = Cu(I), Co(I)] are located in the range from 233 to 219 cm^{-1} [1554]. In $Rh(PPh_3)_3Cl$, the ν(RhP) (550, 465, and 460 cm^{-1}) are higher than those of other ν(MP). This has been attributed to the effect of the Rh($d\pi$)–P($p\pi$) bonding and the delocalization of the phenyl ring charge through the Rh and P atoms [1555].

As stated in Sec. 1.25.1, complexes of the type $Ni(PPh_2R)_2Br_2$ (R = alkyl) exist in two forms (tetrahedral and square–planar), which can be distinguished by the ν(NiBr) and ν(NiP) [1443]. For R = Et, the ν(NiP) of the planar complex is at 243 cm^{-1},

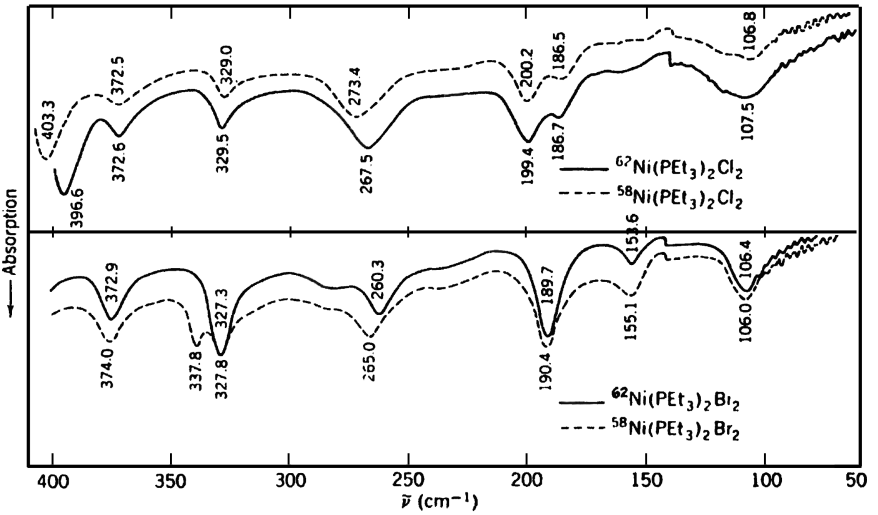

Fig. 1.98. *Far-IR spectra of $^{58}NiX_2(PEt_3)_2$ and its ^{62}Ni analogs (X = Cl,Br) [1430].*

whereas these vibrations are at 195 and 182 cm^{-1} in the tetrahedral complex. Udovich et al. [1431] studied the infrared spectra of Ni(DPE)X_2, where DPE is 1,2-bis (diphenylphosphino)ethane and X is Cl, Br, and I, by using the metal isotope technique. It was found that the ν(NiX) are always lower and ν(NiP) are always higher in the *cis*-Ni(DPE)X_2 than in the corresponding *trans*-Ni$(PEt_3)_2X_2$. This difference has been attributed to the strong *trans* influence of phosphine ligands.

A number of investigators have discussed the nature of the M−P bonding on the basis of electronic, vibrational, and NMR spectra [1556], and controversy has arisen about the degree of π-backbonding in the M−P bond. For example, Park and Hendra

TABLE 1.74. Infrared Frequencies, Isotopic Shifts, and Band Assignments of $NiX_2(PEt_3)_2$ (X = Cl and Br) (cm^{-1}) [1430]

	$^{58}NiCl_2(PEt_3)_2$			$^{58}NiBr_2(PEt_3)_2$		
PEt_3 ν	ν	$\Delta\nu^a$		ν	$\Delta\nu^a$	Assignment[b]
408	416.7	0.0		413.6	1.2	δ(CCP)
—	403.3	6.7		337.8	10.5[c]	ν(NiX)
365	372.5	−0.1		374.0	1.1	δ(CCP)
330	329.0	−0.5		327.8	0.5[c]	δ(CCP)
—	273.4	5.9	4.7	265.0		ν(NiP)
245	(hidden)			(hidden)		δ(CCP)
	200.2	0.8		190.4	0.7	δ(CPC)
	186.2	−0.2		155.1	1.5	δ(NiX)
	161.5	−0.5		(hidden)		δ(NiP)

[a] $\Delta\nu$ indicates metal-isotope shift, $\nu(^{58}Ni)-\nu(^{62}Ni)$.
[b] Ligand vibrations were assigned according to Ref. 1549.
[c] Since these two bands are overlapped (Fig. 1.98), $\Delta\nu$ values are only approximate.

[1557] suggest the presence of a considerable degree of π-bonding in square–planar Pd(II) and Pt(II) complexes of PMe_3 and $AsMe_3$. On the other hand, Venanzi [1558] claims from NMR evidence that the Pt–P π-bonding is much less than originally predicted [1559]. It is rather difficult, however, to discuss the degree of π-bonding from vibrational spectra alone since the MP stretching frequency and force constant are determined by the net effect, which involves both σ- and π-bonding.

1.27.2. Complexes of Arsenic Ligands

Complexes of the type $M(CO)_5L$, where L is arsine (AsH_3) and stibine (SbH_3) and M is Cr, Mo, and W, have been prepared by Fischer et al. [1560]. ν(AsH) and $\delta(AsH_3)$ are near 2200 and 900 cm^{-1}, respectively. Complexes of trimethylarsine ($AsMe_3$) have been studied by several investigators. Goodfellow et al. [1561] and Park and Hendra [1557] measured the infrared spectra of $M(AsMe_3)_2X_2$- (M = Pt,Pd; X = Cl,Br,I)-type complexes and assigned ν(MAs) in the 300–260 cm^{-1} region. The latter workers assigned ν(MSb) of analogous alkylstibine complexes at $\sim$200 cm^{-1}. Konya and Nakamoto [1427] assigned ν(MAs) and ν(MX) of $[M(dias)_2]^{2+}$- and $[M(dias)_2X_2]Y_n$-type complexes by using the metal isotope technique. Figure 1.99 shows the infrared spectra of $[^{58}Ni(dias)_2X_2]X$ and $[^{58}Ni(dias)_2X_2](ClO_4)_2$ (X = Cl,Br) and their ^{62}Ni analogs. Their results show that the ν(MAs) are very weak and appear at 325–295 cm^{-1} for the Ni, Co, and Fe complexes and at 270–210 cm^{-1} for the Pd and Pt complexes. For the ν(MX) of these complexes, see Sec. 1.25.

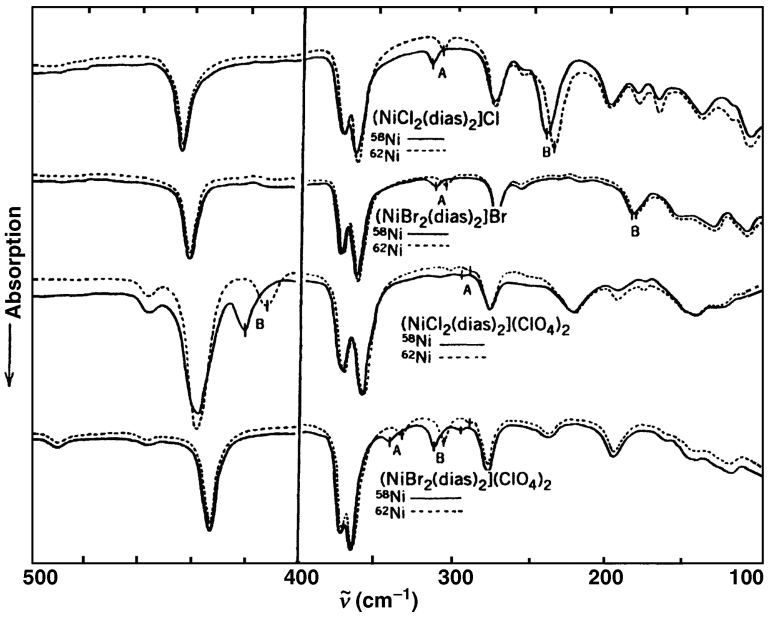

Fig. 1.99. *Far-IR spectra of octahedral nickel dias complexes; vertical lines marked by A and B indicate Ni–As and Ni–X stretching bands, respectively [1427].*

Tertiary phosphine oxides and arsine oxides coordinate to a metal through their O atoms. The ν(P=O) of triphenylphosphine oxide (TPPO) at 1193 cm^{-1} is shifted by $\sim$35 cm^{-1} to a lower frequency when it coordinates to Zn(II) [1562]. The shift is much larger in $MX_4(TPPO)_2$ (160–120 cm^{-1}), where MX_4 is a tetrahalide of Pa, Np, and Pu [1563]. A similar observation has been made for ν(As=O) of arsine oxide and its complexes. Exceptions to this rule are found in $MnX_2(Ph_3AsO)_2$ (X = Cl,Br); their ν(As=O) are higher by 30–20 cm^{-1} than the frequency of the free ligand (880 cm^{-1}) [1564]. Rodley et al. [1565] have assigned the ν(MO) of tertiary arsine oxide complexes at 440–370 cm^{-1}.

1.28. COMPLEXES OF SULFUR AND SELENIUM LIGANDS

A large number of metal complexes of ligands containing sulfur and selenium are known. Here the vibrational spectra of typical compounds are reviewed briefly. For SO_3 and thiourea complexes that form metal–sulfur bonds, see Secs. 1.13 and 1.15, respectively.

1.28.1. Complexes of S_n and Se_n ($n = 2$–6)

According to Müller et al. [1566], most complexes containing the S_2^{2-} ligand take the following structures:

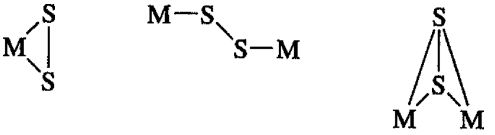

I II (*cis/trans*) III

The $\nu(S_2)$ of free S_2 is 623 cm^{-1} (Table 2.1b of Part A). On coordination, the $\nu(S_2)$ is shifted to 560–510 cm^{-1} in structures I (η^2-S_2) and III {(μ-S)(μ-S)}, and to 510–480 cm^{-1} in structure II(μ-S_2). It is rather difficult, however, to distinguish these structures by vibrational spectroscopy. An extensive compilation of structural and vibrational data of disulfur complexes is found in a review by Müller et al. [1566]. Here, some references for various types of coordination and $\nu(S_2)$ are given: $MoO(S_2)_2$(bipy) (I, 540 cm^{-1}) [1567], Ti(TPP)(S_2) (I, 551 cm^{-1}) [1568], and $Co_2(CO)_6(S_2)$ (III, 615 cm^{-1}). The $\nu(S_2)$ of the last compound is unusually high because the S−S bond is unusually short (1.98 Å) [1569]. The $Mo_3S_{13}^{2-}$ ion contains three type I and three type II S_2 ligands and one bridging S atom, and their $\nu(S_2)$ have been assigned using $^{92}Mo/^{100}Mo$ and $^{32}S/^{34}S$ isotope shift data [1570]. The $\nu(Se_2)$ of the free Se_2^{2-} ion is at 349 cm^{-1}, and this band is shifted to 310 cm^{-1} in [Ir(Se_2)(DME)$_2$]Cl [DME = 1,2-bis(dimethylphosphino)ethane] [1571]. In general, the ν(M−S) and

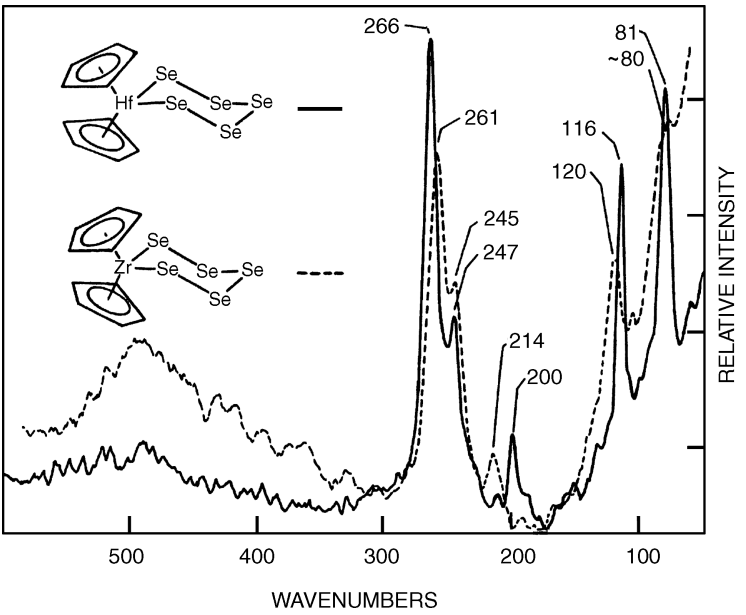

Fig. 1.100. *Raman spectra of solid Cp_2MSe_5 (M = Hf,Zr) in the 600–50 cm^{-1} region (514.5 nm excitation) [1576].*

ν(M−Se) are more difficult to assign empirically; the former is in the 380–300 cm^{-1} region and the latter is lower.

Although the S_n^{2-} and Se_n^{2-} ions ($n = 3$–5) take open-chain configurations in the free state (Sec. 2.18 of Part A), they tend to form chelate rings in metal complexes. The ν(SS) vibrations of the $[Cu(\eta^2\text{-}S_4)_2]^{3-}$ ion were assigned at 474 and 401 cm^{-1} [1572].

The $[M_2O_2(S_2)(S_4)]^{2-}$ (M = Mo,W) exhibits the $\nu(S_2)$ at 521–500 and 490–420 cm^{-1} for the S_2 and S_4 rings, respectively [1573]. The $\nu(Se_2)$ of the $[Zn(Se_4)_2]^{2-}$ ion are observed at 276 and 250 cm^{-1} [1574], while those of the $[Ni(Se_4)_2]^{2-}$ ion are reported to be 364 and 348 cm^{-1} [1575]. Figure 1.100 shows the Raman spectra of $Cp_2M(Se_5)$ (M = Hf and Zr) obtained by Butler et al. [1576]. The bands at 266(261), 247(245), and 200(214) cm^{-1} have been assigned to $\nu_s(Se_2)$, $\nu_a(Se_2)$, and ν(MS), respectively. Raman frequencies are reported for the $[M(S_6)_2]^{2-}$ ion, where M is Zn, Cd, and Hg [1577]. In polymeric $PdCl_2(\eta^1\text{-}Se_6)$, the Se_6 rings are connected to two $PdCl_2$ units by forming Pd−Se bonds, and the ν(Se−Se) ring vibrations are assigned at 275, 256, and 237 cm^{-1} [1578].

1.28.2. Complexes of S- and Se-Containing Ligands

The ν(NS) of N-bonded thionitrosyl (−NS) complexes such as $Cr(NS)(Cp)(CO)_2$ [1579] and $Re(NS)(PMe_2Ph)Cl_2$ [1580] are observed at 1180 cm^{-1}, which is 40 cm^{-1} lower than that of free NS molecule. The ν(NSe) of $[Os(Tp)(NSe)\ Cl_2]$

[Tp = hydro-tris(1-pyrazolyl)borate] is 1156 cm^{-1} [1581]. The ν(SO) of Ru(SO)(Cl)(NO)$(PPh_3)_2$ at 1061 cm^{-1} is 63 cm^{-1} lower than that of free SO (1124 cm^{-1}) [1582].

Thiocarbonyl (CS) may form metal complexes of the following types:

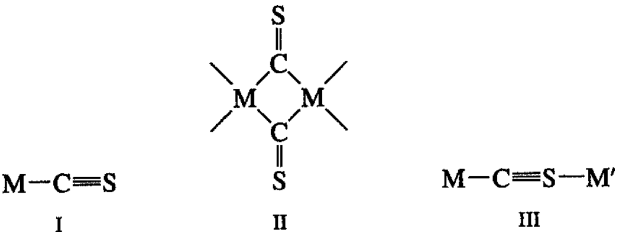

The ν(CS) of free CS is at 1285 cm^{-1}. The ν(CS) of the C-bonded terminal CS group (structure I) is higher than that of free CS (1360–1290 cm^{-1}) [1583–1585]. The C-bonded bridge structure such as shown above (structure II) was found in $[Co_2(\mu\text{-CS})(\mu\text{-}S_2C_2R_2)(CO)_3(\mu\text{-dppm})]$ [R = COOMe,COOEt; dppm = 1,2-bis(diphenylphosphino)methane]. It exhibits the ν(CS) at 1147 cm^{-1} [1586]. The bridging C- and S-bonded structure (III) was suggested for $(DPE)_2(CO)W(\mu\text{-CS})W(CO)_5$ [DPE = 1,2-(diphenylphosphino)ethane], but its ν(CS) was hidden by the DPE band near 1095 cm^{-1} [1587]. An extremely low ν(CS) (910 cm^{-1}) is reported for $Co_3Fe(Cp)(CO)_9(CS)$ in which the CS group acts as a six-electron donor to the three Co atoms [1588]. Normal coordinate analyses have been made on $M(CO)_5(CX)$ (M = Cr,W; X = S,Se) [1589] and $(C_6H_6)Cr(CO)_2(CX)$ (X = O,S,Se) [1590].

On coordination, N_2S_2 may form a chelating ring (η^2-N_2S_2) or a bridge between two metals (μ-N_2S_2, structure II):

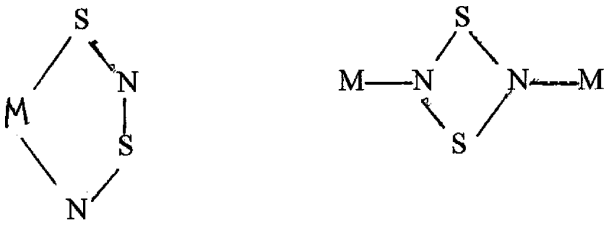

The N_2S_2 ligand in $[Pt(\eta^2\text{-}N_2S_2)(PPh_3)_2]$ forms a five-membered chelate ring (structure I), and exhibits the ν(NS) at 1045 cm^{-1} [1591]. On the other hand, the N_2S_2 ligand in the $[(VCl_5)_2(\mu\text{-}N_2S_2)]^{2-}$ ion forms a bridge between two V atoms (structure II), and exhibits the $\nu(N_2S_2)$ vibration at 858 cm^{-1} [1592].

1.28.3. Complexes of SO_2, CS_2, and Related Ligands

Sulfur dioxide (SO_2) may take one of the following structures when it coordinates to a metal:

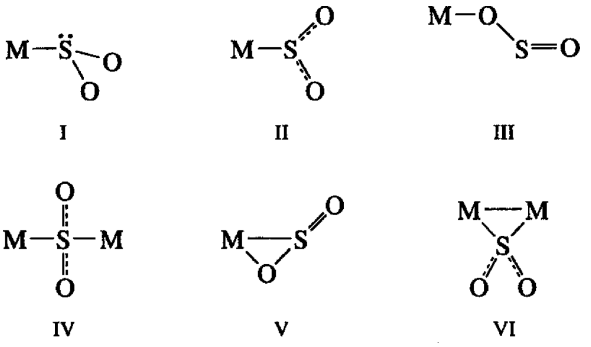

Free SO_2 exhibits the $\nu_a(SO_2)$ and $\nu_s(SO_2)$ at 1351 and 1147 cm^{-1}, respectively (Sec. 2.2 of Part A). Table 1.75 lists the modes of coordination and stretching frequencies of SO_2 complexes. It is clearly not possible to determine the coordination geometry by vibrational data. In fact, most of the structures shown in the table were determined by X-ray analysis. According to Kubas [1608], the coordination geometry of the SO_2 ligand can be deduced by combining spectroscopic and chemical properties. The SO_2 stretching frequencies are useful, however, in distinguishing the O- and S-bonded complexes; a complex is O-bonded if $(\nu_a - \nu_s)$ is larger than 190 cm^{-1}, and S-bonded if it is smaller than 190 cm^{-1} [1600].

Johnson and Dew [1609] first oberved a linkage isomerization of the SO_2 ligand in $[Ru(NH_3)_4(SO_2)Cl]Cl$ that changes from structures II to V by solid-state photolysis (365 nm, 25–195 K). The former stable isomer exhibits the ν_a and ν_b at 1255 and 1110 cm^{-1}, respectively, whereas the latter unstable isomer exhibits them at 1165 and 940 cm^{-1}, respectively. Later, Kovalevsky et al. [1610] confirmed their results by photocrystallographic and IR studies on *trans*-$[Ru(NH_3)_4(H_2O)(SO_2)](C_6H_5SO_3)_2$. In the ground state, the SO_2 ligand coordinates to the Ru as a unidentate (structure II) with

TABLE 1.75. Structures and Observed Frequencies (cm^{-1}) of SO_2 Complexes

Complex	Structure	ν_a	ν_s	Ref.
$IrCl(CO)(PPh_3)_2(SO_2)$	I	1198–1185	1048	1593
$PtBr(C_6H_3(CH_2NMe_2)_2\text{-}o,o')(SO_2)$	I	1231	1074	1594
$[Ru(NH_3)_4(SO_2)Cl]Cl$	II	1301–1278	1100	1595
$[Ru_6C(CO)_{15}(\mu\text{-}SO_2)]^{2-}$	VI	1186	1052	1596
$Fe(CO)_2\{P(OMe_3)\}_2(SO_2)$	II	1225	1095	1597
$RuCl(C_5Me_5)\{P(i\text{-}Pr)_3\}(SO_2)$	II	1249	1095	1598
$Ni\{P(C_6H_5)_3\}_3(SO_2)$	II	1195	1052	1599
$Ni\{P(C_6H_5)Me_2\}_3(SO_2)$	I	1170	1030	1599
$SbF_5(SO_2)$	III	1327	1102	1600
$\{(C_5H_5)Fe(CO)_2\}_2(\mu\text{-}SO_2)$	IV	1135	993	1601
$Fe_2(CO)_8(\mu\text{-}SO_2)$	IV	1203	1048	1602
$RuCl(NO)(PPh_3)_2(SO_2)$	V	—	895	1603
$OsCl(NO)(PPh_3)_2(SO_2)$	V	1133	846	1604
$[Fe_6(CO)_{15}C(\mu\text{-}SO_2)]^{2-}$	VI	1180	1045	1605
$[Pt_3Au(\mu\text{-}CO)_2(\mu\text{-}SO_2)\{P(C_6H_{11})_3\}_4]^+$	VI	1233	1075	1606
$[Pd_3(\mu\text{-}SO_2)_2(\mu\text{-}N_3)(PPh_3)_3]^-$	VI	1202	1062, 1051	1607

the $\nu(SO_2)$ at 1279 and 1126 cm^{-1}. On photolysis (488 nm at 90 K), the metastable MS-2 state (structure V) similar to that of NO complexes (Sec. 1.20.3) is formed. As a result, the ν_a and ν_b are downshifted to 1181 and 946 cm^{-1}, respectively. The increased separation of the ν_a and ν_b reflects the difference in SO_2 bond length between the two structures.

Sulfur dioxide reacts with $[MFe_3(CO)_{14}]^{2-}$ (M = Cr,Mo,W) to form $[Fe_3(CO)_9(\mu_3, \eta^2\text{-}SO_2)]^{2-}$ and $[Fe_3(CO)_8(\mu\text{-}SO_2)(\mu_3\text{-}S)]^{2-}$, shown below [1611] [all as the bistriphenylphosphonium imidium (PPN) salts]:

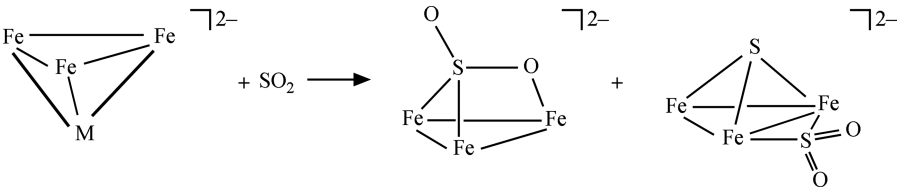

The $\nu(SO)$ of the former are at 1162 and 902 cm^{-1}, while the latter exhibits it at 1066 cm^{-1}.

Vibrational spectra of transition metal complexes of CS_2 and CS have been reviewed by Butler and Fenster [1612]. According to Wilkinson et al. [1584,1613], CS_2 coordinates to the metal in four ways:

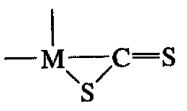

I

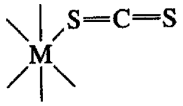

II

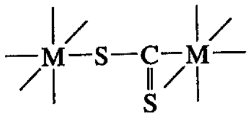

III

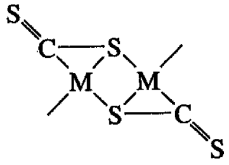

IV

The linear CS_2 molecule in the free state exhibits the $\nu_a(CS_2)$(IR), $\nu_s(CS_2)$ (R), and $\delta(CS_2)$(IR) at 1533, 658, and 397 cm^{-1}, respectively (Sec. 2.2 of Part A). In metal complexes, the SCS bond is bent, except for structure II shown above. Most vibrational studies on CS_2 complexes report only the $\nu(CS_2)$ in the high-frequency region. The $\nu(CS_2)$ of structure I (η^2-bonded) and structure II (η^1-bonded) are at 1100–1150 and 1510 cm^{-1}, respectively. The $\nu(CS_2)$ of the bridging CS_2 groups (structures III–IV) are in the 1155–1120 cm^{-1} region [1613–1615].

From infrared and other evidence, $[Ir(CS_2)(CO)(PPh_3)_3]BPh_4$ was originally thought to be a six-coordinate complex with a η^2-bonded CS_2 [1616]. However, X-ray analysis [1617] revealed an unexpected structure; a five-coordinate complex of the type $[Ir(CO)(PPh_3)_2(S_2C{-}PPh_3)]BPh_4$. Matrix cocondensation reactions of

Ni atoms with CS_2/Ar produce a mixture of $Ni(CS_2)_n$, where $n = 1,2,3$. It was not possible, however, to determine the mode of coordination from their IR spectra [1618]. A mixed-carbon dichalcogenide such as SCSe can form a pair of geometric isomers

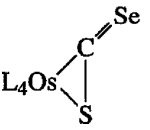

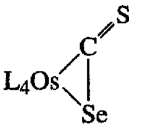

where L_4 represents (CO)(CNR)$(PPh_3)_2$ (R = *p*-tolyl). The *v*(CSe) of the former and the *v*(CS) of the latter have been observed at 1015 and 1066 cm^{-1}, respectively [1619].

The v_a(NSN) and v_s(NSN) of the sulfur–diimine ligand (bent NSN) in Ag(NSN)Ag are at 1115 and 1012 cm^{-1}, respectively (IR) [1620]. Krieglstein and Breitinger [1621] have noted that the two types of sulfito (μ-S,O) bridgings shown below can be distinguished by vibrational spectroscopy:

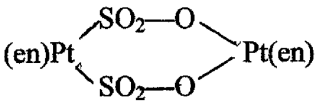

Parallel

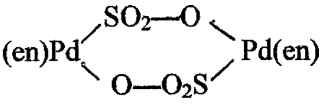

Antiparallel

Complexes of monoalkylsulfides such as $Hg(SR)_2$ ($R = C_nH_{2n+1}$, $n = 1$–10,12) exhibit *v*(HgS) in the 415–220 cm^{-1} region [1622], and the *v*(AgS) of a dialkylsulfide complex, $Ag[S(CH_3)_2]NO_3$, is at 255/240 cm^{-1} in IR spectra [1623].

Allkins and Hendra [1624] carried out an extensive vibrational study on *cis*-and *trans*-$[MX_2Y_2]$ and their halogen-bridged dimers, where M is Pd(II) and Pt(II); X is Cl, Br, and I; and Y is $(CH_3)_2S$, $(CH_3)_2Se$, and $(CH_3)_2Te$. The *v*(ms), *v*(MSe), and *v*(MTe) were assigned in the ranges 350–300, 240–170, and 230–165 cm^{-1}, respectively. The vibrational spectra of PtX_2L_2 [1625], PdX_2L_2, [1626] AuX_3L, and AuXL, [1627], where X is a halogen and L is a dialkylsulfide, have been assigned. Aires et al. [1628] reported the infrared spectra of MX_3L_3-type compounds, where M is Ru(III), Os(III), Rh(III), and Ir(III); X is Cl or Br; and L is Et_2S and Et_2Se. The *v*(MS) and *v*(MSe) of these compounds were assigned at 325–290 and 225–200 cm^{-1}, respectively, based on the *fac* structure. On the other hand, Allen and Wilkinson [1629] proposed the *mer* structure for these compounds, based on far-infrared and other evidence.

According to X-ray analysis, $Pd_2Br_4(Me_2S)_2$ is bridged via Br atoms, whereas $Pt_2Br_4(Et_2S)_2$ is bridged via S atoms [1630]:

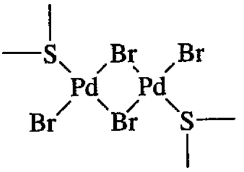

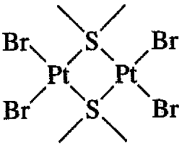

Adams and Chandler [1631] have shown that halogen-bridged $Pd_2Cl_4(SEt_2)_2$ exhibits $\nu(PdCl_t)$, $\nu(PdCl_b)$, and $\nu(PdS)$ at 366, 266, and 358 cm^{-1}, respectively, whereas sulfur-bridged $Pt_2Cl_4(SEt_2)_2$ exhibits $\nu(PtCl_t)$ and $\nu(PtS)$ at 365–325 and 422–401 cm^{-1}, respectively.

1.28.4. Complexes of Thiometalates

Vibrational frequencies of thiometalate ions such as MS_4^{n-}, MS_3O^{n-}, and $MS_2O_3^{n-}$ are found in Sec. 2.2 of Part A. These ions form trinuclear bridging complexes such as shown below:

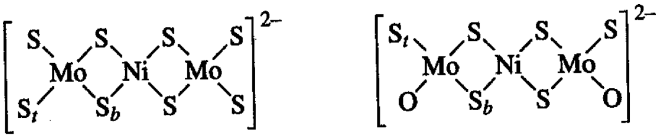

D_{2h} C_{2h} or C_{2v}

Müller and coworkers have carried out an extensive study on structures and spectra of transition metal complexes of thiometalates [1632–1634]. For example, they assigned the IR spectra of the $[Ni(MoS_4)_2]^{2-}$ ion using on normal coordinate analysis involving $^{58}Ni/^{62}Ni$ and $^{92}Mo/^{100}Mo$ isotopes [1635]. The IR-active metal-sulfur stretching frequencies follow the order

	$\nu(MoS_t)$	$\nu(MoS_b)$	$\nu(NiS)$
$\tilde{\nu}(cm^{-1})$	$494(B_{3u})$	$456(B_{2u})*$	$332(B_{3u})*$
		$443(B_{3u})$	$324(B_{2u})$

Here, the asterisks indicate vibrational coupling between them. Figure 1.101 shows the electronic and Raman/RR spectra of the $[Fe(WS_4)_2]^{3-}$ ion obtained by Müller and Hellmann [1636]. It is seen that the excitation at 647.1 nm gives a normal Raman spectrum, whereas those at 514.5 and 488.0 nm yield RR spectra. In the latter case, a series of overtones of ν_2 [totally symmetric $\nu(WS_t)$], as well as a combination with ν(FeS), are observed because the absorption band near 500 nm originates in an electronic transition within the WS_4 ligand. For $[ReOCl(WS_4)2]^{2-}$, the $\nu(WS_t)$ and $\nu(WS_b)$ were observed at ~495 and ~460 cm^{-1}, respectively [1637]. Vibrational spectra are also reported for metal-sulfur bridging complexes formed by the ligands such as PS_4^{3-} [1638] and $PS_2R_2^{2-}$ (R = Me, Ph, etc.) [1639].

The infrared spectra of thiocarbonato complexes of the type $[M(\eta^2\text{-}CS_3)_2]^{2-}$ [M = Ni(II), Pd(II), and Pt(II)] have been studied by Burke and Fackler [1640] and Cormier el al. [1641]. The latter workers carried out normal coordinate analyses on the $[^{58}Ni(\eta^2\text{–}CS_3)_2]^{2-}$ ion and its ^{62}Ni analog. The ν(NiS) were assigned at 385 and 366 cm^{-1}, with a corresponding force constant of 1.41 mdyn/Å (UBF).

The (ν(C=S) and ν(C−S) are at 1010 and 858/507 cm^{-1}, respectively. Band assignments are also reported for the $[AuCl_2(\eta^2\text{-}CS_3)]^-$ [1642] and $[Mo(\eta^2\text{-}CS_3)_4]^{3-}$ [1643]. Vibrational assignments are available for metal complexes of other sulfur

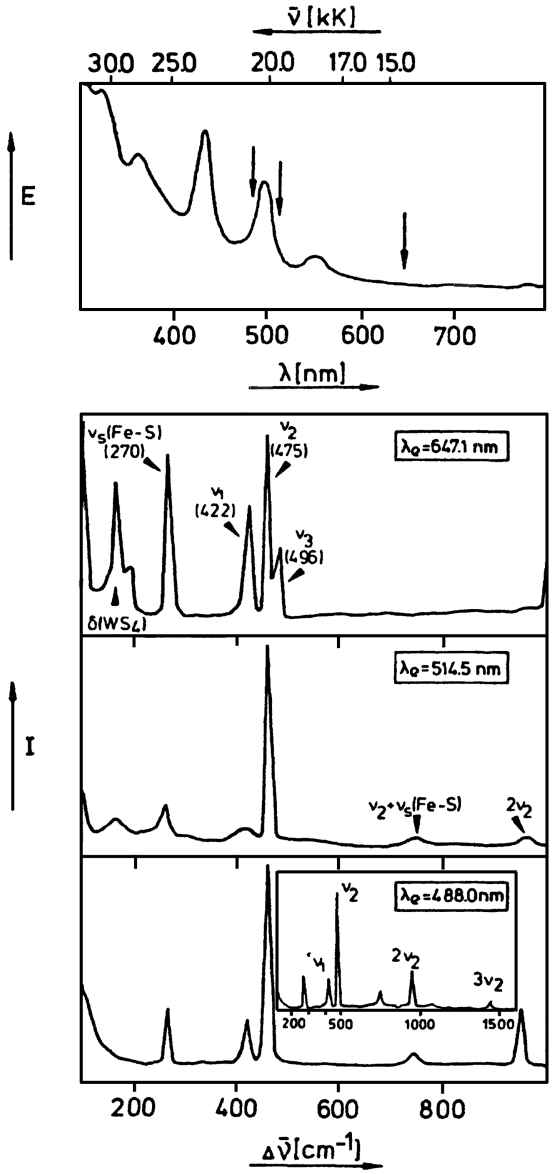

Fig. 1.101. *Electronic absorption (top trace) and Raman/RR spectra (bottom traces) of [(Ph)$_3$PNP(Ph)$_3$]$_2$[N(Et)$_4$][Fe(WS$_4$)$_2$]2CH$_3$CN; the terminal ν(WS$_t$) (ν_2 and ν_3) and bridging ν(WS$_b$) (ν_1) are strongly coupled in this case, and the ν(FeS) is at 270 cm^{-1} [1636].*

ligands such as $K_3[Pu(\eta^2\text{-}PS_4)_3]$ [1644] and $Cp_2Mo(\eta^2\text{–}S_2SO_2)$, which contains a dithiosulfate ion [1645]. Bis(dithioacetato)palladium, $Pd(CH_3CS_2)_2$, exists in three different crystalline forms. Piovesana et al. [1646] characterized each of these forms by IR spectroscopy.

1.28.5. Complexes of Relatively Large Ligands

2,5-Dithiahexane(dth) forms metal complexes such as $[ReCl_3(dth)]_n$ and $Re_3Cl_9(dth)_{1.5}$. Cotton et al. [1647] showed from infrared spectra that dth of the former forms a chelate ring in the *gauche* conformation, whereas that of the latter forms a bridge between two metals by taking the *trans* conformation (see Sec. 1.2.5). Infrared spectra have been used to show that ethanedithiol forms a chelate ring of the *gauche* conformation in $Bi(S_2C_2H_4)X$, where X is Cl and Br [1648]. Schläpfer et al. [1649] assigned the ν(NiS) and ν(NiN) of dth, ete [2-(ethylthio)ethylamine], and mea [mercaptoethylamine] complexes using the metal isotope technique:

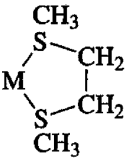

dth

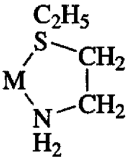

ete

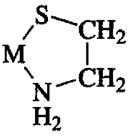

mea

The infrared spectra of *N,N*-dialkyldithiocarbamato complexes have been studied extensively. All these compounds exhibit strong ν(C=N) bands in the 1600–1450 cm^{-1} region. These compounds are roughly classified into two types:

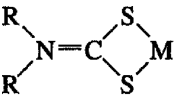

Bidentate coordination

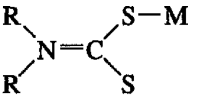

Unidentate coordination

The former exhibits ν(CS) near 1000 cm^{-1} as a single band, whereas the latter shows a doublet in the same region [1650]. Also, the ν(C=N) of the former, (above 1485 cm^{-1}) is higher than that of the latter (below 1485 cm^{-1}) [1651]. The ν(MS) of the bidentate complexes are observed at 400–300 cm^{-1}[1652]. Dithiocarbamato complexes of Fe(III) undergo the high-spin ($^6A_1$)–low-spin ($^2T_2$) crossover. This change can be induced by applying high pressure or by lowering temperature [1653]. Sorai [1654] assigned the ν(FeS) of $Fe(S_2CN(Et)_2)_3$ of the high- and low-spin states to the IR bands at 355 and 552 cm^{-1}, respectively. Hutchinson et al. [1655] have shown by $^{54}Fe - {}^{57}Fe$ isotope shifts and variable-temperature studies that the ν(FeS) of Fe(III) dialkyldithiocarbamates appear at 250–205 and 350–305 cm^{-1}, respectively, for high- and low-spin states, and that intermediate-spin complexes show ν(FeS) in both regions.

Similar ν(FeS) frequencies are reported for high-spin and low-spin Fe(III) complexes of $[Fe(\eta^2\text{-}S_2CNRR')_3]$, where $R = CH_2CH_2OH$, and $R' =$ Me and Et [1656]. Nakamoto et al. [1657] performed normal coordinate analysis on the 1 : 1 (metal/ligand) model of dithiocarbamato Pt(II) complex $[Pt(S_2CNH_2)_2]$ and its ND_2 analog.

The infrared spectra of diselenocarbamato complexes have been reported [1658] and assigned on the basis of normal coordinate analysis [1659]. In the Ni(II) complex,

ν(NiSe) is assigned at 298 cm^{-1}, which is lower by 85 cm^{-1} than the ν(NiS) of the corresponding dithiocarbamato complex. The infrared spectra of xanthato complexes, namely

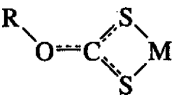

have been studied by Watt and McCormick [1660]. The ν(CO), ν(cs), and ν(MS) were assigned at 1325–1250, 760–540, and 380–340 cm^{-1}, respectively.

Savant et al. [1661] roughly classified monothiobenzoato complexes into three categories:

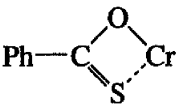

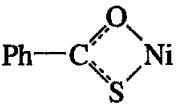

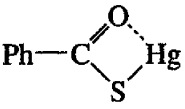

ν(CO) (cm^{-1})	1465	1508	1630
ν(CS) (cm^{-1})	982	958	912

In the Hg(II), Cu(I), and Ag(I) complexes, coordination occurs mainly via sulfur. In the Cr(III) complex, however, the Cr–O bond is stronger than the Cr–S bond. The Ni(II) complex is between these two cases and is close to symmetrical coordination. This is reflected in the frequency trends shown above.

In the $[In(PhCOS)_4]^-$ ion, the ligand is bonded to In(III) through sulfur as a unidentate and exhibits the ν(CO) and ν(CS) vibrations at 1615 and 922 cm^{-1}, respectively [1662]. Similar frequencies (1630 and 910 cm^{-1}) are reported for the S-bonded $As(PhCOS)_3$. In $Bi(PhCOS)_3$, however, the ligand is chelated to the Bi atom through the S and O atoms (1589 and 923 cm^{-1}) [1663]. In thiocarboxylato complexes of the type $Ni(R{-}COS)_2 \cdot \frac{1}{2}(EtOH)$ (R = CH_3, C_2H_5, Ph), the ligand serves as a bridge between two metals as shown

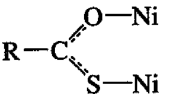

and their ν(CO) are reported to be at 1580–1520 cm^{-1} [1664].

The infrared spectra of metal complexes of thiosemicarbazides

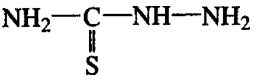

and thiosemicarbazones

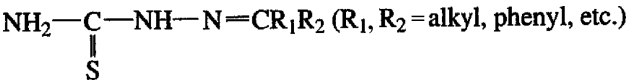

have been reviewed by Campbell [1665]. For metal complexes of dithiocarbazic acid, infrared spectra support the N,S-chelated structure (shown below) rather than the S,S-chelated structure normally found for dithiocarbamato complexes [1666]:

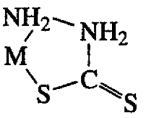

Dithiocarbazato complex

In 1 : 1 complexes of *N*,*N*′-monosubstituted dithiooxamides, Desseyn et al. [1667] concluded from infrared spectra that metals such as Ni(II) and Cu(II) are primarily bonded to the N atom, whereas metals such as Hg(II), Pb(II), and Pd(II) are bonded to the S atom:

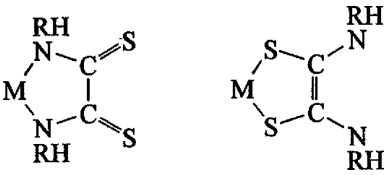

Infrared spectra are reported for $[Au(HL)X_2]$ (HL = dialkylated dithiooxamide; X = Cl or Br) in which the Au(III) atom is chelated to HL via its two S atoms. The ν(Au−S) is observed at 390–380 cm^{-1} [1668].

Monothiooxamide coordinates to Cu(I) as a unidentate via S but as a bidentate to Cu(II) via S and O atoms [1669]. 2-Thiooxamic acid coordinates to Mn(II) as a bidentate via S and O atoms [1670]:

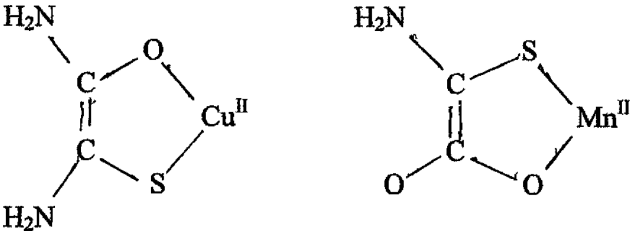

The vibrational spectra and band assignments of these metal complexes are reported.

Dithiooxalato (DTO) complexes $[M(DTO)_2](PPh_4)_2$ [M(II) = Ni,Pd,Pt] are all chelated to the metal via two S atoms, and exhibit two ν(M−S) at 420/370,395/360, and 430/400 cm^{-1}, respectively, in the order of metals shown above [1671]. Two ν(Pt−S) vibrations of $[Pt(mnt)_2]^{2-}$ are observed at 332/318 and 357/330 cm^{-1} for the Pt(II) and Pt(III) complexes, respectively [1672]. Here, mnt^- (maleodinitriledithiolato ion) is an analog of DTO in which its two oxygen atoms are replaced by CN groups. Coucouvanis et al. [1673] synthesized novel tin halide adducts of Ni(II) and Pd(II) dithiooxalto complexes:

The ν(NiS) of the $[Ni(DTO)_2]^{2-}$ ion is at 349 cm^{-1}. In SnX_4 (X = Cl,Br,I) adducts, this band shifts to 385–375 cm^{-1}, indicating a strengthening of the Ni−S bond by complexation. It was found that $Cr(DTO)_3[Cu(PPh_3)_2]_3$ exists in two isomeric forms [1674], one in which the Cr atom is bonded to sulfur, and another in which it is bonded to oxygen of the DTO ion. As expected, ν(C=O), ν(cs), and ν[CrO(S)] are markedly different between these two isomers.

Metal complexes of 1,2-dithiolates (or dithienes) have been of great interest to inorganic chemists because of their redox properties [1675]. Schläpfer and Nakamoto [1676] prepared a series of complexes of the type $[Ni(S_2C_2R_2)2]^n$ where R is H, Ph, CF_3, and CN and n is 0, −1, or −2, and carried out normal coordinate analysis to obtain rough estimates of the charge distribution on the basis of the calculated force constants.

Infrared spectra of metal complexes with thio-β-diketones have been reviewed briefly [1677,1678]. Siimann and Fresco [1679] and Martin et al. [1680] carried out normal coordinate analysis on metal complexes of dithioacetylacotone, monothioacetylacetone, and related ligands. For dithioacetylacetonato complexes, two ν(MS) have been assigned at 390–340 and 300–260 cm^{-1}. Dithiomalonamide(H_2A) is thio-β-acetylacetone in which its two CH_3 groups are replaced by NH_2 groups. The ν(Ni−S) of the $[Ni(H_2A)_2]^{2+}$ ion are at 335 and 233 cm^{-1} in IR spectra [1681].

L-Cysteine has three potential coordination sites (S,N,O), and infrared spectra have been used to determine the structures of its metal complexes. For example, the Zn(II) complex shows no ν(SH), and its carboxylate frequency indicates the presence of a free COO^- group. Thus, the following structure was proposed [1682]:

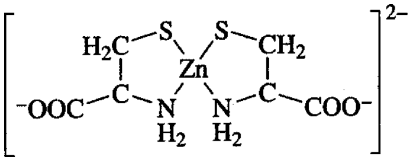

On the other hand, the (S,O) chelation has been suggested for the Pt(II) and Pd(II) complexes [1683]. IR spectra show that the Fe atom in $Fe(cyst)(H_2O)_{1.5}$ is bonded to the S, N, and O atoms whereas that in $Na_2[Fe(cyst)_2]H_2O$ is bonded only to the S and N atoms [1684]. The ν(SS) of L-cystine complexes of Cu(II), Ni(II), and Zn(II), and so on are observed near 500 cm^{-1} [1685].

McAuliffe et al. [1686] studied the IR spectra of metal complexes of methionine [$CH_3-S-CH_2-CH_2-CH(NH_2)-COOH$]. They found that most of the metals they studied [except Ag(I)] coordinate through the NH_2 and COO^- groups, and that the CH_3S groups of these complexes are available for further coordination to other metals. McAuliffe [1687] suggested that complexes of the type M(methionine)Cl_2 [M = Pd(II), Pt(II)] take the polymeric structure:

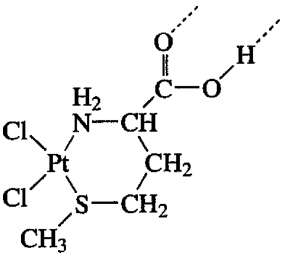

Infrared spectra of metal complexes of sulfur-containing ligands are reported for 2-methylthioaniline, [1688] 8-mercaptoquinoline [1689], cyclic thioethers, [1690], *N*-alkylthiopicolinaimdes [1691], dithizone [1692], and *N*,*N*′-dimethylthioformate [1693].

REFERENCES

1. K. H. Schmidt and A. Müller, *Coord. Chem. Rev.* **19**, 41 (1976).
2. R. Plus, *J. Raman Spectrosc.* **1**, 551 (1973); *Spectrochim. Acta* **32A**, 263 (1976).
3. T. V. Long, II and D. J. B. Penrose, *J. Am. Chem. Soc.* **93**, 632 (1971).
4. K. H. Schmidt and A. Müller, *J. Mol. Struct.* **22**, 343 (1974).
5. K. H. Schmidt and A. Müller, *Inorg. Chem.* **14**, 2183 (1975).
6. A. Deak and J. L. Templeton, *Inorg. Chem.* **19**, 1075 (1980).
7. W. P. Griffith, *J. Chem. Soc. A*, 899 (1966).
8. K. H. Schmidt, W. Hauswirth, and A. Müller, *J. Chem. Soc., Dalton Trans.* 2199 (1975).
9. T. V. Long, II, A. W. Herlinger, E. F. Epstein, and I. Bernal, *Inorg. Chem.* **9**, 459 (1970).
10. M. Gorol, N. C. Mosch-Zanetti, M. Noltemeye, and H. W. Roesky, *Z. Anorg. Allg. Chem.* **626**, 2318 (2000).
11. J. M. Janik, J. A. Janik, G. Pytasz, and J. Sokolowski, *J. Raman Spectrosc.* **4**, 13 (1975).
12. M. J. Nolan and D. W. James, *J. Raman Spectrosc.* **1,** 259, 271 (1973).
13. J. Hiraishi, I. Nakagawa, and T. Shimanouchi, *Spectrochim. Acta* **24A**, 819 (1968).
14. R. Acevedo, G. Diaz, and C. D. Flint, *Spectrochim. Acta* **41A**, 1397 (1985).
15. R. Acevedo, G. Diaz, M. M. Campos-Vallette, and B. Weiss, *Spectrochim. Acta.* **47A**, 355 (1991).
16. A. Müller, P. Christophliemk, and I. Tossidis, *J. Mol. Struct.* **15**, 289 (1973).
17. K. Nakamoto, J. Takemoto, and T. L. Chow, *Appl. Spectrosc.* **25**, 352 (1971).
18. H. Hillebrecht, G. Thiele, A. Koppenhoffer, and H. Vahrenkamp, *Z. Naturforsch.* **49B**, 1163 (1994).
19. D. N. Ishikawa, F. A. De Souza, and S. C. Tellez, *Spectrosc. Lett.* **26**, 803 (1993).
20. M. Manfait, A. J. P. Alix, and J. Delaunay-Zeches, *Inorg. Chim. Acta* **44**, L261 (1980).
21. L. A. Degen and A. J. Rowlands, *Spectrochim. Acta* **47A**, 1263 (1991).
22. M. Manfait, A. J. P. Alix, L. Bernard, and T. Theophanides, *J. Raman Spectrosc.* **7**, 143 (1978).

23. S. J. Cyvin, B. N. Cyvin, K. H. Schmidt, W. Wiegeler, A. Müller, and J. Brunvoll, *J. Mol. Struct.* **30**, 315 (1976).
24. M. Manfait, A. J. P. Alix, and C. Kappenstein, *Inorg. Chim. Acta* **50**, 147 (1981).
25. A. L. Geddes and G. L. Bottger, *Inorg. Chem.* **8**, 802 (1969).
26. P. Nockemann and G. Meyer, *Z. Anorg. Allg. Chem.* **628**, 1636 (2002).
27. M. G. Miles, J. H. Patterson, C. W. Hobbs, M. J. Hopper, J. Overend, and R. S. Tobias, *Inorg. Chem.* **7**, 1721 (1968).
28. S. C. Tellez, *Spectrosc. Lett.* **21**, 871 (1988).
29. R. Essmann, *J. Mol. Struct.* **351,** 87, 91 (1995).
30. B. S. Ault, *J. Am. Chem. Soc.* **100**, 5773 (1978).
31. S. Süzer and L. Andrews, *J. Am. Chem. Soc.* **109**, 300 (1987).
32. J. Szczepanski, M. Szczesniak, and M. Vala, *Chem. Phys. Lett.* **162**, 123 (1989).
33. A. Loutellier, L. Manceron, and J. P. Perchard, *Chem. Phys.* **146**, 179 (1990).
34. B. S. Ault, *J. Phys. Chem. A,* **105**, 4758 (2001).
35. M. Chen, A. Aheng, H. Lu, and M. Ahou, *J. Phys. Chem. A*, **106**, 3077 (2002).
36. H. -J. Himmel, A. J. Downs, J. C. Green, and T. M. Greene, *J. Chem. Soc. Dalton Trans.* 535 (2001).
37. T. Shimanouchi, and I. Nakagawa, *Inorg. Chem.* **3**, 1805 (1964).
38. I. Nakagawa and T. Shimanouchi, *Spectrochim. Acta.* **22**, 759 (1966).
39. Y. Chen, D. H. Christensen, G. O. Sorensen, O. F. Nielsen, and E. Pedersen, *J. Mol. Struct.* **299**, 61 (1993).
40. Y. Chen, D. H. Christensen, G. O. Sorensen, O. F. Nielsen, C. J. H. Jacobsen, and J. Hyldtoft, *J. Mol. Struct.* **319**, 129 (1994).
41. T. M. Loehr, J. Zinich, and T. V. Long, II *Chem. Phys. Lett.* **7**, 183 (1970).
42. M. M. Schmidke and M. Rosner, *Inorg. Chem.* **28**, 2570 (1989).
43. A. F. Schreiner and J. A. McLean, *J. Inorg. Nucl. Chem.* **27**, 253 (1965).
44. A. D. Allen and J. R. Stevens, *Can. J. Chem.* **51**, 92 (1973).
45. M. W. Bee, S. F. A. Kettle, and D. B. Powell, *Spectrochim. Acta* **30A**, 139 (1974).
46. C. Li, L. Jiang, and W. Tang, *Spectrochim. Acta* **49A**, 339 (1993).
47. C. H. Perry, D. P. Athans, E. F. Young, J. R. Durig, and B. R. Mitchell, *Spectrochim. Acta* **23A**, 1137 (1967).
48. P. J. Hendra, *Spectrochim. Acta* **23A**, 1275 (1967).
49. K. Nakaraoto, P. J. McCarthy, J. Fujita, R. A. Condrate, and G. T. Behnke, *Inorg. Chem.* **4**, 36 (1965).
50. P. J. Hendra and N. Sadasivan, *Spectrochim. Acta* **21**, 1271 (1965).
51. R. Layton, D. W. Sink, and J. R. Durig, *J. Inorg. Nucl. Chem.* **28**, 1965 (1966).
52. J. R. Durig, R. Layton, D. W. Sink, and B. R. Mitchell, *Spectrochim. Acta* **21**, 1367 (1965).
53. J. R. Durig and B. R. Mitchell, *Appl. Spectrosc.* **21**, 221 (1967).
54. C. A. Tellez, S. D. N. Ishikawa, and J. G. Lara, *Spectrosc. Lett.* **31**, 313 (1998).
55. E. Bernhardt and W. Preetz, *Z. Anorg. Allg. Chem.* **623**, 1389 (1997).
56. R. J. H. Clark and W. R. Trumble, *Inorg. Chem.* **15**, 1030 (1976).

57. D. M. Adams and J. R. Hall, *J. Chem. Soc., Dalton Trans.* 1450 (1973).
58. J. R. Hall, and D. A. Hirons, *Inorg. Chim. Acta* **34**, L277 (1979).
59. R. J. H. Clark, "Raman and Resonance Raman Spectroscopy of Linear Chain Complexes" in R. J. H. Clark and R. E. Hester, eds., *Advances in Infrared and Raman Spectroscopy*, **Vol. 11**, Wiley, NewYork, 1985, p. 95
60. I. Nakagawa and T. Shimanouchi, *Spectrochim. Acta* **22**, 1707 (1966).
61. T. Grzybek, J. M. Janik, A. Kulczycki, G. Pytasz, J. A. Janik, J. Ściensiński, and E. Ściensiński, *J. Raman Spectrosc.* **1**, 185 (1973).
62. I. Nakagawa, *Bull. Chem. Soc Jpn.* **46**, 3690 (1973).
63. H. Poulet, P. Delorme, and J. P. Mathieu, *Spectrochim. Acta* **20**, 1855 (1964).
64. J. A. Janik, W. Jacob, and J. M. Janik, *Acta Phys. Pol. A*, **38**, 467 (1970).
65. J. M. Janik, A. Magdal-Mikuli, and J. A. Janik, *Acta Phys. Pol. A*, **40**, 741 (1971).
66. K. Niwa, H. Takahashi, and K. Higashi, *Bull. Chem. Soc. Jpn.* **44**, 3010 (1971).
67. K. Brodersen and H. J. Becher, *Chem. Ber.* **89**, 1487 (1956).
68. D. C. Bradley, and M. H. Gitlitz, *J. Chem. Soc. A*, 980 (1969).
69. G. W. Watt, B. B. Hutchinson, and D. S. Klett, *J. Am. Chem. Soc.* **89**, 2007 (1967).
70. M. Goldstein and E. F. Mooney, *J. Inorg. Nucl. Chem.* **27**, 1601 (1965).
71. F. D. Rochon, M. Doyon, and I. S. Butler, *Inorg. Chem.* **32**, 2717 (1993).
72. D. A. Thornton, *J. Coord. Chem.* **24**, 261 (1991).
73. D. Nicholls and R. Swindells, *J. Inorg. Nucl. Chem.* **30**, 2211 (1968).
74. K. H. Linke, F. Dürholz, and P. Hädicke, *Z Anorg. Allg. Chem.* **356**, 113 (1968).
75. H. E. Oosthuizen, E. Singleton, J. S. Field, and G. C. van Niekerk, *J. Organomet. Chem.* **279**, 433 (1985).
76. D. B. Musaev, M. N. Guseinov, N. G. Klyyuchnikov, and R. Ya. Aliev, *Russ. J. Inorg. Chem. (Engl. transl.)* **31**, 641 (1986).
77. Y. Y. Kharitonov, M. A. Sarukhanov, I. B. Baranovskii, and K. U. Ikramov, *Opt. Spektrosk.* **19**, 460 (1965).
78. N. Lehnert, B. E. Wiesler, F. Tuczek, A. Hennige, and D. Selknann, *J. Am. Chem. Soc.* **119**, 8879 (1997).
79. F. A. Andersen, and K. A. Jensen, *J. Mol. Struct.* **141**, 441 (1986).
80. K. Nakatsu, M. Shiro, Y. Saito, and H. Kuroya, *Bull. Chem. Soc. Jpn.* **30**, 158 (1957).
81. K. Nakatsu, *Bull. Chem. Soc. Jpn.* **35**, 832 (1962).
82. R. E. Cramer and J. T. Huneke, *Inorg. Chem.* **14**, 2565 (1975).
83. J. Gouteron, *J. Inorg. Nucl. Chem.* **38**, 63 (1976).
84. G. D. Fleming and R. E. Shepherd, *Spectrochim. Acta* **43A**, 1141 (1987).
85. G. Borch, P. H. Nielsen, and P. Klaeboe, *Acta Chem. Scand.* **31A**, 109 (1977).
86. G. Borch, P. Klaeboe, and P. H. Nielsen, *Spectrochim. Acta* **34A**, 87 (1978).
87. G. Borch, J. Gustavsen, P. Klaeboe, and P. H. Nielsen, *Spectrochim. Acta* **34A**, 93 (1978).
88. B. E. Williamson, L. Dubicki, and S. E. Harnung, *Inorg. Chem.* **27**, 3484 (1988).
89. C. D. Flint and A. P. Matthews, *Inorg. Chem.* **14**, 1219 (1975).
90. Z. Gabelica, *Spectrochim. Acta* **32A**, 327 (1976).

91. Y. Omura, I. Nakagawa, and T. Shimanouchi, *Spectrochim. Acta* **27A**, 2227 (1971).
92. A. M. A. Bennett, G. A. Foulds, and D. A. Thornton, *Spectrochim. Acta* **45A**, 219 (1989).
93. A. M. A. Bennett, G. A. Foulds, D. A. Thornton, and G. M. Watkins, *Spectrochim. Acta* **46A**, 13 (1990).
94. P. Stein, V. Miskowski, W. H. Woodruff, J. P. Griffin, K. G. Werner, B. P. Gaber, and T. G. Spiro, *J. Chem. Phys.* **64**, 2159 (1976).
95. M. Z. Zgierski, *J. Raman Spectrosc.* **6**, 52 (1977).
96. A. B. P. Lever and E. Mantovani, *Can. J. Chem.* **51**, 1567 (1973).
97. G. W. Rayner-Canham and A. B. P. Lever, *Can. J. Chem.* **50**, 3866 (1972).
98. A. B. P. Lever and E. Mantovani, *Inorg. Chem.* **10**, 817 (1971).
99. J. M. Rigg and E. Sherwin, *J. Inorg. Nucl. Chem.* **27**, 653 (1965).
100. M. N. Hughes and W. R. McWhinnie, *J. Inorg. Nucl. Chem.* **28**, 1659 (1966).
101. S. Kida, *Bull. Chem. Soc. Jpn.* **39**, 2415 (1966).
102. E. B. Kipp and R. A. Haines, *Can. J. Chem.* **47**, 1073 (1969).
103. D. B. Powell and N. Sheppard, *J. Chem. Soc.* 3089 (1959).
104. N. Farrell, S. Gama de Almeida, and Y. Qu, *Inorg. Chim. Acta* **178**, 209 (1990).
105. G. Newman and D. B. Powell, *J. Chem. Soc.* 447 (1961); 3447 (1962).
106. K. Brodersen and T. Kahlert, *Z Anorg. Allg. Chem.* **348**, 273 (1966).
107. K. Brodersen, *Z. Anorg. Allg. Chem.* **298**, 142 (1959).
108. T. Iwamoto and D. F. Shriver, *Inorg. Chem.* **10**, 2428 (1971).
109. R. J. H. Clark and V. B. Croud, *Inorg. Chem.* **25**, 1751 (1986).
110. G. C. Papavassiliou, T. Theophanides, and R. Rapsomanikis, *J. Raman Spectrosc.* **8**, 227 (1979).
111. S. P. Love, S. C. Huckett, L. A. Worl, T. M. Frankcom, S. A. Ekberg, and B. I. Swanson, *Phys. Rev. B. Condens. Matter.* **47**, 11107 (1993).
112. J. A. Brozik, B. L. Scott, and B. I. Swanson, *J. Phys. Chem. B,* **103**, 10566 (1999).
113. Y. Omura, I. Nakagawa, and T. Shimanouchi, *Spectrochim. Acta* **27A**, 1153 (1971).
114. R. W. Berg and K. Rasmussen, *Spectrochim. Acta* **29A**, 37 (1973).
115. G. W. Watt and D. S. Klett, *Spectrochim. Acta* **20**, 1053 (1964).
116. A. R. Gainsford and D. A. House, *Inorg. Chim. Acta* **3**, 367 (1969).
117. H. H. Schmidtke and D. Garthoff, *Inorg. Chim. Acta* **2**, 357 (1968).
118. K. W. Kuo and S. K. Madan, *Inorg. Chem.* **8**, 1580 (1969).
119. J. H. Forsberg, T. M. Kubik, T. Moeller, and K. Gucwa, *Inorg. Chem.* **10**, 2656 (1971).
120. D. A. Buckingham and D. Jones, *Inorg. Chem.* **4**, 1387 (1965).
121. K. W. Bowker, E. R. Gardner, and J. Burgess, *Inorg. Chim. Acta* **4**, 626 (1970).
122. S. Mizushima, I. Ichishima, I. Nakagawa, and J. V. Quagliano, *J. Phys. Chem.* **59**, 293 (1955).
123. D. M. Sweeny, S. Mizushima, and J. V. Quagliano, *J. Am. Chem. Soc.* **77**, 6521 (1955).
124. R. J. H. Clark and C. S. Williams, *Inorg. Chem.* **4**, 350 (1965).
125. J. K. Wilmshurst and H. J. Bernstein, *Can. J. Chem.* **35**, 1183 (1957).
126. J. H. S. Green, W. Kynaston, and H. M. Paisley, *Spectrochim. Acta* **19**, 549 (1963).

127. C. Postmus, J. R. Ferraro, A. Quattrochi, K. Shobatake, and K. Nakamoto, *Inorg. Chem.* **8**, 1851 (1969).
128. T. Malyusz and W. Preetz, *Z. Anorg. Allg. Chem.* **622**, 1006 (1996).
129. S. Kolf and W. Preetz, *Z. Anorg. Allg. Chem.* **625**, 411 (1999).
130. H. Junicke, K. Schenzel, F. W. Heinemann, K. Pelz, H. Bogel, and D. Steinborn, *Z. Anorg. Allg. Chem.* **623**, 603 (1997).
131. S. Kolf and W. Preetz, *Z. Anorg. Allg. Chem.* **625**, 43 (1999).
132. S. Kolf and W. Preetz, *Z. Anorg. Allg. Chem.* **623**, 501 (1997).
133. H. -H. Drews and W. Preetz, *Z. Anorg. Allg. Chem.* **623**, 509 (1997).
134. Y. Saito, M. Cordes, and K. Nakamoto, *Spectrochim. Acta* **28A**, 1459 (1972).
135. Y. Saito, C. W. Schläpfer, M. Cordes, and K. Nakamoto, *Appl. Spectrosc.* **27**, 213 (1973).
136. J. E. Ruede and D. A. Thornton, *J. Mol. Struct.* **34**, 75 (1976).
137. D. A. Thornton, *Coord. Chem. Rev.* **104**, 251 (1990).
138. M. Choca, J. R. Ferraro, and K. Nakamoto, *J. Chem. Soc., Dalton Trans*, 2297 (1972).
139. R. H. Nuttall, A. F. Cameron, and D. W. Taylor, *J. Chem. Soc. A*, 3103 (1971).
140. M. Fleischmann, P. J. Hendra, and A. McQuillan, *Chem. Phys. Lett.* **26**, 163 (1974); *J. Electroanal. Chem.* **65**, 933 (1975).
141. D. J. Jeanmaire and R. P. Van Duyne, *J. Electroanal. Chem.* **84**, 1 (1977).
142. R. P. Van Duyne in C. B. Moore, ed., *Chemical and Biological Applications of Lasers*, **Vol. 4**, Academic Press, New York, 1979, p. 101.
143. M. G. Albrecht and J. A. Creighton, *J. Am. Chem. Soc.* **99**, 5215 (1977).
144. J. A. Creighton, M. G. Albrecht, R. E. Hester, and J. A. D. Matthew, *Chem. Phys. Lett.* **55**, 55 (1978).
145. H. Yamada and Y. Yamamoto, *J. Chem. Soc. Faraday Trans. 1*, **75**, 1215 (1979).
146. H. Yamada, *Appl. Spectrosc. Rev.* **17**, 227 (1981).
147. S. A. Bilmes, *Chem. Phys. Lett.* **171**, 141 (1990).
148. S. Farquharson, P. A. Lay, and M. J. Weaver, *Spectrochim. Acta* **40A**, 907 (1984).
149. L. Cattalini, R. J. H. Clark, A. Orio, and C. K. Poon, *Inorg. Chim. Acta* **2**, 62 (1968).
150. J. Burgess, *Spectrochim. Acta* **24A**, 277 (1968).
151. A. B. P. Lever and B. S. Ramaswamy, *Can. J. Chem.* **51**, 1582 (1973).
152. W. R. McWhinnie, *J. Inorg. Nucl. Chem.* **27**, 2573 (1965).
153. D. E. Billing and A. E. Underhill, *J. Inorg. Nucl. Chem.* **30**, 2147 (1968).
154. J. Burgess, *Spectrochim. Acta* **24A**, 1645 (1968).
155. L. El-Sayed and R. O. Ragsdale, *J. Inorg. Nucl. Chem.* **30**, 651 (1968).
156. S. Yurdakul, S. Akyuz, and J. E. D. Davies, *Spectrosc. Lett.* **29**, 175 (1996).
157. M. A. S. Goher, M. A. M. Abu-Youssef, and F. A. Mautner, *Polyhedron* **15**, 453 (1996).
158. M. S. A. Goher, M. A. M. Abu-Youssef, F. A. Mautner, and A. Popitsch, *Polyhedron* **12**, 1751 (1993).
159. R. G. Garvey, J. H. Nelson, and R. O. Ragsdale, *Coord. Chem. Rev.* **3**, 375 (1968).
160. C. P. Prabhakaran and C. C. Patel, *J. Inorg. Nucl. Chem.* **34**, 3485 (1972).
161. I. S. Ahuja and P. Rastogi, *J. Chem. Soc. A* 378 (1970).

162. F. A. Cotton and J. F. Gibson, *J. Chem. Soc. A* 2105 (1970).
163. D. M. L. Goodgame, M. Goodgame, P. J. Hayward, and G. W. Rayner-Canham, *Inorg. Chem.* **7**, 2447 (1968).
164. C. E. Taylor and A. E. Underhill, *J. Chem. Soc. A* 368 (1969).
165. B. Cornilsen and K. Nakamoto, *J. Inorg. Nucl. Chem.* **36**, 2467 (1974).
166. W. J. Eilbeck, F. Holmes, C. E. Taylor, and A. E. Underhill, *J. Chem. Soc. A*, 128 (1968).
167. D. M. L. Goodgame, M. Goodgame, and G. W. Rayner-Canham, *Inorg. Chim. Acta* **3**, 399 (1969).
168. D. M. L. Goodgame, M. Goodgame, and G. W. Rayner-Canham, *Inorg. Chim. Acta* **3**, 406 (1969).
169. W. J. Eilbeck, F. Holmes, C. E. Taylor, and A. E. Underhill, *J. Chem. Soc. A*, 1189 (1968).
170. G. A. Melson and R. H. Nuttall, *J. Mol. Struct.* **1**, 405 (1968).
171. M. M. Cordes and J. L. Walter, *Spectrochim. Acta* **24A**, 1421 (1968).
172. J. B. Hodgson, G. C. Percy, and D. A. Thornton, *J. Mol. Struct.* **66**, 81 (1980).
173. S. Salama and T. G. Spiro, *J. Am. Chem. Soc.* **100**, 1105 (1978).
174. D. S. Caswell and T. G. Spiro, *J. Am. Chem. Soc.* **108**, 6470 (1986).
175. P. Drozdzewski and B. Pawlak, *Spectrochim. Acta, A*, 1527 (2004).
176. P. Drozdzewski and B. Pawlak, *Vib. Spectrosc.* **33**, 15 (2003).
177. P. Drozdzewski and M. Musiala, *J. Mol. Struct.* **704**, 145 (2004).
178. P. Drozdzewski, M. Musiala, M. Kubiak, and T. Lis, *Vib. Spectrosc.* **39**, 59 (2005).
179. B. Hutchinson, J. Takemoto, and K. Nakamoto, *J. Am. Chem. Soc.* **92**, 3335 (1970).
180. Y. Saito, J. Takemoto, B. Hutchinson, and K. Nakamoto, *Inorg. Chem.* **11**, 2003 (1972); J. Takemoto, B. Hutchinson, and K. Nakamoto, *Chem. Commun.* 1007 (1971).
181. E. König and E. Lindner, *Spectrochim. Acta* **28A**, 1393 (1972).
182. R. Wilde, T. K. K. Srinivasan, and N. Ghosh, *J. Inorg. Nucl. Chem.* **35**, 1017 (1973).
183. J. S. Strukl and J. L. Walter, *Spectrochim. Acta* **27A**, 223 (1971).
184. R. J. H. Clark, P. C. Turtle, D. P. Strommen, B. Streusand J. Kincaid, and K. Nakamoto, *Inorg. Chem.* **16**, 84 (1977).
185. J. C. Rubim, *J. Electrochem. Soc.* **140**, 1601 (1993).
186. S. M. Angel, M. K. Dearmond, R. J. Donohoe, and D. W. Wertz, *J. Phys. Chem.* **89**, 282 (1985).
187. R. F. Dallinger and W. H. Woodruff, *J. Am. Chem. Soc.* **101**, 1355 (1979).
188. P. G. Bradley, N. Kress, B. A. Hornberger, R. F. Dallinger, and W. H. Woodruff, *J. Am. Chem. Soc.* **103**, 7441 (1981).
189. M. Forster and R. E. Hester, *Chem. Phys. Lett.* **81**, 42 (1981).
190. S. McClanahan, T. Hayes, and J. Kincaid, *J. Am. Chem. Soc.* **105**, 4486 (1983).
191. W. K. Smothers and M. S. Wrighton, *J. Am. Chem. Soc.* **105**, 1067 (1983).
192. P. K. Mallick, D. P. Strommen, and J. R. Kincaid, *J. Am. Chem. Soc.* **112**, 1686 (1990).
193. R. J. Donohoe, C. D. Tait, M. K. DeArmond, and D. W. Wertz, *Spectrochim. Acta.* **42A**, 233 (1986).
194. P. K. Mallick, G. D. Danzer, D. P. Strommen, and J. R. Kincaid, *J. Phys. Chem.* **92**, 5628 (1988).

195. D. P. Strommen, P. K. Mallick, G. D. Danzer, R. S. Lumpkin, and J. R. Kincaid, *J. Phys. Chem.* **94**, 1357 (1990).
196. G. D. Danzer and J. R. Kincaid, *J. Phys. Chem.* **94**, 3976 (1990).
197. D. J. Ma'nuel, D. P. Strommen, A. Bhuiyan, M. Sykora, and J. R. Kincaid, *J. Raman Spectrosc.* **28**, 933 (1997).
198. H. Su and J. R. Kincaid, *J. Raman Spectrosc.* **34**, 907 (2003).
199. A. A. Bhuiyan and J. R. Kincaid, *Inorg. Chem.* **38**, 4759 (1999).
200. G. D. Danzer, J. A. Golus, and J. R. Kincaid, *J. Am. Chem. Soc.* **115**, 8643 (1993).
201. J. S. Gardner, D. P. Strommen, W. S. Szulbinski, H. Su, and J. R. Kincaid, *J. Phys. Chem. A,* **107**, 351 (2003).
202. J. Wu and J. R. Kincaid, *J. Raman Spectrosc.* **35**, 1001 (2004).
203. J. Takemoto and B. Hutchinson, *Inorg. Nucl. Chem. Lett.* **8**, 769 (1972).
204. E. König and K. J. Watson, *Chem. Phys. Lett.* **6**, 457 (1970).
205. J. Takemoto and B. Hutchinson, *Inorg. Chem.* **12**, 705 (1973).
206. C. L. Zilverentant, G. A. van Albada, A. Boussekson, J. G. Haasnoot, and J. Reedijik, *Inorg. Chim. Acta* **303**, 287 (2000).
207. J. R. Ferraro and J. Takemoto, *Appl. Spectrosc.* **28**, 66 (1974).
208. P. F. B. Barnard, A. T. Chamberlain, G. C. Kulasingam, R. J. Dosser, and W. R. McWhinnie, *Chem. Commun.* 520 (1970).
209. R. H. Herber and L. M. Casson, *Inorg. Chem.* **25**, 847 (1986).
210. D. C. Figg and R. H. Herber, *Inorg. Chem.* **29**, 2170 (1990).
211. D. C. Figg, R. H. Herber, and J. A. Potenza, *Inorg. Chem.* **31**, 2111 (1992).
212. J. J. McGarvey, S. E. J. Bell, and J. N. Bechara, *Inorg. Chem.* **25**, 4325 (1986).
213. C. Turro, Y. C. Chung, N. Leventis, M. E. Kuchenmeister, P. J. Wagner, and G. E. Leroi, *Inorg. Chem.* **35**, 5104 (1996).
214. K. Nakamoto, *Advances in the Chemistry of the Coordination Compounds*, Macmillan, New York, 1961, p. 437.
215. H. van der Poel, G. van Koten, and K. Vrieze, *Inorg. Chem.* **19**, 1145 (1980).
216. J. Takemoto, *Inorg. Chem.* **12**, 949 (1973).
217. B. Hutchinson and A. Sunderland *Inorg. Chem.* **11**, 1948 (1972).
218. A. Bigotto, G. Costa, V. Galasso, and G. DeAlti, *Spectrochim. Acta* **26A**, 1939 (1970).
219. A. Bigotto, V. Galasso, and G. DeAlti, *Spectrochim. Acta* **27A**, 1659 (1971).
220. P. E. Rutherford and D. A. Thornton, *Spectrochim. Acta* **35A**, 711 (1979).
221. N. Ohkaku and K. Nakamoto, *Inorg. Chem.* **10**, 798 (1971).
222. B. Hutchinson, A. Sunderland, M. Neal, and S. Olbricht, *Spectrochim. Acta* **29A**, 2001 (1973).
223. C. Engelter, G. E. Jackson, C. L. Knight, and D. A. Thornton, *J. Mol. Struct.* **213**, 133 (1989).
224. A. H. Jubert, A. C. G. Baro, E. J. Baron, and O. Sala, *J. Raman Spectrosc.* **20**, 555 (1989).
225. P. W. Hansen and R. W. Jensen, *Specrochim. Acta* **50A**, 169 (1994).
226. T. Kitagawa and Y. Ozaki, *Struct. Bonding* (*Berlin*) **64**, 71 (1987).
227. H. Ogoshi, Y. Saito, and K. Nakamoto, *J. Chem. Phys.* **57**, 4194 (1972).

228. H. Susi and J. S. Ard, *Spectrochim. Acta* **33A**, 561 (1977).

229. S. Sunder and H. J. Bernstein, *J. Raman Spectrosc.* **5**, 351 (1976).

230. L. L. Gladkov, A. T. Gradyushko, A. M. Shulga, K. N. Solovyov, and A. S. Starukhin, *J. Mol. Struct.* **47**, 463 (1978).;**45**, 267 (1978).

231. M. Abe, T. Kitagawa, and Y. Kyogoku, *J. Chem. Phys.* **69**, 4526 (1978).

232. X. -Y. Li, R. S. Czernuszewicz, J. R. Kincaid, Y. O. Su, and T. G. Spiro, *J. Phys. Chem.* **94**, 31 (1990).

233. X. -Y. Li, R. S. Czemuszewicz, J. R. Kincaid, P. Stein, and T. G. Spiro, *J. Phys. Chem.* **94**, 47 (1990).

234. X. -Y. Li, R. S. Czernuszewicz, J. R. Kincaid, and T. G. Spiro, *J. Am. Chem. Soc.* **111**, 7012 (1989).

235. J. R. Kincaid and K. Nakamoto, *J. Inorg. Nucl. Chem.* **37**, 85 (1975).

236. V. L. DeVito, and S. A. Asher, *J. Am. Chem. Soc.* **111**, 9143 (1989).

237. V. L. DeVito, M. Z. Cai, H. Zhu, S. A. Asher, L. A. Kehres, and K. M. Smith, *J. Phys. Chem.* **95**, 9320 (1991).

238. T. G. Spiro, P. M. Kozlowski, and M. Z. Zgierrski, *J. Raman Spectrosc.* **29**, 869 (1998).

239. P. M. Kozlowski, T. S. Rush, III, A. A. Jarzecki, M. Z. Zgierski, B. Chase, C. Piffat, B. -H. Ye, X. -Y. Li, P. Pulay, and T. G. Spiro, *J. Phys. Chem. A* **103**, 1357 (1999).

240. T. S. Rush, III, P. M. Kozlowski, C. A. Piffat, R. Kumble, M. Z. Zgierski, and T. G. Spiro, *J. Phys. Chem. B* **104**, 5020 (2000).

241. W. Jentzen, I. Turowska-Tyrk, W. R. Scheidt, and J. A. Shelnutt, *Inorg. Chem.* **35**, 3559 (1996).

242. X. -Z. Song, W. Jentzen, L. Jaquinod, R. G. Khoury, C. J. Medforth, S. -L. Jia, J. -G. Ma, K. M. Smith, and J. A. Shelnutt, *Inorg.Chem.* **37**, 2117 (1998).

243. L. D. Sparks, K. K. Anderson, C. J. Medforth, K. M. Smith, and J. A. Shelnutt, *Inorg. Chem.* **33**, 2297 (1994).

244. J. G. Rankin and R. S. Czernuszewicz, *Org. Geochem.* **20**, 521 (1993).

245. X. -Y. Li, V. I. Petrov, D. Chen, and N. -T. Yu, *J. Raman Spectrosc.* **32**, 503 (2001).

246. Y. Ozaki, K. Iriyama, H. Ogoshi, T. Ochiai, and T. Kitagawa, *J. Phys. Chem.* **90**, 6105 (1986).

247. G. Chottard, P. Battioni, J. -P. Battioni, M. Lange, and D. Mansuy, *Inorg. Chem.* **20**, 1718 (1981).

248. T. Kitagawa, H. Ogoshi, E. Watanabe, and Z. Yoshida, *J. Phys. Chem.* **79**, 2629 (1979).

249. J. Teraoka and T. Kitagawa, *J. Phys. Chem.* **84**, 1928 (1980).

250. T. Kitagawa, M. Abe, Y. Kyogoku, H. Ogoshi, E. Watanabe, and Z. Yoshida, *J. Phys. Chem.* **80**, 1181 (1976).

251. L. M. Proniewicz, K. Bajdor, and K. Nakamoto, *J. Phys. Chem.* **90**, 1760 (1986).

252. W. -D. Wagner and K. Nakamoto, *J. Am. Chem. Soc.* **111**, 1590 (1989).

253. M. Mylrajan, L. A. Andersson, J. Sun, T. M. Loehr, C. S. Thomas, E. P. Sullivan, Jr., M. A. Thomson, K. M. Long, O. P. Anderson, and S. H. Strauss, *Inorg. Chem.* **34**, 3953 (1995).

254. Y. Ozaki, K. Iriyama, H. Ogoshi, T. Ochiai, and T. Kitagawa, *J. Phys. Chem.* **90**, 6113 (1986).

255. K. R. Rodgers, R. A. Reed, Y. O. Su, and T. G. Spiro, *Inorg. Chem.* **31**, 2688 (1992).

256. K. Bütje and K. Nakamoto, *Inorg. Chim. Acta* **167**, 97 (1990).
257. R. S. Czernuszewicz, X. -Y. Li, and T. G. Spiro, *J. Am. Chem. Soc.* **111**, 7024 (1989).
258. U. Bobinger, R. Schweitzer-Stenner, and W. Dreybrodt, *J. Phys. Chem.* **95**, 7625 (1991).
259. J. A. Shelnutt, C. J. Medforth, M. D. Berber, K. M. Barkigia, and K. M. Smith, *J. Am. Chem. Soc.* **113**, 4077 (1991).
260. L. D. Sparks, C. J. Medforth, M. S. Park, J. R. Chamberlain, M. R. Ondrias, M. O. Senge, K. M. Smith, and J. A. Shelnutt, *J. Am. Chem. Soc.* **115**, 581 (1993).
261. A. Stichternath, R. Schweitzer-Stenner, W. Dreybrodt, R. S. W. Mak, X.-Y. Li, L. D. Sparks, J. A. Shelnutt, C. J. Medforth, and K. M. Smith, *J. Phys. Chem.* **97**, 3701 (1993).
262. C. Piffat, D. Melamed, and T. G. Spiro, *J. Phys. Chem.* **97**, 7441 (1993).
263. M. L. Mitchell, X. -Y. Li, J. R. Kincaid, and T. G. Spiro, *J. Phys. Chem.* **91**, 4690 (1987).
264. H. Ogoshi, E. Watanabe, Z. Yoshida, J. R. Kincaid, and K. Nakamoto, *J. Am. Chem. Soc.* **95**, 2845 (1973).
265. P. G. Wright, P. Stein, J. M. Burke, and T. G. Spiro, *J. Am. Chem. Soc.* **101**, 3531 (1979).
266. R. S. Czernuszewicz, W. -D. Wagner, G. B. Ray, and K. Nakamoto, *J. Mol. Struct.* **242**, 99 (1991).
267. H. Oshio, T. Ama, T. Watanabe, and K. Nakamoto, *Inorg. Chim. Acta.* **96**, 61 (1985).
268. L. Galich, H. Hückstädt, and H. Homborg, *J. Porphyrins Phthalocyanines* **1**, 259 (1997).
269. D. Lu, I. R. Paeng, and K. Nakamoto, *J. Coord. Chem.* **23**, 3 (1991).
270. J. R. Kincaid and K. Nakamoto, *Spectrosc. Lett.* **9**, 19 (1976).
271. T. Kitagawa, M. Abe, Y. Kyogoku, H. Ogoshi, E. Watanabe, and Z. Yoshida, *J. Phys. Chem.* **80**, 1181 (1976).
272. T. G. Spiro, "The Resonance Raman Spectroscopy of Metalloporphyrins and Heme Proteins" in A. B. P. Lever and H. B. Gray, eds., *Iron Porphyrins*, Addison-Wesley, Reading, MA, 1983.
273. S. Asher and K. Sauer, *J. Chem. Phys.* **64**, 4115 (1976).
274. H. Ogoshi, E. Watanabe, Z. Yoshida, J. Kincaid, and K. Nakamoto, *Inorg. Chem.* **14**, 1344 (1975).
275. Y. Ozaki, T. Kitagawa, and H. Ogoshi, *Inorg. Chem.* **18**, 1772 (1979).
276. C. D. Tait, J. M. Garner, J. P. Collman, A. P. Sattelberger, and W. H. Woodruff, *J. Am. Chem. Soc.* **111**, 7806 (1989).
277. C. D. Tait, J. M. Garner, J. P. Collman, A. P. Sattelberger, and W. H. Woodruff, *J. Am. Chem. Soc.* **111**, 9072 (1989).
278. T. K. Duchowski and D. F. Bocian, *Inorg. Chem.* **29**, 4158 (1990).
279. J. K. Duchowski and D. F. Bocian, *J. Am. Chem. Soc.* **112**, 8807 (1990).
280. J. A. Shelnutt, *J. Phys. Chem.* **87**, 605 (1983).
281. R. G. Alden, M. R. Ondrias, and J. A. Shelnutt, *J. Am. Chem. Soc.* **112**, 691 (1990).
282. R. A. Reed, B. Purrello, K. Prendergast, and T. G. Spiro, *J. Phys. Chem.* **95**, 9720 (1991).
283. S. Hu, C. -Y. Lin, M. E. Blackwood, Jr., A. Mukherjee, and T. G. Spiro, *J. Phys. Chem.* **99**, 9694 (1995).
284. J. Teraoka, S. Hashimoto, H. Sugimoto, M. Mori, and T. Kitagawa, *J. Am. Chem. Soc.* **109**, 180 (1987).

285. E. Anxolabéhére, G. Chottard, and D. Lexa, *New J. Chem.* **18**, 889 (1994).

286. C. De Silva, K. Czarnecki, and M. D. Ryan, *Inorg. Chim. Acta* **287**, 21 (1999).

287. H. Ogoshi, E. Watanabe, Z. Yoshida, J. Kincaid, and K. Nakamoto, *Inorg. Chem.* **14**, 1344 (1975).

288. M. Atamian, R. J. Donohoe, J. S. Lindsey, and D. F. Bocian, *J. Phys. Chem.* **93**, 2236 (1989).

289. A. D. Procyk, Y. Kim, E. Schmidt, H. N. Fonda, C. K. Chang, G. T. Babcock, and D. F. Bocian, *J. Am. Chem. Soc.* **114**, 6539 (1992).

290. N. J. Boldt, R. J. Donohoe, R. R. Birge, and D. F. Bocian, *J. Am. Chem. Soc.* **109**, 2284 (1987).

291. A. Warshel and A. Lappicirella, *J. Am. Chem. Soc.* **103**, 4664 (1981).

292. A. D. Procyk, Y. Kim, E. Schmidt, H. N. Fonda, C.-K. Chang, G. T. Babcock, and D. F. Bocian, *J. Am. Chem. Soc.* **114**, 6539 (1992).

293. L. A. Anderson, T. M. Loehr, M. T. Stershic, and A. M. Stolzenberg, *Inorg. Chem.* **29**, 2278 (1990).

294. Y. Ozaki, K. Iriyama, H. Ogoshi, T. Ochiai, and T. Kitagawa, *J. Phys. Chem.* **90**, 6105 (1986).

295. Y. Ozaki, K. Iriyama, H. Ogoshi, T. Ochiai, and T. Kitagawa, *J. Phys. Chem.* **90**, 6113 (1986).

296. Y. Ozaki, T. Kitagawa, and H. Ogoshi, *Inorg. Chem.* **18**, 1772 (1979).

297. L. A. Anderson, T. M. Loehr, C. Sotiriou, W. Wu, and C. K. Chang, *J. Am. Chem. Soc.* **108**, 2908 (1986).

298. R. Donohoe, M. Atamian, and D. F. Bocian, *J. Phys. Chem.* **93**, 2244 (1989).

299. L. A. Anderson, T. M. Loehr, R. G. Thompson, and S. H. Strauss, *Inorg. Chem.* **29**, 2142 (1990).

300. C. Zhou, J. R. Diers, and D. F. Bocian, *J. Phys. Chem.* **101**, 9635 (1997).

301. M. Fujiwara and M. Tasumi, *J. Phys. Chem.* **90**, 250 (1986).

302. M. Tasumi and M. Fujiwara, "Vibrational Spectra of Chlorophylls," in R. J. H. Clark and R. E. Hester, eds., *Advances in Infrared and Raman Spectroscopy,* Vol. 14 *(Spectroscopy of Inorganic-Based Materials)*, Wiley, New York, 1987, p. 407.

303. R. Heald and T. M. Cotton, *J. Phys. Chem.* **94**, 3968 (1990).

304. G. A. Schick and D. F. Bocian, *Biochem. Biophys. Acta* **895**, 127 (1987).

305. M. Lutz and B. Robert, "Chlorophylls and the Photosynthetic Membrane" in T. G. Spiro,ed., Vol. 3 *(Biological Applications of Raman Spectroscopy), Resonance Raman Spectra of Heme and Metalloproteins*, Wiley, New York, 1988, p. 347.

306. C. A. Melendres and V. A. Maroni, *J. Raman Spectrosc.* **13**, 319 (1984).

307. B. Hutchinson, B. Spencer, R. Thompson, and P. Neill, *Spectrochim. Acta* **43A**, 631 (1987).

308. R. Aroca, Z. Q. Zeng, and J. Mink, *J. Phys. Chem. Solids* **51**, 135 (1990).

309. G. Ostendrop and H. Homborg, *Z. Anorg. Allg. Chem.* **622**, 873 (1996).

310. G. Ostendorp and H. Homborg, *Z. Anorg. Allg. Chem.* **622**, 235 and 1222 (1996).

311. G. Ostendrop and H. Homborg, *Z. Anorg. Allg. Chem.* **622**, 1358 (1996).

312. M. Goldner, H. Huckstadt, K. S. Murray, B. Moubaraki, and H. Homborg, *Z. Anorg. Allg. Chem.* **624**, 288 (1998).

313. B. Berno, A. Nazri, and R. Aroca, *J. Raman Spectrosc.* **27**, 41 (1996).
314. S. Sievertsen, H. Grunewald, and H. Homborg, *Z. Anorg. Allg. Chem.* **622**, 1573 (1996).
315. H. Huckstadt and H. Homborg, *Z. Anorg. Allg. Chem.* **623**, 292 (1997).
316. H. Schlehahn and H. Homborg, *Z. Anorg. Allg. Chem.* **621**, 1558 (1995).
317. S. Sievertsen, M. Weidemann, O. Tsantsi-Krause, and H. Homborg, *Z. Anorg. Allg. Chem.* **621**, 1567 (1995).
318. K. Schweiger, M. Goldner, H. Huckstadt, and H. Homborg, *Z. Anorg. Allg. Chem.* **625**, 1693 (1999).
319. M. Weidemann, H. Huckstadt, and H. Homborg, *Z. Anorg. Allg. Chem.* **624**, 846 (1998).
320. K. Schweiger, H. Huckstadt, and H. Homborg, *Z. Naturforsch.* **54B**, 963 (1999).
321. A. Kienast, L. Galich, K. S. Murray, B. Moubaraki, G. Lazarev, J. D. Cushion, and H. Homborg, *J. Porphyrins Phthalocyanines* **1**, 141 (1997).
322. M. P. Donzello, C. Ercolani, K. M. Kadish, Z. Ou, and U. Russo, *Inorg. Chem.* **37**, 3682 (1998).
323. M. J. Cook, "Optical and Infrared Spectroscopy of Phthalocyanine Molecular Assemblies," in R. J. H. Clark and R. E. Hester, eds., *(Biomedical Applications of Spectroscopy), Advances in Infrared and Raman Spectroscopy*, Vol. 25, Wiley, New York, 1996, p. 87.
324. I. Nakagawa, T. Shimanouchi, and K. Yamasaki, *Inorg. Chem.* **3**, 772 (1964); **7**, 1332 (1968).
325. M. Le Postolloe, J. P. Mathieu, and H. Poulet, *J. Chim. Phys.* **60**, 1319 (1963).
326. M. J. Cleare and W. P. Griffith, *J. Chem. Soc. A* 1144 (1967).
327. M. J. Nolan and D. W. James, *Aust. J. Chem.* **23**, 1043 (1970).
328. J. T. Huneke, B. Meisner, L. Walford, and R. L. Bain, *Spectrosc. Lett.* **7**, 91 (1974).
329. D. W. James and M. J. Nolan, *Aust J. Chem.* **26**, 1433 (1973).
330. K. Kanamori, A. Shimizu, H. Sekino, S. Hayakawa, Y. Seki, and K. Kawai, *J. Chem. Soc, Dalton Trans.* 1827 (1988).
331. P. E. Merritt and S. E. Wiberley, *J. Phys. Chem.* **59**, 55 (1955).
332. R. B. Hagel and L. F. Druding, *Inorg. Chem.* **9**, 1496 (1970).
333. I. Nakagawa and T. Shimanouchi, *Spectrochim. Acta* **23A**, 2099 (1967).
334. M. J. Nolan and D. W. James, *Aust. J. Chem.* **26**, 1413 (1973).
335. K. Nakamoto, J. Fujita, and H. Murata, *J. Am. Chem. Soc.* **80**, 4817 (1958).
336. D. M. L. Goodgame and M. A. Hitchman, *Inorg. Chem.* **3**, 1389 (1964).
337. W. W. Fee, C. S. Garner, and J. N. M. Harrowfield, *Inorg. Chem.* **6**, 87 (1967).
338. D. M. L. Goodgame, M. A. Hitchman, D. F. Marsham, and C. E. Souter, *J. Chem. Soc. A*, 2464 (1969).
339. D. Ooyama, N. Nagao, H. Nagao, Y. Miura, A. Hasegawa, K. Ando, F. S. Howell, M. Mukaida, and K. Tanaka, *Inorg. Chem.* **34**, 6024 (1995).
340. D. M. L. Goodgame and M. A. Hitchman, *Inorg. Chem.* **6**, 813 (1967).
341. L. El-Sayed and R. O. Ragsdale, *Inorg. Chem.* **6**, 1640 (1967).
342. R. B. Penland, T. J. Lane, and J. V. Quagliano, *J. Am. Chem. Soc.* **78**, 887 (1956).
343. I. R. Beattie and D. P. N. Satchell, *J. Chem. Soc. Faraday Trans.* **52**, 1590 (1956).
344. A. M. Heyns and D. de Waal, *Spectrochim. Acta* **45A**, 905 (1989).

345. J. L. Burmeister, *Coord. Chem. Rev.* **3**, 225 (1968).
346. D. M. L. Goodgame and M. A. Hitchman, *Inorg. Chem.* **4**, 721 (1965).
347. K. L. Leighton, K. R. Grundy, and K. N. Robertson, *J. Organomet. Chem.* **371**, 321 (1989).
348. R. Birdy, D. M. L. Goodgame, J. C. McConway, and D. Rogers, *J. Chem. Soc., Dalton Trans.* 1730 (1977).
349. D. M. L. Goodgame and M. A. Hitchman, *J. Chem. Soc. A*, 612 (1967).
350. D. M. L. Goodgame, M. A. Hitchman, and D. F. Marsham, *J. Chem. Soc. A*, 1933 (1970).
351. I. E. Gray, M. A. Hitchman, G. L. Rowbottom, N. V. Y. Scalett, and J. Wilson, *J. Chem. Soc., Dalton Trans.* 595 (1994).
352. W. J. Lo, M.-Y. Shen, C.-H. Yu, and Y.-P. Lee, *J. Chem. Phys.* **104**, 935 (1996).
353. U. Thewalt and R. E. Marsh, *Inorg. Chem.* **9**, 1604 (1970).
354. S. Kubo, T. Shibahara, and M. Mori, *Bull. Chem. Soc. Jpn.* **52**, 101 (1979).
355. K. Wieghardt and H. Siebert, *Z Anorg. Allg. Chem.* **374**, 186 (1970).
356. D. M. L. Goodgame, M. A. Hitchman, D. F. Marsham, P. Phavanantha, and D. Rogers, *Chem. Commun.* 1383 (1969).
357. D. M. L. Goodgame, M. A. Hitchman, and D. F. Marsham, *J. Chem. Soc. A*, 259 (1971).
358. M. Hass and G. B. B. M. Sutherland, *Proc. Roy. Soc. Lond. A*, **236**, 427 (1956).
359. V. P. Tayal, B. K. Srivastava, D. P. Khandelwal, and H. D. Bist, *Appl. Spectrosc. Rev.* **16**, 43 (1980).
360. J. O. Lundgren and I. Olovsson, *Acta Crystallogr.* **23**, 966 (1967).
361. A. C. Pavia and P. A. Giguère, *J. Chem. Phys.* **52**, 3551 (1970).
362. A. Nakahara, Y. Saito, and H. Kuroya, *Bull. Chem. Soc. Jpn.* **25**, 331 (1952).
363. J. M. Williams, *Inorg. Nucl. Chem. Lett.* **3**, 297 (1967).
364. J. Roziere and J. Potier, *J. Inorg. Nucl. Chem.* **35**, 1179 (1973).
365. I. Nakagawa and T. Shimanouchi, *Spectrochim. Acta* **20**, 429 (1964).
366. V. Stefov, V. M. Petrusevski, and B. Soptajanov, *J. Mol. Struct.* **293**, 97 (1993).
367. C. C. Pye and W. W. Rudolph, *J. Phys. Chem. A*, **102**, 9933 (1998).
368. W. W. Rudorf and G. Irmer, *J. Phys. Chem. B*, **102**, 3564 (1998).
369. W. W. Rudorf, R. Mason, and C. C. Pye, *Phys. Chem. Chem. Phys.* **2**, 5030 (2000).
370. W. W. Rudorf, C. C. Pye, and G. Irmer, *J. Raman Spectrosc.* **33**, 177 (2002).
371. C. R. Clark, C. E. F. Rickard, and M. J. Taylor, *Can. J. Chem.* **64**, 1697 (1986).
372. D. M. Adams and P. J. Lock, *J. Chem. Soc. A*, 2801 (1971).
373. Y. Chen, D. H. Christenson, O. F. Nielsen, and E. Pedersen, *J. Mol. Struct.* **294**, 215 (1993).
374. F. Agullo-Reuda, J. M. Calleja, M. Martini, G. Spinolo, and F. Cariati, *J. Raman Spectrosc.* **18**, 485 (1987).
375. S. P. Best, R. S. Armstrong, and J. K. Beattie, *J. Chem. Soc., Dalton Trans.* 299 (1992).
376. C. W. Bauschlicher, S. R. Langhoff, H. Partridge, J. E. Rice, and A. Komornicki, *J. Chem. Phys.* **95**, 5142 (1991).
377. R. E. Hester and R. A. Plane, *Inorg. Chem.* **3**, 768 (1964).
378. Y. Kameda, K. Sugawara, T. Usuki, and O. Uemura, *Bull. Chem. Soc. Jpn.* **71**, 2769 (1998).

379. Y. Kameda, H. Ebata, and O. Uemura, *Bull. Chem. Soc. Jpn.* **67**, 929 (1994).
380. H. L. Schlafer and H. P. Fritz, *Spectrochim. Acta* **23A**, 1409 (1967).
381. T. G. Chang and D. E. Irish, *Can. J. Chem.* **51**, 118 (1973).
382. H. Boutin, G. J. Safford, and H. R. Danner, *J. Chem. Phys.* **40**, 2670 (1964); H. J. Prask and H. Boutin, *ibid*. **45**, 699, 3284 (1966).
383. J. J. Rush, J. R. Ferraro, and A. Walker, *Inorg. Chem.* **6**, 346 (1967).
384. B. S. Ault, *J. Am. Chem. Soc.* **100**, 2426 (1978).
385. L. Manceron, A. Loutellier, and J. P. Perchard, *Chem. Phys.* **92**, 75 (1985).
386. J. W. Kauffman, R. H. Hauge, and J. L. Margrave, *High Temp. Sci.* **18**, 97 (1984).
387. B. Liang, L. Andrews, J. Li, and B. E. Bursten, *J. Am. Chem. Soc.* **124**, 6723 (2002).
388. M. Zhou, L. Zhang, L. Shao, W. Wang, K. Fan, and Q. Qin, *J. Phys. Chem. A* **105**, 5801 (2001).
389. L. Zhang, J. Dong, and M. Zhou, *J. Phys. Chem. A*, **104**, 8882 (2000).
390. M. Zhou, L. Zhang, J. Dong, and Q. Qin, *J. Am. Chem. Soc.* **122**, 10680 (2000).
391. T. Dupius, C. Duval, and J. Lecomte, *C. R. Hebd. Seances Acad. Sci.* **257**, 3080 (1963).
392. M. Maltese and W. J. Orville-Thomas, *J. Inorg. Nucl. Chem.* **29**, 2533 (1967).
393. R. Minkwitz and S. Schneider, *Angew. Chem. Int. Ed. Engl.* **38**, 210 (1999).
394. J. R. Ferraro and W. R. Walker, *Inorg. Chem.* **4**, 1382 (1965).
395. J. Li, W. Li, and P. R. Sharp, *Inorg. Chem.* **35**, 604 (1996).
396. M. Manfait, A. J. P. Alix, J. Delaunay-Zeches, and T. Theophanides, *Can. J. Chem.* **60**, 2216 (1982).
397. A. Wada, M. Harata, K. Hasegawa, K. Jitsukawa, H. Masuda, M. Mukai, T. Kitagawa, and H. Einaga, *Angew. Chem. Int. Ed. Engl.* **37**, 798 (1998).
398. R. W. Adams, R. L. Martin, and G. Winter, *Aust. J. Chem.* **20**, 773 (1967).
399. R. C. Mehrotra and J. M. Batwara, *Inorg. Chem.* **9**, 2505 (1970).
400. L. M. Brown and K. S. Mazdiyasni, *Inorg. Chem.* **9**, 2783 (1970).
401. G. Tatzel, M. Greune, J. Weidlein, and E. Jocob, *Z. Anorg. Allg. Chem.* **533**, 83 (1986).
402. B. S. Ault and J. B. Everhart, *J. Phys. Chem.* **100**, 15726 (1996).
403. L. Ohrström and I. Michaud-Soret, *J. Am. Chem. Soc.* **118**, 3283 (1996).
404. P. W. N. M. van Leeuwen, *Recl. Trav. Chim. Pays-Bas* **86**, 247 (1967).
405. D. Knetsch and W. L. Groeneveld, *Inorg. Chim. Acta* **7**, 81 (1973).
406. S. Halut-Desportes and E. Musson, *Spectrochim. Acta* **41A**, 661 (1985).
407. H. Wieser and P. J. Knieger, *Spectrochim. Acta* **26A**, 1349 (1970).
408. G. W. A. Fowles, D. A. Rice, and R. A. Walton, *Spectrochim. Acta* **26A**, 143 (1970).
409. S. Magull, K. Dehnicke, and D. Fenske, *Z Anorg. Allg. Chem.* **608**, 17 (1992).
410. A. Neuhaus, G. Frenzen, J. Pebler, and K. Dehnicke, *Z. Anorg. Allg. Chem.* **618**, 93 (1992).
411. L. A. Kloo and M. J. Taylor, *J. Chem. Soc., Dalton Trans.* 2693 (1997).
412. T. Lu, M. Tan, H. Su, and Y. Liu, *Polyhedron* **12**, 1055 (1993).
413. H. Takeuchi, T. Arai, and I. Harada, *J. Mol Struct.* **146**, 197 (1986).
414. W. L. Driessen and W. L. Groeneveld, *Recl. Trav. Chim. Pays-Bas* **88**, 977 (1969).
415. W. L. Driessen and W. L. Groeneveld, *Recl. Trav. Chim. Pays-Bas* **90**, 258 (1971).

416. W. L. Driessen and W. L. Groeneveld, *Recl. Trav. Chim. Pays-Bas* **90**, 87 (1971).
417. W. L. Driessen, W. L. Groeneveld, and F. W. Van der Wey, *Recl. Trav. Chim. Pays-Bas* **89**, 353 (1990).
418. Z. Deng and D. E. Irish, *J. Chem. Soc, Faraday Soc.* **88**, 2891 (1992).
419. D. B. Powell and A. Woollins, *Spectrochim. Acta.* **41A**, 1023 (1985).
420. K. Itoh and H. J. Bernstein, *Can. J. Chem.* **34**, 170 (1956).
421. G. B. Deacon and R. J. Phillips, *Coord. Chem. Rev.* **33**, 227 (1980).
422. P. Drożdżewski, A. Brożyna, and M. Kubiak, *J. Mol. Struct.* **707**, 131 (2004).
423. P. Drożdżewski and A. Brożyna, *Spectrochim. Acta A*, **62**, 701 (2005).
424. T. Giowiak, H. Kozlowski, I. S. Erre, and G. Micera, *Inorg. Chim. Acta*, **236**, 149 (1995).
425. S. D. Robinson and M. F. Uttley, *J. Chem. Soc*, 1912 (1973).
426. B. P. Straughan, W. Moore, and R. McLaughlin, *Spectrochim. Acta* **42A**, 451 (1986).
427. N. W. Alcock, J. Culver, and S. M. Roe, *J. Chem. Soc., Dalton Trans.* 1477 (1992).
428. G. Csontós, B. Heil, and C. Markó, *J. Organomet. Chem.* **37**, 183 (1972).
429. G. Süss-Fink, G. Herrmann, P. Morys, J. Ellermann, and A. Veit, *J. Organomet. Chem.* **284**, 263 (1985).
430. J. P. Bourke, R. D. Cannon, G. Grinter, and U. A. Jayasooriya, *Spectrochim. Acta* **49A**, 685 (1993).
431. S. Pal, J. W. Gohdes, W. C. A. Wilisch, and W. H. Armstrong, *Inorg. Chem.* **31**, 713 (1992).
432. T. A. Stephenson and G. Wilkinson, *J. Inorg. Nucl. Chem.* **29**, 2122 (1967).
433. R. Kapoor, R. Sharma, and P. Kapoor, *Z. Naturforsch.* **39B**, 1702 (1984).
434. H.-M. Gau, C.-T. Chen, T.-T. Jong, and M.-Y. Chien, *J. Organomet. Chem.* **448**, 99 (1993).
435. D. Stoilova, G. Nikolov, and K. Balarev, *Izv. Akad. Nauk SSSR, Ser. Khim.* **9**, 371 (1976).
436. G. Busca and V. Lorenzelli, *Miner. Chem.* **7**, 89 (1982).
437. S. Baba and S. Kawaguchi, *Inorg. Nucl. Chem. Lett.* **9**, 1287 (1973).
438. J. Vicente, M. T. Chicote, M. D. Bermudez, and M. Garcia-Garcia, *J. Organomet. Chem.* **295**, 125 (1985).
439. K. Nakamoto, P. J. McCarthy, and B. Miniatus, *Spectrochim. Acta* **21**, 379 (1965).
440. M. Matzapetakis, N. Karligiano, A. Bino, M. Dakanall, C. P. Raptopoulon, V. Tangoulis, A. Terzis, J. Giapintzakis, and A. Salifoglon, *Inorg. Chem.* **39**, 4044 (2000).
441. M. Tsuboi, T. Onishi, I. Nakagawa, T. Shimanouchi, and S. Mizushima, *Spectrochim. Acta* **12**, 253 (1958).
442. K. Fukushima, T. Onishi, T. Shimanouchi, and S. Mizushima, *Spectrochim. Acta* **14**, 236 (1959).
443. A. J. Stosick, *J. Am. Chem. Soc.* **67**, 365 (1945).
444. K. Nakamoto, Y. Morimoto, and A. E. Martell, *J. Am. Chem. Soc.* **83**, 4528 (1961).
445. R. A. Condrate and K. Nakamoto, *J. Chem. Phys.* **42**, 2590 (1965).
446. J. Kincaid and K. Nakamoto, *Spectrochim. Acta* **32A**, 277 (1976).
447. M. L. Niven and D. A. Thornton, *Inorg. Chim. Acta* **32**, 205 (1979).
448. J. B. Hodgson, G. C. Percy, and D. A. Thornton, *Spectrochim. Acta* **35A**, 949 (1979).

449. G. C. Percy and H. S. Stenton, *J. Chem. Soc., Dalton Trans.* 2429 (1976).
450. A. W. Herlinger, S. L. Wenhold, and T. V. Long, II, *J. Am. Chem. Soc.* **92**, 6474 (1970).
451. A. W. Herlinger and T. V. Long, II, *J. Am. Chem. Soc.* **92**, 6481 (1970).
452. J. A. Kieft and K. Nakamoto, to be published.
453. J. A. Kieft and K. Nakamoto, *J. Inorg. Nucl. Chem.* **29**, 2561 (1967).
454. J. R. Kincaid, J. A. Larrabee, and T. G. Spiro, *J. Am. Chem. Soc.* **100**, 334 (1978).
455. Y. Inomata, A. Shibata, Y. Yukawa, T. Takeuchi, and T. Moriwaki, *Spectrochim. Acta* **44A**, 97 (1988).
456. P. Drożdżewski and E. Kordon, *Spectrochim. Acta* **56A**, 2459 (2000).
457. P. Drożdżewski and E. Kordon, *Spectrochim. Acta* **56A**, 1299 (2000).
458. P. Drożdżewski and E. Kordon, *Vib. Spectrosc.* **24**, 243 (2000).
459. P. Drożdżewski, E. Kordon, and S. Roszak, *Int. J. Quantum Chem.* **96**, 355 (2004).
460. D. H. Busch and J. C. Bailar, Jr., *J. Am. Chem. Soc.,* **75**, 4574 (1953); **78**, 716 (1956); M. L. Morris, D. H. Busch *ibid*. 5178; K. Swaminathan and D. H. Busch, *J. Inorg. Nucl. Chem.* **20**, 159 (1961); R. E. Sievers and J. C. Bailar, Jr., *Inorg. Chem.* **1**, 174 (1962).
461. D. Chapman, *J. Chem. Soc.* 1766 (1955).
462. E. Faulques, D. L. Perry, S. Lott, J. D. Zubkowski, and E. J. Valente, *Spectrochim. Acta* **54A**, 869 (1998).
463. Y. Tomita and K. Ueno, *Bull. Chem. Soc. Jpn.* **36**, 1069 (1963).
464. K. Krishnan and R. A. Plane, *J. Am. Chem. Soc.* **90**, 3195 (1968).
465. A. A. McConnell and R. H. Nuttall, *Spectrochim. Acta* **33A**, 459 (1977).
466. W. S. Caughey, "Methods for Determining Metal Ion Environments," in D. W. Darnell and R. Wilkins, eds., *Proteins: Structure and Function of Metalloproteins*, Elsevier, New York, 1980, p. 95.
467. E. G. Bartick, and R. G. Messerschmidt, *Am. Lab.* Nov. 1984, p. 56.
468. N. A. Marley, J. S. Gaffney, and M. M. Cunningham, *Spectroscopy* **7**, 44 (1992).
469. S. Fronaeus and R. Larsson, *Acta Chem. Scand.* **16,** 1433,1447 (1962).
470. S. Fronaeus and R. Larsson, *Acta Chem. Scand.* **14**, 1364 (1960).
471. R. Larsson, *Acta Chem. Scand.* **19**, 783 (1965).
472. K. Nakamoto, Y. Morimoto, and A. E. Martell, *J. Am. Chem. Soc.* **84**, 2081 (1962).; **85**, 309 (1963).
473. Y. Tomita, T. Ando, and K. Ueno, *J. Phys. Chem.* **69**, 404 (1965).
474. Y. Tomita and K. Ueno, *Bull. Chem. Soc. Jpn.* **36**, 1069 (1963).
475. A. E. Martell and M. K. Kim, *J. Coord. Chem.* **4**, 9 (1974).
476. M. K. Kim and A. E. Martell, *J. Am. Chem. Soc.* **85**, 3080 (1963).
477. M. K. Kim and A. E. Martell, *Biochemistry* **3**, 1169 (1964).
478. M. K. Kim and A. E. Martell, *J. Am. Chem. Soc.* **88**, 914 (1966).
479. M. Tasumi, S. Takahashi, T. Nakata, and T. Miyazawa, *Bull. Chem. Soc. Jpn.* **48**, 1595 (1975).
480. T. P. A. Kruck and B. Sarkar, *Can. J. Chem.* **51**, 3563 (1973).
481. J. Fujita, A. E. Martell, and K. Nakamoto, *J. Chem. Phys.* **36,** 324, 331 (1962).

482. R. D. Hancock and D. A. Thornton, *J. Mol. Struct.* **6**, 441 (1970).
483. J. Gouteron, *J. Inorg. Nucl. Chem.* **38**, 55 (1976).
484. H. G. M. Edwards and P. H. Hardman, *J. Mol Struct.* **273**, 73 (1992).
485. H. Homborg, W. Preetz, G. Barka, and G. Schätzel, *Z Naturforsch*. **35B**, 554 (1980).
486. W. Preetz and A. Krull, *Z. Naturforsch.* **52B**, 315 (1997).
487. J.-G. Uttecht and W. Preetz, *Z. Anorg. Allg. Chem.* **628**, 965 (2002).
488. W. Preetz and J. G. Uttecht, *Z. Naturforsch.* **53B**, 93 (1998).
489. L. Ohrstrum and I. Michaud-Soret, *J. Phys. Chem. A*, **103**, 256 (1999).
490. K. L. Scott, K. Wieghardt, and A. G. Sykes, *Inorg. Chem.* **12**, 655 (1973); K. Wieghardt, *Z. Anorg. Allg. Chem.* **391**, 142 (1972).
491. D. Coucouvanis, K. D. Demadis, C. G. Kim, R. W. Dunham, and J. W. Kampf, *J. Am. Chem. Soc.* **115**, 3344 (1993).
492. V. M. Masters, C. A. Sharkad, P. V. Bernhardt, L. R. Gahan, B. Moubaraki, and K. S. Murray, *J. Chem. Soc., Dalton Trans.* 413 (1998).
493. R. E. Hester and R. A. Plane, *Inorg. Chem.* **3**, 513 (1964); E. C. Gruen and R. A. Plane, *ibid*. **6**, 1123 (1967).
494. P. X. Armendarez and K. Nakamoto, *Inorg. Chem.* **5**, 796 (1966).
495. P. Fischer, R. Graf, and J. Weidlein, *J. Organomet. Chem.* **144**, 95 (1978).
496. F. Quaeyhagens, H. Hofmans, and H. O. Desseyn, *Spectrochim. Acta* **43A**, 531 (1987).
497. B. B. Kedzia, P. X. Armendarez, and K. Nakamoto, *J. Inorg. Nucl. Chem.* **30**, 849 (1968).
498. L. Cavalca, M. Nardelli, and G. Fava, *Acta Crystallogr.* **13**, 594 (1960).
499. Y. Saito, K. Machida, and T. Uno, *Sectrochim. Acta* **26A**, 2089 (1970).
500. T. J. Thamann and T. M. Loehr, *Spectrochim. Acta* **36A**, 751 (1980).
501. K. Nakamoto, J. Fujuta, S. Tanaka, and M. Kobayashi, *J. Am. Chem. Soc.* **79**, 4904 (1957).
502. C. G. Barraclough and M. L. Tobe, *J. Chem. Soc*, 1993 (1961).
503. R. Eskenazi, J. Rasovan, and R. Levitus, *J. Inorg. Nucl. Chem.* **28**, 521 (1966).
504. H. A. dos Santos-Silva, B. R. McGarvey, R. H. de Almeida-Santos, M. Bertotti, V. Mori, and D. W. Franco, *Can. J. Chem.* **79**, 679 (2001).
505. J. R. Ferraro and A. Walker, *J. Chem. Phys.* **42**, 1278 (1965).
506. N. Tanaka, H. Sugi, and J. Fujita, *Bull. Chem. Soc. Jpn.* **37**, 640 (1964).
507. J. A. Goldsmith, A. Hezel, and S. D. Ross, *Spectrochim. Acta* **24A**, 1139 (1968).
508. J. E. Finholt, R. W. Anderson, J. A. Fyfe, and K. G. Caulton, *Inorg. Chem.* **4**, 43 (1965).
509. M. N. Bhattacharjee, M. K. Chaudhuri, and N. S. Islam, *Inorg. Chem.* **28**, 2420 (1989).
510. W. R. McWhinnie, *J. Inorg. Nucl. Chem.* **26**, 21 (1964).
511. I. S. Ahuja, *Inorg. Chim. Acta* **3**, 110 (1969).
512. K. Wieghardt and J. Eckert, *Z. Anorg. Allg. Chem.* **383**, 240 (1971).
513. R. Ugo, F. Conti, S. Cenini, R. Mason, and G. B. Robertson, *Chem. Commun.* 1498 (1968).
514. R. W. Horn, E. Weissberger, and J. P. Collman, *Inorg. Chem.* **9**, 2367 (1970).
515. M. K. Chaudhuri and N. S. Islam, *Inorg. Chem.* **25**, 3749 (1986).

516. V. N. Krasil'nikov, *Russ. J. Inorg. Chem.* (*Engl. transl.*) **30**, 1499 (1985).
517. M. R. Rosenthal, *J. Chem. Educ.* **50**, 331 (1973).
518. B. J. Hathaway and A. E. Underhill, *J. Chem. Soc.* 3091 (1961).
519. B. J. Hathaway, D. G. Holah, and M. Hudson, *J. Chem. Soc.* 4586 (1963).
520. M. E. Farago, J. M. James, and V. C. G. Trew, *J. Chem. Soc. A* 820 (1967).
521. A. E. Wickenden and R. A. Krause, *Inorg. Chem.* **4**, 404 (1965).
522. L. E. Moore, R. B. Gayhart, and W. E. Bull, *J. Inorg. Nucl. Chem.* **26**, 896 (1964).
523. M. Fourati, M. Chaabouni, J. L. Pascal, and J. Potier, *Can. J. Chem.* **67**, 1693 (1989).
524. F. Cunin, C. Deudon, F. Favier, B. Mula, and J. L. Pascal, *Inorg. Chem.* **41**, 4173 (2002).
525. F. Cunin, F. Favier, and J. L. Pascal, *Can. J. Chem.* **78**, 1544 (2000).
526. T. Chausse, A. Potier, and J. Potier, *J. Chem. Res. S*, 316 (1980).
527. M. Fourati, M. Chaabouni, H. F. Ayedi, J. L. Pascal, and J. Potier, *Can. J. Chem.* **63**, 3499 (1985).
528. J. L. Pascal, J. Potier, and C. S. Zhang, *J. Chem. Soc., Dalton Trans*. 297 (1985).
529. F. Favier and J. L. Pascal, *J. Chem. Soc., Dalton Trans.* 1997 (1992).
530. L. S. Skogareva, V. P. Babaeva, and V. Ya. Rosolovskii, *Russ. J. Inorg. Chem.* (*Engl. transl.*) **31**, 500 (1986).
531. Z. K. Nikitina, N. V. Krivtsov, Yu. V. Chuprakov, and V. Ya. Rosolovskii, *Russ. J. Inorg. Chem.* (*Engl. transl.*) **33**, 1143 (1988).
532. S. F. Lincoln and D. R. Stranks, *Aust. J. Chem.* **21**, 37 (1968).
533. T. A. Beech and S. F. Lincoln, *Aust. J. Chem.* **24**, 1065 (1971).
534. R. Coomber and W. P. Griffith, *J. Chem. Soc.* 1128 (1968).
535. S. D. Ross and N. A. Thomas, *Spectrochim. Acta* **26A**, 971 (1970).
536. M. A. Soldatkina, L. B. Serezhkina, and V. N. Serezhkin, *Russ. J. Inorg. Chem.* (*Engl. transl.*) **30**, 1323 (1985).
537. R. I. Bickley, H. G. M. Edwards, R. E. Gustar, and J. K. F. Tait, *J. Mol. Struct.* **273**, 61 (1992).
538. P. A. Tanner, S. T. Hung, T. C. W. Mak, and R. J. Wang, *Polyhedron* **11**, 817 (1992).
539. D. S. Bohle and H. Vahrenkamp, *Inorg. Chem.* **29**, 1097 (1990).
540. A. N. Freedman and B. P. Straughan, *Spectrochim. Acta* **27A**, 1455 (1971).
541. C. F. Edwards, W. P. Griffith, and D. J. Williams, *J. Chem. Soc., Dalton Trans.* 145 (1992).
542. P. A. Yeats, J. R. Sams, and F. Aubke, *Inorg. Chem.* **12**, 328 (1973).
543. S. D. Brown and G. L. Gard, *Inorg. Chem.* **17**, 1363 (1978).
544. P. C. Leung and F. Aubke, *Can. J. Chem.* **62**, 2892 (1984).
545. D. Zhang, S. J. Retting, J. Trotter, and F. Aubke, *Inorg.Chem.* **35**, 6113 (1996).
546. B. M. Gatehouse, S. E. Livingstone, and R. S. Nyholm, *J. Chem. Soc.* 3137 (1958).
547. J. Fujita, A. E. Martell, and K. Nakamoto, *J. Chem. Phys.* **36**, 339 (1962).
548. R. E. Hester and W. E. L. Grossman, *Inorg. Chem.* **5**, 1308 (1966).
549. J. A. Goldsmith and S. D. Ross, *Spectrochim. Acta* **24A**, 993 (1968).
550. M. Dahm and A. Adam, *Z. Anorg. Allg. Chem.* **627**, 2023 (2001).
551. C. Xu, L. Manceron, and J. P. Perchard, *J. Mol. Struct.* **300**, 83 (1993).

552. H. Elliott and B. J. Hathaway, *Spectrochim. Acta* **21**, 1047 (1965).
553. M. R. Churchill, R. A. Lashewycz, K. Koshy, and T. P. Dasgupta, *Inorg. Chem.* **20**, 376 (1981).
554. M. R. Churchill, G. Davies, M. A. El-Sayed, M. F. El-Shazly, J. P. Hutchinson, and M. W. Rupich, *Inorg. Chem.* **19**, 201 (1980).
555. A. Geilenkirchen, P. Neubold, R. Schneider, K. Wieghardt, U. Florke, H.-J. Haupt, and B. Nuber, *J. Chem. Soc., Dalton Trans.* 457 (1994).
556. A. Fscuer, R. Vicente, S. B. Kumar, X. Solans, M. Font-Bardia, and A. Caneschi, *Inorg. Chem.* **35**, 3094 (1996).
557. A. M. Greenaway, T. P. Dasgupta, K. C. Koshy, and G. G. Sadler, *Spectrochim. Acta* **42A**, 954 (1986).
558. J. S. Ogden and S. J. Williams, *J. Chem. Soc., Dalton Trans.* 456 (1981).
559. G. Busca and V. Lorenzelli, *Mater. Chem.* **7**, 89 (1982).
560. C. C. Addison, N. Logan, S. C. Wallwork, and C. D. Barner, *Q. Rev., Chem. Soc.* **25**, 289 (1971).
561. B. M. Gatehouse, S. E. Livinstone, and R. S. Nyholm, *J. Chem. Soc.* 4222 (1957); *J. Inorg. Nucl. Chem.* **8**, 75 (1958).
562. N. F. Curtis and Y. M. Curtis, *Inorg. Chem.* **4**, 804 (1965).
563. C. C. Addison, R. Davis, and N. Logan, *J. Chem. Soc. A* 3333 (1970).
564. B. Lippert, C. J. L. Lock, B. Rosenberg, and M. Zvagulis, *Inorg. Chem.* **16**, 1525 (1977).
565. C. C. Addison and W. B. Simpson, *J. Chem. Soc.* 598 (1965).
566. J. G. Allpress and A. N. Hambly, *Aust. J. Chem.* **12**, 569 (1959).
567. R. J. Fereday, N. Logan, and D. Sutton, *J. Chem. Soc. A* 2699 (1969).
568. D. W. Johnson and D. Sutton, *Can. J. Chem.* **50**, 3326 (1972).
569. N. Logan and W. B. Simpson, *Spectrochim. Acta* **21**, 857 (1965).
570. E. J. Duff, M. N. Hughes, and K. J. Rutt, *J. Chem. Soc. A* 2126 (1969).
571. E. M. Briggs and A. E. Hill, *J. Chem. Soc. A*, 2008 (1970).
572. A. G. M. Al-Daher, K. W. Bagnall, E. Forsellini, F. Benetollo, and G. Bombieri, *J. Chem. Soc, Dalton Trans.* 615 (1986).
573. J. C. G. Bünzli, J. P. Metabanzoulou, P. Froidevaux, and L. Jin, *Inorg. Chem.* **29**, 3875 (1990).
574. D. Grdenic, B. Korpar-Colig, and D. Matkovic-Calogovic, *J. Organomet. Chem.* **522**, 297 (1996).
575. S. Arrowsmith, M. F. A. Dove, N. Logan, and A. Batsanov, *Polyhedron* **17**, 421 (1998).
576. E. L. Varetti, S. A. Brandán, and A. Ben Altabef, *Vib. Spectrosc.* **5**, 219 (1993).
577. A. B. P. Lever, E. Mantovani, and B. S. Ramaswamy, *Can. J. Chem.* **49**, 1957 (1971).
578. J. R. Ferraro, A. Walker, and C. Cristallini, *Inorg. Nucl. Chem. Lett.* **1**, 25 (1965).
579. C. C. Addison, D. W. Amos, D. Sutton, and W. H. H. Hoyle, *J. Chem. Soc.* 808 (1967).
580. R. H. Nuttall and D. W. Taylor, *Chem. Commun.* 1417 (1968).
581. J. I. Bullock and F. W. Parrett, *Chem. Commun.* 157 (1969).
582. J. R. Ferraro and A. Walker, *J. Chem. Phys.* **42**, 1273 (1965).;**43**, 2689 (1965); **45**, 550 (1966).
583. D. E. Irish and G. E. Walrafen, *J. Chem. Phys.* **46**, 378 (1967).

584. P. M. Castro and P. W. Jagodzinski, *Spectrochim. Acta* **47A**, 1707 (1991); *J. Phys. Chem.* **96**, 5296 (1992).
585. R. E. Hester and K. Krishnan, *J. Chem. Phys.* **46**, 3405 (1967).;**47**, 1747 (1967).
586. P. K. Wick, R. Kissner, and W. H. Koppenol, *Helv. Chim. Acta* **83**, 748 (2000).
587. F. A. Cotton and R. Francis, *J. Am. Chem. Soc.* **82**, 2986 (1960).
588. G. Newman and D. B. Powell, *Spectrochim. Acta* **19**, 213 (1963).
589. M. E. Baldwin, *J. Chem. Soc.* 3123 (1961).
590. B. Nyberg and R. Larsson, *Acta Chem. Scand.* **27**, 63 (1973).
591. J. P. Hall and W. P. Griffith, *Inorg. Chim. Acta* **48**, 65 (1981).
592. D. K. Breitinger, H. Meinberg, and A. Bogner, *J. Mol. Struct.* **482/483**, 131 (1999).
593. D. K. Breitinger, A. Bogner, and H. Meinberg, *J. Mol. Struct.* **408/409**, 387 (1997).
594. R. Krieglstein and D. K. Breitinger, *J. Mol. Struct.* **408/409**, 379 (1997).
595. A. D. Fowless and D. R. Stranks, *Inorg. Chem.* **16**, 1271 (1977).
596. R. C. Elder and P. E. Ellis, Jr., *Inorg. Chem.* **17**, 870 (1978).
597. E. Lindner and G. Vitzthum, *Chem. Ber.* **102**, 4062 (1969).
598. G. Vitzthum and E. Lindner, *Angew. Chem. Int. Ed. Engl.* **10**, 315 (1971).
599. K. Nakaraoto and A. E. Martelly, *J. Chem. Phys.* **32**, 588 (1960).
600. M. Mikami, I. Nakagawa, and T. Shiraanouchi, *Spectrochim. Acta* **23A**, 1037 (1967).
601. H. Junge and H. Musso, *Spectrochim. Acta* **24A**, 1219 (1968).
602. K. Nakamoto, C. Udovich, and J. Takemoto, *J. Am. Chem. Soc.* **92**, 3973 (1970).
603. T. Schönherr, U. Rosellen, and H. H. Schmidtke, *Spectrochim. Acta* **49A**, 357 (1993).
604. M. Handa, H. Miyamoto, T. Suzuki, K. Sawada, and Y. Yukawa, *Inorg. Chim. Acta* **203**, 61 (1993).
605. R. C. Fay and R. N. Lowry, *Inorg. Nucl. Chem. Lett.* **3**, 117 (1967).
606. W. D. Courrier, C. J. L. Lock, and G. Turner, *Can. J. Chem.* **50**, 1797 (1972).
607. M. R. Caira, J. M. Haigh, and L. R. Nassimbeni, *J. Inorg. Nucl. Chem.* **34**, 3171 (1972).
608. G. Schätzel and W. Preetz, *Z. Naturforsch.* **31B**, 740 (1976).
609. K. Dallmann and W. Preetz, *Z. Naturforsch.* **53B**, 232 (1998).
610. I. Diaz-Acosta, J. Baker, W. Cordes, and P. Pulay, *J. Phys. Chem. A* **105**, 238 (2001).
611. S. C. Tellez and L. J. Gomez, *Spectrochim. Acta* **51A**, 395 (1995).
612. L. Filotti, G. Bugli, A. Ensuque, and F. Bozon-Verduraz, *Bull. Soc. Chim. Fr.* **133**, 1117 (1996).
613. D. A. Thornton, *Coord. Chem. Rev.* **104**, 173 (1990).
614. M. A. Bush, D. E. Fenton, R. S. Nyholm, and M. R. Truter, *Chem. Commun.* 1335 (1970).
615. I. R. Baird, S. T. Rettig, B. R. James, and K. A. Skov, *Can. J. Chem.* **77**, 1821 (1999).
616. Y. Nakamura, N. Kanehisa, and S. Kawaguchi, *Bull. Chem. Soc. Jpn.* **45**, 485 (1972).
617. F. A. Cotton and R. C. Elder, *J. Am. Chem. Soc.* **86**, 2294 (1964); *Inorg. Chem.* **4**, 1145 (1965).
618. P. W. N. M. van Leeuwen, *Recl. Trav. Chim. Pays-Bas* **87**, 396 (1968).
619. Y. Nakamura and S. Kawaguchi, *Chem. Commun.* 716 (1968).

620. S. Koda, S. Ooi, H. Kuroya, K. Isobe, Y. Nakamura, and S. Kawaguchi, *Chem. Commun.* 1321 (1971).
621. Y. Nakamura, K. Isobe, H. Morita, S. Yamazaki, and S. Kawaguchi, *Inorg. Chem.* **11**, 1573 (1972).
622. S. Koda, S. Ooi, H. Kuroya, Y. Nakamura, and S. Kawaguchi, *Chem. Commun.* 280 (1971).
623. J. Lewis, R. F. Long, and C. Oldham, *J. Chem. Soc.* 6740 (1965); D. Gibson, J. Lewis, and C. Oldham, *J. Chem. Soc. A* 1453 (1966).
624. G. T. Behnke and K. Nakamoto, *Inorg. Chem.* **6**, 433 (1967).
625. G. T. Behnke and K. Nakamoto, *Inorg. Chem.* **6**, 440 (1967).
626. G. T. Behnke and K. Nakamoto, *Inorg. Chem.* **7**, 330 (1968).
627. F. Bonati and G. Minghetti, *Angew. Chem., Int. Ed. Engl.* **7**, 629 (1968).
628. D. Gibson, B. F. G. Johnson, and J. Lewis, *J. Chem. Soc. A* 367 (1970).
629. S. Baba, T. Ogura, and S. Kawaguchi, *Inorg. Nucl. Chem. Lett.* **7**, 1195 (1971).
630. G. Allen, J. Lewis, R. F. Long, and C. Oldham, *Nature* (*London*) **202**, 589 (1964).
631. G. T. Behnke and K. Nakamoto, *Inorg. Chem.* **7**, 2030 (1968).
632. J. Lewis and C. Oldham, *J. Chem. Soc. A* 1456 (1966).
633. Y. Nakamura and K. Nakamoto, *Inorg. Chem.* **14**, 63 (1975).
634. S. Okeya, Y. Nakamura, S. Kawaguchi, and T. Hinomoto, *Inorg. Chem.* **20**, 1576 (1981).
635. Z. Kanda, Y. Nakamura, and S. Kawaguchi, *Inorg. Chem.* **17**, 910 (1978).
636. S. Kawaguchi, *Coord. Chem. Rev.* **70**, 51 (1986).
637. M. Gerisch, C. Bruhn, A. Porzel, and D. Steinborn, *Eur. J. Inorg. Chem.* 1655 (1998).
638. L. G. Hulett and D. A. Thornton, *Spectrochim. Acta* **27A**, 2089 (1971).
639. H. Junge, *Spectrochim. Acta* **24A**, 1957 (1968).
640. B. Hutchinson, D. Eversdyk, and S. Olbricht, *Spectrochim. Acta* **30A**, 1605 (1974).
641. F. Sagara, H. Kobayashi, and K. Ueno, *Bull. Chem. Soc. Jpn.* **45**, 794 (1972).
642. R. B. Penland, S. Mizushima, C. Curran, and J. V. Quagliano, *J. Am. Chem. Soc.* **79**, 1575 (1957).
643. A. Yamaguchi, T. Miyazawa, T. Shimanouchi, and S. Mizushima, *Spectrochim. Acta* **10**, 170 (1957).
644. E. Giesbrecht and M. Kawashita, *J. Inorg. Nucl. Chem.* **32**, 2461 (1970).
645. K. W. Bagnall, M. A. A. Ghany, G. Bombieri, and F. Benetollo, *Inorg. Chim. Acta* **115**, 229 (1986).
646. D. Tudela and J. D. Tornero, *Inorg. Chim. Acta* **214**, 197 (1993).
647. A. Yamaguchi, R. B. Penland S. Mizushima, T. J. Lane, C. Curran, and J. V. Quagliano, *J. Am. Chem. Soc.* **80**, 527 (1958).
648. R. A. Bailey and T. R. Peterson, *Can. J. Chem.* **45**, 1135 (1967).
649. K. Swaminathan and H. M. N. H. Irving, *J. Inorg. Nucl. Chem.* **26**, 1291 (1964).
650. C. D. Flint and M. Goodgame, *J. Chem. Soc. A*, 744 (1966).
651. P. J. Hendra and Z. Jović, *J. Chem. Soc. A*, 735 (1967).
652. D. M. Adams and J. B. Cornell, *J. Chem. Soc. A*, 884 (1967).
653. J. M. Alia, H. G. M. Edwards, and F. J. Garcia-Navarro, *J. Mol. Struct.* **508**, 51 (1999).
654. R. Rivest, *Can. J. Chem.* **40**, 2234 (1962).

655. T. J. Lane, A. Yamaguchi, J. V. Quagliano, J. A. Ryan, and S. Mizushima, *J. Am. Chem. Soc.* **81**, 3824 (1959).
656. D. Gambino, E. Kremer, E. J. Baran, A. Mombru, L. Suescum, R. Mariezcurrena, M. Kieninger, and O. N. Ventura, *Z. Anorg. Allg. Chem.* **625**, 813 (1999).
657. M. Schafer and C. Curran, *Inorg. Chem.* **5**, 265 (1966).
658. R. K. Gosavi and C. N. R. Rao, *J. Inorg. Nucl. Chem.* **29**, 1937 (1967).
659. G. B. Aitken, J. L. Duncan, and G. P. McQuillan, *J. Chem. Soc., Dalton Trans.* 2103 (1972).
660. P. J. Hendra and Z. Jović, *Spectrochim. Acta* **24A**, 1713 (1968).
661. R. J. Balahura and R. B. Jordan, *J. Am. Chem. Soc.* **92**, 1533 (1970).
662. F. A. Cotton, R. Francis, and W. D. Horrocks, *J. Phys. Chem.* **64**, 1534 (1960).
663. R. S. Drago and D. W. Meek, *J. Phys. Chem.* **65**, 1446 (1961); D. W. Meek, D. K. Straub, and R. S. Drago, *J. Am. Chem. Soc.* **82**, 6013 (1960).
664. B. B. Wayland and R. F. Schramm, *Inorg. Chem.,* **8**, 971 (1969); *Chem. Commun.* 1465 (1968).
665. V. N. Krishnamarthy and S. Soundararajan, *J. Inorg. Nucl. Chem.* **29**, 517 (1967); S. K. Ramalingam and S. Soundararajan, *Z. Anorg. Allg. Chem.* **353**, 216 (1967).
666. C. G. Fuentes and S. J. Patel, *J. Inorg. Nucl. Chem.* **32**, 1575 (1970).
667. F. Gaizer, *Polyhedron* **4**, 1909 (1985).
668. C. V. Senoff, E. Maslowsky, Jr. and R. G. Goel, *Can. J. Chem.* **49**, 3585 (1971).
669. D. A. Langs, C. R. Hare, and R. G. Little, *Chem. Commun.* 1080 (1967).
670. W. Kitchings, C. J. Moore, and D. Doddrell, *Inorg. Chem.* **9**, 541 (1970).
671. M. van Beusichem and N. Farrell, *Inorg. Chem.* **31**, 634 (1992).
672. V. Yu. Kukushkin, V. K. Bel'skii, V. E. Konovalov, R. R. Shifrina, A. I. Moiseev, and R. A. Vlasova, *Inorg. Chim. Acta* **183**, 57 (1991).
673. D. P. Riley, and J. D. Oliver, *Inorg. Chem.* **25**, 1814 (1986).
674. I. P. Evans, A. Spencer, and G. Wilkinson, *J. Chem. Soc., Dalton Trans.* 204 (1973).
675. A. Mercer and J. Trotter, *J. Chem. Soc., Dalton Trans.* 2480 (1975).
676. P. G. Antonov, Y. N. Kukushkin, V. I. Konnov, and B. I. Ionin, *Russ. J. Inorg. Chem. (Engl. transl.)* **23**, 245 (1978).
677. U. C. Sarma, K. P. Sarma, and R. K. Poddar, *Polyhedron* **7**, 1727 (1988).
678. E. Alessio, G. Balducci, A. Lutman, G. Mestroni, M. Calligaris, and W. M. Attia, *Inorg. Chim. Acta* **203**, 205 (1993).
679. E. Alessio, B. Milani, M. Bolle, G. Mestroni, P. Faleschini, F. Todone, G. Geremia, and M. Calligaris, *Inorg. Chem.* **34**, 4722 (1995).
680. S. Geremia, S. Mestroni, M. Calligaris, and E. Alessio, *J. Chem. Soc., Dalton Trans.* 2447 (1998).
681. A. Milicic-Tang and J. C. G. Bunzli, *Inorg. Chim. Acta* **192**, 201 (1992).
682. R. Minkwitz and W. Molsbeck, *Z. Anorg. Allg. Chem.* **612**, 35 (1992).
683. M. Tranquille and M. T. Forel, *Spectrochim. Acta* **28A**, 1305 (1972).
684. C. V. Berney and J. H. Weber, *Inorg. Chem.* **7**, 283 (1968).
685. G. Griffiths and D. A. Thornton, *J. Mol. Struct.* **52**, 39 (1979).
686. B. R. James and R. H. Morris, *Spectrochim. Acta* **34A**, 577 (1978).

687. P. W. N. M. Van Leeuwen, *Recl. Trav. Chim. Pays-Bos* **86**, 201 (1967); P. W. N. M. Van Leeuwen and W. L. Groeneveld *ibid*. 721.
688. S. K. Madan, C. M. Hull, and L. J. Herman, *Inorg. Chem.* **7**, 491 (1968).
689. K. A. Jensen and K. Krishnan, *Scand. Chim. Acta* **21**, 1988 (1967).
690. A. G. Sharp, *The Chemistry of Cyano Complexes of the Transition Metals*, Academic Press, New York, (1976).
691. W. P. Griffith, *Coord. Chem. Rev.* **17**, 177 (1975).
692. P. Rigo and A. Turco, *Coord. Chem. Rev.* **13**, 133 (1974).
693. L. H. Jones and B. I. Swanson, *Acc. Chem. Res.* **9**, 128 (1976).
694. H. Stammreich, B. M. Chadwick, and S. G. Frankiss, *J. Mol. Struct.* **1**, 191 (1968).
695. B. M. Chadwick and S. G. Frankiss, *J. Mol. Struct.* **31**, 1 (1976).
696. B. M. Chadwick and S. G. Frankiss, *J. Mol. Struct.* **2**, 281 (1968).
697. G. J. Kubas and L. H. Jones, *Inorg. Chem.* **13**, 2816 (1974).
698. W. P. Griffith and J. R. Lane, *J. Chem. Soc., Dalton Trans.* 158 (1972).
699. W. P. Griffith and G. T. Turner, *J. Chem. Soc. A*, 858 (1970).
700. P. W. Jensen, *J. Raman Spectrosc.* **4**, 75 (1975).
701. H. Siebert and A. Siebert, *Angew. Chem., Int. Ed. Engl.* **8**, 6009 (1969); *Z. Anorg. Allg. Chem.* **378**, 160 (1970).
702. M. F. A. El-Sayed and R. K. Sheline, *J. Inorg. Nucl. Chem.* **6**, 187 (1958).
703. R. Nast and D. Rehder, *Chem. Ber.* **104**, 1709 (1971).
704. R. A. Penneman and L. H. Jones, *J. Inorg. Nucl. Chem.* **20**, 19 (1961).
705. J. Fernandez-Beltran, J. Blanco-Pascual, and E. Reguera-Edilao, *Spectrochim. Acta* **46A**, 685 (1990).
706. C. Kappenstein and R. P. Hugel, *Inorg. Chem.* **16**, 250 (1977).
707. C. Kappenstein and R. P. Hugel, *Inorg. Chem.* **17**, 1945 (1978).
708. B. M. Chadwick, D. A. Long, and S. U. Qureshi, *J. Mol. Struct.* **63**, 167 (1980).
709. L. H. Jones and B. I. Swanson, *J. Chem. Phys.* **63**, 5401 (1975).
710. E. Bernhardt, G. Henkel, and H. Willner, *Z. Anorg. Allg. Chem.* **626**, 560 (2000).
711. W. E. Buschmann, A. M. Arif, and J. S. Miller, *Angew. Chem. Int. Ed. Engl.* **37**, 781 (1998).
712. G. R. Rossman, F. -D. Tsay, and H. B. Gray, *Inorg. Chem.* **12**, 824 (1973).
713. P. M. Kiernan and W. P. Griffith, *Inorg. Nucl. Chem. Lett.* **12**, 377 (1976).
714. W. P. Griffith, P. M. Kiernan and J. -M. Brégeault, *J. Chem. Soc., Dalton Trans.* 1411 (1978).
715. H. S. Trop, A. G. Jones, and A. Davison, *Inorg. Chem.* **19**, 1993 (1980).
716. A. M. Soares, P. M. Kiernan, D. J. Cole-Hamilton, and W. P. Griffith, *Chem. Commun.* 84 (1981).
717. J. L. Hoard, T. A. Hamor, and M. D. Glick, *J. Am. Chem. Soc*. **90**, 3177 (1968).
718. H. Stammreich and O. Sala, *Z. Elektrochem.* **64**, 741 (1960).;**65**, 149 (1961).
719. K. O. Hartman and F. A. Miller, *Spectrochim. Acta* **24A**, 669 (1968).
720. B. V. Parish, P. G. Simms, M. A. Wells, and L. A. Woodward, *J. Chem. Soc*. 2882 (1968).
721. P. M. Kiernan and W. P. Griffith, *J. Chem. Soc., Dalton Trans.* 2489 (1975).

722. T. V. Long, II, and G. A. Vernon, *J. Am. Chem. Soc.* **93**, 1919 (1971).
723. M. B. Hursthouse and A. M. Galas, *Chem. Commun.* 1167 (1980).
724. K. N. Raymond, P. W. R. Corfield, and J. A. Ibers, *Inorg. Chem.* **7**, 1362 (1968).
725. A. Terzis, K. N. Raymond, and T. G. Spiro, *Inorg. Chem.* **9**, 2415 (1970).
726. L. J. Basile, J. R. Ferraro, M. Choca, and K. Nakamoto, *Inorg. Chem.* **13**, 496 (1974).
727. E. Hellner, H. Ahsbahs, G. Dehnicke, and K. Dehnicke, *Ber. Bunsensenges. Phys. Chem.* **77**, 277 (1973).
728. V. Caglioti, G. Sartori, and C. Furlani, *J. Inorg. Nucl. Chem.* **13**, 22 (1960); **8**, 87 (1958).
729. L. H. Jones, *J. Chem. Phys.* **41**, 856 (1964).
730. I. Nakagawa and T. Shimanouchi, *Spectrochim. Acta* **18**, 101 (1962).
731. L. H. Jones, *Inorg. Chem.* **2**, 777 (1963).
732. I. Nakagawa and T. Shimanouchi, *Spectrochim. Acta* **26A**, 131 (1970).
733. L. H. Jones, B. I. Swanson, and G. J. Kubas, *J. Chem. Phys.* **61**, 4650 (1974); B. I. Swanson and L. H. Jones, *Inorg. Chem.* **13**, 313 (1974).
734. L. H. Jones, *J. Chem. Phys.* **29**, 463 (1958).
735. H. Poulet and J. P. Mathieu, *Spectrochim. Acta* **15**, 932 (1959).
736. L. H. Jones, *Spectrochim. Acta* **17**, 188 (1961).
737. D. M. Sweeny, I. Nakagawa, S. Mizushima, and J. V. Quagliano, *J. Am. Chem. Soc.* **78**, 889 (1956).
738. C. W. F. T. Pistorius, *Z. Phys. Chem.* **23**, 197 (1960).
739. R. L. McCullough, L. H. Jones, and G. A. Crosby, *Spectrochim. Acta* **16**, 929 (1960).
740. L. H. Jones and J. M. Smith, *J. Chem. Phys.* **41**, 2507 (1964).
741. L. H. Jones, *J. Chem. Phys.* **27**, 665 (1957).
742. L. H. Jones, *Spectrochim. Acta* **19**, 1675 (1963).
743. L. H. Jones, *J. Chem. Phys.* **26**, 1578 (1957); **25**, 379 (1956).
744. L. H. Jones, *J. Chem. Phys.* **27**, 468 (1957); **21**, 1891 (1953); **22**, 1135 (1954).
745. V. Lorenzelli and P. Delorme, *Spectrochim. Acta* **19**, 2033 (1963).
746. J. C. Coleman, H. Peterson, and R. A. Penneman, *Inorg. Chem.* **4**, 135 (1965).
747. L. H. Jones, *Inorg. Chem.* **3**, 1581 (1964); **4**, 1472 (1965); J. M. Smith, L. H. Jones, I. K. Kressin, and R. A. Penneman, *ibid*. 369
748. L. H. Jones and J. M. Smith, *Inorg. Chem.* **4**, 1677 (1965).
749. M. N. Memering, L. H. Jones, and J. C. Bailar, Jr., *Inorg. Chem.* **12**, 2793 (1973).
750. D. B. Soria and P. J. Aymonino, *Specrochim. Acta, A*, **55**, 1243 (1999).
751. M. E. C. Villalba, E. L. Varetti, and P. J. Aymonino, *Vib. Spectrosc.* **14**, 275 (1997).
752. M. E. C. Villalba, E. L. Varetti, and P. J. Aymonino, *Specrochim. Acta A,* **55**, 1545 (1999).
753. H. Chun, E. M. Maes, R. S. Czernuszewicz, and I. Bernal, *Polyhedron*, **20**, 2597 (2001).
754. D. F. Shriver, *J. Am. Chem. Soc.* **84**, 4610 (1962); **85**, 1405 (1963); D. F. Shriver and J. -Posner, *ibid*. **88**, 1672 (1966).
755. D. F. Shriver, S. A. Shriver, and S. E. Anderson, *Inorg. Chem.* **4**, 725 (1965).
756. D. B. Brown, D. F. Shriver, and L. H. Schwartz, *Inorg. Chem.* **7**, 77 (1968).
757. B. I. Swanson and J. J. Rafalko, *Inorg. Chem.* **15**, 249 (1976).

758. B. I. Swanson, *Inorg. Chem.* **15**, 253 (1976).
759. R. E. Hester and E. M. Nour, *J. Chem. Soc., Dalton Trans.* 939 (1981).
760. H. G. Nadler, J. Pebler, and K. Dehnicke, *Z. Anorg. Allg. Chem.* **404**, 230 (1974).
761. R. E. Wilde, S. N. Ghosh, and B. J. Marshall, *Inorg. Chem.* **9**, 2513 (1970).
762. I. Escorihuela, L. R. Falvello, and M. Tomás, *Inorg. Chem.* **40**, 636 (2001).
763. G. A. Bowmaker, H. Hartl, and V. Urban, *Inorg. Chem.* **39**, 4548 (2000).
764. P. Forlano, F. D. Cukiernik, O. Poizat, and J. A. Olabe, *J. Chem. Soc. Dalton Trans.* 595 (1997).
765. P. Forlano, L. M. Baraldo, J. A. Olabe, and C. O. della Vedova, *Inorg. Chim. Acta* **223**, 37 (1994).
766. B. W. Pfennig, Y. Wu, R. Kumble, T. G. Spiro, and A. B. Bocarsly, *J. Phys. Chem.* **100**, 5745 (1996).
767. B. W. Pfennig, J. V. Lockard, J. L. Cohen, D. F. Watson, D. M. Ho, and A. B. Bocarsly, *Inorg. Chem.* **38**, 2941 (1999).
768. J. R. Ferraro, *Coord. Chem. Rev.* **43**, 205 (1982).
769. J. R. Ferraro, L. J. Basile, J. M. Williams, J. I. McOmber, D. F. Shriver, and D. R. Greig, *J. Chem. Phys.* **69**, 3871 (1978).
770. M. Maliarik, J. Glaser, and I. Toth, *Inorg. Chem.* **37**, 5452 (1998).
771. F. Jalilehvand M. Maliarik, M. Sandström, J. Mink, I. Persson, P. Persson, I. Toth, and J. Glaser, *Inorg. Chem.* **40**, 3889 (2001).
772. R. A. Walton, *Spectrochim. Acta* **21**, 1795 (1965); *Can. J. Chem.* **44**, 1480 (1966).
773. R. E. Clarke and P. C. Ford, *Inorg. Chem.* **9**, 227 (1970).
774. D. P. Fairlie, W. G. Jackson, B. W. Skelton, H. Wen, A. H. White, W. A. Wickramasinghe, T. C. Woon, and H. Taube, *Inorg. Chem.* **36**, 1020 (1997).
775. B. von Ahsen, B. Bley, S. Proemmel, R. Wartchow, H. Willner, and F. Aubke, *Z. Anorg. Allg. Chem.* **624**, 1225 (1998).
776. J. C. Evans and G. Y. -S. Lo, *Spectrochim. Acta* **21**, 1033 (1965).
777. J. Reedijk and W. L. Groeneveld, *Rec. Trav. Chim. Pays-Bas* **86**, 1127 (1967).
778. R. Birk, H. Berke, H. -U. Hund, G. Huttner, L. Szolnai, L. Dahlenburg, U. Behrens, and T. Sielisch, *J. Organomet. Chem.* **372**, 397 (1989).
779. T. C. Wright, G. Wilkinson, M. Motevalli, and M. B. Hursthouse, *J. Chem. Soc., Dalton Trans.* 2017 (1986).
780. M. F. Farona and K. F. Kraus, *Inorg. Chem.* **9**, 1700 (1970).
781. Y. Kinoshita, I. Matsubara, and Y. Saito, *Bull. Chem. Soc. Jpn.* **32**, 741 (1959).
782. M. Kubota, D. L. Johnston, and I. Matsubara, *Inorg. Chem.* **5**, 386 (1966).
783. Y. Kinoshita, I. Matsubara, and Y. Saito, *Bull. Chem. Soc. Jpn.* **32**, 1216 (1959).
784. I. Matsubara, *Bull. Chem. Soc. Jpn.* **34**, 1719 (1961); *J. Chem. Phys.* **35**, 373 (1961).
785. J. K. Brown, N. Sheppard, and D. M. Simpson, *Philos. Trans. Roy. Soc., Lond.* **A247**, 35 (1954).
786. M. Kubota and D. L. Johnston, *J. Am. Chem. Soc.* **88**, 2451 (1966).
787. I. Matsubara, *Bull. Chem. Soc. Jpn.* **35**, 27 (1962).
788. F. A. Cotton and F. Zingales, *J. Am. Chem. Soc.* **83**, 351 (1961).
789. A. Sacco and F. A. Cotton, *J. Am. Chem. Soc.* **84**, 2043 (1962).

790. J. W. Dart, M. K. Lloyd, R. Mason, J. A. McCleverty, and J. Williams, *J. Chem. Soc., Dalton Trans.* 1747 (1973).
791. P. M. Boorman, P. J. Craig, and T. W. Swaddle, *Can. J. Chem.* **48**, 838 (1970).
792. J. P. Al-Dulaimi, R. J. H. Clark, S. M. Saavedra, and M. A. Salam, *Inorg. Chim. Acta* **300–302**, 175 (2000).
793. J. L. Burmeister, *Coord. Chem. Rev.* **3**, 225 (1968); **1**, 205 (1966).
794. R. A. Bailey, S. L. Kozak, T. W. Michelsen, and W. N. Mills, *Coord. Chem. Rev.* **6**, 407 (1971).
795. A. H. Norbury, *Adv. Inorg. Chem. Radiochem.* **17**, 231 (1975).
796. S. Ahrland J. Chatt, and N. R. Davies, *Q. Rev. Chem. Soc.* **12**, 265 (1958).
797. P. C. H. Mitchell and R. J. P. Williams, *J. Chem. Soc.* 1912 (1960).
798. J. Lewis, R. S. Nyholm, and P. W. Smith, *J. Chem. Soc.* 4590 (1961).
799. A. Sabatini and I. Bertini, *Inorg. Chem.* **4**, 959 (1965).
800. C. Pecile, *Inorg. Chem.* **5**, 210 (1966).
801. R. A. Bailey, T. W. Michelsen, and W. N. Mills, *J. Inorg. Nucl. Chem.* **33**, 3206 (1971).
802. R. Larsson and A. Miezis, *Acta Chem. Scand.* **23**, 37 (1969).
803. R. J. H. Clark and C. S. Williams, *Spectrochim. Acta* **22**, 1081 (1966).
804. D. Forster and D. M. L. Goodgame, *Inorg. Chem.* **4**, 715 (1965).
805. M. A. Bennett, R. J. H. Clark, and A. D. J. Goodwin, *Inorg. Chem.* **6**, 1625 (1967).
806. D. Forster and D. M. L. Goodgame, *Inorg. Chem.* **4**, 823 (1965).
807. H. H. Schmidtke and D. Garthoff, *Helv. Chim Acta* **50**, 1631 (1967).
808. K. H. Schmidt, A. Müller, and M. Chakravorti, *Spectrochim Acta* **32A**, 907 (1976).
809. C. Engelter and D. A. Thornton, *J. Mol. Struct.* **33**, 119 (1976).
810. H. -H. Fricke and W. Preetz, *Z. Naturforsch.* **38B**, 917 (1983).
811. K. Bütje and W. Preetz, *Z. Naturforsch.* **43B,** 371, 382 (1988).
812. L. Homolya and W. Preetz, *Z. Naturforsch.* **55B**, 178 (2000).
813. L. Homolya, S. Struess, and W. Preetz, *Z. Naturforsch.* **54B**, 767 (1999).
814. O. Stahler and W. Preetz, *Z. Anorg. Allg. Chem.* **626**, 2077 (2000).
815. M. Semraw and W. Preetz, *Z. Anorg. Allg. Chem.* **622**, 1287 (1996).
816. J. Seemann and W. Preetz, *Z. Naturforsch.* **53B**, 13 (1998).
817. J. -U. Rohde and W. Preetz, *Z. Anorg. Allg. Chem.* **624**, 1319 (1998).
818. O. Stahler and W. Preetz, *Z. Anorg. Allg. Chem.* **626**, 2077 (2000).
819. M. Karbowiak, J. Hanuza, J. Janczak, and J. Drożdżyński, *J. Alloys and Compounds.* **225**, 338 (1995).
820. T. Yamaguchi, K. Yamamoto, and H. Ohtaki, *Bull. Chem. Soc. Jpn.* **58**, 3235 (1985).
821. I. Persson, A. Iverfeldt, and S. Ahrland *Acta Chem. Scand.* **A35**, 295 (1981).
822. M. M. Chamberlain and J. C. Bailar, Jr., *J. Am. Chem. Soc.* **81**, 6412 (1959).
823. A. B. P. Lever, B. S. Ramaswamy, S. H. Simonsen, and L. K. Thompson, *Can. J. Chem.* **48**, 3076 (1970).
824. A. Turco and C. Pecile, *Nature (London)* **191**, 66 (1961).
825. J. J. MacDougall, J. H. Nelson, M. W. Babich, C. C. Fuller, and R. A. Jacobson, *Inorg. Chim. Acta* **27**, 201 (1978).

826. G. Contreras and R. Schmidt, *J. Inorg. Nucl. Chem.* **32**,1295, 127 (1970).
827. F. Basolo, J. L. Bunneister, and A. J. Poe, *J. Am. Chem. Soc.* **85**, 1700 (1963).
828. A. Sabatini and I. Bertini, *Inorg. Chem.* **4**, 1665 (1965).
829. D. M. L. Goodgame, and B. W. Malerbi, *Spectrochim. Acta* **24A**, 1254 (1968).
830. J. L. Burmeister and F. Basolo, *Inorg. Chem.* **3**, 1587 (1964).
831. T. E. Sloan and A. Wojcicki, *Inorg. Chem.* **7**, 1268 (1968).
832. I. Stotz, W. K. Wilmarth, and A. Haim, *Inorg. Chem.* **7**, 1250 (1968).
833. R. L. Hassel and J. L. Burmeister, *Chem. Commun.* 568 (1971).
834. L. A. Epps and L. G. Marzilli, *Inorg. Chem.* **12**, 1514 (1973).
835. W. Preetz and M. Semrau, *Z. Anorg. Allg. Chem.* **621**, 725 (1995).
836. O. Stahler, M. Semrau, and W. Preetz, *Z. Anorg. Allg. Chem.* **626**, 1845 (2000).
837. M. Semrau, W. Preetz, and L. Homolya, *Z. Anorg. Allg. Chem.* **623**, 179 (1997).
838. I. Homolya and W. Preetz, *Z. Naturforsch.* **54B**, 1009 (1999).
839. J. -U. Rohde and W. Preetz, *Z. Anorg. Allg. Chem.* **623**, 1774 (1997).
840. I. Bertini and A. Sabatini, *Inorg. Chem.* **5**, 1025 (1966).
841. G. R. Clark, G. J. Palenik, and D. W. Meek, *J. Am. Chem. Soc.* **92**, 1077 (1970).
842. G. P. McQuillan and I. A. Oxton, *J. Chem. Soc., Dalton Trans.* 1460 (1978).
843. K. K. Chow, W. Levason, and C. A. McAuliffe, *Inorg. Chim. Acta* **15**, 79 (1975).
844. D. W. Meek, P. E. Nicpon, and V. I. Meek, *J. Am. Chem. Soc.* **92**, 5351 (1970).
845. M. J. Coyer, M. Croft, J. Chen, and R. H. Herber, *Inorg. Chem.* **31**, 1752 (1992).
846. S. M. Nelson and J. Rodgers, *Inorg. Chem.* **6**, 1390 (1967).
847. J. L. Burmeister, R. L. Hassel, and R. J. Phelan, *Inorg. Chem.* **10**, 2032 (1971).
848. J. Chatt and L. A. Duncanson, *Nature* (*London*) **178**, 997 (1956).
849. J. Chatt, L. A. Duncanson, F. A. Hart, and P. G. Owston, *Nature* (*London*) **181**, 43 (1958).
850. P. G. Owston and J. M. Rowe, *Acta Crystallogr.* **13**, 253 (1960).
851. J. Chatt and F. A. Hart, *J. Chem. Soc.* 1416 (1961).
852. B. R. Chamberlain and W. Moser, *J. Chem. Soc. A,* 354 (1969).
853. G. Liptay, K. Burger, E. Papp-Molnár, and Sz. Szebeni, *J. Inorg. Nucl. Chem.* **31**, 2359 (1969).
854. J. M. Homan, J. M. Kawamoto, and G. L. Morgan, *Inorg. Chem.* **9**, 2533 (1970).
855. R. A. Bailey and T. W. Michelsen, *J. Inorg. Nucl. Chem.* **34**, 2671 (1972).
856. F. A. Cotton, A. Davison, W. H. Ilsley, and H. S. Trop, *Inorg. Chem.* **18**, 2719 (1979).
857. N. K. Karan, S. Mitra, T. Matsyshita, V. Gramlich, and G. Rosair, *Inorg. Chim. Acta* **332**, 87 (2002).
858. F. A. Cotton, D. M. L. Goodgame, M. Goodgame, and T. E. Hass, *Inorg. Chem.* **1**, 565 (1962).
859. J. Chatt and L. A. Duncanson, *Nature* (*London*) **178**, 997 (1956).
860. M. E. Farago and J. M. James, *Inorg. Chem.* **4**, 1706 (1965).
861. A. Turco, C. Pecile, and M. Nicolini, *J. Chem. Soc.* 3008 (1962).
862. J. L. Burmeister and Y. Al-Janabi, *Inorg. Chem.* **4**, 962 (1965).
863. D. Forster and D. M. L. Goodgame, *Inorg. Chem.* **4**, 1712 (1965).
864. J. L. Burmeister and H. J. Gysling, *Inorg. Chim. Acta* **1**, 100 (1967).

865. M. A. Jennings and A. Wojcicki, *Inorg. Chim. Acta* **3**, 335 (1969).
866. J. L. Burmeister, H. J. Gysling, and J. C. Lim, *J. Am. Chem. Soc.* **91**, 44 (1969).
867. K. Bütje and W. Preetz, *Z. Naturforsch.* **43B**, 574 (1988).
868. U. Klopp and W. Preetz, *Z. Anorg. Allg. Chem.* **619**, 1336 (1993).
869. S. Struess and W. Preetz, *Z. Naturforsch.* **54B**, 1222 (1999).
870. S. Struess and W. Preetz, *Z. Naturforsch.* **54B**, 357 (1999).
871. J.-U. Rohde, B. von Malottki, and W. Preetz, *Z. Anorg. Allg. Chem.* **626**, 905 (2000).
872. V. Palaniappan and U. C. Agarwala, *Inorg. Chem.* **25**, 4064 (1986).
873. F. A. Miller and G. L. Carlson, *Spectrochim. Acta* **17**, 977 (1961).
874. D. Forster and W. D. Horrocks, *Inorg. Chem.* **6**, 339 (1967).
875. D. Forster and D. M. L. Goodgame, *J. Chem. Soc.* 262 (1965).
876. A. R. Chugtai and R. N. Keller, *J. Inorg. Nucl. Chem.* **31**, 633 (1969).
877. D. Forster and D. M. L. Goodgame, *J. Chem. Soc.* 1286 (1965).
878. E. J. Peterson, A. Galliart, and J. M. Brown, *Inorg. Nucl. Chem. Lett.* **9**, 241 (1973).
879. R. A. Bailey and S. L. Kozak, *J. Inorg. Nucl. Chem.* **31**, 689 (1969).
880. H.-D. Amberger, R. D. Fischer, and G. G. Rosenbauer, *Z. Naturforsch.* **31B**, 1 (1976).
881. A. H. Norbury and A. I. P. Sinha, *J. Chem. Soc. A* 1598 (1968).
882. S. J. Patel and D. G. Tuck, *J. Chem. Soc. A* 1870 (1968).
883. E. Bonfada, U. Abram, and J. Strähle, *Z. Anorg. Allg. Chem.* **624**, 757 (1998).
884. H. G. M. Edwards, D. W. Farwell, I. R. Lewis, and N. Webb, *J. Mol. Struct.* **271**, 27 (1992).
885. S. J. Anderson and A. H. Norbury, *Chem. Commun.* 37 (1974).
886. K. Seppelt and H. Oberhammer, *Inorg. Chem.* **24**, 1227 (1985).
887. J. Nelson and S. M. Nelson, *J. Chem. Soc. A,* 1597 (1969).
888. R. B. Saillant, *J. Organomet. Chem.* **39**, C71 (1972).
889. T. Schönherr, *Inorg. Chem.* **25**, 171 (1986).
890. R. Vicente, A. Escuer, E. Pefialba, X. Solans, and M. Font-Bardia, *J. Chem. Soc., Dalton Trans.* 3005 (1994).
891. W. Beck, *Chem. Ber.* **95**, 341 (1962).
892. W. Beck, P. Swoboda, K. Feldl, and E. Schuierer, *Chem. Ber.* **103**, 3591 (1970).
893. W. Beck and E. Schuierer, *Z. Anorg. Allg. Chem.* **347**, 304 (1966).
894. W. Beck and E. Schuierer, *Chem. Ber.* **98**, 298 (1965).
895. W. Beck, C. Oetker, and P. Swoboda, *Z. Naturforsch.* **28B**, 229 (1973).
896. W. Weigand U. Nagel, and W. Beck, *J. Organomet. Chem.* **314**, C55 (1986).
897. W. Beck, *Organomet. Chem. Rev.* **A7**, 159 (1971).
898. W. Beck and W. P. Fehlhammer, *J. Organomet. Chem.* **279**, C22 (1985).
899. W. Beck, W. P. Fehlhammer, P. Pöllmann, E. Schuierer, and K. Feldl, *Chem. Ber.* **100**, 2335 (1967).
900. W. Beck, W. P. Fehlhammer, P. Pöllmann, E. Schuierer, and K. Feldl, *Angew. Chem.* **77**, 458 (1965).
901. D. Forster and W. D. Horrocks, *Inorg. Chem.* **5**, 1510 (1966).

902. K. Steiner, W. Willing, U. Müller, and K. Dehnicke, *Z. Anorg. Allg. Chem.* **555**, 7 (1987).
903. W.-M. Dyck, K. Dehnicke, F. Weller, and U. Müller, *Z. Anorg. Allg. Chem.* **470**, 89 (1980).
904. D. Seybold and K. Dehnicke, *Z. Anorg. Allg. Chem.* **361**, 277 (1968).
905. L. F. Druding, H. C. Wang, R. E. Lohen, and F. D. Sancilio, *J. Coord Chem.* **3**, 105 (1973).
906. I. Agrell, *Acta Chem. Scand.* **25**, 2965 (1971).
907. W. Beck, T. M. Klapötke, P. Klüfers, G. Kramer, and C. M. Rienäcker, *Z. Anorg. Allg. Chem.* **627**, 1669 (2001).
908. K. Karaghiosoff, T. M. Klapötke, B. Krumm, H. Nöth, T. Schütt, and M. Suter, *Inorg. Chem.* **41**, 170 (2002).
909. S. Schröder and W. Preetz, *Z. Anorg. Allg. Chem.* **627**, 390 (2001).
910. S. Schröder and W. Preetz, *Z. Anorg. Allg. Chem.* **626**, 1915 (2000).
911. T. M. Klapötke, H. Nöth, T. Schütt, and M. Warchhold, *Z. Anorg. Allg. Chem.* **627**, 81 (2001).
912. T. M. Klapötke, K. Polborn, and T. Schutt, *Z. Anorg. Allg. Chem.* **626**, 1444 (2000).
913. S. Schröder and W. Preetz, *Z. Anorg. Allg. Chem.* **626,** 1757, 1915 (2000).
914. M. Stumme and W. Preetz, *Z. Anorg. Allg. Chem.* **626**, 1186 (2000).
915. B. C. Dave and R. S. Czernuszewicz, *J. Coord. Chem.* **33**, 257 (1994).
916. W. Beck, W. P. Felhammer, P. Pöllman, and R. S. Tobias, *Inorg. Chim. Acta* **2**, 467 (1968).
917. D. R. Herrington and L. J. Boucher, *Inorg. Nucl. Chem. Lett.* **7**, 1091 (1971).
918. R. Vicente, A. Escuer, J. Ribas, M. S. El-Fallah, X. Solans, and M. Font-Bardia, *Inorg. Chem.* **32**, 1920 (1993).
919. A. L. Balch, L. A. Fossett, R. R. Guimerans, M. M. Olmstead, P. E. Reedy, and F. E. Wood, *Inorg. Chem.* **25**, 1248 (1986).
920. M. Herberhold, A. Goller, and W. Milius, *Z. Anorg. Allg. Chem.* **627**, 891 (2001).
921. M. Herberhold, A. M. Dietel, and W. Milius, *Z. Anorg. Allg. Chem.* **625**, 1885 (1999).
922. F. A. Mautner, S. Hanna, R. Cortes, L. Lezama, M. G. Barandike, and T. Rojo, *Inorg. Chem.* **38**, 4647 (1999).
923. M. H. V. Huynh, R. T. Baker, D. L. Jameson, A. Labouriau, and T. J. Meyer, *J. Am. Chem. Soc.* **124**, 4580 (2002).
924. P. S. Braterman, *Metal Carbonyl Spectra*, Academic Press, New York, 1974.
925. M. Bigorgne, *J. Organomet Chem.* **94**, 161 (1975).
926. S. F. A. Kettle, *Top. Curr. Chem.* **71**, 111 (1977).
927. C. P. Horwitz and D. F. Shriver, *Adv. Organomet, Chem.* **23**, 219 (1984).
928. C. de la Cruz and N. Sheppard, *J. Mol. Struct.* **224**, 141 (1990).
929. J. S. Kristoff and D. F. Shriver, *Inorg. Chem.* **13**, 499 (1974).
930. G. Bouquet and M. Bigorgne, *Spectrochim. Acta* **27A**, 139 (1971).
931. W. F. Edgell and J. Lyford, IV, *J. Chem. Phys.* **52**, 4329 (1970).
932. H. Stammreich, K. Kawai, Y. Tavares, P. Krumholz, J. Behmoiras, and S. Bril, *J. Chem. Phys.* **32**, 1482 (1960).

933. H. Willner, M. Bodenbinder, R. Bröchler, G. Hwang, S. J. Rettig, J. Trotter, B. von Ahsen, U. Westphal, V. Jonas, W. Thiel, and F. Aubke, *J. Am. Chem. Soc.* **123**, 588 (2001).
934. M. Bigorgne, *J. Organomet. Chem.* **24**, 211 (1970).
935. L. H. Jones, R. S. McDowell, M. Goldblatt, and B. I. Swanson, *J. Chem. Phys.* **57**, 2050 (1972).
936. L. H. Jones, R. S. McDowell, and M. Goldblatt, *Inorg. Chem.* **8**, 2349 (1969).
937. E. Bernhardt, B. Bley, R. Wartchow, H. Willner, E. Bill, P. Kuhn, I. H. T. Shah, M. Bodenbinder, R. Bröchler, and F. Aubke, *J. Am. Chem. Soc.* **121**, 7188 (1999).
938. B. von Absen, M. Berkei, G. Henkel, H. Willer, and F. Aubke, *J. Am. Chem. Soc.* **124**, 8371 (2002).
939. E. W. Abel, R. A. N. McLean, S. P. Tyfield, P. S. Braterman, A. P. Walker, and P. J. Hendra, *J. Mol. Spectrosc.* **30**, 29 (1969).
940. R. A. N. McLean, *Can. J. Chem.* **52**, 213 (1974).
941. A. Terzis and T. G. Spiro, *Inorg. Chem.* **10**, 643 (1971).
942. P. J. Hendra and M. M. Qurashi, *J. Chem. Soc. A* 2963 (1968).
943. S. F. A. Kettle, I. Paul, and P. J. Stamper, *J. Chem. Soc., Chem. Commun.* 1724 (1970).
944. S. F. A. Kettle, I. Paul, and P. J. Stamper, *Inorg. Chim. Acta* **7**, 11 (1973).
945. S. F. A. Kettle and N. Luknar, *J. Chem. Phys.* **68**, 2264 (1978).
946. M. R. Afiz, R. J. H. Clark, and N. R. D'Urso, *J. Chem. Soc., Dalton Trans.* 250 (1977).
947. W. Scheuermann and K. Nakamoto, *J. Raman Spectrosc.* **7**, 341 (1978).
948. D. Adelman and D. P. Gerrity, *J. Phys. Chem.* **94**, 4055 (1990).
949. C. J. Jameson, D. Rehder, and M. Hoch, *Inorg. Chem.* **27**, 3490 (1988).
950. J. M. Allen, W. W. Brennessel, C. E. Buss, J. E. Ellis, M. E. Minyaev, M. Pink, G. F. Warnock, M. L. Winzenburg, and V. G. Young, *Inorg. Chem.* **40**, 5279 (2001).
951. J. E. Ellis, P. T. Barger, M. L. Winzenburg, and G. I. Warnock, *J. Organomet. Chem.* **383**, 521 (1990).
952. J. E. Ellis, C. P. Parnell, and G. P. Hagen, *J. Am. Chem. Soc.* **100**, 3605 (1978).
953. M. Bodenbinder, G. Balzer-Jollenbeck, H. Willner, R. J. Batchelor, F. W. B. Einstein, C. Wang, and F. Aubke, *Inorg. Chem.* **35**, 82 (1996).
954. H. Willner, J. Schaebs, G. Hwang, F. Mistry, R. Jones, J. Trotter, and F. Aubke, *J. Am. Chem. Soc.* **114**, 8972 (1992).
955. G. Hwang, M. Bodenbinder, H. Willner, and F. Aubke, *Inorg. Chem.* **32**, 4667 (1993).
956. W. F. Edgell, J. Lyford, R. Wright, W. M. Risen, Jr., and A. T. Watts, *J. Am. Chem. Soc.* **92**, 2240 (1970); W. F. Edgell and J. Lyford, *ibid*. **93**, 6407 (1971).
957. W. F. Edgell, S. Hegde, and A. Barbetta, *J. Am. Chem. Soc.* **100**, 1406 (1978).
958. F. Kitamura, M. Takahashi, and M. Ito, *Surf. Sci.* **223**, 493 (1989).
959. J. Mink, *Mikrochim. Acta* (*Wien*) **III**, 63 (1987).
960. B. E. Hayden and A. M. Bradshow, *Surf. Sci.* **125**, 787 (1983).
961. M. Ichikawa and T. Fukushima, *J. Phys. Chem.* **89**, 1564 (1985).
962. C. Wang, M. Bodenbinder, H. Willner, S. Rettig, J. Trotter, and F. Aubke, *Inorg. Chem.* **33**, 779 (1994).

963. Q. Xu, B. T. Heaton, C. Jacob, K. Mogi, Y. Ichihashi, Y. Souma, K. Kanamori, and T. Eguchi, *J. Am. Chem. Soc.* **122**, 6862 (2000).
964. G. G. Summer, H. P. Klug, and L. E. Alexander, *Acta Crystallogr.* **17**, 732 (1964).
965. F. A. Cotton and R. R. Monchamp, *J. Chem. Soc.* 1882 (1960).
966. R. L. Sweany and T. L. Brown, *Inorg. Chem.* **16**, 415 (1977).
967. R. K. Sheline and K. S. Pitzer, *J. Am. Chem. Soc.* **72**, 1107 (1950).
968. H. M. Powell and R. V. G. Ewens, *J. Chem. Soc.* 286 (1939).
969. L. F. Dahl and R. E. Rundle, *Acta Crystallogr.* **16**, 419 (1963).
970. D. M. Adams, M. A. Hooper, and A. Squire, *J. Chem. Soc. A* 71 (1971).
971. G. Bor, *Chem. Commun.* 641 (1969).
972. R. A. Levenson, H. B. Gray, and G. P. Ceasar, *J. Am. Chem. Soc.* **92**, 3653 (1970).
973. I. J. Hyams, D. Jones, and E. R. Lippincott, *J. Chem. Soc. A* 1987 (1967).
974. N. Flitcroft, D. K. Huggins, and H. D. Kaesz, *Inorg. Chem.* **3**, 1123 (1964).
975. G. D. Michels and H. J. Svec, *Inorg. Chem.* **20**, 3445 (1981).
976. P. D. Harvey and I. S. Butler, *Can. J. Chem.* **63**, 1510 (1985).
977. D. M. Adams, P. D. Hatton, and A. C. Shaw, *J. Phys., Condens. Matter* **3**, 6145 (1991).
978. L. F. Dahl and J. F. Blount, *Inorg. Chem.* **4**, 1373 (1965); C. H. Wei and L. F. Dahl, *J. Am. Chem. Soc.* **91**, 1351 (1969).
979. N. E. Erickson and A. W. Fairhall, *Inorg. Chem.* **4**, 1320 (1965).
980. F. A. Cotton and D. L. Hunter, *Inorg. Chim. Acta* **11**, L9 (1974).
981. B. F. G. Johnson, *Chem. Commun.* 703 (1976).
982. J. H. Jang, J. G. Lee, H. Lee, Y. Xie, and H. F. Schaefer, III, *J. Phys. Chem. A*, **102**, 5298 (1998).
983. E. R. Corey and L. F. Dahl, *Inorg. Chem.* **1**, 521 (1962).
984. D. K. Huggins, N. Flitcroft, and H. D. Kaesz, *Inorg. Chem.* **4**, 166 (1965).
985. C. O. Quicksall and T. G. Spiro, *Inorg. Chem.* **7**, 2365 (1968).
986. C. E. Anson and U. A. Jayasooriya, *Spectrochim. Acta* **46A**, 967 (1990).
987. G. A. Battiston, G. Bor, U. K. Dietler, S. F. A. Kettle, R. Rossetti, G. Sbrignadello, and P. L. Stanghellini, *Inorg. Chem.* **19**, 1961 (1980).
988. I. T. Horvath, G. Bor, M. Garland, and P. Pino, *Organometallics*, **5**, 1441 (1986).
989. P. Corradini, *J. Chem. Phys.* **31**, 1676 (1959).
990. G. Bor, G. Sbrignadello, and K. Noack, *Helv. Chim. Acta* **58**, 815 (1975).
991. P. C. Steinhardt, W. L. Gladfelter, A. D. Harley, J. R. Fox, and G. L. Geoffroy, *Inorg. Chem.* **19**, 332 (1980).
992. N. T. Lucas, J. P. Blitz, S. Petrie, R. Stranger, M. G. Humphrey, G. A. Heath, and Y. Otieno-Alego, *J. Am. Chem. Soc.* **124**, 5139 (2002).
993. H. Stammreich, K. Kawai, O. Sala, and P. Krumholz, *J. Chem. Phys.* **35**, 2175 (1961).
994. G. Bor, *Inorg. Chim. Acta* **3**, 196 (1969).
995. R. J. Ziegler, J. M. Burlitch, S. E. Hayes, and W. M. Risen, Jr., *Inorg. Chem.* **11**, 702 (1972).
996. F. A. Cotton, L. Kruczynski, and B. A. Frenz, *J. Organomet. Chem.* **160**, 93 (1978).
997. W. D. Jones, M. A. White, and R. G. Bergman, *J. Am. Chem. Soc.* **100**, 6770 (1978).

998. P. Braunstein, C. de Méric de Bellefon, and B. Oswald, *Inorg. Chem.* **32**, 1649 (1993).
999. W. A. Herrmann, M. L. Ziegler, K. Weidenhammer, and H. Biersack, *Angew. Chem., Int. Ed. Engl.* **18**, 960 (1979).
1000. S. F. A. Kettle, E. Diana, P. L. Stanghellini, R. della Pergola, and A. Fumagalli, *Inorg. Chim. Acta* **235**, 407 (1995).
1001. R. della Pergola, A. Cinquantini, G. Garlashelli, F. Laschi, P. Luzzini, M. Manassero, A. Repossi, M. Sansoni, P. L. Stanghellini, and P. Zannello, *Inorg. Chem.* **36**, 3761 (1997).
1002. S. F. Parker, N. A. Marsh, L. M. Camus, M. K. Whittlesey, U. A. Jayasooriya, and G. J. Kearley, *J. Phys. Chem. A* **106**, 5797 (2002).
1003. S. Martinengo, G. Ciani, and A. Sironi, *Chem. Commun.* 1405 (1992).
1004. N. T. Tran, M. Kawano, D. R. Powell, and L. F. Dahl, *J. Chem. Soc., Dalton Trans.* 4138 (2000).
1005. J. Zhang and L. F. Dahl, *J. Chem. Soc., Dalton Trans.* 1269 (2002).
1006. F. Fabrizi de Biani, C. Femoni, M. C. Iapalucci, G. Longoni, P. Zanello, and A. Ceriott, *Inorg. Chem.* **38**, 3721 (1999).
1007. J. D. Roth, G. J. Lewis, L. K. Safford, X. Jiang, L. F. Dahl, and M. J. Weaver, *J. Am. Chem. Soc.* **114**, 6159 (1992).
1008. J. D. Roth, G. J. Lewis, X. Jiang, L. F. Dahl, and M. J. Weaver, *J. Phys. Chem.* **96**, 7219 (1992).
1009. N. J. Nelson, N. E. Kime, and D. F. Shriver, *J. Am. Chem. Soc.* **91**, 5173 (1969).
1010. P. L. Stanghellini, M. J. Sailor, P. Kuznesof, K. H. Whitmire, J. A. Hriljac, J. W. Kolis, Y. Zheng, and D. F. Shriver, *Inorg. Chem.* **26**, 2950 (1987).
1011. C. E. Anson, D. B. Powell, A. G. Cowie, B. F. G. Johnson, J. Lewis, W. J. H. Nelson, J. M. Nicholls, and D. A. Welch, *J. Mol Struct.* **159**, 11 (1987).
1012. G. Bor and P. L. Stanghellini, *Chem. Commun.* 886 (1979).
1013. P. F. Jackson, B. F. G. Johnson, J. Lewis, M. McPartlin, and W. J. H. Nelson, *Chem. Commun.* 224 (1980).
1014. I. A. Oxton, S. G. A. Kettle, P. F. Jackson, B. F. G. Johnson, and J. Lewis, *J. Mol Struct.* **71**, 117 (1981).
1015. M. J. Sailor and D. F. Shriver, *J. Am. Chem. Soc.* **109**, 5039 (1987).
1016. P. Künding, M. Moskovits, and G. A. Ozin, *J. Mol Struct.* **14**, 137 (1972).
1017. J. Mink and P. L. Goggin, *Can. J. Chem.* **69**, 1857 (1991).
1018. B. von Ahsen, R. Wartchow, H. Willner, V. Jonas, and F. Aubke, *Inorg. Chem.* **39**, 4424 (2000).
1019. C. Crocker, P. L. Goggin, and R. J. Goodfellow, *Chem. Commun.* 1056 (1978).
1020. M. Bruns and W. Preetz, *Z. Naturforsch.* **41B**, 25 (1986).
1021. I. J. Hyams and E. R. Lippincott, *Spectrochim. Acta* **25A**, 1845 (1969).
1022. D. K. Ottesen, H. B. Gray, L. H. Jones, and M. Goldblatt, *Inorg. Chem.* **12**, 1051 (1973).
1023. M. J. Cleare and W. P. Griffith, *J. Chem. Soc. A* 372 (1969).
1024. F. H. Johannsen, W. Preetz, and A. Scheffler, *J. Organomet. Chem.* **102**, 527 (1975).
1025. F. H. Johannsen, W. Preetz, and *Z. Naturforsch.* **32B**, 625 (1977).
1026. P. Goggin and J. Mink, *J. Chem. Soc., Dalton Trans.* 534 (1974).

1027. M. A. El-Sayed and H. D. Kaesz, *Inorg. Chem.* **2**, 158 (1963).
1028. C. W. Garland and J. R. Wilt, *J. Chem. Phys.* **36**, 1094 (1962).
1029. L. F. Dahl, C. Martell, and D. L. Wampler, *J. Am. Chem. Soc.* **83**, 1761 (1961).
1030. B. F. G. Johnson, J. Lewis, P. W. Robinson, and J. R. Miller, *J. Chem. Soc. A* 2693 (1969).
1031. F. A. Cotton and B. F. G. Johnson, *Inorg. Chem.* **6**, 2113 (1967).
1032. D. F. Rieck, J. A. Gavney, R. L. Norman, R. K. Hayashi, and L. F. Dahl, *J. Am. Chem. Soc.* **114**, 10369 (1992).
1033. A. Loutellier and M. Bigorgne, *J. Chim. Phys.* **67,** 78, 99, 107 (1970).
1034. M. Bigorgne, *J. Organomet. Chem.* **24**, 211 (1970).
1035. J. Dalton, I. Paul, J. G. Smith, and F. G. A. Stone, *J. Chem. Soc. A* 1195 (1968).
1036. R. J. Angelici and M. D. Malone, *Inorg. Chem.* **6**, 1731 (1967).
1037. B. Hutchinson and K. Nakamoto, *Inorg. Chim. Acta* **3**, 591 (1969).
1038. H. Gäbelein and J. Ellermann, *J. Organomet. Chem.* **156**, 389 (1978).
1039. S. Schmitzer, U. Weis, H. Käb, W. Buchner, W. Malisch, T. Polzer, U. Posset, and W. Kiefer, *Inorg. Chem.* **32**, 303 (1993).
1040. A. M. English, K. R. Plowman, and I. S. Butler, *Inorg. Chem.* **20**, 2553 (1981).
1041. B. H. Weiller, *J. Am. Chem. Soc.* **114**, 10910 (1992).
1042. A. A. Chalmers, J. Lewis, and R. Whyman, *J. Chem. Soc. A* 1817 (1967).
1043. M. F. Farona, J. G. Grasselli, and B. L. Ross, *Spectrochim. Acta* **23A**, 1875 (1967).
1044. S. Singh, P. P. Singh, and R. Rivest, *Inorg. Chem.* **7**, 1236 (1968).
1045. A. Terheiden, E. Bernhardt, H. Willner, and A. Aubke, *Angew. Chem. Int. Ed. Engl.* **41**, 799 (2002).
1046. C. Wang, A. R. Lewis, R. J. Batchelor, F. W. B. Einstein, H. Willner, and A. Aubke, *Inorg. Chem.* **35**, 1279 (1996).
1047. N.-T. Yu, *Methods in Enzymology*, Vol. 130, Academic Press, New York, 1986, p. 350.
1048. M. Kozuka and K. Nakamoto, *J. Am. Chem. Soc.* **103**, 2162 (1981).
1049. B. B. Wayland L. F. Mehne, and J. Swartz, *J. Am. Chem. Soc.* **100**, 2379 (1978).
1050. G. Eaton and S. Eaton, *J. Am. Chem. Soc.* **97**, 235 (1975).
1051. E. A. Kerr, H. C. Mackin, and N.-T. Yu, *Biochemistry* **22**, 4373 (1983).
1052. N.-T. Yu, E. A. Kerr, B. Ward, and C. K. Chang, *Biochemistry* **22**, 4534 (1983).
1053. A. Desbois, M. Momenteau, and M. Lutz, *Inorg. Chem.* **28**, 825 (1989).
1054. H. D. Kaesz and R. B. Saillant, *Chem. Rev.* **72**, 231 (1972).
1055. W. F. Edgell, C. Magee, and G. Gallup, *J. Am. Chem. Soc.* **78** 4185, 4188 (1956); W. F. Edgell and R. Summitt, *ibid*. **83**, 1772 (1961).
1056. S. J. LaPlaca, W. C. Hamilton, and J. A. Ibers, *Inorg. Chem.* **3**, 1491 (1964); *J. Am. Chem. Soc.* **86**, 2288 (1964).
1057. D. K. Huggins and H. D. Kaesz, *J. Am. Chem. Soc.* **86**, 2734 (1964).
1058. P. S. Braterman, R. W. Harrill, and H. D. Kaesz, *J. Am. Chem. Soc.* **89**, 2851 (1967).
1059. A. Davison and J. W. Falter, *Inorg. Chem.* **6**, 845 (1967).
1060. W. F. Edgell, J. W. Fisher, G. Asato, and W. M. Risen, Jr., *Inorg. Chem.* **8**, 1103 (1969).
1061. K. Farmery and M. Kilner, *J. Chem. Soc. A* 634 (1970).
1062. S. S. Bath and L. Vaska, *J. Am. Chem. Soc.* **85**, 3500 (1963).

1063. J. Chatt, N. P. Johnson, and B. L. Shaw, *J. Chem. Soc.* 1625 (1964).
1064. L. Vaska, *J. Am. Chem. Soc.* **88**, 4100 (1966).
1065. F. L'Eplattenier and F. Calderazzo, *Inorg. Chem.* **7**, 1290 (1968).
1066. D. K. Huggins, W. Fellman, J. M. Smith, and H. D. Kaesz, *J. Am. Chem. Soc.* **86**, 4841 (1964).
1067. J. M. Smith, W. Fellmann, and L. H. Jones, *Inorg. Chem.* **4**, 1361 (1965).
1068. R. G. Hayter, *J. Am. Chem. Soc.* **88**, 4376 (1966).
1069. R. Bau and T. F. Koetzle, *Pure Appl Chem.* **50**, 55 (1978).
1070. C. B. Cooper, III, D. F. Shriver, D. J. Darensbourg, and J. A. Froelich, *Inorg. Chem.* **18**, 1407 (1979); C. B. Cooper, III, D. F. Shriver, and S. Onaka, *Adv. Chem. Ser.* **167**, 232 (1978).
1071. A. P. Ginsberg and M. J. Hawkes, *J. Am. Chem. Soc.* **90**, 5931 (1968).
1072. M. J. Mays and R. N. F. Simpson, *J. Chem. Soc. A* 1444 (1968); *Chem. Commun.* 1024 (1967).
1073. H. D. Kaesz, F. Fontal, R. Bau, S. W. Kirtley, and M. R. Churchill, *J. Am. Chem. Soc.* **91**, 1021 (1969).
1074. M. J. Bennett, W. A. G. Graham, J. K. Hoyano, and W. L. Hutcheon, *J. Am. Chem. Soc.* **94**, 6232 (1972).
1075. S. A. R. Knox, J. W. Koepke, M. A. Andrews, and H. D. Kaesz, *J. Am. Chem. Soc.* **97**, 3942 (1975).
1076. S. A. R. Knox and H. D. Kaesz, *J. Am. Chem. Soc.* **93**, 4594 (1971).
1077. C. E. Anson, U. A. Jayasooriya, S. F. A. Kettle, P. L. Stranghellini, and R. Rosetti, *Inorg. Chem.* **30**, 2282 (1991).
1078. C. R. Eady, B. F. G. Johnson, J. Lewis, M. C. Malatesta, P. Machin, and M. McPartlin, *Chem. Commun.* 945 (1976).
1079. I. A. Oxton, S. F. A. Kettle, P. F. Jackson, B. F. G. Johnson, and J. Lewis, *Chem. Commun.* 687 (1979).
1080. J. W. White and C. J. Wright, *Chem. Commun.* 971 (1970).
1081. M. Zhou, L. Andrews, and C. W. Bauschlicher, Jr., *Chem. Rev.* **101**, 1931 (2001).
1082. L. Manceron and M. E. Alikhani, *Chem. Phys.* **244**, 215 (1999).
1083. B. Tremblay and L. Monceron, *Chem. Phys.* **250**, 187 (1999).
1084. M. Zhou and L. Andrews, *J. Chem. Phys.* **110**, 10370 (1999).
1085. M. Zhou and L. Andrews, *J. Am. Chem. Soc.* **120**, 11499 (1998).
1086. A. J. Downs, T. M. Greene, and C. M. Gordon, *Inorg. Chem.* **34**, 6191 (1995).
1087. L. Shao, L. Zhang, M. Zhou, and Q. Qin, *Organometallics* **20**, 1137 (2001).
1088. M. Zhou and L. Andrews, *J. Phys. Chem. A* **103**, 7785 (1999).
1089. C. N. Krishnan, R. H. Hauge, and J. L. Margrave, *J. Mol. Struct.* **157**, 187 (1987).
1090. D. McIntosh and G. A. Ozin, *Inorg. Chem.* **16**, 51 (1977).
1091. L. Andrews and T. J. Tague, Jr., *J. Am. Chem. Soc.* **116**, 6856 (1994).
1092. M. Poliakoff and J. J. Turner, *J. Chem. Soc., Dalton Trans.* 1351 (1973); 2276 (1974).
1093. M. A. Graham, M. Poliakoff, and J. J. Turner, *J. Chem. Soc. A* 2939 (1971).
1094. E. P. Kündig and G. A. Ozin, *J. Am. Chem. Soc.* **96**, 3820 (1974).
1095. J. D. Black and P. S. Braterman, *J. Am. Chem. Soc.* **97**, 2908 (1975).

1096. R. N. Perutz and J. J. Turner, *Inorg. Chem.* **14**, 262 (1975).
1097. S. C. Fletcher, M. Poliakoff, and J. J. Turner, *Inorg. Chem.* **25**, 3597 (1986).
1098. I. R. Dunkin, P. Härter, and C. J. Shields, *J. Am. Chem. Soc.* **106**, 7248 (1984).
1099. A. F. Hepp and M. J. Wrighton, *J. Am. Chem. Soc.* **105**, 5934 (1983).
1100. S. Firth, P. M. Hodges, M. Poliakoff, and J. J. Turner, *Inorg. Chem.* **25**, 4608 (1986).
1101. D. A. Van Leirsburg and C. W. DeKock, *J. Phys. Chem.* **78**, 134 (1974).
1102. D. Tevault and K. Nakamoto, *Inorg. Chem.* **15**, 1282 (1976).
1103. B. I. Swanson, L. H. Jones, and R. R. Ryan, *J. Mol. Spectrosc.* **45**, 324 (1973).
1104. M. Poliakoff and J. J. Turner, *J. Chem. Soc. A* 654 (1971).
1105. D. Tevault and K. Nakamoto, *Inorg. Chem.* **14**, 2371 (1975); A. Cormier, J. D. Brown, and K. Nakamoto, *ibid*. **12**, 3011 (1973).
1106. F. A. Cotton, and C. S. Kraihanzel, *J. Am. Chem. Soc.* **84**, 4432 (1962); *Inorg. Chem.* **2**, 533 (1963); **3**, 702 (1964).
1107. F. A. Cotton, M. Musco, and G. Yagupsky, *Inorg. Chem.* **6**, 1357 (1967).
1108. L. H. Jones, *Inorg. Chem.* **7**, 1681 (*1968);* **6**, 1269 (1967).
1109. F. A. Cotton, *Inorg. Chem.* **7**, 1683 (1968).
1110. M. B. Hall and R. F. Fenske, *Inorg. Chem.* **11**, 1619 (1972).
1111. A. C. Sarapu and R. F. Fenske, *Inorg. Chem.* **14**, 247 (1975).
1112. I. Castro-Rodriguez, H. Nakai, L. N. Zakharov, A. L. Rheingold, and K. Meyer, *Science* **305**, 1757 (2004).
1113. K. Toyohara, K. Tsuge, and K. Tanaka, *Organometallics* **14**, 5099 (1995).
1114. K. Tanaka, Y. Kushi, K. Tsuge, K. Toyohara, T. Nishioka, and K. Isobe, *Inorg. Chem.* **37**, 120 (1998).
1115. C. Jegat, M. Fouassier, M. Tranquille, and J. Mascetti, *Inorg. Chem.* **30**, 1529 (1991).
1116. C. Jegat, M. Fouassier, and J. Mascetti, *Inorg. Chem.* **30**, 1521 (1991).
1117. C. Jegat, M. Fouassier, M. Tranquille, J. Mascetti, I. Tommasi, M. Aresta, F. Ingold, and A. Dedieu, *Inorg. Chem.* **32**, 1279 (1993).
1118. M. Aresta and C. F. Nobile, *J. Chem. Soc., Dalton Trans.* 708 (1977).
1119. M. Aresta and C. F. Nobile, *Inorg. Chim. Acta* **24**, L49 (1977).
1120. J. Mascetti and M. Tranquille, *J. Phys. Chem.* **92**, 2177 (1988).
1121. V. N. Solov'ev, E. V. Polikarpov, A. V. Nemukhin, and G. B. Sergeev, *J. Phys. Chem. A*, **103**, 6721 (1999).
1122. A. M. Le Quere, C. Xu, and L. Manceron, *J. Phys. Chem.* **95**, 3031 (1991).
1123. G. A. Ozin, H. Huber, and D. McIntosh, *Inorg. Chem.* **17**, 1472 (1978).
1124. B. Liang and L. Andrews, *J. Phys. Chem. A* **106**, 595 (2002).
1125. M. Zhou, L. Zhang, M. Chen, Q. Zheng, and Q. Qin, *J. Phys. Chem. A* **104**, 10159 (2000).
1126. J. A. McGinnety, *MTP Int. Rev. Sci. Inorg. Chem.* **5**, 229 (1972).
1127. B. L. Haymore and J. A. Ibers, *Inorg. Chem.* **14**, 3060 (1975).
1128. P. Gans, A. Sabatini, and L. Sacconi, *Coord. Chem. Rev.* **1**, 187 (1966).
1129. J. Masek, *Inorg. Chim. Acta, Rev.* **3**, 99 (1969).
1130. B. F. G. Johnson and J. A. McCleverty, *Progr. Inorg. Chem.* **7**, 277 (1966).

1131. W. P. Griffith, *Adv. Organomet. Chem.* **7**, 211 (1968).
1132. J. H. Enemark and R. D. Feltham, *Coord. Chem. Rev.* **13**, 339 (1974).
1133. M. Herberhold and A. Razavi, *Angew. Chem., Int. Ed. Engl.* **11**, 1092 (1972).
1134. I. H. Sabberwal and A. B. Burg, *Chem. Commun.* 1001 (1970).
1135. A. Keller, *Inorg. Chim. Acta* **133**, 207 (1987).
1136. J. A. Timney and C. A. Barnes, *Spectrochim. Acta* **48A**, 953 (1992).
1137. L. H. Jones, R. S. McDowell, and B. I. Swanson, *J. Chem. Phys.* **58**, 3757 (1973).
1138. G. Barna and I. S. Butler, *Can. J. Spectrosc.* **17**, 2 (1972).
1139. O. Crichton and A. J. Rest, *Inorg. Nucl. Chem. Lett.* **9**, 391 (1973).
1140. B. F. G. Johnson, *J. Chem. Soc. A* 475 (1967).
1141. Z. Iqbal and T. C. Waddington, *J. Chem. Soc. A* 1092 (1969).
1142. E. Miki, T. Ishimori, H. Yamatera, and H. Okuno, *J. Chem. Soc. Jpn.* **87**, 703 (1966).
1143. J. R. Durig, W. A. McAllister, J. N. Willis, Jr., and E. E. Mercer, *Spectrochim. Acta* **22**, 1091 (1966).
1144. K. E. Linder, J. C. Dewan, C. E. Costello, and S. Maleknia, *Inorg. Chem.* **25**, 2085 (1986).
1145. M. Quinby-Hunt and R. D. Feltham, *Inorg. Chem.* **17**, 2515 (1978).
1146. J. H. Swinebart, *Coord. Chem. Rev.* **2**, 385 (1967).
1147. R. K. Khanna, C. W. Brown, and L. H. Jones, *Inorg. Chem.* **8**, 2195 (1969).
1148. J. B. Bates and R. K. Khanna, *Inorg. Chem.* **9**, 1376 (1970).
1149. D. B. Brown, *Inorg. Chim. Acta* **5**, 314 (1971).
1150. L. Tosi and J. Danon, *Inorg. Chem.* **3**, 150 (1964).
1151. E. L. Varetti, M. M. Vergara, G. Rigotti, and A. Navaza, *J. Phys. Chem. Solids* **51**, 381 (1990).
1152. J. A. Güida, O. E. Piro, P. J. Aymonino, and O. Sala, *J. Raman Spectrosc.* **23**, 131 (1992).
1153. M. E. Chacón Villalba, E. L. Varetti, and P. J. Aymonino, *Vib. Spectrosc.* **4**, 109 (1992).
1154. A. Poletti, A. Santucci, and G. Paliani, *Spectrochim. Acta* **27A**, 2061 (1971).
1155. E. Miki, S. Kubo, K. Mizumachi, T. Ishimori, and H. Okuno, *Bull. Chem. Soc. Jpn.* **44**, 1024 (1971).
1156. C. G. Pierpont, D. G. Van Derveer, W. Durland, and R. Eisenberg, *J. Am. Chem. Soc.* **92**, 4760 (1970).
1157. C. P. Brock, J. P. Collman, G. Dolcetti, P. H. Farnham, J. A. Ibers, J. E. Lester, and C. A. Reed, *Inorg. Chem.* **12**, 1304 (1973).
1158. J. Müller and S. Schmitt, *J. Organomet. Chem.* **160**, 109 (1978).
1159. R. G. Ball, B. W. Hames, P. Legzdins, and J. Trotter, *Inorg. Chem.* **19**, 3626 (1980).
1160. J. R. Norton, J. P. Collman, G. Dolcetti, and W. T. Robinson, *Inorg. Chem.* **11**, 382 (1972).
1161. H. Nagao, N. Nagao, Y. Yukawa, D. Ooyama, Y. Sato, T. Oosawa, H. Kuroda, F. S. Howell, and M. Mukaida, *Bull. Chem. Soc. Jpn.* **72**, 1273 (1999).
1162. J. Muller and C. Hirsch, *Z. Anorg. Allg. Chem.* **621**, 1478 (1995).
1163. B. W. Fitzsimmons, L. F. Larkworthy, and K. A. Rogers, *Inorg. Chim. Acta* **44**, L53 (1980).

1164. S. K. Satija, B. I. Swanson, O. Crichton, and A. J. Rest, *Inorg. Chem.* **17**, 1737 (1978).
1165. O. Crichton and A. J. Rest, *J. Chem. Soc., Dalton Trans.* **202**, 208 (1978).
1166. O. Crichton and A. J. Rest, *Chem. Commun.* 407 (1973).
1167. B. B. Wayland L. W. Olson, and Z. U. Siddiqui, *J. Am. Chem. Soc.* **98**, 94 (1976).
1168. B. B. Wayland and L. W. Olson, *J. Am. Chem. Soc.* **96**, 6037 (1974).
1169. D. S. Bohle, C.-H. Hung, A. K. Powell, B. D. Smith, and S. Wocadlo, *Inorg. Chem.* **36**, 1992 (1997).
1170. K. M. Kadish, V. A. Adamian, E. van Caemelbecke, Z. Tan, P. Tagliatesta, P. Bianco, T. Boschi, G.-B. Yi, M. A. Khan, and G. B. Rechter-Addo, *Inorg. Chem.* **35**, 1343 (1996).
1171. J. C. Maxwell and W. S. Caughey, *Biochemistry* **15**, 388 (1976).
1172. I. K. Choi, Y. Liu, D. W. Feng, K. J. Paeng, and M. D. Ryan, *Inorg. Chem.* **30**, 1832 (1991).
1173. N.-T. Yu, S. H. Lin, C. K. Chang, and K. Gersonde, *Biophys. J.*, **55**, 1137 (1989).
1174. L. A. Lipscomb, B. S. Lee, and N.-T. Yu, *Inorg. Chem.* **32**, 281 (1993).
1175. J. A. Güida, P. J. Aymonino, O. E. Piro, and E. E. Castellano, *Spectrochim. Acta* **49A**, 535 (1993).
1176. J. A. Güida, O. E. Piro, and P. J. Aymonino, *Solid State Commun* **57**, 175 (1986).
1177. F. Bottomly and P. S. White, *Acta Crystallogr.* **B35**, 2193 (1979).
1178. M. D. Carducci, M. R. Pressprich, and P. Coppens, *J. Am. Chem. Soc.* **119**, 2669 (1997).
1179. Y. Morioka, S. Takeda, H. Tomizawa, and E. Miki, *Chem. Phys. Lett.* **292**, 625 (1998).
1180. M. E. Chacón Villalba, J. A. Guida, E. L. Varetti, and P. J. Aymonino, *Spectrochim. Acta* **57A**, 367 (2001).
1181. M. E. Chacón Villalba, J. A. Guida, E. L. Varetti, and P. J. Aymonino, *Inorg. Chem.* **42**, 2622 (2003).
1182. D. V. Fomitchev and P. Coppens, *Inorg. Chem.* **35**, 7021 (1996).
1183. A. Puig-Molina, H. Muller, A.-M. Le Quere, G. Vaughan, H. Graafsma, and A. Kvick, *Z. Anorg. Allg. Chem.* **626**, 2379 (2000).
1184. C. Kim, I. Novozhilova, M. S. Goodman, K. A. Bagley, and P. Coppens, *Inorg. Chem.* **39**, 5791 (2000).
1185. J. A. Guida, M. A. Ramos, O. E. Piro, and P. J. Aymonino, *J. Mol. Struct.* **609**, 39 (2002).
1186. M. Kawano, A. Ishikawa, Y. Morioka, H. Tomizawa, E.-I. Miki, and Y. Ohashi, *J. Chem. Soc., Dalton Trans.* 2425 (2000).
1187. Y. Morioka, A. Ishikawa, H. Tomizawa, and E.-I. Miki, *J. Chem. Soc., Dalton Trans.* 781 (2000).
1188. K. Ookubo, Y. Morioka, H. Tomizawa, and E. Miki, *J. Mol. Struct.* **379**, 241 (1996).
1189. D. V. Fomitchev, P. Coppenns, T. Li, K. A. Bagley, L. Chen, and G. B. Richter-Addo, *Chem. Commun.* 2013 (1999).
1190. J. A. Güida, O. E. Piro, and P. J. Aymonino, *Inorg. Chem.* **34**, 4113 (1995).
1191. P. S. Schaiquevich, J. A. Güida, and P. J. Aymonino, *Inorg. Chim. Acta* **303**, 277 (2000).
1192. P. Coppens, I. Novozhilova, and A. Kovalevsky, *Chem. Rev.* **102**, 861 (2002).
1193. P. Gütlich, Y. Garcia, and T. Woike, *Coord. Chem. Rev.* **219/221**, 839 (2001).
1194. L. Andrews and A. Citra, *Chem. Rev.* **102**, 885 (2002).
1195. M. Zhou and L. Andrews, *J. Phys. Chem. A* **102**, 7452 (1998).

1196. V. J. Choy and C. H. O'Connor, *Coord. Chem. Rev.* **9**, 145 (1972/1973).
1197. F. Basolo, B. M. Hoffman, and J. A. Ibers, *Acc. Chem. Res.* **8**, 384 (1975).
1198. L. Vaska, *Acc. Chem. Res.* **9**, 175 (1976).
1199. J. P. Collman, *Acc. Chem. Res.* **10**, 265 (1977).
1200. G. McLendon and A. E. Martell, *Coord. Chem. Rev.* **19**, 1 (1976).
1201. R. W. Erskine and B. O. Field, *Struct. Bonding* (*Berlin*) **28**, 1 (1976).
1202. R. D. Jones, D. A. Summerville, and F. Basolo, *Chem. Rev.* **79**, 139 (1979).
1203. T. D. Smith and J. R. Pilbrow, *Coord. Chem. Rev.* **39**, 295 (1981).
1204. M. H. Gubelmann and A. F. Williams, *Struct. Bonding* (*Berlin*) **55**, 1 (1983).
1205. E. C. Niederhoffer, J. H. Timmons, and A. E. Martell, *Chem. Rev.* **84**, 137 (1984).
1206. L. Andrews, "Infrared and Raman Spectroscopic Studies of Alkali-Metal-Atom Matrix-Reaction Products" in M. Moskovits and G. A. Ozin, eds., *Cryochemistry*, Wiley-Interscience, New York, 1976, p. 211.
1207. D. Mclntosh and G. A. Ozin, *Inorg. Chem.* **16**, 59 (1977).
1208. A. J. L. Hanlan and G. A. Ozin, *Inorg. Chem.* **16**, 2848 (1977).
1209. M. J. Zehe, D. A. Lynch, Jr., B. J. Kelsali, and K. D. Carlson, *J. Phys. Chem.* **83**, 656 (1979).
1210. D. McIntosh and G. A. Ozin, *Inorg. Chem.* **15**, 2869 (1976).
1211. B. J. Kelsall and K. D. Carlson, *J. Phys. Chem.* **84**, 951 (1980).
1212. H. Huber, W. Klotzbücher, G. A. Ozin, and A. Vander Voet, *Can. J. Chem.* **51**, 2722 (1973).
1213. S. Chang, G. Blyholder, and J. Fernandez, *Inorg. Chem.* **20**, 2813 (1981).
1214. A. B. P. Lever, G. A. Ozin, and H. B. Gray, *Inorg. Chem.* **19**, 1823 (1980).
1215. L. Andrews, *J. Chem. Phys.* **50**, 4288 (1969).
1216. J. C. Evans, *Chem. Commun.* 682 (1969).
1217. H. H. Eysel and S. Thym, *Z. Anorg. Allg. Chem.* **411**, 97 (1975).
1218. A. Citra, G. V. Chertihin, L. Andrews, and M. Neurock, *J. Phys. Chem. A* **101**, 3109 (1997).
1219. A. Bakac, S. L. Scott, J. H. Espenson, and K. R. Rodgers, *J. Am. Chem. Soc.* **117**, 6483 (1995).
1220. X. Zhang, G. R. Loppnow, R. Mcdonald, and J. Takats, *J. Am.Chem. Soc.* **117**, 7828 (1995).
1221. M. K. Chaudhuri and B. Das, *Inorg. Chem.* **25**, 168 (1986).
1222. E. M. Nour and S. Morsy, *Inorg. Chim. Acta* **117**, 45 (1986).
1223. M. T. H. Trafder and A. A. M. A. Islam, *Polyhedron* **8**, 109 (1989).
1224. C. R. Bhattacharjee, M. Bhattacharjee, M. K. Chaudhuri, and M. Choudhury, *Polyhedron* **9**, 1653 (1990).
1225. R. Schmidt, G. Pausewang, and W. Massa, *Z Anorg. Allg. Chem.* **535**, 135 (1986).
1226. N. J. Campbell, A. C. Dengel, and W. P. Griffith, *Polyhedron* **8**, 1379 (1989).
1227. M. C. Chakravorti, S. Ganguly, G. V. B. Subrahmanyam, and M. Bhattacharjee, *Polyhedron* **12**, 683 (1993).
1228. A. C. Dengel, W. P. Griffith, and B. C. Parkin, *J. Chem. Soc., Dalton Trans.* 2683 (1993).

1229. S. Ahmad, J. D. McCallum, A. K. Shiemke, E. H. Appelman, T. M. Loehr, and J. Sanders-Loehr, *Inorg. Chem.* **27**, 2230 (1988).

1230. J. K. Basumatary, M. K. Chaudhuri, and R. N. Dutta Purkayastha, *J. Chem. Soc., Dalton Trans.* 709 (1986).

1231. J. A. Crayston and G. Davidson, *Spectrochim. Acta* **42A**, 1311 (1986).

1232. A. Nakamura, Y. Tatsuno, M. Yamamoto, and S. Otsuka, *J. Am. Chem. Soc.* **93**, 6052 (1971).

1233. N. Kitajima, K. Fujisawa, C. Fujimoto, Y. Moro-oka, S. Hashimoto, T. Kitagawa, K. Toriumi, K. Tatsumi, and A. Nakamura, *J. Am. Chem. Soc.* **114**, 1277 (1992).

1234. K. Nakamoto, Y. Nonaka, T. Ishiguro, M. W. Urban, M. Suzuki, M. Kozuka, Y. Nishida, and S. Kida, *J. Am. Chem. Soc.* **104**, 3386 (1982).

1235. K. Bajdor, K. Nakamoto, H. Kanatomi, and I. Murase, *Inorg. Chim. Acta* **82**, 207 (1984).

1236. T. Shibahara and M. Mori, *Bull. Chem. Soc. Jpn.* **51**, 1374 (1978).

1237. C. G. Barraclough, G. A. Lawrence, and P. A. Lay, *Inorg. Chem.* **17**, 3317 (1978).

1238. R. E. Hester and E. M. Nour, *J. Roman Spectrosc.* **11**, 43 (1981).

1239. M. Suzuki, T. Ishiguro, M. Kozuka, and K. Nakamoto, *Inorg. Chem.* **20**, 1993 (1981).

1240. E. M. Nour and R. E. Hester, *J. Mol. Struct.* **62**, 77 (1980).

1241. K. Nakamoto, M. Suzuki, T. Ishiguro, M. Kozuka, Y. Nishida, and S. Kida, *Inorg. Chem.* **19**, 2822 (1980).

1242. R. E. Hester and E. M. Nour, *J. Raman Spectrosc.* **11**, 59 (1981).

1243. T. Tsumaki, *Bull. Chem. Soc. Jpn.* **13**, 252 (1938).

1244. M. Kozuka and K. Nakamoto, *J. Am. Chem. Soc.* **103**, 2162 (1981).

1245. M. W. Urban, K. Nakamoto, and J. Kincaid, *Inorg. Chem.* **61**, 77 (1983).

1246. L. M. Proniewicz, A. Kulczycki, A. Weselucha-Birczybska, H. Majcherczyk, and K. Nakamoto, *New J. Chem.* **23**, 71 (1999).

1247. L. M. Proniewicz and K. Nakamoto, to be published.

1248. T. Watanabe, T. Ama, and K. Nakamoto, *J. Phys. Chem.* **88**, 440 (1984).

1249. W.-D. Wagner, I. R. Paeng, and K. Nakamoto, *J. Am. Chem. Soc.* **110**, 5565 (1988).

1250. K. Bajdor, H. Oshio, and K. Nakamoto, *J. Am. Chem. Soc.* **106**, 7273 (1984).

1251. L. M. Proniewicz, T. Isobe, and K. Nakamoto, *Inorg. Chim. Acta* **155**, 91 (1989).

1252. W. Lewandowski, L. M. Proniewicz, and K. Nakamoto, *Inorg. Chim. Acta* **190**, 145 (1991).

1253. M. W. Urban, K. Nakamoto, and F. Basolo, *Inorg. Chem.* **21**, 3406 (1982).

1254. A. Weselucha-Birczynska, L. M. Proniewicz, K. Bajdor, and K. Nakamoto, *J. Raman Spectrosc.* **22**, 315 (1991).

1255. T. Watanabe, T. Ama, and K. Nakamoto, *Inorg. Chem.* **22**, 2470 (1983).

1256. K. Hasegawa T. Imamura, and M. Fujimoto, *Inorg. Chem.* **25**, 2154 (1986).

1257. K. Nakamoto, *Coord. Chem. Rev.* **100**, 363 (1990).

1258. K. Bajdor, J. R. Kincaid, and K. Nakamoto, *J. Am. Chem. Soc.* **106**, 7741 (1984).

1259. K. Nakamoto, I. R. Paeng, T. Kuroi, T. Isobe, and H. Oshio, *J. Mol. Struct.* **189**, 293 (1988).

1260. P. Doppelt and R. Weiss, *Nouv. J. Chim.* **7**, 341 (1983).

1261. J. P. Collman, J. I. Brauman, T. R. Halbert, and K. S. Suslick, *Proc. Natl. Acad. Sci. USA* **73**, 3333 (1976).

1262. J. M. Burke, J. R. Kincaid, S. Peters, R. R. Gagne, J. P. Collman, and T. G. Spiro, *J. Am. Chem. Soc.* **100**, 6083 (1978).
1263. G. Chottard, M. Schappacher, L. Richard, and R. Weiss, *Inorg. Chem.* **23**, 4557 (1984).
1264. J. R. Kincaid, L. M. Proniewicz, K. Bajdor, A. Bruha, and K. Nakamoto, *J. Am. Chem. Soc.* **107**, 6775 (1985).
1265. K. Nakamoto and H. Oshio, *J. Am. Chem. Soc.* **107**, 6518 (1985).
1266. M. Matsu-ura, F. Tani, S. Nakayama, N. Nakamura, and Y. Naruta, *Angew. Chem., Int. Ed. Engl.* **39**, 1989 (2000).
1267. J. Odo, H. Imai, E. Kyuno, and K. Nakamoto, *J. Am. Chem. Soc.* **110**, 742 (1988).
1268. L. M. Proniewicz, J. Odo, J. Goral, C. K. Chang, and K. Nakamoto, *J. Am. Chem. Soc.* **111**, 2105 (1989).
1269. L. M. Proniewicz, J. Golus, K. Nakamoto, and J. R. Kincaid, *J. Raman Spectrosc.* **26**, 27 (1995).
1270. L. M. Proniewicz, A. Bruha, K. Nakamoto, E. Kyuno, and J. R. Kincaid, *J. Am. Chem. Soc.* **111**, 7050 (1989).
1271. L. M. Proniewicz, A. Bruha, K. Nakamoto, Y. Uemori, E. Kyuno, and J. R. Kincaid, *J. Am. Chem. Soc.* **113**, 9100 (1991).
1272. L. M. Proniewicz and J. R. Kincaid, *J. Am. Chem. Soc.* **112**, 675 (1990).
1273. J. P. Fox, B. Ramdhanie, A. A. Zareba, R. S. Czernuszewicz, and D. P. Goldberg, *Inorg. Chem.* **43**, 6600 (2004).
1274. B. S. Mandimutsira, B. Ramdhanie, R. C. Todd, H. Wang, A. A. Zareba, R. S. Czernuszewicz, and D. P. Goldberg, *J. Am. Chem. Soc.* **124**, 15170 (2002).
1275. M. Chatterjee, B. Achari, S. Das, R. Banerjee, C. Chakrabarti, J. K. Dattagupta, and S. Banerjee, *Inorg. Chem.* **37**, 5424 (1998).
1276. M. Kim, W. K. Seok, H. N. Lee, S. H. Han, Y. Dong, and H. Yun, *Z. Naturforsch.* **56B**, 747 (2001).
1277. K. Wieghardt, G. Backes-Dahmann, B. Nuber, and J. Weiss, *Angew. Chem., Int. Ed. Engl.* **24**, 777 (1985).
1278. A. Bashall, V. C. Gibson, T. P. Kee, M. McPartlin, O. B. Robinson, and A. Shaw, *Angew. Chem., Int. Ed. Engl.* **30**, 980 (1991).
1279. W. P. Griffith and J. D. Wickins, *J. Chem. Soc. A* 400 (1968).
1280. J. C. Dobson, K. J. Takeuchi, D. W. Pipes, D. A. Geselowitz, T. J. Meyer *Inorg. Chem.* **25**, 2357 (1986).
1281. C. S. Johnson, C. Mottley, J. T. Hupp, and G. D. Danzer, *Inorg. Chem.* **31**, 5143 (1992).
1282. G. Pausewang and K. Dehnicke, *Z. Anorg. Allg. Chem.* **369**, 265 (1969).
1283. F. W. Moore and R. E. Rice, *Inorg. Chem.* **7**, 2510 (1968).
1284. A. Syamal and M. R. Maurya, *Transition Met. Chem.* **11**, 255 (1986).
1285. K. Dreisch, C. Anderson, and C. Stalhandske, *Polyhedron* **11**, 2143 (1992).
1286. B. Šoptrjanov, A. Nikolovski, and I. Petrov, *Spectrochim. Acta* **24A**, 1617 (1968).
1287. W. Willing, F. Schmock, U. Müller, and K. Dehnicke, *Z. Anorg. Allg. Chem.* **532**, 137 (1986).
1288. I. R. Paeng and K. Nakamoto, *J. Am. Chem. Soc.* **112**, 3289 (1990).
1289. J. T. Groves and K. H. Ahn, *Inorg. Chem.* **26**, 3831 (1987).

1290. V. R. Reddy, D. F. Berning, K. V. Ketti, C. I. Bernes, W. A. Volkert, and A. R. Ketring, *Inorg. Chem.* **35**, 1753 (1996).

1291. E. Lengo, E. Zangranddo, S. Mestroni, G. Fronzoni, M. Stener, and E. Alessio, *J. Chem. Soc., Dalton Trans.* 1338 (2001).

1292. A. Struess and W. Preetz, *Z. Naturforsch.* **53B**, 1338 (1998).

1293. M. K. Chaudhin, D. T. Khathing, and P. Srinivas, *J. Fluorine Chem.* **56**, 305 (1992).

1294. G. Asgedom, A. Sreedhara, J. Kovikoski, J. Volkonen, F. Kohlemainen, and C. P. Rao, *Inorg. Chem.* **35**, 5674 (1996).

1295. W. J. Casteel, D. M. Mcleod, H. P. A. Mercier, and G. J. Schrobilgen, *Inorg. Chem.* **35**, 7279 (1996).

1296. W. L. Casteel, D. A. Dixon, N. LeBlond, P. E. Lock, H. P. A. Mercier, and G. J. Schrobilgen, *Inorg. Chem.* **38**, 2340 (1999).

1297. K. O. Kriste, D. A. Dixon, H. G. Mack, H. Oberhammer, A. Pagelot, J. C. P. Sanders, and G. J. Schrobilgen, *J. Am. Chem. Soc.* **115**, 11279 (1993).

1298. J. M. Burke, J. R. Kincaid, and T. G. Spiro, *J. Am. Chem. Soc.* **100**, 6077 (1978).

1299. N. J. Boldt, and D. F. Bocian, *J. Phys. Chem.* **92**, 581 (1988).

1300. D. J. Liston and B. O. West, *Inorg. Chem.* **24**, 1568 (1985).

1301. D. J. Liston, B. J. Kennedy, K. Murray, and B. O. West, *Inorg. Chem.* **24**, 1561 (1985).

1302. P. C. Junk, B. J. McCool, B. Moubaraki, K. S. Murray, J. D. Casion, and J. W. Steed, *J. Chem. Soc., Dalton Trans.* 1024 (2002).

1303. K. Kanamori, M. Teraoka, H. Maeda, and K. Okamoto, *Chem. Lett.* 1731 (1993).

1304. K. Wieghardt, K. Pohl, and W. Gebert, *Angew. Chem., Int. Ed. Engl.* **22**, 727 (1983).

1305. R. S. Czernuszewicz, J. E. Sheats, and T. G. Spiro, *Inorg. Chem.* **26**, 2963 (1987).

1306. M. R. Bond, R. S. Czernuszewicz, B. C. Dave, Q. Yan, M. Mohan, R. Verastegue, and C. J. Carrano, *Inorg. Chem.* **34**, 5857 (1995).

1307. J. Sanders-Loehr, W. D. Wheeler, A. K. Shiemke, B. A. Averill, and T. M. Loehr, *J. Am. Chem. Soc.* **111**, 8084 (1989).

1308. M. A. Cinellu, G. Minghetti, M. V. Pinna, S. Stoccoro, A. Zucca, and M. Manassero, *J. Chem. Soc., Dalton Trans.* 1261 (2000).

1309. Y. Funahashi, K. Nakaya, S. Hirota, and O. Yamauchi, *Chem. Lett.* 1172 (2000).

1310. C. E. Anson, N. Chai-Sa'ard, J. P. Bourke, R. D. Cannon, U. A. Jayasooriya, and A. K. Powell, *Inorg. Chem.* **32**, 1502 (1993).

1311. K. Bajdor and K. Nakamoto, *J. Am. Chem. Soc.* **106**, 3045 (1984).

1312. L. M. Proniewicz, K. Bajdor, and K. Nakamoto, *J. Phys. Chem.* **90**, 1760 (1986).

1313. R. S. Czernuszewicz and K. A. Macor, *J. Raman Spectrosc.* **19**, 553 (1988).

1314. R. S. Czernuszewicz, Y. O. Su, M. K. Stem, K. A. Macor, D. Kim, J. T. Groves, and T. G. Spiro, *J. Am. Chem. Soc.* **110**, 4158 (1988).

1315. W.-D. Wagner and K. Nakamoto, *J. Am. Chem. Soc.* **110**, 4044 (1988).

1316. L. M. Proniewicz, I. R. Paeng, and K. Nakamoto, *J. Am. Chem. Soc.* **113**, 3294 (1991).

1317. S. Hashimoto, Y. Tatsuno, and T. Kitagawa, *J. Am. Chem. Soc.* **109**, 8096 (1987).

1318. J. R. Kincaid, A. J. Schneider, and K.-J. Paeng, *J. Am. Chem. Soc.* **111**, 735 (1989).

1319. K. Czarnecki, S. Nimri, Z. Gross, L. M. Proniewicz, and J. R. Kincaid, *J. Am. Chem. Soc.* **118**, 2929 (1996).
1320. R. S. Czernuszewicz, K. A. Macor, X.-Y. Li, J. R. Kincaid, and T. G. Spiro, *J. Am. Chem. Soc.* **111**, 3860 (1989).
1321. W. A. Oertling, A. Salehi, C. K. Chang, and G. T. Bobcock, *J. Phys. Chem.* **93**, 1311 (1989).
1322. K. A. Macor, R. S. Czernuszewicz, and T. G. Spiro, *Inorg. Chem.* **29**, 1996 (1990).
1323. Y. O. Su, R. S. Czernuszewicz, L. A. Miller, and T. G. Spiro, *J. Am. Chem. Soc.* **110**, 4150 (1988).
1324. K. Czarnecki, L. M. Proniewicz, H. Fujii, R. S. Czernuszewicz, and J. R. Kincaid, *J. Am. Chem. Soc.* **118**, 4680 (1996).
1325. S. Hu and T. G. Spiro, *J. Am. Chem. Soc.* **115**, 12029 (1993).
1326. T. Kitagawa and Y. Mizutani, *Coord. Chem. Rev.* **135/136**, 685 (1994).
1327. K. Nakamoto, *Coord. Chem. Rev.* **226**, 153 (2002).
1328. A. D. Allen and C. V. Senoff, *Chem. Commun.* 621 (1965).
1329. A. D. Allen and F. Bottomley, *Acc. Chem. Res.* **1**, 360 (1968).
1330. P. C. Ford, *Coord. Chem. Rev.* **5**, 75 (1970).
1331. R. Murray and D. C. Smith, *Coord. Chem. Rev.* **3**, 429 (1968).
1332. G. Henrici-Olive and S. Olive, *Angew. Chem., Int. Ed. Engl.* **8**, 650 (1969).
1333. A. D. Allen, F. Bottomley, R. O. Harris, V. P. Reinsalu, and C. V. Senoff, *J. Am. Chem. Soc.* **89**, 5595 (1967).
1334. M. Hirano, M. Akita, T. Morikita, H. Kubo, A. Fukuoka, and S. Komiya, *J. Chem. Soc., Dalton Trans.* 3453 (1997).
1335. B. E. Wiesler, N. Lehnert, F. Tuczek, J. Neuhausen, and W. Tremel, *Angew. Chem., Int. Ed. Engl.* **37**, 815 (1998).
1336. S. Pell, R. H. Mann, H. Taube, and J. N. Armor, *Inorg. Chem.* **13**, 479 (1974).
1337. M. W. Bee, S. F. A. Kettle, and D. B. Powell, *Spectrochim. Acta* **30A**, 585 (1974).
1338. A. D. Allen and J. R. Stevens, *Chem. Commun.* 1147 (1967).
1339. G. Albertin, S. Antoniutti, D. Baldan, and E. Bordignon, *Inorg. Chem.* **34**, 6205 (1995).
1340. G. Speier and L. Markó, *Inorg. Chim. Acta* **3**, 126 (1969).
1341. J. H. Enemark, B. R. Davis, J. A. McGinnety, and J. A. Ibers, *Chem. Commun.* 96 (1968).
1342. J. P. Collman, M. Kubota, F. D. Vastine, J. Y. Sun, and J. W. Kang, *J. Am. Chem. Soc.* **90**, 5430 (1968).
1343. H. Bauer and W. Beck, *J. Organomet. Chem.* **308**, 73 (1986).
1344. M. Hidai, K. Tominari, Y. Uchida, and A. Misono, *Chem. Commun.* 1392 (1969).
1345. B. Bell, J. Chatt, and G. J. Leigh, *Chem. Commun.* 842 (1970).
1346. G. Speier, and L. Markó, *J. Organomet. Chem.* **21**, P46 (1970).
1347. H. Miessner, *J. Am. Chem. Soc.* **116**, 11522 (1994).
1348. S. C. Srivastava and M. Bigorgne, *J. Organomet. Chem.* **19**, 241 (1969).
1349. D. J. Darensbourg, *Inorg. Chem.* **11**, 1436 (1972).
1350. J. N. Armor and H. Taube, *J. Am. Chem. Soc.* **92**, 2560 (1970).
1351. C. Krüger and Y.-H. Tsay, *Angew. Chem., Int. Ed. Engl.* **12**, 998 (1973).

1352. D. V. Fomichev, K. A. Bagley, and P. Coppens, *J. Am. Chem. Soc.* **122**, 532 (2000).
1353. J. Chatt, A. B. Nikolsky, R. L. Richards, and J. R. Sanders, *Chem. Commun.* 154 (1969).
1354. C. E. Laplaza, M. J. A. Johnson, J. Peters, A. L. Odom, E. Kim, C. C. Commins, G. N. Graham, and I. J. Pickering, *J. Am. Chem. Soc.* **118**, 8623 (1996).
1355. J. Chatt, R. C. Fay, and R. L. Richards, *J. Chem. Soc. A* 702 (1971).
1356. M. Mercer, R. H. Crabtree, and R. L. Richards, *Chem. Commun.* 808 (1973).
1357. D. Sellman, A. Brandl, and R. Endell, *J. Organomet. Chem.* **49**, C22 (1973).
1358. J. D. Cohen, M. Mylvaganam, M. D. Fryzuk, and T. M. Loehr, *J. Am. Chem. Soc.* **116**, 9529 (1994).
1359. H. Huber, E. P. Kündig, M. Moskovits, and G. A. Ozin, *J. Am. Chem. Soc.* **95**, 332 (1973).
1359a. L. Manceron, M. E. Alikhani, and H. A. July, *Chem. Phys.* **228**, 73 (1998).
1360. G. A. Ozin and A. Vander Voet, *Can. J. Chem.* **51**, 637 (1973).
1361. E. P. Kündig, M. Moskovits, and G. A. Ozin, *Can. J. Chem.* **51**, 2710 (1973).
1362. H. Huber, T. A. Ford, W. Klotzbücher, and G. A. Ozin, *J. Am. Chem. Soc.* **98**, 3176 (1976).
1363. D. W. Green, R. V. Hodges, and D. M. Gruen, *Inorg. Chem.* **15**, 970 (1976).
1364. T. C. DeVore, *Inorg. Chem.* **15**, 1315 (1976).
1365. D. W. Gieen and G. T. Reedy, *J. Mol. Spectrosc.* **74**, 423 (1979).
1366. G. A. Ozin and A. Vander Voet, *Can. J. Chem.* **51**, 3332 (1973).
1367. G. V. Chertihin, L. Andrews, and M. Neurock, *J. Phys. Chem.* **100**, 14609 (1996).
1368. C. A. Thompson and L. Andrews, *J. Phys. Chem.* **99**, 7913 (1995).
1369. A. Citra, X. Wang, W. D. Bare, and L. Andrews, *J. Phys. Chem. A,* **105**, 7799 (2001).
1370. G. Maier, H. P. Reisenauer, and J. Glatthaar, *Organometallics* **19**, 4775 (2000).
1371. W. P. Griffith, *Coord. Chem. Rev.* **8**, 369 (1972).
1372. M. J. Cleare and W. P. Griffith, *J. Chem. Soc. A*, 1117 (1970).
1373. S. M. Sinitsyn and N. A. Razorenova, *Russ. J. Inorg. Chem. (Engl. transl)* **31**, 1618 (1986).
1374. J. T. Groves, T. Takahashi, and W. M. Butler, *Inorg. Chem.* **22**, 884 (1983).
1375. J. Bendix, K. Meyer, T. Weyhermuller, E. Bill, N. Metzler-Nolte, and K. Wieghardt, *Inorg. Chem.* **37**, 1767 (1998).
1376. D. M.-T. Chan, M. H. Chisholm, H. Folting, J. C. Huffman, and N. S. Marchant, *Inorg. Chem.* **25**, 4170 (1986).
1377. J. C. Kim, W. S. Rees, and V. L. Goedken, *Inorg. Chem.* **33**, 3191 (1994).
1378. C. Campochiara, J. A. Hofmann, and D. F. Bocian, *Inorg. Chem.* **24**, 449 (1985).
1379. U. Abram, S. Abram, H. Spies, R. Kirmse, J. Stach, and K. Kohler, *Z. Anorg. Allg. Chem.* **544**, 167 (1987).
1380. W. P. Griffith and D. Pawson, *J. Chem. Soc., Dalton Trans.* 1315 (1973).
1381. M. Stumme and W. Preetz, *Z. Anorg. Allg. Chem.* **626**, 1186 (2000).
1382. W.-D. Wagner and K. Nakamoto, *J. Am. Chem. Soc.* **111**, 1590 (1989).
1383. K. Meyer, E. Bill, B. Mienert, T. Weyhermuller, and K. Wieghardt, *J. Am. Chem. Soc.* **121**, 4859 (1999).

1384. M. Horner, K. P. Frank, and J. Strahle, *Z. Naturforsch.* **41B**, 423 (1986).

1385. T. Godemeyer, A. Berg, H.-D. Gross, U. Müller, and K. Dehnicke, *Z. Naturforsch.* **40B**, 999 (1985).

1386. J. Bendix, T. Weyhermuller, E. Bill, and K. Wieghardt, *Angew. Chem. Int. Ed. Engl.* **38**, 2766 (1999).

1387. V. M. DeFlon, E. Niqet, and J. Strahle, *Z. Anorg. Allg. Chem.* **625**, 1357 (1999).

1388. G. A. Schick and D. F. Bocian, *J. Am. Chem. Soc.* **105**, 1830 (1983).

1389. G. J. Kubas, *Comments Inorg. Chem.* **7**, 17 (1988).

1390. G. E. Gadd, R. K. Upmacis, M. Poliakoff, and J. J. Turner, *J. Am. Chem. Soc.* **108**, 2547 (1986).

1391. R. K. Upmacis, M. Poliakoff, and J. J. Turner, *J. Am. Chem. Soc.* **108**, 3645 (1986).

1392. R. L. Sweany and A. Moroz, *J. Am. Chem. Soc.* **111**, 3577 (1989).

1393. M. W. George, M. T. Haward, P. A. Hamley, C. Hughes, E. P. A. Johnson, V. K. Popov, and M. Poliakoff, *J. Am. Chem. Soc.* **115**, 2286 (1993).

1394. S. A. Jackson, P. M. Hodges, M. Poliakoff, J. J. Turner, and F. W. Grevels, *J. Am. Chem. Soc.* **112**, 1221 (1990).

1395. G. J. Kubas, R. R. Ryan, B. I. Swanson, P. J. Vergamini, and H. J. Wasserman, *J. Am. Chem. Soc.* **106**, 451 (1984).

1396. G. J. Kubas, C. J. Unkefer, B. I. Swanson, and E. Fukushima, *J. Am. Chem. Soc.* **108**, 7000 (1986).

1397. B. R. Bender, G. J. Kubas, L. H. Jones, B. I. Swanson, K. Eckert, K. B. Capps, and C. D. Hoff, *J. Am. Chem. Soc.* **119**, 9179 (1997).

1398. M. Chopra, K. F. Wong, G. Jia, and N. T. Yu, *J. Mol. Struct.* **379**, 93 (1996).

1399. G. J. Kubas, J. E. Nelson, J. C. Bryan, J. Eckert, L. Wisniewski, and K. Zilm, *Inorg. Chem.* **33**, 2954 (1994).

1400. J. Pauls and B. Neumuller, *Inorg. Chem.* **40**, 121 (2001).

1401. E. Johnsen, A. J. Downs, T. M. Greene, P. F. Souter, K. Aarset, E. M. Page, D. A. Rice, A. N. Richardson, P. T. Brain, D. W. H. Rankin, and C. R. Pulham, *Inorg. Chem.* **39**, 719 (2000).

1402. A. A. H. van der Zeijden, T. Burgi, and H. Berke, *Inorg. Chim, Acta* **201**, 131 (1992).

1403. M. J. Mockford and W. P. Griffith, *J. Chem. Soc., Dalton Trans.* 717 (1985).

1404. C. E. Ash, C. M. Kim, M. Y. Darensbourg, and A. L. Rheingold, *Inorg. Chem.* **26**, 1357 (1987).

1405. J. Chatt and R. G. Hayter, *J. Chem. Soc.* 5507 (1961).

1406. R. G. S. Banks and J. M. Pratt, *J. Chem. Soc. A*, 854 (1968).

1407. E. Bonfada, C. Maichle-Mössmer, J. Strähle, and U. Abram, *Z. Anorg. Allg. Chem.* **625**, 1327 (1999).

1408. D. V. Yandulov, D. Huang, J. C. Huffman, and K. G. Gaulton, *Inorg. Chem.* **39**, 1919 (2000).

1409. M. J. Fernandez, M. A. Esteruelas, M. Covarrubias, and L. A. Oro, *J. Organomet. Chem.* **316**, 343 (1986).

1410. J. Chatt, L. A. Duncanson, and B. L. Shaw, *Chem. Ind. (London)*, 859 (1958).

1411. M. J. Church, and M. J. Mays, *J. Chem. Soc.* 3074 (1968).; 1938 (1970).

1412. P. W. Atkins, J. C. Green, and M. L. H. Green, *J. Chem. Soc. A* 2275 (1968).

1413. S. C. Abrahams, A. P. Ginsberg, T. F. Koetzle, S. P. Marsh, and C. R. Sprinkle, *Inorg. Chem.* **25**, 2500 (1986).

1414. M. D. Fryzuk and D. H. McConville, *Inorg. Chem.* **28**, 1613 (1989).

1415. T. M. Arkhireeva, B. M. Bulychev, T. A. Sokolova, G. L. Soloveichik, V. K. Belsky, and G. N. Boiko, *Inorg. Chim. Acta* **141**, 221 (1988).

1416. D. W. Hart, R. G. Teller, C. Y. Wei, R. Bau, G. Longoni, S. Campanella, P. Chini, and T. F. Koetzle, *J. Am. Chem. Soc.* **103**, 1458 (1981); *Angew. Chem., Int. Ed. Engl.* **18**, 80 (1979).

1417. D. Graham, J. Howard, and T. C. Waddington, *J. Chem. Soc., Faraday Trans.* 2, **79**, 1713 (1983).

1418. P. L. Stanghellini and G. Longoni, *J. Chem. Soc., Dalton Trans.* 685 (1987).

1419. J. D. Corbett, J. Eckert, U. A. Jayasooriya, G. J. Kearley, R. P. White, and J. Zhang, *J. Ptys. Chem.* **97**, 8386 (1993).

1420. S. F. Parker, U. A. Jayasooriya, J. C. Sprunt, M. Bortz, and K. Yvon, *J. Chem. Soc., Faraday Trans.* **94**, 2595 (1998).

1421. M. Olofsson-Martensson, U. Haussermann, J. Tomkinson, and D. Noreus, *J. Am. Chem. Soc.* **122**, 6960 (2000).

1422. L. Andrews, *Chem. Soc. Rev.* **33**, 123 (2004).

1423. T. J. Tague, Jr. and L. Andrews, *J. Phys. Chem.* **98**, 8611 (1994).

1424. R. J. H. Clark, in V. Gutmann,ed., *Halogen Chemistry*, **Vol. 3**, Academic Press, New York, 1967, p. 85.

1425. A. J. Carty, *Coord. Chem. Rev.* **4**, 29 (1969).

1426. R. J. H. Clark, *Spectrochim. Acta* **21**, 955 (1965).

1427. K. Konya and K. Nakamoto, *Spectrochim. Acta* **29A**, 1965 (1973).

1428. S. J. Higgins, W. Levason, M. C. Feiters, and A. T. Steel, *J. Chem. Soc., Dalton Trans.* 317 (1986).

1429. K. Thompson and K. Carlson, *J. Chem. Phys.* **49**, 4379 (1968).

1430. K. Shobatake and K. Nakamoto, *J. Am. Chem. Soc.* **92**, 3332 (1970).

1431. C. Udovich, J. Takemoto, and K. Nakamoto, *J. Coord Chem.* **1**, 89 (1971).

1432. P. M. Boorman and A. J. Carty, *Inorg. Nucl. Chem. Lett.* **4**, 101 (1968).

1433. I. Wharf and D. F. Shriver, *Inorg. Chem.* **8**, 914 (1969).

1434. D. F. Shriver and M. P. Johnson, *Inorg. Chem.* **6**, 1265 (1967).

1435. J. H. Nelson, W. L. Wilson, L. W. Cary, N. W. Alcock, H. J. Clase, G. S. Jas, L. Ramsey-Tassin, and J. W. Kenney, *Inorg. Chem.* **35**, 883 (1996).

1436. B. Crociani, T. Boschi, and M. Nicolini, *Inorg. Chim. Acta* **4**, 577 (1970).

1437. F. H. Herbelin, J. D. Herbelin, J. P. Mathieu, and H. Poulet, *Spectrochim. Acta* **22**, 1515 (1966).

1438. D. M. Adams, J. Chatt, J. Gerratt, and A. D. Westland *J. Chem. Soc.* 734 (1964).

1439. T. G. Appleton, H. C. Clark, and L. E. Manzer, *Coord. Chem. Rev.* **10**, 335 (1973).

1440. R. J. Goodfellow, P. L. Goggin, and D. A. Duddell, *J. Chem. Soc. A*, 504 (1968).

1441. M. A. Bennett, R. J. H. Clark, and D. L. Milner, *Inorg. Chem.* **6**, 1647 (1967).

1442. J. Fujita, K. Konya, K. Nakamoto *Inorg. Chem.* **9**, 2794 (1970).

1443. J. T. Wang, C. Udovich, K. Nakamoto, A. Quattrochi, and J. R. Ferraro, *Inorg. Chem.* **9**, 2675 (1970).
1444. B. T. Kilbourn and H. M. Powell, *J. Chem. Soc. A*, 1688 (1970).
1445. J. R. Ferraro, K. Nakamoto, J. T. Wang, and L. Lauer, *Chem. Commun.* 266 (1973).
1446. C. Postmus, K. Nakamoto, and J. R. Ferraro, *Inorg. Chem.* **6**, 2194 (1967).
1447. J. R. Ferraro, *Vibrational Spectroscopy at High External Pressures. The Diamond Anvil Cell*, Academic Press, New York, 1984.
1448. J. R. Ferraro, *Coord. Chem. Rev.* **29**, 1 (1979).
1449. D. M. Adams and P. J. Chandler, *J. Chem. Soc. A*, 1009 (1967).
1450. N. Ohkaku and K. Nakamoto, *Inorg. Chem.* **12,** 2440, 2446 (1973).
1451. D. M. Adams and D. C. Newton, *J. Chem. Soc., Dalton Trans.* 681 (1972).
1452. R. J. Goodfellow, P. L. Goggin, and L. M. Venanzi, *J. Chem. Soc. A*, 1897 (1967).
1453. D. M. Adams and P. J. Chandler, *Chem. Common.* 69 (1966).
1454. M. Goldstein, and W. D. Unsworth, *Inorg. Chim. Acta* **4**, 342 (1970).
1455. I. Reese and W. Preetz, *Z. Anorg. Allg. Chem.* **626**, 911 (2000).
1456. H. Hillebrecht, G. Thiele, P. Hollmann, and W. Preetz, *Z. Naturforsch.* **47B**, 1099 (1992).
1457. R. S. Armstrong, W. A. Horsfield, and K. W. Nugent, *Inorg. Chem.* **29**, 4551 (1990).
1458. G. Thiele, H. W. Rotter, and W. Bachle, *Z. Anorg. Allg. Chem.* **620**, 1271 (1994).
1459. P. Hassanzadeh, A. Citra, L. Andrews, and M. Neurock, *J. Phys. Chem.* **100** 7317 (1996).
1460. T. G. Spiro, *Prog. Inorg. Chem.* **11**, 1 (1970).
1461. K. L. Watters and W. M. Risen, Jr. *Inorg. Chim. Acta Rev.* **3**, 129 (1969).
1462. E. Jr. Maslowsky, *Chem. Rev.* **71**, 507 (1971).
1463. B. J. Bulkin and C. A. Rundell, *Coord. Chem. Rev.* **2**, 371 (1967).
1464. D. F. Shriver and C. B. Cooper, III, *Adv. Infrared Raman Spectrosc.* **6**, 127 (1980).
1465. C.-M. Che, M.-C. Tse, M. C. W. Chan, K.-K. Cheung, D. L. Phillips, and K.-H. Leung, *J. Am. Chem. Soc.* **122**, 2464 (2000).
1466. K.-H. Leung, D. L. Phillips, M. C. Tse, C. M. Che, and V. M. Miskowski, *J. Am. Chem. Soc.* **121**, 4799 (1999).
1467. E. C. C. Cheng, K.-H. Leung, V. M. Miskowski, V. W. W. Yam, and D. L. Phillips, *Inorg. Chem.* **39**, 3690 (2000).
1468. H. Huckstadt and H. Homborg, *Z. Anorg. Allg. Chem.* **623**, 369 (1997).
1469. F. Jalilehvand, M. Maliarik, M. Sandstrom, J. Mink, I. Persson, I. Toth, and J. Glaser, *Inorg.Chem.* **40**, 3889 (2001).
1470. G. Ma, A. Fischer, and J. Glaser, *Eur. J. Inorg. Chem.* 1307 (2002).
1471. P. D. Harvey, K. D. Truong, K. T. Aya, M. Droulin, and A. D. Bandrauk, *Inorg. Chem.* **33**, 2347 (1994).
1472. G. A. Bowmaker, R. K. Harris, and D. C. Apperley, *Inorg. Chem.* **38**, 4956 (1999).
1473. F. A. Cotton, *Chem. Soc. Rev.* 27 (1975); *Acc. Chem. Res.* **11**, 225 (1978).
1474. R. J. H. Clark and M. L. Franks, *J. Am. Chem. Soc.* **98**, 2763 (1976).
1475. F. A. Cotton, B. A. Frenz, B. R. Stults, and T. R. Webb, *J. Am. Chem. Soc.* **98**, 2768 (1976).

1476. J. Jr. San Filippo, and H. J. Sniadoch, *Inorg. Chem.* **12**, 2326 (1973).
1477. A. J. Hempleman, R. J. H. Clark, and C. D. Flint, *Inorg. Chem.* **25**, 2915 (1986).
1478. C. L. Angell, F. A. Cotton, B. A. Frenz, and T. R. Webb, *Chem. Commun.* 399 (1973).
1479. A. Loewenschuss, J. Shamir, and M. Ardon, *Inorg. Chem.* **15**, 238 (1976).
1480. D. J. Santure, J. C. Huffman, and A. P. Sattelberger, *Inorg. Chem.* **24**, 371 (1985).
1481. R. J. H. Clark, A. J. Hempleman, and D. A. Tocher, *J. Am. Chem. Soc.* **110**, 5968 (1988).
1482. R. J. H. Clark, A. J. Hempleman, and C. D. Flint, *J. Am, Chem. Soc.* **108**, 518 (1986).
1483. R. J. H. Clark and A. J. Hempleman, *Inorg. Chem.* **27**, 2225 (1988).
1484. R. J. H. Clark, A. J. Hempleman, H. M. Dawes, M. B. Hursthouse, and C. D. Flint, *J. Chem. Soc., Dalton Trans.* 1775 (1985).
1485. R. J. H. Clark, D. J. West, and R. Withnall, *Inorg. Chem.* **31**, 456 (1992).
1486. R. J. H. Clark, S. Firth, A. Sella, V. M. Miskowski, and M. D. Hopkins, *J. Chem. Soc., Dalton Trans.* 2928 (2000).
1487. I. M. Bell, R. J. H. Clark, and D. G. Humphrey, *J. Chem. Soc., Dalton Trans.*, 1225 (1997).
1488. J. C. Littrell, C. E. Talley, R. F. Dallinger, and T. M. Gillbert, *Inorg. Chem.* **36**, 760 (1997).
1489. G. Estiu, F. D. Cukiernik, P. Maldivi, and O. Poizai, *Inorg. Chem.* **38**, 3030 (1999).
1490. B. Hutchinson, J. Morgan, C. B. Cooper, III Y. Mathey, and D. F. Shriver, *Inorg. Chem.* **18**, 2048 (1979).
1491. W. K. Bratton, F. A. Cotton, M. Debeau, and R. A. Walton, *J. Coord. Chem.* **1**, 121 (1971).
1492. A. P. Ketteringham, C. Oldham, and C. J. Peacock, *J. Chem. Soc., Dalton Trans.* 1640 (1976).
1493. C. O. Quicksall and T. G. Spiro, *Inorg. Chem.* **8**, 2363 (1969).
1494. J. R. Johnson, R. J. Ziegler, and W. M. Risen, Jr. *Inorg. Chem.* **12**, 2349 (1973).
1495. K. L. Watters, J. N. Britain, and W. M. Risen, Jr. *Inorg. Chem.* **8**, 1347 (1969).
1496. K. L. Watters, W. M. Butler, and W. M. Risen, Jr. *Inorg. Chem.* **10**, 1970 (1971).
1497. K. M. Mackay and S. R. Stobart, *J. Chem. Soc, Dalton Trans.* 214 (1973).
1498. S. Onaka, C. B. Cooper, III and D. F. Shriver, *Inorg. Chim. Acta* **37**, L467 (1979).
1499. P. L. Goggin and R. J. Goodfellow, *J. Chem. Soc., Dalton Trans.* 2355 (1973).
1500. J. San Filippo Jr. and H. J. Sniadoch, *Inorg. Chem.* **12**, 2326 (1973).
1501. B. I. Swanson, J. J. Rafalko, D. F. Shriver, J. San Filippo, Jr. and T. G. Spiro, *Inorg. Chem.* **14**, 1737 (1975).
1502. C. B. Cooper, III, S. Onaka, D. F. Shriver, L. Daniels, R. L. Hance, B. Hutchinson, and R. Shipley, *Inorg. Chim. Acta* **24**, L92 (1977).
1503. S. Onaka and D. F. Shriver, *Inorg. Chem.* **15**, 915 (1976).
1504. M. Vitale, K. K. Lee, C. F. Hemann, R. Hills, T. L. Gustafson, and B. E. Bursten, *J. Am. Chem. Soc.* **117**, 2286 (1995).
1505. S. F. A. Kettle and P. L. Stanghellini, *Inorg. Chem.* **18**, 2749 (1979).
1506. G. A. Battiston, G. Bor, U. K. Dietler, S. F. A. Kettle, R. Rossetti, G. Sbrignadello, and P. L. Stanghellini, *Inorg. Chem.* **19**, 1961 (1980).

1507. H. W. Martin, P. Skinner, R. K. Bhardwaj, V. A. Jayasooriya, D. B. Powell, and N. Sheppard, *Inorg. Chem.* **25**, 2846 (1986).

1508. V. A. Jayasooriya and P. Skinner, *Inorg. Chem.* **25**, 2850 (1986).

1509. V. A. Jayasooriya, S. J. Stotesbury, R. Grinter, D. B. Powell, and N. Sheppard, *Inorg. Chem.* **25**, 2853 (1986).

1510. S. F. A. Kettle, E. Diana, R. Rossetti, E. Boccaleri, U. A. Jayasooryia, and P. L. Stanghellini, *Inorg. Chem.* **39**, 5690 (2000).

1511. C. O. Quicksall and T. G. Spiro, *Inorg. Chem.* **8**, 2011 (1969).

1512. C. O. Quicksall and T. G. Spiro, *Chem. Commun.* 839 (1967).

1513. J. A. Creighton and B. T. Heaton, *J. Chem. Soc., Dalton Trans.* 1498 (1981).

1514. C. Sourisseau, *J. Raman Spectrosc.* **6**, 303 (1977).

1515. S. F. A. Kettle and P. L. Stanghellini, *Inorg. Chem.* **26**, 1626 (1987).

1516. H. K. Mahtani and P. Stein, *J. Am. Chem. Soc.* **111**, 1505 (1989).

1517. M. Mitsumi, T. Murase, H. Kishida, T. Yoshinari, Y. Ozawa, K. Toriumi, T. Sonoyama, H. Kitagawa, and T. Mitani, *J. Am. Chem. Soc.* **123**, 11179 (2001).

1518. T. G. Appleton, J. R. Hall, and D. W. Neale, *Inorg.Chim. Acta* **104**, 19 (1985).

1519. R. J. H. Clark, J. H. Tocher, J. P. Fackler, R. Neira, H. H. Murray, and H. Knackel, *J. Organomet. Chem.* **303**, 437 (1986).

1520. R. Bender, P. Braunstein, A. Dedieu, P. D. Ellis, B. Huggins, P. D. Harvey, E. Sappa, and A. Tiripicchio, *Inorg. Chem.* **35**, 1223 (1996).

1521. R. F. Dallinger, *J. Am. Ckem. Soc.* **107**, 7202 (1985).

1522. R. F. Dallinger, V. M. Miskowski, H. B. Gray, and W. H. Woodruff, *J. Am. Chem. Soc.* **103**, 1595 (1981).

1523. R. F. Dallinger, M. J. Carlson, V. M. Miskowski, and H. B. Gray, *Inorg. Chem.* **37**, 5011 (1998).

1524. V. M. Miskowski, S. F. Rice, H. B. Gray, R. F. Dallinger, S. J. Milder, M. G. Hill, C. L. Exstrom, and K. R. Mann, *Inorg. Chem.* **33**, 2799 (1994).

1525. K. H. Leung, D. L. Phillips, Z. Mao, C. -M. Che, V. M. Miskowski, and C. K. Chan, *Inorg. Chem.* **41**, 2054 (2002).

1526. C. -M. Che, L. G. Butler, H. B. Gray, R. M. Crooks, and W. H. Woodruff, *J. Am. Chem. Soc.* **105**, 5492 (1983).

1527. P. D. Harvey, R. F. Dallinger, W. H. Woodruff, and H. B. Gray, *Inorg. Chem.* **28**, 3057 (1989).

1528. D. E. Morris and W. H. Woodruff, "Vibrational Spectra and the Structure of Electronically Excited Molecules in Solution" in R. J. H. Clark and R. E. Hester, eds., *Advances in Spectroscopy*, Vol. 14, Wiley, New York, 1987, p. 285.

1529. M. Trabelsi, A. Loutellier, and M. Bigorgne, *J. Organomet. Chem.* **40**, C45 (1972).

1530. M. Bigorgne, A. Loutellier, and M. Pańkowski, *J. Organomet. Chem.* **23**, 201 (1970).

1531. M. Trabelsi, A. Loutellier, and M. Bigorgne, *J. Organomet. Chem.* **56**, 369 (1973).

1532. M. Trabelsi and A. Loutellier, *J. Mol. Struct.* **43**, 151 (1978).

1533. A. Loutellier, M. Trabelsi, and M. Bigorgne, *J. Organomet. Chem.* **133**, 201 (1977).

1534. Th. Kruck, *Angew. Chem., Int. Ed. Engl.* **6**, 53 (1967).

1535. Th. Kruck and K. Bauer, *Z. Anorg. Allg. Chem.* **364**, 192 (1969).

1536. Th. Kruck and A. Prasch, *Z. Anorg. Allg. Chem.* **356**, 118 (1968).

1537. W. Collong and Th. Kruck, *Chem. Ber.* **123**, 1655 (1990).
1538. W. Fuss and M. Ruhe, *Z. Naturforsch.* **47B**, 591 (1992).
1539. Th. Kruck and A. Prasch, *Z. Anorg. Allg. Chem.* **371**, 1 (1969).
1540. S. Bénazeth, A. Loutellier, and M. Bigorgne, *J. Organomet. Chem.* **24**, 479 (1970).
1541. L. A. Woodward and J. R. Hall, *Spectrochim. Acta* **16**, 654 (1960); H. G. M. Edwards and L. A. Woodward, *ibid*. **26A**, 897 (1970).
1542. H. G. M. Edwards and L. A. Woodward, *Spectrochim. Acta* **26A**, 1077 (1970).
1543. H. G. M. Edwards, *Spectrochim. Acta* **42A**, 431 (1986).
1544. H. G. M. Edwards, *J. Mol. Struct.* **158**, 153 (1987).
1545. H. G. M. Edwards, *Spectrochim. Acta* **42A**, 1401 (1986).
1546. K. Angermair, G. A. Bowmaker, E. N. de Silva, P. C. Healy, B. E. Jones, and H. Schmidbaur, *J. Chem. Soc., Dalton Trans.* 3121 (1998).
1547. P. L. Goggin and R. J. Goodfellow, *J. Chem. Soc. A*, 1462 (1966).
1548. G. D. Coates and C. Parkin, *J. Chem. Soc.* 421 (1963).
1549. M. A. Bennett, R. J. H. Clark, and A. D. J. Goodwin, *Inorg. Chem.* **6**, 1625 (1967).
1550. J. H. S. Green, *Spectrochim. Acta* **24A**, 137 (1968).
1551. K. Shobatake, C. Postmus, J. R. Ferraro, and K. Nakamoto, *Appl. Spectrosc.* **23**, 12 (1969).
1552. R. J. H. Clark, C. D. Flint, and A. J. Hempleman, *Spectrochim. Acta* **43A**, 805 (1987).
1553. J. Bradbury, K. P. Forest, R. H. Nuttall, and D. W. A. Sharp, *Spectrochim. Acta* **23A**, 2701 (1967).
1554. H. G. M. Edwards, I. R. Lewis, and P. H. Turner, *Inorg. Chim. Acta* **216**, 191 (1994).
1555. H. G. M. Edwards, A. F. Johnson, and I. R. Lewis, *Spectrochim. Acta* **49A**, 707 (1993).
1556. J. G. Verkade, *Coord. Chem. Rev.* **9**, 1 (1972).
1557. P. J. D. Park and P. J. Hendra, *Spectrochim. Acta* **25A,** 227, 909 (1969).
1558. L. M. Venanzi, *Chem. Brit.* **4**, 162 (1968).
1559. J. Chatt, G. A. Gamlen, and L. E. Orgel, *J. Chem. Soc.* 486 (1958).
1560. E. O. Fischer, W. Bathelt, and J. Müller, *Chem. Ber.* **103**, 1815 (1970).
1561. R. J. Goodfellow, J. G. Evans, P. L. Goggin, and D. A. Duddell, *J. Chem. Soc. A*, 1604 (1968).
1562. G. B. Deacon and J. H. S. Green, *Spectrochim. Acta* **24A**, 845 (1968).
1563. D. Brown, J. Hill, and C. E. F. Richard, *J. Chem. Soc. A*, 497 (1970).
1564. D. M. L. Goodgame and F. A. Cotton, *J. Chem. Soc.* 2298, 3735 (1961).
1565. G. A. Rodley, D. M. L. Goodgame, and F. A. Cotton, *J. Chem. Soc.* 1499 (1965).
1566. A. Müller, W. Jaegermann, and J. H. Enemark, *Coord. Chem. Rev.* **46**, 245 (1982).
1567. P. K. Chakrabarty, S. Bhattacharya, C. G. Pierpont, and R. Bhattacharyya, *Inorg. Chem.* **31**, 3573 (1992).
1568. R. Guilard, C. Ratti, A. Tabard, P. Richard, D. Dubois, and K. M. Kadish, *Inorg. Chem.* **29**, 2532 (1990).
1569. R. Minkwitz, H. Borrmann, and J. Nowicki, *Z. Naturforsch.* **47B**, 915 (1992).
1570. V. P. Fedin, B. A. Kolesov, Yu. V. Mironov, and V. Ye. Fedorov, *Polyhedron* **8**, 2419 (1989).
1571. A. P. Ginsberg and W. E. Lindsell, *Chem. Commm.* 232 (1971).

1572. D. M. Young, G. L. Schimek, and J. W. Kolis, *Inorg. Chem.* **35**, 7620 (1996).

1573. R. Bhattacharyya, P. K. Chakrabarty, P. N. Ghosh, A. K. Mukherjee, D. Podder, and M. Mukherjee, *Inorg. Chem.* **30**, 3948 (1991).

1574. B. Neumüller, M. L. Ha-Eierdanz, U. Müller, S. Magull, G. Kräuter, and K. Dehnicke, *Z. Anorg. Allg. Chem.* **609**, 12 (1992).

1575. A. Ahle, B. Neumüller, J. Pebler, M. Atanasov, and K. Dehnicke, *Z. Anorg. Allg. Chem.* **615**, 131 (1992).

1576. I. S. Butler, P. D. Harvey, J. McCall, and A. Shaver, *J. Raman Spectrosc.* **17**, 221 (1986).

1577. A. Müller, J. Schimanski, U. Schmanski, and H. Bögge, *Z. Naturforsch.* **40B**, 1277 (1985).

1578. K. Neininger, H. W. Rotter, and G. Thiele, *Z. Anorg. Allg. Chem.* **622**, 1814 (1996).

1579. T. J. Greenhough, B. W. S. Kolthammer, P. Legzdins, and J. Trotter, *Inorg. Chem.* **18**, 3548 (1979).

1580. M. W. Bishop, J. Chatt, and J. R. Dilworth, *Chem. Commun.* 780 (1975).

1581. T. J. Crevier, S. Lovell, J. M. Mayer, A. L. Rheingold, and L. A. Guzei, *J. Am. Chem. Soc.* **120**, 6607 (1998).

1582. H. Adamsa, L. V. Y. Guio, M. J. Morris, and A. J. Pratt, *J. Chem. Soc., Dalton Trans.* 3489 (2000).

1583. W. Petz, *Inorg. Chim. Acta* **201**, 203 (1992).

1584. M. C. Baird, G. Hartwell, and G. Wilkinson, *J. Chem. Soc. A*, 2037 (1967).

1585. J. D. Gilbert, M. C. Baird, and G. Wilkinson, *J. Chem. Soc. A*, 2198 (1968).

1586. H. Adams, L. V. Y. Guio, M. J. Morris, and A. J. Pratt, *J. Chem. Soc., Dalton Trans.* 3489 (2000).

1587. B. D. Dombek and R. J. Angeloci, *J. Am. Chem. Soc.* **96**, 7568 (1974).

1588. L. Busetto, V. Zanotti, V. G. Albano, D. Braga, and M. Honari, *J. Chem. Soc., Dalton Trans.* 1791 (1986).

1589. A. M. English, K. R. Plowman, and I. S. Butler, *Inorg. Chem.* **20**, 2553 (1981).

1590. A. M. English, K. R. Plowman, and I. S. Butler, *Inorg. Chem.* **21**, 338 (1982).

1591. P. A. Bates, M. B. Hursthouse, P. F. Kelly, and J. D. Woollins, *J. Chem. Soc., Dalton Trans.* 2367 (1986).

1592. J. Hanich, M. Krestel, U. Muller, and K. Dehnicke, *Z. Anorg. Allg. Chem.* **522**, 92 (1985).

1593. L. Vaska and S. S. Bath, *J. Am. Chem. Soc.* **88**, 1333 (1966).

1594. J. Terheijden, G. van Koten, W. P. Mul, D. J. Stufkens, F. Muller, and C. H. Stam, *Organometallics* **5**, 519 (1986).

1595. L. H. Vogt, J. L. Katz, and S. E. Wiberley, *Inorg. Chem.* **4**, 1157 (1965).

1596. T. Chihara, H. Kubota, M. Fukumoto, H. Ogawa, Y. Yamamoto, and Y. Wakatsuki, *Inorg. Chem.* **36**, 5488 (1997).

1597. F. Meier-Brocks, R. Albrecht, and E. Weiss, *J. Organomet. Chem.* **439**, 65 (1992).

1598. W. A. Schenck and U. Karl, *Z. Naturforsch.* **44B**, 988 (1989).

1599. U. Schimmelpfennig, R. Kalähne, K. D. Schleinitz, and E. Wenschuh, *Z. Anorg. Allg. Chem.* **603**, 21 (1991).

1600. D. M. Byler and D. F. Shriver, *Inorg. Chem.* **15**, 32 (1976).

1601. P. Reich-Rohrwig, A. C. Clark, R. L. Downs, and A. Wojcicki, *J. Organomet. Chem.* **145**, 57 (1978).
1602. C. Sourisseau and J. Corset, *Inorg. Chim. Acta* **39**, 153 (1980).
1603. R. D. Wilson and J. A. Ibers, *Inorg. Chem.* **17**, 2134 (1978).
1604. M. Herberhold and A. F. Hill, *J. Organomet Chem.* **387**, 323 (1990).
1605. P. L. Bogdan, M. Sabat, S. A. Sunshine, C. Woodcock, and D. F. Shriver, *Inorg. Chem.* **27**, 1904 (1988).
1606. D. M. P. Mingos and R. W. M. Wardle, *J. Chem. Soc., Dalton Trans.* 73 (1986).
1607. A. D. Burrows, A. A. Gosden, C. M. Hill, and D. M. P. Mingos, *J. Organomet. Chem.* **452**, 251 (1993).
1608. G. J. Kubas, *Inorg. Chem.* **18**, 182 (1979).
1609. D. A. Johnson and V. C. Dew, *Inorg. Chem.* **18**, 3273 (1979).
1610. A. Y. Kovalevsky, K. A. Bagley, and P. Coppens, *J. Am. Chem. Soc.* **124**, 9241 (2002).
1611. R. W. Eveland C. C. Raymond, T. E. Albrecht-Schmitt, and D. F. Shriver, *Inorg. Chem.* **38**, 1282 (1999).
1612. I. S. Butler and A. E. Fenster, *J. Organomet. Chem.* **66**, 161 (1974).
1613. M. C. Baird and G. Wilkinson, *J. Chem. Soc. A*, 865 (1967).
1614. D. S. Barratt and C. A. McAuliffe, *Inorg. Chim. Acta* **97**, 37 (1985).
1615. Y. Yamamoto and H. Yamazaki, *J. Chem. Soc., Dalton Trans.* 677 (1986).
1616. M. P. Yagupsky and G. Wilkinson, *J. Chem. Soc. A*, 2813 (1968).
1617. G. R. Clark, T. J. Collins, S. M. James, W. R. Roper, and K. G. Town, *Chem. Commun.* 475 (1976).
1618. H. Huber, G. A. Ozin, and W. J. Power, *Inorg. Chem.* **16**, 2234 (1977).
1619. P. J. Brothers, C. E. L. Headford, and W. R. Roper, *J. Organomet. Chem.* **195**, C29 (1980).
1620. A. Haas, U. Fleischer, M. Matschke, and V. Staemmler, *Z. Anorg. Allg. Chem.* **625**, 681 (1999).
1621. R. Krieglstein and D. K. Breitinger, *J. Mol. Struct.* **408/409**, 379 (1997).
1622. G. G. Hoffmann, W. Brockner, and I. Steinfatt, *Inorg. Chem.* **40**, 977 (2001).
1623. M. M. El-Etri and W. M. Scovell, *Inorg. Chim. Acta* **187**, 201 (1991).
1624. J. R. Allkins and P. J. Hendra, *J. Chem. Soc. A*, 1325 (1967); *Spectrochim. Acta* **22**, 2075 (1966); **23A**, 1671 (1967); **24A**, 1305 (1968).
1625. E. A. Allen and W. Wilkinson, *Spectrochim. Acta* **28A**, 725 (1972).
1626. R. J. H. Clark, G. Natile, U. Belluco, L. Cattalini, and C. Filippin, *J. Chem. Soc. A*, 659 (1970).
1627. E. A. Allen and W. Wilkinson, *Spectrochim. Acta* **28A**, 2257 (1972).
1628. B. E. Aires, J. E. Fergusson, D. T. Howarth, and J. M. Miller, *J. Chem. Soc. A*, 1144 (1971).
1629. E. A. Allen and W. Wilkinson, *J. Chem. Soc., Dalton Trans.* 613 (1972).
1630. P. L. Goggin, R. J. Goodfellow, D. L. Sales, J. Stokes, and P. Woodward, *Chem. Commun.* 31 (1968).
1631. D. M. Adams and P. J. Chandler, *J. Chem. Soc. A*, 588 (1969).
1632. K. H. Schmidt and A. Müller, *Coord. Chem. Rev.* **14**, 115 (1974).

1633. A. Müller, E. Diemann, R. Jostes, and H. Bögge, *Angew. Chem., Int. Ed. Engl.* **20**, 934 (1981).
1634. A. Müller, "Thiometallato Complexes: Vibrational Spectra and Structural Chemistry" in J. R. Durig, ed., *Vibrational Spectra and Structure*, Vol. 15, Elsevier, New York, 1986, p. 251.
1635. E. Königer-Ahlborn, A. Müller, A. D. Cormier, J. D. Brown, and K. Nakamoto, *Inorg. Chem.* **14**, 2009 (1975).
1636. A. Müller and W. Hellman, *Spectrochim. Acta* **41A**, 359 (1985).
1637. R. Pradhan and R. Bhattacharyya, *Transition Met. Chem.* **24**, 64 (1999).
1638. U. Pätzmann, W. Brockner, S. N. Cyvin, and S. J. Cyvin, *J. Raman Spectrosc.* **17**, 257 (1986).
1639. R. G. Cavell, W. Byers, E. D. Day, and P. M. Watkins, *Inorg. Chem.* **11**, 1598 (1972).
1640. J. M. Burke and J. P. Fackler, *Inorg. Chem.* **11**, 2744 (1972).
1641. A. Cormier, K. Nakamoto, P. Christophliemk, and A. Müller, *Spectrochim Acta* **30A**, 1059 (1974).
1642. J. Vicente, M.-T. Chicote, P. Gonzalez-Herrero, and P. G. Jones, *Inorg. Chem.* **36**, 5735 (1997).
1643. C. Simonnnet-Jégat, E. Cadusseau, R. Dessapt, and F. Sécheresse, *Inorg. Chem.* **38**, 2335 (1999).
1644. R. F. Hess, P. L. Gordon, C. D. Tait, K. D. Abney, and P. K. Dorhout, *J. Am. Chem. Soc.* **124**, 1327 (2002).
1645. A. Z. Rys, A.-M. Lebuis, A. Shaver, and D. N. Harpp, *Inorg.Chem.* **41**, 3653 (2002).
1646. O. Piovesana, C. Bellitto, A. Flamini, and P. F. Zanazzi, *Inorg. Chem.* **18**, 2258 (1979).
1647. F. A. Cotton, C. Oldham, and R. A. Walton, *Inorg. Chem.* **6**, 214 (1967).
1648. M. Ikram and D. B. Powell, *Spectrochim. Acta* **28A**, 59 (1972).
1649. C. W. Schläpfer, Y. Saito, and K. Nakamoto, *Inorg. Chim. Acta* **6**, 284 (1972); C.W. Schläpfer and K. Nakamoto ibid. 177.
1650. F. Bonati and R. Ugo, *J. Organomet. Chem.* **10**, 257 (1967).
1651. C. O'Connor, J. D. Gilbert, and G. Wilkinson, *J. Chem. Soc. A*, 84 (1969).
1652. D. C. Bradley, and M. H. Gitlitz, *J. Chem. Soc. A*, 1152 (1969).
1653. R. J. Butcher, J. R. Ferraro, and E. Sinn, *Inorg. Chem.* **15**, 2077 (1976).
1654. M. Sorai, *J. Inorg. Nucl. Chem.* **40**, 1031 (1978).
1655. B. Hutchinson, P. Neill, A. Finkelstein, and J. Takemoto, *Inorg. Chem.* **20**, 2000 (1981).
1656. S. Singhal, C. L. Sharma, A. N. Garg, and K. Chandra, *Polyhedron* **21**, 2489 (2002).
1657. K. Nakamoto, J. Fujita, R. A. Condrate, and Y. Morimoto, *J. Chem. Phys.* **39**, 423 (1963).
1658. K. A. Jensen and V. Krishnan, *Acta Chem. Scand.* **24**, 1088 (1970).
1659. K. Jensen, B. M. Dahl, P. Nielsen, and G. Borch, *Acta Chem. Scand.* **26**, 2241 (1972).
1660. G. W. Watt and B. J. McCormick, *Spectmchim. Acta* **21**, 753 (1965).
1661. V. V. Savant, J. Gopalakrishnan, and C. C. Patel, *Inorg. Chem.* **9**, 748 (1970).
1662. P. Singh, S. Bhattacharyya, V. D. Gupta, and H. Noth, *Chem. Ber.* **129**, 1093 (1996).
1663. P. Singh, S. Singh, V. D. Gupta, and H. Noth, *Z. Naturforsch.* **53B**, 1475 (1998).
1664. G. A. Melson, N. P. Crawford, and B. J. Geddes, *Inorg. Chem.* **9**, 1123 (1970).

1665. M. J. M. Campbell, *Coord. Chem. Rev.* **15**, 279 (1975).
1666. M. A. Ali, S. E. Linvingstone, and D. J. Phillips, *Inorg. Chim. Acta* **5**, 119 (1971).
1667. H. O. Desseyn, W. A. Jacob, and M. A. Herman, *Spectrochim. Acta* **25A**, 1685 (1969).
1668. B. Stootmaekers, E. Manessi-Zoupa, S. P. Perlepes, and H. O. Desseyn, *Spectrochim. Acta* **52A**, 1255 (1996).
1669. E. Manessi-Zoupa, S. P. Perlepes, A. C. Fabretti, and H. O. Desseyn, *Spectrosp. Lett.* **27**, 119 (1994).
1670. M. L. B. F. Hereygers, H. O. Desseyn, K. A. F. Verhulst, A. T. H. Lenstra, and S. P. Perlepes, *Polyhedron* **15**, 3437 (1996).
1671. P. Román, J. J. Beitia, A. Luque, and C. Guzmán-Miralles, *Polyhedron* **14**, 1091 (1995).
1672. J. Bremi, E. D'Agostino, V. Gramlich, W. Caseri, and P. Smith, *Inorg. Chim. Acta* **335**, 15 (2002).
1673. D. Coucouvanis, N. C. Baenziger, and S. M. Johnson, *J. Am. Chem. Soc.* **95**, 3875 (1973).
1674. D. Coucouvanis and D. Piltingsrud, *J. Am. Chem. Soc.* **95**, 5556 (1973).
1675. J. A. McCleverty, *Prog. Inorg. Chem.* **10**, 49 (1968).
1676. C. W. Schläpfer and K. Nakamoto, *Inorg. Chem.* **14**, 1338 (1975).
1677. M. Cox and J. Darken, *Coord. Chem. Rev.* **7**, 29 (1971).
1678. S. E. Linvingstone, *Coord. Chem. Rev.* **7**, 59 (1971).
1679. O. Siimann and J. Fresco, *Inorg. Chem.* **8**, 1846 (1969); *J. Chem. Phys.* **54**, 734, 740 (1971).
1680. C. G. Barraclough, R. L. Martin, and I. M. Stewart, *Aust. J. Chem.* **22**, 891 (1969); G. A. Heath and R. L. Martin, *ibid*. **23**, 1721 (1970).
1681. S. H. J. de Beukeleer and H. O. Desseyn, *Spectrochim. Acta* **51A**, 1617 (1995).
1682. H. Shindo and T. L. Brown, *J. Am. Chem. Soc.* **87**, 1904 (1965).
1683. M. Chandrasekharan, M. R. Udupa, and G. Aravamudan, *Inorg. Chim. Acta* **7**, 88 (1973).
1684. R. Panossian, G. Tenrian, and M. Guiliano, *Spectrosc. Lett.* **12**, 715 (1979).
1685. R. J. Gale and C. A. Winkler, *Inorg. Chim. Acta* **21**, 151 (1977).
1686. C. A. McAuliffe, J. V. Quagliano, and L. M. Vallarino, *Inorg. Chem.* **5**, 1996 (1966).
1687. C. A. McAuliffe, *J. Chem. Soc. A*, 641 (1967).
1688. M. Ikram and D. B. Powell, *Spectrochim. Acta* **27A**, 1845 (1971).
1689. Y. Mido and E. Sekido, *Bull. Chem. Soc. Jpn.* **44**, 2130 (1971).
1690. J. A. W. Dalziel, M. J. Hitch, and S. D. Ross, *Spectrochim. Acta* **25A**, 1055 (1969).
1691. W. W. Fee and J. D. Pulsford, *Inorg. Nucl. Chem. Lett.* **4**, 227 (1968).
1692. D. Michalska and A. T. Kowal, *Spectrochim. Acta* **41A**, 1119 (1985).
1693. C. M. V. Státhandske, I. Persson, M. Sandström, and E. Kamienska-Piotrowicz, *Inorg. Chem.* **36**, 3174 (1997).

Chapter 2

Applications in Organometallic Chemistry

Vibrational spectra of organometallic compounds have been reported extensively [1], and comprehensive reviews are found in several monographs [2,3]. More limited reviews are available on specific metal elements or functional groups, and will be quoted in respective sections. Reference books on vibrational spectra of organic compounds [4–6] are useful in making band assignments since vibrational spectra of organometallic compounds in the high-frequency region are largely due to organic ligands or moieties. Spectral charts [7,8] and an index [9] of vibrational spectra of organic and organometallic compounds are also useful for this purpose. In the following, we review vibrational spectra of organometallic compounds with emphasis on metal-carbon streching vibrations in the low-frequency region since they provide structural and bonding information on the metal-carbon skeleton.

2.1. METHYLENE, METHYL, AND ETHYL COMPOUNDS

The smallest organometallic compound may be a metal carbene in which the carbon atom of the methylene group is σ-bonded to a metal ($M-CH_2$). Such a compound can be prepared via cocondensation reaction of metal atom vapor with diazomethane in inert gas matrices:

$$M + CH_2N_2 \rightarrow M-CH_2 + N_2$$

Infrared and Raman Spectra of Inorganic and Coordination Compounds, Part B: Applications in Coordination, Organometallic, and Bioinorganic Chemistry, Sixth Edition, by Kazuo Nakamoto

Margrave and co-workers obtained the IR spectra of $CuCH_2$ [10], $FeCH_2$ [11], and $CrCH_2$ [12] in Ar matrices. These molecules are planar and exhibit the six normal vibrations shown in Fig. 1.33. In the case of $CrCH_2$, the $\nu_a(CH_2)$, $\nu_s(CH_2)$, $\delta(CH_2)$, $\rho_r(CH_2)$ and $\nu(Cr-C)$ are observed at 2967, 2907, 688, 450, and 567 cm^{-1}, respectively. The $\nu(Cu-C)$ in $CuCH_2$ is at 614 cm^{-1}, and the $\nu(Fe-C)$ in $FeCH_2$ is at 624 cm^{-1}. Bare et al. [13] also obtained $MgCH_2$ and its carbenoid radicals $XMgCH_2$ by the reaction of laser-ablated Mg atoms with CH_3X (X = H,F,Cl,Br) diluted in Ar. The $\nu(Mg-C)$ of $MgCH_2$ was at 502.2 cm^{-1}.

There are many compounds in which the carbon atom of the methyl group is σ-bonded to a metal ($M-CH_3$). Vibrational spectra of these methyl compounds can be interpreted in terms of the normal modes of a 1:1 (metal/methyl) model as shown in Fig. 1.2. The $\nu_a(CH_3)$, $\nu_s(CH_3)$, $\delta_d(CH_3)$, $\delta_s(CH_3)$, and $\rho_r(CH_3)$, and $\nu(M-C)$ are at 3000–2800, 3000–2700, 1400–1350, 1300–1100, 950–700, and 700–400 cm^{-1}, respectively. The simplest is the 1:1 (metal/methyl) complex such as $NaCH_3$ and KCH_3, which can be prepared in Ar matrices at 20 K [14]. Table 2.1 lists the Raman frequencies of typical $M(CH_3)_4$-type compounds. Figure 2.1 shows the Raman spectra of $Si(CH_3)_4$ and $Si(CD_3)_4$ obtained by Fischer et al. [17]. In Fig. 2.2, the observed frequencies are plotted as a function of the atomic mass of the group IVB elements [18]. It is seen that the $\delta_s(CH_3)$, $\rho_r(CH_3)$, $\nu(M-C)$, and $\delta(CMC)$ are shifted progressively to lower frequencies as the atomic mass increases. The $\rho_r(CH_3)$ and $\nu(M-C)$ are particularly sensitive to the nature of these metals. Under $\mathbf{T}_d$ symmetry, two $\nu(M-C)$ (A_1 and F_2) are expected for the $M(CH_3)_4$-type molecule. These vibrations are reported to be 508 and 530 cm^{-1}, respectively, for $Sn(CH_3)_4$, [19] and 598 and 696 cm^{-1}, respectively, for $Si(CH_3)_4$ [20].

Tables 2.2 and 2.3 list the MC stretching and CMC bending frequencies of various $M(CH_3)_n$-type molecules and ions observed in IR and/or Raman spectra. The number of IR- and Raman-active skeletal vibrations expected for each structure are found in Appendix V of Part A. As already seen in the $M(CH_3)_4$ series, both $\nu(M-C)$ bands are downshifted progressively as the mass of the central metal increases in the same family of the periodic table. Thus, the orders of $\nu(M-C)$ are

$$Al(CH_3)_3 > Ga(CH_3)_3 > In(CH_3)_3$$

TABLE 2.1. Raman Frequencies[a] of $M(CH_3)_4$-Type Molecules (cm^{-1}) [15,16]

Compound	$\nu_a(CH_3)$	$\nu_s(CH_3)$	$\delta_d(CH_3)$	$\delta_s(CH_3)$	$\rho_r(CH_3)$	ν(MC)	δ(CMC)
$C(CH_3)_4$	2959	2922	(1475)	—	926	733	418
	2963		1457		(926)	1260	332
$Si(CH_3)_4$	(2959)	2913	(1430)	1271	870	593	239
	2964		1421		(870)	698	190
	(2910)						
$Ge(CH_3)_4$	(2981)	2920	(1430)	1259	—	561	196
	2982		1420		(828)	599	188
$Sn(CH_3)_4$	(2984)	2920	(1447)	1211	—	509	137
	2988		—		(768)	527	133
$Pb(CH_3)_4$	2996	2924	1450	1170	767	478	145
	2924		1400	1154	700	459	130

[a] ( ) = IR frequency.

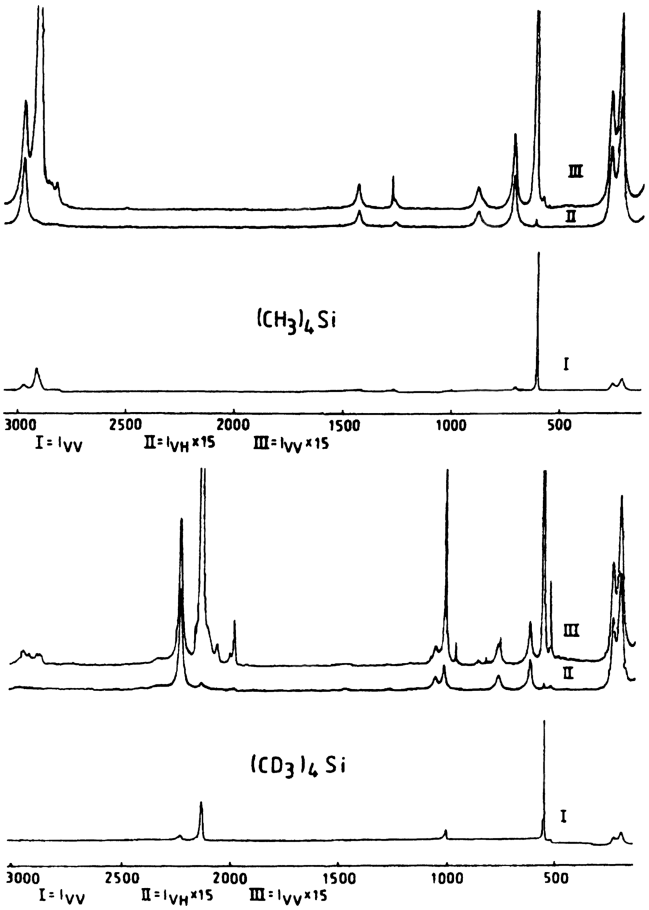

Fig. 2.1. *Polarized and depolarized Raman spectra of $Si(CH_3)_4$ and $Si(CD_3)_4$ [17].*

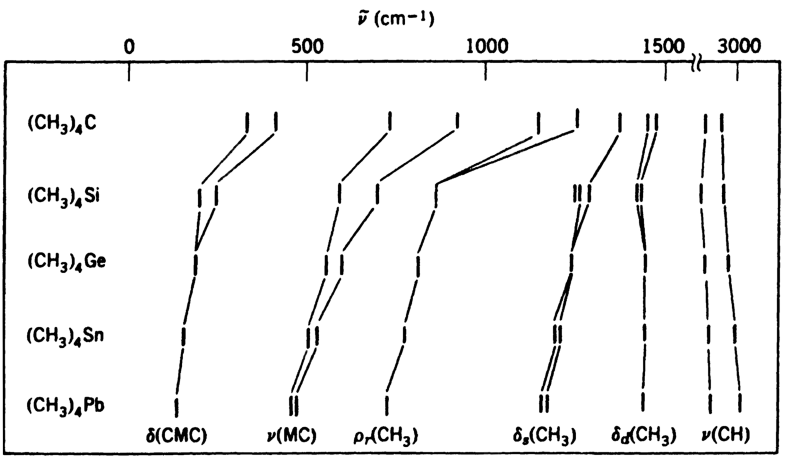

Fig. 2.2. *Vibrational frequencies of $M(CH_3)_4$-type compounds [18].*

TABLE 2.2. Metal–Carbon Skeletal Frequencies of $M(CH_3)_n$-Type Compounds (cm^{-1})

Compound	Structure	ν_a(MC)	ν_s(MC)	δ(CMC)	Ref.
$Be(CH_3)_2$	Linear	1081	—	—	21
$Zn(CH_3)_2$	Linear	604	503	157	22–26
$Cd(CH_3)_2$	Linear	525	460	140	22,24–27
$Hg(CH_3)_2$	Linear	538	515	160	22,24–26
$Se(CH_3)_2$[a]	Bent	604	589	233	28,29,31
$Te(CH_3)_2$[a]	Bent	528	528	198	28–31
$B(CH_3)_3$	Planar	1177	680	341,321	32–34
$Al(CH_3)_3$	Planar	760	530	170	35–37
$Ga(CH_3)_3$	Planar	577	521.5	162.5	36–40
$In(CH_3)_3$	Planar	500	467	132	39,41,42
$P(CH_3)_3$	Pyramidal	703	653	305,263	43–45
$As(CH_3)_3$	Pyramidal	583	568	238,223	43,44,46
$Sb(CH_3)_3$	Pyramidal	513	513	188	47
$Bi(CH_3)_3$	Pyramidal	460	460	171	47
$Si(CH_3)_4$	Tetrahedral	696	598	239,202	48,49
$Ge(CH_3)_4$	Tetrahedral	595	558	195,175	16,49
$Sn(CH_3)_4$	Tetrahedral	529	508	157	18,49
$Pb(CH_3)_4$	Tetrahedral	476	459	120	49,50
$Ti(CH_3)_4$	Tetrahedral	577	489	180	51
$Sb(CH_3)_5$	Trigonal–bipyramidal	514[b]	493[b]	213[b]	52
		456[c]	414[c]	199[b]	
				104[c]	
$W(CH_3)_6$	Octahedral	482	—	—	53

[a] New assignments have been proposed on the basis of $\mathbf{D}_{3d}$ model containing a linear C–M–C skeleton (see Ref. 31).
[b] Equatorial.
[c] Axial.

TABLE 2.3. Metal–Carbon Skeletal Frequencies of $[M(CH_3)_n]^{m+}$-Type Compounds (cm^{-1})

Compound	Structure	ν_a(MC)	ν_s(MC)	δ(CMC)	Refs.
$[Zn(CH_3)]^+$	—	—	557	—	54
$[In(CH_3)_2]^+$	Linear	566	502	—	55
$[Tl(CH_3)_2]^+$	Linear	559	498	114	56,57
$[Sn(CH_3)_2]^{2+}$	Linear	582	529	180	58
$[Sn(CH_3)_3]^+$	Planar	557	521	152	59
$[Sb(CH_3)_3]^{2+}$	Planar	582	536	166	60
$[Se(CH_3)_3]^+$	Nonplanar	602	580	272	61
$[Te(CH_3)_3]^+$	Nonplanar	534	—	—	62
$[P(CH_3)_4]^+$	Tetrahedral	783	649	285	63
				170	64
$[As(CH_3)_4]^+$	Tetrahedral	652	590	217	47
$[Sb(CH_3)_4]^+$	Tetrahedral	574	535	178	47

and

$$P(CH_3)_3 > As(CH_3)_3 > Sb(CH_3)_3 > Bi(CH_3)_3$$

An exception is found in the linear $M(CH_3)_2$ series:

	$Zn(CH_3)_2$		$Cd(CH_3)_2$		$Hg(CH_3)_2$
ν_s(M−C) (cm^{-1})	503	>	460	<	515
ν_a(M−C) (cm^{-1})	604	>	525	<	538

Apparently, this is due to an irregular variation in the M−C bond order. Figure 2.3 shows the matrix-isolation IR spectra of the series above obtained by Bochmann et al. [26]. The two strong bands below 800 cm^{-1} are due to the $\rho_r(CH_3)$ and ν_a(M−C) vibrations. In this case, the latter bands are observed at 613(Zn), 538(Cd), and 538(Hg) cm^{-1}. Vibrational spectra are reported for methyl compounds such as $M(^{12,13}CH_3)_2$ (M = Zn,Cd, Hg) [65], $Te(CH_3)_2$ [66], and $M(CH_3)_3$ (M = In, Tl) [67].

H_3C-M-H-type compounds are produced by matrix cocondensation reactions of laser-ablated metal atoms with CH_4 in Ar (M = Be,Mg,Ca [68]; Zn,Cd, Hg [69]), and their IR spectra are available. Matrix cocondensation reactions of $Cd(CH_3)_2$ with a ligand such as H_2S and NH_3 form 1 : 1 adducts in which the ligand is bonded to the linear $H_3C-Cd-CH_3$ by taking a T-shaped structure. As a result, the $\nu_a(CdC_2)$ is lower by 6–22 cm^{-1} relative to free $Cd(CH_3)_2$ [70].

Vibrational assignments are reported for CF_3 compounds such as $Cd(CF_3)_2$ [71], $Pb(CF_3)_4$ [72] and $B(CF_3)_3(NH_3)$ [73]. For example, the Raman spectrum of $Cd(CF_3)_2$ in the solid state exhibits the $\nu_s(CF_3)$ at 1157 and 1135, $\nu_a(CF_3)$ at 980 and 960, and $\delta(CF_3)$ at 696 cm^{-1}. The ν_s(Cd−C) are observed at 218 and 196 cm^{-1}. Normal coordinate analyses were carried out on $Hg(CF_3)_2$, $Hg(CCl_3)_2$, and related compounds [74].

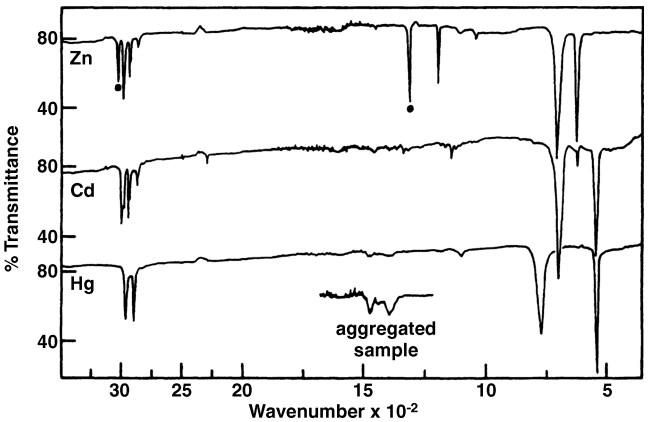

Fig. 2.3. *Infrared spectra of $M(CH_3)_2$ (M = Zn,Cd,Hg) in Ar matrices; • indicates bands due to methane in the $Zn(CH_3)_2$ spectrum [26].*

Some metal alkyls are polymerized in condensed phases. $Li(CH_3)$ forms a tetramer containing $Li-CH_3-Li$ bridges in the solid state [75], and its CH_3 frequencies are lower than those of nonbridging compounds [$\nu_a(CH_3)$ and $\nu_s(CH_3)$ are 2840 and 2780 cm^{-1}, respectively] [76].

Solid $Be(CH_3)_2$ and $Mg(CH_3)_2$ also form long-chain polymers through CH_3 bridges [77] while $A1(CH_3)_3$ is dimeric in the solid state [78]. The infrared spectra of $Li[Al(CH_3)_4]$ and $Li_2[Zn(CH_3)_4]$ have been interpreted on the basis of linear polymeric chains in which the Al (or Zn) atom and the Li atom are bonded alternately through two CH_3 groups [79]. Normal coordinate analyses have been carried out on $M(CH_3)_2^-$ (M = Zn,Cd,Hg) [22,25,80], dimeric $Al(CH_3)_3^-$ [36,78] and linear $[M(CH_3)_2]^{n+}$-type cations [55,58].

The ethyl group bonded to a metal ($M-CH_2-CH_3$) exhibits bands characteristic of both the CH_3 and CH_2 groups. It is difficult, however, to give complete assignments of the $M-C_2H_5$ group vibrations because of band over-lapping and vibrational coupling. Table 2.4 lists the MC_n skeletal frequencies of typical $M(C_2H_5)_n$-type compounds. The MC stretching frequencies of the ethyl compounds are lower than those of the corresponding methyl compounds (Table 2.2) due to the larger mass of the ethyl, relative to the methyl group.

$Li(C_2H_5)$ is hexameric in hydrocarbon solvents [97] and is polymeric in the solid state [98]. The LiC stretching bands of these polymers are at 530–300 cm^{-1} [99]. The vibrational spectra of other polymeric ethyl compounds such as $Be(C_2,H_5)_2$ (dimer) [100] $Mg(C_2H_5)_2$, [101], $A1(C_2H_5)_3$ (dimer) [102], and $Li[Al(C_2H_5)_4]$ (polymer) [103] have been reported. There are many other compounds containing higher alkyl groups. References for some typical compounds are as follows: $[T1(n\text{-}C_3H_7)_2]C1$ (57), $Ge(n\text{-}C_4H_9)_4$ [104], and $[Li(t\text{-}C_4H_9)]_4$ [105]. Vibrational spectra have also been reported for cycloalkyl compounds such as $Zn(c\text{-}C_3H_5)_2$ [106], $M(c\text{-}C_3H_5)_4$ (M = Si,Ge,Sn) [107], $Pb(c\text{-}C_3H_5)_4$ [108], and $Sb(c\text{-}C_3H_5)_5$ [109].

TABLE 2.4. Metal–Carbon Skeletal Frequencies of $M(C_2H_5)_n$-Type Compounds (cm^{-1})

Compound	Structure	ν_a(MC)	ν_s(MC)	δ(MCC)	δ(CMC)	Ref.
$Zn(C_2H_5)_2$	Linear	563	474	261	205	81,82
$Cd(C_2H_4)_2$	Linear	498	445			37
$Hg(C_2H_5)_2$	Linear	515	488	267	140	83,84
$^{10}B(C_2H_5)_3$	Planar	1135	—	—	287	32,85
$Al(C_2H_5)_3$	Planar	662	489			36
$Ga(C_2H_5)_3$	Planar	496	—	—	—	86
$In(C_2H_5)_3$	Planar	457	447			44
$P(C_2H_5)_3$	Pyramidal	697, 669	619	410, 249	—	87,88
$As(C_2H_5)_3$	Pyramidal	540	570, 563	—	—	88,89
$Sb(C_2H_5)_3$	Pyramidal	505	505	—	—	87,90
$Bi(C_2H_5)_3$	Pyramidal	450	450	253	124	91
$Si(C_2H_5)_4$	Tetrahedral	731	549	392, 233	170	63,92
$Ge(C_2H_5)_4$	Tetrahedral	572	532	332	152	93,94
$Sn(C_2H_5)_4$	Tetrahedral	508	490	272	132, 86	95,96
$Pb(C_2H_5)_4$	Tetrahedral	461	443	243, 213	107	91,95

An unusual three-center, two-electron bridging interaction was proposed for the ethyl group in $(Cp^*)_2Sc(CH_2-CH_3)$ ($Cp^* = \eta^5$-$Cp{\cdot}Me_5$):

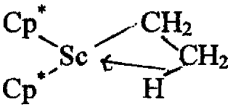

IR spectra provide strong support for this "agostic" interaction between β C−H bond and the Sc atom; it exhibits three prominent, low-frequency ν(C−H) bands at 2593, 2503, and 2440 cm^{-1}, whereas the corresponding methyl compound shows no such bands in the 2700–1600 cm^{-1} region [110].

2.2. VINYL, ALLYL, ACETYLENIC, AND PHENYL COMPOUNDS

Table 2.5 lists the CC and MC stretching frequencies of metal vinyl (M−CH=CH_2), allyl (M−CH_2−CH=CH_2), and acetylenic (M−C≡CH) compounds in which the organic ligands are σ-bonded to the central metal. The ν(C=C) and ν(C≡C) are generally strong in the Raman. However, their infrared intensities depend on the metal involved.

Vibrational spectra of vinyl compounds such as $B(CH=CH_2)_2(OCH_3)$ [128] and $SiHCl_2(CH=CH_2)$ [129] have been assigned. Vibrational spectra of halovinyl

TABLE 2.5. Carbon–Carbon and Metal–Carbon Stretching Frequencies of Vinyl, Allyl, and Acetylenic Compounds (cm^{-1})

Compound	ν(C=C) or ν(C≡C)	ν(M−C)	Ref.
$Zn(CH=CH_2)_2$	1565	—	111
$Hg(CH=CH_2)_2$	1603	541, 513	112
$^{10}B(CH=CH_2)_3$	1604	1186, 651	113–116
$P(CH=CH_2)_3$	1590	715, 667	117
$Si(CH=CH_2)_4$	1591	725,578,541	118–120
$Ge(CH=CH_2)_4$	1595	600, 561	119
$Sn(CH=CH_2)_4$	1583	531,490	119–120
$Pb(CH=CH_2)_4$	1580	495,479	119
$Si(CH_2-CH=CH_2)_4$	1631	707,597,526	121
$Sn(CH_2-CH=CH_2)_4$	1624	487,475	121
$Hg(CH_2-CH=CH_2)_2$	1617	495,475	122
$Si(C\equiv CH)_4$	2062,2053	708,534	123–125
$Ge(C\equiv CH)_4$	2062,2057	523,507	123–125
$Sn(C\equiv CH)_4$	2043	504,447	123–125
$P(C\equiv CH)_3$	2061	646,615	126
$As(C\equiv CH)_3$	2053	526,517	126,127
$Sb(C\equiv CH)_3$	2033	477,450	126,127
$(CH_3)_2Si(C\equiv CH)_2$[a]	2041	548, 385,377,300	123–126
$(CH_3)_2Ge(C\equiv CH)_2$[a]	2041	538,521	123–126
$(CH_3)_2Sn(C\equiv CH)_2$[a]	2016	454	123–126

[a]For these compounas, the ν(M−C) indicates that of the M−C≡CH group.

compounds have been reported for $Hg(CH{=}CHCl)_2$ [130] and $M(CF{=}CF_2)_n$ (M = Hg, As, and Sn) [131]. Complete vibrational assignments, are available for metal allyl compounds such as $M(CH_2{-}CH{=}CH_2)_4$(M = Si,Sn) [132], $(M(CH_2{-}CH{=}CH_2)_3$ (M = P,As) [133], and $Hg(CH_2{-}CH{=}CH_2)_2$ [134,135].

Matrix cocondensation reactions of laser-ablated Be atoms with C_2H_2/Ar produce $HBe(C{\equiv}CH)$ and $Be(C{\equiv}CH)$, which exhibit the $\nu(C{\equiv}C)$ at 2119.4 and 2108.9 cm^{-1}, respectively [136]. Raman spectra of metal acetylides of the type $M^{2+}(C_2{}^{2-})$ (M^{2+} = Ca,Sr,Ba) show the $\nu(C_2{}^{2-})$ in the 1871–1798 cm^{-1} region [137].

The phenyl group σ-bonded to a metal ($M{-}C_6H_5$) exhibits bands characteristic of monosubstituted benzenes [138]. The $M{-}C_6H_5$ group exhibits 30 $(3 \times 12 - 6)$ fundamentals, only six of which, shown in Fig. 2.4, are sensitive to the change in metals. Table 2.6 lists the observed frequencies of these six modes for typical phenyl compounds. It is seen that most of these bands are shifted progressively to lower frequencies as the metal is changed in the order

$$\begin{aligned} &Al > Ga > In \\ &Si > Ge > Sn > Pb \\ &P > As > Sb > Bi \end{aligned}$$

Among the six modes, t and u are particularly metal-sensitive because they correspond to the ν(MC) and δ(CMC), respectively. The number of these bands reflects the local symmetry of the MC_n skeleton. For example, in the $M(C_6H_5)_3$ (M = P, As,Sb,Bi) series, two ν(MC) bands (A_1 and E) are expected in IR as well as in Raman

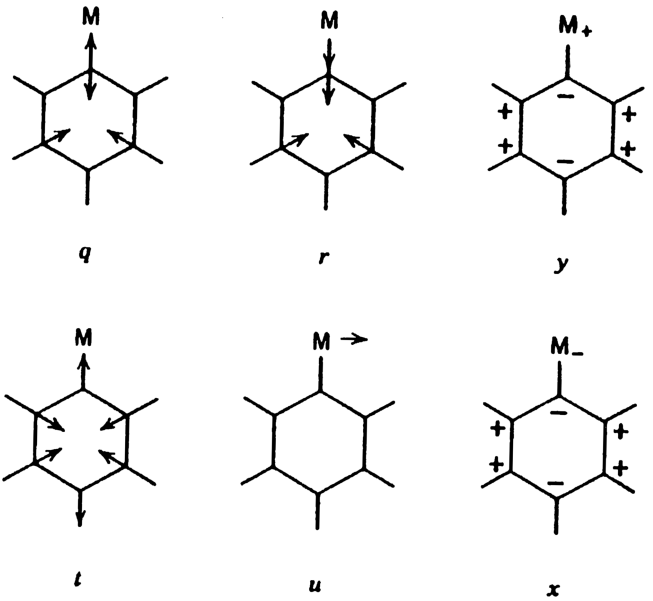

Fig. 2.4. *Metal-sensitive modes of the $M{-}C_6H_5$ moiety.*

TABLE 2.6. Vibrational Frequencies of Metal-Sensitive Modes of Metal Phenyls (cm^{-1})

Compound	*q*	*r*	*y*	*t*	*x*	*u*	Ref.
$Hg(C_6H_5)_2$	1067	661	456	258 252 248	—	207	139,140
$^{10}B(C_6H_5)_3$	1285 1248	893	600	650	245	408	141,142
$Al(C_6H_5)_3$	1085	670 643	460	420	207	332	142,143
$Ga(C_6H_5)_3$	1085	665	453 445	315	180	245 225	142
$In(C_6H_5)_3$	1070	673	465	270	180	248 195	142,144
$Si(C_6H_5)_4$	1108	709	519 511	435 239	185 171	261 223	145
$Ge(C_6H_5)_4$	1091	—	481 465	332	187 168	232 214	145,146
$Sn(C_6H_5)_4$	1075	616	459 448	268 212	193 152	225	145,147,148
$Pb(C_6H_5)_4$	1061	645	450 440	223 201	147	181	145
$P(C_6H_5)_3$	1089	—	501 509	428 398	248 268	209 190	147,149
$As(C_6H_5)_3$	1082 1074	667	474	313	237	192 183	147,149
$Sb(C_6H_5)_3$	1065	651	457	270 257	216	166	147,149
$Bi(C_6H_5)_3$	1055	—	448	237 220	207	157	147,149,150

spectra since, the symmetry of the MC_3 skeleton is $\mathbf{C}_{3v}$. This is clearly demonstrated in Fig. 2.5, where the IR and Raman spectra of these compounds in benzene solution are shown [149]. The spectra obtained in the solid state [149] show further band splittings due to lowering of symmetry and intermolecular interaction.

2.3. HALOGENO, PSEUDOHALOGENO, AND ACIDO COMPOUNDS

There are many organometallic compounds containing functional groups other than those discussed in the preceding sections. Vibrational spectra of these compounds can be interpreted approximately as the overlap of bands discussed previously and those described below.

2.3.1. Halogeno Compounds

Table 2.7 lists metal-carbon and metal-halogen stretching frequencies of typical compounds. The $\nu(M-CH_3)$ and $\nu(M-C_6H_5)$ are observed in the, 750–450 and

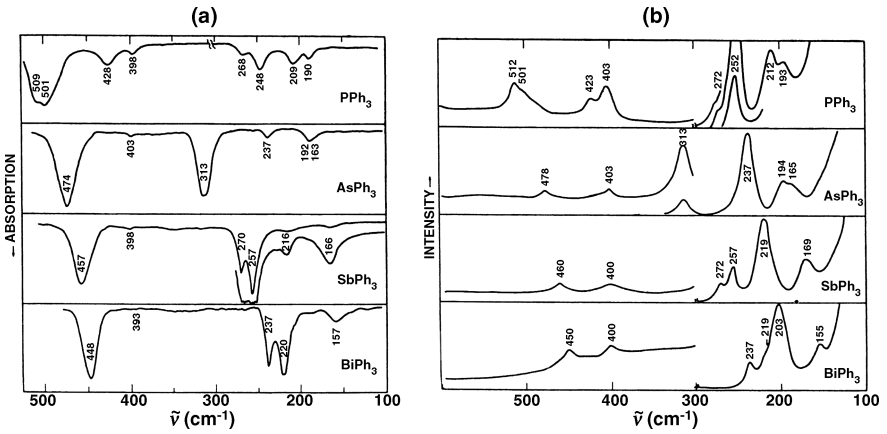

Fig. 2.5. *(a) Infrared and (b) Raman spectra of $M(C_6H_5)_3$ (M = P, As, Sb, Bi) in benzene solution [149].*

300–190 cm^{-1} regions, respectively, as previously found in methyl and phenyl compounds. The ν(M–X) (terminal) vibrations (Sec. 1.23) appear in the following regions:

ν(MF)	ν(MCl)	ν(MBr)	ν(MI)	
800–400	550–200	450–140	260–100	(cm^{-1})

These ranges are rather wide because the ν(MX) varies markedly depending on the structure. This is clearly demonstrated in Table 2.7. As shown previously for ν(MC), the ν(MX) also becomes lower as the mass of M increases in the same family of the periodic table:

	$Si(CH_3)_3Cl$		$Ge(CH_3)_3Cl$		$Sn(CH_3)_3Cl$
$\nu(M-Cl)\,(cm^{-1})$	472	>	378	>	318
	$Si(C_6H_5)Cl_3$		$Ge(C_6H_5)Cl_3$		$Sn(C_6H_5)Cl_3$
$\nu(M-Cl)\,(cm^{-1})$	596,518	>	427,407	>	383,363

The same trends are observed for the $\nu(M-CH_3)$ and $\nu(M-C_6H_5)$ of these compounds.

Normal coordinate analyses have been carried out on $Si(CH_3)_3Cl$ [165], $Si(CH_3)_2Cl_2$ [166], $Si(CH_3)Cl_3$ [167], $Si(CH_3)Cl_3$ [168], $Si(^tBu)X_3$(X = F, Cl, Br, etc.) [169], $Sb(CH_3)_3X_2$ [159], $Ti(CH_3)Cl_3$ [152], *cis*-$[Au(CH_3)_2X_2]^-$ [160], $Si(C_2H_5)_3F$[170], and $Tl(C_6H_5)X_2$ [162]. Detailed band assignments are reported for the $Sn(CH_3)_nCl_{4-n}$ [19] and $M(C_6H_5)Cl_3$ (M = Si,Ge,Sn) series [171].

TABLE 2.7. Metal–Carbon and Metal–Halogen Stretching Frequencies of Organometal Halogeno Compounds (cm^{-1})

Compound	ν(MC)	ν(MX)	Ref.	Compound	ν(MC)	ν(MX)	Ref.
$Cd(CH_3)Cl$	476	247	151	$Sb(CH_3)_3Cl_2$[a]	577	282	158
$Cd(CH_3)Br$	475	206	151		538	272	159
$Cd(CH_3)I$	482	167	151	$Sb(CH_3)_3Br_2$[a]	569	215	158
$Ti(CH_3)Cl_3$	536	551	152		526	168	159
		390		$Sb(CH_3)_3I_2$[a]	559	144	158
$Al(CH_3)Cl_2$	653	564	153		508	122	
		425		$[Au(CH_3)_2Cl_2]^-$	572	272	160
$Al(CH_3)_2Cl$	603	691	153	(*cis*)	563	268	
		453		$[Au(CH_3)_2Br_2]^-$	558	197	160
$Si(CH_3)_3F$	704	898	154	(*cis*)	552	179	
	635			$Tl(C_6H_5)F_2$	283	525	161
$Si(CH_3)_3Cl$	704	472	155			500	
	635			$Tl(C_6H_5)Cl_2$	273	382	162
$Ge(CH_3)_3F$	623	623	156			332	
	576			$Tl(C_6H_5)Br_2$	206	270	162
$Ge(CH_3)_3Cl$	612	378	157			258	
	569			$Bi(C_6H_5)_3F_2$[a]	202	445	163
$Sn(CH_3)_3Cl$	548	318	19	$Bi(C_6H_5)_3Cl_2$[a]	213	253	163
	518				195		
$Sb(CH_3)_3F_2$[a]	591	484	158	$Bi(C_6H_5)_3Br_2$[a]	215	153	163
	546	465	159		195		
				$Sn(C_6H_5)_3Cl$	276	339	164
					232		

[a] The halogens occupy the axial positions of trigonal bipyramias.

In condensed phases, halogeno compounds tend to polymerize by forming halogeno bridges between two metal atoms. As discussed in Sec. 1.25, the bridging frequencies are much lower than the terminal frequencies. For example, in $[Al(CH_3)Cl_2]_2$

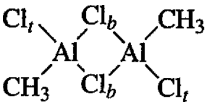

(C_{2h})

the $\nu(Al-Cl_t)$ are at 495 (A_g) and 485 (B_u), whereas the $\nu(Al-Cl_b)$ are at 345 (A_g), 380 (A_u), and 322 cm^{-1} (B_u) [153]. As shown in Table 2.7, the $\nu(Al-Cl)$ of monomeric $Al(CH_3)Cl_2$ are at 425 (ν_s) and 564 cm^{-1} (ν_a). Thus, it is possible to distinguish monomeric and polymeric structures by vibrational spectroscopy.

It was found that $B(CH_3)_2X$ (X = F,Cl,Br) is monomeric [172], whereas $Al(CH_3)_2F$, $Ga(CH_3)_2F$, and $In(CH_3)_2Cl$ are tetrameric [173], trimeric [174], and dimeric [175], respectively, in benzene solution. Alkyl silicon and germanium halides tend to be monomeric, whereas alkyl tin and lead halides tend to be polymeric in the

liquid and solid phases. For example, $Sn(CH_3)_2F_2$ and $Sn(CH_3)_3F$ are polymerized through the fluorine bridges [176]:

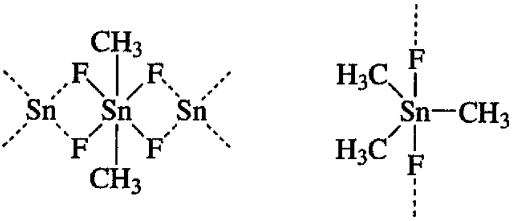

The ν(SnF) for terminal bonds are at 650–625 cm^{-1}, whereas those for bridging bonds are at 425–335 cm^{-1}. In the solid state, the coordination number of tin is five or six. Dialkyl compounds prefer six-coordinate structures, while trialkyl compounds tend to form five-coordinate structures. In both cases, the favored positions of the alkyl groups are those shown in the diagrams above. Normal coordinate calculations have been made on the *trans*-$[Sn(CH_3)_2X_4]^{2-}$ (X = F,Cl,Br) series [177].

$Pb(CH_3)_3X$ (X = F,Cl,Br,I) are monomeric in benzene but polymeric in the solid state; ν(PbCl) of the monomer and polymer are observed at 281 and 191 cm^{-1}, respectively [178]. In the $[Au(CH_3)_2X]_2$ series, the Au atom takes a square–planar arrangement with two bridging halogens. The $\nu(Au-X_b)$ of these compounds are at 273 and 256 for X = Cl, 181 for X = Br, and 144 and 131 cm^{-1} for X = I [179]. Figure 2.6 shows the tetrameric structure of $[Pt(CH_3)_3X]_4$-type compounds. Vibrational spectra have been reported for $[Pt(CH)_3X]_4$ (X = Cl,Br,I) [180,181] and $[Pt(CH_3)_2X_2]_n$ (X = Cl,Br,I; n is probably 4) [182].

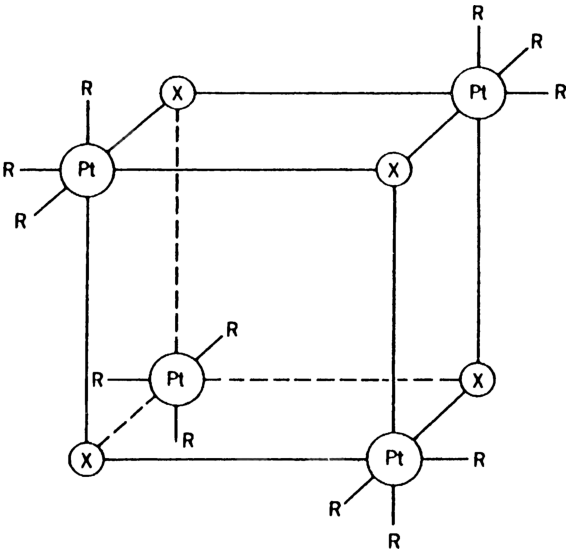

Fig. 2.6. *Structure of $[Pt(CH_3)_3X]_4$; R denotes CH_3.*

2.3.2. Pseudohalogeno Compounds

Vibrational spectra of coordination compounds containing pseudohalogeno groups such as CN^-, SCN^-, CNO^-, and N_3^- ions were discussed in Sec. 1.17. The IR spectra of organometallic compounds involving these ligands have been reviewed by Thayer and West [183]. Although these compounds may have corresponding linkage isomers, only one of the isomers is generally stable for a given metal. The linear triatomic pseudohalogeno groups exhibit three vibrations in the regions 2300–2000 (ν_a), 1500–850 (ν_s), and 700–450 cm^{-1} (δ).

The ν_a is most useful as a diagnostic test of these groups because of its strong appearance in the, IR region, which is free from interference by other bands. As an example, Fig. 2.7 shows the IR spectrum of $Si(CH_3)_3N_3$ obtained by Thayer and Strommen [184].

Vibrational spectra of azido compounds are reported for $Zn(CH_3)N_3$ [185], $Hg(CH_3)N_3$ [186], $A1(CH_3)_2N_3$ [187], $Ga(CH_3)_2N_3$ [188], $Ge(CF_3)_3N_3$ [189], $Si(CH_3)_3N_3$ [190], and $Sn(CH_3)_3N_3$ [191]. The ν(M−N) of these compounds are in the 600–400 cm^{-1} region. The NCO group is always bonded to the metal via the N atom (isocyanato compound). Vibrational spectra of monomeric CH_3Hg−NCO [192], $(CH_3)_3Si$−NCO [190,193], $(CH_3)_3Ge$−NCO [194], $(CH_3)_3Sb(NCO)_2$ [192], and $(C_6H_5)_3Bi(NCO)_2$ [163] have been reported.

The NCS group may be bonded to a metal through the N or S atom or may form a bridge between two metals by using the N, the S, or both atoms. It is not easy to distinguish all these possible structures by vibrational spectra. Table 2.8 lists the modes of coordination and the vibrational frequencies of the M−NCS group. The NCSe group is N-bonded in $(CH_3)_3Si$−NCSe [200] and $(CH_3)_3Ge$−NCSe [201] but is Se-bonded in $(CH_3)_3Pb$−SeCN [202]. Only a very few compounds containing the M−CNO (fulminato) group are known. The spectrum of $(CH_3)_2Tl(CNO)$ is similar to that of K[CNO], and the Tl−CNO bond may be ionic [203]. No isofulminato complexes are reported. The CN group is usually bonded to the metal through the C atom. In the case of $(CH_3)_3M(CN)$ (M = Si,Ge), however, the cyano and isocyano complexes are in equilibrium in the liquid phase, although the mole fraction of the latter is rather small. The CN stretching frequencies (cm^{-1}) of these isomers are as follows:

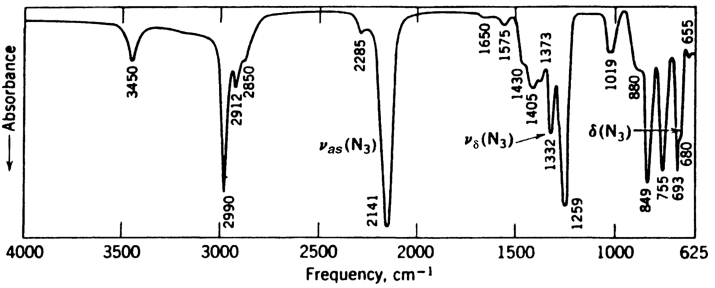

Fig. 2.7. *Infrared spectrum of $Si(CH_3)_3N_3$ (liquid film) [184].*

TABLE 2.8. Vibrational Frequencies of Thiocyanato and Isothiocyanato Compounds (cm^{-1})

Compound	Mode of Coordination	ν(CN)	ν(CS)	δ(NCS)	ν(MS) or ν(MN)	Ref.
$[CH_3Zn(SCN)]_\infty$	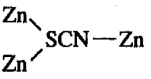	2190 2140	685	445	—	195
$[CH_3Hg(SCN)_3]^{2-}$	Hg—SCN	2119	—	—	276	196
$[(CH_3)_3A1(SCN)]^-$	Al—SCN	2097	845	485	335	197
$[(CH_3)_2A1(SCN)]_3$		2075	627	501 438	—	198
$(CH_3)_3Sn(NCS)$, solid (polymer)	Sn—NCS—Sn	2098 2079 2046	779	474 467	—	199
$(CH_3)_3Sn(NCS)$, CS_2 solution (monomer)	Sn—NCS	2050	781	485	478	199
$[(CH_3)_2Au(NCS)]_2$		2163	775	444 430 [a]	—	179

[a] These bands may be assigned to ν(AuN).

	$(CH_3)_3M-CN$	$(CH_3)_3M-NC$	
M = Si	2198	2095	(gas phase) [204]
M = Ge	2182	2090	($CHC1_3$ solution) [205]

Complete band assignments for $(CH_3)_3GeCN$ and its deuterated analog have been made based on normal coordinate analysis [206].

2.3.3. Acido Compounds

The free acetate ion (CH_3COO^-) exhibits the ν_a(COO) and ν_s(COO) at 1578 and 1414 cm^{-1}, respectively (Sec. 1.9.4). If it is covalently bonded to a metal as a unidentate ligand, the ν_a and ν_s are shifted to higher and lower frequencies, respectively:

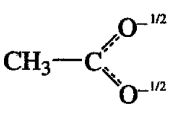

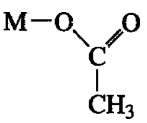

Figure 2.8 shows the IR spectra of the $Si(CH_3)_n(CH_3COO)_{4-n}$ ($n = 0$–3) obtained by Okawara et al. [207]. The ν(C=O) are observed at 1765, 1748, 1732, and 1725 cm^{-1}, respectively, for $n = 0,1,2,3$. In contrast, analogous Sn compounds such as $Sn(CH_3)_3(CH_3COO)$ and $Sn(CH_3)_2Cl(CH_3COO)$ exhibit two ν(COO) near 1600

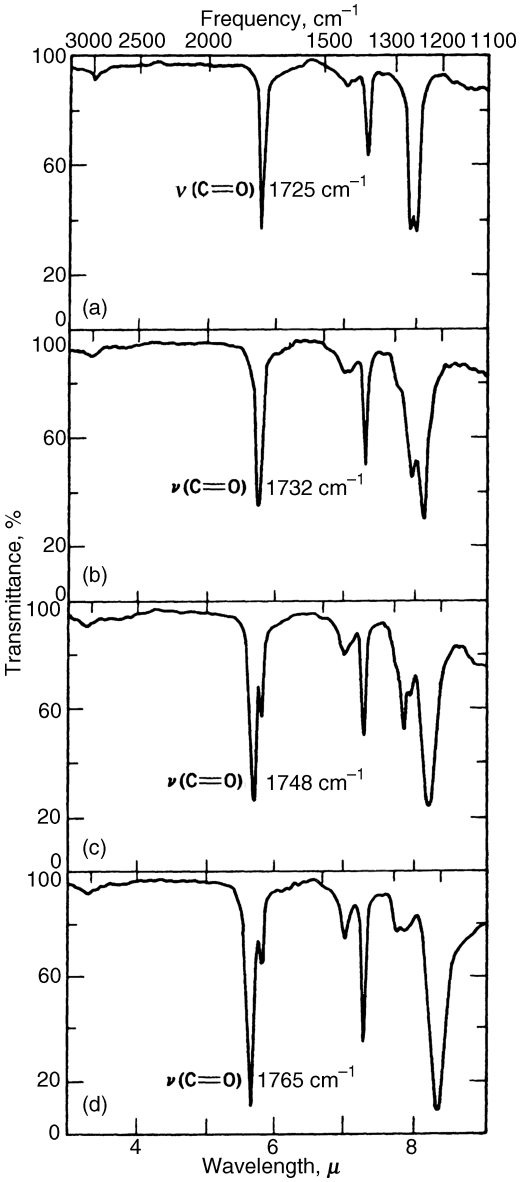

Fig. 2.8. *Infrared spectra of (a) $Si(CH_3)_3(OCOCH_3)$, (b) $Si(CH_3)_2(OCOCH_3)_2$, (c) $Si(CH_3)(OCOCH_3)_3$, (d) $Si(OCOCH_3)_4$ [207].*

and 1420 cm^{-1}, indicating the ionic character of the tin-acetate interaction [207,208]. In $Sb(CH_3)_3(CH_3COO)_2$, however, the two acetate groups occupy the axial positions of the trigonal–bipyramidal structure, and are covalently bonded to the metal as unidentate ligands [209].

As stated earlier, the trigonal-planar $Sn(CH_3)_3$ group in $Sn(CH_3)_3F$ is polymerized by forming the Sn−F−Sn bridges in the solid state. Similar polymerization occurs in $Sn(CH_3)_3L$ where L is CH_3COO^- [210], NO_3^- [211], ClO_4^- [212], and other acido groups:

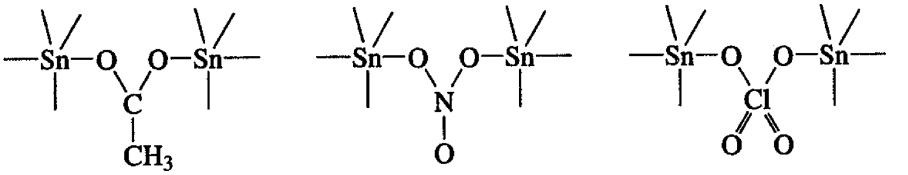

As expected for symmetric bidentate coordination, the separation of the ν_a (1600 cm^{-1}) and ν_s (1363 cm^{-1}) of the first compound (237 cm^{-1}) is much smaller than those observed for unidentate coordination (~460 cm^{-1}) [207]. In agreement with the local symmetry of the NO_3 group in the structure shown above ($\mathbf{C}_{2v}$ or lower), $Sn(CH_3)_3(NO_3)$ exhibits three ν(NO) (1452, 1300, and 1021 cm^{-1}) in IR spectra [211]. Symmetric bidentate coordination of the ClO_4 group in $Sn(CH_3)_3(ClO_4)$ is also confirmed by the observation of four ν(ClO) at 1212, 1112, 998, and 908 cm^{-1} in IR spectral [212].

If $Sn(CH_3)_3L$ is tetrahedral, two ν(Sn−C) vibrations should be IR-active. Thus, the tetrahedral $Sn(CH_3)_3Cl$ molecule exhibits two ν(Sn−C) bands at 545 and 513 cm^{-1} [207]. On the other hand, only one ν(Sn−C) vibration is expected in IR spectra if it contains a trigonal-planar $Sn(CH_3)_3$ group. Examples of the latter are found in the polymeric $Sn(CH_3)_3$ L-type compounds discussed above. These compounds exhibit only one ν(Sn−C) band near 550 cm^{-1}.

Tetrahedral $Sn(CH_3)_2X_2$ (X = Cl,Br,I) molecules exhibit two ν(Sn−C) vibrations at ~560 and 515 cm^{-1} in IR spectra because their C−Sn−C groups are bent [207]. The C−Sn−C groups in polymeric $[Sn(CH_3)_2]_2O(CO_3)$ and $[Sn(CH_3)_2(NCS)]_2O$ may be bent since they show two ν(Sn−C) bands in IR spectra [213]. Only one ν(Sn−C) vibration is expected for a linear C−Sn−C group.

2.4. COMPOUNDS CONTAINING OTHER FUNCTIONAL GROUPS

2.4.1. Nitrogen Donors

The ν(MN) of ammine and related ligands have been discussed in Sec. 1.l. The ν(MN) of $[Hg(CH_3)(NH_3)]^+$ [214], $Ga(CH_3)_3(NH_3)$ [215], and $[Sn(CH_3)_3(NH_3)]^+$ [216] are observed at 585, 350, and 503 cm^{-1}, respectively. The IR spectrum of $Al(CH_3)_3(NH_3)$ in Ar matrices shows significant nonplanarity of the AlC_3 skeleton [217]. In

$Sn(CH_3)_2(bipy)Cl_2$, the $Sn(CH_3)_2$ group is linear because its IR spectrum shows only one ν(Sn−C) near 575 cm^{-1} [218]. The IR bands at 427 and 346 cm^{-1} were tentatively assigned to the ν(Sn−N). The IR and Raman spectra of $[Pt(CH_3)_3(NH_3)_3]^+$ are interpreted on the basis of the *fac* structure ($\mathbf{C}_{3v}$): the ν(PtN) are at 390 (A_1, Raman) and 410 and 377 cm^{-1} (E, IR) [219].

2.4.2. Oxygen and Sulfur Donors

Compounds containing the hydroxo (OH) group exhibit ν(OH), δ(MOH), and ν(MO) at 3760–3000, 1200–700, and 900–300 cm^{-1}, respectively. As expected, these frequencies depend heavily on the metal and the strength of the hydrogen bond involved. The ν(SiO) of $Si(CH_3)_3(OH)$ is at 915 cm^{-1} [220], whereas the ν(SnO) of $Sn(CH_3)_3(OH)$ is at 370 cm^{-1} [221,222]. Polymeric structures involving the trigonal-planar $Sn(CH_3)_3$ group and Sn−OH−Sn bridges were proposed for the latter compound because it exhibits only one ν(Sn−C) at 540 cm^{-1}. Figure 2.9 shows the IR spectra of $Sn(CH_3)_3(OH)$ obtained by Okawara and Yasuda [221]. References on other hydroxo compounds are as follows: $Si(C_2H_5)_2(OH)_2$ [223], $Sb(CH_3)_4(OH)$ [224], $M(CH_3)_2(OH)_2$ (M = Ge,Sn,Pb) [225], $[Ga(CH_3)_2(OH)]_4$ [226], and $[Pt(CH_3)_3(OH)]_4$ [227]. $Si(CH_3)_3(SH)$ exhibits the ν(SH) and ν(SiS) at 2580 and 454 cm^{-1}, respectively, in the liquid state [228].

The IR spectra of $Sn(CH_3)_2(OR)_2$ (R = Me, Et, etc.) exhibit the ν(C−O) and ν(Sn−O) in the 1070–1000 and 650–550 cm^{-1}, respectively [229]. Other pertinent references are $Al(CH_3)_2(OCH_3)$ [230] and $Si(CH_3)_2(OCH_3)_2$ [231]. The ν(M−S) of $Si(CH_3)_3(SC_2H_5)$ [232], $Si(CH_3)_3(SC_6H_5)$ [233], $Ge(CH_3)_3(SCH_3)$ [234], and $Sn(CH_3)_2(SCH_3)_2$ [235] are assigned at 486, 459, 394, and 347 cm^{-1}, respectively.

The vibrational spectra of aquo complexes are characterized by the bands discussed in Sec. 1.82. References are cited for $[Sn(CH_3)_3(OH_2)_2]^+$ [236], $[Hg(CH_3)(OH_2)]^+$ [237], and $[Pt(CH_3)_3(OH_2)_3]^+$ [238]. Vibrational assignments are also reported for the IR spectrum of $Ge(CH_3)_2O$, which exhibits the ν(Ge=O), $\nu_a(GeC_2)$ and $\nu_s(GeC_2)$ at 943, 584, and 546 cm^{-1}, respectively [239]. Methyltrioxorhenium(VII), $Re(CH_3)O_3$, exhibits the ν_s(ReO), ν_a(ReO), and ν(ReC) at 998, 947, and 575 cm^{-1}, respectively, in IR spectra [240].

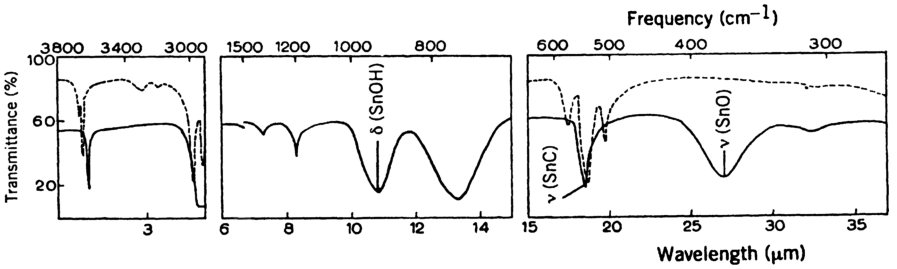

Fig. 2.9. *IR spectra of $Sn(CH_3)_3(OH)$. — and ------ indicate the spectra obtained in Nujol (or hexachlorobutadiene) mull and CCl_4 solution, respectively [221].*

Vibrational spectra of O-bonded (chelated) acetylacetonato (acac) complexes were discussed in Sec. 1.14. Some references for acac complexes of metal alkyls are $Ga(CH_3)_2(acac)$ [226], $Sn(CH_3)_2(acac)_2$ [241], $Pb(CH_3)_2(acac)_2$ [242], $Sb(CH_3)_2(acac)Cl_2$ [243], and $Au(CH_3)_2(acac)$ [244]. The structure of $Sn(CH_3)_2(acac)_2$ was originally suggested to be *trans* in solution and in the solid state on the basis of NMR and vibrational spectra [245]. Later, the *cis* structure was proposed because of the large dipole moment (2.95 D) in benzene solution [246]. X-Ray analysis showed, however, that the compound is *trans* in the solid state [247]. Ramos and Tobias [241] suggest that the structure remains *trans* in solution and that the large dipole moment may originate in the nonplanarity of the SnO_4 plane with the remainder of the acac ring.

2.4.3. Hydrido Compounds

Metal hydrido (H) complexes exhibit the ν(MH) and δ(MH) in the 2250–1700 and 800–600 cm^{-1} regions, respectively (Sec. 1.24.2). The ν(MH) and ν(MC) of typical compounds are listed in Table 2.9. It is seen that the ν(MH) decreases as the mass of the metal increases in the same family of the periodic table and as more methyl groups are bonded to the metal in the $M(CH_3)_nH_{4-n}$ ($n = 1$–3) series. Vibrational spectra of B_2H_6-type molecules were discussed in Sec. 2.10 of Part A. Methyldiboranes, $(CH_3)_nB_2H_{6-n}$ ($n = 1$–4), exhibit terminal and bridging ν(BH) at 2600–2500 and 2150–1525 cm^{-1}, respectively [258]. The dimeric $[(CH_3)_2AlH]_2$ species is predominant in the gaseous dimethylaluminum hydride; the ν_a(AlH) and ν_s(AlH) of the Al−H−Al bridges are observed at ~1353 and 1215 cm^{-1}, respectively [259].

TABLE 2.9. Metal–Hydrogen and Metal–Carbon Stretching Frequencies of Typical Hydrido Compounds (cm^{-1})

Compound	ν(MH)	ν(MC)	Ref.
CH_3SiH_3	2166,2169	701	248
$(CH_3)_2SiH_2$	2145, 2142	728,659	249
$(CH_3)_3SiH$	2123	711,624	249
$(CH_3)_2GaH$	1869.5	589.5	250
CH_3GeH_3	2086,2085	604	251
$(CH_3)_2GeH_2$	2080,2062	604,590	252
$(CH_3)_3GeH$	2049	601,573	252
CH_3SnH_3	1875	527	253
$(CH_3)_2SnH_2$	1869	536,514	254
$(CH_3)_3SnH$	1837	521,516	254
$(CH_3)_3PbH$	1709	—	255
$(CH_3)_2PH$	2288	703,660	256
$(CH_3)_2AsH$	2080	580, 565	257

TABLE 2.10. Metal–Metal Stretching Frequencies of Metal Alkyl Compounds (cm^{-1})

Compound	ν(MM′)	Ref.
$(CH_3)_3Si-Mn(CO)_5$	297 (R)	260
$(CH_3)_3Ge-Cr(CO)_3(\pi\text{-Cp})$	119 (R)	261
$(CH_3)_3Ge-Mn(CO)_5$	191 (R)	262
$(CH_3)_3Ge-Co(CO)_4$	192 (R)	263
$(CH_3)_3Sn-Mo(CO)_3(\pi\text{-Cp})$	172 (IR)	264
$(CH_3)_3Sn-Mn(CO)_5$	182 (IR, R)	264
$(CH_3)_3Sn-Re(CO)_5$	147 (R)	262
$(CH_3)_3Sn-Co(CO)_4$	176 (IR, R)	263

2.4.4. Metal–Metal Bonded Compounds

As discussed in Sec. 1.26, the ν(MM′) of metal–metal bonded compounds are generally strong in the Raman and weak in the infrared. Table 2.10 lists the ν(MM′) of some metal–metal bonded compounds. Figure 2.10 shows the ν(SnMn) bands observed in far-IR spectra of $(CH_3)_{3-n}Cl_nSn-Mn(CO)_5$-type compounds [264]. The vibrational spectra of $(CH_3)_3M-M(CH_3)_3$ (M = Si,Ge,Sn,Pb) [265] and M[Si $(CH_3)_3]_4$ (M = Si,Ge,Sn) [266] are reported.

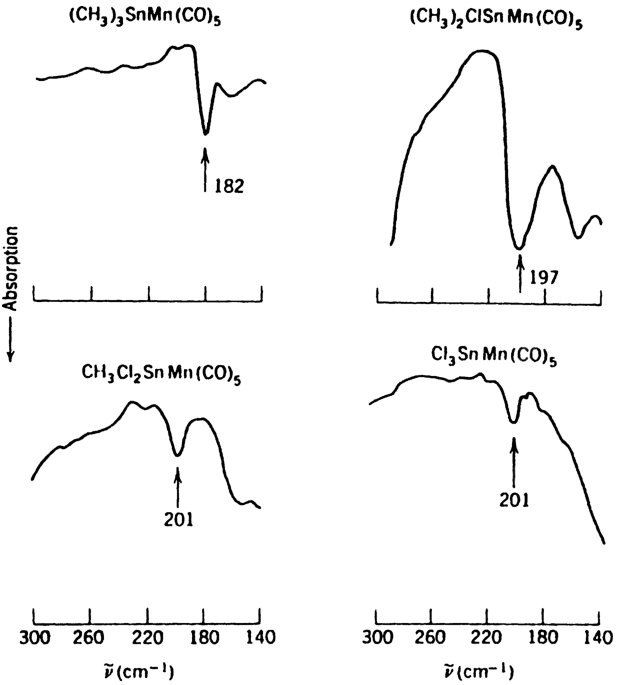

Fig. 2.10. *Far-IR spectra of $(CH_3)_{3-n}Cl_nSnMn(CO)_5$ where n = 0, 1, 2, or 3; the arrow indicates the ν(Sn–Mn) band [264].*

2.5. π-BONDED COMPLEXES OF OLEFINS, ACETYLENES, AND RELATED LIGANDS

Vibrational spectra of π-bonded complexes of ethylene, acetylene, and related ligands have been reviewed by Davidson [267]. In contrast to σ-bonded complexes (Sec. 2.2), the ν(C=C) and ν(C≡C) bands of π-bonded complexes show marked shifts to lower frequencies relative to those of free ligands.

2.5.1. Complexes of Monoolefins

Ethylene and other olefins form π-complexes with transition metals. Free ethylene Exhibits 12 ($3 \times 6 - 6$) normal modes that are classified into $3A_g(\mathrm{R}) + A_u$ (i.a.) + $2B_{1g}(R) + \mathrm{B}_{1u}(\mathrm{IR}) + B_{2g}(\mathrm{R}) + 2\mathrm{B}_{2u}(\mathrm{IR}) + 2\mathrm{B}_{3u}(\mathrm{IR})$ under $\mathbf{D}_{2h}(\mathbf{V}_h)$ symmetry. Figure 2.11 shows the approximate normal modes and observed frequencies of these vibrations [6].

The simplest and best-studied complex is Zeise's salt, $K[Pt(C_2H_4)Cl_3]H_2O$, in which the ethylene molecule replaces one of the Cl atoms of the square–planar $PtCl_4^{2-}$ ion with its C=C axis perpendicular to the $PtCl_4$ plane. According to Chatt et al. [268], the Pt(II)–ethylene interaction is described in terms of two bonding schemes: (A) a σ-type bond is formed by electron donation from the filled $2p\pi$ bonding orbital of the olefin to the vacant dsp^2 bonding orbital of the metal, and (B) a π-type bond is formed

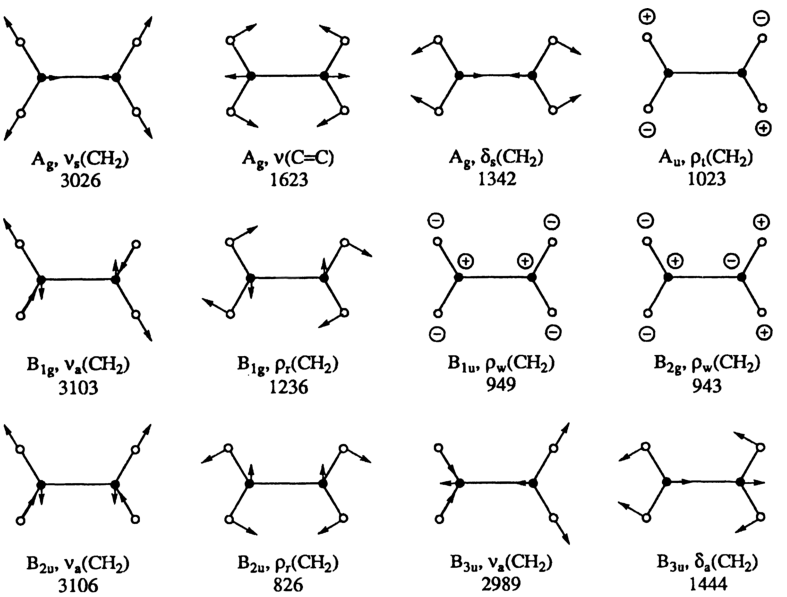

Fig. 2.11. *Approximate normal modes of vibration of ethylene; symmetry, vibrational assignments, and observed frequencies (cm^{-1}) are given for each vibration; the ν(C=C) and $\delta_s(CH_2)$ are vibrationally coupled in the A_g species.*

by backdonation of electron from a filled *dp* hybrid orbital of the metal to the $2p\pi^*$ antibonding orbital of the olefin. This is illustrated below:

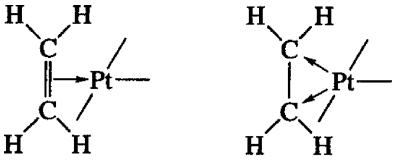

The real bonding is somewhere between A and B, and the latter becomes more predominant as the oxidation state of the metal becomes lower. The results of X-ray analysis [269] as well as MO calculations [270] seem to indicate that bonding scheme A is predominant in the case of Zeise's salt.

The vibrational spectra of Zeise's salt have been studied by several investigators [271–274]. The effects of coordination on the vibrational frequencies of free ethylene are (l) The ν(C=C) coupled with the $\delta_s(CH_2)$ is shifted markedly from 1623 to 1526 [271] or 1243 cm^{-1} [273], (2) the $\rho_r(CH_2)$ are shifted to lower frequencies ($\sim$1030 to 840/720 cm^{-1}), and (3) the $\rho_w(CH_2)$ and ρ_t (CH_2) are shifted to higher frequencies ($\sim$945 to 1010/975 and 1023 to 1180 cm^{-1}, respectively) [273]. The directions of these shifts are anticipated since (1) and (2) are in-plane, whereas (3) are out-of-plane vibrations.

Approximate band assignments of IR spectra of Zeise's salt and its deuterated analog were first made by assuming that Zeise's anion is a composite of a perturbed C_2H_4 and the $PtCl_3$ moiety [271]. The band at 407 cm^{-1} was assigned to the $\nu(Pt-C_2H_4)$ (scheme A) since it did not belong to either components. More elaborate treatments employ a triangular model involving two Pt−C bonds (scheme B). Hiraishi [273] carried out normal coordinate analysis on such a model and assigned the Raman bands at 493 (*dp*) and 405 cm^{-1} (*p*) to the $\nu_a(Pt-C_2H_4)$ and $\nu_s(Pt-C_2H_4)$, respectively. The corresponding force constants for these two modes were calculated to be 1.92 and 1.45 mdyn/Å, respectively. The $\nu_a(Pt-C_2H_4)$ may be called the "tilt" mode since it involves a tilting motion of the ethylene against the rest of the anion. Crayston and Davidson [274] carried out similar calculations on several ethylene complexes. These workers assigned the bands at 455 and 380 cm^{-1} to the $\nu_a(Pt-C_2H_4)$ and $\nu_s(Pt-C_2H_4)$ of $Pt(0)(C_2H_4)(PPh_3)_2$. Both bands are downshifted on going from the Pt(II) to Pt(O) complexes because a "metallocyclopropane" form (scheme B) becomes more predominant in the latter.

Mink and coworkers [275,276] have assigned the IR and Raman spectra of $M(C_2H_4)_3$ (M = Pt,Pd,Ni) using normal coordinate analysis. These molecules take a $\mathbf{D}_{3h}$ structure, as shown in Fig. 2.12, and their 51 ($3 \times 19 - 6$) normal vibrations are grouped into:

$$5A'_1(\mathrm{R}) + 4A'_2(\mathrm{i.a.}) + 10E'(\mathrm{IR},R) + 4A''_1(\mathrm{i.a.}) + 4A''_2(\mathrm{IR}) + 7E''(\mathrm{R})$$

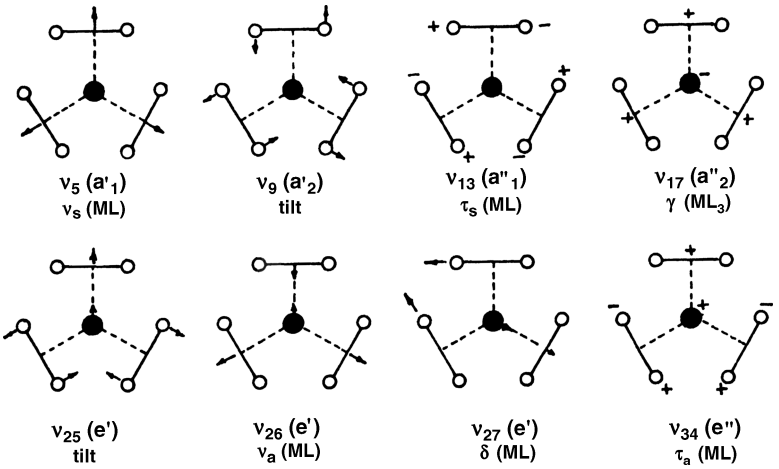

Fig. 2.12. *Skeletal modes of tris(ethylene)metal complexes; symmetry and vibrational assignments are indicated for each mode (L denotes ethylene) [276].*

Figure 2.12 illustrates their skeletal modes, and Table 2.11 compares their band assignments and force constants for $Pt(C_2H_4)_3$ and Zeise's anion.

Figure 2.13 shows the IR and Raman spectra of $Pt(C_2H_4)_3$ obtained by Csaszar et al. [276]. As shown in Table 2.11, the calculated force constants for the tilt and symmetric stretching modes are relatively close in Zeise's anion, whereas the former is larger in $Pt(C_2H_4)_3$. This result may suggest that the π-bonding (scheme B) is more predominant in the latter compound [275].

Vibrational spectra are reported for many other complexes of ethylene. Some references are $Li(C_2H_4)$(in Ar matrix) [277], $Ni(C_2H_4)$(in Ar matrix) [278], $[Pd(C_2H_4)Cl_3]^-$ [279], *trans*-$M(C_2H_4)_2(CO)_4$ (M = Mo,W) [280], $Fe(C_2H_4)(CO)_4$ [281], $[Rh(C_2H_4)_2Cl]_2$ [282], $Ir(C_2H_4)_4Cl$ [283], and $[Pt(C_2H_4)Cl_2]_2$ [271].

TABLE 2.11. Observed Frequencies, Band Assignments, and Force Constants of Zeise's Anion and $Pt(C_2H_4)_3$ [275,276]

$[Pt(C_2H_4)Cl_3]^-$ (C_{2v})	$Pt(C_2H_4)_3$ ($\mathbf{D}_{3h}$)	Band Assignment
	Observed Frequencies (cm^{-1})	
1517 (A_1)	1617 (A'_1) 1501 (E')	ν(C=C) + $\delta(CH_2)$
501 (B_1)	448(E')	Tilt
408 (A_1)	398 (A'_1) 332 (E')	ν(Pt−C_2H_4)
	Force Constants (mdyn/Å)	
2.84	2.04	Tilt
2.54	1.66	Pt−C_2H_4 stretch

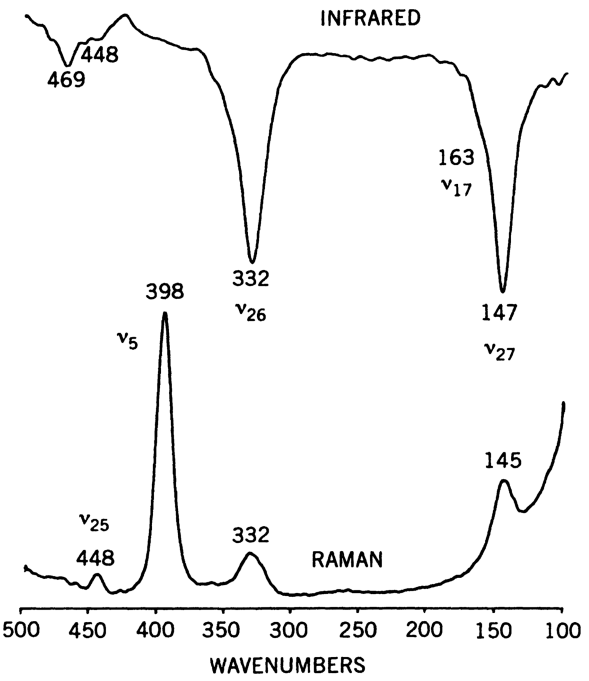

Fig. 2.13. *Far-IR and low-frequency Raman spectra of $Pt(C_2H_4)_3$ in petroleum ether [276].*

Tetracyanoethylene (TCNE) also forms π-complexes with transition metals, and their vibrational spectra are reported for M(TCNE)$(CO)_5$ (M = Cr, W) [284], Fe(TCNE)$(CO)_4$ [285], and Pt(TCNE)$(PPh_3)_2$ [286].

Mrozek and Weaver [287] measured surface-enhanced Raman spectra (Sec. 1.3.2) of chemisorbed ethylene on metal electrode surfaces of Au, Pd, Rh, Pt, and Ir. The results indicate the extensive formation of π-bonded ethylene on each metal surface. The ν(C=C) coupled with $\delta(CH_2)$ vibrations (cm^{-1}) were observed at

Au	Pd	Rh	Pt	Ir
1540	1514	1506	1495	1495
1275	1244	1232	1210	1188

These values were obtained at the electrode potential of −0.2 V versus SCE. The decreasing order of these frequencies indicates the increasing order of π-backbonding from the metal to the $2p\pi^*$ orbital of ethylene. It was noted that the formation of ethylidyne ($\equiv C-CH_3$) from chemisobed ethylene increases as the electrode potential is lowered. This was confirmed by the appearance of the bands characteristic of the CH_3 group vibrations.

2.5.2. Allyl Complexes

According to X-ray analysis [288], the two Pd atoms in $[Pd(\pi\text{-allyl})Cl]_2$ are bridged by two Cl atoms to form a square–planar $(PdCl)_2$ group, and the ally (C_3H_5) groups are bonded to the Pd atoms with their planes tilted by 112° with respect to the $(PdCl)_2$ plane so that the overall symmetry is $\mathbf{C}_{2h}$:

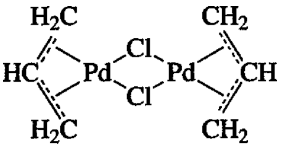

Vibrational spectra of $[Pd(\pi\text{-allyl})Cl]_2$ and related compounds in the low-frequency region were assigned on the basis of isotope shifts due to $^{104}Pd/^{110}Pd$ substitution. The bands at 402 and 379 cm^{-1} were assigned to the ν_a(Pd-allyl) and ν_s(Pd-allyl), respectively, since both bands are downshifted by 3 cm^{-1} by such substitution [289]. References on other allyl complexes are $M(\pi\text{-}C_3H_5)_2$ (M = Ni,Pd), $M(\pi\text{-}C_3H_5)_3$ (M = Rh,Ir) [290], $[Pd(\pi\text{-}C_3H_5)X]_2$ (X = CL,Br) [291], $Fe(\pi\text{-}C_3H_5)(CO)_3X$ (X = Br,NO_3) [292], and $Mn(\pi\text{-}C_3H_5)(CO)_4$ [293]. Chenskaya et al. [294] assigned the metal-olefin and metal-halogen vibrations of π-allyl complexes of transition metals.

2.5.3. Complexes of Diolefins and Oligoolefins

Nonconjugated diolefins such as norbornadiene (NBD, C_7H_g) and 1,5-hexadiene (C_6H_{10}) form metal complexes via their C=C double bonds (Figs. 2.14a, 2.14b). Complete vibrational assignments have been made for $M(NBD)(CO)_4$ (M = Cr,Mo, W) [295], $Cr(NBD)(CO)_4$ [296], and $Pd(NBD)X_2$ (X = Cl,Br) [296]. The metal–olefin vibrations are assigned in the region from 305 to 200 cm^{-1}. The spectrum of $K_2[(PtCl_3)_2(C_6H_{10})]$ is similar to that of the free ligand in the *trans* conformation [297]. Thus, its structure may be shown as in Fig. 2.14b. However, the spectrum of $Pt(C_6H_{10})Cl_2$ is more complicated than that of the free ligand and suggests a chelate structure such as that shown in Fig. 2.14a.

Free butadiene (C_4H_6) is *trans*-planar. However, it takes a *cis*-planar structure in $Fe(C_4H_6)(CO)_3$ [298] and $Fe(C_4H_6)_2CO$ [299]. For $K_2[C_4H_6(PtCl_3)_2]$, the infrared spectrum indicates the *trans*-planar structure of the olefin [300]. In $[Rh(COT)Cl]_2$, cyclooctatetraene (COT) takes a tub conformation and coordinates to a metal via the 1,5 C=C double bonds, the 3,7 C=C double bonds being free (Fig. 2.14c). The C=C stretching bands of free COT are at 1630 and 1605 cm^{-1}, whereas those of the complex are at 1630 (free) and 1410 (bonded) cm^{-1} [301]. According to X-ray analysis [302], only two of the four C=C double bonds of COT are bonded to the metal in Fe(COT) $(CO)_3$ (Fig. 2.14d). In this case, the C=C stretching band for free C=C double bonds is at 1562 cm^{-1}, whereas that for coordinated C=C double bonds is at 1460 cm^{-1} [303]. In $[Rh(COD)Cl]_2$ (COD, C_8H_{12}, 1,5-cyclooctadiene), the Rh atom is bonded to COD via the 1,5 C=C bonds in a manner similar to its COT analog (Fig. 2.14c).

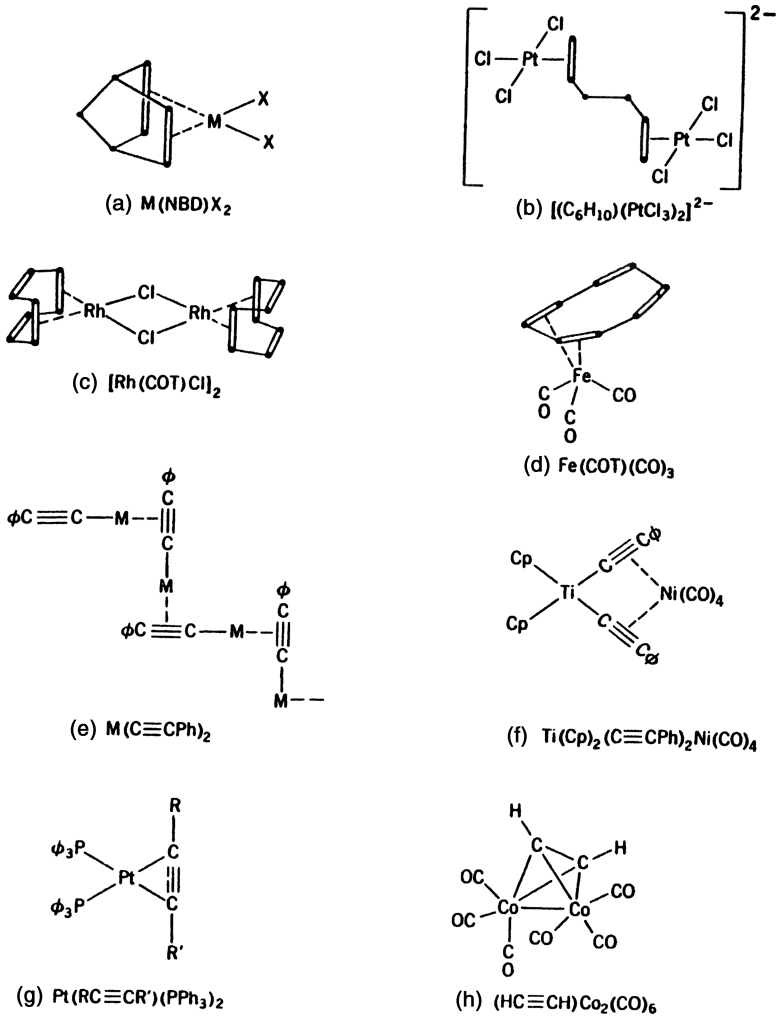

Fig. 2.14. Structures of π-complexes.

The Rh–olefin stretching vibrations were assigned in the range from 490 to 385 cm^{-1} [304]. Bailey et al. [305] measured the resonance Raman excitation profiles of Co(Cp)(COD), and noted interference effects between multiple excited states. The ν(Co−COD) and ν(Co−Cp) were assigned at 470 and 354 cm^{-1}, respectively.

Figure 2.15 shows the far-IR spectra of $^{104}Pd(COT)Cl_2$, $^{104}Pd(COD)Cl_2$, and their ^{110}Pd analogs [306]. The COT complex exhibits four isotope-sensitive bands at 344, 319, 238, and 219 cm^{-1}. The first two are assigned to the ν_a(Pd−Cl) and ν_s(Pd−Cl), respectively, whereas the last two are attributed to the ν_a(Pd-olefin) and ν_s(Pd-olefin), respectively. Similar assignments can be made for the COD complex. These ν(Pd-olefin) frequencies are much lower than the $\nu(Pd-C_2H_4)$ (427 cm^{-1}) because of weaker metal-olefin bonds and larger olefin masses.

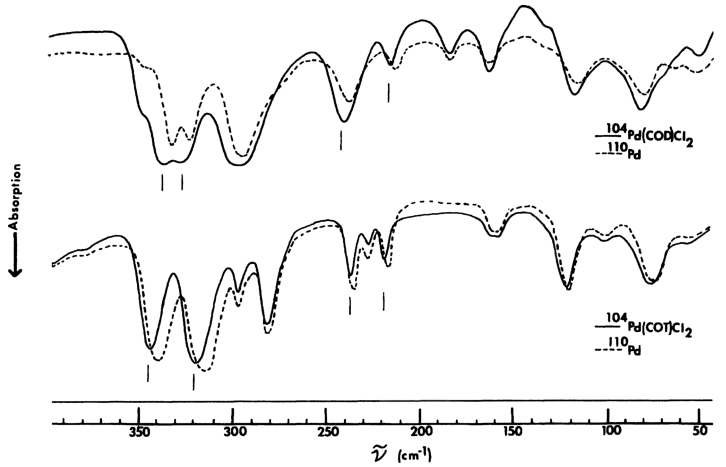

Fig. 2.15. *Far-IR spectra of $Pd(COD)Cl_2$ and $Pd(COT)Cl_2$; the solid and dashed lines indicate the spectra of the complexes containing ^{104}Pd and ^{110}Pd isotopes, respectively; vertical lines show metal–isotope-sensitive bands [306].*

2.5.4. Complexes of Acetylene and Related Ligands

Free $HC\equiv C(C_6H_5)$ exhibits the $C\equiv C$ stretching band at 2111 cm^{-1}. In the case of σ-bonded complexes (Sec. 2.2), this band shifts slightly to a lower frequency (2062–2016 cm^{-1}) [307]. In $M[-C\equiv C(C_6H_5)]_2$ [M = Cu(I) and Ag(I)], it shifts to 1926 cm^{-1}. This relatively large shift was attributed to the formation of both σ- and π-type bonding, shown in Fig. 2.14e [308]. $Ti[C\equiv C(C_6H_5)]_2(\pi\text{-}Cp)_2$ reacts with $Ni(CO)_4$ to form the complex shown in Fig. 2.14f. The $C\equiv C$ stretching band of the parent compound at 2070 cm^{-1} is shifted to 1850 cm^{-1} by complex formation [309]. According to Chart and coworkers [310], the $C\equiv C$ stretching bands of disubstituted alkynes (2260–2190 cm^{-1}) are lowered to ~2000 cm^{-1} in $Na[Pt(RC\equiv CR')Cl_3]$ and $[Pt(RC\equiv CR')Cl_2]_2$, and to ~1700 cm^{-1} in $Pt(RC\equiv CR')(PPh_3)_2$. Here R and R′ denote various alkyl groups. The former represents a relatively weak π-bonding similar to that found for Zeise's salt, whereas the latter indicates strong π-bonding in which the $C\equiv C$ triple bond is almost reduced to the double bond (Fig. 2.14g). Similar results were found for $(RC\equiv CR')Co_2(CO)_6$, which exhibits the $C\equiv C$ stretching bands near 1600 cm^{-1} [311]. In the case of $(HC\equiv CH)Co_2(CO)_6$, the $C\equiv C$ stretching band was observed at 1402 cm^{-1}, which is ~570 cm^{-1} lower than the value for free acetylene (1974 cm^{-1}). The spectrum of the coordinated acetylene in this complex is similar to that of free acetylene in its first excited state, at which the molecule takes a *trans*-bent structure. Considering possible steric repulsion between the hydrogens and the $Co(CO)_3$ moiety, a structure such as that shown in Fig. 2.14h was proposed [312].

There are many other π-bonded acetylenic complexes for which vibrational data are available. For example, the chloro-bridged dimer, $[WCl_4(IC\equiv Cl)]_2$, exhibits the $\nu(C\equiv C)$ at 1619 and 1590 and the $\nu(WC)$ at 928 865 and 848 cm^{-1}. The former are ~510 cm^{-1} lower than that of free $IC\equiv CI$ (2118 cm^{-1}) [313]. In the case

of $(t\text{-Bu}-C\equiv C-t\text{-Bu})_2Fe_2(CO)_4$, the $C\equiv C$ bonds are π-bonded to the Fe–Fe bridge as shown below:

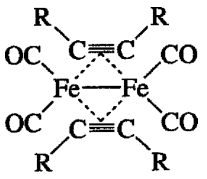

R = *t*-Bu

Its IR spectrum shows a very weak $\nu(C\equiv C)$ at 1670 cm^{-1}. The weak band at 531 cm^{-1} and a strong band at 284 cm^{-1} were assigned to the ν(Fe-acetylene) coupled with δ(FeCO) and ν(Fe–Fe), respectively. According to normal coordinate analysis [314], the Fe–Fe stretching force constant (3.0 mdyn/Å) is about twice that of the Fe–Fe single bond (1.3 mdyn/Å) of $Fe_2S_2(CO)_6$ [315]. Thus, the Fe–Fe bond of the compound shown above must be close to a double bond.

2.5.5. Complexes of Nitriles

The $C\equiv N$ stretching frequency of $CF_3-C\equiv N$ is 2271 cm^{-1}. This band is shifted to 1734 cm^{-1} in $Pt(CF_3CN)(PPh_3)_2$ because of the formation of a Pt–nitrile π-bond [316]. A similar π-bonding has been proposed for $Mn(CO)_3IL$, where L is *o*-cyanophenyldiphenylphosphine:

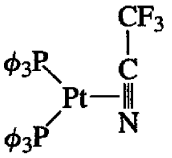

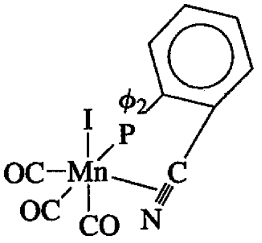

(ϕ = phenyl)

In the latter case, the $C\equiv N$ stretching band of the free ligand at 2225 cm^{-1} is shifted to 1973 cm^{-1} in the complex [317].

2.5.6. Metal–Olefin Complexes in Inert Gas Matrices

A number of olefin complexes of the type $M(olefin)_n$ have been prepared via cocondensation reactions of metal vapors with olefins in inert gas matrices:

$$M + n(\text{olefin}) \rightarrow M(\text{olefin})_n$$

Vibrational studies show that the olefins in these cocondensation products are all π-bonded to metal atoms. Moskovitz and Ozin [318] report the IR spectra of $M(C_2H_4)_n$

where **M** is Co, Ni, Cu, Pd, Ag, and Au. Andrews and coworkers measured and assigned the IR spectra of $Li(C_2H_4)_n$ ($n = 1,2,3$) [319] and $In(C_2H_4)$ [320]. In the latter, the ν(C=C) coupled with the $\delta(CH_2)$ and ν(In−C) were observed at 1201 and 238 cm^{-1}, respectively. These frequencies are also reported for $Ni(C_2H_4)_n$ ($n = 1,2,3$) [321]. The first RR spectrum of such a cocondensation product was obtained for $Cu(C_2H_4)_3$, which exhibits the ν(C=C) and ν(Cu−C) at 1530 and 302 cm^{-1}, respectively [322].

Similar studies have been extended to $Li(C_2H_2)$ [323], $Ni(C_2H_2)$ [324], $Ni(C_4H_6)$ [325], $(HgCl_2)$(olefin) [326], and $Fe(TPP)(C_2H_4)$ [327]. Matrix cocondensation reaction of $Mo(CO)_6$ with acethylene in Ar matrices yield: $Mo(CO)_6(C_2H_2)$, which exhibits a very low $\nu(C \equiv C)$ at 1820 cm^{-1} [328].

2.5.7. Metal Methylidenes and Metylidynes

Metal methylidene, $H_2C{=}Re(O)_2(OH)$, was obtained by photoexcitation (254 nm) of CH_3ReO_3 in Ar matrices. The ν(C=Re) vibration was located at ~780 cm [329]. Metal methylidyne, *trans*-$[HC \equiv W(PMe_3)_4Cl]$, exhibits the $\nu(C \equiv W)$ band at 911 cm^{-1} that is shifted to 871 cm^{-1} by deuteration of the CH hydrogen [330]. Similar frequencies are reported for $HC \equiv W(CO)_2(Tp)$ where Tp is hydridotris(3,5-diethylpyrazolyl) borate [331].

2.6. CYCLOPENTADIENYL COMPOUNDS

The infrared spectra of cyclopentadienyl (C_5H_5 or Cp) complexes have been reviewed extensively by Fritz [332], who roughly classified them into four groups, each of which exhibits its own characteristic spectrum.

2.6.1. Ionic Complexes

These are complexes such as MCp ($M = K^+$, Rb^+, Cs^+) and MCp_2 ($M = Ca^{2+}$, Sr^{2+}, Ba^{2+}, Mn^{2+}) [333,334], in which M^{n+} and Cp^- are ionically bonded. The spectra of these compounds are essentially the same as that of the $C_5H_5^-$ ion, which takes a planar pentagonal structure of $\mathbf{D}_{5h}$, symmetry. The 24 ($3 \times 10 - 6$) normal vibrations of this ion are classifed into

$$2A'_1(R) + A'_2(i.a.) + A''_2(IR) + 3E'_1(IR) + E''_1(R) + 4E'_2(R) + 2E''_2(ia)$$

Figure 2.16 illustrates the approximate normal modes and observed frequencies (K^+Cp^-) of these vibrations. Four IR-active and seven Raman-active vibrations are expected for the Cp^- ion. In fact, the ionic complexes mentioned above exhibit four IR bands: ν(CH), 3100–3000 cm^{-1}, ν(CC), 1500–1400 cm^{-1}, δ(CH), 1010–1000 cm^{-1}, and π(CH), 750–650 cm^{-1}.

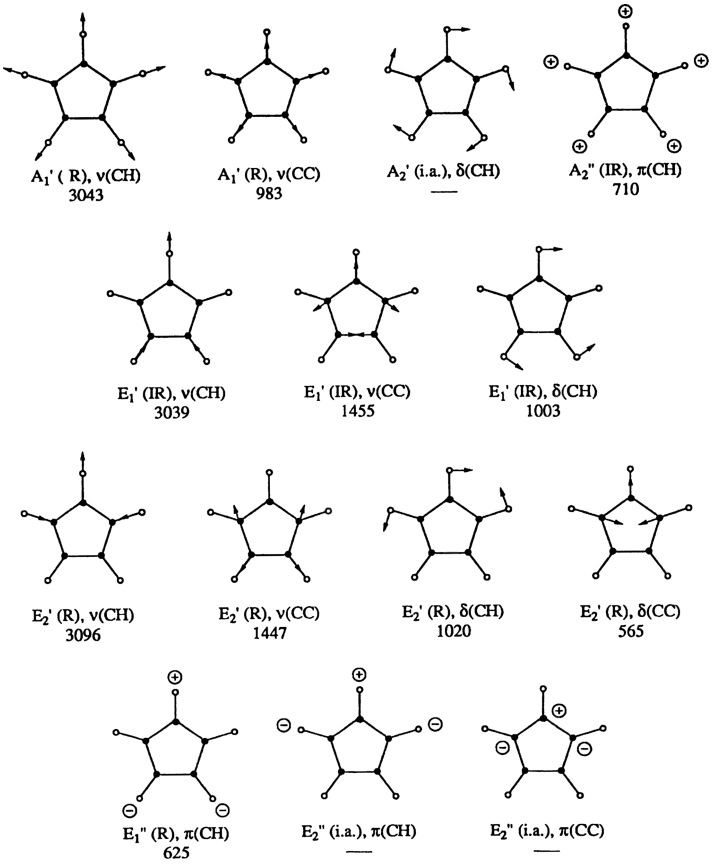

Fig. 2.16. *Normal modes of vibration of the cyclopentadienyl group. These figures are approximate, and only the displacements of the H or C atoms are shown. Symmetry, band assignments, and observed frequencies (cm^{-1}) are given for each mode.*

2.6.2. Ion-Paired and Centrally σ-Bonded Complexes

These are complexes such as MCp (M = Li,Na), in which the metal ion is bonded to the center of the ring by forming a tight ion pair, or MCp_2 (M = Be,Mg,Ca) [333–336], in which the metal is covalently bonded to the center of the ring. In this case, the local symmetry of the Cp ring is regarded as $\mathbf{C}_{5v}$, and its 24 normal vibrations are classified into

$$3A_1(\mathrm{IR},R) + A_2(\mathrm{i.a.}) + 4E_1(\mathrm{IR},R) + 6E_2(\mathrm{R})$$

Thus, seven bands are expected to appear in IR spectra. These vibrations are observed in the following regions: ν(CH), 3100–3000 cm^{-1}; ν(CH), 2950–2900 cm^{-1}; ν(CC), 1450–1400 cm^{-1}; ν(CC), 1150–1100 cm^{-1}; δ(CH), 1010–990 cm^{-1}; two π(CH), 890–700 cm^{-1}. In addition, these complexes are expected

to show one ν(M−Cp) (A_1) and one ring-tilt (E_1) vibration in the low-frequency region. The former is observed at 426 cm^{-1} for Li^+Cp^- and at 196 cm^{-1} for Na^+Cp^- in IR spectra [337] and the latter, the 150–130 cm^{-1} region in Raman spectra [338].

According to electron diffraction studies [339], the two rings of $SnCp_2$ and $PbCp_2$ form angles of 45° and 55°, respectively, in the vapor state. On the assumption of angular structure in the solid state, two bands at 240 and 170 cm^{-1} of $SnCp_2$ have been assigned to the antisymmetric and symmetric M−Cp stretching modes, respectively [340]. The IR spectrum of $BeCp_2$ in solution [341] exhibits the bands characteristic of the centrally σ-bonded ring (similar to CpBeCl) and those of the diene-type (σ-bonded) ring ($HgCp_2$) discussed in the later subsection. Thus, a structure such as (A) shown below, has been proposed. X-Ray analysis [342] as well as IR studies [343] show that $BeCp_2$ in the gaseous and solid phases take a "slip-sandwich" structure as shown in B. A highly symmetric ferrocene-like structure (η^5-ring, $\mathbf{D}_{5d}$) and a centrally σ-bonded structure (η^1-ring, $\mathbf{C}_{5v}$) can be ruled out because seven IR bands are observed in the ν(CH) region:

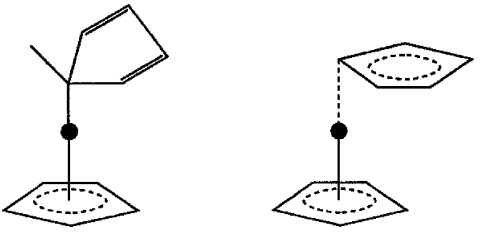

A **B**

On the basis of vibrational analysis of metal–ligand and out-of-plane ρ(CH) vibrations, a similar "slip-sandwich" structure was proposed for $ZnCp_2$ in THF solution. The ν_s(Zn−Cp_2), ν_a(Zn−Cp_2), and δ(CpZnCp) were assigned at 315,344, and 171 cm^{-1} respectively. The η^5-ring exhibits the tilt vibrations at 494 and 349 cm^{-1}, while the δ(ZnCC) of the η^1-ring is observed at 260 cm^{-1} [344].

2.6.3. Centrally π-Bonded Complexes*

These are η^5-complexes such as $FeCp_2$ and $RuCp_2$, in which the transition metals are bonded to the center of the ring via the d–π-bond.

It is interesting to note that two rings in solid ferrocene take the staggered configuration ($\mathbf{D}_{5d}$), while those in ruthenocene take the eclipsed configuration ($\mathbf{D}_{5h}$):

$\mathbf{D}_{5d}$ $\mathbf{D}_{5h}$

* Or pentahapto (η^5) complexes.

Since the number of infrared- or Raman-active fundamentals is the same for both conformations, they cannot be distinguished on the basis of the number of fundamentals observed.

Under $\mathbf{D}_{5d}$ symmetry, the 57 $(3 \times 21 - 6)$ normal vibrations of ferrocene are classified into

$$4A_{1g}(\mathrm{R}) + 2A_{1u}(\mathrm{i.a.}) + A_{2g}(\mathrm{i.a.}) + 4A_{2u}(\mathrm{IR}) + 5E_{1g}(\mathrm{R})$$
$$+ 6E_{1u}(\mathrm{IR}) + 6E_{2g}(\mathrm{R}) + 6E_{2u}(\mathrm{ia})$$

Thus, 10 vibrations are expected to be IR-active. These include the seven Cp bands discussed previously and three skeletal modes (ν_3, ν_5, and ν_6) illustrated in Fig. 2.17. Table 2.12 lists the observed IR frequencies of the centrally π-bonded MCp_2-type complexes, and Fig. 2.18 shows the IR spectra of $NiCp_2$ and $FeCp_2$. As shown in Table 2.12, the IR bands at 492 and 478 cm^{-1} of $FeCp_2$ have been assigned to the ring-tilt (ν_5) and ν(M−Cp) (ν_3), respectively. Both bands show marked isotope shifts (7–8 cm^{-1}) by $^{54}Fe/^{57}Fe$ substitution [350]. The Raman spectra of $Fe(Cp_2)^+$ [351] and $Fe(Cp_2^*)^+$ [352] exhibit the ν_s(M−Cp or M−Cp*) of these complexes at 311 and 173/160 cm^{-1}, respectively. Here Cp* denotes the pentamethyl derivative of Cp.

Lippincott and Nelson [346] carried out normal coordinate analysis on the C_5H_5 ring of ferrocene assuming $\mathbf{D}_{5h}$ symmetry. Fritz [332] calculated the approximate M−Cp stretching force constants using the equation available for the antisymmetric stretching vibration of a linear YXY-type molecule:

$$(5.89 \times 10^{-2})\tilde{\nu}_3^2 = \left(1 + \frac{2m_y}{m_x}\right)\frac{k}{m_y}$$

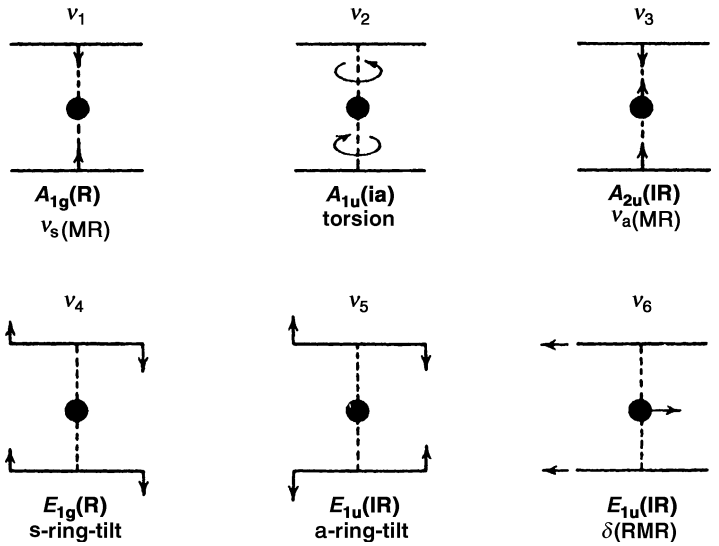

Fig. 2.17. *Skeletal modes of dicyclopentadienyl metal complexes ($\mathbf{D}_{5h}$ symmetry); R denotes the C_5H_5 ring in band assignments.*

TABLE 2.12. Observed Infrared Frequencies and Band Assignments of Centrally π-Bonded MCp_2-Type Compounds (cm^{-1})

Compound	ν(CH)		ν(CC)		δ(CH)	π(CH)		Ring Tilt	ν(MR)[a]	δ(RMR)[a]	Ref.
$FeCp_2$	—	3077	1110	1410	1005	820	855	492	478	179	344
$RuCp_2$	—	3076	1095	1410	1005	808	834	450	380	170	344
$OsCp_2$	3061	3061	1098	1400	998	823	831	428	353	160	332,345
$CoCp_2$	3041	3041	1101	1412	995	778	828	464	355	—	332,345
$NiCp_2$	3075	3075	1110	1430	1000	773	839	355	355	—	346
$FeCp_2^+$	3108	3108	1116	1421	1017	805	860	501	423	—	347
	3100	3100	1110	1412	1001	779	841	490	405		
$CoCp_2^+$	3094	3094	1113	1419	1010	860	895	495	455	172	348
$IrCp_2^+$	3077	3077	1106	1409	1009	818	862	—	—	—	348

[a]R denotes the Cp ring. For the Raman spectra of MCp_2 (M = Mn, Cr, V, Ru, Os), see Ref. 349.

Here, $\tilde{\nu}_3$ is the observed ν_a(M−Cp) in cm^{-1}, m_x and m_y are the point masses (atomic weight unit) of the metal and the Cp ring, respectively, and k is the M−Cp stretching force constant in mdyn/Å. The results are

	Os		Fe		Ru		Cr	Co	V	Ni	Zn
k(M−Cp)(mdyn/Å)	2.8	>	2.7	>	2.4	≫	1.6	∼1.5	∼1.5	∼1.5	∼1.5
ν_a(M−Cp)(cm^{-1})	353		478		379		408	355	379	355	345

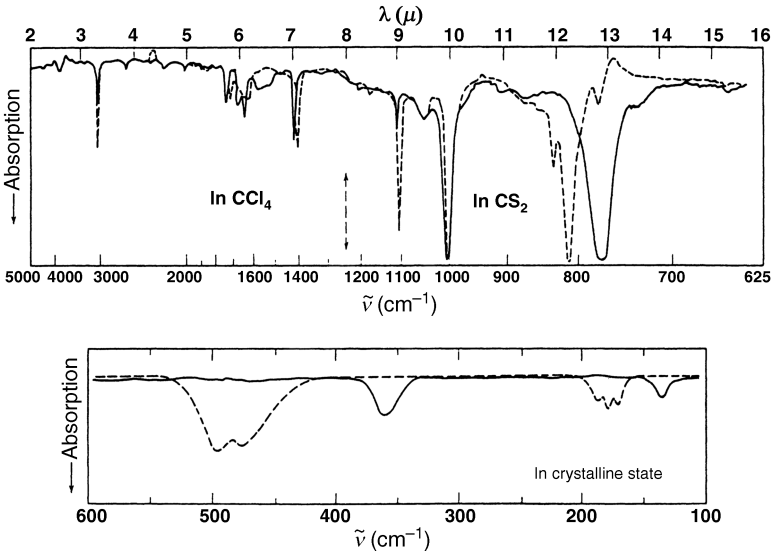

Fig. 2.18. *Infrared spectra of $Ni(C_5H_5)_2$ (solid line) and $Fe(C_5H_5)_2$ (dashed line).*

This may indicate the order of the M−Cp bond strength. Table 2.12 shows that the M−Cp stretching band of $FeCp_2$ at 478 cm^{-1} is shifted to a lower frequency when it is ionized to $FeCp_2^+$. Apparently, the deviation from the inert gas electronic configuration due to the ionization weakens the M−Cp bond. More accurate calculations on M−Cp stretching force constants of ferrocene and its derivatives have been made by Phillips et al. [353], who employed two observed frequencies [478 (ν_3) and 306 (ν_1) for ferrocene]. The Fe−Cp stretching force constant was 3.11 mdyn/Å with the stretch-stretch interaction constant of 0.48 mdyn/Å. In another approach, Hyam [354] considered five Fe−C bonds between the Fe atom and the Cp ring, and obtained a "pseudoring"-Fe stretching force constant of 1.4 mdyn/Å. Schäfer et al. [355,356] carried out the most complete normal coordinate analysis by assuming 10 Fe−C bonds between the Fe atom and the two Cp rings ($\mathbf{D}_{5h}$ symmetry).

According to Yokoyama et al. [357], the observed skeletal frequencies of $FeCp_2$ and $NiCp_2$ are as follows (cm^{-1}):

	ν_1 (R)	ν_3(IR)	ν_4(R)	ν_5(IR)
$FeCp_2$	306	476	390	400
$NiCp_2$	245	355	198	355

These workers have explained the marked difference in ν_4 on the basis of their electronic structures. More references are available on vibrational spectra of $FeCp_2$ [353–359] and RuCp [360]. Diana et al. [361] carried out approximate normal coordinate calculations of the M-(η^5-Cp) units of a variety of metal–Cp complexes, and found a correlation between the metal–ring stretching force constant and the metal–carbon distance.

2.6.4. Diene-Type (σ-Bonded) Complexes*

These are complexes such as $HgCp_2$ and CH_3HgCp [362,363] in which the metal is σ-bonded to one of the C atoms of the Cp ring:

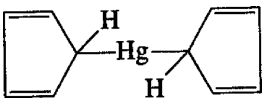

The spectra of these compounds are similar to that of C_5H_6 (cyclopentadiene), and are markedly different from those of the other groups discussed previously.

Figure 2.19 shows the infrared spectrum of $HgCp_2$ [364]. Band assignments of these compounds can be made on the basis of those obtained for C_5H_6 [365]. Infrared and NMR evidence suggests the presence of diene-type bonding for $(Cp)M(CH_3)_3$ (M = Si,Ge,Sn) [366].

There are many other complexes in which the π-bonded (η^5) and the σ-bonded (η^1) cyclopentadienyl groups are mixed. As expected, these compounds exhibit

* Or monohapto (η^1) complexes

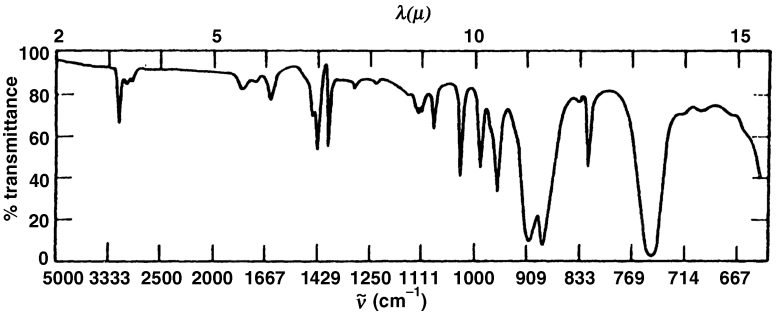

Fig. 2.19. *Infrared spectrum of $Hg(C_5H_5)_2$ in CS_2 (2–6 μm and 7.1–15.5 μm). $CHCl_3$ (6–6.6 μm), and CCl_4 (6.6–7.1 μ) [364].*

bands characteristic of both groups. Typical examples are as follows: VCp_3 (two π and one σ) [367], $NbCp_4$ (two π and two σ) [368], $ZrCp_4$ (three π and one σ) [369–371] and $MoCp_4$ (three π and one σ) [372]. Infrared [368], X-ray [370], and NMR [373] evidence indicates the presence of two π- and two σ-bonded Cp rings in $TiCp_4$.

In addition to the η^5- and η^1-bondings discussed above, X-ray analysis [374] reveals the presence of η^3-type bonding in allylic $[Ni(Cp)(C_3H_4)]_2$.

2.7. CYCLOPENTADIENYL COMPOUNDS CONTAINING OTHER GROUPS

2.7.1. Carbonyl Compounds

The vibrational spectra of carbonyl compounds were discussed in Sec. 1.18. Here we discuss only those containing cyclopentadienyl rings. It has been well established that the number of CO stretching bands observed in the infrared depends on the local symmetry of the $M(CO)_n$ group in $M(Cp)_m(CO)_n$-type compounds [332]. For example, only two CO stretching bands have been observed for the following compounds, in accordance with the prediction from local symmetry:

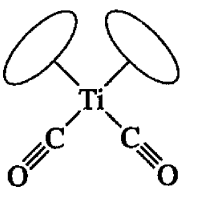

C_{2v}
1890(B_2)
1969(A_1)

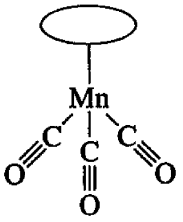

C_{3v}
1938(E)
2025(A_1)

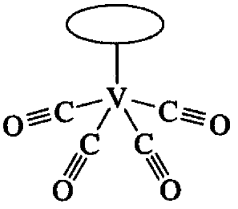

C_{4v}
1916(E)
2016(A_1)

In the case of $MCp(CO)_3$ (M = Mn, Re), breakdown of the $\mathbf{C}_{5v}$ selection rule for the Cp vibrations was noted in solution IR spectra [375]. The FT Raman spectra of $MnCp(CO)_3$ as well as $Cr(arene)(CO)_3$ are reported [376]. Other references for carbonyl compounds are $[M(Cp)(CO)_3]^-$ (M = Cr,Mo,W) [377], $Mn(Cp)(CO)_3$ [378], $Re(Cp)(CO)_3$ [379], and $V(Cp)(CO)_4$ [380]. In $M(Cp)(CO)_3$-type compounds [381], the CO stretching frequencies increase in the order $V^{-1} < Cr^0 < Mn^{+1} < Fe^{2+}$. This indicates that the higher the oxidation state of the metal, the less the M−C π-backbonding and the higher the CO stretching frequency.

Originally, $Fe(Cp)_2(CO)_2$ was thought to contain two π-bonded Cp rings [382]. However, an infrared and NMR study [383] showed that one ring is π-bonded and the other σ-bonded to the metal. Later, X-ray analysis confirmed this structure [384]. The structure of $Fe_2(Cp)_2(CO)_4$ has been studied extensively. In the solid state, it takes a *trans*-bridged structure (Fig. 2.20a) [385], or a *cis*-bridged structure (Fig. 2.20b) if crystallized in polar solvents at lower temperatures [386]. The *cis*-isomer exhibits two terminal (1975 and 1933 cm^{-1}) and two bridging (1801 and 1766 cm^{-1}) bands. Although the *trans*-isomer also exhibits two terminal (1956 and 1935 cm^{-1}) and two bridging (1769 and 1755 cm^{-1}) bands, these splittings are probably due to the crystal field effect.

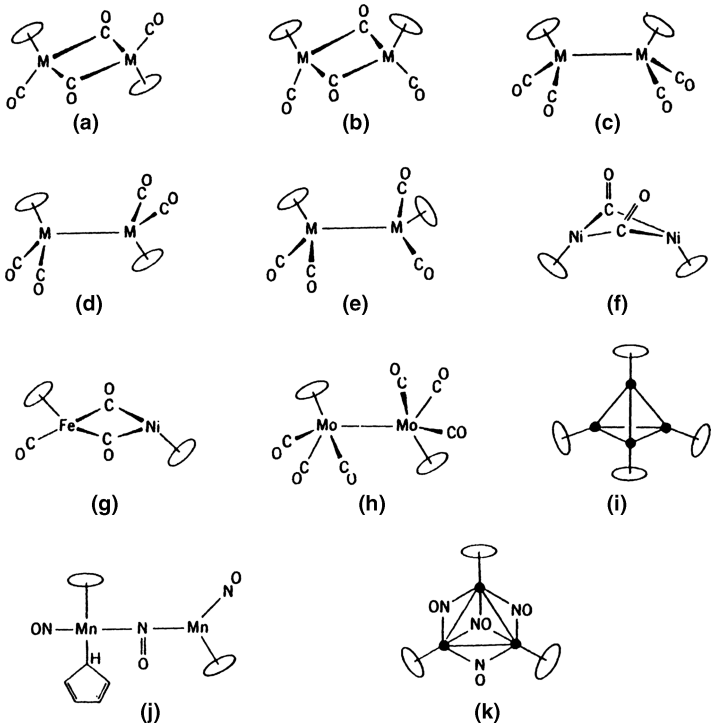

Fig. 2.20. *Structures of cyclopentadienyl carbonyl and nitrosyl complexes. The bridging CO groups are not shown in (i).*

The structure of $Fe_2(Cp)_2(CO)_4$ in solution has been controversial. Early infrared studies [387] suggested the presence of the *cis*-bridged structure (Fig. 2.20b) mixed with a trace of noncentrosymmetric, nonbridging isomer (Fig. 2.20c). Manning [388] proposed, however, an equilibrium involving the three isomers, *a*, *b*, and *c*, of Fig. 2.20. This was confirmed by Bullet et al. [389] who gave the following assignments for the spectrum in a $CS_2-C_6D_5CD_3$ solution: *trans*-isomer (a), 1954 and 1781 cm^{-1}; *cis*-isomer (b), 1998, 1954, 1810, and 1777 cm^{-1}. The frequencies of nonbridged species could not be determined because of their very low concentration. In the case of $Ru_2(Cp)_2(CO)_4$, Bullitt et al. [389] proposed an equilibrium containing four isomers: *a*, *b*, *d*, and *e* of Fig. 2.20.

It is interesting to note that the bridging CO groups of $Fe_2(Cp)_2(CO)_4$ form an adduct with trialkylaluminum [390] (see Sec. 1.18):

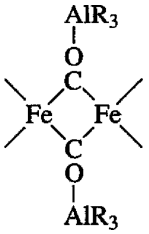

This indicates that the basicity of the bridging CO group is greater than that of the terminal CO group. The CO stretching bands of the parent compound (R: isobutyl) are at 2005 and 1962 (terminal) and 1794 (bridging) cm^{-1} in heptane solution. These bands are shifted to 2041 and 2003 (terminal) and 1680 (bridging) cm^{-1} by adduct formation. X-Ray analysis has been carried out on $[Fe_2(Cp)_2(CO)_4][Al(C_2H_5)_3]_2$ [391]. Formation of adducts such as $[Fe_2(Cp)_2(CO)_4]BX_3$ (X = Cl,Br) and $[Fe(Cp)(CO)]_4 \cdot BX_3$ (X = F,Cl,Br) has also been confirmed [392]. These compounds exhibit bands at 1470–1290 cm^{-1} for bridging CO groups, which are bonded to a Lewis acid via the O atom.

$Ni_2(Cp)_2(CO)_2$ exhibits two bridging CO stretching bands at 1854 and 1896 cm^{-1} in heptane solution. The structure shown in Fig. 2.20f with a puckered $Ni(CO)_2Ni$ bridge was proposed for this compound [393]. In heptane solution $FeNi(Cp)_2(CO)_3$ shows a strong terminal CO stretching at 2004 cm^{-1} and two bridging CO stretching bands at 1855 and 1825 cm^{-1}. Since the 1855 cm^{-1} band (symmetric type) is very weak, the $Ni(CO)_2Fe$ bridge in this compound was thought to be virtually planar, as shown in Fig. 2.20g [393].

According to X-ray analysis [394], the structure of $Mo_2(Cp)_2(CO)_6$ is *trans*-centrosymmetric, as shown in Fig. 2.20h. The infrared spectrum in the CO sketching region is consistent with this structure, both in the solid state and in solution [395]. In solvents of high dielectric constants, however, the *trans*-rotamer is rearranged into the *gauche*-rotamer [396]. For the infrared spectra of analogous tungsten compounds, see Refs. [377] and [397]. According to X-ray analysis [398], $Fe_4(Cp)_4(CO)_4$ takes a regular tetrahedral structure such as that shown in Fig. 2.20i. It exhibits a bridging CO

stretching band at 1649 cm [390] in the infrared and a FeFe stretching band at 214 cm^{-1} [399] in the Raman.

2.7.2. Halogeno Compounds

Cyclopentadienyl complexes containing metal-halogen bonds exhibit metal–halogen vibrations (Sec. 1.25), together with those of the cyclopentadienyl rings. The low-frequency spectra of these compounds are complicated [400,401] because metal–ring skeletal modes couple with metal–halogen modes. The infrared spectra of $M(Cp)_2X_2$-type compounds (M = Ti,Zr,Hf; X = Cl,Br,I) have been studied by several investigators [400–403]. Also, infrared spectra have been reported for $Mo(Cp)(CO)_3X$ [375] and $Mo(Cp)-(CO)_2X_3$ (X = Cl,Br,I) [404].

2.7.3. Nitrosyl Compounds

Vibrational spectra of nitrosyl compounds were discussed in Sec. 1.20. The vibrational spectra of Ni(Cp)(NO) and its deuterated and ^{15}N species have been assigned completely [405]; the NO stretching, NiN stretching, NiCp stretching, and NiCp tilt vibrations are at 1809, 649, 322, and 290 cm^{-1}, respectively. If this compound in an Ar matrix is irradiated by UV light, the bands near 1830 cm^{-1} disappear and a new band emerges at 1390 cm^{-1} [406]. This has been interpreted as indicating the following photoionization:

$$(Cp)NiNO \xrightarrow{h\nu} (Cp)Ni^{+}NO^{-}$$

$Mn_2(Cp)_3(NO)_3$ exhibits two NO stretching bands at 1732 and 1510 cm^{-1} [407]. With the former attributed to the terminal and the latter to the bridging NO, the structure that is shown in Fig. 2.20j was proposed. The infrared spectrum of $Mo(Cp)(CO)_2(NO)$ has been reported [408,375]. Figure 2.20k shows the structure of $Mn_3(Cp)_3(NO)_4$, containing doubly and triply bridging NO groups. The bands at 1530 and 1480 cm^{-1} were assigned to the doubly bridged NO groups, whereas the 1320-cm^{-1} band was attributed to the triply bridged NO group [409].

2.7.4. Hydrido Complexes

Vibrational spectra of hydrido complexes were reviewed in Sec. 1.24. The metal-hydrogen stretching bands for $Mo(Cp)_2H_2$ [410], $Re(Cp)_2H_2$, and $W(Cp)_2H_2$ [411,412] have been observed in the 2100–1800 cm^{-1} region. X-Ray analysis on $Mo(Cp)_2H_2$ [413] suggests that the coordination around the Mo atom is approximately tetrahedral. In polymeric $[Zr(Cp)_2H_2]_n$ [414], the bridging ZnH stretching vibration is observed as a strong, broad band a 1540 cm^{-1} [415]. A similar bridging TiH vibration is found at 1450 cm^{-1} for $[Ti(Cp)_2H]_2$ [416]. In $\{[Rh(Cp^*)]_2HCl_3\}$, where Cp* denotes the pentamethyl-Cp group, the bridging RhH vibration was assigned at 1151 cm^{-1} [417]:

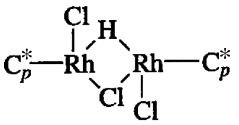

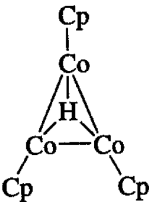

An extremely low CoH stretching frequency (950 cm^{-1}), together with an unusually high-field proton chemical shift observed for $[Co(Cp)H]_4$, was attributed to the triply bridged structure shown above (only one face of the tetrahedron is shown) [418].

2.7.5. Complexes Containing Other Groups

As discussed in Sec. 1.17 the mode of coordination of the pseudohalide ion can be determined by vibrational spectroscopy. Burmeister et al. [419] found that all NCS and NCSe groups are N-bonded in $M(Cp)_2X_2$-type compounds, where M is Ti, Zr, Hf, or V, and X is NCS or NCSe. In the case of analogous NCO complexes, Ti, Zr, and Hf form O-bonded complexes, whereas V forms an N-bonded complex. Later, Jensen et al. [420] suggested the N-bonded structure for the titanium complex.

The ν(CH) (3311 cm^{-1}) and ν(CN) (2097 cm^{-1}) of free HCN are shifted to 3188 and 2155 cm^{-1}, respectively, when it coordinates to the Ti atom in the $[Ti(Cp)_2(HCN)_2]^{2+}$ ion. This result has been attributed to the Ti ← HCN σ-donation [421]. The *cis*- and *trans*-isomers of the isonitrile complex, $MoCp(CO)_2$ (*t*-BuNC)I, exhibit the ν(NC) at 2153 and 2138 cm^{-1}, respectively:

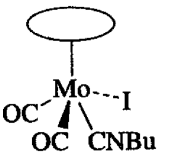

(*cis*)

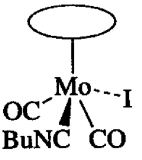

(*trans*)

The ν(NC) of the *trans* isomer is lower because its I → CN π-donation may be larger relative to the *cis* isomer [422]. The ν(NC) of $MoCp(CO)_2(EtNC)I$ at 2168 cm^{-1} is shifted to 1869 cm^{-1} in Na $[MoCp(CO)_2(EtNC)]$. The marked downshift of ν(NC) may reflect a lower oxidation state (O) of the Mo atom in the latter since the Mo → CN-Et π-backdonation increases as the oxidation state becomes lower [423].

A strong N ≡ N stretching band is observed at 1910 cm^{-1} in the Raman spectrum of $L_2(Cp)Mo-N\equiv N-Mo(Cp)L_2$ (L: PPh_3) [424]. Thiocarbonyl complexes of the (Cp) $Mn(CO)_{3-n}(CS)_n$-($n = 1,2,3$) type exhibit the C ≡ S stretching bands at 1340–1235 cm^{-1} [425]. In $(Cp)Nb(S_2)X$-type compounds (X = Cl,Br,I,SCN), the S_2 is

probably coordinated to the metal in a side-on fashion, and its SS stretching band may be assigned at 540 cm^{-1} [426].

2.8. COMPLEXES OF OTHER CYCLIC UNSATURATED LIGANDS

In addition to those discussed in the preceding sections, there are many other cyclic unsaturated ligands that form π-complexes with transition metals. Some of these complexes are discussed below.

2.8.1. Complexes of Cyclobutadiene (C_4H_4)

The local symmetry of the C_4H_4 ring in $Fe(C_4H_4)(CO)_3$ is regarded as $\mathbf{C}_{4v}$, and its 18 ($3 \times 8-6$) vibrations are classified into

$$3A_1(\mathrm{IR,R}) + A_2(\mathrm{ia}) + 4B_1(\mathrm{ia}) + 2B_2(\mathrm{ia}) + 4E(\mathrm{IR,R})$$

Thus, seven vibrations are IR- as well as Raman-active. Two skeletal modes, ring tilt (E) and ν_s (Fe$-C_4H_4$) (A_1) should be added if the Fe atom is included. These vibrations were observed near 475 and 406 cm^{-1}, respectively [427,428]. Normal coordinate analysis on $Fe(C_4H_4)(CO)_3$ was carried out by Andrews and Davidson [429]. The IR spectra of $Ni(C_4(CH_3)_4)Cl_2$, $M(C_4(C_6H_s)_4)X_2$ (M = Ni,Pd; X = Cl,Br,I) and $Pt(C_4R_4)Cl_2$ (R = alkyl) [430] are reported [431].

2.8.2. Cyclopentadiene (C_5H_6) and Cyclohexadienyl (C_6H_7) Complexes

Cyclopentadiene forms π-complexes such as $MCp(C_5H_6)$ (M = Co,Rh) in which the two H atoms of the CH_2 group exhibit two separate bands; $\nu(CH_{endo})$ and $\nu(CH_{exo})$ at 2750 and 2945 cm^{-1}, respectively [432]:

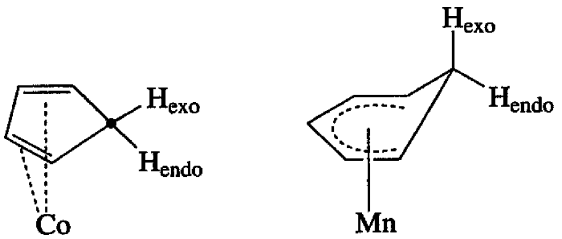

A later study [433] shows, however, that the lower-frequency band at 2750 cm^{-1} must be assigned to $\nu(CH_{exo})$, since replacement of the exo hydrogen by the phenyl or perfluorophenyl group results in the disappearance of this band. In a cyclohexadienyl complex such as $Mn(C_6H_7)(CO)_3$, the bands at 2970 and 2830 cm^{-1} were assigned to $\nu(CH_{endo})$ and $\nu(CH_{exo})$, respectively [434].

2.8.3. Complexes of Benzene (C_6H_6)

Under $\mathbf{D}_{6h}$ symmetry, the 30 ($3 \times 12-6$) normal vibrations of benzene are classified into

$$2A_{1g}(\mathrm{R}) + A_{2g}(\mathrm{ia}) + A_{2u}(\mathrm{IR}) + 2B_{1u}(\mathrm{ia}) + 2B_{2g}(\mathrm{ia}) + 2B_{2u}(\mathrm{ia})$$
$$+ E_{1g}(\mathrm{R}) + 3E_{1u}(\mathrm{IR}) + 4E_{2g}(\mathrm{R}) + 2E_{2u}(\mathrm{ia})$$

Thus only four vibrations are IR-active and only seven vibrations are Raman-active. Figure 2.21 shows the normal modes and observed frequencies of these vibrations.

Dibenzene chromium, $Cr(C_6H_6)_2$, takes a ferrocene-like sandwich structure of $\mathbf{D}_{6h}$ symmetry (eclipsed form). Then, its 69 ($3 \times 25-6$) normal vibrations are grouped into

$$4A_{1g} + 2A_{1u} + A_{2g} + 4A_{2u} + 2B_{1g} + 4B_{1u} + 4B_{2g} + 2B_{2u} + 5E_{1g} + 6E_{1u} + 6E_{2g} + 6E_{2u}$$

of which only A_{2u} and E_{1u} vibrations are IR-active and A_{1g}, E_{1g}, and E_{2g} vibrations are Raman-active. Thus 10- (4 A_{2u} and 6 E_{1u}) bands should be observed in IR spectra. Table 2.13 lists these 10 frequencies, including the ring tilt, $\nu_s(\mathrm{Cr-C_6H_6})$, and $\delta(\mathrm{C_6H_6-Cr-C_6H_6})$. Figure 2.22 shows the IR spectrum of $Cr(C_6H_6)_2$ [436]. Using the same approximation as used previously for ferrocene (Sec. 2.6.3), the $Cr-C_6H_6$ stretching force constant of $Cr(C_6H_6)_2$ is calculated to be 2.43 mdyn/Å, which is smaller than that of ferrocene (2.7 mdyn/Å). Cyvin et al. [437] carried out normal coordinate analysis on $Cr(C_6H_6)_2$.

Infrared spectra have been reported for $V(C_6H_6)_2$ [438] and $Fe(C_6H_6)_2$ [439], which were prepared by matrix cocondensation techniques (Sec. 2.5.6). Resonance Raman spectra of $V(C_6H_6)_2$ thus prepared exhibit the progression of the $\nu(\mathrm{V-C_6H_6})$ (257 cm^{-1}) up to the ninth overtone [440]. The IR spectra of $V(C_6H_6)^+$ and $V(C_6H_6)_2{}^+$ in the gaseous state have been assigned [441]. The CH out-of-plane vibrations of aromatic rings tend to shift to higher frequencies by forming sandwich complexes. Saito et al. [442] noted, however, that some vibrations are upshifted, while others are downshifted, when benzene forms the sandwich complex $[Cr(C_6H_6)_2]I$.

The IR and Raman spectra of $Cr(C_6H_6)(C_6F_6)$ ($\mathbf{C}_{6v}$ symmetry) have been assigned empirically [443]. Normal coordinate analyses of $Cr(C_6H_6)(CO)_3$ ($\mathbf{C}_{3v}$ symmetry) have been made by two groups of investigators [444,445]. The UV photolysis of $Cr(C_6H_6)(CO)_3$ in the gas phase produces $Cr(C_6H_6)(CO)_{1,2}$, which is characterized by ν(CO); $Cr(C_6H_6)(CO)_2$ is predominant on 355 nm photolysis [446].

2.8.4. Tropylium Cation ($C_7H_7{}^+$) and π-C_7H_7 Metal Complexes

Under $\mathbf{D}_{7h}$, symmetry, the 36 ($3 \times 14 - 6$) normal vibrations of the planar tropylium cation are classified into

$$2A'_1 + A'_2 + A''_2 + 3E'_1 + E''_1 + 4E'_2 + 2E''_2 + 4E'_3 + 2E''_3$$

of which A''_2 and E'_1 vibrations are IR-active, whereas A'_1, E''_1, and E'_2 vibrations are Raman-active. Thus, four IR and seven Raman bands are expected for the $C_7H_7{}^+$ cation. The four IR bands of $(C_7H_7)Br$ are observed at 3020 [ν(CH)], 1477 [ν(CC)], 992 [δ(CH)], and 633 cm^{-1} [π(CH)] [447].

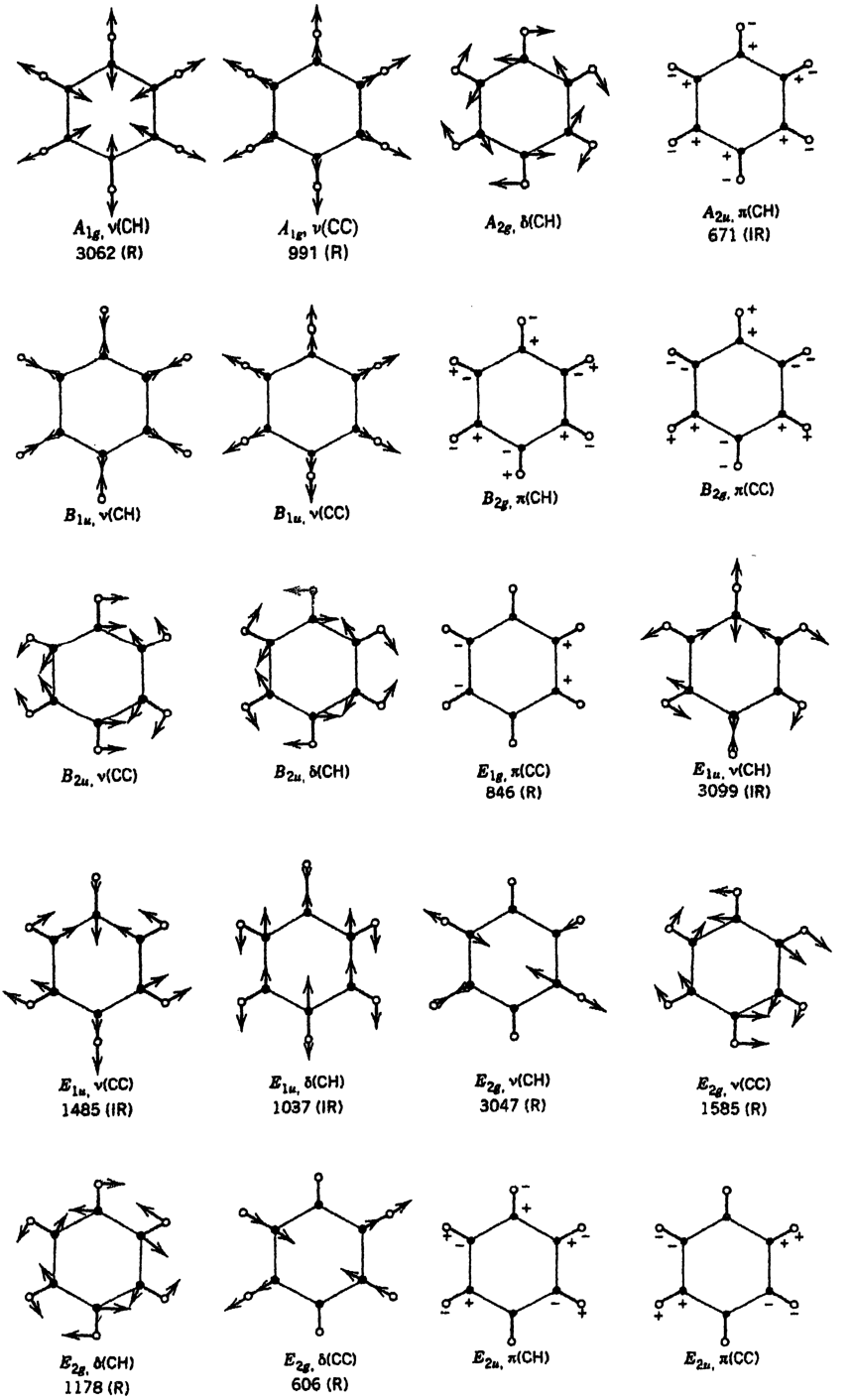

Fig. 2.21. *Approximate normal modes of vibration of benzene. Symmetry, band, assignments, and observed frequencies (cm^{-1}) of representative modes are given.*

TABLE 2.13. Infrared Frequencies of Dibenzene-Metal Complexes (cm^{-1}) [332,435]

Complex	ν(CH)		ν(CC)	δ(CH)	ν(CC)	π(CH)	Ring Tilt		ν(MR)[a]	δ(RMR)[a]
$Cr(C_6H_6)_2$	3037	—	1426	999	971	833	794	490	459	(140)
$Cr(C_6H_6)_2^+$	3040	—	1430	1000	972	857	795	466	415	(144)
$Mo(C_6H_6)_2$	3030	2916	1425	995	966	811	773	424	362	—
$W(C_6H_6)_2$	3012	2898	1412	985	963	882	798	386	331	—
$V(C_6H_6)_2$	3058	—	1416	985	959	818	739	470	424	—

[a] R denotes the C_6H_6 ring.

The IR frequencies of several metal π-complexes such as $M(C_7H_7)(CO)_3$ (M = Cr, Mo) are summarized by Fritz [332]. In these complexes, the symmetry of the $M(C_7H_7)$ moiety is regarded as $\mathbf{C}_{7v}$, and its 39 ($3 \times 15 - 6$) vibrations are grouped into

$$4A_1(\text{IR, R}) + A_2(\text{ia}) + 5E_1(\text{IR, R}) + 6E_2(\text{R}) + 6E_3(\text{ia})$$

Thus, nine vibrations are IR-active while 15 vibrations are Raman-active. These vibrations include the ring tilt (E_1) and $\nu_s(M{-}C_7H_7)$ (A_1), which are IR- as well as Raman-active. The Raman spectrum of $[Mo(C_7H_7)(CO)_3]BF_4$ in the solid state exhibits the ring tilt at 331 and 324 cm^{-1}, and the $\nu_s(Mo{-}C_7H_7)$ at 309 cm^{-1}, with two shoulder bands at 302 and 295 cm^{-1}. The observed splitting of the former is due to lowering of symmetry in the crystalline state (site symmetry, $\mathbf{C}_1$) [448].

2.8.5. Complexes of Cyclooctadienyl Anion ($C_8H_8^{2-}$)

The $C_8H_8^{2-}$ ion takes an octagonal planar structure of $\mathbf{D}_{8h}$ symmetry, and its 42 ($3 \times 16 - 6$) vibrations are grouped into

$$2A_{1g} + A_{2g} + A_{2u} + 2B_{1u} + 2B_{2g} + 2B_{2u} + E_{1g} + 3E_{1u} + 4E_{2g} + 2E_{2u} + 4E_{3g} + 2E_{3u}$$

of which A_{2u} and E_{1u} vibrations are IR-active, whereas A_{1g}, E_{1g}, and E_{2g} vibrations are Raman-active. Thus, four vibrations are IR-active and seven vibrations are Raman-active. The former bands of $K_2(C_8H_8)$ are observed at 2994 [ν(CH)], 1431

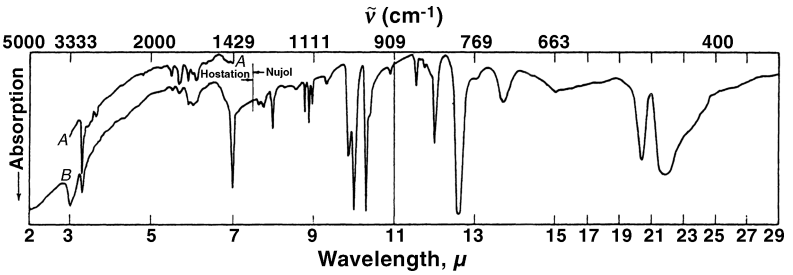

Fig. 2.22. *Infrared spectra of crystalline $Cr(C_6H_6)_2$ in (A) KBr pellet and (B) Hostaflon oil suspension (2–7.5 μm) and Nujol mull suspension (7.5–29 μm) [436].*

[ν(CC)], 880 [δ(CH)], and 684 cm^{-1} [π(CH)] [332]. Metal complexes such as $M(C_8H_g)_2$ (M = Th,U) take sandwich structures similar to that of ferrocene, but the two rings are eclipsed so that the overall symmetry becomes $\mathbf{D}_{8h}$. In this case, the 93 ($3 \times 33 - 6$) normal vibrations are classified as

$$4A_{1g} + 2A_{1u} + A_{2g} + 4A_{2u} + 2B_{1g} + 4B_{1u} + 4B_{2g} + 2B_{2u} + 5E_{1g} + 6E_{1u} + 6E_{2g} + 6E_{2u} + 6E_{3g} + 6E_{3u}$$

Then, 10 vibrations ($4A_{2u} + 6E_{1u}$) are IR-active and 15 vibrations ($4A_{1g} + 5E_{1g} + 6E_{2g}$) are Raman-active. The IR spectra of biscyclooctadienyl complexes mentioned above have been assigned by Hocks et al. [449]. The ring tilt (E_{1u}) and $\nu_a(M-C_8H_8)$ (A_{2u}) of these complexes are observed at 695(698) and 250(240) cm^{-1}, respectively (the numbers in parentheses are for the uranium complex).

In $Ti(C_8H_8)_2$, however, one ring is symmetrically bonded (local symmetry, $\mathbf{C}_{8h}$), while the other is asymmetrically bonded to the metal (local symmetry, $\mathbf{C}_s$). Under $\mathbf{C}_{8h}$, symmetry, the 45 ($3 \times 17 - 6$) vibrations of the $M(C_8H_8)$ moiety are classified into

$$4A_1 + A_2 + 2B_1 + 4B_2 + 5E_1 + 6E_2 + 6E_3$$

Then, nine ($4A_1 + 5E_1$) vibrations are IR-active, whereas 15 ($4A_1 + 5E_1 + 6E_2$) vibrations are Raman-active. The IR spectra of $M(C_8H_8)_2$ (M = Ti,V) have been assigned partly on this basis [449]. Similar assignments can be made for the $Ti(C_8H_8)$ moiety of $Ti(C_8H_8)(C_5H_5)$ [450]. The IR spectra of the $K[Ln(C_8H_8)_2]$ (Ln = Ce,Pr,Nd, Sm) can be assigned on the basis of the sandwich structure ($\mathbf{D}_{8h}$) [451].

Cyclooctatetrane (COT) takes a tub conformation in the free state. As discussed in Sec. 2.5.3, it takes a tub conformation in $[Rh(COT)Cl]_2$ and a chair conformation in $Fe(COT)(CO)_3$.

2.8.6. Indenyl Complexes

The indenyl group may coordinate to the metal through a σ- or a π-bond:

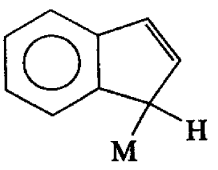

σ-Complex

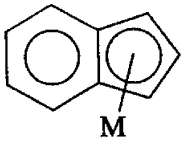

π-Complex

An example of the former is seen in $Hg(C_9H_7)Cl$, which exhibits an aromatic CH stretching at 3060–3050 cm^{-1} and an aliphatic CH stretching band at 2920–2850 cm^{-1}. The latter band should be absent in the π-bonded complex [452].

The IR spectra of π-bonded sandwich complexes such as $Ru(C_9H_7)_2$ (fully eclipsed) and $Fe(C_9H_7)_2$ (staggered) have been assigned. No appreciable differences were noted between these two complexes in the low-frequency region [452].

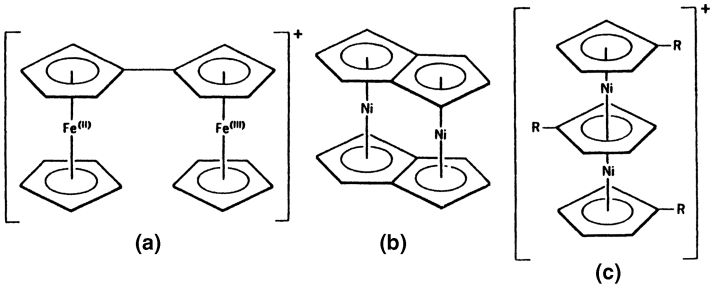

Fig. 2.23. Structures of some metal sandwich compounds.

2.8.7. Complexes of Larger Ligands

Infrared spectra are reported for a mixed-valence-state complex, biferrocene (Fe^{2+}, Fe^{3+}) picrate [453] and bis(pentalenyl)Ni [454], whose structures are shown in Fig. 2.23a and 2.23b, respectively. The two ferrocene moieties in the former are not independent since only one set of the skeletal modes is observed. The spectrum of a triple-decker compound, $[Ni_2(Cp')_3]BF_4(Cp': CH_3-Cp)$ (Fig. 2.23c), is similar to that of $Ni(Cp')_2$ [455]. In the case of the $[Ni_2Cp_3]^+$ ion, the skeletal frequencies of the Ni−Cp (terminal) moiety was found to be 25–10 cm^{-1} higher than those of the Ni−Cp (bridging) moiety [456].

2.9. MISCELLANEOUS COMPOUNDS

There are many other organometallic compounds that have not been covered in the preceding sections. For these, the reader should consult general references cited previously. Other review articles on specific groups of compounds are listed below:

Alkyldiboranes: W. J. Lehmann and I. Shapiro, *Spectrochim. Acta* **17**, 396 (1961).

Organoaluminum compounds: E. G. Hoffman, Z. Elektrochem. **64**, 616 (1960).

Organosilicon compounds: A. L. Smith, *Spectrochim. Acta* **16**, 87 (1960).

Organogermanes: R. J. Cross and R. Glockling, *J. Organomet. Chem.* **3**, 146 (1965).

Organotin compounds: R. Okawara and W. Wada, *Adv. Organomet. Chem.* **5**, 137 (1967).

Organophosphorus compounds: D. E. C. Corbridge, *The Structural Chemistry of Phosphorus*, Elsevier, Amsterdam, 1974; L. C. Thomas, *Interpretation of the Infrared Spectra of Organophosphorus Compounds*, Heyden, London, 1974.

Organometallic compounds of P, As, Sb, and Bi: E. Maslowsky, Jr., *J. Organomet. Chem.* **70**, 153 (1974).

REFERENCES

1. *Spectroscopic Properties of Inorganic and Organometallic Compounds*, Vol. 1 to present, The Chemical Society, London.
2. K. Nakaraoto, "Characterization of Organometallic Compounds by Infrared Spectroscopy," in M. Tsutsui,ed., *Characterization of Organometallic Compounds*, Part I, Wiley, New York, (1969).
3. E. Maslowsky, Jr., *Vibrational Spectra of Organometallic Compounds*, Wiley, New York, (1977).
4. L. J. Bellamy, *The Infrared Spectra of Complex Molecules*, 3rd ed., Chapman and Hall, London, Vol. 1, 1975; Vol. 2, 1980.
5. D. Lin-Vien, N. B. Colthup, W. G. Fateley, and J. G. Grasselli, *The Handbook of Infrared and Raman Characteristic Frequencies of Organic Molecules*, Academic Press, San Diego, CA, (1991).
6. T. Shimanpuchi, *Tables of MolecularVibrational Frequencies, Consolidated Volume*, Natl. Stand. Ref. Data Ser., US Natl. Bur. Stand. Vol. 39, June (1972).
7. B. Schrader, *Raman/IR Atlas of Organic Compomias*, VCH, New York, (1989).
8. *The Sadtler Standard Spectra*, Sadtler Research Laboratories, Division of Bio-Rad Laboratories, Inc., Philadelphia, PA.
9. N. N. Greenwood, E. J. F. Ross, and B. P. Straughan, *Index of Vibrational Spectra of Inorganic and Organometallic Compounds*, Vols. 1–3, Butterworth, London, 1972–1977.
10. S. C. Chang, Z. H. Kafafi, R. H. Hauge, W. E. Billups, and J. L. Margrave, *J. Am. Chem. Soc.* **109**, 4508 (1987).
11. S. C. Chang, R. H. Hauge, Z. H. Kafafi, J. L. Margrave, and W. E. Billups, *J. Am. Chem. Soc.* **110**, 7975 (1988).
12. W.E. Billups, S. C. Chang, R. H. Hauge, and J. L. Margrave, *Inorg. Chem.* **32**, 1529 (1993).
13. W. D. Bare, A. Citra, C. Trindle, and L. Andrews, *Inorg. Chem.* **39**, 1204 (2000).
14. K. Burczyk and A. J. Downs, *J. Chem. Soc. Dalton Trans.* 2351 (1990).
15. E. Maslowsky, Jr., *Chem. Soc. Rev.* **9**, 25 (1980).
16. A. M. Pyndyk, M. R. Aliev, and V. T. Aleksanyan, *Opt. Spectrosc. (Engl. transl.)* **36**, 393 (1974).
17. D. Fischer, K. Klostermann, and K. -L. Oehme, *J. Raman Spectrosc.* **22**, 19 (1990).
18. W. F. Edgell and C. H. Ward, *J. Am. Chem. Soc.* **77**, 6486 (1955).
19. W. F. Edgell and C. H. Ward, *J. Mol. Spectrosc.* **8**, 343 (1962).
20. K. Shimizu and H. Murata, *J. Mol. Spectrosc.* **5**, 44 (1960).
21. R. A. Kovar and G. L. Morgan, *Inorg. Chem.* **8**, 1099 (1969).
22. I. S. Butler and M. L. Newbury, *Spectrochim. Acta.* **33A**, 669 (1977).
23. B. Nagel and W. Brüser, *Z. Anorg. Allg. Chem.* **468**, 148 (1980).
24. J. R. Dung, and S. C. Brown, *J. Mol. Spectrosc.* **45**, 338 (1973).
25. C. Kippels, W. Thiel, D. C. McKean, and A. M. Coats, *Spectrochim. Acta* **48A**, 1067 (1992).
26. M. A. Bochmann, M. A. Chesters, A. R. Coleman, R. Grinter, and D. R. Linder, *Spectrochim. Acta* **48A**, 1173 (1992).

27. M. J. Almond, C. E. Jenkins, D. A. Rice, and C. A. Yates, *J. Mol. Struct.* **222**, 219 (1990).
28. J. R. Allkins and P. L. Hendra, *Spectrochim. Acta* **22**, 2075 (1966).
29. J. R. Durig, C. M. Plater, Jr., J. Bragin, and Y. S. Li, *J. Chem. Phys.* **55**, 2895 (1971).
30. K. Aida, Y. Yamaguchi, and Y. Imai, *Spectrochim. Acta* **43A**, 837 (1987).
31. K. Hamada and H. Morishita, *J. Mol. Struct.* **44**, 119 (1978).
32. W. J. Lehmann, C. O. Wilson, and I. Shapiro, *J. Chem. Phys.* **31**, 1071 (1959).
33. L. A. Woodward, J. R. Hall, R. N. Nixon, and N. Sheppard, *Spectrochim. Acta* **15**, 249 (1959).
34. H. J. Becher and F. Bramsiepe, *Spectrochim. Acta* **35A**, 53 (1979).
35. R. J. O'Brien and G. A. Ozin, *J. Chem. Soc. A* **1136**, (1971).
36. S. Kvisle and E. Rytter, *Spectrochim. Acta* **40A**, 939 (1984).
37. G. A. Atiyah, A. S. Grady, D. K. Russell, and T. A. Claxton, *Spectrochim. Acta* **47A**, 467 (1991).
38. H. G. E. Coates and A. J. Downs, *J. Chem. Soc.* 3353 (1964).
39. J. R. Hall, L. A. Woodward, and E. A. V. Ebsworth, *Spectrochim. Acta.* **20**, 1249 (1964).
40. J. R. Durig and K. K. Chatterjee, *J. Raman Spectrosc.* **11**, 168 (1981).
41. Z. S. Huang, C. Park, and T. J. Anderson, *J. Organomet. Chem.* **449**, 77 (1993).
42. A. J. Blake and S. Cradock, *J. Chem. Soc. Dalton Trans.* 2393 (1990).
43. G. Bouquet and M. Bigorgne, *Spectrochim. Acta* **23A**, 1231 (1967).
44. P. J. D. Park and P. J. Hendra, *Spectrochim. Acta* **24A**, 2081 (1968).
45. H. Rojhantalab, J. W. Nibler, and C. J. Wilkins, *Spectrochim. Adta* **32A**, 519 (1976).
46. H. Rojhantalab and J. W. Nibler, *Spectrochim. Acta* **32A**, 947 (1976).
47. H. Siebert and Z. Anorg, *Allg. Chem.* **273**, 161 (1953).
48. S. Sportouch, C. Lacoste, and R. Gaufrès, *J. Mol. Struct.* **9**, 119 (1971).
49. F. Watari, *Spectrochim. Acta* **34A**, 1239 (1978).
50. G. A. Crowder, G. Gorin, F. H. Kruse, and D. W. Scott, *J. Mol. Spectrosc.* **16**, 115 (1965).
51. H. H. Eysel, H. Siebert, G. Groh, and H. J. Berthold, *Spectrochim. Acta* **26A**, 1595 (1970).
52. A. J. Downs, R. Schrautzler, and I. A. Steer, *Chem. Commun.* 221 (1966).
53. A. J. Shortland and G. Wilkinson, *J. Chem. Soc. Dalton Trans.* 872 (1973).
54. J. W. Nibler and T. H. Cook, *J. Chem. Phys.* **58**, 1596 (1973).
55. C. W. Hobbs and R. S. Tobias, *Inorg. Chem.* **9**, 1998 (1970).
56. P. L. Goggin and L. A. Woodward, *Trans. Faraday Soc.* **56**, 1591 (1960).
57. G. B. Deacon and J. H. S. Green, *Spectrochim. Acta* **24A**, 885 (1968).
58. M. G. Miles, J. H. Patterson, C. W. Hobbs, M. J. Hopper, J. Overend, and R. S. Tobias, *Inorg. Chem.* **7**, 1721 (1968).
59. H. Kriegsmann, S. Pischtscfaan, and Z. Anorg, *Allg. Chem.* **308**, 212 (1961).
60. A. J. Downs and I. A. Steer, *J. Orgcmomet. Chem.* **8**, P21 (1967).
61. K. J. Wynne and J. W. George, *J. Am. Chem. Soc.* **91**, 1649 (1969).
62. M. T. Chen and J. W. George, *J. Am. Chem. Soc.* **90**, 4580 (1968).
63. J. A. Creighton, G. B. Deacon, and J. H. S. Green, *Aust. J. Chem.* **20**, 583 (1967).
64. R. Baumgärtner, W. Sawodny, J. Goubeau, and Z. Anorg, *Allg. Chem.* **333**, 171 (1964).

65. A. M. Coats, D. C. McKean, H. G. M. Edwards, and V. Fawcett, *J. Mol. Struct.* **320**, 159 (1994).
66. M. G. M. van der Vis, E. H. P. Cordfunke, R. J. M. Konings, and A. Oskam, *J. Chem. Soc., Faraday Trans.* **92**, 973 (1996).
67. A. P. Kurbakova, S. S. Bukalov, L. A. Leites, L. M. Golubinskaya, and V. I. Bregadze, *J. Organometal. Chem.* **536/537**, 519 (1997).
68. T. M. Greene, L. Andrews, and A. J. Downs, *J. Am. Chem. Soc.* **117**, 8180 (1995).
69. T. M. Greene, D. V. Lanzisera, L. Andrews, and A. J. Downs, *J. Am. Chem. Soc.* **120**, 6097 (1998).
70. H. Bai and B. S. Ault, *J. Mol. Struct.* **377**, 235 (1996).
71. R. Eujen and B. Hoge, *J. Organometal. Chem.* **503**, C51 (1995).
72. R. Eujen and A. Potorra, *J. Organomet. Chem.* **438**, C1 (1992).
73. A. Ansorge, D. J. Brauer, H. Burger, B. Krumm, and G. Pawelke, *J. Organomet. Chem.* **446**, 25 (1993).
74. J. Mink and P. L. Goggin, *J. Organomet. Chem.* **246**, 115 (1983).
75. E. Weiss and E. A. Lucken, *J. Organomet. Chem.* **2**, 197 (1964).
76. R. West and W. Glaze, *J. Am. Chem. Soc.* **83**, 3580 (1961).
77. P. Krohmer and J. Goubeau, *Z Anorg. Allg. Chem.* **369**, 238 (1969).
78. T. Ogawa, *Spectrochim. Acta* **23A**, 15 (1968).
79. J. Yamamoto and C. A. Wilkie, *Inorg. Chem.* **10**, 1129 (1971).
80. J. Mink and B. Gellai, *J. Organomet. Chem.* **66**, 1 (1974).
81. S. Inoue and T. Yamada, *J. Organomet. Chem.* **25**, 1 (1970).
82. B. Nagel and W. Brüser, *Z. Anorg. Allg. Chem.* **468**, 148 (1980).
83. J. Mink and Y. A. Pentin, *J. Organomet. Chem.* **23**, 293 (1970).
84. J. L. Bribes and R. Gaufrès, *Spectrochim. Acta* **27A**, 2133 (1971).
85. W. J. Lehmann, C. O. Wilson, and I. Shapiro, *J. Chem. Phys.* **28**, 781 (1958).
86. J. Chouteau, G. Davidovics, F. D'Amato, and L. Savidan, *C. R. Hebd. Seances Acad. Sci.* **260**, 2759 (1965).
87. J. H. S. Green, *Spectrochim. Acta* **24A**, 137 (1968).
88. C. Crocker and P. L. Goggin, *J. Chem. Soc., Dalton Trans.* 388 (1978).
89. A. E. Borisov, N. V. Novikova, N. A. Chumaevski, and E. B. Shkirtil, *Dokl. Akad. Nauk SSSR* **173**, 855 (1967).
90. R. L. McKenney and H. H. Sisler, *Inorg. Chem.* **6**, 1178 (1967).
91. J. A. Jackson and R. J. Nielson, *J. Mol. Spectrosc.* **14**, 320 (1964).
92. M. I. Batuev, A. D. Petrov, V. A. Ponomarenko, and A. D. Mateeva, *Izv. Akad. Nauk SSSR, Otd. Kim. Nauk* 1070 (1956).
93. L. A. Leites, Y. P. Egorov, J. Y. Zueva, and V. A. Ponomarenko, *Izv. Akad. Nauk SSSR, Otd. Kim. Nauk* 2132 (1961).
94. W. R. Cullen, G. B. Deacon, and J. H. S. Green, *Can. J. Chem.* **43**, 3193 (1965).
95. P. Taimasalu and J. L. Wood, *Trans. Faraday Soc.* **59**, 1754 (1963).
96. C. R. Dillard and J. R. Lawson, *J. Opt. Soc. Am.* **50**, 1271 (1960).
97. T. L. Brown, R. L. Gerteis, D. A. Bafus, and J. A. Ladd, *J. Am. Chem. Soc.* **86**, 2134 (1964); T. L. Brown, J. A. Ladd, and C. N. Newmann, *J. Organomet. Chem.* **3**, 1 (1965).

98. H. Dietrich, *Acta Crystallogr.* **16**, 681 (1963).
99. T. L. Brown,in F. G. A. Stone and R. West,eds., *Advances in Organometallic Chemistry*, Vol. 3, Academic Press, New York, 1965, p. 374.
100. C. N. Atam, H. Müller, and K. Dehnicke, *J. Organomet. Chem.* **37**, 15 (1972).
101. J. Kress and A. Novak, *J. Organomet. Chem.* **121**, 7 (1976).
102. O. Yamamoto, *Bull. Chem. Soc. Jpn.* **35**, 619 (1962).
103. C. A. Wilkie, *J. Organomet. Chem.* **32**, 161 (1971).
104. R. J. Cross and F. Glocking, *J. Organomet. Chem.* **3**, 146 (1965).
105. W. M. Scovell, B. Y. Kimura, and T. G. Spiro, *J. Coord. Chem.* **1**, 107 (1971).
106. K. H. Thiele, S. Wilcke, and M. Ehrhardt, *J. Organomet. Chem.* **14**, 13 (1968).
107. B. Busch and K. Dehnicke, *J. Organomet. Chem.* **67**, 237 (1974).
108. L. Czuchajowski, J. Habdas, S. A. Kucharski, and K. Rogosz, *J. Organomet. Chem.* **155**, 185 (1978).
109. A. H. Cowley, J. L. Mills, T. M. Leohr, and T. V. Long, *J. Am. Chem. Soc.* **93**, 2150 (1971).
110. M. E. Thompson, S. M. Baxter, R. Bulls, B. J. Burger, M. C. Nolan, B. D. Santarsiero, W. P. Schaefer, and J. E. Bercaw, *J. Am. Chem. Soc.* **109**, 203 (1987).
111. P. W. Jolly, M. I. Bruce, and P. G. A. Stone, *J. Chem. Soc.* 5830 (1965).
112. J. Mink and Y. A. Pentin, *Acta Chim. Acad. Sci. Hung.* **66**, 277 (1970).
113. A. K. Holliday, W. Reade, K. R. Seddon, and I. A. Steer, *J. Organomet. Chem.* **67**, 1 (1974).
114. J. D. Odom, L. W. Hall, S. Riethmiller, and J. R. Durig, *Inorg. Chem.* **13**, 170 (1974).
115. D. C. Andrews and G. Davidson, *J. Organomet. Chem.* **36**, 349 (1972).
116. D. C. Andrews and G. Davidson, *J. Organomet. Chem.* **76**, 373 (1974).
117. G. Davidson and S. Phillips, *Spectrochim. Acta* **34A**, 949 (1978).
118. G. Davidson, *Spectrochim. Acta.* **27A**, 1161 (1971).
119. G. Masetti and G. Zerbi, *Spectrochim. Acta* **26A**, 1891 (1970).
120. U. Kunze, E. Lindner, and J. Koola, *J. Organomet. Chem.* **57**, 319 (1973).
121. R. S. P. Coutts and P. C. Wailes, *Aust. J. Chem.* **22**, 1547 (1969).
122. C. L. Sloan and W. A. Barber, *J. Am. Chem. Soc.* **81**, 1364 (1959).
123. D. I. Maclean and R. E. Sacher, *J. Organomet. Chem.* **74**, 197 (1974).
124. J. G. Contreras and D. G. Tuck, *Inorg. Chem.* **12**, 2596 (1973).
125. J. G. Contreras and D. G. Tuck, *J. Organomet. Chem.* **66**, 405 (1974).
126. P. Krommes and J. Lorberth, *J. Organomet. Chem.* **88**, 329 (1975).
127. W. M. A. Smit and G. Dijkstra, *J. Mol. Struct.* **8**, 263 (1971).
128. E. J. Stampf, J. D. Odom, Y. H. Kim, A. R. Garber, F. M. Wasacz, and J. R. Durig, *Spectrochim. Acta* **49A**, 2117 (1993).
129. G. A. Guirgis, P. Zhen, and J. R. Durig, *Spectrochim. Acta.* **56A**, 1957 (2000).
130. A. N. Nesmeyanov, A. E. Borisov, N. V. Novikova, and E. I. Fedin, *J. Organomet. Chem.* **15**, 279 (1968).
131. S. L. Stafford and F. G. A. Stone, *Spectrochim. Acta* **17**, 412 (1961).
132. G. Davidson, P. G. Harrison, and E. M. Riley, *Spectrochim. Acta* **29A**, 1265 (1973).
133. G. Davidson and S. Phillips, *Spectrochim. Acta* **35A**, 83 (1979).

134. J. Mink and Y. A. Pentin, *J. Organomet. Chem.* **23**, 293 (1970).
135. C. Souresseau and B. Pasquier, *J. Organomet. Chem.* **39**, 51 (1972).
136. C. A. Thompson and L. Andrews, *J. Am. Chem. Soc.* **118**, 10242 (1996).
137. O. Reckeweg, A. Baumann, H. A. Mayer, J. Glaser, and H. -J. Meyer, *Z. Anorg. Allg. Chem.* **625**, 1686 (1999).
138. D. H. Whiffen, *J. Chem. Soc.* 1350 (1956).
139. J. Mink, G. Végh, and Y. A. Pentin, *J. Organomet. Chem.* **35**, 225 (1972).
140. C. G. Barraclough, G. E. Berkovic, and G. B. Deacon, *Aust. J. Chem.* **30**, 1905 (1977).
141. G. Costa, A. Camus, N. Marsich, and L. Gatti, *J. Organomet. Chem.* **8**, 339 (1967).
142. A. N. Rodionov, N. I. Rucheva, I. M. Viktorova, D. N. Shigorin, N. I. Sheverdina, and K. A. Kocheshkov, *Izv. Akad. Nauk SSSR, Ser. Khim.* 1047 (1969).
143. H. F. Shurvell, *Spectrochim. Acta* **23A**, 2925 (1967).
144. N. Kumar, B. L. Kalsotra, and R. K. Multani, *J. Inorg. Nucl. Chem.* **35**, 3019 (1973).
145. A. L. Smith, *Spectrochim. Acta* **24A**, 695 (1968).
146. J. R. Durig, C. W. Sink, and J. B. Turner, *Spectrochim. Acta* **26A**, 557 (1970).
147. D. H. Brown, A. Mohammed, and D. W. A. Sharp, *Spectrochim. Acta* **21**, 663 (1965).
148. N. S. Dance, W. R. McWhinnie, and R. C. Poller, *J. Chem. Soc., Dalton Trans.* 2349 (1976).
149. K. Shobatake, C. Postmus, J. R. Ferraro, and K. Nakamoto, *Appl. Spectrosc.* **23**, 12 (1969).
150. C. Ludwig and H. J. Gotze, *Spectrochim. Acta* **51A**, 2019 (1995).
151. K. Cavanaugh and D. F. Evans, *J. Chem. Soc. A* 2890 (1969).
152. D. C. McKean, G. P. McQuillan, I. Torto, N. C. Bednell, A. J. Downs, and J. M. Dickinson, *J. Mol. Struct.* **247**, 73 (1991).
153. E. Rytter and S. Kvisle, *Inorg. Chem.* **25**, 3796 (1986).
154. H. Kriegsmann, *Z. Anorg. Allg. Chem.* **294**, 113 (1958).
155. H. Bürger, *Spectrochim. Acta* **24A**, 2015 (1968).
156. K. Licht and P. Koehler, *Z Anorg. Allg. Chem.* **383**, 174 (1971).
157. J. R. Durig, K. K. Lau, J. B. Turner, and J. Bragin, *J. Mol. Spectrosc.* **31**, 419 (1971).
158. B. A. Nevett and A. Perry, *J. Organomet. Chem.* **71**, 399 (1974).
159. R. G. Goel, E. Maslowsky, Jr., and C. V. Senoff, *Inorg. Chem.* **10**, 2572 (1971).
160. W. M. Scovell and R. S. Tobias, *Inorg. Chem.* **9**, 945 (1970).
161. B. P. Asthana and C. M. Pathak, *Spectrochim. Acta.* **41A**, 595 (1985).
162. B. P. Asthana and C. M. Pathak, *Spectrochim. Acta* **41A**, 1235 (1985).
163. R. G. Goel and H. S. Prasad, *Spectrochim. Acta* **32A**, 569 (1976).
164. D. Tudela and J. M. Calleja, *Spectrochim. Acta* **49A**, 1023 (1993).
165. K. Shimizu and H. Murata, *J. Mol. Spectrosc.* **4**, 201 (1960).
166. K. Shimizu and H. Murata, *J. Mol. Spectrosc.* **4**, 214 (1960).
167. K. Shimizu and H. Murata, *Bull. Chem. Soc. Jpn.* **32**, 46 (1959).
168. M. A. Othaitat, A. B. Mohamad, T. A. Mohamed, D. J. Gerson, A. Q. McArver, M. S. Afifi, and J. R. Durig, *Spectrochim. Acta* **50A**, 621 (1994).
169. K. Hassler and M. Weidenbruch, *J. Organomet. Chem.* **465**, 127 (1994).
170. T. Tanaka and S. Murakami, *Bull. Chem. Soc. Jpn.* **38**, 1465 (1965).

171. J. R. Dung, C. W. Sink, and S. R. Bush, *J. Chem. Phys.* **45**, 66 (1966).
172. H. J. Becher, *Z. Anorg. Allg. Chem.* **294**, 183 (1958).
173. J. Weidlein and V. Krieg, *J. Organomet. Chem.* **11**, 9 (1968).
174. H. Schmidbaur, J. Weidlein, H. F. Klein, and K. Eiglmeier, *Chem. Ber.* **101**, 2268 (1968).
175. H. C. Clark and A. L. Pichard, *J. Organomet. Chem.* **8**, 427 (1967).
176. L. E. Levchuk, J. R. Sams, and F. Aubke, *Inorg. Chem.* **11**, 43 (1972).
177. C. W. Hobbs and R. S. Tobias, *Inorg. Chem.* **9**, 1037 (1970).
178. E. Amberger and R. Honigschmid-Grossich, *Chem. Ber.* **98**, 3795 (1965).
179. W. M. Scovell, G. C. Stocco, and R. S. Tobias, *Inorg. Chem.* **9**, 2682 (1970).
180. D. E. Clegg and J. R. Hall, *J. Organomet. Chem.* **22**, 491 (1970).
181. P. A. Bulliner, V. A. Maroni, and T. G. Spiro, *Inorg. Chem.* **9**, 1887 (1970).
182. J. R. Hall and G. A. Swile, *J. Organomet. Chem.* **56**, 419 (1973).
183. J. S. Thayer and R. West, *Adv. Organomet. Chem.* **5**, 169 (1967).
184. J. S. Thayer and D. P. Strommen, *J. Organomet. Chem.* **5**, 383 (1966).
185. H. Müller and K. Dehnicke, *J. Organomet. Chem.* **10**, P1 (1967).
186. K. Dehnicke and D. Seybold, *J. Organomet. Chem.* **11**, 227 (1968).
187. J. Müller and K. Dehnicke, *J. Organomet. Chem.* **12**, 37 (1968).
188. T. W. Bitner and J. I. Zink, *Inorg. Chem.* **40**, 3252 (2001).
189. T. M. Klapötke and A. Schulz, *Inorg. Chem.* **35**, 4995 (1996).
190. J. R. Durig, J. F. Sullivan, A. W. Cox, Jr., and B. J. Streusand, *Spectrochim. Acta* **34A**, 719 (1978).
191. J. Müller, *Z Naturforsch.* **34B**, 536 (1979).
192. H. Leimeister and K. Dehnicke, *J. Organomet. Chem.* **31**, C3 (1971).
193. R. G. Goel and D. R. Ridley, *Inorg. Chem.* **13**, 1252 (1974).
194. J. R. Durig, J. F. Sullivan, and A. W. Cox, Jr., *J. Mol. Struct.* **44**, 31 (1978).
195. J. E. Förster, M. Vargas, and H. Müller, *J. Organomet. Chem.* **59**, 97 (1973).
196. J. Relf, R. P. Cooney, and H. F. Henneike, *Organomet. Chem.* **39**, 75 (1972).
197. F. Weller, I. L. Wilson, and K. Dehnicke, *J. Organomet. Chem.* **30**, Cl (1971).
198. K. Dehnicke, *Angew. Chem.* **79**, 942 (1967).
199. M. Wada and R. Okawara, *J. Organomet. Chem.* **8**, 261 (1967).
200. H. Bürger and U. Goetze, *J. Organomet. Chem.* **10**, 380 (1967).
201. J. S. Thayer, *Inorg. Chem.* **7**, 2599 (1968).
202. E. E. Aynsley, N. N. Greenwood, G. Hunter, and M. J. Sprague, *J. Chem. Soc. A* 1344 (1966).
203. W. Beck and E. Schuierer, *J. Organomet. Chem.* **3**, 55 (1965).
204. M. R. Booth and S. G. Frankiss, *Spectrochim. Acta* **26A**, 859 (1970).
205. J. R. Durig, Y. S. Li, and J. B. Turner, *Inorg. Chem.* **13**, 1495 (1974).
206. F. Watari, *J. Mol. Struct.* **32**, 285 (1976).
207. R. Okawara, D. E. Webster, and E. G. Rochow, *J. Am. Chem. Soc.* **82**, 3287 (1960).
208. M. P. Brown, R. Okawara, and E. G. Rochow, *Spectrochim. Acta* **16**, 595 (1960).
209. M. Shindo and R. Okawara, *J. Organomet. Chem.* **5**, 537 (1966).

210. R. Okawara and M. Ohara, *J. Organomet. Chem.* **1**, 360 (1964).
211. K. Yasuda and R. Okawara, *J. Organomet. Chem.* **3**, 76 (1965).
212. H. C. Clark and R. J. O'Brien, *Inorg. Chem.* **2**, 740 (1963).
213. R. G. Goel, H. S. Prasad, G. M. Bancroft, and T. K. Sham, *Can. J. Chem.* **54**, 711 (1976).
214. N. Q. Dao and D. Breitinger, *Spectochim. Acta* **27A**, 905 (1971).
215. M. J. Almond, C. E. Jenkins, D. A. Rice, and K. Hagen, *J. Organomet. Chem.* **439**, 251 (1992).
216. H. C. Clark, R. J. O'Brien and A. L. Pickard, *J. Organomet. Chem.* **4**, 43 (1965).
217. B. S. Ault, *J. Phys. Chem.* **96**, 7908 (1992).
218. T. Tanaka, M. Komura, Y. Kawasaki, and R. Okawara, *J. Organomet. Chem.* **1**, 484 (1964).
219. D. E. Clegg and J. R. Hall, *Spectrochim. Acta* **23A**, 263 (1967).
220. G. Ferguson, R. G. Goel, F. C. March, D. R. Ridley, and H. S. Prasad, *J. Chem. Soc. Dalton Trans.* 1547 (1971).
221. R. Okawara and K. Yasuda, *J. Organomet. Chem.* **1**, 356 (1964).
222. J. M. Brown, A. C. Chapman, R. Harper, D. J. Mowthorpe, A. G. Davies, and P. J. Smith, *J. Chem. Soc. Dalton Trans.* 338 (1972).
223. P. I. Paetzold, *Z Anorg. Allg. Chem.* **326**, 53 (1963).
224. J. F. Helling and D. M. Braitsch, *J. Am. Chem. Soc.* **92**, 7207 (1970).
225. R. S. Tobias and S. Hutcheson, *J. Organomet. Chem.* **6**, 535 (1966).
226. R. S. Tobias, M. J. Sprague, and G. Glass, E. *Inorg. Chem.* **7**, 1714 (1968).
227. P. A. Bulliner and T. G. Spiro, *Inorg. Chem.* **8**, 1023 (1969).
228. H. Kriegsmann, *Z Anorg. Allg. Chem.* **294**, 113 (1958).
229. F. K. Butcher, W. Gerrard, E. F. Mooney, R. G. Rees, and H. A. Willis, *Spectrochim. Acta* **20**, 51 (1964).
230. G. Mann, A. Haaland, and J. Weidlein, *Z. Anorg. Allg. Chem.* **398**, 231 (1973).
231. T. Tanaka, *Bull. Chem. Soc. Jpn.* **33**, 446 (1960).
232. E. W. Abel, *J. Chem. Soc.* 4406 (1960).
233. K. A. Hooton and A. L. Allred, *Inorg. Chem.* **4**, 671 (1965).
234. J. E. Drake, H. E. Henderson, and L. N. Khasrou, *Spectrochim. Acta* **38A**, 31 (1982).
235. P. G. Harrison and S. R. Stobart, *J. Organomet. Chem.* **47**, 89 (1973).
236. M. Wada and R. Okawara, *J. Organomet. Chem.* **4**, 487 (1965).
237. P. L. Goggin and L. A. Woodward, *Trans. Faraday Soc.* **58**, 1495 (1962).
238. D. E. Clegg and J. R. Hall, *J. Organomet. Chem.* **17**, 175 (1969) *Spectrochim. Acta* **21**, 357 (1965).
239. V. N. Khabashesku, S. E. Boganov, K. N. Kudin, J. L. Margrave, and O. M. Nefedov, *Organometallics* **17**, 5041 (1998).
240. W. A. Herrmann, P. Kiprof, K. Rypdal, J. Tremmel, R. Blom, R. Alberto, J. Behm, R. W. Albach, H. Bock, B. Solouki, D. Lichtenberger, and N. E. Gruhn, *J. Am. Chem. Soc.* **113**, 6527 (1991).
241. V. B. Ramos and R. S. Tobias, *Spectrochim. Acta* **29A**, 953 (1973).
242. Y. Kawasaki, T. Tanaka, and R. Okawara, *Spectrochim. Acta* **22**, 1571 (1966).
243. H. A. Meinema, A. Mackor, and J. G. Noltes, *J. Organomet. Chem.* **37**, 285 (1972).
244. M. G. Miles, G. E. Glass, and R. S. Tobias, *J. Am. Chem. Sec.* **88**, 5738 (1966).

245. M. M. McGrady and R. S. Tobias, *Inorg. Chem.* **3**, 1161 (1964); *J. Am. Chem. Soc.* **87**, 1909 (1965).
246. C. Z. Moore and W. H. Nelson, *Inorg. Chem.* **8**, 138 (1969).
247. G. A. Miller and E. O. Schlemper, *Inorg. Chem.* **12**, 677 (1973).
248. D. F. Ball, T. Carter, D. C. McKean, and L. A. Woodward, *Spectrochim. Acta* **20**, 1721 (1964).
249. D. F. Ball, P. L. Goggin, D. C. McKean, and L. A. Woodward, *Spectrochim. Acta* **16**, 1358 (1960).
250. J. Muller, H. Sternkicker, U. Bergmann, and B. Atakan, *J. Phys. Chem. A* **104** 3627 (2000).
251. M. W. Mackenzie, *Spectrochim. Acta* **38A**, 1083 (1982).
252. D. F. Van de Vondel and G. P. Van der Kelen, *Bull Soc. Chim. Belg.* **74**, 467 (1965).
253. H. Kimmel and C. R. Dillard, *Spectrochim. Acta* **24A**, 909 (1968).
254. C. R. Dillard and L. May, *J. Mol. Spectrosc.* **14**, 250 (1964).
255. E. Amberger, *Angew. Chem.* **72**, 494 (1960).
256. A. J. F. Clark and J. E. Drake, *Spectrochim. Acta* **34A**, 307 (1978).
257. A. J. F. Clark, J. E. Drake, and Q. Shen, *Spectrochim. Acta* **34A**, 311 (1978).
258. W. J. Lehmann, C. O. Wilson, and I. Shapiro, *J. Chem. Phys.* **32**,1088, 1786 (1960); **33**, 590 (1960); **34**, 476, 783 (1961).
259. A. S. Grady, S. G. Puntambekar, and D. K. Russell, *Spectrochim. Acta* **47A**, 47 (1991).
260. R. A. Burnham and S. R. Stobart, *J. Chem. Soc. Dalton Trans.* 1269 (1973).
261. D. J. Cardin, S. A. Keppie, and M. F. Lappert, *Inorg. Nucl. Chem. Lett.* **4**, 365 (1968).
262. A. Terzis, T. C. Strekas, and T. G. Spiro, *Inorg. Chem.* **13**, 1346 (1974).
263. G. F. Bradley and S. R. Stobart, *J. Chem. Soc. Dalton Trans.* 264 (1974).
264. N. A. D. Carey and H. C. Clark, *Chem. Commun.* 292 (1967); *Inorg. Chem.* **7**, 94 (1968).
265. B. Fontal and T. G. Spiro, *Inorg. Chem.* **10**, 9 (1971).
266. H. Bürger and U. Goetze, *Spectrochim. Acta* **26A**, 685 (1970).
267. G. Davidson, *Organomet. Rev. A* **8**, 303 (1972).
268. J. Chatt, L. A. Duncanson, and R. G. Guy, *Nature (Lond.)* **184**, 526 (1959).
269. J. A. J. Jarvis, B. T. Kilbourn, and P. G. Owston, *Acta Crystallogr.* **B27**, 366 (1971).
270. N. Rösch, R. P. Messmer, and K. H. Johnson, *J. Am. Chem. Soc.* **96**, 3855 (1974).
271. M. J. Grogan and K. Nakamota, *J. Am. Chem. Soc.* **88**, 5454 (1966); **90**, 918 (1968).
272. J. P. Sorzano and J. P. Fackler, *J. Mol. Spectrosc.* **22**, 80 (1967).
273. J. Hiraishi, *Spectrochim. Acta* **25A**, 749 (1969).
274. J. A. Crayston and G. Davidson, *Spectrochim. Acta* **43A**, 559 (1987).
275. J. Mink, M. Gal, P. L. Goggin, and J. L. Spencer, *J. Mol. Struct.* **142**, 467 (1986).
276. P. Csaszar, P. L. Goggin, J. Mink, and J. L. Spencer, *J. Organomet. Chem.* **379**, 337 (1989).
277. Y. K. Lee and L. Manceron, *J. Mol. Struct.* **415**, 197 (1997).
278. Y. K. Lee, Y. Hannachi, C. Xu, L. Andrews, and L. Manceron, *J. Phys. Chem.* **100**, 11228 (1996).
279. E. Bencze, I. Papai, J. Mink, and P. L. Goggin, *J. Organomet Chem.* **584**, 118 (1999).
280. G. Davidson and C. L. Davies, *Inorg. Chim. Acta* **165**, 231 (1989).
281. D. C. Andrews and G. Davidson, *J. Organomet. Chem.* **35**, 161 (1972).

282. M. A. Bennett, R. J. H. Clark, and D. L. Miller, *Inorg. Chem.* **6**, 1647 (1967).
283. J. Howard and T. C. Waddington, *J. Chem. Soc. Faraday Trans. 2*, **74**, 1275 (1978).
284. D. J. Stufkens, T. L. Snoeck, W. Kaim, T. Roth, and B. Olbrich-Deussner, *J. Organomet. Chem.* **409**, 189 (1991).
285. M. Bigorgne, *J. Organomet. Chem.* **127**, 55 (1977).
286. J. A. Crayston and G. Davidson, *Spectrochim. Acta* **42A**, 1385 (1986).
287. M. F. Mrozek and M. J. Weaver, *J. Phys. Chem. B* **105**, 8931 (2001).
288. A. E. Smith, *Acta Crystallogr.* **18**, 331 (1965).
289. K. Shobatake and K. Nakamota, *J. Am. Chem. Soc.* **92**, 3332 (1970).
290. D. C. Andrews and G. Davidson, *J. Organomet. Chem.* **55**, 383 (1973).
291. D. M. Adams and A. Squire, *J. Chem. Soc. A* 1808 (1970).
292. D. C. Andrews and G. Davidson, *J. Organomet. Chem.* **124**, 181 (1977).
293. G. Davidson and D. C. Andrews, *J. Chem. Soc. Dalton Trans.* 126 (1972).
294. T. B. Chenskaya, L. A. Leites, and V. T. Aleksanyan, *J. Organomet. Chem.* **148**, 85 (1978).
295. I. S. Butler and G. G. Barna, *J. Raman Spectrosc.* **1**, 141 (1973).
296. J. Howard and T. C. Waddington, *Spectrochim. Acta* **34A**, 807 (1978).
297. P. J. Hendra and D. B. Powell, *Spectrochim. Acta* **17**, 909 (1961).
298. G. Davidson, *Inorg. Chim. Acta* **3**, 596 (1969).
299. G. Davidson and D. A. Duce, *J. Organomet. Chem.* **44**, 365 (1972).
300. M. J. Grogan and K. Nakamoto, *Inorg. Chim. Acta* **1**, 228 (1967).
301. M. A. Bennett and J. D. Saxby, *Inorg. Chem.* **7**, 321 (1968).
302. B. Dickens and W. N. Lipscomb, *J. Am. Chem. Soc.* **83**, 4062 (1961); *J. Chem. Phys.* **37**, 2084 (1962).
303. R. T. Bailey, E. R. Lippincott, and D. Steele, *J. Am. Chem. Soc.* **87**, 5346 (1965).
304. G. G. Barna and I. S. Butler, *J. Raman Spectrosc.* **7**, 168 (1978).
305. S. E. Bailey, J. S. Cohan, and J. I. Zink, *J. Phys. Chem. B* **104**, 10743 (2000).
306. C. Udovich, J. Takemoto, K. Shobatake, and K. Nakamoto, unpublished.
307. M. A. Coles and F. A. Hart, *J. Organomet. Chem.* **32**, 279 (1971).
308. I. A. Garbusova, V. T. Alexanjan, L. A. Leites, I. R. Golding, and A. M. Sladkov, *J. Organomet. Chem.* **54**, 341 (1973).
309. K. Yasufuku and H. Yamazaki, *Bull. Chem. Soc. Jpn.* **45**, 2664 (1972).
310. J. Chatt, G. A. Rowe, and A. A. Williams, *Proc. Chem. Soc.* 208 (1957); J. Chatt, R. Guy, and L. A. Duncanson, *J. Chem. Soc.* 827 (1961).
311. Y. Iwashita, A. Ishikawa, and M. Kainosho, *Spectrochim. Acta* **27A**, 271 (1971).
312. Y. Iwashita, F. Tamura, and A. Nakamura, *Inorg. Chem.* **8**, 1179 (1969).
313. K. Stahl, U. Müller, and K. Dehnicke, *Z. Anorg. Allg. Chem.* **527**, 7 (1985).
314. G. J. Kubas and T. G. Spiro, *Inorg. Chem.* **12**, 1797 (1973).
315. W. M. Scovell and T. G. Spiro, *Inorg. Chem.* **13**, 304 (1974).
316. W. J. Bland, R. D. Kemmitt, and R. D. Moore, *J. Chem. Soc., Dalton Trans.* 1292 (1973).
317. D. H. Payne, Z. A. Payne, R. Rohmer, and H. Frye, *Inorg. Chem.* **12**, 2540 (1973).
318. M. Moskovitz and G. A. Ozin, *Cryochemistry*, Wiely, New York, 1976, p 263.
319. L. Manceron and L. Andrews, *J. Phys. Chem.* **90**, 4514 (1986).

320. L. Manceron and L. Andrews, *J. Phys. Chem.* **94**, 3513 (1990).
321. T. Merle-Méjean, C. Cosse-Mertens, S. Bouchareb, J. Mascetti, and M. Tranquille, *J. Phys. Chem.* **96**, 9148 (1992).
322. T. Merle-Méjean, S. Bouchareb, and M. Tranquille, *J. Phys. Chem.* **93**, 1197 (1989).
323. L. Manceron and L. Andrews, *J. Am. Chem. Soc.* **107**, 563 (1985).
324. E. S. Kline, Z. H. Kafafi, R. H. Hauge, and J. L. Margrave, *J. Am. Chem. Soc.* **109**, 2402 (1987).
325. G. A. Ozin and W. J. Power, *Inorg. Chem.* **19**, 3860 (1980).
326. D. Tevault, D. P. Strommen, and K. Nakamoto, *J. Am. Chem. Soc.* **99**, 2997 (1977).
327. A. Weselucha-Birczynska, I. R. Paeng, A. A. Shabana, and K. Nakamoto, *New J. Chem.* **16**, 563 (1992).
328. T. Szymanska-Buzar, A. J. Downs, T. M. Greene, and A. S. Marshall, *J. Organomet. Chem.* **495**, 149 (1995).
329. L. J. Morris, A. J. Downs, T. M. Greene, G. S. McGrady, W. A. Herrmann, P. Sirsch, W. Scherer, and O. Gropen, *Organometallics* **20**, 2344 (2001).
330. J. Manna, R. F. Dallinger, V. M. Miskowski, and M. D. Hopkins, *J. Phys. Chem. B.* **104**, 10928 (2000).
331. A. E. Enriquez, P. S. White, and J. L. Templeton, *J. Am. Chem. Soc.* **123**, 4992 (2001).
332. H. P. Fritz, *Adv. Organomet. Chem.* **1**, 239 (1964).
333. H. P. Fritz and L. Schäfer, *Chem. Ber.* **97**, 1827 (1964).
334. E. R. Lippincott, J. Xavier, and D. Steele, *J. Am. Chem. Soc.* **83**, 2262 (1961).
335. J. Lusztyk and K. B. Starowieyski, *J. Organomet. Chem.* **170**, 293 (1979).
336. K. A. Allan, B. G. Gowenlock, and W. E. Lindsell, *J. Organomet. Chem.* **55**, 229 (1973).
337. O. G. Garkusha, I. A. Garbuzova, B. V. Lokshin, and G. K. Borisov, *J. Organomet. Chem.* **336**, 13 (1987).
338. I. A. Garbuzova, O. G. Garkusha, B. V. Lokshin, G. K. Borisov, and T. S. Morozova, *J. Organomet. Chem.* **279**, 327 (1985).
339. A. Almenningen, A. Haaland, and T. Motzfeldt, *J. Organomet. Chem.* **7**, 97 (1967).
340. P. G. Harrison and M. A. Healy, *J. Organomet. Chem.* **51**, 153 (1973).
341. S. J. Pratten, M. K. Cooper, and M. J. Aroney, *Polyhedron* **3**, 1347 (1984).
342. K. W. Nugent, J. K. Beattie, T. W. Hambley, and M. R. Snow, *Aust. J. Chem.* **37**, 1601 (1984).
343. K. W. Nugent and J. K. Beattie, *Inorg. Chem.* **27**, 4269 (1988).
344. G. G. Garkushin, B. V. Lokshin, and G. K. Borisov, *J. Organomet. Chem.* **553**, 59 (1998).
345. B. V. Lokshin, V. T. Aleksanian, and E. B. Rusach, *J. Organomet. Chem.* **86**, 253 (1975).
346. E. R. Lippincott and R. D. Nelson, *Spectrochim. Acta* **10**, 307 (1958).
347. I. Pavlik and J. Klilorka, *Collect. Czech. Chem. Commun.* **30**, 664 (1965).
348. D. Hartley and M. J. Ware, *J. Chem. Soc. A* 138 (1969).
349. V. T. Aleksanyan, B. V. Lokshin, G. K. Borisov, G. G. Devyatykh, A. S. Smirnov, R. V. Nazarova, J. A. Koningstein, and B. F. Gachter, *J. Organomet. Chem.* **124**, 293 (1977).
350. K. Nakamoto, C. Udovich, J. R. Ferraro, and A. Quattrochi, *Appl. Spectrosc.* **24**, 606 (1970).
351. S. Sievertsen, L. Galich, and H. Homborg, *Z. Naturforsch.* **50A**, 881 (1995).
352. P. L. Stanghellini, G. Diana, E. Boccaceri, and R. Rossetti, *J. Organometal. Chem.* **593/594**, 36 (2000).

353. L. Phillips, A. R. Lacey, and M. K. Cooper, *J. Chem. Soc. Dalton Trans.* 1383 (1988).
354. I. J. Hyams, *Chem. Phys. Lett.* **15**, 88 (1972).
355. L. Schäfer, J. Brunvoll, and S. J. Cyvin, *J. Mol. Struct.* **11**, 459 (1972).
356. J. Brunvoll, S. J. Cyvin, and L. Schäfer, *J. Organomet. Chem.* **27**, 107 (1971).
357. K. Yokoyama, S. Kobinata, and S. Maeda, *Bull. Chem. Soc. Jpn.* **49**, 2182 (1976).
358. I. J. Hyams, *Spectrochim. Acta* **29A**, 839 (1973).
359. F. Rocquet, L. Berreby, and J. P. Marsault, *Spectrochim. Acta* **29A**, 1101 (1973).
360. D. M. Adams and W. S. Fernado, *J. Chem. Soc. Dalton Trans.* 2507 (1972).
361. E. Diana, R. Rossetti, P. L. Stanghellini, and S. F. A. Kettle, *Inorg. Chem.* **36**, 382 (1997).
362. E. Maslowsky, Jr. and K. Nakamoto, *Inorg. Chem.* **8**, 1108 (1969).
363. F. A. Cotton and T. J. Marks, *J. Am. Chem. Soc.* **91**, 7281 (1969).
364. G. Wilkinson and T. S. Piper, *J. Inorg. Nucl. Chem.* **2**, 32 (1956).
365. E. Gallinella, B. Fortunato, and P. Mirone, *J. Mol. Spectrosc.* **24**, 345 (1967).
366. A. Davison and P. E. Rakita, *Inorg. Chem.* **9**, 289 (1970).
367. F. W. Siegert and H. J. de Liefde Meijer, *J. Organomet. Chem.* **15**, 131 (1968).
368. F. W. Siegert and H. J. de Liefde Meijer, *J. Organomet. Chem.* **20**, 141 (1969).
369. V. I. Kulishov, E. M. Brainina, N. G. Bokiy, and Yu. T. Struchkov, *Chem. Commun.* 475 (1970).
370. J. L. Calderon, F. A. Cotton, B. G. DeBoer, and J. Takats, *J. Am. Chem. Soc.* **93**, 3592 (1971).
371. R. D. Rogers, R. V. Bynum, and J. L. Atwood, *J. Am. Chem. Soc.* **100**, 5238 (1978).
372. E. O. Fischer and Y. Hristidu, *Chem. Ber.* **95**, 253 (1962).
373. J. L. Calderon, F. A. Cotton, and J. Takats, *J. Am. Chem. Soc.* **93**, 3587 (1971).
374. A. E. Smith, *Inorg. Chem.* **11**, 165 (1972).
375. P. J. Fitzpatrick, Y. Le Page, J. Sedman, and I. S. Butler, *Inorg. Chem.* **20**, 2852 (1981).
376. S. M. Barnett, F. Dicaire, and A. A. Ismail, *Can. J. Chem.* **68**, 1196 (1990).
377. R. Feld, E. Hellner, A. Klopsch, and K. Dehnicke, *Z. Anorg. Allg. Chem.* **442**, 173 (1978).
378. D. M. Adams and A. Squire, *J. Organomet. Chem.* **63**, 381 (1973).
379. B. V. Lokshin, Z. S. Klemmenkova, and Yu. V. Makarov, *Spectrochim. Acta***28A**, 2209 (1972).
380. J. R. Durig, R. B. King, L. W. Houk, and A. L. Marston, *J. Organomet. Chem.* **16**, 425 (1969).
381. A. Davison, M. L. H. Green, and G. Wilkinson, *J. Chem. Soc.* 3172 (1961).
382. B. F. Hallam and P. L. Pauson, *Chem. Ind. (London)* **23**, 653 (1955).
383. T. S. Piper and G. Wilkinson, *Chem. Ind. (London)* **23**, 1296 (1955); *J. Inorg. Nucl. Chem.* **3**, 104 (1956).
384. M. J. Bennett, F. A. Cotton, A. Davison, J. W. Faller, S. J. Lippard, and S. M. Morehouse, *J. Am. Chem. Soc.* **88**, 4371 (1966).
385. O. S. Mills, *Acta Crystallogr.* **11**, 620 (1958); R. F. Bryan and P. T. Greene, *J. Chem. Soc. A* 3064 (1970).
386. R. F. Bryan, P. T. Greene, M. J. Newlands, and D. S. Field, *J. Chem. Soc. A* 3068 (1970).
387. F. A. Cotton and G. Yagupsky, *Inorg. Chem.* **6**, 15 (1967).

388. A. R. Manning, *J. Chem. Soc. A* 1319 (1968).
389. J. G. Bullitt, F. A. Cotton, and T. J. Marks, *Inorg. Chem.* **11**, 671 (1972).
390. A. Alich, N. J. Nelson, D. Strope, and D. F. Shriver, *Inorg. Chem.* **11**, 2976 (1972); N. J. Nelson, N. E. Kime, and D. F. Shriver, *J. Am. Chem. Soc.* **91**, 5173 (1969).
391. N. E. Kim, N. J. Nelson, and D. F. Shriver, *Inorg. Chim. Acta* **7**, 393 (1973).
392. J. S. Kristoff and D. F. Shriver, *Inorg. Chem.* **13**, 499 (1974).
393. P. McArdle and A. R. Manning, *J. Chem. Soc. A* 717 (1971).
394. F. C. Wilson and D. P. Shoemaker, *J. Chem. Phys.* **27**, 809 (1957).
395. G. Davidson and E. M. Riley, *J. Organomet. Chem.* **51**, 297 (1973).
396. R. D. Adams and F. A. Cotton, *Inorg. Chim. Acta* **7**, 153 (1973).
397. A. Davison, W. McFarlane, E. Pratt, and G. Wilkinson, *J. Chem. Soc.* 3653 (1962).
398. M. A. Neuman, Trin-Toan, and L. F. Dahl, *J. Am. Chem. Soc.* **94**, 3383 (1972).
399. A. Terzis and T. G. Spiro, *Chem. Commun.* 1160 (1970).
400. E. Maslowsky, Jr. and K. Nakamoto, *Appl. Spectrosc.* **25**, 187 (1971).
401. E. Samuel, R. Ferner, and M. Bigorgne, *Inorg. Chem.* **12**, 881 (1973).
402. P. M. Druce, B. M. Kingston, M. F. Lappert, and R. C. Srivastava, *J. Chem. Soc. A* 2106 (1969).
403. G. Balducci, L. Bencivenni, G. DeRosa, R. Gigli, B. Martini, and S. Nunziante, *J. Mol. Struct.* **64**, 163 (1980).
404. R. J. Haines, R. S. Nyholm, and M. H. B. Stiddard, *J. Chem. Soc. A* 1606 (1966).
405. G. Paliani, R. Cataliotti, A. Poletti, and A. Foffani, *J. Chem. Soc. Dalton Trans.* 1741 (1972).
406. O. Crichton and A. J. Rest, *Chem. Commun.* 407 (1973).
407. T. S. Piper and G. Wilkinson, *J. Inorg. Nucl. Chem.* **2**, 38 (1956).
408. H. Brunner, *J. Organomet. Chem.* **16**, 119 (1969).
409. R. C. Elder, F. A. Cotton, and R. A. Schunn, *J. Am. Chem. Soc.* **99**, 3645 (1967).
410. M. J. D'Aniello, Jr. and E. K. Barefield, *J. Organomet. Chem.* **76**, C50 (1974).
411. R. L. Cooper, M. L. H. Green, and J. T. Moelwyn-Hughes, *J. Organomet. Chem.* **3**, 261 (1965).
412. M. P. Johnson and D. F. Shriver, *J. Am. Chem. Soc.* **88**, 301 (1966).
413. M. Gerloch and R. Mason, *J. Chem. Soc.* 296 (1965).
414. B. D. James, R. K. Nanda, and M. G. H. Wallbridge, *Inorg. Chem.* **6**, 1979 (1967).
415. L. Banford and G. E. Coates, *J. Chem. Soc.* 5591 (1964).
416. J. E. Bercaw and H. H. Brintzinger, *J. Am. Chem. Soc.* **91**, 7301 (1969).
417. C. White, D. S. Gill, J. W. Kang, H. B. Lee, and P. M. Maitlis, *Chem. Commun.* 734 (1971).
418. J. Müller and H. Dorner, *Angew. Chem. Int. Ed. Engl.* **12**, 843 (1973).
419. J. L. Burmeister, E. A. Deardorff, A. Jensen, and V. H. Christiansen, *Inorg. Chem.* **9**, 58 (1970).
420. A. Jensen, V. H. Christiansen, J. F. Hansen, T. Likowski, and J. L. Burmeister, *Acta Chem. Scand.* **26**, 2898 (1972).
421. A. Schulz and T. M. Klapötke, *J. Organomet. Chem.* **436**, 179 (1992).
422. A. C. Filippou, W. Grünleitner, and E. Herdtweck, *J. Organomet. Chem.* **373**, 325 (1989).
423. A. C. Filippou, E. O. Fischer, and W. Grünleitner, *J. Organomet. Chem.* **386**, 333 (1990).

424. M. L. H. Green and W. E. Silverthorn, *Chem. Commun.* 557 (1971).
425. A. E. Fenster and I. S. Butler, *Can. J. Chem.* **50**, 598 (1972).
426. P. M. Treichel and G. P. Werber, *J. Am. Chem. Soc.* **90**, 1753 (1968).
427. D. C. Andrews and G. Davidson, *J. Organomet. Chem.* **36**, 349 (1972).
428. J. Howard and T. C. Waddington, *Spectrochim. Acta* **34A**, 445 (1978).
429. D. C. Andrews and G. Davidson, *J. Organomet. Chem.* **76**, 373 (1974).
430. D. Steinborn, M. Gerisch, F. W. Heinemann, J. Scholz, and K. Schenzel, *Z. Anorg. Allg. Chem.* **621**, 1421 (1995).
431. H. P. Fritz, *Z Naturforsch.* **16B**, 415 (1961).
432. M. L. H. Green, L. Pratt, and G. Wilkinson, *J. Chem. Soc.* 3753 (1959).
433. P. M. Treichel and R. L. Shubkin, *Inorg. Chem.* **6**, 1328 (1967).
434. G. Winkhaus, L. Pratt, and G. Wilkinson, *J. Chem. Soc.* 3807 (1961).
435. H. P. Fritz and E. O. Fischer, *J. Organomet. Chem.* **7**, 121 (1967).
436. H. P. Fritz, W. Lüttke, H. Stammreich, and R. Forneris, *Spectrochim. Acta* **17**, 1068 (1961).
437. S. J. Cyvin, J. Brunvoll, and L. S. Schäfer, *J. Chem. Phys.* **54**, 1517 (1971).
438. K. Judai, K. Sera, S. Amatsutsumi, K. Yagi, T. Yasuike, S. Yabushita, A. Nakajima, and K. Kaya, *Chem. Phys. Lett.* **334**, 277 (2001).
439. D. W. Ball, Z. H. Kafafi, R. H. Hauge, and J. L. Margrave, *J. Am. Chem. Soc.* **108**, 6621 (1986).
440. A. McCamley and R. N. Perutz, *J. Phys. Chen.* **95**, 2738 (1991).
441. D. van Heijnsbergen, G. von Helden, G. Meijer, P. Maitre, and M. A. Duncan, *J. Am. Chem. Soc.* **124**, 1562 (2002).
442. H. Saito, Y. Kakiuchi, and M. Tsutsui, *Spectrochim. Acta* **23A**, 3013 (1967).
443. J. D. Laposa, N. Hao, B. G. Sayer, and M. J. McGlinchey, *J. Organomet. Chem.* **195**, 193 (1980).
444. D. M. Adams, R. E. Christopher, and D. C. Stevens, *Inorg. Chem.* **14**, 1562 (1975).
445. E. M. Bisby, G. Davidson, and D. A. Duce, *J. Mol. Stract.* **48**, 93 (1978).
446. W. Wang, P. Jin, Y. Liu, Y. She, and K. Fu, *J. Phys. Chem.* **96**, 1278 (1992).
447. R. D. Nelson, W. G. Fateley, and E. R. Lippincott, *J. Am. Chem. Soc.* **78**, 4870 (1956).
448. P. D. Harvey, I. S. Butler, and D. F. R. Gilson, *Inorg. Chem.* **26**, 32 (1987).
449. L. Hocks, J. Gorrart, G. Duyckaerts, and P. Teyssié, *Spectrochim. Acta* **30A**, 907 (1974).
450. J. Goffart and L. Hocks, *Spectrochim. Acta* **37A**, 609 (1981).
451. K. O. Hodgson, F. Mares, D. F. Starks, and A. Streitwieser, Jr., *J. Am. Chem. Soc.* **95**, 8650 (1973).
452. E. Samuel and M. Bigorgne, *J. Organomet. Chem.* **19**, 9 (1969); **30**, 235 (1971).
453. F. Kaufman and D. O. Cowan, *J. Am. Chem. Soc.* **92**, 6198 (1970).
454. T. J. Katz and N. Acton, *J. Am. Chem. Soc* **94**, 3281 (1972).
455. A. Salzer and H. Werner, *Angew. Chem. Int. Ed. Engl.* **11**, 930 (1972).
456. L. A. Garbuzova, O. G. Garkusha, B. V. Lockshin, A. R. Kudinov, and K. I. Rybin-skaya, *J. Organomet. Chem.* **408**, 247 (1991).

Chapter 3

Applications in Bioinorganic Chemistry

Metal ions in biological systems are divided into two classes. The first class consists of ions such as K^+, Na^+, Mg^{2+}, and Ca^{2+}, which are found in relatively high concentrations. These ions are important in maintaining the structure of proteins by neutralizing negative charges of peptide chains and in controlling the function of cell membranes that selectively pass certain molecules. In the second class, ionic forms of Mn, Fe, Co, Cu, Zn, Mo, and so on exist in small to trace quantities, and are often incorporated into proteins (metalloproteins). The latter class is divided into two categories: (A) transport and storage proteins and (B) enzymes. Type A includes oxygen transport proteins such as hemoglobin (Fe), myoglobin (Fe), hemerythrin (Fe), and hemocyanin (Cu), electron transfer proteins such as cytochromes (Fe), iron–sulfur proteins (Fe), blue-copper proteins (Cu), and metal storage proteins such as ferritin (Fe) and ceruloplasmin Cu). Type B includes hydrolases such as carboxypeptidase (Zn) and aminopeptidase (Zn,Mg), oxidoreductases such as oxidase (Fe,Cu,Mo) and nitrogenase Mo,Fe), and isomerases such as vitamin B_{12} coenzyme (Co).

To understand the roles of these metal ions in metalloproteins, it is first necessary to know the coordination chemistry (structure and bonding) of metal ions in their active sites. Such information is difficult to obtain since these active sites are buried in a large and complex protein backbone. Although X-ray crystallography would be ideal for this purpose, its application is hampered by the difficulties in growing single crystals of large protein molecules and in analyzing diffraction data with high resolution. As will

Infrared and Raman Spectra of Inorganic and Coordination Compounds, Part B: Applications in Coordination, Organometallic, and Bioinorganic Chemistry, Sixth Edition, by Kazuo Nakamoto

be discussed later, these difficulties have been overcome in some cases, and knowledge of precise geometries has made great contribution to our understandings of their biological functions in terms of molecular structure. In other cases where X-ray structural information is not available or definitive, a variety of physicochemical techniques have been employed to gain structural and bonding information about the metal and its environment. These include electronic, infrared, resonance Raman, ESR, NMR, ORD, CD, Mössbauer spectroscopy, EXAFS, and electrochemical, thermodynamic, and kinetic measurements.

Resonance Raman (RR) spectroscopy (Sec. 1.22 of Part A) has been used extensively for the study of active sites of metalloproteins. The reason for this is twofold:

(1) Most metalloproteins have strong electronic absorptions in the UV–visible region that originate in a chromophore containing a metal center. By tuning the laser wavelength into these bands, it is possible to selectively enhance the vibrations localized in this chromophore without interference from the rest of the protein.

(2) Owing to strong resonance enhancement of these vibrations, only a dilute solution is needed to observe their RR spectra. This enables one to obtain spectra from a small volume of dilute aqueous solution under biological conditions. This is particularly significant in assigning metal–ligand vibrations by using metal–isotope techniques, because isotopes such as ^{54}Fe and ^{68}Zn are expensive.

In some cases, however, the vibrations of interest may not be enhanced with sufficient intensity. A typical example is the $\nu(O_2)$ of oxyhemoglobin. Then, one must resort to IR spectroscopy, which exhibits all vibrations allowed by IR selection rules. It should be noted, however, that IR measurements in aqueous media are generally limited to the regions where water does not absorb strongly (Sec. 1.11). Furthermore, it is often necessary to use difference techniques to cancel out interfering bands due to the solvent and some solute bands.

In the following, we will review typical results to demonstrate the utility of vibrational spectroscopy in deducing structural and bonding information about large and complex biological molecules. Marked progress has been made in biomimetic chemistry where the active site is modeled by relatively simple coordination compounds. For example, a number of iron porphyrins have been prepared to mimic heme proteins, and the vibrational spectra of some of these compounds have been discussed in Sec. 1.5 and other sections. Thus, we compare vibrational spectra of biological molecules and their model systems whenever appropriate or necessary.

Since biospectroscopy is one of the most exciting areas of modern research, the volume of literature on biological compounds is increasing explosively. It is clearly not possible to cover all important topics in a limited space. Several excellent monographs [1–6] and review articles cited in each section should be consulted for further information.

3.1. MYOGLOBIN AND HEMOGLOBIN

Myoglobin (Mb, MW $\sim$ 16,000) is an oxygen storage protein found in animal muscles. Figure 3.1 shows the structure of sperm-whale myoglobin as determined by X-ray analysis. It is a monomer consisting of 153 amino acids, and its active site is an iron protoporphyrin (see Fig. 1.24) that is linked axially to the proximal histidine (F8). In the deoxy state, the iron is divalent and high-spin, and the Fe atom is out of the porphyrin core plane by $\sim$0.6 Å as shown in Fig. 3.2. On oxygenation, the dioxygen molecule coordinates to the vacant axial position, and the heme core becomes planar. The Fe atom in oxy-Mb is low spin, and its oxidation state is close to Fe(III) (see discussion below).

Hemoglobin (Hb, MW $\sim$ 64,000) is an oxygen transport protein found in animal blood. It consists of four subunits (α_1, α_2, β_1, and β_2), each of which takes a structure similar to that of Mb. However, these four subunits are not completely independent of each other. Oxygen uptake studies show that the oxygen affinity of each subunit depends on the number of other subunits that are already oxygenated (cooperativity).

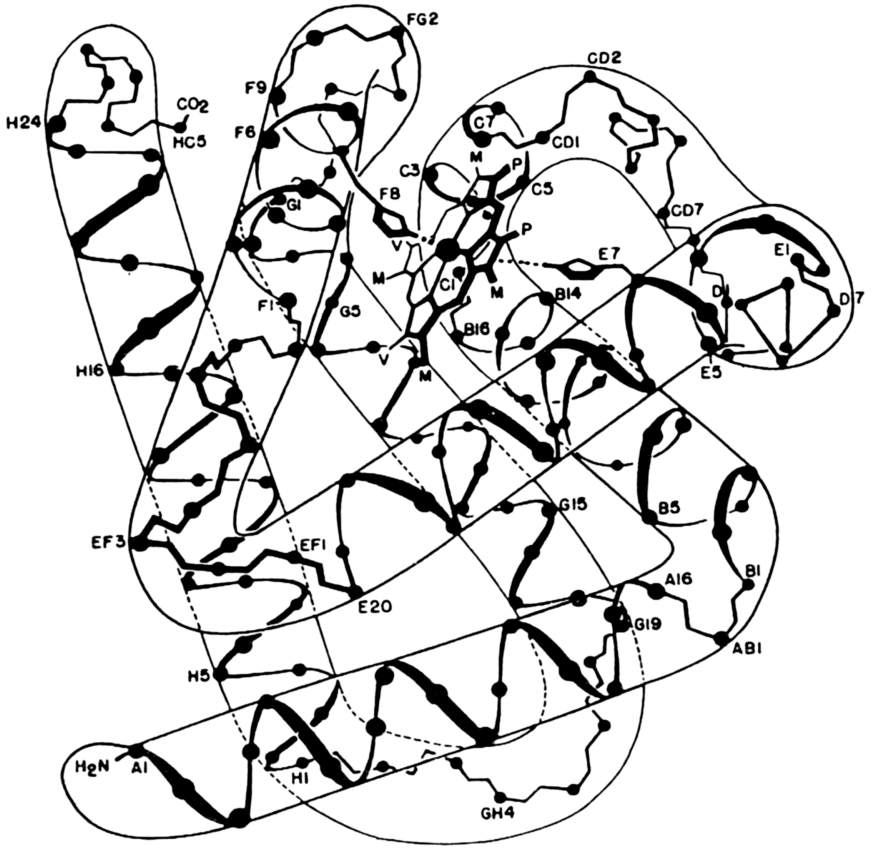

Fig. 3.1. *Structure of sperm whale myoglobin.*

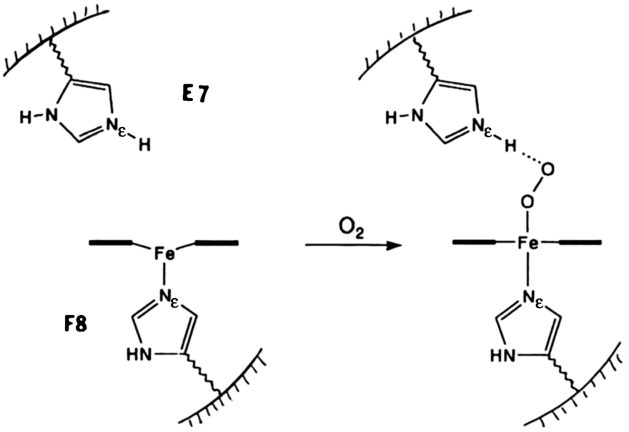

Fig. 3.2. *Structures of deoxy- and oxymyoglobins.*

This phenomenon has been explained in terms of two quaternary structures called the T and R (tense and relaxed) states. Deoxy-Hb is in the T_0 (most tense) state. As it gradually absorbs dioxygen, the R state becomes more stable than the corresponding T state. Finally, oxy-Hb assumes the R_4 (most relaxed) state [7].

Several review articles are available on RR [8–11] and IR [12] spectra of heme proteins.

3.1.1. Selective Excitation of RR Spectra

As stated previously, one of the great advantages of RR spectroscopy is its ability to selectively enhance chromophor vibrations by tuning the excitation wavelength to the electronic transition of a particular chromophor in a large and complex molecule such as myoglobin and hemoglobin. This is clearly demonstarated in Fig. 3.3, obtained by Asher [13]. The absorption spectrum of the fluoride complex of sperm whale myoglobin is shown in the bottom (b). The absorption near 500 nm is due to the Fe−F (axial ligand) CT and/or the π–π^* transition of the porphyrin core. Thus, the RR spectrum obtained by excitation near 500 nm (inset f) shows strong enhancement of the porphyrin core as well as the ν(Fe−F) vibrations. Excitation at the Soret band near 400 nm (π–π^* transition of the porphyrin core) produces the RR spectrum (inset e) in which totally symmetric porphyrin vibrations are strongly enhanced (Sec. 1.23 of Part A).

In contrast, excitation below 300 nm produces RR spectra that exhibit peptide chain vibrations with no major interference from porphyrin core vibrations. The absorption band in the 270–220 nm region originates in the π–π^* transitions of aromatic amino acids such as tyrosine and tryptophan (structures shown). Thus, their phenyl and indole ring vibrations are enhanced by excitation in this region (inset c). Strong enhancement of peptide chain vibrations can occur by excitation below 220 nm (inset d), since the electronic absorption in this region is due to the π–π^* transition of the peptide backboned [14].

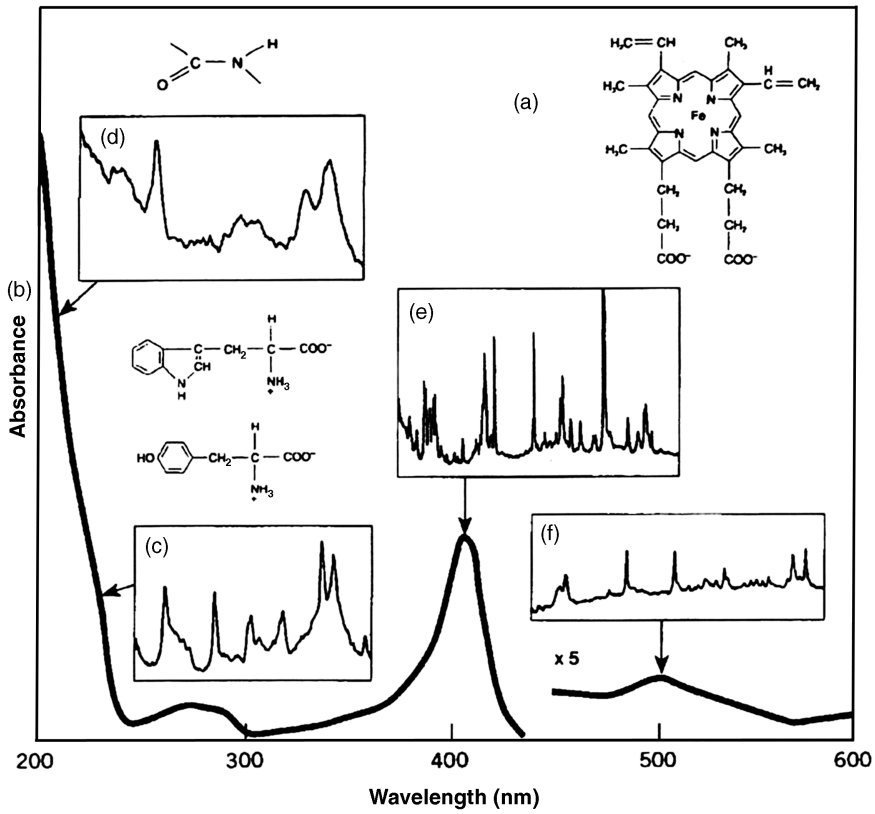

Fig. 3.3. (a) *Structure of iron protoporphyrin;* (b) *absorption spectrum of Mb fluoride;* (c) *UV excitation at 225 nm enhances tyrosine and tryptophan bands;* (d) *excitation further in the UV region enhances amide vibrations;* (e) *excitation near 400 nm enhances totally symmetric vibrations of the heme core;* (f) *the absorption bands in the 600–500 nm region are due to the porphyrin core as well as Fe–axial ligand CT transitions, and excitation in this region enhances nontotally symmetric porphyrin core vibrations as well as Fe–axial ligand vibrations [13].*

In Mb(III)F, Hb(III)F and their model compounds, the vinyl group vibrations of protoporphyrin (PP) such as the ν(C=C) near 1620 cm^{-1} are overlapped by strong porphyrin core vibrations when RR spectra are measured by Soret excitation [15]. In the case of the $[Fe(PP)(CN)_2]^-$ ion, however, the vinyl stretching as well as the vinyl–heme stretching (1125 cm^{-1}) vibrations are observed without interference by porphyrin core vibrations if excitation lines in the UV region (225 nm) are used [16]. UVRR techniques* have been utilized extensively to elucidate the structures of biological macromolecules [17].

*UV laser lines down to 175 nm can be obtained by combining the third (355 nm) and fourth (266 nm) harmonics of the Nd–YAG laser with dye lasers or hydrogen Raman shifters.

Deoxy-Hb and deoxy-Mb exhibit a weak charge transfer absorption near 764 nm (not shown in Fig. 3.3). RR spectra obtained by excitation in this region are markedly different from those obtained by B- and Q-state excitations; such an excitation exhibits a number of relatively intense low-frequency modes including those at 168 and 115 cm^{-1}, which may be due to out-of-plane deformation of the porphyrin ring [19].

3.1.2. Porphyrin Core Vibrations

"Structure-sensitive bands" of porphyrin core vibrations in heme proteins were first discovered by Spiro and Strekas [19] in 1974. Table 3.1 lists four structure-sensitive bands reported by these workers. Bands I and IV are an oxidation-state-marker and a spin-state marker, respectively, while bands II and V are sensitive to both oxidation and spin states. On the basis of these results, they proposed that the $Fe-O_2$ bond in oxy-Hb should be formulated as $Fe(III)-O_2^-$. In Sec. 1.5, we discussed structure-sensitive bands of model compounds such as Ni(OEP) and Ni(TPP) on the basis of the results of normal coordinate analyses. The normal modes obtained for these model systems are not directly transferable to heme proteins since the effects of peripheral substituents, axial ligands, and peptide chains on porphyrin core vibrations must be considered. Approximate correlations may be made, however, between these two systems. Thus, bands I, II, IV, and V listed in Table 3.1 are often referred to as the ν_4, ν_3, ν_{19}, and ν_{10} of the model compound, respectively (see Table 1.10).

The oxidation-state-sensitive bands (I, II, IV, and V) contain $\nu(C_\alpha C_m)$ or $\nu(C_\alpha N)$ as the major contributors in their potential energy distribution. By lowering the oxidation state, backdonation of *d*-electrons to the porphyrin π^* orbitals increases. Thus, the porphyrin π-bonds are weakened, and their stretching frequencies are lowered. As seen in Table 3.1, this is most clearly demonstrated by band I, which is a relatively pure oxidation-state marker. In general, axial coordination of π-acceptor ligands (CO, O_2, etc.) raises its frequency, while that of π-donor ligands (RS^-, etc.) lowers it. In fact, cytochrome P450 [Fe(II), high spin] exhibits band I at 1346 cm^{-1}, which is much lower than that of deoxy-Hb (1358 cm^{-1}) because its axial ligand is a mercaptide sulfur of a cysteinyl residue [20].

TABLE 3.1. Structure-Sensitive Bands of Heme Proteins (cm^{-1})[a]

Protein	Oxidation State	Spin State	Band I (*p*)	Band II (*p*)	Band IV (*ap*)	Band V (*dp*)
Ferricytochrome *c*	Fe(III)	Low spin	1374	1502	1582	1636
CN-Met-Hb	Fe(III)	Low spin	1374	1508	1588	1642
F-Met-Hb	Fe(III)	High spin	1374	1482	1555	1608
deoxy-Hb	Fe(II)	High spin	1358	1473	1552	1607
Ferrocytochrome *c*	Fe(II)	Low spin	1362	1493	1584	1620
oxy-Hb	Fe(II)	Low spin	1377	1506	1586	1640

[a] The bands are numbered following the convention given by T. G. Spiro and J. M. Burke [*J. Am. Chem. Soc.* **98**, 5482 (1976)]. Bands I, II, IV, and V (where *p* = polarized, *ap* = anonymous polarization, *dp* = depolarized) correspond approximately to ν_4, ν_3, ν_{19}, and ν_{10}, respectively, of metalloporphyrins (see Sec. 1.5.2). For a more complete listing, see Ref. 8.

As discussed in Sec. 1.5, the sensitivity of RR bands to spin state is attributed to expansion or out-of-plane deformation of the porphyrin core. In high-spin iron, electrons populate the antibonding $d_{x^2-y^2}$ orbital, and the lengthened Fe−N bonds are accommodated by expansion of the porphyrin core or displacement of the Fe atom from the porphyrin core plane. This results in weakening of the methine bridge bonds in high-spin complexes. Thus, the frequencies of spin-state-sensitive bands (ν_3, ν_{19}, and ν_{10}) are lower in high-spin than in low-spin complexes since all these vibrations contain $\nu(C_\alpha C_m)$ as the major contributor in their normal modes (see Table 1.10). The spin-state-sensitive bands are also metal sensitive since electron occupation in the antibonding $d_{x^2-y^2}$ orbital is varied in a series of transition metals [21].

3.1.3. Fe–Histidine Vibrations [22]

As shown in Fig. 3.2, the iron protoporphyrin is linked to the nitrogen (N_ϵ) atom of the proximal histidine (F8) in Mb, Hb, and many other heme proteins. Thus, the ν[Fe−N_ϵ(His)] vibration is highly important in understanding the nature of the *T* and *R* states mentioned previously. Nagai et al. [23] have shown definitively that the ν[Fe−N_ϵ(His)] is near 220 cm^{-1}, which is much lower than those proposed by others. Their assignments were confirmed by the observed $^{54}Fe/^{58}Fe$ isotope shifts ($\sim$2 cm^{-1}) of these bands. As seen in Fig. 3.4, this band is at 215 cm^{-1} for the *T* state of deoxy Hb,

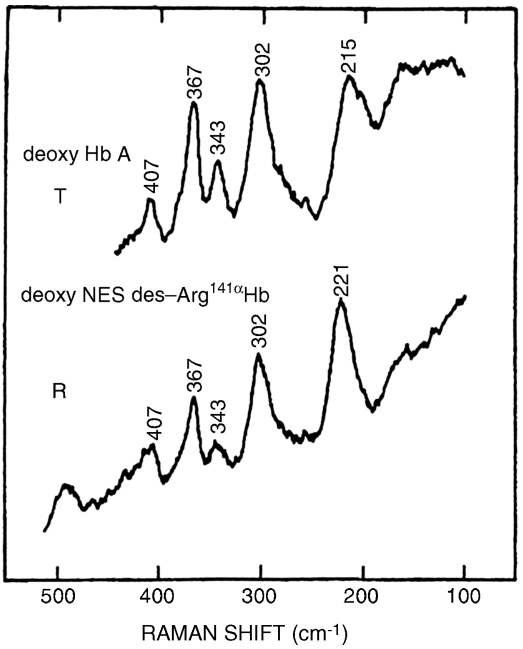

Fig. 3.4. *The RR spectra (441.6 nm excitation) of deoxy-Hb at the T and R states; Hb A and NES des-Arg (141 α)Hb were used to represent these states, respectively; the 215 cm^{-1} band is asymmetric and broad because contributions from the α and β chains are not equivalent [23].*

and at 221 cm^{-1} for the *R* state of deoxy NES des–$Arg^{141\alpha}$ Hb [23]. It is the only band that can differentiate between the *T* and *R* states of deoxy Hb. The observed upshift in going from the *T* to *R* state indicates that the Fe−N_ϵ bond is stretched in the *T* state because of a strain exerted by the globin [24]. Stein et al. [25] proposed an alternative explanation that partial donation of the $N_\delta H$ proton to an acceptor such as the COO^- group of the peptide backbone would strengthen the Fe−N_ϵ bond, and that the degree of such partial donation might be less in the *T* than in the *R* state.

The ν[Fe−N_ϵ(His)] of oxyMb [Fe(III), low spin] is much higher (271 cm^{-1}) [9] than that of deoxyMb [Fe(II), high spin] (218 cm^{-1}). Extensive isotope labeling studies have shown that the latter should be regarded as a vibration of the whole imidazole moiety against the Fe center, and not as a simple Fe−N_ϵ diatomic vibrator [26].

The RR spectrum of horse myoglobin exhibits the ν[Fe−N(His)] at 220 cm^{-1} in solution at atmospheric pressure (0.1 MPa). This band is upshifted by 2.8 cm^{-1} when high pressure (175 MPa) is applied to the sample in a hydrostatic cell. The observed upshift may be due to the sliding of the F helix (Fig. 3.1), which alters the tilt angle of the proximal histidine (F8) relative to the heme plane [27]. The ν(Fe−N(His)] of Ni-reconstututed Hb was located at 236 cm^{-1}. This band is shifted to 229 cm^{-1} by $^{58}Ni/^{64}Ni$ substitution [28].

3.1.4. Low-Frequency Vibrations

Resonance Raman spectra of Hb in the low-frequency region provide structural information on the subtle differences between two types of subunits (α and β). Deconvolution studies show that the intense band at 300 cm^{-1} of Hb consists of two bands at 299 and 304 cm^{-1}, which are attributed to the α- and β-subunits, respectively. These bands are due largely to the out-of-plane bending vibrations of the methane carbons, which are useful for detecting distorsion resulting from interactions between subunits [29].

3.2. LIGAND BINDING TO MYOGLOBIN AND HEMOGLOBIN

When a diatomic (XY) ligand such as CO, NO, and O_2 binds to myoglobin and hemoglobin, the ν(XY) as well as the ν(Fe−XY) and δ(FeXY) vibrations are expected in IR and Raman spectra. In RR spectra, the origin of resonance enhancement of these axial vibrations is attributed to "direct coupling" between the ν(Fe−XY) vibration and the porphyrin π–π^* electronic transition [9]. These axial vibrations provide valuable information about the steric and electronic effects of the heme cavity on the Fe−X−Y moiety.

3.2.1. CO Adducts [5,30]

In general, the ν(CO) is strong in IR but weak in RR spectra. The opposite trend holds for the ν(Fe−CO) and δ(FeCO) in the low-frequency region. Tsubaki et al. [31] first

assigned the ν(CO), δ(FeCO), and ν(Fe−CO) of HbCO at 1951, 578, and 507 cm^{-1}, respectively. Isotopic substitution experiments show

	$^{12}C^{16}O$		$^{13}C^{16}O$		$^{12}C^{18}O$		$^{13}C^{18}O$
δ(FeCO) (cm^{-1})	578	>	563	<	576	>	560
ν(Fe−CO) (cm^{-1})	507	>	503	>	498	>	494

These assignments were supported by approximate normal coordinate analysis on a linear (tilted) Fe−C≡O model. The δ(FeCO) exhibits a "zigzag" pattern (Sec. 1.18.7), whereas the ν(Fe−CO) changes monotonously as the mass of CO increases. Although the trend δ(FeCO) > ν(Fe−CO) is somewhat unusual, it has been reported for some metal carbonyls (Table 1.48). Hirota et al. [32] assigned the δ(FeCO) at 365 cm^{-1} and attributed the band at 578 cm^{-1} to a combination of the δ(FeCO) with a porphyrin or a Fe−C deformation mode (displacement of the C atom parallel to the porphyrin plane). Their assignments are based on the Raman difference spectra of HbCO obtained by using four isotopomers of CO. On the other hand, Hu et al. [33] observed two strong bands at 574 and 495 cm^{-1} in the IR spectrum of Fe(OEP)(py)(CO) that were downshifted by 17 and 5 cm^{-1}, respectively, by $^{12}CO/^{13}CO$ substitution. However, they could not observe any isotope-sensitive bands near 360 cm^{-1}. This observation led them to support the original assignment by Tsubaki et al. Further support was provided by RR studies of selectively deuterated hemes [34] and DFT calculations [35,36].

As discussed in Sec. 1.18, σ-donation from the CO to the metal tends to raise the ν(CO) while π-backdonation from the metal to the CO tends to lower the ν(CO). It is expected, therefore, that the Fe−C bond order would increase, and the CO bond order would decrease, as π-backbonding increases. In fact, a negative linear relationship was found between the ν(CO) and ν(Fe−CO) in a series of heme proteins containing imidazole as the axial ligand [37]. Deviation from the straight-line relationship occurs when (1) electron-donating substituents are introduced in the porphyrin ring, (2) the donor strength of the *trans* axial ligand is increased, and (3) the coordinated CO interacts with the distal histidine.

In a protein-free environment, the Fe−C≡O bond is perpendicular to the porphyrin plane. In the heme cavity, however, it may be bent and/or tilted owing, to steric hindrance and/or electronic interaction with distal histidine (E7). Three probable geometries are illustrated in Fig. 3.5. According to X-ray analysis [38], the Fe−C≡O bond in MbCO is linear but tilted by 13° from the normal to the porphyrin plane. Such distortion is expected to raise the ν(CO) since it decreases the Fe($d\pi$) → CO(π^*)

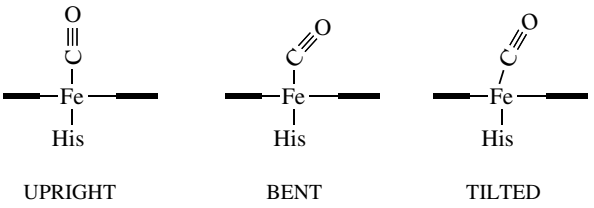

Fig. 3.5. *Three geometries of Fe−C≡O bond in heme proteins.*

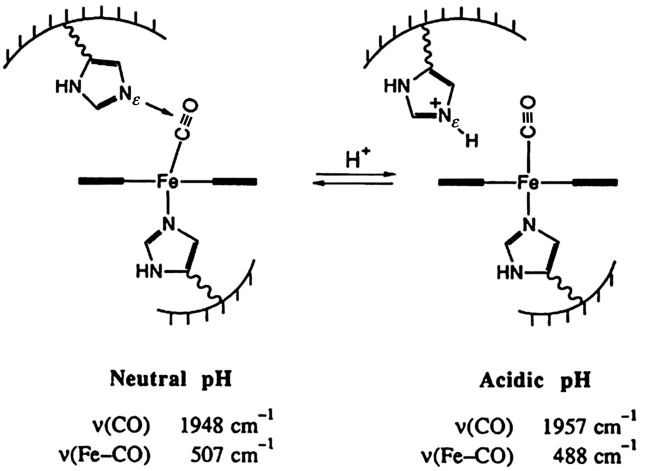

Fig. 3.6. *Orientation of distal histidine at neutral and acidic pH.*

backbonding. However, this effect is overcome by an increase in the pyrrole (π)−CO (π^*) overlap resulting from such tilting. As a result, tilting lowers the ν(CO) and raises the ν(Fe−CO) as discussed for "strapped" porphyrins in Sec. 1.18.4.

In heme proteins, the upright $\rightleftharpoons$ tilted conformational change is observed by changing the pH of the solution. Thus, the ν(Fe−CO) of the sperm whale MbCO at 507 cm^{-1} in neutral pH solution is shifted to 488 cm^{-1} in acidic solution [39]. This result corresponds to the previous IR observation that the ν(CO) of soybean legHbCO at 1947.5 cm^{-1} in neutral pH is upshifted to 1957 cm^{-1} in acidic solution [40]. As illustrated in Fig. 3.6, the N_ε atom of the distal histidine is protonated in acidic solution. This may induce the displacement of the histidine to accommodate the upright geometry of the Fe−C≡O bond. Similar upshifts of the ν(CO) are observed when the β-chain distal histidine of Hb is replaced by nonpolar residues such as glycine and valine [41], and when the degree of hydration of hydrated films of Hb and Mb is changed [42].

The IR spectra of sperm whale MbCO exhibit three ν(CO) near 1967, 1944, and 1933 cm^{-1} in solution as well as in the crystalline state. Three different environments of the Fe−C≡O moiety were proposed to account for this observation [43]. In human HbCO, two ν(CO) bands of α and β subunits overlap to give a single band at 1951 cm^{-1}. In contrast, rabbit HbCO exhibits two ν(CO) at 1951 (β) and 1928 (α) cm^{-1}; the latter frequently is unusually low, and its intensity is about half that of the former. It has been suggested that the distal histidine acts as a nucleophilic donor to the CO in the α subunit [44]. All the observations of ν(CO) mentioned above were made by using aqueous IR techniques (Sec. 1.11).

3.2.2. O_2 Adducts [5,30]

As discussed in Sec. 1.21, dioxygen coordinated to metalloporphyrins can take end-on, side-on, and bridging structures. However, the bridging structure is too bulky to occur in a heme cavity. Although the side-on coordination is stereochemically

possible, it may be too unstable under biological conditions. Thus, the end-on coordination, such as shown in Fig. 3.2, is most probable. In fact, this structure was found by X-ray [45] and neutron diffraction [46] on MbO_2 and X-ray diffraction on HbO_2 [47]. These studies also revealed the presence of hydrogen bonding between the bound O_2 and the N_ε atom of the distal imidazole (Fig. 3.2). The $N-H\cdots O_2$ distance in MbO_2 is 2.97 Å, whereas in HbO_2 it is 3.7 and 3.2–3.4 Å, respectively, for the α- and β-subunits.

The coordinated dioxygen of the end-on type exhibits the $\nu(O_2)$, $\nu(Fe-O_2)$, and $\delta(FeOO)$. Thus far, the $\nu(O_2)$ of heme proteins have been observed only in IR spectra. Attempts to resonance-enhance this mode have been unsuccessful because the "direct coupling" mechanism invoked for CO adducts does not work or because the oscillator strength of the $Fe \rightarrow O_2$ CT transition is too small [9]. Exceptions are found in five-coordinate $Fe(TPP)O_2$ (Sec. 1.21) and O_2 adducts of cytochrome P450 (Sec. 3.3). In contrast, the $\nu(Fe-O_2)$ and $\delta(FeOO)$ in the low-frequency region have been observed exclusively by RR spectroscopy. Thus, the $\nu(Fe-O_2)$ vibration of HbO_2 was first observed at 567 cm^{-1} by Brunner [48], and the end-on geometry was confirmed by $^{16}O^{18}O$ experiments that showed two $\nu(Fe-O_2)$ vibrations due to mixing of the $Fe-^{16}O-^{18}O$ and $Fe-^{18}O-^{16}O$ bonds [49]. Hirota et al. [50] were able to locate the $\delta(FeOO)$ of HbO_2 at 425 cm^{-1} using Raman difference techniques. As shown in Fig. 3.7, difference features are observed at 568 and 425 cm^{-1}. The same results were obtained independently by Jeyarajah et al. [51].

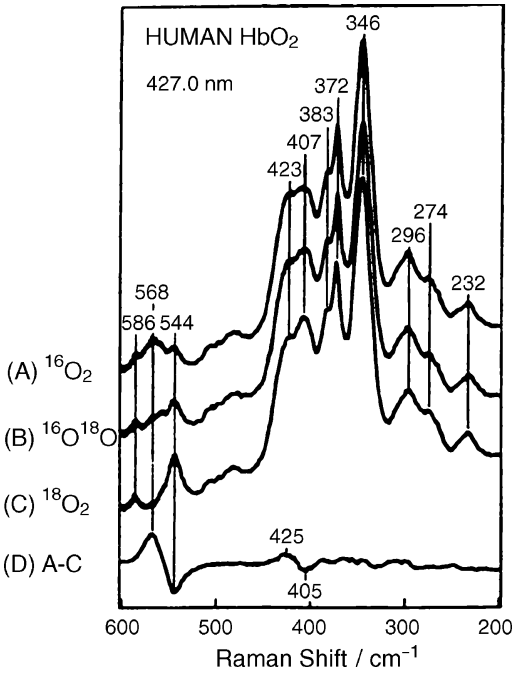

Fig. 3.7. *The RR spectra (427.0 nm excitation) of HbO_2 and their difference spectrum as specified [50].*

The $\nu(O_2)$ of HbO_2 was first located at 1107 cm^{-1} by IR spectroscopy [52]. This was followed by similar work on MbO_2 that gave almost the same frequency [53]. Later IR studies revealed, however, that HbO_2 exhibits two $\nu(O_2)$ bands at 1156 and 1107 cm^{-1}, although a single $\nu(^{18}O_2)$ was observed at 1065 cm^{-1}. Therefore, the observed splitting was attributed to Fermi resonance between $\nu(^{16}O_2)$ near 1130 cm^{-1} and the first overtone of the $\nu(Fe-O_2)$ at 567 cm^{-1} [11].

The interpretation presented above was challenged by Tsubaki and Yu [54], who observed the $\nu(O_2)$ of cobalt(II)-reconstituted HbO_2 ($CoHbO_2$) using Soret excitation, which is in resonance with the $Co-O_2$ CT transition. These workers observed three oxygen–isotope-sensitive bands at 1152 (weak), 1137 (strong), and 1107 cm^{-1} (very weak). The origin of this multiple-band structure was attributed to the presence of two conformers; conformer I is responsible for the bands at 1137 and 1107 cm^{-1}, which result from Fermi resonance between the unperturbed $\nu(O_2)$ ($\sim$1122 cm) and the porphyrin mode at 1121 cm^{-1}, whereas conformer II is responsible for the 1152 cm^{-1} band. This interpretation is based on X-ray analysis of MbO_2 in which the $Fe-O-O$ plane can take two orientations relative to the porphyrin plane [45]. Thus, in conformer I, the $Co-O-O$ plane is in the direction that permits the formation of the $N-H\cdots O_2$ bond mentioned earlier. In conformer II, this plane is rotated by about 40° from that of conformer I so that the O_2 is free from hydrogen bonding. As a result, the $\nu(O_2)$ of the latter (1152 cm^{-1}) is much higher than that of the former ($\sim$1122 cm^{-1}). The observed upshift of the 1137 cm^{-1} band (2 cm^{-1}) by D_2O/H_2O (solvent) exchange was regarded as evidence to support their interpretation [55]. More recent IR studies by Potter et al. [56] confirmed the presence of the three bands mentioned above. These workers noted, however, that the observed difference in $\nu(O_2)$ (30 cm^{-1}) between the two conformers is too large to attribute it to the effect of hydrogen bonding alone, and proposed a structure of conformer I in which the $Fe-O-O$ and imidazole planes are eclipsed on the $N-Fe-N$ axis of the porphyrin ring since π-electron donation from the imidazole to the O_2 mediated through the metal would cause a marked reduction in the $\nu(O_2)$.

Quite contrary to these investigations, Bruha and Kincaid [57] interpret the RR spectra of $CoMbO_2$ and $CoHbO_2$ in terms of a single conformer. Figure 3.8 shows the RR spectra of $CoHbO_2$ obtained by these authors. The complicated features arise because of two reasons. First, several porphyrin vibrations appear in this region. They are easily identified at 1228, 1174, $\sim$1136, and $\sim$1123 cm^{-1} because they show no oxygen–isotope shifts and appear in all the compounds studied. Second, the remaining oxygen–isotope-sensitive bands are analyzed by considering the possibilities of vibrational couplings between the $\nu(O_2)$ fundamental and internal modes of imidazole (proximal or distal). In this case, vibrational coupling occurs between the $\nu(^{16}O_2)$ near 1136 cm^{-1} and the imidazole mode near 1160 cm^{-1}. Similar coupling occurs between the $\nu(^{18}O_2)$ near 1063 cm^{-1} and the second imidazole mode near 1100 cm^{-1} (these imidazole bands are seen in the spectrum of histidine shown by the dotted line in trace A). Thus, the $\nu(^{16}O_2)$ and $\nu(^{18}O_2)$ of HbO_2 are assigned near 1136 and 1063 cm^{-1}, respectively. As stated in Sec. 1.21.5, these vibrational couplings have been analyzed quantitatively by using the Fermi resonance scheme.

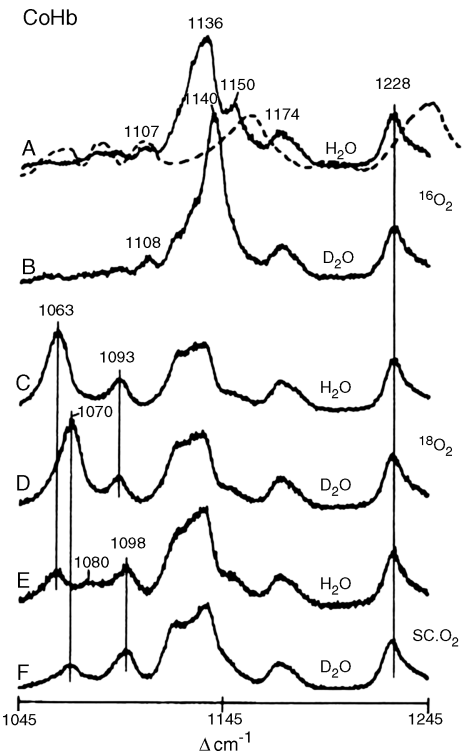

Fig. 3.8. *The RR spectra (406.7 nm excitation) of CoHbO_2 and its $^{18}O_{2_a}$ and scrambled O_2 adducts in H_2O and D_2O. The dashed line in* (A) *indicates the Raman spectrum of* L*-histidine [57].*

Vibrational spectra of O_2 adducts of heme protein model compounds such as "picket-fence" and "strapped" porphyrins have also been discussed in Sec. 1.21.5.

3.2.3. NO Adducts [12,30]

Similar to the case of O_2 adducts, the NO groups bonded to ferrous Mb and Hb take a bent end-on geometry. The bent Fe−N−O group is expected to show the ν(NO) at 1700–1600 cm^{-1}, and the ν(Fe−NO) and δ(FeNO) in the 600–400 cm^{-1} region. The NO has been used to probe conformational changes of the heme moiety when the quaternary structure of Hb is switched from the *R* to the *T* state. Human HbNO in the *R* state has four six-coordinate hemes, whereas the *T* state is a hybrid of five- and six-coordinate NO moieties. Using IR spectroscopy, Maxwell and Caughey [58] observed the ν(NO) of six-coordinate heme (*R* state) at 1618 cm^{-1} and that of five-coordinate heme (*T* state induced by adding IHP (inositol hexaphosphate) at 1668 cm^{-1}. The lack of discernible pH effects on these frequencies suggested that a polar (donor–acceptor) interaction is more likely than hydrogen bonding between the NO and the distal imidazole. Spiro and coworkers [59,60] observed the ν(Fe−NO) of these six- and five-coordinate hemes near 550 and 590 cm^{-1}, respectively (413.1 and 454.5 nm

excitation). However, Yu and coworkers [61,62] could not detect the latter by 406.7 nm excitation. According to Benko and Yu [63], the band near 554 cm^{-1} in ferrous MbNO is the δ(FeNO) and not ν(Fe−NO). Their assignment is based on the zigzag isotopic shift pattern in the order of $NO(554\ cm^{-1}) > {}^{15}NO(545\ cm^{-1}) < N^{18}O(554\ cm^{-1})$.

Figure 3.9 shows the RR spectra of NO adducts of ferrous Mb obtained by Hu and Kincaid [64]. These workers assigned the bands at 554 and 449 cm^{-1} to the ν(Fe−NO) and δ(FeNO), respectively, although substantial mode mixing was noted. The former shows a zigzag isotope shift pattern, whereas the frequency of the latter decreases monotonously as the total mass of the NO ligand increases. Thus, the observation of a zigzag isotope shift pattern does not necessarily indicate a bending mode. Normal coordinate analysis on a bent FeNO model shows that local internal coordinates are mixed substantially and the degree of contribution of each coordinate to these vibrations depends on the FeNO bending angle.

The NO can also bind to ferric heme proteins, although ferric nitrosyl complexes have a tendency for spontaneous autoreduction. Since the Fe(III)−NO is isoelectronic with the Fe(II)−CO, it may take a linear geometry which would be distorted in a heme cavity. The ν[Fe(III)−NO] and δ[Fe(III)NO] of MbNO are observed at 595 and 573 cm^{-1}, respectively [63]. In this case, the latter shows a zigzag isotope shift pattern.

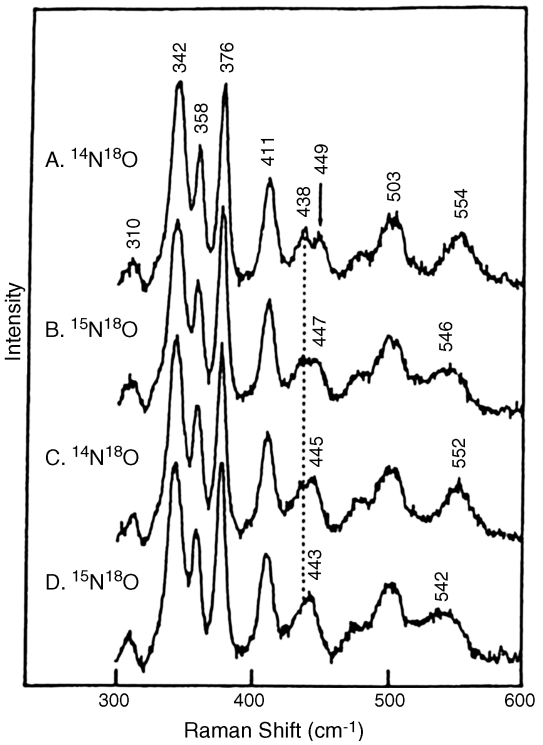

Fig. 3.9. *The RR spectra (406.7 nm excitation) of MbNO with four NO isotopomers [64].*

The NO group vibrations are also reported for the NO adducts of Co(II)-[65,66] and Mn(II)-reconstituted [67] Mb and Hb. The following trend is found in the Mb series:

	ν[Mn(II)−NO]	> ν[Fe(III)−NO]	> ν[Co(II)−NO]	> ν[Fe(II)−NO]
$\tilde{\nu}$(cm^{-1})	627	595	576	554

The RR spectra of NO adducts of Mn(II) complexes of "unprotected" and "strapped" porphyrins (Fig. 1.64b) have been compared to study the steric effects of the "strap" [68]. Vibrational spectra of NO adducts of heme proteins have been reviewed by Wang et al. [69].

3.2.4. Adducts of Other Axial Ligands [11,30]

The CN^- ion binds strongly to ferric heme proteins. The ν(CN) of ferric MbCN and HbCN are observed at 2125 cm^{-1} in IR spectra [70]. This frequency is higher than that of free CN^- ion (2083 cm^{-1}) for the reason discussed in Sec. 1.16. Since the Fe(III)−C≡N bond is linear, it may be distorted in a heme cavity. Although an X-ray diffraction study on ferric (or met) HbCN confirmed such a distortion, the exact geometry has not yet been known because of poor resolution (2.8 Å) [71]. Yu et al. [72] suggest that the linear Fe−C≡N bond is tilted only because both the ν(Fe–^{13}C≡N) and ν(Fe–C≡^{15}N) bands appear at 450 cm^{-1}. The CN^- ion can also bind to ferrous heme proteins, but its affinity is much lower and the corresponding complexes are readily photodissociated.

The N_3^- ion binds to ferric heme proteins to form a mixture of high-spin (hs) and low-spin (ls) complexes at room temperature. Thus, the IR spectrum of metMbN_3 exhibits two $\nu_a(N_3)$ bands at 2045 and 2023 cm^{-1} that were assigned to the hs and ls complexes, respectively. Similar bands were observed at 2047 (hs) and 2025 (ls) cm^{-1} for metHbN_3 [70]. In RR spectra, Tsubaki et al. [73] observed two sets of porphyrin vibrations corresponding to the low- and high-spin states of metMbN_3. They also assigned the RR band at 411 cm^{-1} to the ν(Fe−N_3) of the low-spin complex, although the band at 413 cm^{-1} was previously assigned to the high-spin complex [74].

The ν(Fe−OH) of metHbOH is observed at 495 cm^{-1} [75]. In the abnormal subunit of Hb M Boston, the heme iron is bonded to the phenolate oxygen of tyrosine (E7) [76] instead of the proximal histidine (F8). Nagai et al. [77] assigned the band at 603 cm^{-1} to the ν[Fe−O(tyrosine)].

In metMbF, the ν(Fe−F) vibrations were observed at 461 and 421 cm^{-1} which were attributed to the nonhydrogen-bonded and hydrogen-bonded (to water) Fe−F moieties, respectively [78].

3.2.5. Photochemistry of HbCO and HbO_2

Time-resolved resonance Raman (TR^3) spectroscopy (Sec. 1.4.2) has been utilized extensively to study the structures and dynamics of extremely short-lived transient species [in the order of nanosecond (10^{-9}) and picosecond (10^{-12})] that are created by photolysis of HbCO, HbO_2, and other proteins [79–81].

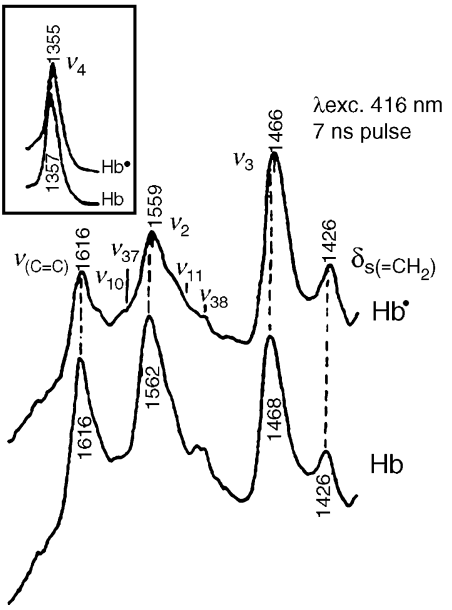

Fig. 3.10. *Soret band excited RR spectrum of deoxyHb and Hb* with 416-nm, 7-ns pulses [82].*

Dasgupta and Spiro [82] measured the RR spectra of deoxy-Hb and the photoproduct of HbCO (abbreviated as Hb*) using 7 ns Nd–YAG laser pulses at wavelengths of 416 and 533 nm. As stated in Sec. 1.23 of Part A, Soret excitation (416 nm) enhances the totally symmetric modes (ν_2, ν_3, and ν_4), whereas Q excitation (532 nm) enhances nontotally symmetric modes (ν_{10}, ν_{11}, and ν_{19}). Figure 3.10 compares the RR spectra (Soret excitation) of these two compounds. It is seen that the bands at 1562 (ν_2), 1468 (ν_3), and 1357 cm^{-1} (ν_4; see Fig. 3.10 inset) of deoxy-Hb are downshifted by 2–3 cm^{-1} in Hb*. Similar downshifts are observed for nontotally symmetric vibrations of Hb*. These results suggest that the photoproduct, Hb*, has a slightly expanded porphyrin core because of the out-of-plane displacement of the Fe atom by ~0.1 Å relative to the deoxy-Hb structure. To gain more detailed information, Kincaid et al. [83] prepared two hybrid Hb such as $(\alpha\beta^*)_2$ and $(\alpha^*\beta)_2$ where α^* and β^* denote protoheme-*d*4 subunits, and measured the RR spectra of their native states and the photoproducts of HbCO with 10 ns Nd–YAG laser line at 532.1 nm. The ν_{19} frequency (subunit-specific structural marker band) shows no difference between the two photoproducts of the above two hybrid Hb in spite of significant differences observed for their equilibrium deoxy forms. Thus, subunit heterogeneity does not exist in the photoproducts. Similar work on HbO_2 [84] shows that the photoproduct obtained by ~30-ps pulses (532 nm) exhibits the ν_{10} and ν_{11} at frequencies lower by 10 and 5 cm^{-1}, respectively, than the HbCO photoproduct. These large shifts were attributed tentatively to the formation of an electronically excited deoxy-Hb.

Kaminaka et al. [85] studied the dynamics of quaternary structural changes of HbCO after the photolysis by using UV TR^3 spectroscopy (218 nm). Finally, ultrafast

femtosecond (10^{-15}) IR spectroscopy was used to characterize ^{13}CO bonded to the α- and β-subunits of Hb M Boston [86].

Mizutani and Kitagawa [87] carried out an extensive TR^3 study on ultrafast dynamics of photodecomposition of MbCO and its derivatives. Since Mb has no quaternary structures, their interest was focused on the structure and the timeframe of the photodissociated product (Mb*). Figure 3.11 compares temporal changes of the Raman intensities of the ν(Fe−N) of the proximal histidine at 220 cm^{-1} and the porphyrin core (out-of-plane) vibrations, γ_7, at 301 cm^{-1}. These vibrations serve as monitors in detecting structural changes in the protein matrix and the porphyrin core, respectively. As seen in the figure, the temporal intensity change of γ_7 shows that structural changes in the porphyrin core by photodissociation are completed within the instrumental response time of the apparatus used (~2 ps) and the equilibrium structure is reached within a few picoseconds. On the other hand, the temporal intensity change

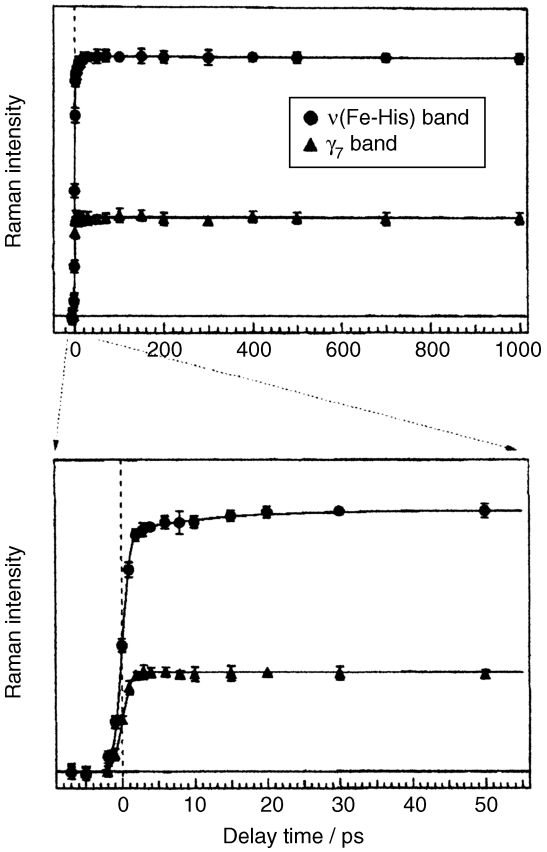

Fig. 3.11. *Temporal changes of Raman intensities of the Stokes ν(Fe−His) (circles) and γ_7 (triangles) of photo-dissociated MbCO. The solid lines indicate the calculated fits. The lower panel shows a close-up of the curve in the early time region [87].*

of the ν(Fe−N) shows a gradual increase up to ~20 ps after instantaneous rise on photodissociation. Thus, changes in the tertiary structure of the protein are much slower than that of the heme core caused by the Fe−CO bond cleavage.

3.3. CYTOCHROMES AND OTHER HEME PROTEINS

3.3.1. Cytochrome *c* [88]

Cytochromes (*a*, *b*, and *c*) are electron carriers in the mitochondrial respiratory chain. Among them, cytochromes *c* are relatively small (MW ~ 13,000) and relatively easily crystallized. The structures of cytochromes *c* from various sources have been determined by X-ray crystallography [89]. These studies show that the prosthetic group of cytochrome *c* is a heme in which the vinyl sidechains of iron protoporphyrin are replaced by cysteinyl thioether bonds and to which the imidazole (His 18) nitrogen and the methionine (Met 80) sulfur (thioether) atoms are coordinated axially. One of the structural features of cytochrome *c* is the presence of an "opening" at the edge of the heme cavity through which the electron transfer may occur. In most cytochrome *c*, the iron atoms are in the low-spin state, and the basic structure of the heme is unchanged by changing the oxidation state of the iron [90]. As shown in Table 3.1, bands I (ν_4), II (ν_3), and V (ν_{10}) are shifted markedly to higher frequencies in going from the ferrous to ferric states [19].

Cytochrome *c* takes five different structures depending on the pH with

I		II		III		IV		V
	0.42		2.50		9.35		12.76	

p*K* values shown above [91]. As stated above, the heme iron is axially bonded to the imidazole nitrogen (His 18) and the methionine sulfur (Met 80) at neutral pH (III). However, these axial ligands are replaced by water at acidic pH (I and II). At alkaline pH, the Fe−S (Met 80) bond is cleaved and may be replaced by another ligand (Lys 79), although the Fe−N (His 18) bond is intact (IV). At extremely alkaline pH, both of these axial ligands may be replaced by other ligands. Thus, vibrational studies of cytochrome *c* as a function of pH are of particular interest.

The RR spectra of ferricytochrome *c* as a function of pH were first studied by Kitagawa et al. [92]. These workers noted that the bands at 1375 (ν_4), 1504 (ν_3), 1563 (ν_{11}), and 1637 cm (ν_{10}) are shifted by 2–3 cm^{-1} to higher frequencies when the pH is increased from 7 to 10.8. This result is expected since a weak π-backdonation from the Met 80 to the porphyrin (π^*) via the Fe(dπ) orbital is disrupted at alkaline pH. As mentioned above, both axial ligands are replaced by water at pH = 2.5. Lanir et al. [93] observed that the bands at 1563 (ν_{11}), 1585 (ν_{19}), and 1637 cm (ν_{10}) are downshifted to 1556, 1569, and 1623 cm^{-1}, respectively, by decreasing the pH from 7.0 to 2.0. Thus, these workers concluded that structure II mentioned above is high spin.

The RR spectra of ferrocytochrome *c* at pH = 7–11.2 exhibit many bands below 500 cm^{-1}. At pH = 13.6, however, this feature is replaced by a much simpler spectrum in this region. Valance and Strekas [94] interpret this result as follows. In neutral to alkaline solution, the heme is rigidly held by the peptide chain, and the resulting asymmetric heme activates many Raman bands. At pH over 13, however, the protein structure is relaxed (unfolded) and the symmetry of the heme becomes effectively higher, resulting in fewer Raman bands. Thus far, not much information is available on axial vibrations. The ν[Fe−N (His 18)] is observed at 182 cm^{-1}, and the ν[Fe−S (Met 80)] is estimated to be near 344 cm^{-1} [95].

Hu et al. [96] measured the RR spectra (Soret and Q excitation) of ferrocytochrome *c* and its isotopomers (*meso-d*4 and pyrrole-^{15}N, etc.) at neutral pH, and assigned most of the in-plane and out-of-plane skeletal modes according to the assignments obtained for Ni(OEP) (Sec. 1.5). This is justifiable because cytochrome *c* does not have the conjugating vinyl groups of protoporphyrins that complicate the vibrational assignments. Their results manifest the out-of-plane distorsions of the porphyrin core found by high-resolution X-ray diffraction studies [97]. For example, two anomalously polarized bands (ν_{19} and ν_{21}) gain substantial intensity by Soret excitation, and the depolarized band (ν_{15}) becomes extraordinarily strong. These and other observations suggest that the $\mathbf{D}_{4h}$ symmetry of the porphyrin core is lowered by "suddle-shaped distortion" [96].

X-Ray analysis has been reported on several model compounds of cytochrome *c* such as [Fe(TPP)(THT)$_2$]ClO_4 and [Fe(TPP)(PMS)$_2$]ClO_4, where THT and PMS denote tetrahydrothiophene and pentamethylene sulfide, respectively [98,99]. Oshio et al. [100] assigned the ν_a(S−Fe−S) of these compounds at 328 and 323.5 cm^{-1}, respectively, based on $^{54}Fe/^{56}Fe$ isotope shifts observed in IR spectra.

3.3.2. Cytochrome P450 [101]

Cytochromes P450 (MW ∼ 50,000) are monooxygenase enzymes that catalyze hydroxylation reactions of substrates such as drugs, steroids, pesticides, and carcinogens:

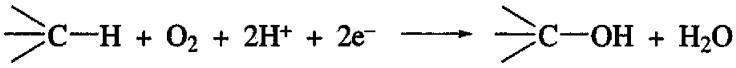

One of the microbial species in which cytochrome P450 is found is *Pseudomonas putida*. When this bacterium is grown in air with camphor as the substrate, cytochrome $P450_{cam}$ can be isolated in a crystalline form. Thus far, most spectroscopic studies have been made on this compound. The term P450 was used because its CO adduct exhibits the Soret band at 450 nm.

The active site of cytochrome P450 is an iron protoporphyrin with the iron center axially bound to the mercaptide sulfur of a cysteinyl residue. The axial Fe−S linkage is retained throughout its reaction cycle shown in Fig. 1.12 [101]. This was confirmed by X-ray analysis [102] of cytochrome $P450_{cam}$ (b state). The resting state (a) is a six-coordinate ferric low-spin porphyrin with H_2O as the axial ligand *trans* to the Fe−S linkage. Binding of a substrate (SH) disrupts the Fe−OH_2 bond and converts it to

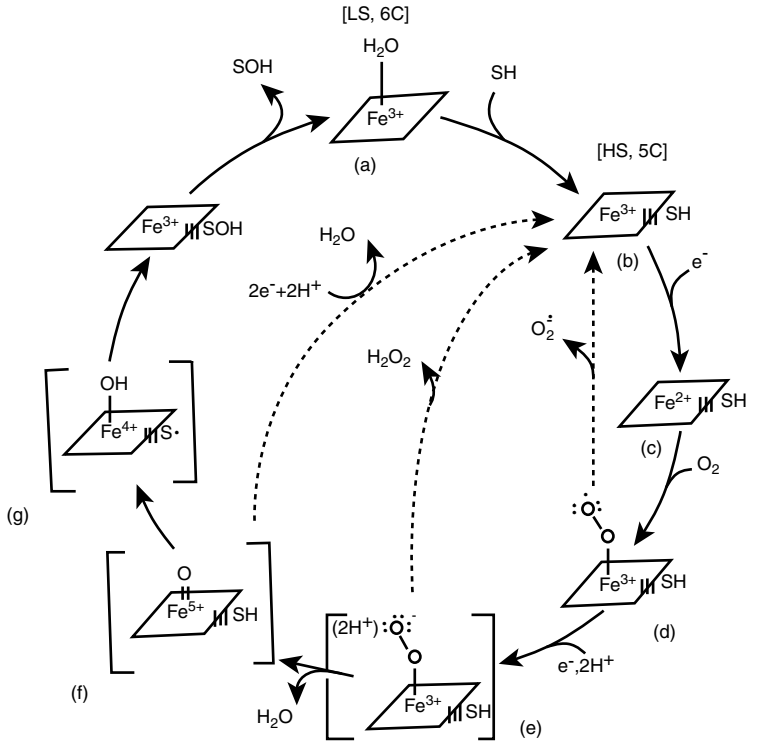

Fig. 3.12. *Catalytic cycle of cytochrome P450 [101]. The axial Fe–S bond is not shown.*

b state, which is a ferric five-coordinate (5C) high-spin (HS) state. In general, this conversion produces a mixture of high- and low-spin complexes, and the fraction of the high-spin species depends on the substrate; it is 95% for a large substrate such as camphor but only 43% for a small substrate such as norcamphor [103].

b state is converted to c state (five-coordinate, ferrous, high-spin complex) by accepting electrons from iron–sulfur proteins (Sec. 3.8) and other reducing agents. Oxygenation of c state yields an O_2 adduct (d state) that is the last detectable intermediate in the reaction cycle. Thus, the structures of e–g states shown in Fig. 3.12 were proposed without definitive evidence.

As stated in Sec. 3.1, Ozaki et al. [20] observed the oxidation-state marker band of cytochrome $P450_{cam}$ in the c state at 1346 cm^{-1}, which is much lower than those of other Fe(II) porphyrins. Similar observations have been made for cytochromes P450 from other sources [104]. This anomaly was attributed to the extra negative charge transmitted to the porphyrin $\pi^*(e_g)$ orbital from the mercaptide sulfur (RS^-), which has two lone-pair electrons. Champion et al. [105] first observed the ν(Fe–S) of cytochrome $P450_{cam}$ (b state) at 351 cm^{-1} in the RR spectrum (364 nm excitation). This band is shifted by $^{54}Fe/^{56}Fe$ and $^{32}S/^{34}S$ substitutions by 2.5 ± 0.2 and 4.9 ± 0.3 cm^{-1}, respectively. Later, excitation profile studies on the ν(Fe–S) and other modes were carried out by Bangcharoenpaurpong et al. [106]. The ν(Fe–S) of model compounds such as Fe(TPP)(SC_6H_5) are observed at 345–335 cm^{-1} in IR spectra [100].

According to IR studies by O'Keefe et al. [107], cytochrome $P450_{cam}-CO$ exhibits the $\nu(CO)$ at 1940 cm^{-1} (nonlinear FeCO bond), whereas the camphor-free compound exhibits two $\nu(CO)$ at 1963 (linear) and 1942 cm^{-1} (nonlinear). The $\nu(CO)$ of model compounds such as $Fe(T_{piv}PP)(CH_3S)(CO)$ is observed at 1945 cm^{-1} [108]. Uno et al. [109] assigned the bands at 1940, 558, and 481 cm^{-1} to the $\nu(CO)$, $\delta(FeCO)$, and $\nu(Fe-CO)$, respectively. This $\nu(Fe-CO)$ is markedly lower than that of HbCO (507 cm^{-1}) because of the *trans* effect of the mercaptide sulfur discussed earlier.

The $\nu(O_2)$ of cytochrome $P450_{cam}-O_2$ (d state) was first observed at 1140 cm^{-1} in RR spectra (420 nm excitation) by Bangcharoenpaurpong et al. [110]. This frequency is very close to the $\nu(O_2)$ of a model compound, $[Fe(T_{piv}PP)(SC_6HF_4)(O_2)]^-$ (1139 cm^{-1}), observed in IR [111] as well as in RR spectra [112]. In a Co(II)-substituted model compound, $[Co(TPP)(SC_6H_5)(O_2)]^-$, the $\nu(O_2)$ is at 1122 cm^{-1}, which is 22 cm^{-1} lower than that of Co(TPP)(py-d_5)(O_2) [113].

The $\nu(Fe-O_2)$ of cytochrome $P450_{cam}-O_2$ was first located at 541 cm^{-1} in RR spectra by Hu et al. [114]. As seen in Fig. 3.13, this band is rather weak, but its presence is confirmed by the difference spectrum (trace C). These workers also noted that two $\nu(O_2)$ are observed at 1139 and 1147 cm^{-1} when camphor is replaced by adamantanone. This may indicate the existence of two conformers that have different types of interactions between the bound O_2 and the substrate. The

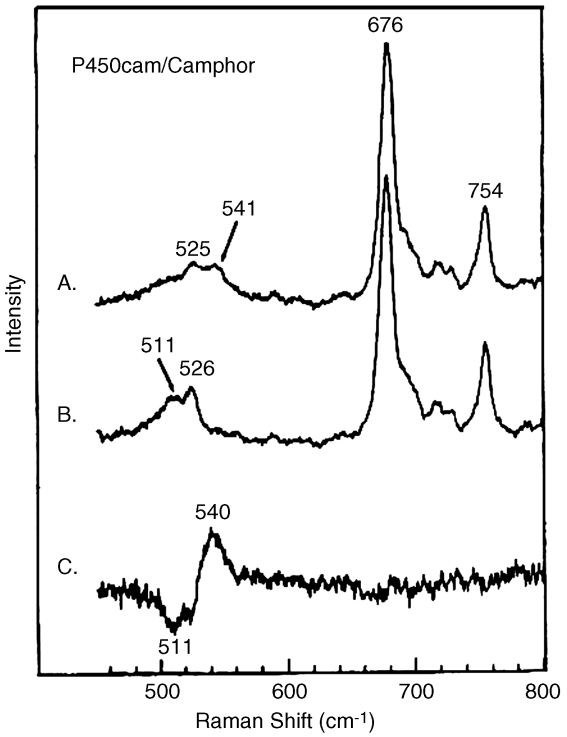

Fig. 3.13. *The RR spectra (441.6 nm excitation) of O_2 adducts of cytochrome $P450_{cam}$:* (A) $^{16}O_2$, (B) $^{18}O_2$ *and their difference spectrum* (C) *[114].*

TABLE 3.2. Effect of Substrates on FeNO Group Vibrations of Cytochrome P450–NO (cm^{-1}) [117]

	Fe(III)–NO (Linear)		Fe(II)–NO (Bent)	
Substrate	ν(Fe–NO)	δ(FeNO)	ν(Fe–NO)	δ(FeNO)
Substrate-free	528	—	547	444
Norcamphor	524	—	545	441
Camphor	522	546	553	445
Adamantanone	520	542	554	446
Mb–NO	594[a]	573[a]	554[b,c]	450[b]

[a] Reference 63
[b] Reference 64
[c] This band was previously (Ref. 63) assigned to the δ(FeNO).

$\nu(Fe-O_2)$ of a model compound of cytochrome $P450_{cam}$, "twin-coronet" iron porphyrin with an axial thiolate ligand, was observed at 578 cm^{-1} (413.1 nm excitation, −80° C). This band is shifted to 552 cm^{-1} by $^{16}O_2/^{18}O_2$ substitution [115]. Macdonald et al. [116] located the δ(Fe−O−O) mode of oxycytochrome $P450_{cam}$ at 401 cm^{-1}. A simple three-body calculation gives the Fe−O−O angle of 125–130°. This frequency is higher than those of the corresponding modes of MbO_2 and HbO_2, suggesting a strained Fe−O−O moiety relative to those of the latter.

Hu and Kincaid [117] studied the effect of changing the substrate structure on the Fe(III)−NO bond of cytochrome P450. Table 3.2 summarizes their results together with those obtained for the Fe(II)−NO series. The Fe(III)−NO bond is expected to be linear since it is isoelectronic with the Fe(II)−CO bond. It is seen that the ν(Fe−NO) of ferricytochrome P450−NO is by 70 cm^{-1} lower than that of ferriMb−NO because of the thiolate ligand in the former. Furthermore, this band is shifted sensitively by changing the substrate. These results have been explained by considering electronic and kinematic effects for a slightly bent Fe(III)−NO bond in the substrate-bound form. Their work has been extended to the cyanide adducts of cytochrome $P450_{cam}$ [118].

According to Fig. 3.12, hydroxylation of the substrate molecule is accomplished by the activated oxygen released from the oxoferrylporphyrin (f state). Although such a state has not yet been characterized spectroscopically, oxoferryl stretching [Fe(IV)= O] vibrations have been observed for model compounds such as FeO(TPP) (852 cm^{-1}) (Sec. 1.22.3) and for horseradish peroxidase compound II (HRP-II) at ~780 cm^{-1}.

3.3.3. Horseradish Peroxidase [119,120]

Peroxidases are enzymes that catalyze the oxidation of a substrate, AH_2, by H_2O_2:

$$AH_2 + H_2O_2 \rightarrow A + 2H_2O$$

Among them, reaction mechanisms of horseradish peroxidase (HRP) (MW ~ 40,000) have been studied most extensively. The active site of HRP is the same as that of Mb, namely, iron protoporphyrin, which is axially bonded to the proximal histidine. However, there are marked differences between the two; HRP binds O_2 irreversibly,

whereas Mb does so reversibly. Also, HRP is active biologically in the ferric state, whereas Mb is active in the ferrous state. This may be due to the difference in the heme environment; the proximal histidine in HRP is strongly hydrogen-bonded to nearby amino acid residues, and this hydrogen bonding increases σ-basicity of the proximal histidine. As a result, the ν[Fe−N(His)] of HRP is at 244 cm^{-1}, which is much higher than that of Mb (220 cm^{-1}) [121].

The reaction cycle of HRP involves two intermediates, HRP-I and HRP-II:

$$\begin{aligned} \text{HRP(ferric)} + H_2O_2 &\rightarrow \text{HRP-I} + H_2O \\ \text{HRP-I} + AH_2 &\rightarrow \text{HRP-II} + AH \\ \text{HRP-II} + AH &\rightarrow \text{HRP(ferric)} + A + H_2O \end{aligned}$$

Thus, HRP-I (green) and HRP-H (red) have oxidation states higher than the native Fe (III) state by two and one oxidizing equivalents, respectively. It has been found that both intermediates are oxoferryl [Fe(IV)=O] porphyrins and that HRP-II is low-spin Fe(IV), whereas HRP-I is its π-cation radical, which is one electron deficient in the porphyrin π-orbital of HRP-II.

As expected from its high oxidation state, HRP-II exhibits the ν_4 at 1381 cm^{-1}, which is the highest among heme proteins [122]. The ν(Fe=O) of HRP-II was reported by Hashimoto et al. [123] and Terner et al. [124] almost simultaneously. Figure 3.14 shows the RR spectra of HRP-II obtained by the former workers. On reacting HRP with H_2O_2 at alkaline pH, a new band appears at 787 cm^{-1} (trace C) that is shifted to 790 cm^{-1} by $^{56}Fe/^{54}Fe$ substitution (trace B), and to 753 cm^{-1} by $H_2{}^{16}O_2/H_2{}^{18}O_2$ substitution (trace D). Thus, this band was assigned to the ν(Fe=O) of HRP-II. In neutral solution, the ν(Fe=O) band was observed at 774 cm^{-1}, which was shifted to 740 cm^{-1} by $H_2{}^{16}O_2/H_2{}^{18}O_2$ substitution. The observed downshift (from 787 to 774 cm^{-1}) in going from alkaline solution to neutral solution has been attributed to the formation of a hydrogen bond between the oxoferryl oxygen and the NH group of the distal histidine, which disappears in alkaline pH.

As discussed in Sec. 1.22.3, the ν(Fe=O) of model compounds such as FeO(TPP) were first observed near 852 cm^{-1} in O_2 matrices. These frequencies are much higher than that of HRP-II because the former is a five-coordinate complex. In fact, the ν(Fe=O) of six-coordinate model compounds such as FeO(TPP)(1-MeIm) (820 cm^{-1}) are lower than that of five-coordinate complexes.

HRP-I is a π-cation radical (Sec. 1.22.5) produced by one-electron oxidation of HRP-II, and is much more unstable and photolabile than HRP-II. Thus several groups of workers reported different RR spectra. Ogura and Kitagawa [125] measured the RR (406.7 nm excitation) and electronic absorption spectra of HRP-I. However, they could not determine the radical type ($^2A_{1u}$ or $^2A_{2u}$) because no prominent band shifts were observed between HRP-I and HRP-II in the 1700–1200 cm^{-1} region. They suggested that a clear cation radical state may not exist for HRP-I because of delocalization of electrons through the metal atom and the axial ligand. Oertling and Babcock [126] measured the RR spectrum (390 nm excitation, 10-ns pulses) using the rapid mixing and flow sample techniques, and also noted similarity between them; the ν(Fe=O) of HRP-I was 791 cm^{-1}, which was almost identical to that of HRP-II

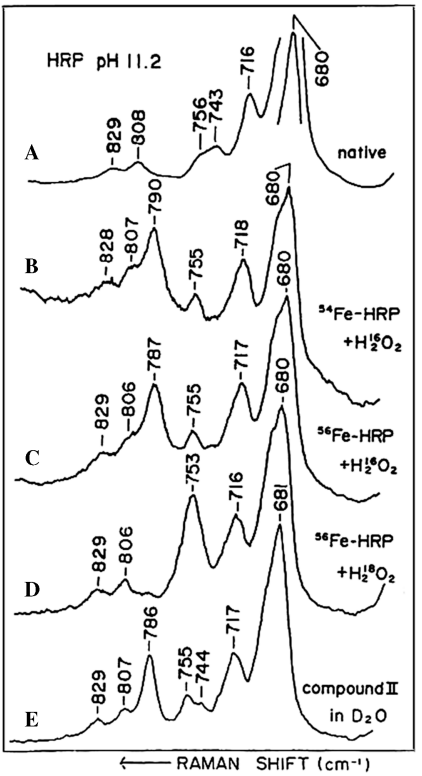

Fig. 3.14. *The RR spectra (406.7 nm excitation) of HRP-II (pH = 11.2) containing isotopomers as indicated [123].*

(787 cm^{-1}). These workers suggested two possibilities: (1) the electron delocalization proposed by Ogura and Kitagawa [125] and (2) conversion of HRP-I to HRP-I* via rapid and efficient photoinduced electron transfer. The latter symbol indicates a nonradical porphyrin similar to HRP-II produced by one electron transfer from a nearby amino acid residue to the porphyrin cation radical.

Paeng and Kincaid [127] used a microdroplet sample device to reduce the sample residence time in the laser beam (406.7 nm) to less than 5 μs, and assigned the ν(Fe=O) of HRP-I at 737 cm^{-1}. Their spectrum in the high-frequency region suggested $^2A_{2u}$ formulation. Using a similar device, Chuang and Van Wart [128] observed it at 721 cm^{-1}. Palaniappan and Terner [129] obtained a spectrum ($\sim$350 nm excitation) that is definitely different from that of HRP-II. Their spectrum in the high-frequency region suggested the $^2A_{2u}$ formulation of HRP-I. Finally, Kincaid and co-workers [130] measured the RR spectra of HRP-I with 356.4 nm excitation as a function of laser power. They found that, with low laser power (1 mW), the conversion of HPR-I to HRP-I* and/or HRP (resting state) [129] is minimized, and concluded that the spectrum obtained by Palaniappan and Turner [129] is due to HRP-I. It exhibits the ν(Fe=O) at 790 cm^{-1} (pH = 7.5), which is similar to that reported by Oertling and

Babcock [126], but markedly different from that of Paeng and Kincaid [127]. Their RR spectra obtained by high laser power ($5 \sim 25$ mW) [130] suggest the conversion of HRP-I to a HRP-II-like photoproduct. Nakamoto [131] reviewed the RR spectra and biological significance of high-valence iron (IV,V) porphyrins including the ν(Fe=O) of other heme proteins.

Resonance Raman studies of cyanide-coordinated HRP in the 5.5–12.5 pH range indicate the presence of two conformers [132]. In conformer I, the Fe−C−N linkage is essentially linear with the axial ν(Fe−CN) and δ(Fe−C−N) at 453 and 405 cm^{-1}, respectively (pH = 5.5). In conformer II, the Fe−C−N linkage is bent and the corresponding frequencies are 360 and 422 cm^{-1}, respectively, at the same pH. The ν(Fe−CN) of these conformers are pH-dependent, and the origins of their pH-dependent shifts have been discussed.

3.3.4. Cytochrome c Oxidase

Cytochrome *c* oxidases (CcO) are the terminal enzymes in the respiratory chains of mitochondria and aerobic bacteria, and catalyze the O_2-reducing and proton-pumping reaction:

$$4[\text{cyt. c, Fe(II)}] + O_2 \xrightarrow[\text{CcO}]{4H^+,\,4e} 4[\text{cyt. c, Fe(III)}] + 2H_2O$$

The number of subunits depends on the source of CcO. Bovine cytochrome *c* oxidase (MW, 2.1×10^5) in the mitochondrial inner membrane consists of 13 subunits. However, only subunits I and II are involved in the enzymatic reaction above. Figure 3.15 is a schematic representation of the structures of these subunits in the fully oxidized form of bovine heart CcO based on X-ray analysis by Tsukihira et al. [133,134]. Subunit I contains one Cu_B atom and one five-coordinate high-spin heme a_3

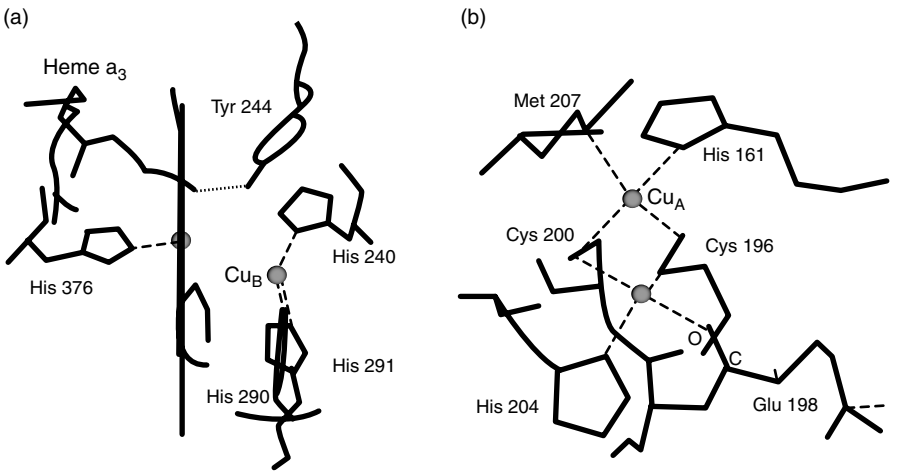

Fig. 3.15. *Structures of subunit I (a) and subunit II (b). In (b), heme a is not shown [133].*

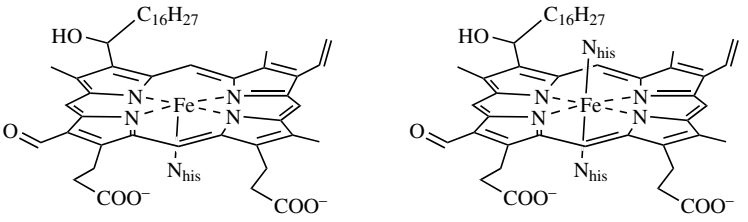

Fig. 3.16. *Structures of the hemes (heme a_3 and heme a) and Cu sites in subunits I and II of CcO. $C_{16}H_{27}$ = CH_2-[CH_2CH=$C(CH_3)CH_2]_2$–CH_2–CH=$C(CH_3)_2$.*

(Fig. 3.16) with the N atom of His 376 occupying one axial position, and the other axial position is utilized for O_2 coordination. The distance between the Fe(a_3) and Cu_B atoms is 4.9 Å, but no bridging ligands are detected between them despite their strong antiferomagnetic coupling. Subunit II contains one six-coordinate low-spin heme a (Fig. 3.16) and two Cu_A atoms that are bridged by two sulfur atoms of Cys196 and Cys200 to form a planar Cu_2S_2 ring, as shown in Fig. 3.15b. Electrons from cytochrome *c* are transferred to heme a via $Cu^I \leftrightarrow Cu^{II}$ shuttling, and eventually transferred to heme a_3 of subunit I.

Resonance Raman spectra (840 nm excitation) of bovine CcO exhibit the Cu_A–N (His) and Cu_A–S(Cys) stretching vibrations of subunit II at 356 and 330 cm^{-1}, respectively [135]. The CcO fragment obtained from bacterium *Paracoccus denitrificans* contains a similar bridging structure, and Andrew et al. [136] made complete assignments of its dinuclear Cu_A center by combining isotopic shift data with normal coordinate analysus ($\mathbf{C}_{2h}$ symmetry). Figure 3.17 shows the RR spectra (488 nm excitation) of six isotopic species ($^{32}S/^{34}$, $^{63}Cu/^{65}Cu$, and $^{14}N/^{15}N$) in the 375–200 cm^{-1} region. Most of these bands are due to coupled vibrations of ν(Cu–S), ν(Cu–N), and ν(Cu–Cu), and the vibrations at 339 (A_g), 260 (A_g), and 216 cm^{-1}(B_u) have major contributions from the ν(Cu–S), as they are shifted by 5.1, 4.1 and 1.5 cm^{-1}, respectively, to lower frequencies on $^{32}S/S^{34}$ substitution.

Since the enzymatic reaction occurs in subunit I, it is important to identify the structure of the intermediate species involved in the passageway. Ogura and Kitagawa [137,138] carried out TR^3 studies coupled with electronic absorption spectroscopy on CcO obtained from bovine heart muscle. On the basis of isotope shift data coupled with temperature dependence studies, they were able to characterize the intermediate species in the catalytic cycle.

The vacant axial position of heme a_3 can also be coordinated by other ligands such as CO, CN^-, and NO. Hosler et al. [139] obtained the IR and Raman spectra of the CO adduct of wild-type *Rb. sphaeroides* CcO, and assigned the ν(CO) at Cu_B, ν(CO) at Fe(a_3), ν(Fe–CO), and ν(Fe–N) at 2060, 1964, 516, and 214 cm^{-1}, respectively. Other investigations include UV resonance studies of model compounds of the Cu_B site [140,141]. Kim et al. [142] reviewed synthetic models of CcO.

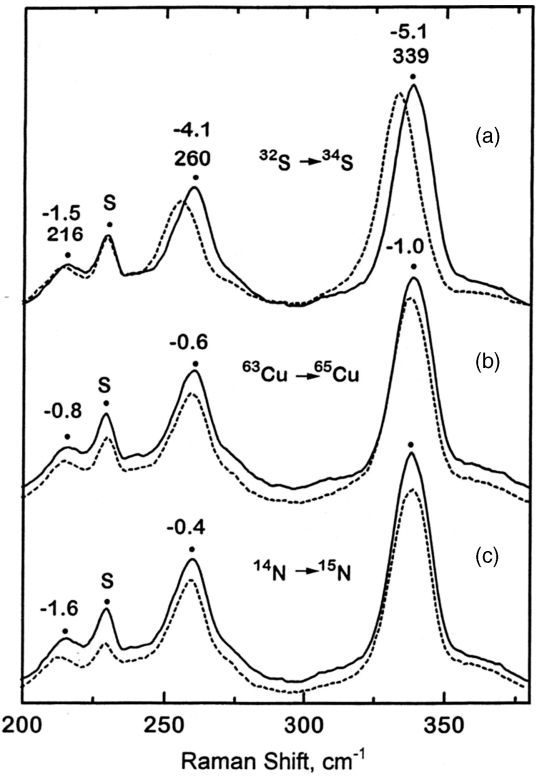

Fig. 3.17. *Effect of isotope substitution on RR spectra (488 nm excitation) of P. denitrificans Cu_A: (a) Cu_A fragment from cells grown on ^{32}S- or -^{3} ^{4}S-sulfate; (b) Cu_A apoprotein fragment reconstituted with ^{63}Cu or ^{65}Cu; (c) Cu_A fragment from cells grown on ^{14}N- or ^{15}N-ammonium chloride. Peak frequencies are listed for the lighter isotope spectra (—) with frequency shifts for the heavier isotope spectra (···) indicated above [136].*

3.3.5. Other Heme Proteins

Infrared and Raman studies have also been made on many other heme proteins. These include cytochrome *c* peroxidase (CCP), myeloperoxidase (MPO), lactoperoxidase (LPO), and catalase (CAT). Several review articles mentioned previously should be consulted for vibrational studies of these and other heme proteins.

3.4. BACTERIOCHLOROPHYLLS

In purple photosynthetic bacterium such as *Rb. sphaeroides*, the reaction center (RC) contains four bacteriochlorophylls (BChl), two bacteriopheophytins (BPh), two quinones, a carotinoid, and a nonheme iron or manganese atom. Figure 3.18 compares the structure of BChl *a* with that of chlorophyll *a* (Sec. 1.6). The structure of BPh is the

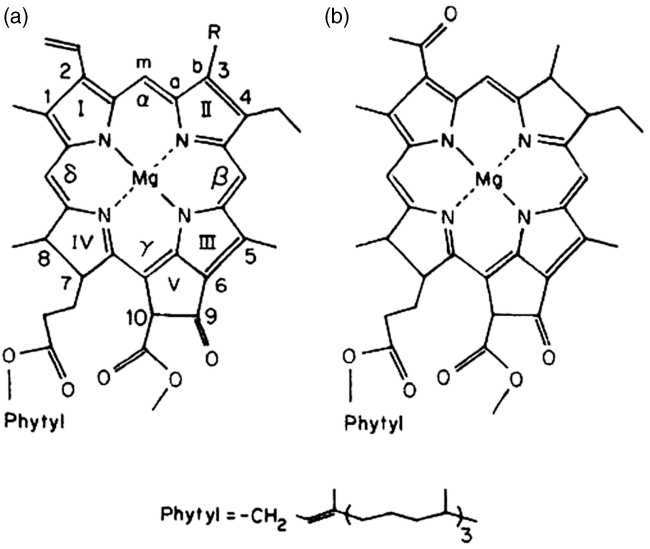

Fig. 3.18. *Structures of (a) chlorophyll a (R = CH_3) and (b) bacteriochlorophyll a.*

same as that of BChl with the Mg^{2+} ion replaced by two protons. Similar to chlorophylls, BChl is a Mg^{2+} macrocycle in which the two pyrrole rings (II and IV) are reduced and the fifth isocyclic ring (V) is fused to ring III. Figure 3.19 illustrates the arrangement of the BChl and BPh cofactors in the RC that was adapted by Czarnecki

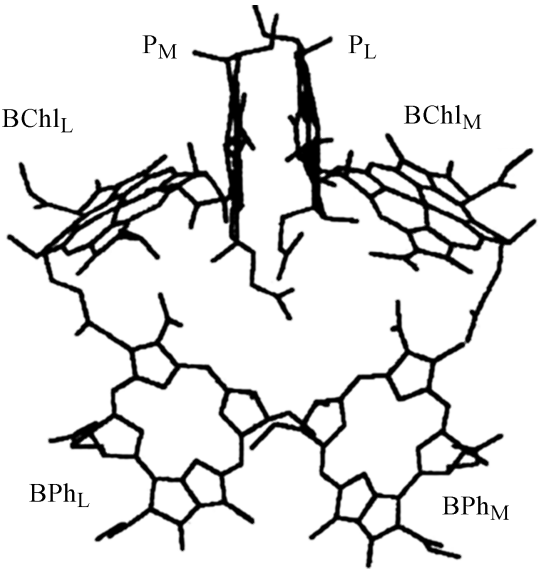

Fig. 3.19. *Arrangement of the BChl and BPh cofactors in RCs from Rb. sphaeroides; for clarity, the protein matrix, the other cofactors, and the phytyl substituents of the BChls and BPhs have been removed [143,144].*

et al. [143] from the results of X-ray analysis of *Rb. sphaeroides* [144]. Here, P denotes a special BChl pair where the primary charge separation for electron transfer occurs. The subscripts "L" and "M" denote the L and M peptide subunits, respectively.

Robert and Lutz [145] measured the RR spectra of the RC of this bacterium at 20–80 K with 363.8 nm excitation (Soret resonance) in the high-frequency region, and proposed the structure and bonding of the P_MP_L pair in the ground state on the basis of observed ν(C=O) frequencies. Raman difference techniques were used because the Soret bands of P and BChl are almost perfectly overlapped. The band at 1684 cm^{-1} was assigned to the keto carbonyl group of P, which is moderately interacting with the peptide chain. Two bands at 1660 and 1637 cm^{-1} were assigned to the two acetyl group of P; the former to the ν(C=O) group free from intermolecular interaction, and the latter to the acetyl group interacting with the peptide chain. No binding interactions were proposed between the two BChl's.

Czarnecki et al. [143] studied the RR spectra of the RC of *Rb. sphaeroides* in the low-frequency region. Figure 3.20 shows the electronic absorption spectrum of the RC in the near-IR region at 10 K. These workers were able to resonance-enhance the vibrations due to P, BChl, and BPh separately with excitation lines near 900, 800, and 760 nm, respectively, and obtained the RR spectra (894 nm excitation, 25 K) of P for the naturally abundant, ^{26}Mg-labeled and ^{15}N-labeled RCs. The SERDS (shifted excitation Raman difference spectroscopy) technique [146] was used to remove the large fluorescence background. In this method, RR spectra are measured with two exciting lines of slightly different wavenumbers (typically 10 cm^{-1}), and

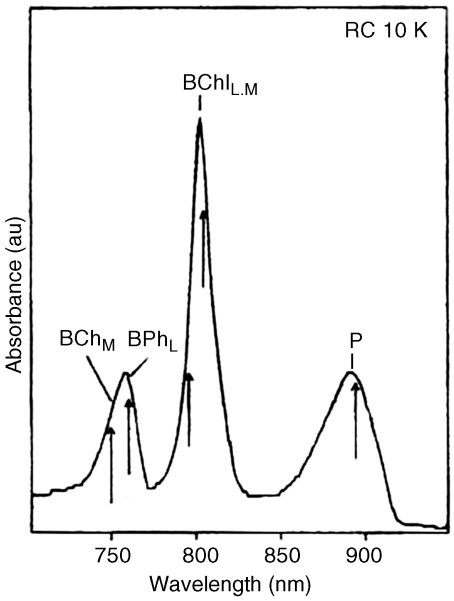

Fig. 3.20. *Low-temperature (10-K) near-infrared absorption spectrum of RCs from Rb. sphaeroides. The cofactors contributing to the various absorptions are indicated. The arrows mark the different excitation wavelengths used to acquire RR spectra [143].*

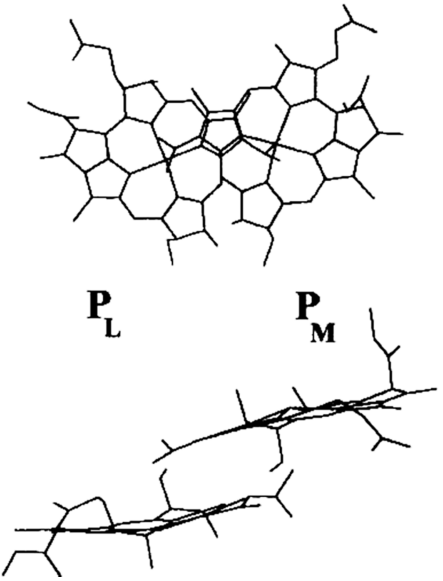

Fig. 3.21. *Two views of P in RCs from Rb. sphaeroides. The bottom view is along the approximate C_2 symmetry axis of the dimmer; the top view in approximately orthogonal to this axis [143].*

then the subtraction between them yields a spectrum that is free from background interference. The RR spectrum of P thus obtained exhibits a band near 137 cm^{-1} that is known to be a marker band of the primary electron donor. On the basis of observed isotope shifts and normal coordinate calculations, it was assigned to a strongly coupled vibration involving the in-plane deformation of the C_2 acetyl group, a doming motion of the Mg^{2+} ion, and a core deformation that includes all four pyrrole rings. Such vibrational coupling may be intrinsic of the structure of P shown in Fig. 3.21 [144] since the overlap between P_L and P_M primarily involves ring I of BChl and the positions of the two C_2-acetyl groups are close to the core of the neighboring macrocycle.

As stated earlier, the RC of *Rb. sphaeroides* contains two quinone molecules (Q_A and Q_B) that play different roles; Q_A is a one-electron carrier while Q_B leaves the RC as dihydroquinone after accepting two electrons and two protons. To account for this difference, Zhao et al. [147] measured the RR spectra of $Q_A^{\bullet -}$ and $Q_B^{\bullet -}$ and their ^{13}C analogs to assign the ν(C=O) and ν(C=C) vibrations, and concluded that environmental differences are responsible for their different roles at the RC.

Figure 3.22 illustrates the X-ray crystal structure of one subunit of the BChl *a*–protein complex from *Prosthecochloris aestuari* [148]. It contains seven BChl *a* molecules that are noncovalently bonded to protein. Lutz et al. [149] measured the RR spectra of this complex in the 1710–1630 cm^{-1} region and observed many acetyl- and ketocarbonyl bands. A review article, "Chlorophylls and the Photosynthetic Membrane" by Lutz and Robert [150], is available.

Fig. 3.22. *One subunit of the bacteriochlorophyll protein showing the seven bacteriochlorophylls enclosed within an envelope of protein. For clarity, the phytyl tails of each bacteriochlorophyll have been omitted. In this figure, the threefold symmetry axis extends from left to right across the front of the molecule [148].*

3.5. HEMERYTHRINS [151–155]

Hemerythrins (Hr) are molecular oxygen carriers found in invertebrate plyla. Different from Hb and Mb, Hr have no heme groups. Thus far, spectroscopic investigations have been concentrated on hemerythrin isolated from *Golfingia gouldii*, a sipunculan worm (MW 108,000) consisting of eight identical subunits. Each unit contains 113 amino acids and two Fe atoms, and each pair of Fe atoms binds one molecule of dioxygen. However, its oxygen affinity is slightly lower than hemoglobin, and no cooperativity is found in its oxygenation reaction. Deoxy-Hr (colorless) turns to pink on oxygenation ("pink blood"). Figure 3.23 shows the primary structure of Hr obtained from *G. gouldii*, while Fig. 3.24 shows the tertiary structure of monomeric myohemerythrin obtained by low-resolution X-ray analysis [156]; it consists of four nearly parallel helical segments, 30–40 Å long, connected by sharp nonhelical turns.

Figure 3.25 shows the electronic spectra of deoxy-, oxy-, and Met-Hr obtained by Dunn et al. [157]. The oxy form exhibits a band at 500 nm that does not exist in the deoxy form. When the laser wavelength falls under this electronic absorption, two bands are resonance-enhanced at 844 and 500 cm^{-1} that are shifted to 798 and 478 cm^{-1}, respectively, by $^{16}O_2$–$^{18}O_2$ substitution (Fig. 3.26). These two bands are assigned to the $\nu(O_2)$ and $\nu(Fe-O_2)$ of the oxy form, respectively. Apparently, the

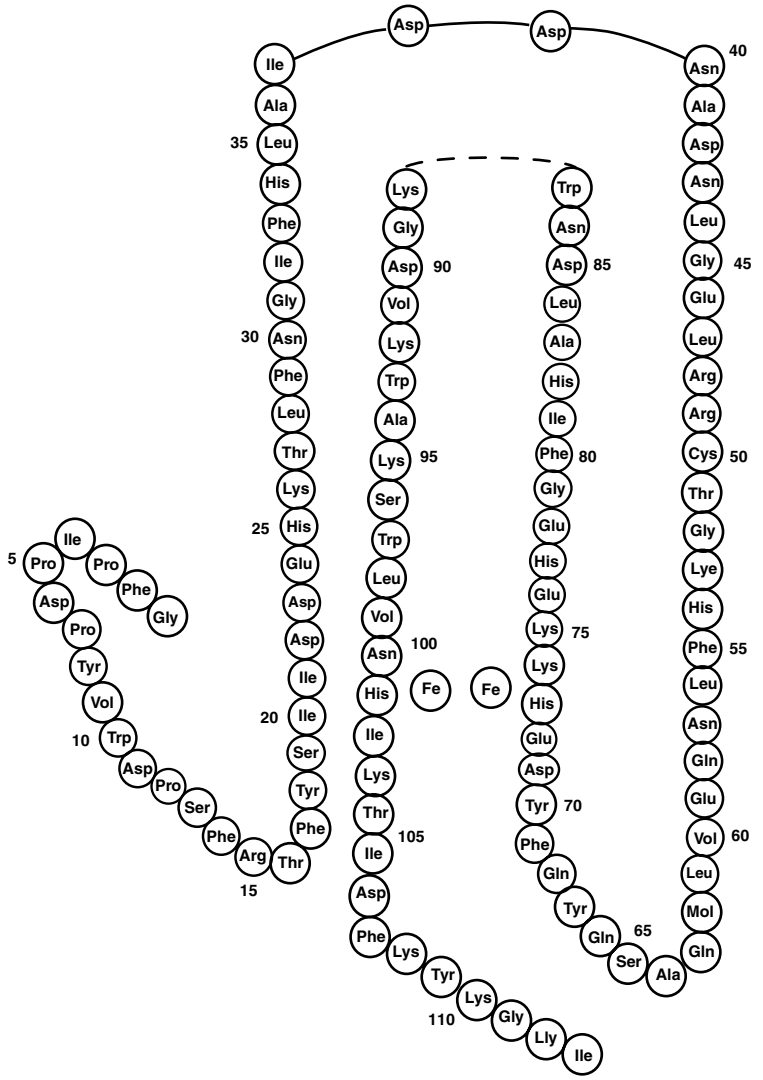

Fig. 3.23. *Primary structure of hemerythrin from erythrocytes of G. gouldii [156].*

electronic transition at 500 nm is due to $Fe \rightarrow O_2$ charge transfer. Also, the observed frequency of $\nu(O_2)$ (844 cm^{-1}) suggests that the dioxygen is not of "superoxo" but of "peroxo" type (Sec. 1.21).

In order to gain more information about the geometry of O_2 binding, Kurtz et al. [158] measured the RR spectra of the oxy-Hr with isotopically scrambled oxygen ($^{16}O_2/^{16}O^{18}O/^{18}O \approx 1/2/1$). Figure 3.27 shows that the central band due to the $^{16}O^{18}O$ adduct clearly splits into two peaks, indicating the nonequivalence of the two oxygen atoms. This conclusion is also supported by the RR spectrum in the $\nu(Fe-O_2)$

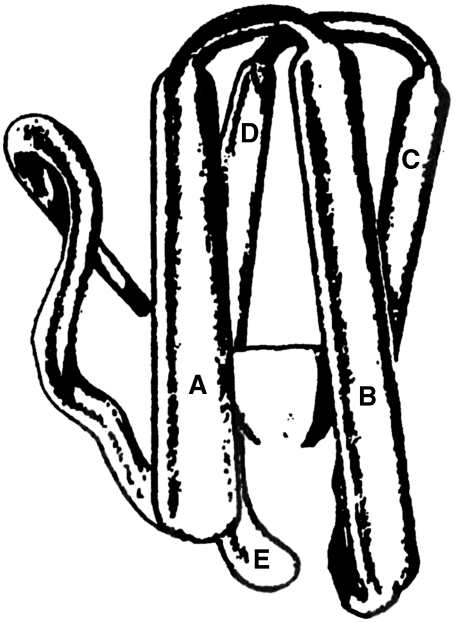

Fig. 3.24. *Tertiary structure of monomeric myohemerythrin [156].*

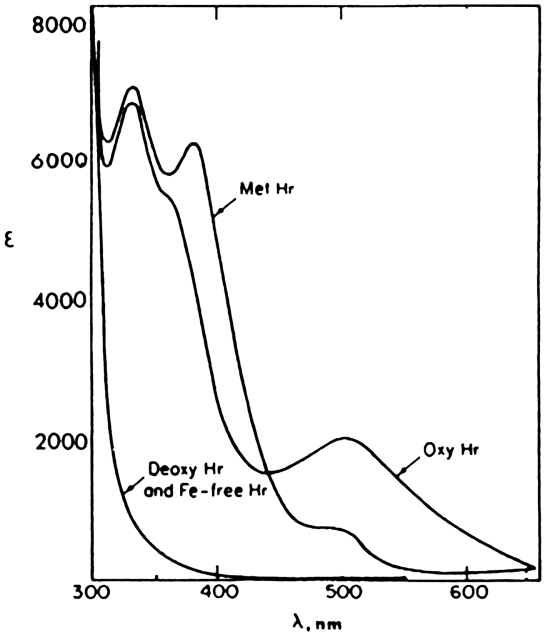

Fig. 3.25. *Electronic spectra of hemerythrin in the deoxy, oxy, and Met forms [157].*

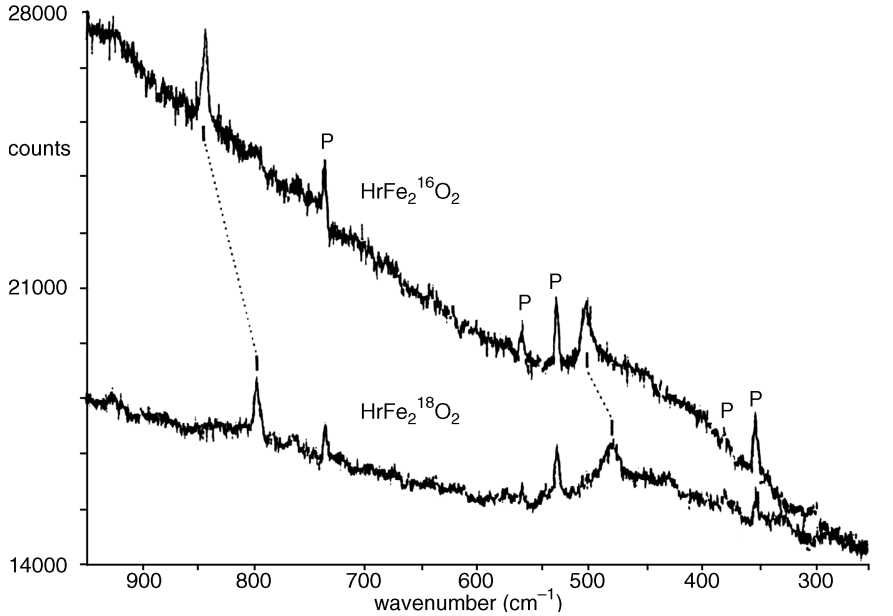

Fig. 3.26. *The RR spectra (488.0 nm excitation) of oxyhemerythrin ($^{16}O_2$ and $^{18}O_2$), where P denotes laser plasma lines [157].*

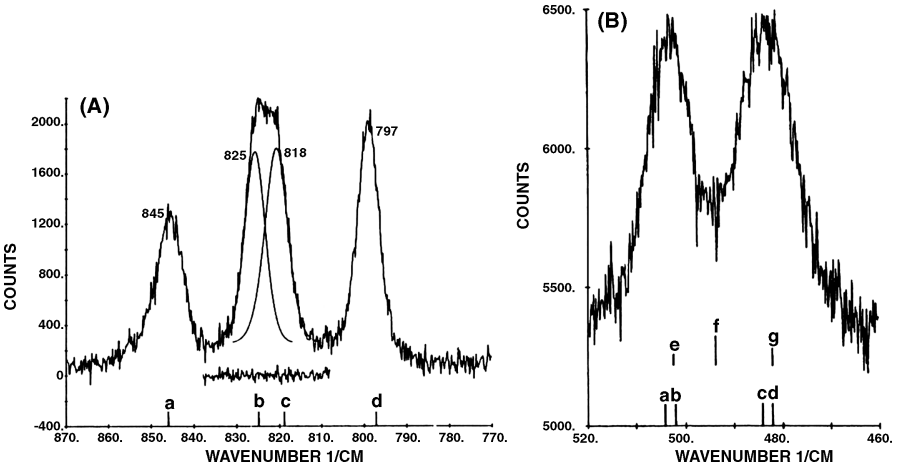

Fig. 3.27. *The RR spectra (514.5 nm excitation) of oxyhemerythrin ($^{16}O_2$/$^{16}O^{18}O$/^{18}O/$^{18}O_2$ = 1/2/1 [158].* (A) *The $\upsilon(O_2)$ region. The smooth curves represent deconvolution of the 822 cm^{-1} feature into two components. The difference between the observed and fitted curves is shown below the spectrum near 822 cm^{-1}. Lines a–d show the calculated peak positions for models I and II of Fe-$^{16}O_2$ (845 cm^{-1}), Fe–$^{16}O^{18}O$ (825 cm^{-1}), Fe–$^{18}O^{16}O$ (818 cm), and Fe–$^{18}O_2$ (797 cm^{-1}), respectively.* (B) *The ν(Fe–O_2) region. Lines a–d represent calculated positions for the isotopic species defined in* (A). *Lines e–g show, for models III and IV, the calculated peak positions and estimated relative intensitives for $^{16}O_2$ (502 cm^{-1}), $^{16}O^{18}O$ (495 cm^{-1}), and $^{18}O_2$ (489 cm^{-1}), respectively.*

region. As is seen in Fig. 3.27B, the spectrum consists of two composite bands, one near 502 cm^{-1} and the other near 483 cm^{-1}. Simple normal coordinate calculations on models I and II indicate

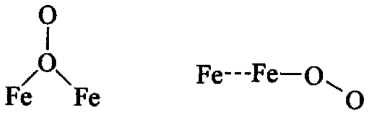

I II

that the $\nu(Fe-O_2)$ of the $Fe-^{16}O^{16}O$ (a) and $Fe-^{16}O^{18}O$ (b) adducts nearly overlap, as do those of the $Fe-^{18}O^{16}O$ (c) and $Fe-^{18}O^{18}O$ (d) adducts (a–d refer to the vertical lines in Fig. 3.27B). If the two oxygen atoms were equivalent as shown below

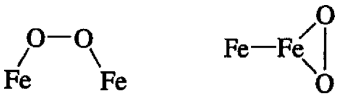

III IV

a three-peak spectrum with 1 : 2 : 1 intensity ratio would have appeared in the positions indicated by e–g in Fig. 3.27B.

Later, X-ray analyses were carried out on *met*-azidohemerythrin [159] and oxyhemerythrin [160]. Figure 3.28 shows the structure of the active site of the latter; the two Fe atoms are separated by 3.25 Å, and bridged by an oxo atom and two carboxylate groups of the peptide chain. The structure of the former is similar except that the protonated peroxide ion is replaced by the azide ion. Shiemke et al. [161] observed the ν_a(FeOFe) and ν_s(FeOFe) of the oxo bridge at 753 and 486 cm^{-1}, respectively, in the RR spectrum (363.8 nm excitation). They also noted that both $\nu(O_2)$ (844 cm^{-1}) and $\nu(Fe-O_2)$ (503 cm^{-1}) of oxy-Hr in H_2O are shifted by +4 and −3 cm^{-1}, respectively, in D_2O solution. These shifts are consistent with the protonated peroxide structure shown in Fig. 3.28. Their subsequent study [162] revealed the

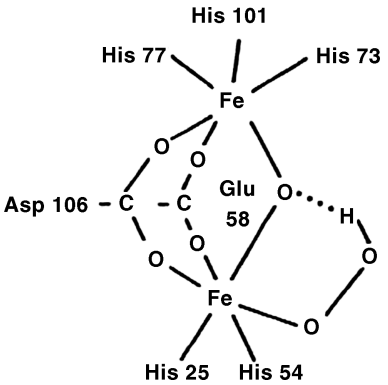

Fig. 3.28. *Structures of the active site of hemerythrin in the oxy form [160].*

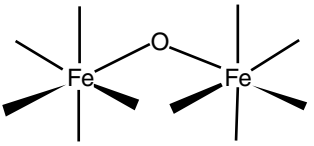

Monobridged

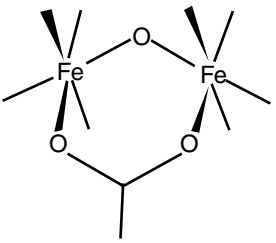

Dibridged

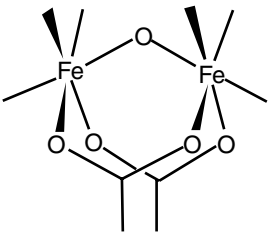

Tribridged

Fig. 3.29. *Structures of three types of oxo bridges [164].*

presence of two ν_s(FeOFe) vibrations at 492 and 506 cm^{-1}, which correspond to the *cis*-isomer involving the intramolecular hydrogen bond shown in Fig. 3.28 and its *trans*-isomer having a free OH group, respectively.

Kaminaka et al. [163] found via RR studies that, in a cooperative hemerythrin (*Lingula unguis*), hydrogen bonding between bound O_2 and a nearby amino acid residue is responsible for cooperativity in oxygen affinity. As seen in Fig. 3.28, oxyhemerythrin takes a tribridged structure with one oxo bridge. Figure 3.29 illustrates three types of oxo bridges [164]. Vibrational spectra of oxo-bridged complexes containing a variety of metals have been discussed in Sec. 1.22.3. RR spectra of dibridged compounds containing one oxo group and one carboxylate group are reported for ribonucleotide reductase [165] and stearoyl–ACP desaturase [166].

3.6. HEMOCYANINS [151,167]

Hemocyanins (Hc) are oxygen transport nonheme proteins (MW 10^5–10^7) found in the blood of some insects, crustaceans, and other invertebrates. One of the smallest Hc (MW 450,000) extracted from spiny lobster *Panulirus interruptus* consists of six subunits each containing two Cu atoms. On oxygenation, the deoxy form [Cu(I), colorless] turns blue [Cu(II), "blue blood"] by binding one O_2 molecule per two Cu atoms.

Oxy-Hc extracted from *Cancer magister* (Pacific crab) and *Busycon canaliculatum* (channeled whelk) exhibit absorption bands near 570 and 490 nm. Freedman et al. [168] measured the RR spectra of these compounds with 530.9 and 457.9 nm

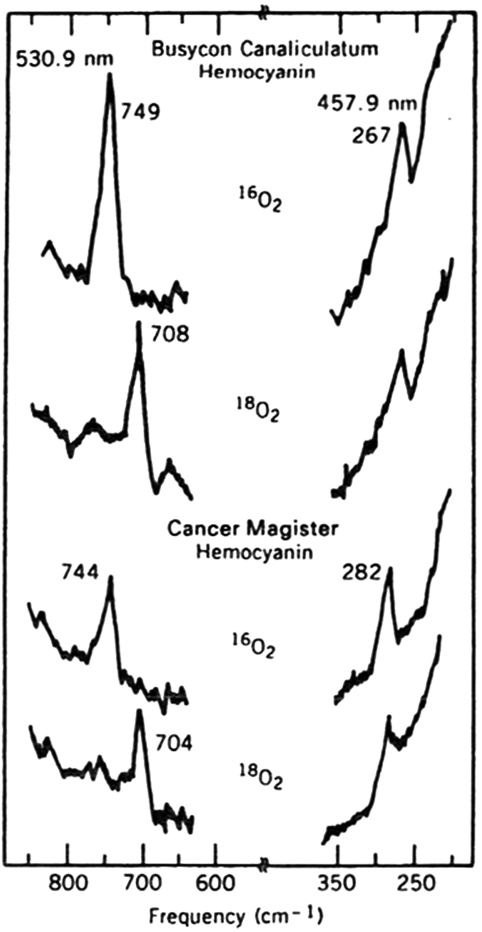

Fig. 3.30. *The RR spectra of oxyhemocyanins ($^{16}O_2$ and $^{18}O_2$) with 530.9 and 457.9 nm excitation [168].*

excitations. The results shown in Fig. 3.30 clearly indicate that the bands near 747 cm^{-1} are sensitive to $^{16}O_2$–$^{18}O_2$ substitution and must be assigned to the $\nu(O_2)$ characteristic of the peroxo(O_2^{2-}) type. Excitation profiles of the $\nu(O_2)$ consist of two components and indicate that the absorption bands near 570 and 490 nm are due to $O_2^{2-} \rightarrow$ Cu(II) charge transfer. These workers proposed a nonplanar ($\mathbf{C}_2$) structure to account for the appearance of the two CT bands:

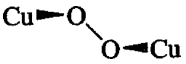

The equivalence of the two oxygen atoms in this structure was confirmed by the RR spectrum of oxy-Hc, which exhibits a single $\nu(O_2)$ band at 728 cm^{-1} for the $^{16}O^{18}O$ adduct [169]. This is a marked contrast to oxy-Hr discussed in the preceding section.

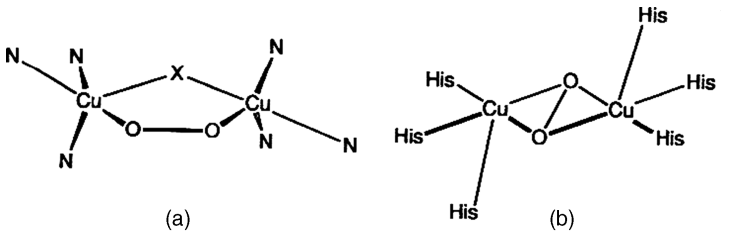

Fig. 3.31. *Structures of the active site of oxyhemocyanin.*

The bands in the 290–260 cm^{-1} region in Fig. 3.30 are not sensitive to $^{16}O_2/^{18}O_2$ substitution, and are assigned to the ν[Cu−N(His)] vibrations. Larrabee and Spiro [170] observed ν(Cu−N(Im)) below 300 cm^{-1} in the RR spectra of oxy-Hc with 363.8 nm excitation. Their assignments were confirmed by ^{63}Cu–^{65}Cu and H_2O-D_2O frequency shifts.

In 1980, Brown et al. [171] carried out an EXAFS study on oxy- and deoxy-Hc of *B. canaliculatum*, and proposed the structure shown in Fig. 3.31a for the oxy form; the two Cu atoms are bound to the protein via three histidine ligands each, and bridged by the O_2^{2-} and an X atom from a protein, possibly tyrosine. Later, Gaykema et al. [172] carried out X-ray analysis (3.2 Å resolution) on colorless single crystals of Hc extracted from *Panulirus interruptus*. This molecule consists of six subunits (MW 75,000), each folded into three domains. The structure of the second domain in which two Cu atoms are located is shown in Fig. 3.32. The Cu−Cu distance is 3.8 Å, and each Cu atom is coordinated by three histidyl residues as suggested by Brown et al. [171] for the deoxy form. No evidence for a bridging protein ligand was found, although it was not possible to rule out such a possibility from low-resolution X-ray analysis.

X-Ray analysis by Magnus et al. [173] revealed that the two Cu(II) atoms in oxy-Hc (from *Limulus polyphemus*) are bridged by a side-on peroxide as shown in Fig. 3.31b. Here, each Cu(II) atom takes a square–pramidal structure with four equatorial bonds (two Cu−N and two Cu−O bonds) and one axial Cu−N bond so as to obtain the overall $\mathbf{C}_{2h}$ symmetry. Ling et al. [174] have measured the RR spectra of oxy-Hc from several sources, and made complete band assignments via normal coordinate analysis using isotopic shift data ($^{16}O/^{18}O$, $^{63}Cu/^{65}Cu$, and H/D). The ν_a (Cu_2O_2) and its first overtone are located at 542 and 1085 cm^{-1}, respectively, for oxy-Hc from *Octopus dofleini*. The ν[Cu−N(His)] of oxy-Hc (*L. polyphemus*) appear in the 370–190 cm^{-1} region, although some of these are coupled with the ν(Cu−O) modes.

Fager and Alben [175] studied the FTIR spectra of HcCO using $^{13}C^{16}O$ and $^{12}C^{18}O$, and proposed a structure in which the CO is coordinated to one Cu via the O atom in a trigonal–planar fashion while the second Cu is free from such interaction. Pate et al. [176] proposed the μ-1,3 bridging structure for *met*-HcN_3 based on RR spectra obtained by using the isotopic $^{14}N_2{}^{15}N^-$ ligand:

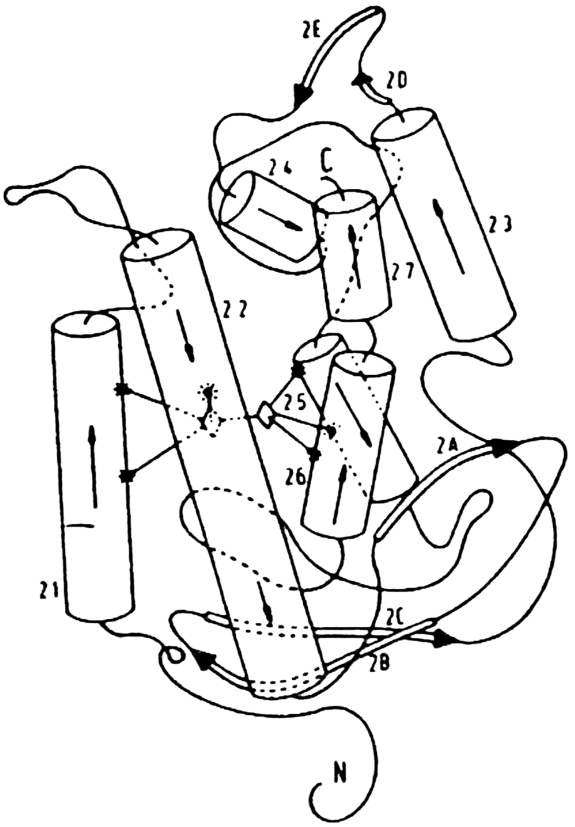

Fig. 3.32. *Structures of the second domain of Hc extracted from P. interruptus. The Cu atoms are indicated by diamonds. The cylinders (2.1–2.7) indicate the α-helical structure, while the strips (2A–2E) represent the β structure of the peptide chain [172].*

For the $^{14}N-^{14}N-^{15}N$ ion, two $\nu(N_3)$ bands were observed at 2035 and 2024 cm^{-1}. This observation suggests nonequivalence in the two Cu−N interactions that originates in differences between the two Cu environments in the protein.

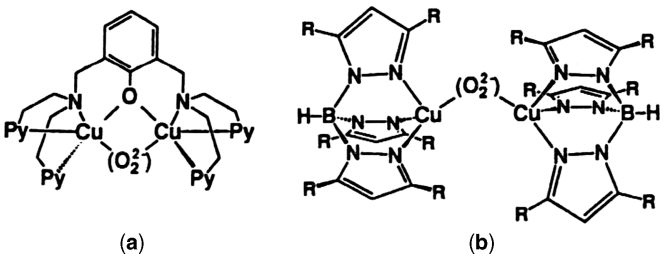

Fig. 3.33. *Structures of model compounds of oxyhemocyanin: (a) Py denotes the 2-pyridyl group; (b) R denotes the Me, i-Pr, or Ph group.*

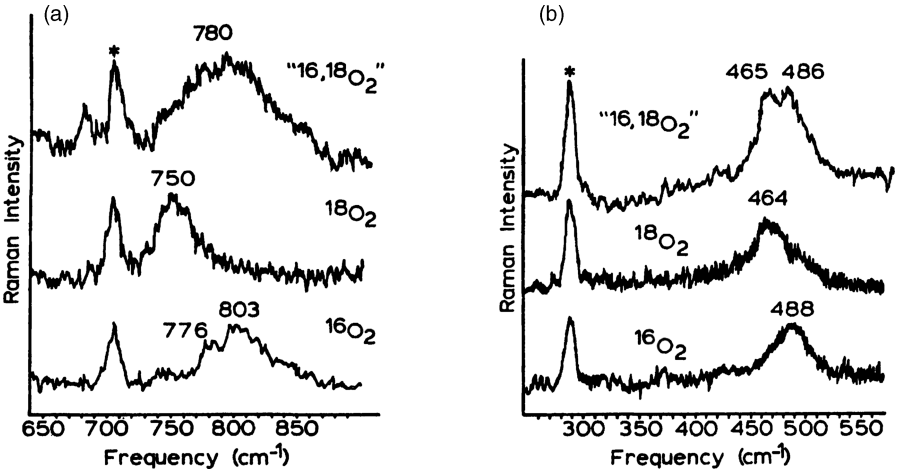

Fig. 3.34. *The RR spectra of model compound A (Fig. 3.33) with $^{16}O_2$, $^{18}O_2$, and $^{16}O^{18}O$ (a mixture of $^{16}O_2$, $^{16}O^{18}O$, and $^{18}O_2$ in 1/2/1 ratio): (a) the $\nu(O_2)$ region (488.0 nm excitation). The asterisk indicates the peak due to CH_2Cl_2; (b) the ν(Cu–O) region (647.1 nm) excitation [178].*

Karlin et al. [177] first prepared a model compound of Hc, which is shown in Fig. 3.33a. This complex performs reversible oxygenation at $-70°C$. As seen in Fig. 3.34, the $^{16}O^{18}O$ adduct exhibits a broad $\nu(O_2)$ centered at 780 cm^{-1} (peroxide-type) and two ν(Cu–O) bands at 486 and 465 cm^{-1} in RR spectra. Through normal coordinate analyses and computer simulations of the observed band shapes. Pate et al. [178] have shown that the peroxide is asymmetrically bonded to the Cu atoms, although the nature of asymmetry is not clear.

Kitajima et al. [179] prepared another type of model compounds that mimic HcO_2. As shown in Fig. 3.33b, their compounds contain two Cu atoms that are bonded via the peroxo bridge without a phenoxo bridge. Figure 3.35 shows the RR spectra of one of their complexes, $[Cu(HB(3,5\text{-}R_2pz)_3)]_2(O_2)$ (R = *i*-Pr), which were obtained with $^{16}O_2$ (A) and isotopically scrambled dioxygen ($^{16}O_2/^{16}O^{18}O/^{18}O_2 = 1/2/1$) (B) at $-40°C$. The latter spectrum shows that the intensity ratio of the three $\nu(O_2)$ is close to 1/2/1 and their band widths are nearly identical. These results confirm that the $\nu(^{16}O_2)$ is at 741 cm^{-1}, and that the peroxide is symmetrically coordinated as that shown in Fig. 3.31b (μ-η^2 η^2-type). Electronic and vibrational spectra of the model compound shown in Fig. 3.33a were also studied by Baldwin et al. [180]. Karlin [181] reviewed the reaction of O_2 with copper complexes.

As shown above, the peroxo bridging complex of oxy-Hc exhibits the $\nu(O_2)$ at $\sim$750 cm^{-1}, [174]. A similar μ-η^2 η^2 peroxo structure was also proposed for the dioxygen adduct of the dinuclear Co(II) complex $[Co(HB(3,5\text{-}R_2pz)_3)]_2(O_2)$ ($R = i$-Pr) [182]. It exhibits an electronic absorption band at 350 nm (ϵ (8900 M^{-1} cm^{-1}) with an intensity less than half that of the corresponding Cu(II) complex (340 nm, ϵ (21,000 M^{-1} cm^{-1}). The RR spectrum of the Co(II) complex (514.5 nm excitation) in acetone at $-80°C$ exhibits the peroxo $\nu(O_2)$ at 651 cm^{-1}, which is shifted to 617 cm^{-1} by $^{16}O_2/^{18}O_2$ substitution. This may be the lowest $\nu(O_2)$ thus far

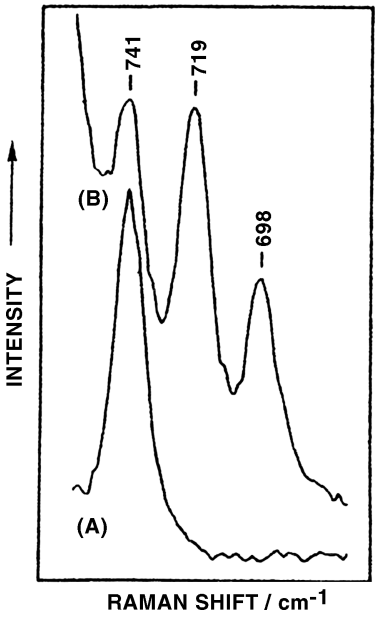

Fig. 3.35. *The RR spectra (514.5 nm excitation) of model compound b (Fig. 3.33) in acetone at −40° C;* (A) $^{16}O_2$; (B) *a mixture of* $^{16}O_2$, $^{16}O^{18}O$, *and* $^{18}O_2$ *in 1/2/1 ratio [179].*

observed. High electron density on both of the antibonding peroxo orbitals might weaken the O−O bond more in the Co(II), complex than in the Cu(II) complex [179].

3.7. BLUE COPPER PROTEINS [183,167]

Blue copper proteins are found widely in nature. For example, oxidized plastocyanin (electron transport protein) and azurin (copper oxidase) contain one Cu(II) atom per protein, and exhibit an intense absorption band near 600 nm that is due to the S (Cys) → Cu charge transfer near 600 nm. In addition, these copper proteins have unusual properties such as extremely small hyperfine splitting constants ($0.003 \sim 0.009\,cm^{-1}$) in ESR spectra and rather high redox potential ($+0.2 \sim 0.8$ V) compared to the Cu(II)/Cu(I) couple in aqueous solution.

In 1978 the crystal structure of poplar plastocyanin was first determined by X-ray diffraction with 2.7 Å resolution [184], and later refined to 1.6 Å resolution [185]. Figures 3.36a and 3.36b show the location of the Cu atom in the peptide chain and the environment around the Cu atom, respectively. It was found that Cu atom is coordinated by two histidyl nitrogens (His 37 and 87), one cysteinyl sulfur (Cys 84), and one methionyl sulfur (Met 92) in a distorted tetrahedral environment. The two Cu−N(His) distances are 2.10 and 2.04 Å, and the Cu−S(Cys) distance is 2.13 Å, while the Cu−S(Met) is 2.90 Å. This distorted tetrahedral structure approaches to the distorted trigonal–planar structure as the Cu−S(Met) bond lengthens. These

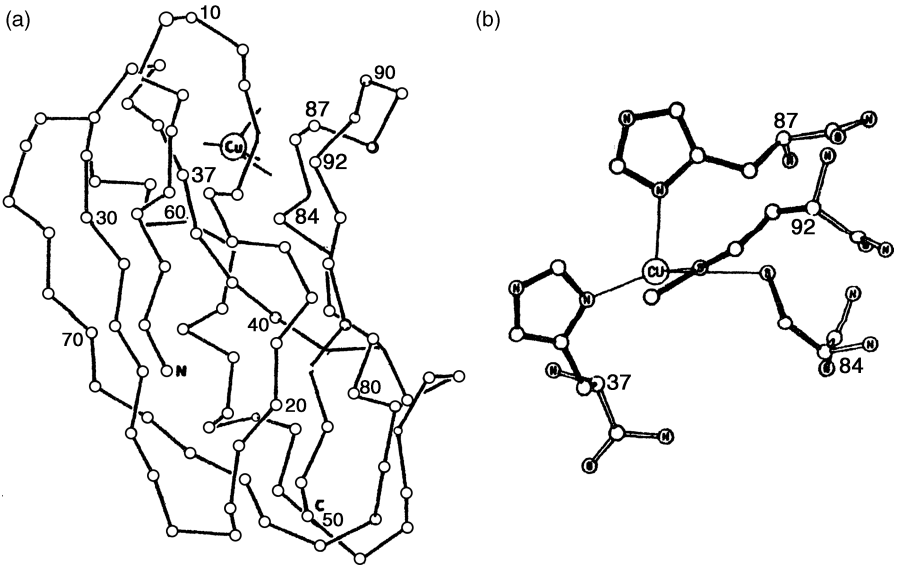

Fig. 3.36. *Crystal structure of plastocyanin:* (a) *location of the Cu atom in the peptide chain;* (b) *environment around the Cu atom [184].*

structures (type 1 site) are responsible for the unusual properties of blue copper proteins mentioned above.

Since then, several groups of investigators measured the RR spectra of type 1 blue copper proteins with excitation lines near the S(Cys) → Cu charge transfer band, and assigned the ν[Cu−N(His)], ν[Cu−S(Cys)], and ν[Cu−S(Met)] vibrations on the basis of isotopic shifts (^{63}Cu/^{65}Cu, ^{32}S/^{34}S and ^{14}N/^{15}N). Although these low-frequency vibrations are strongly coupled with each other, the vibration containing the larger contribution from the ν[Cu−S(Cys)] coordinate is expected to be more strongly resonance-enhanced and to show the larger isotope shift by ^{32}S/^{34}S substitution. Figure 3.37 shows the RR spectra (647.1 nm excitation) of naturally abundant (NA) and isotopically labeled poplar plastocyanins obtained by Qui et al. [186]. Two intense bands at 429.1 and 419.9 cm^{-1} of the NA show the largest isotope shifts (~2.2 cm^{-1}) due to major contribution from the ν[Cu−S(Cys)] coordinate. As expected, the ν[Cu−N(His)] band at 267.3 cm^{-1} (not shown) gives no isotope shift by ^{32}S/^{34}S substitution. Dong and Spiro [187] measured the RR spectra (647.1 nm excitation) of isotopically labeled plastocyanins (H/D, and ^{14}N/^{15}N) in the 1500–150 cm^{-1} region at low-temperature. Their results revealed the presence of vibrational coupling between the ν[Cu−S(Cys)] and ligand internal vibrations that helped in assigning internal modes of cysteine and histidine residues.

Wu et al. [188] measured UVRR spectra (229 nm excitation) of poplar plastocyanine in H_2O/D_2O solution, and compared the NH/ND exchange rate of His 37 and His 87 (Fig. 3.36b). Intensity variations of their imidazole ring modes at 1389 and 1344 cm^{-1} caused by H/D exchange were slower than those of the pair at 1398

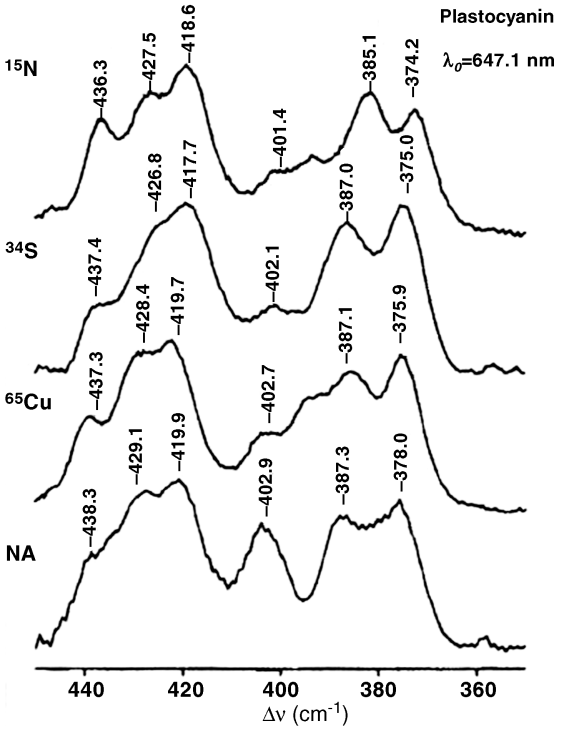

Fig. 3.37. *647.1-nm excited resonance Raman spectra of isotopically labeled and natural abundance plastocyanin from poplar [186].*

and 1354 cm^{-1}. Thus, the former pair was assigned to His 37, which is hydrogen-bonded to the backbone carbonyl group, whereas the latter pair was assigned to His 87, which is exposed to the solvent. The frequencies of the former pair are ~10 cm^{-1} lower than those of the latter due to hydrogen bonding.

The X-ray crystal structure of azurin (*Alcaligenes denitriflavans*) shows that the Cu site takes a distorted trigonal–planar or a trigonal–bipyramodal structure rather than a distorted tetrahedral structure [189]. Dave et al. [190] measured the RR spectra (568.2 nm excitation) of azurin from *Pseudomonas aeruginosa* in natural abundance (WT), and its two mutants, M121G (Met 121 is replaced by Gly) and H46D (His 46 is replaced by Asp) to study the relationship between the ν[Cu−S(Cys)] frequency and metal site geometry. Figure 3.38 shows the RR spectra of these three azurins and their ^{34}S(Cys)-labeled analogs. Each spectrum consists of four bands in the 430–360 cm^{-1} region, which is typical of type 1 structure. The two strong bands near 400 cm^{-1} are of primary interest because the remaining two bands near 428 and 373 cm^{-1} show only small or no $^{32}S/^{34}S$ isotope shifts. Wild-type azurin exhibits the most intense band at 408.6 cm^{-1} with a shoulder at ~400 cm^{-1}. The former is down-shifted by 3.8 cm^{-1}, while the latter shows almost no shift. In mutant M121G and H46D, these bands are separated more distinctly into two bands of almost equal intensities. In WT, the higher

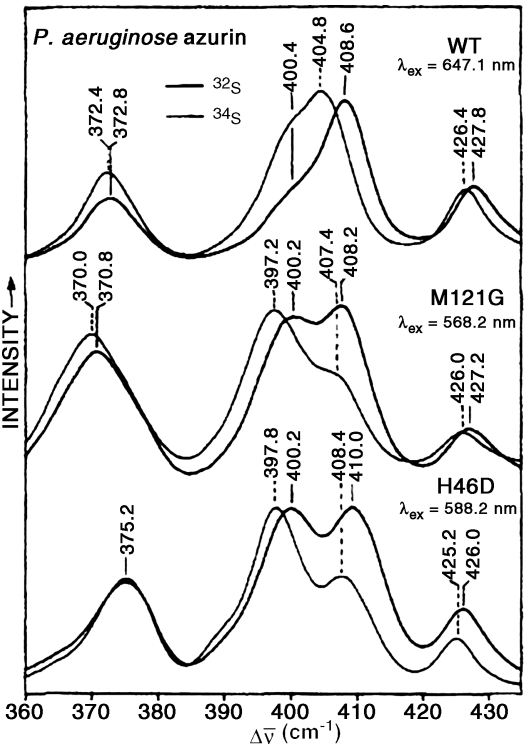

Fig. 3.38. *Low-temperature (77-K) RR spectra of P. aeruginosa azurins (thick-line traces) and their ^{34}S-Cys-labeled proteins (thin-line traces) in the region between 360 and 435 cm^{-1}: top, wild type (WT) excited at 647.1 nm; middle, M121G mutant, and bottom, H46D mutant, both excited at 568.2 nm [190].*

frequency band at 408.6 cm^{-1} can be definitively assigned to the ν[Cu−S(Cys)] vibration. In the mutant azurins, however, the lower-frequency bands near 400 cm^{-1} show much larger isotope shifts than do the higher frequency bands. Thus, the lower-frequency bands are due mainly to the ν[Cu-S(Cys)] vibration. These results suggest that the Cu−S(Cys) bonds of the mutant azurins are lengthened relative to WT azurin probably because the Cu atoms are displaced from the trigonal N_2S plane because of strong interaction with an axial ligand [191]. Van Gastel et al. [192] measured the RR spectra (635.5 nm excitation) of azurin from *P. aeruginosa* and observed that the bands at 409.0 and 401.9 cm^{-1} are downshifted by 4.6 and 5.9 cm^{-1}, respectively, in D_2O solution probably because these vibrations contain δ (Cu−S−H) character.

Ni(II)-substituted *P. aeruginosa* azurin exhibits the S(Cys) → Ni(II) charge transfer absorption at 440 nm (pale yellow). Czernuszewicz et al. [193] measured the RR spectra of Ni(II)(^{58}Ni/^{62}Ni)-reconstituted azurins with 413.1 nm excitation at 77 K. The strong bands at 360 and 346 cm^{-1} were assigned to the ν[Ni–S(Cys)] coupled with δ(SCC) and δ(CCN) vibrations, respectively. These frequencies are much lower than those of the corresponding ν[Cu−S(Cys)] vibrations (408 and 401 cm^{-1}). Their excitation profile

studies show that the intensities of these ν[Ni−S(Cys)] bands are maximized with exciting lines close to the S(Cys) → Ni(II) charge transfer band.

As described above, type 1 (blue) copper proteins are characterized by the electronic absorption near 600 nm and the ν[Cu−S(Cys)] near 400 cm^{-1}. On the other hand, type 2 (yellow) copper proteins such as amine oxidase and superoxide dismutase are characterized by the electronic absorption near 400 nm and the ν[Cu−S (Cys)] near 320–290 cm^{-1}, indicating that the Cu−S(Cys) bond in type 2 is longer and weaker than that of type 1. The Cu center of *P. aeruginosa* azurin mutant, H117G (His 117 is replaced by Gly), is accessible to exogenous ligands through the opening on the surface created by the removal of the endogenous imidazole ligand. den Blaauwen et al.[194] measured the RR spectra of the solution of H117G mutant by adding unidentate ligands such as Cl^-, Br^- and N_3^- and bidentate ligands such as histidine and histamine. Excitation lines at 647.1 and 413.1 nm were used for the solutions containing unidentate and bidentate ligands, respectively. Similar to those mentioned above, the former solutions exhibit strong ν[Cu−S(Cys)] bands in the 410–390 cm^{-1} region, which are typical of type 1 copper site, whereas the latter solutions show them in the 320–290 cm^{-1} region, which are characteristic of type 2 copper site. For example, the histidine mutant exhibits strong bands at 319 and 298 cm^{-1} as shown in Fig. 3.39a. A similar spectrum was obtained for the aqueous solution of H117G

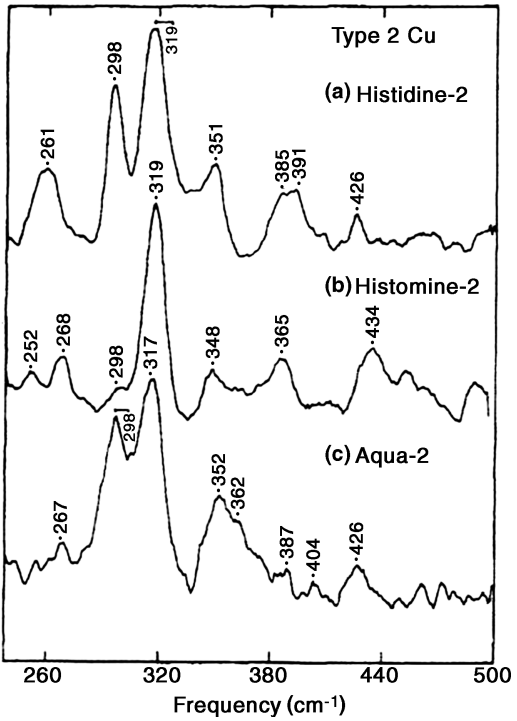

Fig. 3.39. *Resonance Raman spectra of type 2 sites in H117G azurins obtained with 413.1 nm excited:* (a) *H117G plus histidine;* (b) *H117G plus histamine;* (c) *H117G in H_2O (no ligand added) [194].*

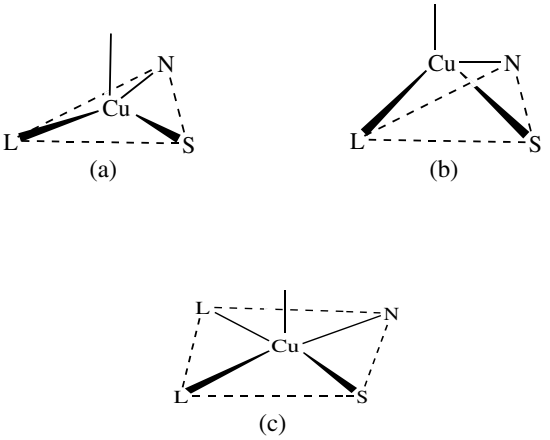

Fig. 3.40. *Proposed structures for types 1 and 2 sites in H117G azurin: (a) trigonal type 1 site, with Cys 112 (S), His 46 (N), and an exogenous ligand (L) in a trigonal–planar array (in wild type, L = His 117 with met 121 as a weak axial ligand); (b) tetrahedral type 1 site, where Cu is displaced from the trigonal ligand plane owing to stronger coordination of the axial ligand; (c) tetragonal type 2 site, which has four strong ligands [e.g., Cys 112 (S), His 46 (N), and a bidentate exogenous ligand (2L)] in a square–planar array with one or more ligands at a longer distance [194].*

(no ligand added) This may imply that two H_2O molecules occupy two coordination sites like one bidentate ligand.

Figure 3.40 illustrates the structures of types 1 and 2 copper sites of H117G azurin proposed by these workers [194]. Here, an exogenous ligand coordinates as a unidentate (L) or a bidentate (L–L). The type 1 site has two possible structures: trigonal (a) and tetrahedral (b). For the type 2 site, the tetragonal geometry (c) was proposed on the basis of on electronic absorption, RR and ESR studies. Andrew and Sanders-Loehr [195] reviewed the relationship between RR spectra and coordination chemistry of copper–sulfur sites.

3.8. IRON–SULFUR PROTEINS [196,197]

Iron–sulfur proteins are found in a variety of organisms, bacteria, plants, and animals, and serve as electron transfer agents via a one-electron oxidation–reduction step [redox potential (E_m), -0.43 V in chloroplasts to $+0.35$ V in photosynthetic bacteria]. For example, ferredoxin in green plants (chloroplasts) is involved in the electron transfer system of photosynthesis. The molecular weights of iron–sulfur proteins range from 5600 (rubredoxin from *Clostridium pasteurianum*, *Cp*) to 83,000 (beef heart aconitase). All these compounds show strong absorptions in the visible and near-UV regions that are due to Fe $\leftarrow$ S CT transitions. Thus, laser excitation in these regions is expected to resonance-enhance ν(Fe$-$S) vibrations of iron–sulfur proteins.

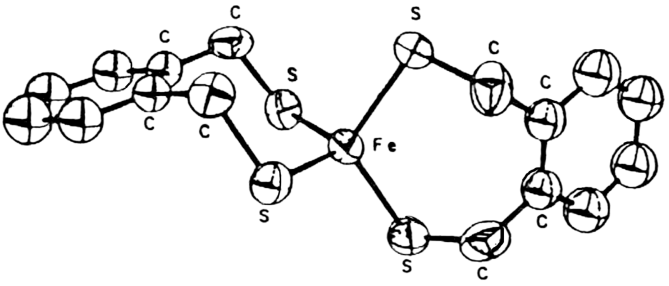

Fig. 3.41. *ORTEP drawing of $[Fe(S_2\text{-}o\text{-}xyl)_2]^-$ viewed down the C_2 axis [198].*

The most simple iron–sulfur protein is rubredoxin (Rd), which contains one Fe atom per protein. The Fe atom is coordinated by four sulfur atoms of cysteinyl residues in a tetrahedral environment. Figure 3.41 shows the crystal structure of a model compound, $[Fe(S_2\text{-}o\text{-}xyl)_2]^-$ (S_2-*o*-xyl = *o*-xylene-α,α'-dithiolate) [198]. Long et al. [199] first obtained the RR spectrum of oxidized rubredoxin, and assigned two bands at 368(ν_3) and 314(ν_1) cm^{-1} to the ν(Fe−S) and those at 150(ν_4) and 126(ν_2) cm^{-1} to the $\delta(FeS_4)$ of the FeS_4 tetrahedron. Later, Yachandra et al. [200] attributed three bands observed near 371, 359, and 325 cm^{-1} of oxidized rabredoxins to the splitting components of the $\nu_3(F_2)$ vibration. Figure 3.42 shows the RR spectra of oxidized rubredoxin from *Desulfovibrio gigas* (D_g) at 77 K obtained by Czernuszewicz et al. [201]. The split components are clearly seen at 376, 363, and 348 cm^{-1} with the $\nu(A_1)$ at 314 cm^{-1}. These workers were able to assign all the fundamentals as well as overtones and combination bands as indicated in Fig. 3.42. Czernuszewicz et al. [202]

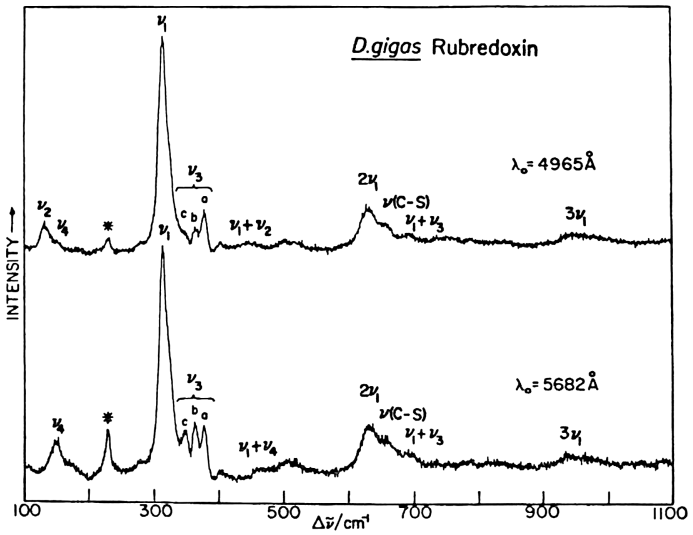

Fig. 3.42. *The RR spectra of oxidized D. gigas rubredoxin obtained in a liquid N_2 Dewar using the excitation lines indicated; the asterisk indicates a band due to ice [201].*

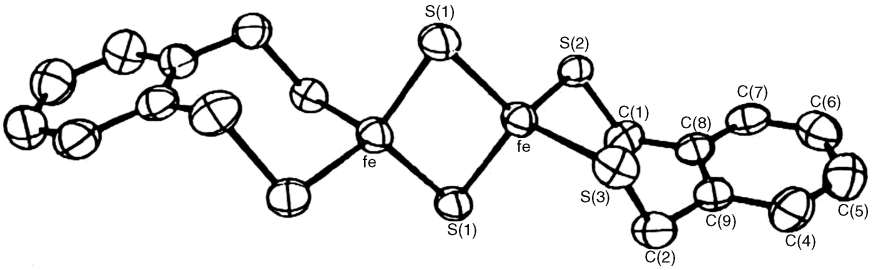

Fig. 3.43. *ORTEP drawing of* $[Fe_2S_2(S_2\text{-}o\text{-}xyl)_2]^{2-}$ *in its* Et_4N^+ *salt [206].*

studied the origins of the F_2 mode splitting by using model compounds, $[FeL_4]^-$ (L=SMe^-; and SEt^-; $(L)_2$=S_2-*o*-xyl). Saito et al. [203] carried out normal coordinate analysis on rubredoxins, considering over 1000 internal coordinates around the FeS_4 site. Their results show the presence of extensive vibrational couplings between the ν(Fe−S) and bending modes of the peptide skeleton.

The RR spectra of rubrerythrin (from *Desulfovibrio vulgaris*) demonstrates the presence of a rubredoxin-type FeS_4 site as well as a (μ-oxo) diiron(III) cluster [204].

Two-iron proteins are found in ferredoxin from chloroplast (MW $\sim$ 10,000) and in adrenodoxin from adrena cortex of mammals (MW $\sim$ 13,000), and so on. These proteins contain the Fe_2S_2(cysteinyl)$_4$ cluster in which two Fe atoms are bridged by two "labile" (inorganic) sulfur atoms and each Fe atom is tetrahedrally coordinated by two bridging and two cysteinyl sulfur atoms (2Fe−2S cluster). This structure was confirmed by X-ray analysis of the ferredoxin from *Spirulina platensis* (*Sp* Fd) [205]. The $Fe_2S_2S'_4$ core ($\mathbf{D}_{2h}$ symmetry) is modeled by the $[Fe_2S_2(S_2\text{-}o\text{-}xyl)_2]^{2-}$ ion whose structure is shown in Fig. 3.43 [206]. Yachandra et al. [207] measured the RR spectra of oxidized spinach ferredoxin and its ^{34}S-enriched analog containing such a 2Fe−2S cluster. Later, Han et al. [208] remeasured the RR spectra of bovine adrenodoxin (Ado) and ferredoxin (Fd) from *Porphyra umbilicalis* with ^{34}S substituted at the bridge positions. Figure 3.44 shows the RR spectra of the native and $^{34}S_b$-reconstituted Fd measured at 77 K, and Table 3.3 lists the band assignments for Fd and its model compound, which were confirmed by normal coordinate calculations. These workers also carried out normal coordinate analysis on model compounds for the $[Fe_2S_2]S'_4$-type proteins to study vibrational couplings between ν(Fe−S) and bending modes [209]. Kuila et al. [210] measured the RR spectra of *Thermus*(*thermophilus*) Rieske protein (TRP) and phthalate dioxygenase (PDO) from *Pseudomonas cepacia* and discussed possible structures for the $[Fe_2S_2]S'_2N_2$-type core.

Vidakovic and coworkers [211] prepared the Ala45Ser mutant of the 2Fe−2S ferredoxin from vegetative cells of the cyanobacterium *Anabaena sp.* 7120, and studied its biochemical and biophysical properties. The RR spectrum was distinctly different from that of the wild-type (WT) protein and showed exceptional similarity to those of higher plant ferredoxins such as spinach ferredoxin. However, the terminal Fe−S stretching vibration of the mutant showed a considerably larger deuterium isotope shift than that of the WT protein. This was attributed to the formation of more hydrogen bonding between the protein matrix and the cysteinyl sulfur atoms in the

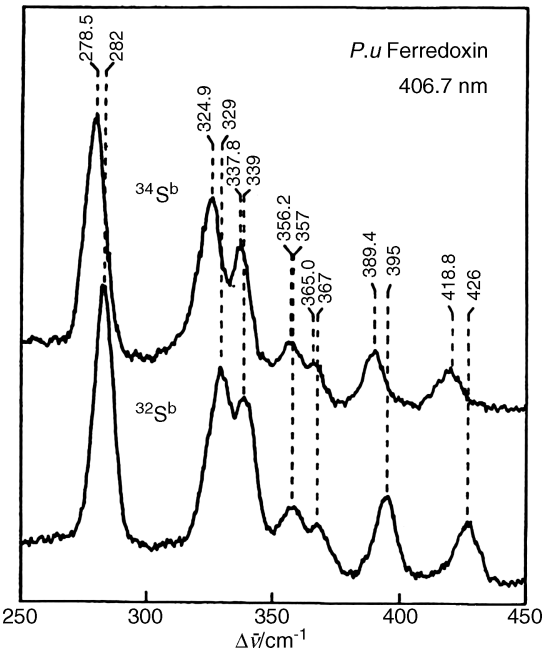

Fig. 3.44. *The RR spectra (77 K) of native and $^{34}S_b$-reconstituted P. umbilicalis Fd [208].*

mutant than in the WT protein. For example, the sidechain hydroxyl group of Ser 45 in the mutant is hydrogen-bonded to the sulfur atom of Cys 41.

One of the most common Fe–S clusters in iron–sulfur proteins is the 4Fe–4S cube containing interpenetrating Fe_4 and S_4 tetrahedra, the Fe corners of which are bound to cysteinyl sulfur atoms. Figure 3.45 shows the X-ray crystal structure of a bacterial ferrodoxin from *Peptococcus aewgenes* (MW $\sim$ 6000) containing two such clusters

TABLE 3.3. RR frequencies and Vibrational Assignments of the $Fe_2S_2(SR)_4$ Core (cm^{-1}) [208]

Vibrational Mode[a]	Symmetry[b]	Fd[c]	$[Fe_2S_2(S_2\text{-}o\text{-xyl})_2]^{2-,c}$
ν(Fe–S_b)	B_{2u}	426(7.2)	415(6.0)
ν(Fe–S_b)	A_g	395(5.6)	391(5.9)
ν(Fe–S_b)	B_{3u}	367 (2.0)	342(3.2)
ν(Fe–S_t)	B_{1u}	357(0.8)	—
ν(Fe–S_t)	B_{2g}		
ν(Fe–S_t)	A_g	339(1.2)	323(2.0)
ν(Fe–S_b)	B_{1g}	329(4.1)	313(3.2)
ν(Fe–S_t)	B_{3u}	282(3.5)	276(3.2)

[a] S_b and S_t denote the bridging and terminal sulfur atoms, respectively.
[b] $\mathbf{D}_{2h}$ symmetry.
[c] Numbers in parentheses indicate the $^{32}S - {}^{34}S$ isotopic shift.

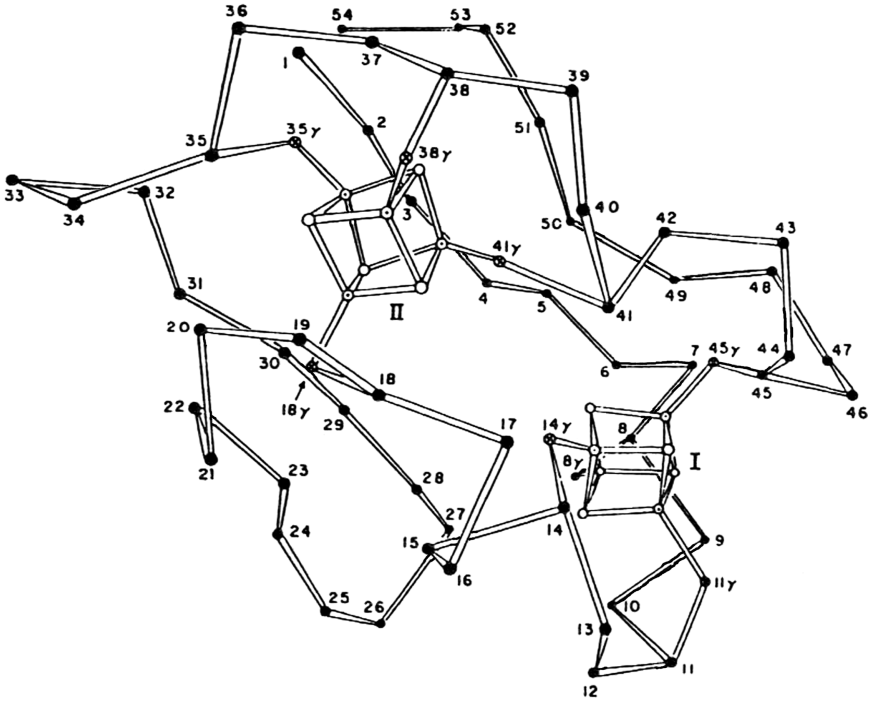

Fig. 3.45. *Structure of bacterial ferredoxin: ⊙, ○, ⊗, and ● indicate Fe, S (inorganic), S (cysteinyl), and C atoms, respectively [212].*

[212]. The geometry of this 4Fe−4S cluster is in good agreement with that of the synthetic analog, $[Fe_4S_4(SR)_4]^{2-}$ (R=$CH_2C_6H_5$, C_6H_5, etc.) prepared by Berg and Holm [213]. In both cases, the 4Fe−4S cube is slightly squashed with four short and eight long Fe−S bonds (approximately $\mathbf{D}_{2d}$ symmetry).

The RR spectra of 4Fe−4S proteins have been reported by several investfgators [214–217]. Figure 3.46 shows the RR spectra of the high-potential iron protein (HiPIP) from *Chromatium vinosum* (*Cv*), ferredoxin from *Clostridium pasteurianum* (*Cp*), and their model compounds, $(Et_4N)_2$ $[Fe_4S_4(SCH_2Ph)_4]$, in the solid state and in solution obtained by Czernuszewicz et al. [216]. Table 3.4 lists the observed frequencies and band assignments for these compounds. From normal coordinate calculations using $^{32}S/^{34}S$ isotopic shift data, these workers confirmed that the symmetry of the model compound above is $\mathbf{T}_d$ in solution but $\mathbf{D}_{2d}$ in the solid state. If the symmetry of the $(Fe_4S_4)S'_4$ core shown in Fig. 3.47 is $\mathbf{T}_d$, it should give five ν(Fe-S_b) ($A_1+E+F_1+2F_2$) and two ν(Fe−S_t) (A_1+F_2) modes. Here, S_b and S_t denote the bridging and terminal S atoms, respectively. If it is $\mathbf{D}_{2d}$, all the degenerate vibrations under $\mathbf{T}_d$ symmetry should split into two bands. As a result, a total of 12 vibrations are expected.

Thus, the results shown in Table 3.4 and Fig. 3.46 support their conclusions. Furthermore, the RR spectra of HiPIP and *Cp Fd* are similar to that of the model compound in solution and in the solid state, respectively. Thus, the symmetries of the Fe_4S_4 cores of these proteins must be $\mathbf{T}_d$ and $\mathbf{D}_{2d}$, respectively.

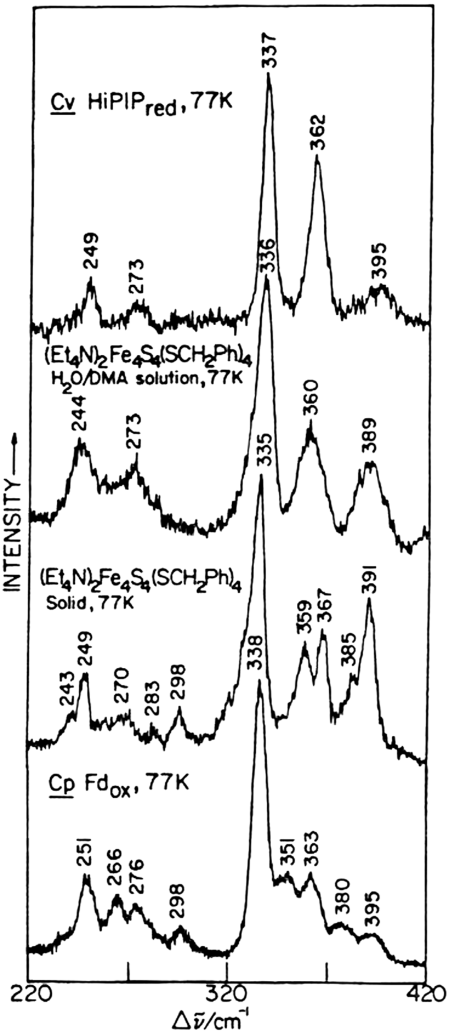

Fig. 3.46. *The RR spectra (77 K) of Cv* HiPIP$_{red}$ (457.9 nm excitation), *Cp* Fd_{ox} *(488.0 nm excitation), and* $(Et_4N)_2[Fe_4S_4(SCH_2Ph)_4]$ *in solution (room temperature, 457.9 nm excitation) and solid state (KCl pellet, 488.0 nm excitation) [216].*

Maes et al. [218] measured the RR spectra of a series of 4Fe−4S proteins of the type $(n\text{-}Bu_4N)_2[Fe_4S_4(SR^-)_4]$, where SR^- is thiophenol (tp) and its dimethyl derivatives at positions 3.5, 2.4, and 2.6. Assignments of their Fe−S vibrations were based on $^{32}S/^{34}S$ isotope shifts and normal coordinate analysis. It was found that the Fe_4S_4 cores of these proteins take a significantly distorted $\mathbf{D}_{2d}$ structure, and that the general rule $\nu(Fe-S_t) > \nu(Fe-S_b)$ is violated when their frequencies are compared for the thiphenolate and 2,6-dimethylthiophenolate clusters as shown in Fig. 3.48.

TABLE 3.4. RR Frequencies (cm^{-1}) and Band Assignments for the $[Fe_4S_4(SCH_2Ph)_4]^{2-}$ Ion, Oxidized *Cp Fd* and Reduced *Cv* HiPIP[a]

D_{2d}	$[Fe_4S_4(SCH_2Ph)_4]^{2-}$ (Solid)	*Cp Fd*	*Cv* HiPIP	$Fe_4S_4(SCH_2Ph)_4]^{2-}$ (Solution)	T_d
		Mainly Terminal ν (Fe–S)			
A_1	391(1)	395(3.9)	395	384(1)	A_1
$B_2(F_2)$	367(1)	351(0.7)	362	358(1)	F_2
$E(F_2)$	359(2)	363(2.0)			
		Mainly Bridging ν(Fe–S)			
$B_2(F_2)$	385(6)	380(5.6)	395	384(1)	F_2
$E(F_2)$	—	—			
A_1	335(8)	338(7.0)	337	333(7)	A_1
A_1(E)	298(5)	298(4.9)	273	268(3)	E
B_1(E)	283(4)	276(4.5)			
$E(F_1)$	283(4)	276(4.5)	273	268(3)	F_1
$A_2(F_1)$	270(3)	266(4.0)			
$B_2(F_2)$	249(6)	251(6.2)	249	241(6)	F_2
$E(F_2)$	243(5)	—			

[a] Numbers in parentheses indicate downshifts due to S substitution for the bridging S atoms [216].

In the active form of aconitase that catalyzes the isomerization of citrate to isocitrate, one of the Fe atoms in the Fe_4S_4 cluster is coordinated by an OH_x ($x = 1$ or 2) group instead of a cysteinyl residue. Kilpatrick et al. [219] assigned the ν(Fe−S) of aconitase and its model compounds via normal coordinate analysis.

A number of Fe−S proteins contain 3Fe centers. ln some cases, the 3Fe center can be converted to the 4Fe center, and vice versa. The structures of 3Fe clusters were controversial. In 1980, Stout et al. [220] determined the crystal structure of ferredoxin I extracted from *Azotobacter vinelandii* (*Av* Fd I; MW, 14,000) which contains a 3Fe−3S cluster in addition to a 4Fe−4S cluster. For the former, they proposed a novel Fe_3S_3 planar ring structure. However, Beinert et al. showed that four labile sulfides, not three, are associated with the 3Fe center [221]. Thus, these workers as well as Johnson et al. [214] proposed cubane-like structures in which one of the corner Fe atoms is lost (Fig. 3.49).

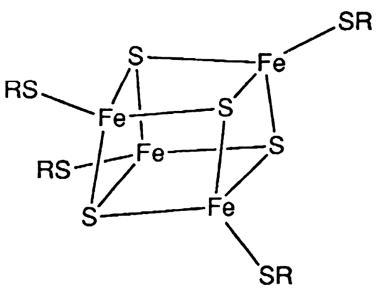

Fig. 3.47. *Structure of the $(Fe_4S_4)S'_4$ cluster.*

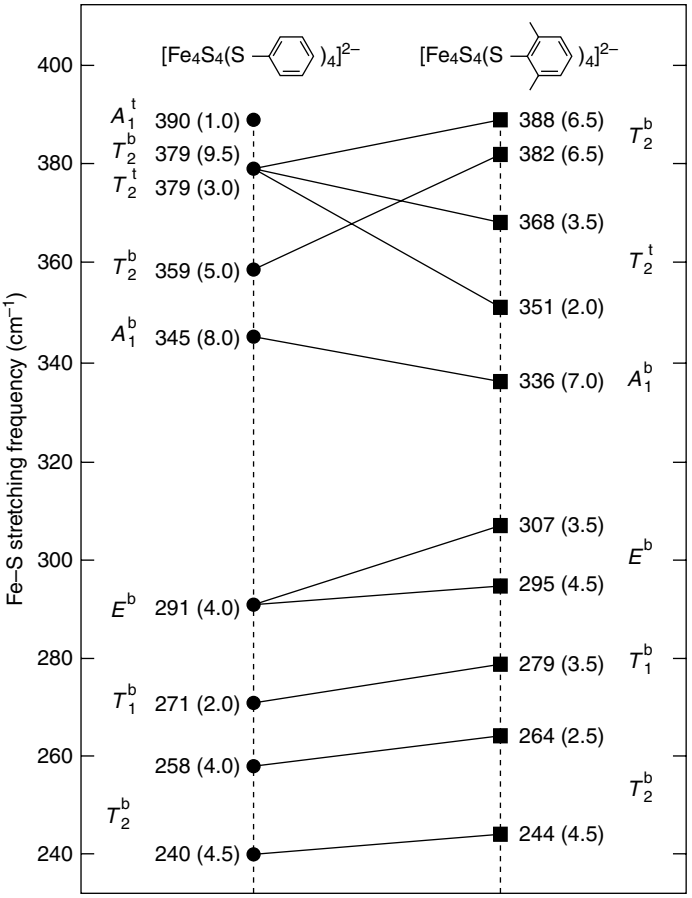

Fig. 3.48. *Correlation diagram of RR frequencies for $[Fe_4S_4(tp)_4]^{2-}$ and $[Fe_4S_4(2,6\text{-dmtp})_4]^{2-}$ (b refers to bridging Fe–S modes; t refers to terminal Fe–S (aryl) modes) [218].*

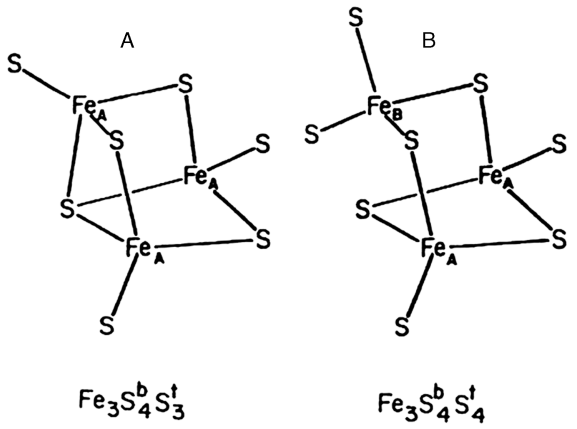

Fig. 3.49. *Structures proposed for 3Fe–4S clusters [221].*

Johnson et al. [214] first measured the RR spectra of *Av* Fd I and *Tt* Fd (from *Thermus thermophilus*), both of which contain 3Fe as well as 4Fe clusters. As seen in Fig. 3.50, their RR spectra are dominated by the 3Fe spectra, which exhibit bands at 390, 368, 347,

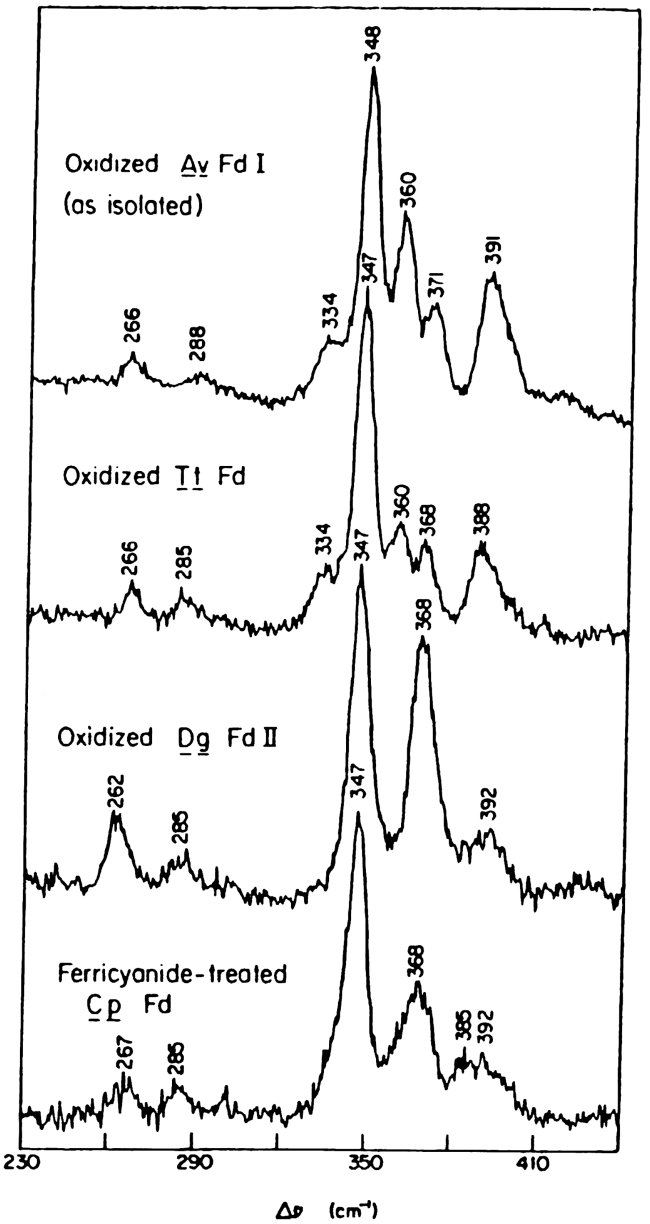

Fig. 3.50. *Low-temperature RR spectra (488.0 nm excitation) of oxidized Av Fd I, oxidized Tt Fd, oxidized Dg Fd II, and ferricyanide-tetrated Cp Fd [222].*

285, and 266 cm^{-1}. The weak band at 334 cm^{-1} is attributed to the 4Fe−4S cluster. Oxidized *Dg* Fd II [222] and ferricyanide-treated C_p Fd, [223], which are known to contain only 3Fe clusters, show no such bands. The ^{34}S sulfide substitution in *Tt* Fd and ferricyanide-treated *Cp* Fd produced downshifts of the bands near 266, 285, and 347 cm^{-1}. Therefore, these bands must be assigned to the bridging ν(Fe−S). The strong band at 347 cm^{-1} is due to the totally symmetric breathing-cluster mode, while the remaining bands near 390 and 368 cm^{-1} are assigned to the terminal ν(Fe−S).

Normal coordinate calculations by Johnson et al. [214] have shown that the RR spectra of *Av* Fd I crystals and 3Fe-bacterial ferredoxins (*Cp* Fd and *Tt* Fd) are compatible with cubane-like 3Fe−4S structures shown in Fig. 3.49, but not with the 3Fe−3S structure reported by Stout et al. The RR spectra of aconitase (inactive form) and *Desulfovibrio desulfuricans* [224] are also very similar to those mentioned above, indicating the possibility of the cubane-like 3Fe−4S structures in these proteins. Later, the planar Fe_3S_3 structure originally proposed by Stout et al. [220] was found to be in error [225].

3.9. INTERACTIONS OF METAL COMPLEXES WITH NUCLEIC ACIDS

Nucleic acids interact with a variety of ligands such as metal ions, metal complexes, anticancer drugs, and carcinogens. Their modes of interactions with DNA can be classified into *intercalation, groove binding, covalent bonding,* and *strand-breaking,* and these are often reinforced by hydrogen bonding and/or Coulombic interactions. Figure 3.51 shows the structure of one strand of DNA backbone consisting of deoxyriboses connected via phosphate groups Bases such as guanine (G), cytosine (C), adenine (A), and thymine (T) are attached to deoxyriboses, and the chain direction is defined as 5′O to 3′O (5′ → 3′). The well-known double-helix structure is formed by hydrogen bondings between G–C and A–T bases on the complementary strands (Fig. 3.52). Interaction of DNA with a ligand results in changes in the double-helix structure, thereby inhibiting DNA replication and transcription, which are necessary preconditions for cell division. In the following, vibrational studies on interactions of metal complexes with nucleic acids are discussed using two examples. More detailed and extensive discussions are found in several review articles [226] and monographs [227,228].

3.9.1. Cisplatin [229]

A square–planar platinum complex, *cis*-diamminedichloroplatinum(II), *cis*-$[Pt(NH_3)_2Cl_2]$ (abbreviated as *cisplatin*) and its derivative, carboplatin, shown in Fig. 3.53a are well-known anticancer drugs that are currently in clinical use. When reacted with DNA, cisplatin forms *covalent* Pt−N bonds by replacing its two Cl ligands with the N_7 atoms of guanine (G) or adenine (A) bases. Although four types of platinum–DNA complexes shown in Fig. 3.53b (structures **a**, **b**, **c**, and **d**) are formed, the major products are the *1,2-intrastrand crosslinking* complexes at the 5′-GG-3′ sequence (**a**, 60%) and 5′-AG-3′ sequence (**b**, 25%). Minor products are *1,3-intrastrand crosslinking* (**c**) and *1,2-interstrand crosslinking* (**d**) complexes between two G bases that are formed less than 10%.

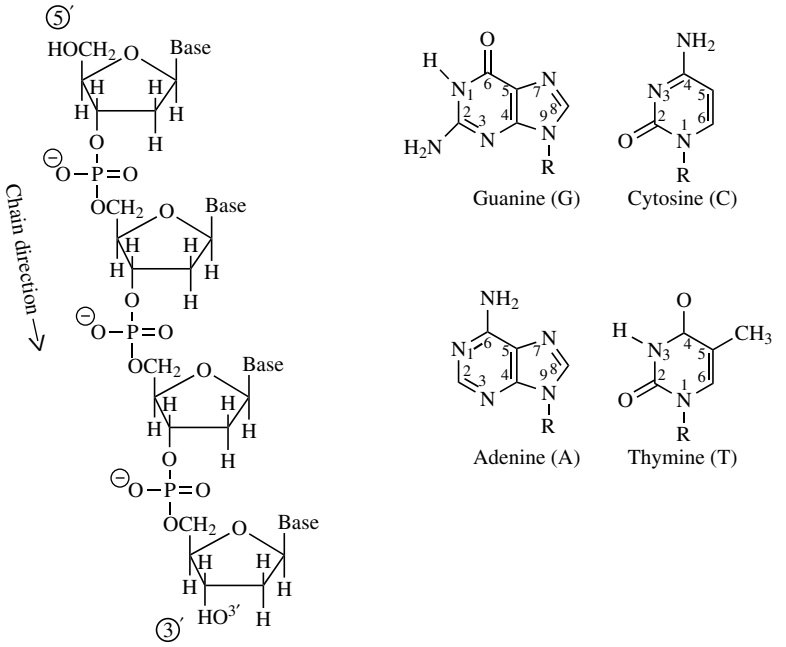

Fig. 3.51. *Structures of one strand of DNA chain (left) and four bases attached to it (right). (R denotes the attached sugar ring; R = H for isolated bases).*

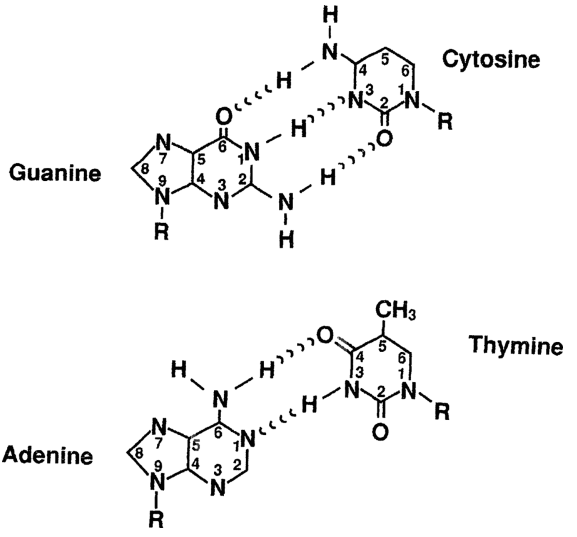

Fig. 3.52. *Watson–Crick base-pairing schemes via hydrogen bonding.*

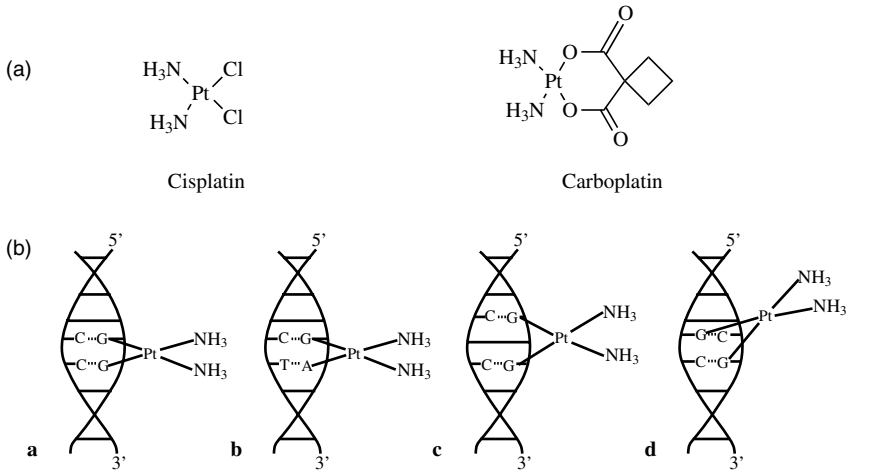

Fig. 3.53. *(a) Structures of cisplatin and carboplatin; (b) four modes of interactions of cisplatin with DNA.*

Lippard and coworkers [230] carried out X-ray analysis of cisplatin complexed to the dodecamer, d(CCTCTG*G*TCTCC)·d(GGAGACCAGAGG), where G*G* denotes the binding site of cisplatin. It was found that the duplex is bent significantly at this site, and such a severely bent structure with a widened minor groove resembles the DNA structures in complexes with proteins containing the high-mobility group (HMG). This similarity suggests how HMG-domain protein may recognize the presence of the cisplatin–DNA complex, thus explaining the origin of the anticancer activity of cisplatin.

Figure 3.54 shows the UVRR spectra (209 nm excitation) of 5′-GMP (guanosine-5′-monophosphate) [panel (*a*)] and its complex with cisplatin [panel (*b*)] obtained by Benson et al. [231]. The guanine bands at 1686 [$\nu(C_6{=}O)$], 1586 (six-membered ring vibration) and 1368 cm^{-1} (five-membered ring vibration) are weakened considerably as a result of the $Pt{-}N_7$ bonding. In particular, the band at 1368 cm^{-1} disappears almost completely by platination. In the 1300–1100 cm^{-1} region, the 1180 cm^{-1} band (five-membered ring vibration) is shifted to higher frequencies (1245 and 1218 cm^{-1}) with increased intensities. Similar results [panel (*c*)] were obtained for 5′-GMP reacted with carboplatin (Fig. 3.53a), although the changes observed were less pronounced than those for cisplatin. The band near 1178 cm^{-1} of $d(GGCCGGCC)_2$ is also shifted on interaction with cisplatin, thus demonstrating the effect of forming the $Pt{-}N_7$ bond on the guanine ring.

3.9.2. Water-Soluble Metalloporphyrins

Cationic water-soluble *meso*-tetra(*N*-methyl-4-pyridyl) porphyrins, H_2(TMpy-P4) and its metal complexes shown in Fig. 3.55 can be activated chemically or by light to cleave a DNA strand, and may be used in treating cancer and other deseases [232].

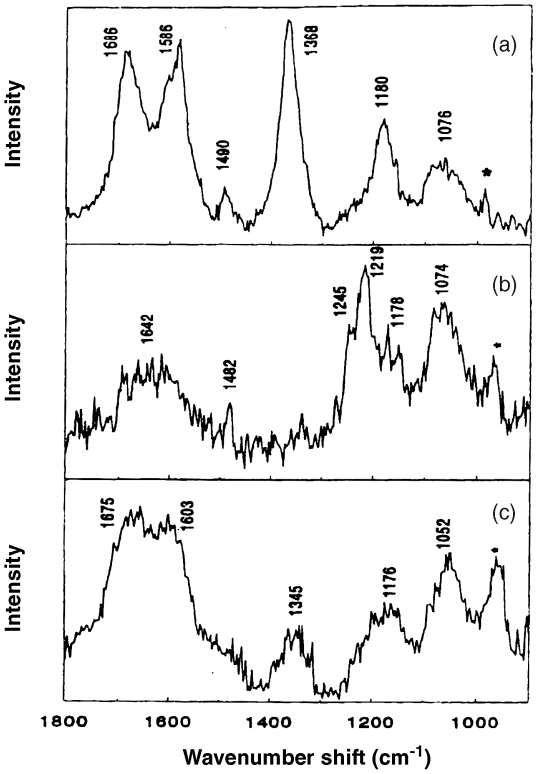

Fig. 3.54. *UV RR spectra (209 nm excitation) of 5′-GMP* (a)*, its complex with cisplatin* (b)*, and carboplatin* (c) *[231].*

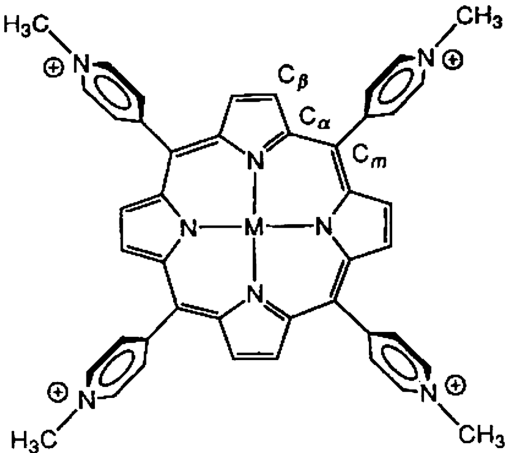

Fig. 3.55. *Structure of M(TMpy-P4).*

Interactions of these porphyrins with DNA have been studied by a variety of physicochemical techniques. It is known that H_2(TMpy-P4) and its Cu(II) and Ni(II) derivatives with no axial ligands *intercalate* at the GC-rich region, whereas the Zn(II), Co(III), Fe(III), and Mn(III) derivatives with axial water coordination form *outside-bound* or *groove-bound* complexes at the AT-rich region of DNA [233].

The porphyrin–DNA system is ideal for RR studies because only porphyrin vibrations can be resonance-enhanced by using excitation lines in the 400–500 nm region. Schneider et al. [234] were the first to measure band shifts of metalloporphyrins resulting from interaction with nucleic acids by using Raman difference techniques. Figure 3.56 shows the RR spectra of Cu(TMpy-P4) (trace **A**) and its mixture with poly $(dG–dC)_2$ (porphyrin/phosphate ratio = 0.04) in dilute solution (trace **B**). Although nine bands are observed in this region, only six (I, II, V, VI, VIII, and IX) are shifted by interaction with poly$(dG–dC)_2$. Among them, band II near 1100 cm^{-1} shows the largest shift (+6.8 cm). This band corresponds to the ν_9 of Ni(TPP) (Table 1.10), and is due largely to the $\delta(C_\beta–H)$ mode. In free Cu(TMpy-P4), the *N*-methylpyridyl (pyr) rings are nearly perpendicular to the porphyrin plane. In order to form an *intercalated*

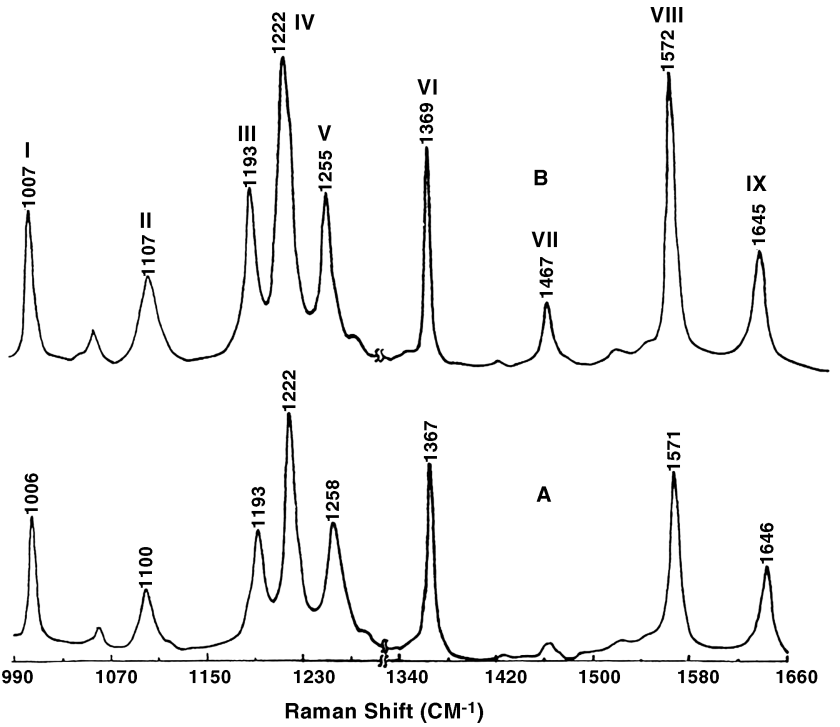

Fig. 3.56. *The RR spectra (441.6 nm excitation) of (A) Cu (TMpy-P4) and (B) Cu(TMpy-P4) + poly(dG–dC)$_2$ (R = 0.04). The frequencies given are only approximate. For accurate values, see Ref. 234.*

complex with poly(dG–dC)$_2$, however, it is necessary to rotate the pyr ring toward the porphyrin plane. This would increase repulsion between the C_β–H and the hydrogen of the pyr ring at the ortho position, resulting in an upshift of the $\delta(C_\beta–H)$ vibration. Conversely, the observation of such a trend signals *intercalation* of the metalloporphyrin between base pairs of nucleic acids. In fact, a mixture of Cu(TMpy-P4) with poly(dA–dT)$_2$, which is known to be *groove-bound*, shows only a small upshift (0.2 cm^{-1}) of this band. Similar observation is made for Co(III)(TMpy-P4) mixed with poly(dG–dC)$_2$ or poly(dA–dT)$_2$. Bands V ($\sim$1258 cm^{-1}) and IX ($\sim$1646 cm^{-1}) originate in the *N*-methylpyridyl group, and show small downshifts regardless of the mode of interaction. Later, Nonaka et al. [235] observed that the $\nu_a(PO_2)$ at 1221 cm^{-1} and $\nu_s(PO_2)$ at 1086 cm^{-1} of DNA are upshifted by 17–12 cm^{-1} and downshifted by 26–18 cm^{-1}, respectively, when DNA is mixed with M(TMpy-P4). These results

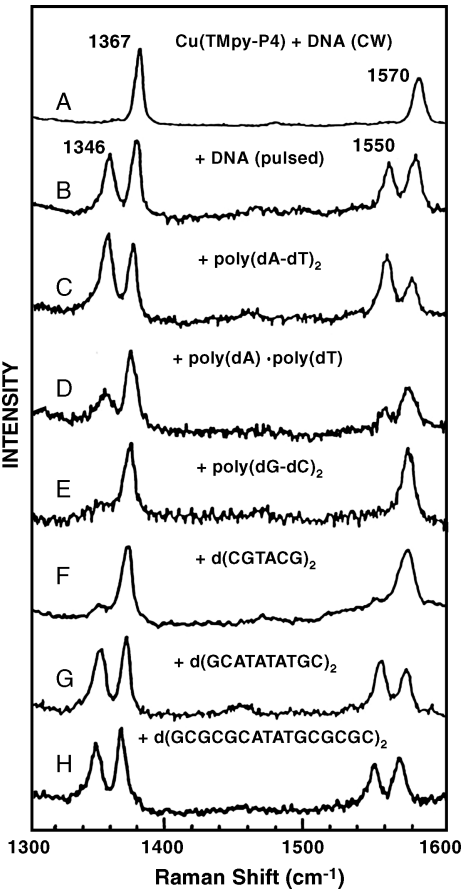

Fig. 3.57. *The RR spectra of Cu(TMpy-P4)–nucleic acid complexes. All the spectra were obtained by using a pulsed-laser excitation (416 nm) except for the top spectrum (CW 406.7 nm excitation) [237].*

indicate the presence of strong *Coulombic interaction* between the N^+-CH_3 group of M(TMpy-P4) and the O atom of the PO_2 group of the DNA backbone, which strengthens their interaction. In fact, X-ray analysis on Cu(TMpy-P4) complexed to $d(CGATCG)_2$ shows that the porphyrin ring is *hemiintercalated* at the C−G step of one strand of 5′-TCG-3′, and that two positively charged pyridyl groups in the minor groove are close to several negatively charged phosphate oxygen atoms, although other two pyridyl groups in the major groove are relatively far from them [236].

Strahan et al. [237] found that the Cu(TMpy-P4) *intercalated* between the GC/CG sequence of DNA is translocated to the ATAT site upon electronic excitation by a pulsed laser. As seen in Fig. 3.57, the RR spectrum of Cu(TMpy-P4) obtained by high-power pulsed laser exhibits new bands at 1550 and 1346 cm^{-1} (trace B) that are not observed by CW laser excitation (trace A). These new bands do not appear with low-power pulsed-laser excitation. They are observed with poly(dA–dT)$_2$ (trace C) but not with poly(dG–dC)$_2$ (trace E). These new bands have been attributed to an electronically excited Cu(TMpy-P4) that is stabilized by forming a π-cation radical exciplex, $(Cu(TMpy\text{-}P4))^{+*}(AT)^-$, at an AT site [238]. If oligonucleotides contain GC/CG as well as ATAT or a longer A/T sequence, the exciplex bands are observed as shown in traces G and H. More elaborate experiments show that, in these cases, some of the *intercalated* porphyrin at the GC/CG site is translocated to the ATAT site (major *groove binding*) [237].

Photochemistry of Cu(II) complexes including Cu(TMpy-P4) was reviewed by McMillin and McNett [239]. Mettach et al. [240] prepared a series of non-*meso*-substututed cationic porphyrins and studied their interactions with DNA and photocleavage properties.

REFERENCES

1. T. G. Spiro, ed., *Biological Applications of Raman Spectroscopy*, Vols. 1–3, Wiley, New York, 1987–1988.
2. A. T. Tu, *Raman Spectroscopy in Biology*, Wiley, New York, 1982.
3. P. B. Carey, *Biochemical Applications of Raman and Resonance Raman Spectroscopies*, Academic Press, New York, 1982.
4. F. S. Parker, *Application of Infrared Raman and Resonance Raman Spectroscopy in Biochemistry*, Plenum Press, New York, 1983.
5. K. Nakamoto and R. S. Czernuszewicz, "Infrared Spectroscopy," in J. F. Riordan and B. L. Vallee, eds., *Methods in Enzymology*, Vol. 226, Part C, Academic Press, San Diego, CA, 1993.
6. T. G. Spiro and R. S. Czernuszewicz, "Resonance Raman Spectroscopy of Metalloproteins," in K. Sauer, ed., *Methods in Enzymology*, Vol. 246, Academic Press, San Diego, CA, 1995. p. 416.
7. R. G. Shulman, J. J. Hopfield, and S. Ogawa, *Q. Rev. Biophys.* **8**, 325 (1975).
8. R. H. Felton, and N.-T. Yu, "Resonance Raman Scattering from Metalloporphyrins and Hemopreteins," in D. Dolphin,ed., *The Porphyrins* Vol. 3, Part A, Academic Press, New York, 1978, p. 347.

9. T. G. Spiro, "The Resonance Raman Spectroscopy of Metalloporphyrins and Heme Proteins," in A. B. P. Lever and H. B. Gray, eds., *Iron Porphyrins*, Addison-Wesley, Reading, MA, 1983.
10. S. A. Asher, "Resonance Raman Spectroscopy of Hemoglobin," in S. P. Colowick and N. O. Kaplan, eds., *Methods in Enzymology*, Vol. 76, Academic Press, New York, 1981, p. 371.
11. J. R. Kincaid, "Resonance Raman Spectroscopy of Heme Proteins and Model Compounds," in K. M. Kadish, K. M. Smith, and R. Guillard, eds., *The Porphyrin Handbook*, Vol. 7, Academic Press, San Diego, CA, 1999, Chapter 51.
12. J. O. Alben, "Infrared Spectroscopy of Porphyrins," in D. Dolphin, ed., *The Porphyrins*, Vol. 3, Part A, Academic Press, New York, 1978, p. 323.
13. S. A. Asher, *Anal. Chem.* **65**, 59A, 201A (1993).
14. X. Zhao and T. G. Spiro, *J. Raman Spectrosc.* **29**, 49 (1996).
15. S. Choi, T. G. Spiro, K. C. Langry, K. M. Smith, D. L. Budd, and G. N. La Mar, *J. Am. Chem. Soc.* **104**, 4345 (1982).
16. V. L. DeVito and S. A. Asher, *J. Am. Chem. Soc.* **111**, 9143 (1989).
17. P. G. Hildebrandt, R. A. Copeland, T. G. Spiro, J. Otlewski, M. Laskowski, Jr., and F. G. Prendergast, *Biochemistry* **27**, 5426 (1988).
18. V. Palaniappan and D. F. Bocian, *J. Am. Chem. Soc.* **116**, 8839 (1994).
19. T. G. Spiro and T. C. Strekas, *J. Am. Chem. Soc.* **96**, 338 (1974).
20. H. Ozaki, T. Kitagawa, Y. Kyogoku, H. Shimada, T. Iizuka, and Y. Ishimura, *J. Biochem.* **80**, 1447 (1976).
21. H. Oshio, T. Ama, T. Watanabe, J. Kincaid, and K. Nakamoto, *Spectrochim. Acta* **40A**, 863 (1984).
22. T. Kitagawa, "Heme Protein Structure and the Iron-Histidine Stretching Mode," in T. G. Spiro, ed., *Biological Applications of Raman Spectroscopy*, Vol. 3, Wiley, New York, 1988, p. 97.
23. K. Nagai, T. Kitagawa, and H. Morimoto, *J. Mol. Biol.* **136**, 271 (1980).
24. S. Matsukawa, K. Mawatari, Y. Yoneyama, and T. Kitagawa, *J. Am. Chem. Soc.* **107**, 1108 (1985).
25. P. Stein, M. Mitchell, and T. G. Spiro, *J. Am. Chem. Soc.* **102**, 7795 (1980).
26. A. V. Wells, J. T. Sage, D. Morikis, P. M. Champion, M. L. Chiu, and S. G. Sligar, *J. Am. Chem. Soc.* **113**, 9655 (1991).
27. A. Schulte, S. Buchter, O. Galkin, and C. Williams, *J. Am. Chem. Soc.* **117**, 10149. (1995).
28. J. A. Shelnutt, K. Alston, J.-Y. Ho, N.-T. Yu, T. Yamamoto, and J. M. Rifkind, *Biochemistry* **25**, 620 (1986).
29. E. Podstawka, C. Rajani, J. R. Kincaid, and L. M. Proniewicz, *Biopolymers* **57**, 201 (2000).
30. N.-T. Yu, "Vibrational Modes of Coordinated CO, CN^-, O_2 and NO," in T. G. Spiro, ed., *Biological Applications of Raman Spectroscopy*, Vol. 3, Wiley, New York, 1988, p. 39.
31. M. Tsubaki, R. B. Srivastava, and N.-T. Yu, *Biochemistry* **21**, 1132 (1982).
32. S. Hirota, T. Ogura, K. Shinzawa-Itoh, S. Yoshikawa, M. Nagai, and T. Kitagawa, *J. Phys. Chem.* **98**, 6652 (1994).
33. S. Hu, K. M. Vogel, and T. G. Spiro, *J. Am. Chem. Soc.* **116**, 11187 (1994).

34. C. Rajani and J. R. Kincaid, *J. Am. Chem. Soc.* **120**, 7278 (1998).
35. A. Ghosh and D. F. Bocian, *J. Phys. Chem.* **100**, 6363 (1996).
36. I. Pápai, A. Stirling, J. Mink, and K. Nakamoto, *Chem. Phys. Lett.* **287**, 531 (1998).
37. X.-Y. Li and T. G. Spiro, *J. Am. Chem. Soc.* **110**, 6024. (1988).
38. J. M. Baldwin, *J. Mol. Biol.* **136**, 103 (1980).
39. J. Ramsden and T. G. Spiro, *Biochemistry* **28**, 3125 (1989).
40. W. H. Fuchsman and G. A. Appleby, *Biochemistry* **18**, 1309 (1979).
41. R. Hoffman, M. M. L. Chen, and D. L. Thorn, *Inorg. Chem.* **16**, 503 (1977).
42. W. E. Brown, III, J. W. Sutcliffe, and P. D. Pulsinelli, *Biochemistry* **22**, 2914 (1983).
43. M. W. Makinen, R. A. Houtchens, and W. S. Caughey, *Proc. Natl. Acad. Sci. USA* **76**, 6042 (1979).
44. J. D. Sattwellee, M. Teintze, and J. H. Richards, *Biochemistry* **27**, 1456 (1978).
45. S. E. V. Philips, *J. Mol. Biol* **142**, 521 (1980).
46. S. E. V. Philips and B. P. Schoenborn, *Nature* **292**, 81, (1981).
47. B. Shaanan, *Nature* **296**, 683 (1982).
48. H. Brunner, *Naturwissenschaften* **61**, 129 (1974).
49. L. L. Duff, E. H. Applelman, D. F. Shriver, and I. M. Klotz, *Biochem. Biophys. Res. Commun.* **90**, 1098 (1979).
50. S. Hirota, T. Ogura, E. H. Applelman, K. Shinzawa-Itoh, S. Yoshikawa, and T. Kitagawa, *J. Am. Chem. Soc.* **116**, 10564, (1994).
51. S. Jeyarajah, L. M. Proniewicz, H. Bronder, and J. R. Kincaid, *J. Biol. Chem.* **269**, 31047 (1994).
52. C. H. Barlow, J. C. Maxwell, W. J. Wallace, and W. S. Caughey, *Biochem. Biophys. Res. Commun.* **55**, 91 (1973).
53. J. C. Maxwell and W. S. Caughey, *Biochem. Biophys. Res. Commun.* **60**, 1309 (1974).
54. M. Tsubaki and N.-T. Yu, *Proc. Natl. Acad. Sci. USA* **78**, 3581 (1981).
55. T. Kitagawa, M. R. Ondrias, D. L. Rousseau, M. Ikeda-Saito, and T. Yonetani, *Nature* **298**, 869 (1982).
56. W. T. Potter, M. P. Tucker, R. A. Houtchens, and W. S. Caughey, *Biochemistry* **26**, 4699 (1987).
57. A. Bruha and J. R. Kincaid, *J. Am. Chem. Soc.* **110**, 6006 (1988).
58. J. C. Maxwell and W. S. Caughey, *Biochemistry* **15**, 388 (1976).
59. J. D. Stong, J. M. Burke, P. Daly, P. Wright, and T. G. Spiro, *J. Am. Chem. Soc.* **102**, 5815 (1980).
60. M. A. Walters and T. G. Spiro, *Biochemistry* **21**, 6989 (1982).
61. M. Tsubaki and N.-T. Yu, *Biochemistry* **21**, 1140 (1982).
62. H. C. Mackin, B. Benko, N.-T. Yu, and K. Gersonde, *FEBS Lett*. **158**, 199 (1983).
63. B. Benko and N.-T. Yu, *Proc. Natl. Acad. Sci. USA* **80**, 7042 (1983).
64. S. Hu and J. R. Kincaid, *J. Am. Chem. Soc.* **113**, 9760 (1991).
65. N.-T. Yu, H. M. Thompson, H. Mizukami, and K. Gersonde, *Eur. J. Biochem.* **159**, 129 (1986).
66. S. Hu, *Inorg. Chem.* **32**, 1081 (1993).

67. N. Parthasarathi and T. G. Spiro, *Inorg. Chem.* **26**, 2280, 3792 (1987).
68. N.-T. Yu, S. H. Lin, C. K. Chang, and K. Gersonde, *J. Biophys.* **55**, 1137 (1989).
69. J.-L. Wang, W. S. Caughey, and D. L. Rousseau, in M. Feelisch and J. S. Stamler, eds., *Methods in Nitric Oxide Research*, Wiley, New York, (1996).
70. S. McCoy and W. S. Caughey, *Biochemistry* **9**, 2387 (1970).
71. J. F. Deatherage, R. S. Loe, C. M. Anderson, and K. Moffat, *J. Mol. Biol.* **104**, 687 (1976).
72. N.-T. Yu, B. Benko, E. A. Kerr, and K. Gersonde, *Proc. Natl. Sci. USA* **81**, 5106 (1984).
73. M. Tsubaki, R. B. Srivastava, and N.-T. Yu, *Biochemistry* **20**, 946 (1981).
74. S. A. Asher and T. M. Schuster, *Biochemistry* **18**, 5377 (1979).
75. S. A. Asher, L. E. Vickery, T. M. Schuster, and K. Sauer, *Biochemistry* **16**, 5849 (1977).
76. D. D. Pulsinelli, M. F. Perutz, and R. L. Nagel, *Proc. Natl. Acad. Sci. USA* **70**, 3870 (1973).
77. K. Nagai, T. Kagimoto, A. Hayashi, F. Taketa, and T. Kitagawa, *Biochemistry* **22**, 1305 (1983).
78. S. A. Asher, M. L. Adams, and T. M. Schuster, *Biochemistry* **20**, 3339 (1981).
79. D. L. Rousseau and J. M. Friedman, "Transient and Cryogenic Studies of Photodissociated Hemoglobin and Myoglobin," in T. G. Spiro, ed., *Biological Applications of Raman Spectroscopy*, Vol. 3, Wiley, New York, 1988, p. 133.
80. J. R. Kincaid, "Structure and Dynamics of Transient Species Using Time-Resolved Resonance Raman Spectroscopy," in K. Sauer, ed., *Methods in Enzymology*, Vol. 246, Academic Press, San Diego, CA, 1995, p. 460.
81. J. Terner, J. D. Stong, T. G. Spiro, M. Nagumo, M. Nicol, and M. A. El-Sayed, *Proc. Natl. Sci. USA* **78**, 1313 (1981).
82. S. Dasgupta and T. G. Spiro, *Biochemistry* **25**, 5941 (1986).
83. J. R. Kincaid, C. Rajani, L. M. Proniewicz, and K. Maruszewski, *J. Am. Chem. Soc.* **119**, 9073 (1997).
84. J. Terner, D. F. Voss, C. Paddock, R. B. Miles, and T. G. Spiro, *J. Phys. Chem.* **86**, 859 (1982).
85. S. Kaminaka, T. Ogura, and T. Kitagawa, *J. Am. Chem. Soc.* **112**, 23 (1990).
86. T. Lian, B. Locke, T. Kitagawa, M. Nagai, and R. M. Hochstrasser, *Biochemistry* **32**, 5809 (1993).
87. Y. Mizutani, and T. Kitagawa, *J. Phys. Chem. B* **105**, 10992 (2001).
88. B. Cartling, "Cytochrome c," in T. G. Spiro, ed., *Biological Applications of Raman Spectroscopy*, Vol. 3, Wiley, New York, 1988, p. 217.
89. R. Timkovich, "Cytochrome c," in D. Dolphin, ed., *The Porphyrins*, Vol.7 Part B, Academic Press, New York, 1979.
90. T. Takano and R. E. Dickerson, *Proc. Natl. Acad. Sci. USA* **77**, 6371 (1980).
91. R. E. Dickerson, and R. Timkovich, "Cytochromes c" in P. D. Boyer, ed., *The Enzymes*, Vol. 11, Academic Press, New York, 1975, p. 397.
92. T. Kitagawa, Y. Ozaki, J. Teraoka, Y. Kyogoku, and T. Yamanaka, *Biochim. Biophys. Acta* **494**, 100 (1977).
93. A. Lanir, N.-T. Yu, and R. H. Felton, *Biochemistry* **18**, 1656 (1979).
94. W. G. Valance and T. C. Strekas, *J. Phys. Chem.* **86**, 1804 (1982).
95. B. Carling, *Biophys J.* **43**, 191 (1983).

96. S. Hu, I. K. Morris, J. P. Singh, K. M. Smith, and T. G. Spiro, *J. Am. Chem. Soc.* **115**, 12446 (1993).
97. R. E. Dickerson, M. L. Kopka, C. L. Borders, Jr., J. C. Varnum, J. E. Weinziert, and E. Margoliash, *J. Mol. Biol.* **29**, 77 (1967).
98. T. Mashiko, J.-C. Marchon, D. T. Musser, C. A. Reed, M. E. Kastner, and W. R. Scheidt, *J. Am. Chem. Soc.* **101**, 3653 (1979).
99. T. Mashiko, C. A. Reed, K. J. Haller, M. E. Kastner, and W. R. Scheidt, *J. Am. Chem. Soc.* **103**, 5758 (1981).
100. H. Oshio, T. Ama, T. Watanabe, and K. Nakamoto, *Inorg. Chim. Acta* **96**, 61 (1985).
101. J. R. Kincaid, "Resonance Raman Spectra of Heme Proteins and Model Compounds," in K. M. Kadish, K. M. Smith, and R. Guilard, eds., *The Porphyrin Handbook*, Vol. 7, Academic Press, San Diego, CA, 2000, pp. 225–291.
102. T. L. Poulos, B. C. Finzel, I. C. Gunsalus, G. C. Wagner, and J. Kraut, *J. Biol. Chem.* **260**, 16122 (1985).
103. M. T. Fisher and S. G. Sligar, *Biochemistry* **24**, 6696 (1985).
104. Y. Ozaki, T. Kitagawa, Y. Kyogoku, Y. Imai, C. Hashimoto-Yutsudo, and R. Sato, *Biochemistry* **17**, 5826 (1978).
105. P. M. Champion, B. R. Stallard, G. C. Wagner, and I. C. Gunsalus, *J. Am. Chem. Soc.* **104**, 5469 (1982).
106. O. Bangcharoenpaupong, P. M. Champion, S. A. Martinis, and S. G. Sligar, *J. Chem. Phys.* **87**, 4273 (1987).
107. D. H. O'Keefe, R. E. Ebel, J. A. Peterson, J. C. Maxwell, and W. S. Caughey, *Biochemistry* **17**, 5845 (1978).
108. J. P. Collman and T. N. Sorrell, *J. Am. Chem. Soc.* **97**, 4133 (1975).
109. T. Uno, Y. Nishimura, R. Makino, T. Iizuka, Y. Ishimura, and M. Tsuboi, *J. Biol. Chem.* **260**, 2023 (1985).
110. O. Bangcharoenpaurpong, A. K. Rizos, P. M. Champion, D. Jollie, and S. G. Sligar, *J. Biol. Chem.* **261**, 8089 (1986).
111. M. Schappacher, L. Richard, R. Weiss, R. Montiel-Montoya, E. Bill, U. Gonser, and A. Trautwein, *J. Am. Chem. Soc.* **103**, 7646 (1981).
112. G. Chottard, M. Schappacher, L. Richard, and R. Weiss, *Inorg. Chem.* **23**, 4557 (1984).
113. K. Nakamoto and H. Oshio, *J. Am. Chem. Soc.* **107**, 6518 (1985).
114. S. Hu, A. J. Schreider, and J. R. Kincaid, *J. Am. Chem. Soc.* **113**, 4815 (1991).
115. F. Tani, S. Nakayama, M. Ichimura, N. Nakamura, and Y. Naruta, *Chem. Lett*. 729 (1999).
116. I. D. G. Macdonald, S. G. Sligar, J. F. Christian, M. Unno, and P. M. champion, *J. Am. Chem. Soc.* **121**, 376 (1999).
117. S. Hu and J. R. Kincaid, *J. Am. Chem. Soc.* **113**, 2843 (1991).
118. M. C. Simianu and J. R. Kincaid, *J. Am. Chem. Soc.* **117**, 4628 (1995).
119. T. Kitagawa, "Resonance Raman Spectra of Reaction Intermediates of Heme Proteins," in R. J. H. Clark and R. E. Hester, eds., *Raman Spectroscopy of Biological Systems*, Vol. 13, Wiley, New York, 1986, p. 443.
120. T. Kitagawa and Y. Mizutani, *Coord. Chem. Rev.* **135/136**, 685 (1994).
121. J. Teraoka and T. Kitagawa, *J. Biol. Chem.* **256**, 3969 (1981).
122. G. Rakhit, T. G. Spiro, and M. Uyeda, *Biochem. Biophys. Res. Commun.* **71**, 803 (1976).

123. S. Hashimoto, Y. Tatsuno, and T. Kitagawa, *Proc. Jpn. Acad.* **60B**, 345 (1984); *Proc. Natl. Acad. Sci. USA* **83**, 2417 (1986).
124. J. Terner, A. J. Sitter, and M. Reczek, *Biochem. Biophys. Acta* **828**, 73 (1985); *J. Biol. Chem.* **260**, 7515 (1985).
125. T. Ogura and T. Kitagawa, *J. Am. Chem. Soc.* **109**, 2177 1987; *Rev. Sci. Instrum.* **59**, 1316 (1988).
126. W. A. Oertling and G. T. Babcock, *Biochemistry* **27**, 3331 (1988).
127. K. J. Paeng and J. R. Kincaid, *J. Am. Chem. Soc.* **110**, 7913 (1988).
128. W.-J. Chuang and H. E. Van Wart *J. Biol. Chem.* **267**, 13293 (1992).
129. V. Palaniappan and J. Turner, *J. Biol. Chem.* **264**, 16046 (1989).
130. J. R. Kincaid, Y. Zheng, J. Al-Mustafa, and K. Czarnecki, *J. Biol. Chem.* **271**, 2880 (1996).
131. K. Nakamoto, *Coord. Chem. Rev.* **226**, 153 (2002).
132. J. Al-Mustafa and J. R. Kincaid, *Biochemistry* **33**, 2191 (1994).
133. T. Tsukihara, H. Aoyama, E. Yamashita, T. Tomizaki, H. Yamaguchi, K. Shinzawa-Itoh, R. Nakashima, R. Yaono, and S. Yoshikawa, *Science* **269**, 1069 (1995).
134. S. Yoshikawa, K. Shinzawa-Itoh, R. Nakashima, R. Yaono, E. Yamashita, N. Inoue, M. Yao, M. J. Fei, C. P. Libeu, T. Mizushima, H. Yamaguchi, T. Tomizaki, and T. Tsukihara, *Science* **280**, 1723 (1998).
135. S. Takahashi, T. Ogura, K., Shinzawa-Itoh S. Yoshikawa, and T. Kitagawa, *Biochemistry* **32**, 3664 (1993).
136. C. R. Andrew, R. Fraczkiewicz, R. S. Czernuszewicz, P. Lappalainen, M. Saraste, and J. Sanders-Loehr, *J. Am. Chem. Soc.* **118**, 10436 (1996).
137. T. Ogura, S. Takahashi, S. Hirota, K. Shinzawa-Itoh, S. Yoshikawa, E. H. Appleman, and T. Kitagawa, *J. Am. Chem. Soc.* **115**, 8527 (1993).
138. T. Kitagwa, *J. Inorg. Biochem.* **82**, 9 (2000).
139. J. P. Hosler, Y. Kim, J. Shapleigh, R. Gennis, J. Alben, S. Ferguson-Miller, and G. T. Babcock, *J. Am. Chem. Soc.* **116**, 5515 (1994).
140. Y. Nagano, J.-G. Liu, Y. Naruta, and T. Kitagawa, *J. Mol. Struct.* **735/736**, 279 (2005).
141. M. Aki, T. Ogura, Y. Naruta, T. H. Le, T. Sato, and T. Kitagawa, *J. Phys. Chem. A* **106**, 3436 (2002).
142. E. Kim, E. E. Chufan, K. Kamaraj, and K. D. Karlin, *Chem. Rev.* **104**, 1077 (2004).
143. K. Czarnecki, J. R. Diers, V. Chynwat, J. P. Erickson, H. A. Frank, and D. F. Bocian, *J. Am. Chem. Soc.* **119**, 415 (1997).
144. U. Ermler, G. Fritzsch, S. Buchanan, and H. Michel, *Structure* **2**, 925 (1994).
145. B. Robert and M. Lutz, *Biochemistry* **25**, 2303 (1986).
146. A. P. Shreve, N. J. Cherepy, and R. A. Mathies, *Appl. Spectrosc.* **46**, 707 (1992).
147. X. Zhao, T. Ogura, M. Okamura, and T. Kitagawa, *J. Am. Chem. Soc.* **119**, 5263 (1997).
148. B. W. Matthews and R. E. Fenna, *Acc. Chem. Res.* **13**, 309 (1980).
149. M. Lutz, A. J. Hoff, and L. Brehamet, *Biochim. Biophys. Acta* **679**, 331 (1982).
150. M. Lutz, B. Robert, "Chlorophylls and the Photosynthetic Membrane," in T. G. Spiro, ed., *Biological Applications of Raman Spectroscopy*, Vol. 3, Wiley, New York, 1988, p. 347.
151. T. M. Loehr and A. K. Shiemke, "Nonheme Respiratory Proteins," in T. G. Spiro, ed., *Biological Applications of Raman Spectroscopy*, Vol. 3, Wiley, New York, 1988, p. 439.

152. D. M. Kurtz, Jr., *Chem. Rev.* **90**, 585 (1990).
153. J. B. Vincent, G. L. Oliver-Lilley, B. A. Averill, *Chem. Rev.* **90**, 1447 (1990).
154. I. M. Klotz and D. M. Kurtz, Jr., *Acc. Chem. Res.* **17**, 16 (1984).
155. D. M. Kurtz, Jr., D. F. Shriver, and I. M. Klotz, *Coord. Chem. Rev.* **24**, 145 (1977).
156. W. A. Henderickson, G. L. Klippenstein, and K. B. Ward, *Proc. Natl. Acad. Sci. USA* **72**, 2160 (1975).
157. J. B. R. Dunn, D. F. Shriver, and I. M. Klotz, *Proc. Natl. Acad. Sci. USA* **70**, 2582 (1973).
158. D. M. Kurtz, Jr., D. F. Shriver, and I. M. Klotz, *J. Am. Chem. Soc.* **98**, 5033 (1976).
159. R. E. Stenkamp, L. C. Sieker, and L. H. Jensen, *J. Am. Chem. Soc.* **106**, 618 (1984).
160. R. E. Stenkamp, L. C. Sieker, L. H. Jensen, J. D. McCallum, and J. Sanders-Loehr, *Proc. Natl. Acad. Sci. USA* **82**, 713 (1985).
161. A. K. Shiemke, T. M. Loehr, and J. Sanders-Loehr, *J. Am. Chem. Soc.* **106**, 4951 (1984).
162. A. K. Shiemke, T. M. Loehr, and J. Sanders-Loehr, *J. Am. Chem. Soc.* **108**, 2437 (1986).
163. S. Kaminaka, H. Takizawa, T. Handa, H. Kihara, and T. Kitagawa, *Biochemistry* **31**, 6997 (1992).
164. J. Sanders-Loehr, W. D. Wheeler, A. K. Shiemke, B. A. Averill, and T. M. Loehr, *J. Am. Chem. Soc.* **111**, 8084 (1989).
165. J. Ling, M. Sahlin, B.-M. Sjöberg, T. M. Loehr, and J. Sanders-Loehr, *J. Biol. Chem.* **269**, 5595 (1994).
166. B. G. Fox, J. Shanklin, J. Ai, T. M. Loehr, and J. Sanders-Loehr, *Biochemistry* **33**, 12776 (1994).
167. "Copper Proteins," in: T. G. Spiro, ed., *Metal Ions in Biology*, Vol. 3, Wiley, New York, 1981.
168. T. B. Freedman, J. S. Loehr, and T. M. Loehr, *J. Am. Chem. Soc.* **98**, 2809 (1976). J. S. Loehr, T. B. Freedman, and T. M. Loehr, *Biochem. Biophys. Res. Commun.* **56**, 510 (1974).
169. T. J. Thamann, J. S. Loehr, and T. M. Loehr, *J. Am. Chem. Soc.* **99**, 4187 (1977).
170. J. A. Larrabee and T. G. Spiro, *J. Am. Chem. Soc.* **102**, 4217 (1980).
171. J. M. Brown, L. Powers, B. Kincaid, J. A. Larrabee, and T. G. Spiro, *J. Am. Chem. Soc.* **102**, 4210 (1980).
172. W. P. J. Gaykema, W. G. J. Hol, J. M. Vereijken, N. M. Soeter, H. J. Bak, and J. J. Beintema, *Nature* **309**, 23 (1984).
173. K. A. Magnus, B. Hazes, H. Ton-That, C. Bonaventura, J. Bonaventura, and W. G. J. Hol, *Proteins* **19**, 302 (1994).
174. J. Ling, L. P. Nestor, R. S. Czernuszewicz, T. G. Spiro, R. Fraczkiewicz, K. D. Sharma, T. M. Loehr, and J. Sanders-Loehr, *J. Am. Chem. Soc.* **116**, 7682 (1994).
175. L. Y. Fager and J. O. Alben, *Biochemistry* **11**, 4786 (1972).
176. J. E. Pate, T. J. Thamann, and E. I. Solomon, *Spectrochim. Acta* **42A**, 313 (1986).
177. K. D. Karlin, R. W. Cruse, Y. Gultneh, J. C. Hayes, and J. Zubieta, *J. Am. Chem. Soc.* **106**, 3372 (1984).
178. J. E. Pate, R. W. Cruse, K. D. Karlin, and E. I. Solomon, *J. Am. Chem. Soc.* **109**, 2624 (1987).

179. N. Kitajima, K. Fujisawa, C. Fujimoto, Y. Moro-oka, S. Hashimoto, T. Kitagawa, K. Toriumi, K. Tatsumi, and A. Nakamura, *J. Am. Chem. Soc.* **114**, 1277 (1992).

180. M. J. Baldwin, D. E. Root, J. E. Pate, K. Fujisawa, N. Kitajima, and E. I. Solomon, *J. Am. Chem. Soc.* **114**, 10421 (1992).

181. K. D. Karlin, *Prog. Inorg. Chem.* **35**, 219 (1987).

182. S. Hikichi, H. Komatsuzaki, N. Kitajima, M. Akita, M. Mukai, T. Kitagawa, and Y. Moro-oka, *Inorg. Chem.* **36**, 266 (1997).

183. W. H. Woodruff, R. B. Dyer, J. R. Schoonover, "Resonance Raman Spectroscopy of Blue Copper Proteins," in T. G. Spiro, ed., *Biological Applications of Raman Spectroscopy*, Vol. 3, Wiley, New York, 1988, p. 413.

184. P. M. Colman, H. C. Freeman, J. M. Guss, M. Morata, V. A. Norris, J. A. M. Ramshaw, and M. P. Venkatappa, *Nature* **272**, 319 (1978).

185. J. M. Guss and H. C. Freeman, *J. Mol. Biol.* **169**, 521 (1983).

186. D. Qiu, S. Dong, J. A. Ybe, M. H. Hecht, and T. G. Spiro, *J. Am. Chem. Soc.* **117**, 6443 (1995).

187. S. Dong and T. G. Spiro, *J. Am. Chem. Soc.* **120**, 10434 (1998).

188. Q. Wu, F. Li, W. Wang, M. H. Hecht, and T. G. Spiro, *J. Inorg. Biochem.* **88**, 381 (2002).

189. G. E. Norris, B. G. Anderson, and E. N. Baker, *J. Mol. Biol.* **165**, 501 (1983). *J. Am. Chem. Soc.* **108**, 2784 (1986).

190. B. C. Dave, J. P. Germanas, and R. S. Czernuszewicz, *J. Am. Chem. Soc.* **115**, 12175 (1993).

191. A. Romero, C. W. G. Hoitink, H. Nar, A. Messerschmidt, and G. W. Canters, *J. Mol. Biol.* **229**, 1007 (1993).

192. M. van Gastel, Y. Nagano, R. Zondervan, G. W. Canters, L. J. C. Leuken, G. C. M. Warmerdam, E. C. de Waal, and E. J. J. Groenen, *J. Phys. Chem. B* **106**, 4018 (2002).

193. R. S. Czernuszewicz, G. Fraczkiewicz, and A. A. Zareba, *Inorg. Chem.* **44**, 5746 (2005).

194. T. den Blaauwen, C. W. G. Hoitink, G. W. Canters, J. Han, T. M. Loehr, and J. Sanders-Loehr, *Biochemistry* **32**, 12455 (1993).

195. C. R. Andrew and J. Sanders-Loehr *Acc. Chem. Res.* **29**, 365 (1996).

196. T. G. Spiro, J. Hare, V. Yachandra, A. Gowirth, M. K. Johnson, E. Remsen, "Resonance Raman Spectra of Iron-Sulfur Proteins and Analogs," in T. G. Spiro, ed., *Iron-Sulfur Proteins*, Wiley-Interscience, New York, 1982, p. 409.

197. T. G. Spiro, R. S. Czernuswicz, S. Han, "Iron-Sulfur Proteins and Analog Complexes," in T. G. Spiro, ed., *Biological Applications of Raman Spectroscopy*, Vol. 3, Wiley, New York, 1988, p. 523.

198. R. W. Lane, J. A. Ibers, R. B. Frankel, R. H. Holm, and G. C. Papaefthymiou, *J. Am. Chem. Soc.* **99**, 84 (1977).

199. T. V. Long, and T. M. Loehr, *J. Am. Chem. Soc.* **92**, 6384 (1970); T. V. Long, T. M. Loehr, J. R. Alkins, and W. Lovenberg, *ibid*. **93**, 1809 (1971).

200. V. K. Yachandra, J. Hare, I. Moura, and T. G. Spiro, *J. Am. Chem. Soc.* **105**, 6455 (1983).

201. R. S. Czernuszewicz, J. LeGall, I. Moura, and T. G. Spiro, *Inorg. Chem.* **25**, 696 (1986).

202. R. S. Czernuszewicz, L. K. Kilpatrick, S. A. Koch, and T. G. Spiro, *J. Am. Chem. Soc.* **116**, 7134 (1994).

203. H. Saito, T. Imai, K. Wakita, A. Urushiyama, and T. Yagi, *Bull. Chem. Soc. Jpn.* **64**, 829 (1991).
204. B. C. Dave, R. S. Czernuszewicz, B. C. Prickril, and D. M. Kurtz, Jr., *Biochemistry* **33**, 3572 (1994).
205. K. Fukuyama, T. Hase, S. Matsumoto, T. Tsukihara, Y. Katsube, N. Tanaka, M. Kakudo, K. Wada, and H. Matsubara, *Nature* **286**, 522 (1980).
206. J. J. Mayerle, S. E. Denmark, B. V. DePamphilis, J. A. Ibers, and R. H. Holm, *J. Am. Chem. Soc.* **97**, 1032 (1975).
207. V. K. Yachandra, J. Hare, A. Gewirth, R. S. Czernuszewicz, T. Kimura, R. H. Holm, and T. G. Spiro, *J. Am. Chem. Soc.* **105**, 6462 (1983).
208. S. Han, R. S. Czernuszewicz, T. Kimura, M. W. W. Adams, and T. G. Spiro, *J. Am. Chem. Soc.* **111**, 3505 (1989).
209. S. Han, R. S. Czernuszewicz, and T. G. Spiro, *J. Am. Chem. Soc.* **111**, 3496 (1989).
210. D. Kuila, J. A. Fee, J. R. Schoonover, W. H. Woodruff, C. J. Batie, and D. P. Ballou, *J. Am. Chem. Soc.* **109**, 1559 (1987).
211. M. Vidakovic, G. Fraczkiewicz, B. C. Dave, R. S. Czernuszewicz, and J. P. Germanas, *Biochemstry* **34**, 13906 (1995).
212. E. T. Adman, L. C. Sieker, and L. H. Jensen, *J. Biol. Chem.* **248**, 3987 (1973).
213. T. M. Berg, R. H. Holm, "Iron-Sulfur Proteins," in T. G. Spiro, ed., *Metal Ions in Biology*, Vol. 4, Wiley, New York, 1982, Chapter 1.
214. M. K. Johnson, R. S. Czernuszewicz, T. G. Spiro, J. A. Fee, and W. V. Sweeney, *J. Am. Chem. Soc.* **105**, 6671 (1983).
215. J.-M. Moulis, J. Meyer, and M. Lutz, *Biochem. J.* **219**, 829 (1984). *Biochemistry* **23**, 6605 (1984).
216. R. S. Czernuszewicz, K. A. Macor, M. K. Johnson, A. Gewirth, and T. G. Spiro, *J. Am. Chem. Soc.* **109**, 7178 (1987).
217. G. Backes, Y. Mino, T. M. Loehr, T. E. Meyer, M. A. Cusanovich, W. V. Sweeney, A. T. Adman, and J. Sanders-Loehr, *J. Am. Chem. Soc.* **113**, 2055 (1991).
218. E. M. Maes, M. J. Knapp, R. S. Czernuszewicz, and D. N. Hendrickson, *J. Phys. Chem. B* **104**, 10878 (2000).
219. L. K. Kilpatrick, M. C. Kennedy, H. Beinert, R. S. Czernuszewicz, T. G. Spiro, and D. Qiu, *J. Am. Chem. Soc.* **116**, 4053 (1994).
220. C. D. Stout, D. Ghosh, V. Pattabhi, and A. H. Robbins, *J. Biol. Chem.* **255**, 1797 (1980); D. Ghosh, W. Furey, Jr., S. O'Donnell, and C. D. Stout, *ibid*. **256**, 4185 (1981); D. Ghosh, S. O'Donnell, W. Furey, Jr., A. H. Robinson, and C. D. Stout, *J. Mol. Biol.* **158**, 73 (1982).
221. H. Beinert, M. H. Emptage, J. L. Dryer, R. A. Scott, J. E. Kahn, K. O. Hodgson, and A. Y. Thompson, *Proc. Natl. Acad. Sci. USA* **80**, 393 (1983).
222. M. K. Johnson, J. W. Hare, T. G. Spiro, J. J. G. Moura, A. V. Xavier, and J. Legall, *J. Biol. Chem.* **256**, 9006 (1981).
223. M. K. Johnson, T. G. Spiro, and L. E. Mortenson, *J. Biol. Chem.* **257**, 2447 (1982).
224. M. K. Johnson, R. S. Czernuszewicz, T. G. Spiro, R. R. Ramsey, and T. P. Singer, *J. Biol. Chem.* **258**, 12771 (1983).
225. C. D. Stout, *J. Biol. Chem.* **263**, 9256 1988; *J. Mol. Biol.* **205**, 545 (1989).
226. M. J. Waring, *Annu. Rev. Biochem.* **50**, 159 (1981).

227. M. Manfait and T. Theophanides, "Drug-Nucleic Acid Interactions," in R. J. H. Clark and R. E. Hester, eds., *Spectroscopy of Biological Systems*, Vol. 13, Wiley, New York, 1986, p. 311.

228. K. Nakamoto, M. Tsuboi, and G. D. Strahan, *Drug–DNA Interactions: Structures and Spectra*, Wiley, Hoboken, NJ, 2008.

229. E. R. Jamieson and S. J. Lippard, *Chem. Rev.* **99**, 2467 (1999).

230. P. M. Takahara, C. A. Frederick, and S. J. Lippard, *J. Am. Chem. Soc.* **118**, 12309 (1996).

231. R. L. Benson, K. Iwata, W. L. Weaver, and T. L. Gustafson, *Appl. Spectrosc.* **46**, 240 (1992).

232. R. Fiel, B. Jenkins, and J. Alderfer, "Cationic Porphyrins-DNA Complexes," in B. Pullman and J. Jortner, eds., *Proc. 23rd Jerusalem Symp. Quantum Chemistry and Biochemistry*, Kluwer Academic Press, Amsterdam, 1990.

233. R. F. Pasternack, E. J. Gibbs, and J. J. Villafranca, *Biochemisty* **22**, 2406 (1983).

234. J. H. Schneider, J. Odo, and K. Nakamoto, *Nucleic Acids Res.* **16**, 10323 (1988).

235. Y. Nonaka, D. S. Lu, A. Dwivedi, D. P. Strommen, and K. Nakamoto, *Biopolymers* **29**, 999 (1990).

236. L. A. Lipscomb, F. X. Zhou, S. R. Presnell, R. J. Woo, M. E. Peek, R. R. Plaskon, and L. D. Williams, *Biochemistry* **35**, 2818 (1996).

237. G. D. Strahan, D. S. Lu, M. Tsuboi, and K. Nakamoto, *J. Phys. Chem.* **96**, 6450 (1992).

238. P. Y. Turpin, L. Chinsky, A. Laigle, M. Tsuboi, J. R. Kincaid, and K. Nakamoto, *Photochem. Photobiol.* **51**, 519 (1990).

239. D. R. McMillin and K. M. McNett, *Chem. Rev.* **98**, 1201 (1998).

240. S. Mettath, B. R. Munson, and R. K. Pandey, *Bioconj. Chem.* **10**, 94 (1999).

Index

Since the number of compounds included in this volume is numerous, entries for most of individual compounds are collected under general entries listed below. Tables of vibrational frequencies, and figures of vibrational (Infrared, Raman) spectra and normal modes of vibration are listed separately under respective entries. Abbreviations used are: M (metal), L (ligand), X (a halogen), and R(alkyl).

Infrared and Raman Spectra of Inorganic and Coordination Compounds, Part B: Applications in Coordination, Organometallic, and Bioinorganic Chemistry, Sixth Edition, by Kazuo Nakamoto

Tables of Vibrational Frequencies

Vibrational Spectra

Matrix Cocondensation Reactions

Normal Modes of Vibration